ON THE

SERVICE LIFE MODELLING

OF

TASMANIAN CONCRETE BRIDGES

by

Rodney William

Rodney W. M^{c}Gee ESM FIEAust CPEng
BE(Hons), ME, GDipBusProfMan, ADEM, BSocSc(EmMan)

Submitted in fulfilment of
the requirements for the Degree of
Doctor of Philosophy

Civil & Mechanical Engineering

University of Tasmania

November 2001

ORIGINALITY

This thesis contains no material which has been accepted for a degree or diploma by the University of Tasmania or any other institution, except by way of background information and duly acknowledged in the thesis, and to the best of the candidate's knowledge and belief no material previously published or written by another person except where due acknowledgment is made in the test of the thesis.

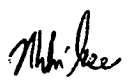

Signed:
(Rodney W. M^{c}Gee)

AUTHORITY OF ACCESS

This thesis may be made available for loan and limited copying in accordance with the Copyright Act 1968.

ABSTRACT

Various forms of concrete have been used for buildings since the time of Egyptian civilisation. The art of cement manufacture was however lost during the Middle Ages. The rediscovery of the art in the nineteenth century and the subsequent development of reinforced and prestressed concrete have seen concrete become the most commonly used construction material throughout the world.

While concrete structures perform well in many situations, lack of durability in others over the last two or three decades in particular has emerged as a significant issue for asset owners internationally. While there is a number of mechanisms by which concrete deteriorates, chloride induced corrosion of bridge and marine structures and carbonation induced damage of buildings are perhaps the most significant.

The various concrete deterioration mechanisms and, to a lesser extent, cover to reinforcement have been researched and reported extensively, particularly in the last twenty years. The research has however tended to focus on specific aspects of the durability performance of concrete structures.

From an asset owner's perspective, it is the interaction of the various aspects of the deterioration processes that determines management strategies for affected structures and code and specification requirements for new structures. The literature relating to the interaction of the chloride and carbonation deterioration mechanisms and cover to reinforcement is however limited.

The Tasmanian Department of Infrastructure, Energy and Resources is responsible for the management of a substantial bridge asset with a high proportion of its value in close proximity to salt water. The durability of its concrete structures is a significant management issue. A series of corrosion investigations and structural surveys have provided a substantial body of data which has been analysed and reported in this thesis to assist with the management of the asset and provide the basis for enhancements to specifications and codes.

This work has highlighted the high variability in the parameters used to describe the durability related properties of insitu aged concrete and in cover to reinforcement. The high variability leads to high probabilities of corrosion initiation, particularly for

chloride induced corrosion, that are reflected in the durability related performance of the bridge asset. A high and continuing demand for maintenance, rehabilitation and replacement of corrosion affected structures is indicated.

The high variabilities also suggest that incremental changes to existing approaches to durability in aggressive environments will not achieve the improvements in performance required to increase materials related reliability to levels that are consistent with, albeit lower than, levels of structural reliability. Approaches to enhance the durability, reflecting the significant level of change required, of concrete structures are proposed.

ACKNOWLEDGMENTS

The author would like to especially thank the following:

My wife, Margie, daughter Heather, and son Andrew for their tolerance and forebearance over many years; initially during the period that I spent as bridge asset manager, involving considerable travelling and time away from home, both intrastate and interstate, on bridge inspections and subsequently during the period of analysis and thesis preparation.

The Department of Infrastructure, Energy and Resources for providing the opportunity to develop my interests in bridges and concrete durability through my employment as a bridge designer and bridge manager and making the data available for the preparation of the thesis; the views expressed in the thesis are not however necessarily those of the Department.

Dr Allan Beasley for his guidance, support, encouragement and advice during the preparation of this thesis and in previous study.

Professor Frank Bullen for his encouragement and critical comment.

My colleagues Fred Andrews-Phaedonos, Dr Alan Carse, Howard Morris, Dr Ahmad Shayan, Gordon Chaplin, Terry White, Frank Collins, Vute Sirivivatnanon, Trinh Cao, Fred Salome, Samia Guirguis, Steen Rostam, Gro Markeset and Leif Hartøft for stimulating my interest in concrete durability.

Carmen Andrade for her inspiration and checks on validity of processes and analyses for determining chloride ingress parameters.

Judy Jensen for her assistance with locating and obtaining references.

1 INTRODUCTION

1.1 GENERAL

Humans have sought materials that would bind stones together from the time that the first buildings were erected. Lime and gypsum mortar was used by the Egyptians to build the pyramids, with the Greeks using similar but improved material. The Romans developed an hydraulic cement, that produced highly durable structures, by combining slaked lime with pozzolana, a volcanic ash. Examples of Roman concrete include the Colosseum, Roman baths and the Basilica of Constantine in Rome.

The art of cement manufacture was lost during the Middle Ages. Its rediscovery is generally attributed to Smeaton, who developed a cement made from limestone and clay that was used to rebuild the Eddystone lighthouse after several failures. His reconstruction stood for 126 years before it was replaced. The discovery of portland cement, which provides the basis for virtually all contemporary concretes, is generally credited to Joseph Aspdin who, in 1824, was granted a patent for a cement made by pulverising a mixture of limestone and clay, and burning them at high temperature to form a clinker, which was then ground to form cement.

The early use of concrete for structural purposes was limited by its low tensile capacity. The principle of reinforcing concrete to provide a tensile capacity seems to have appeared in the 1850's (Warner et al, 1982). Wilkinson, of Newcastle-upon-Tyne in England, was probably the first to take out a patent in 1854 for reinforcing concrete with flat bars and wire rope. Other patents included Lambøt in 1855 and Coignet in 1861 and 1867. In Britain, early reinforced concrete structures used the Hennebique system, which was patented in both England and France. In Australia, two reinforced concrete arch spans were constructed in 1895 at Forest Lodge, Sydney. Further developments in reinforcing came with the introduction of prestressing by Freyssinet in the 1930's.

Concrete has since become the most commonly used construction material, with worldwide consumption having grown to approximately eight billion tonnes per annum (Mehta, 1997).

From the 1930's until perhaps the 1970's, it was generally believed that concrete structures would last for periods in excess of 50 years with little or no maintenance because of the chemical and physical protection afforded to reinforcing steel by the cover concrete. The belief is highlighted in the description of concrete and steel structures being built of permanent materials. The perception that concrete will require minimal maintenance over long periods in even the most aggressive environments remains in some quarters.

While concrete structures continue to perform well in many situations, lack of durability in others has over the last two or three decades emerged as a significant issue for asset owners throughout the world. Of a backlog of bridgework in the United States in 1991 of US$70b, US$28b was attributed to corrosion of reinforcing steel (Weyers, 1998). Similar deficiencies are reported in other countries (Nilsson et al, 1996, The Concrete Society, 1996, Austroads, 1997). Much of the deterioration of bridges in the United States is due to the use of deicing salts on roads (Frangopol et al, 1997). Marine exposures, rising salt in soils and the use of calcium chloride as a set accelerator are other common sources of chlorides. Carbonation is likely to be a more significant cause of corrosion damage necessitating repair in buildings because of the lower covers to reinforcement and construction standards that commonly apply in the building industry and their usual locations away from direct contact with sources of chlorides.

Other concrete deterioration mechanisms, including alkali aggregate reaction and sulfate attack, have also affected structures. Chloride induced damage is likely to be the most significant economically throughout the world, and this is certainly the case with the Tasmanian bridge stock.

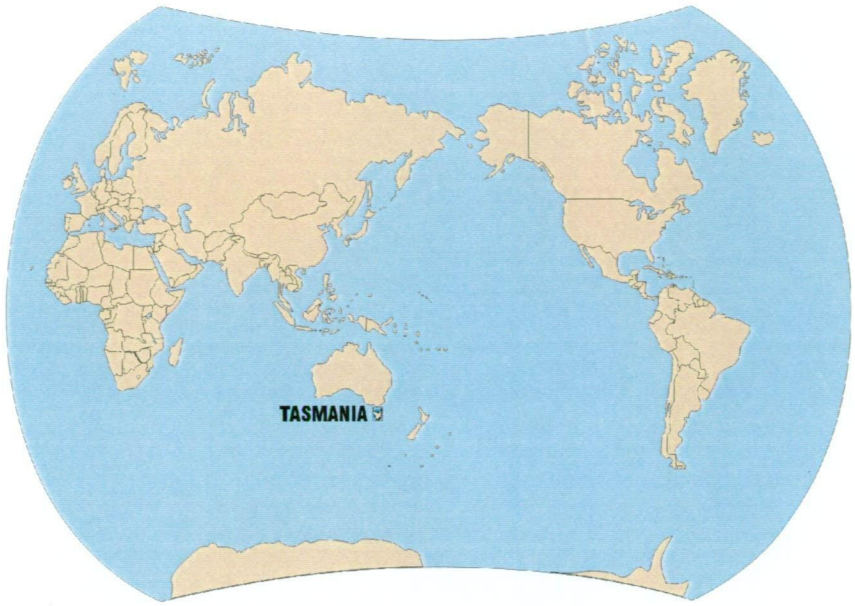

Figure 1.1 – Location of Tasmania

The literature on concrete properties, chloride ingress, carbonation and the other deterioration mechanisms affecting the concrete matrix is extensive. There is however only limited and infrequent publication of data and analysis relating to the variability of cover to reinforcement.

While there are a number of publications relating to service lives of structures, it appears to the author that few have used data on the variability of chloride ingress, carbonation and cover to reinforcement for the probabilistic modelling of durability performance. This compares with structural disciplines where reliability concepts are an integral part of design processes and codes.

The aim of this thesis is to contribute to the enhancement of the durability of concrete bridges and their management, particularly in Tasmania. It focuses on chloride induced corrosion because of the high proportion of the Tasmanian bridge stock affected and the severity and economic consequences of the damage. Carbonation is also considered.

1.2 BACKGROUND TO RESEARCH

The Tasmanian Department of Infrastructure, Energy and Resources (DIER), and its predecessors, are and have been responsible for a substantial bridge asset which currently comprises some 1200 bridges, box culverts, retaining walls and other civil engineering structures with an estimated replacement cost of approximately A$1.1b. The Department previously had responsibility for approximately 50 marine structures,

including jetties, wharves, slipways and training walls. Concrete is the dominant material of construction and, because of the island nature of the State and the distribution of its population, much of the bridge asset is exposed to chlorides and many structures are affected by chloride induced corrosion of reinforcing steel. Oother concrete deterioration mechanisms include carbonation, alkali aggregate reaction, freeze thaw, acid attack and physical damage.

Available funds for road construction and maintenance in Tasmania are extremely limited, with some 5 to 6% of the $70m annual budget allocated to bridge operation and maintenance. The bridge funding needs to be distributed amongst a range of activities including repainting of structural steelwork, lead paint removal, joint and bearing rehabilitation, timber bridge maintenance, conservation of heritage (principally masonry) bridges, concrete works, strengthening for increased vehicle loadings, tidal flow traffic operation of Tasman Bridge, operation of the two moveable bridges at Bridgewater and Dunalley, and replacement of structurally and functionally deficient bridges. Durability related deficiencies of concrete structures are placing increased demands on the available funding.

The author had primary responsibility for management of the bridge stock from 1990 to 1997 and retains a significant involvement as part of a broader asset management role. He was responsible for introducing a systematic bridge inspection and maintenance program that highlighted the significance of concrete durability as an issue for the Department. Because of the dominance of concrete as a material for structures, the frequency and severity of much of the corrosion and the limited funding which is available for roads and bridges generally, the author became particularly interested in the durability of concrete as part his role as manager of the bridge asset.

Addressing concrete deterioration problems required an understanding of the causes and state of corrosion in each structure so that appropriate remedial measures could be implemented, and a program of corrosion investigations was thus established. A number of impressed current cathodic protection systems have now been installed to address chloride induced corrosion and more will be installed as funds become available. Concrete patch repairs, penetrating sealers and coatings have been applied to a number of structures. Other bridges have been replaced because of the severity and extent of corrosion and other deficiencies.

Inspections of structures at the completion of construction and as part of other investigations indicated the accuracy to which structures could be built, particularly in terms of cover to reinforcement.

The author also had a major role in the full scale testing of Princess River Bridge, a reinforced concrete T-beam structure on Tasmania's west coast, prior to its inundation by a hydro-electric power development. In addition to static and dynamic tests at working loads and an ultimate load test, the test program included analysis of dimensional accuracy and concrete durability and structural performance.

Data from the various inspections and investigations and bridge testing provided a substantial body of data which could be analysed to better understand and predict the likely performance of part of the bridge stock and hence enhance the effectiveness of asset management in the Department. The various data have been supplemented as required for the research involved in preparing this thesis.

Prior to assuming responsibility for bridge management, the author had designed a range of bridges of various structural forms and materials for more than 11 years and was thus well aware of the differences in approach between structural design, with a range of well developed models and computer software, and the simplistic qualitative approach to materials design. Structural design philosophies have changed in recent years from working stress to limit state and load and resistance factor design (LRFD) approaches to recognise variability in loading and structural properties and provide consistent reliabilities.

It became evident in managing the bridge stock, with few critical structural problems but many related to material and detailing factors, that improving the durability of new structures would require enhancing the materials design process so that those factors were properly considered in design and implemented during construction and it was likely that a LRFD approach would help to ensure proper consideration by designers because of a consistency of approach with structural design. To develop such an approach would however require quantitative models. The author became aware of early progress towards such an approach from his roles as Convenor of the AUSTROADS project group on concrete durability, and membership of Fédération Internationale de la Précontrainte (*fip*) Commission 10 "Management, Maintenance and Strengthening of Concrete Structures and subsequently, after the merger of *fip* and

Comité European du Beton (CEB), of Fédération Internationale du Beton (*fib*) Commission C5 – Structural Service Life Aspects.

It is hoped that this thesis will contribute to the development of those models and their incorporation in relevant codes, standards and specifications. In the shorter term, implications are being addressed in Departmental specifications and the results used to assist with the programming of remedial and preventative works on affected and exposed structures. Results are being presented in technical papers and will also be submitted to Code committees for consideration, particularly in relation to the variability in cover to reinforcement.

1.3 OBJECTIVES OF THE RESEARCH

Objectives of the research were:

- to collate and analyse data on the durability performance of existing Tasmanian concrete bridges, particularly in relation to concrete properties, chloride ingress, carbonation and cover to reinforcement
- to develop models for assessing the durability performance of Tasmanian concrete bridges
- to provide a basis for the review of specifications and codes to enhance the durability performance of new concrete bridges.

1.4 ORGANISATIONAL OUTLINE OF THESIS

The thesis is structured to provide background information on the deterioration of concrete and the structures from which the data have been collected. Various aspects of concrete durability are then examined individually, and drawn together with the modelling of service lives. The work is then summarised, conclusions drawn and recommendations made.

Chapter 2 defines the shorthand notation which is used in the thesis.

Chapter 3 provides a general introduction to the various mechanisms by which concrete deteriorates to establish the context for the remainder of the thesis.

Chapter 4 provides an overview of the size and condition of the entire structural asset for which DIER is responsible. Investigations of a number of bridge, culvert and marine structures located throughout Tasmania, including the Bass Strait islands,

provided the data on which this thesis is based. The structures which were examined and the environments in which they are located are described in more detail in the appendices.

Chapter 5 examines the strength and compositional characteristics of sampled concretes from the various structures.

In Chapter 6, the penetration of chloride ions into concrete and models to describe it are discussed. Data from the corrosion investigations are then analysed to investigate possible correlations with concrete strength, compositional properties and other factors, and a model developed for service life modelling.

Chapter 7 similarly examines the carbonation of concrete.

Chapter 8 discusses the work of a number of researchers in the field of variability of cover to reinforcement and analyses data from cover surveys of Tasmanian bridges to develop a model for service life assessment.

In Chapter 9, the models for chloride ingress and carbonation are combined with those for cover to reinforcement to assess the service lives of Tasmanian bridges from a concrete durability perspective, using both deterministic and probabilistic approaches. A number of recommendations to improve service lives, particularly with chloride exposures, are made.

Chapter 10 contains summaries of the thesis and findings of the research. Is also discusses implications for the bridge asset and for codes and specifications. Suggested areas for further research are presented.

Additional data for climate, exposure, concrete performance, chloride ingress, carbonation, cover to reinforcement and service life modelling are included in an appendix.

The appendix also includes copies of technical papers based on the research for this thesis that have been written by the author, subject to peer review, presented at international conferences in Sydney and Paris, and published in proceedings of those conferences.

2 NOTATION

2.1 CHAPTER 1 – INTRODUCTION

AUSTROADS	Association of Australian and New Zealand Road Authorities
CEB	Comité European du Beton
DIER	Department of Infrastructure, Energy and Resources
fib	Fédération Internationale du Beton
fip	Fédération Internationale de la Précontrainte

2.2 CHAPTER 3 – CONCRETE DETERIORATION MECHANISMS

AAR	Alkali aggregate reaction
ASR	Alkali silica reaction

2.3 CHAPTER 5 – CONCRETE PERFORMANCE

f'_c	- characteristic concrete compressive strength
f_{c_28}	- 28 day concrete compressive strength
f_{cm}	- target mean concrete compressive strength
f_t	- compressive strength of concrete at time t
F_1	- strength/diameter relationship factor
F_2	- strength/diameter relationship factor
k	- statistical constant
t	- time, age
σ	- standard deviation

2.4 CHAPTER 6 – CHLORIDES

c	- chloride ion concentration
c_s	- chloride ion concentration at surface
D	- chloride diffusion coefficient
D_{eff}	- effective chloride diffusion coefficient
e	- depth of layer boundary
F	- flow of chloride ions

K	- diffusion coefficient ratio
R	- layer boundary resistance
T	- temperature
t	- time
x	- distance
α	- coefficient
μ	- viscosity of solution

2.5 CHAPTER 7 - CARBONATION

a	- coefficient
c	- calcium oxide content
D	- depth of cover
$\overline{D}$	- carbonation coefficient
D	- carbonation depth
f_c	- concrete compressive strength
k	- air permeability of concrete, carbonation coefficient
m	- coefficient for air permeability of concrete
n	- humidity exponent
r	- relative humidity
t, t_m	- time of exposure
w/c	- water cement ratio
x	- depth of carbonation

2.6 CHAPTER 8 – COVER TO REINFORCEMENT

C_m	- mean cover
C_s	- specified cover
k	- statistical constant
M	- difference between mean and specified cover
n	- number of cover measurements
SD	- standard deviation of cover
t	- tolerance for cover

AASHO	American association of State Highway Officials
CIA	Concrete Institute of Australia
NAASRA	National Association of Australian State Road Authorities

2.7 CHAPTER 9 – SERVICE LIFE MODELLING

$C(D)$, c	- chloride concentration
C_T	- chloride threshold concentration
c_s	- surface chloride concentration
c	- specified cover
D	- diffusion coefficient
$F_C(.)$, $F_D(.)$	- cumulative distribution function
$F_R(R)$	- load probability density function
$g(D)$, $G()$	- limit state function
k	- carbonation parameter
P, P_f	- probability
R	- resistance
S	- load effect
t	- time
X	- nominal cover, depth
V_{CO2}	- carbonation rate
α	- diffusion coefficient exponent
β	- reliability index
δ	- partial ponderation factor
φ	- reinforcement accuracy factor
$\Phi(.)$	- standard normal cumulative distribution function
λ_D	- lognormal distribution parameter
ξ_D	- lognormal distribution parameter

3 CONCRETE DETERIORATION MECHANISMS

3.1 GENERAL

As noted in the introduction, concrete has little strength in tension and most contemporary concrete structures are consequently either reinforced or prestressed with steel bar or tendons to give them adequate structural capacity. The steel is normally protected from corrosion by sound cover concrete and the development of a passive oxide layer on the steel in the alkaline environment created by the pore water. While concrete generally performs well from both structural and durability perspectives, deterioration of structures, potentially with a loss of load capacity, may occur through a number of mechanisms.

This chapter provides a general introduction to the range of mechanisms and causes which lead to the deterioration of concrete structures. Additional detail on two of the distress mechanisms, namely chloride ingress and carbonation leading to reinforcement corrosion, is provided later in the thesis. The deterioration mechanisms represent complex interactions between a structure and its surrounding environment and sometimes between the components within the concrete matrix (AUSTROADS, 1997).

The primary distress mechanisms are summarised in Table 3.1 and described in more detail in the remainder of the chapter.

Mechanism	Causes
Reinforcement corrosion	Chloride ingress Carbonation
Disintegration of matrix	Alkali aggregate reaction (AAR) Sulphate attack Thaumasite Delayed ettringite formation (DEF) Acid attack Freeze-thaw
Physical damage	Overloading Impact Abrasion

Table 3.1 – Concrete deterioration mechanisms

3.2 CHLORIDE INGRESS

Chloride ions may be present in three forms within hardened concrete:

- chemically bound

- physically adsorbed
- free chlorides.

Only the free chloride ions are available for transport to an anode for the corrosion process to begin. It is however likely that most of the bound chloride is released and can thus contribute to the corrosion process after initiation (Glass et al, 2000).

Corrosion of steel reinforcement in chloride contaminated concrete is an electrochemical process that requires oxygen and moisture for the reaction to continue and may occur even in alkaline environments. The oxygen is reduced at the cathode and moisture is necessary for the electrolytic process. Hence, corrosion activity will be greatest where oxygen, moisture and chloride ion concentrations are high such as in the splash zone of marine structures. A simplified model of the corrosion process is shown in Figure 3.1. The corrosion process model for carbonation damage is similar.

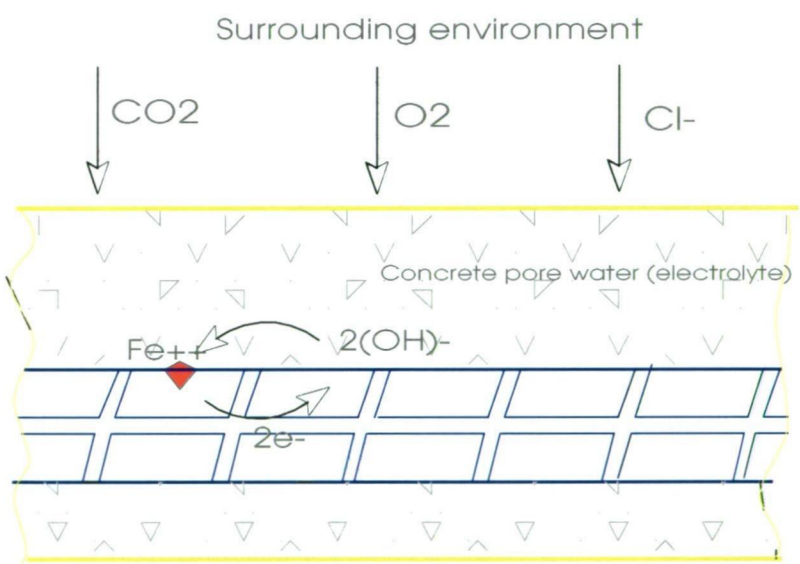

Figure 3.1 – Corrosion process

Chloride ions may enter a concrete structure by a range of transport processes including diffusion for structures where chlorides are present at the surface, such as those located in salt water, or by capillary absorption for structures above water. Chlorides may also be present either from contamination of the constituent materials or as a component of concrete additives. More comprehensive descriptions of transport processes are provided in Chapter 6.

3.3 CARBONATION

Carbonation of the cover concrete occurs when carbon dioxide from the atmosphere reacts with calcium hydroxide produced from the cement hydration reactions and the CSH gel. As a result, the pH of the pore water reduces to the level represented by a saturated calcium carbonate solution of pH 8.3. As the carbonation front approaches the reinforcing, the protective passive film on the steel surface may break down and the corrosion process, in the presence of water and oxygen, may take place.

In conditions of high levels of saturation of concrete, the rate of carbonation is low due to the slower diffusion of carbon dioxide in the water filled pores. Conversely, in very dry environments, there is insufficient water in the pores of the concrete for the gas to dissolve. Carbonation occurs most rapidly at relative humidities between 50% and 70%.

3.4 ALKALI AGGREGATE REACTION

The reaction between alkali hydroxides (usually derived from cement), present in the pore solution of concrete, and aggregates is termed alkali-aggregate reaction (AAR). Depending on its severity, this reaction can be of an expansive nature, causing cracking, and in extreme cases spalling, to occur in a structure. In addition, the cracking exposes the interior of the concrete, and may lead to penetration by aggressive agents (e.g. oxygen, moisture, carbon dioxide, sulphates and salt solution) which cause further accelerated deterioration of the affected concrete.

For deleterious AAR to occur in a structure and lead to significant expansion and cracking, the concrete must contain sufficient amounts of reactive aggregates, alkali and moisture. The absence of one or more of these will inhibit the reaction.

Three types of AAR have been identified, viz. :

- alkali-silica reaction;
- alkali-silicate reaction;
- alkali-carbonate reaction.

Alkali-silica reaction (ASR) occurs between the various forms of silica (including cryptocrystalline and amorphous silica) and the alkali hydroxides.

Alkali-silicate reaction has not been well defined and is considered to occur with aggregates of complex mineralogy such as greywacke, phyllite and argillite. However, it appears that it is basically similar to ASR as far as the reaction products are concerned, but the rate of reaction is lower. In general, no distinction is made between these two types of reaction. In both, an expansive gel is formed which produces large swelling pressures on absorbing water, and may crack the affected concrete. After cracking, the gel penetrates some of the cracks and some of the pressure is relieved.

Alkali-carbonate reaction occurs between the alkali hydroxides of the pore solution of concrete and certain dolomitic carbonate rocks, but this is far less common than ASR, and has not been reported in Australia.

3.5 SULPHATE ATTACK

Sulphates are found in natural water, industrial or domestic sewage and in soils which contain iron pyrite. In sulphate attack, damage to concrete is caused by an expansive chemical reaction between tricalcium aluminate in the cement and sulphates in solution which produces both gypsum and calcium sulphoaluminate (ettringite). The crystals of ettringite occupy a larger volume than the original compounds. The larger volume leads to concrete expansion, cracking, and disintegration.

The primary requirements of sulphate attack are :

- the availability of soluble sulphates;
- a relatively permeable concrete matrix that allows sulphate solution to penetrate;
- the availability of tricalcium aluminate component.

In contrast to the usual increase in corrosion with increase in temperature, sulphate attack diminishes with increasing temperature in the range 0^{o} - $80^{o}C$.

3.6 THAUMASITE

Thaumasite has relatively recently been identified, particularly in the United Kingdom. It is a form of sulphate attack in which there is significant damage to the concrete matrix as a consequence of the replacement of cement hydrates by thaumasite. Thaumasite formation renders the cement paste soft with comcomitant loss of strength and disintegration of the concrete. Advanced attack typically exhibits a white pulpy mass at the surface of the affected buried concrete.

Primary risk factors are:

- presence of sulphates and/or sulphides in the ground
- presence of mobile groundwater
- presence of carbonate, generally in the concrete aggregates
- low temperatures, generally below 15^0C.

3.7 DELAYED ETTRINGITE FORMATION

This mechanism refers to the delayed formation of ettringite (tricalcium aluminate trisulphate hydrate), usually due to the excessive heating of the concrete during its early hardening stage. As a result of the high temperature, the formation of the stable ettringite is suppressed and the metastable monosulphate compound, tricalcium aluminate sulfate hydrate, is formed. The stable ettringite may form subsequently. However, due to the amount of crystalline water contained in the formed ettringite, large expansive forces are generated in the hardened concrete.

Ettringite may form in cracks in concrete which occur due to other primary mechanisms eg. alkali-silica reaction. This type of ettringite formation is a secondary effect and generally harmless.

3.8 ACID ATTACK

In contrast to sulphate attack where only certain compounds in the cement system react, acid attack destroys the complete system. Acids in concentrations common in natural waters and soils tend to dissolve the carbonate layer on the surface of concrete, allowing further carbonation. Concrete will deteriorate because the calcium hydroxide and the hydrated silicate and aluminate phases in the concrete and the acids attacking it form water soluble salts which are subsequently leached.

The resistance to acid attack is independent of the permeability of the concrete and dependent upon the amount of acid available to attack the structure.

The rate of acid attack of any concrete is controlled by the nature of the acid, by the concentration of free hydrogen ions (the pH), by the availability of the acid and by the solubility of the calcium salts formed by exchange reactions with the salts dissolved in the water.

3.9 FREEZE THAW

The transition of water to ice produces an increase in volume of 9%. For saturated concrete this volume increase will cause spalling of the affected concrete. The limiting value of the water content causing damage to occur depends on :

- the age of the concrete;
- pore size distribution;
- the rate of cooling and frequency of freeze-thaw cycles;
- any drying out which may occur between freeze-thaw cycles.

3.10 PHYSICAL DAMAGE

Physical damage is defined as the damage caused to a concrete structure due to an external force or loading pattern as distinct from the chemical attack of the concrete matrix. The following types and causes of physical damage are noted, particularly for bridges:

- cracking due to overloading of structural elements;
- impact damage and abrasion of surfaces due to vehicles, particularly those that exceed legal height limits;
- abrasion of surfaces due to water-borne debris and suspended sediments in high velocity streams.

3.11 CRACKING AND CORROSION

The presence of initial cracking may allow aggressive substances to penetrate faster into the cover concrete and hence increase the rate of deterioration of a given structure.

Before a structure is placed in service it may already have some early age cracking due to:

- plastic shrinkage;
- plastic settlement;
- thermal effects;
- differential and restrained shrinkage;
- applied construction loads.

Later age cracking may also occur due to the following reasons :

- drying shrinkage;

- alkali-aggregate reaction (AAR);
- reinforcement corrosion;
- applied service loads.

Later age cracking such as drying shrinkage and AAR may utilise part of any existing early age crack network and in the process increase its width and extent.

Beeby (1983) discusses a number of investigations aimed at establishing a relationship between crack width and corrosion. Work undertaken at the Technical University, Munich has been reported by authors including Rehm and Moll, Martin and Schieβl. Other investigations have been reported by Houston, Atimtay and Ferguson, Tremper, Raphael and Shalon, and O'Neil. Husain and Ferguson and others have shown that a wide surface crack does not necessarily imply a wide internal crack at the level of the reinforcement. Beeby concludes that crack widths have little influence on corrosion.

Schieβl and Raupach (1997) reported the results of tests involving the measurement of corrosion currents in reinforcing steel in concrete beams with defined crack widths. They found that the influence of crack width declined significantly with test duration until after a period of 2 years when no clear relationship between crack widths and steel removal rates in the crack zone was observable.

Bridge inspections undertaken as part of the Department of Infrastructure, Energy and Resources' management of its bridges show that visible distress leading to decisions to investigate and remediate chloride induced and carbonation damage takes the form of cracking reflecting the underlying reinforcing steel, as a result of its corrosion, and is not usually related to cracking from causes such as flexural behaviour or shrinkage. The amount of visible cracking in all elements of structures from causes other than deterioration of concrete is in fact small.

Because of the lack of a clear relationship between cracking and corrosion, the investigation reported in this thesis is thus based on the penetration of chlorides and carbon dioxide into the concrete matrix.

3.12 SUMMARY

While concrete generally performs well from structural and durability perspectives, it is subject to a number of deterioration mechanisms. Chloride ingress and carbonation

may lead to corrosion of the reinforcing or prestressing steel. Alkali aggregate reaction, sulphate attack, delayed ettringite formation, acid attack and freeze-thaw action lead to deterioration of the concrete matrix. Physical damage may result from overloading, impact or abrasion.

The remainder of this thesis mostly examines chloride ingress and carbonation with a view to assessing implications for the existing bridge stock and proposing models for service life prediction of reinforced and prestressed concrete structures.

4 TASMANIAN BRIDGE STOCK

4.1 GENERAL

The aim of this chapter is to establish the context for the development of cover and deterioration parameters for service life modelling.

The bridge stock managed by DIER is described in terms of numbers, replacement cost, materials of construction, age, environmental exposure and condition. The author has analysed data from the database on bridge inventory and condition that he established during his period of responsibility for management of the bridge stock to describe the bridge stock.

An overview is also provided of the nature and scope of the corrosion investigations that have provided much of the data for the project. Details of individual bridges are provided in the appendix.

4.2 BRIDGE STOCK

Tasmania is an island state with an extensive coastline. Much of its early white settlement took place from the sea, with many towns established near the mouths of rivers. Jetties were built for coastal shipping and roads constructed to provide access to the hinterland. The nature of settlement was reflected in the enactment of the Roads and Jetties Act in 1935 to enable the Public Works Department, a predecessor of DIER, to manage roads, bridges and coastal structures, including jetties. Responsibility for marine facilities to serve amateur and professional fishers continued until June 1997.

With the growth of vehicular transport, roads were built to connect the townships and bridges were built to cross the mouths and estuaries of rivers. Early bridges were made of masonry and timber, but most of the timber bridges have progressively been replaced by and supplemented with steel and concrete structures, concrete being the dominant material of construction. Many of the masonry bridges however remain; these include Richmond Bridge which is Australia's oldest extant bridge with construction having commenced in 1823. The estuarine locations mean that bridges in coastal exposures tend to be larger than the average for the State network.

A substantial proportion of the State's population continues to live near to the coast.

Virtually all the State's bridge stock is managed by government authorities, including DIER, the Forestry Corporation, the Hydro-Electric Corporation and local government. Responsibility for bridges on arterial roads, including highways and main roads, rests with DIER and discussion in this document is based on the performance of its bridge asset.

During his period of responsibility for the management of the State's bridge stock, the author was responsible for the development of a computerised database of structure inventory and condition. Those data have been analysed to provide the following overview of the asset and condition.

The Department's bridge stock includes structures built from a range of materials, including reinforced and prestressed concrete, steel, timber, stone and brick. At 1 July 1998 it comprised 1158 structures with an estimated replacement cost of $1.077b.

Figures 4.1 and 4.2 show the distribution of the numbers and replacement costs of bridge stock by age in 1998. Replacement cost provides a better indication of funding needs than does numbers of structures. The figures highlight the major construction period of the 1960's. In addition to the large number of structures, that decade saw the construction of large bridges such as Tasman Bridge and Batman Bridge.

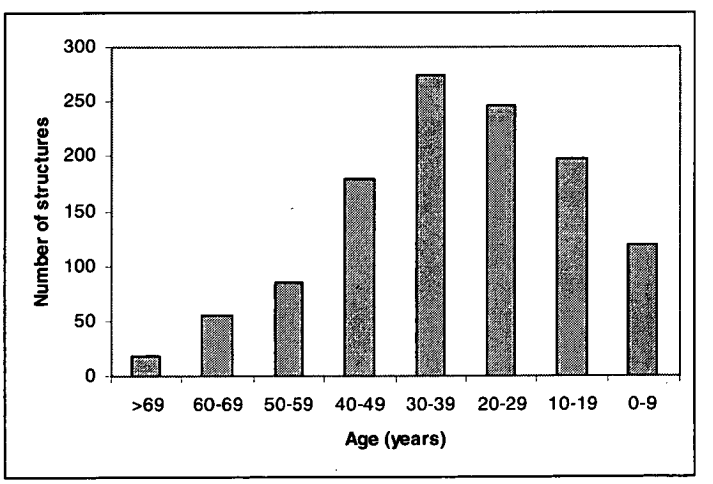

Figure 4.1 – Bridge stock age distribution

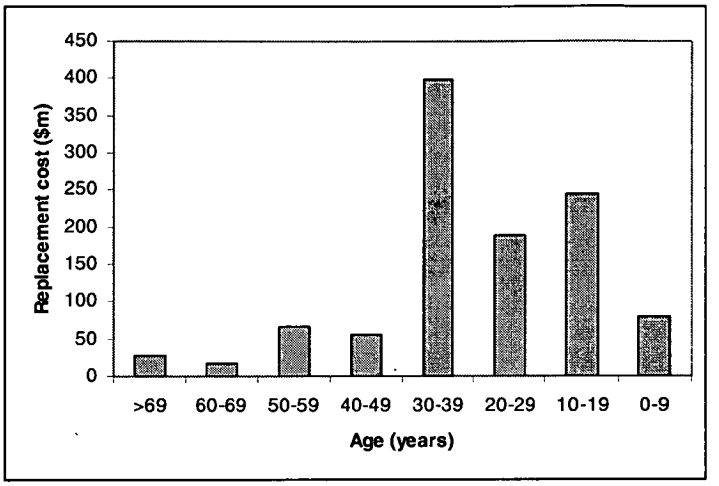

Figure 4.2 - Bridge distribution by replacement cost

Figures 4.3 and 4.4 show the distribution of structures by the material of principal superstructure element construction, both in terms of the numbers of structures and of their replacement cost. The figures show that concrete is the dominant material of construction, particularly when it is considered that concrete is generally used for the substructures and decks of steel bridges, and may be used for piers and abutments of timber bridges.

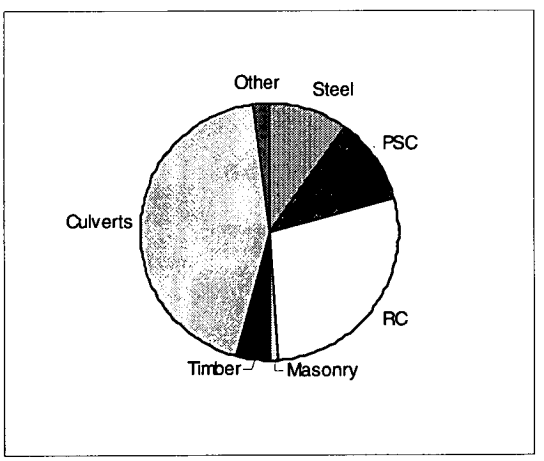

Figure 4.3 – Bridge distribution by type
(RC = reinforced concrete, PSC = prestressed concrete)

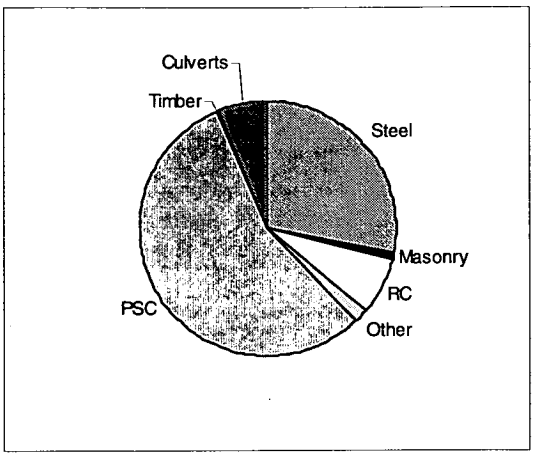

Figure 4.4 – Bridge distribution by replacement cost

4.3 BRIDGE EXPOSURES

Figure 4.5 details DIER's bridge stock in terms of distance from the coastline. For the purposes of this study, coastline is defined as the distance from the ocean (Tasman Sea, Indian Ocean or Bass Strait), the distance from large masses of salt water such as Macquarie Harbour, Pittwater or Tamar River or the estuaries of tidal rivers including Derwent River, Mersey River and Rubicon River. Distance from the coast provides a first indicator of the exposure to chlorides from marine sources. Conversely, structures located a considerable distance from the coast may be at greater risk of damage from other deterioration mechanisms such as carbonation or freeze-thaw damage because of lower relative humidities or greater ranges of temperature.

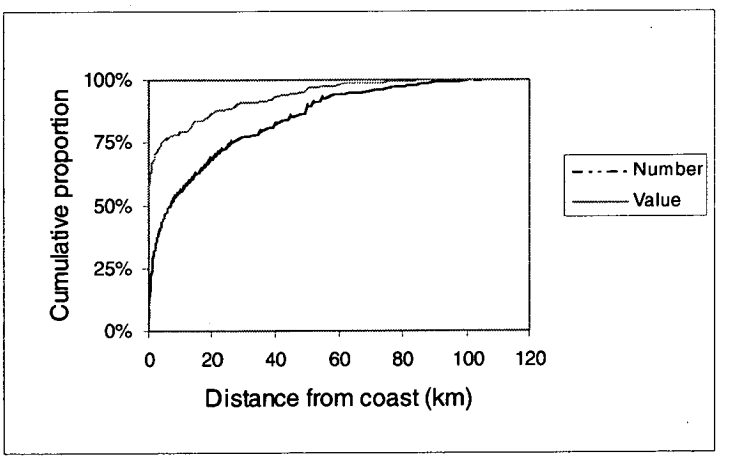

Figure 4.5 – Bridge exposures

The distributions further highlight the coastal nature of settlement within Tasmania and the consequent location of many bridges in tidal estuaries and near to salt water.

The distribution varies little with structures having no concrete superstructure elements excluded, because a number of larger bridges such as Batman Bridge are located close to salt water.

Selected points from figure 4.5 and the distribution for bridges without concrete superstructures are detailed in Table 4.1.

Distance from coast (km)	Cumulative proportions			
	All structures		Structures with concrete elements only	
	By number	By value	By number	By value
0	4.7%	51.5%	4.4%	65.6%
1	26.3%	64.7%	26.1%	65.6%
5	46.4%	76.3%	47.0%	77.0%
10	56.0%	79.2%	56.6%	80.0%
20	68.7%	86.5%	68.9%	87.0%
50	89.6%	96.6%	89.9%	96.8%
75	96.8%	99.1%	96.8%	99.2%
102	99.9%	99.9%	100%	100%
105	100%	100%	100%	100%

Table 4.1 – Bridge exposures

Water samples were taken from various bridge and culvert sites to examine whether environmental exposures could be better determined. Descriptions of the nature of stream flows and results of analysis are included in Chapter 3 of the Appendix. While pH of the water ranges only from mildly acid (pH 5.7) to mildly alkaline (pH 8.7), there are substantial differences in the chloride concentrations of water at the bridge sites, ranging from 4.2 mg/l to 20,000 mg/l, as shown in Figure 4.6. The figure also shows that high chloride concentrations only occur in the ocean and estuaries.

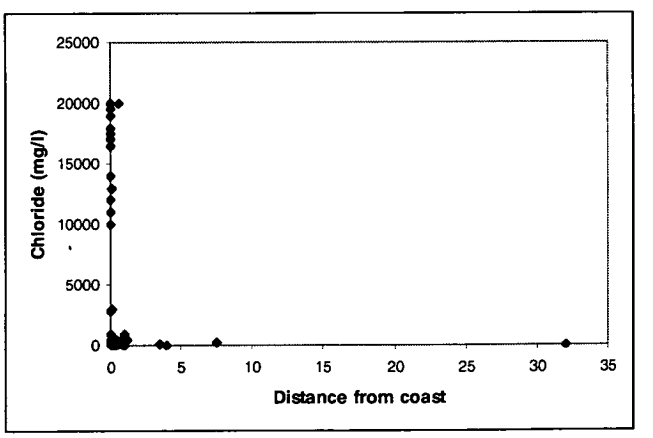

Figure 4.6 - Relationship between stream chloride concentration and distance from coast

Although a number of bridges are in close proximity to large bodies of salt water, this is not necessarily reflected in the chloride concentrations of water in contact with or immediately adjacent to the structure. Particular examples are Bridgewater Bridge, which is located where freshwater from upstream meets the salt water from downstream and it likely that sampling has been from the freshwater wedge. Bridges such as Wrinklers Lagoon, Kelvedon Creek, Denison River, Emu River, Flights Creek and Pats River are protected from direct contact with sea water for much of the time by sand bars. Breaching or overtopping of the bars or weirs as a result of waves, high stream flows and spring tides will however result in intermittent contact of bridge elements to high chloride concentrations. The structures will also be subject to aerosol chloride exposure.

Additionally, the exposure to chlorides for structures located in salt water may be affected by the tidal range at the site. Tidal ranges around Tasmania vary significantly, with the highest ranges in Bass Strait, and are described in Table 4.2 (Port Authorities, 1997).

Location	Range (m)
Hobart	0.9
Spring Bay	0.8
Burnie	3.5
Devonport	2.9
Georgetown	3.3

Table 4.2 - Tidal ranges for Tasmanian ports

Tasmania's prevailing winds are generally westerly but, as shown in Figure 4.14, other wind directions are likely to be dominant in terms of windborne chlorides for the majority of structures involved in the study. In many cases, post-cyclonic winds from the east are more likely significant. Data on prevailing wind directions and associated core orientations were not included in the research. Corrosivity or similar surveys to examine the effects of windborne chlorides were additionally not available for the various sites, given that little or no work has been undertaken in this area in Tasmania.

4.4 CLIMATIC CONDITIONS

In addition to exposure to chlorides and carbonation, corrosion processes in concrete may be affected by climatic factors. In particular, temperature and humidity will affect corrosion and carbonation rates.

Chapter 3 of the Appendix presents detailed climatic data for each of the bridges and culverts involved in the research. Data are distance from the coast, AUSTROADS exposure classification, median rainfall, mean temperature, 'frost' days, and humidities.

The temperate nature of the Tasmanian climate is highlighted by the mean temperatures ranging only from 8^0C to 14^0C and mean relative humidities from 63% to 76%, notwithstanding distances from the coast ranging from 0 to 90 km. There is a greater range in average annual rainfall from 530 mm to 2340 mm. It should be noted that the values presented are at a macroscopic level and there may be localised effects which influence microclimate at a site. These include factors such as the proximity of water and topography which may result in differences in relative humidity, temperature and rainfall. It is unlikely that microclimatic data would generally be available for the design or management of bridges, and the use of macroclimatic factors was thus considered appropriate.

Additional microclimatic factors include the effects of structural form on airflows around structures with implications for the deposition of aerosol and splash chlorides and the degree of exposure to rain with the associated washing of chlorides from the surface. These factors are similarly not considered except for possible omission of the surface layer in the determination of chloride ingress parameters.

4.5 BRIDGE CONDITION

The systematic inspection program established by the author had identified a number of structures affected to varying degrees by one or more of the various forms of concrete deterioration. Figure 4.7 shows a severe case of chloride induced corrosion of a wharf structure which has resulted in delamination and spalling of cover concrete on both beams and deck slab soffits and significant loss of section of reinforcing steel. Scaffolding in the background of the photograph is supporting the delaminated deck slab soffit cover concrete for reasons of public safety.

Figure 4.7 - Stanley Dock beam and slab

Condition data from the database have been analysed by the author to determine the relationship between the numbers and replacement costs of bridges with concrete elements affected by corrosion and the distance from the coastline. Assessments of severity are generally based on visual assessment, supplemented by detailed corrosion assessments for many of the more severely affected structures and a broad knowledge of the performance of the asset. Severe corrosion of bridge structures is generally due to chloride ingress, although there is one significant case of alkali aggregate reaction within the asset. For culverts distant from the coast, delayed ettringite formation and thaumasite attack may contribute to the degradation, although this is as yet unconfirmed.

Severity of corrosion is defined as follows:

- severe corrosion – corrosion which has resulted in significant deterioration of the structure in the form of cracking, staining and/or reinforcement corrosion which has or will require remedial measures, such as the installation of a cathodic protection system or structure replacement, in the short term
- moderate corrosion – significant corrosion that will require remedial measures in the medium term

- mild corrosion – limited corrosion, typically of kerbs and fences, which will not affect structural capacity in the medium term.

Results of the analysis in terms of distance from the coast are shown in figures 4.8 and 4.9. The figures show that a high proportion of affected structures is located close to the coast, but that structures in all locations are affected.

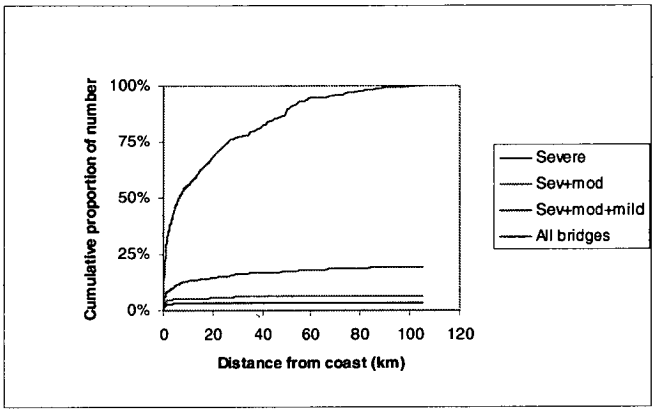

Figure 4.8 – Numbers of corrosion affected bridges

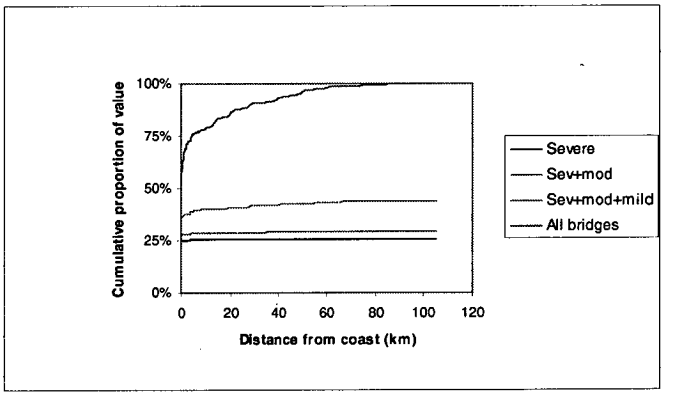

Figure 4.9 – Replacement cost of corrosion affected bridges

Figures 4.10 and 4.11 describe the proportions of bridges affected by corrosion in terms of their ages. Figures 4.12 and 4.13 express the same data as stacked histograms grouped into class intervals of 10 years. The figures show significant proportions of structures affected by corrosion throughout the entire age distribution, including some at quite young ages. The discontinuity in figure 4.11 showing the cumulative proportion of the replacement cost of bridges affected corresponds to corrosion damage in some of the large bridges built during the 1960's. Furthermore, a high

proportion of structures older than 30 years is affected to some degree by the deterioration of concrete.

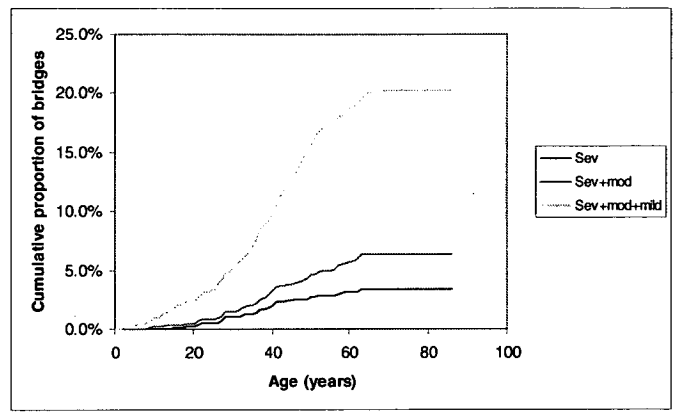

Figure 4.10 – Cumulative proportion of bridge stock affected by corrosion

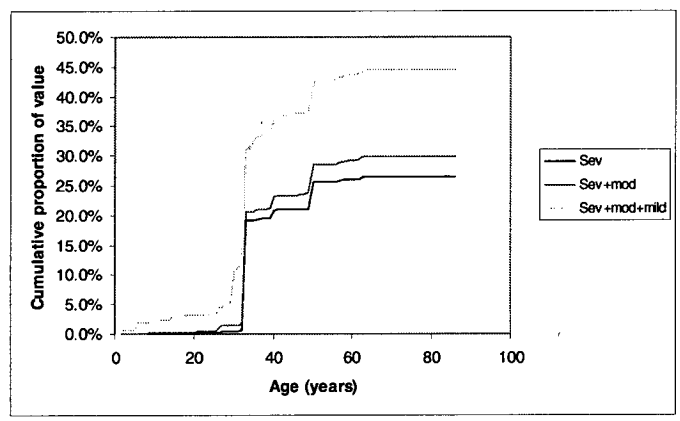

Figure 4.11 – Cumulative proportion of value of bridge stock affected by corrosion

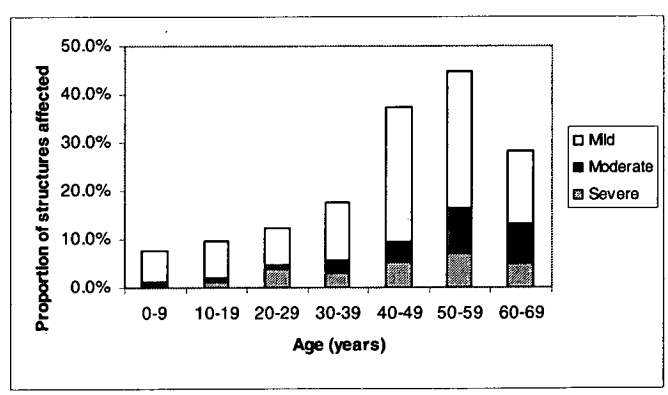

Figure 4.12 – Numbers of corrosion affected bridges

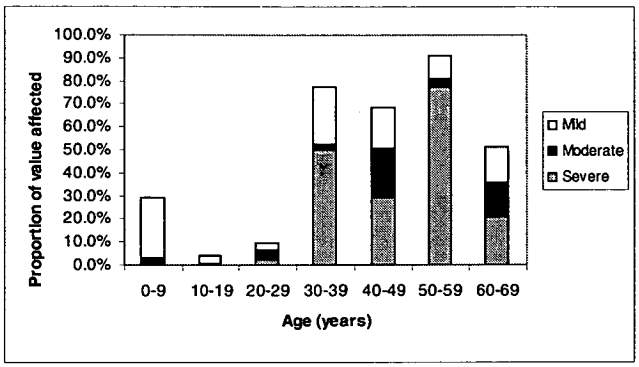

Figure 4.13 – Replacement costs of corrosion affected bridges

The chapter has so far shown that the Department's bridge stock has an average age of approximately 35 years and that about 65% by value is located within 1 km of direct contact with salt water. The analysis of the condition data has shown that a significant proportion of the bridge stock is already visibly affected to some degree by one or more of the various forms of concrete deterioration. Limited funding controls the rate at which remedial measures can be implemented and severely affected structures can be replaced, and it is consequently expected that the significance of concrete deterioration as an issue will become even greater as the asset ages further.

4.6 CORROSION INVESTIGATIONS

DIER, and its predecessors, have been for a number of years been undertaking corrosion investigations to assist with the management of the Tasmanian bridge stock by assessing the nature, cause, severity and extent of corrosion. The results of the investigations are used to assist with understanding the causes of the corrosion and determining appropriate management strategies for affected structures. The corrosion investigations have been supplemented by a program of investigation into poorer than expected durability performance of precast box culvert crown units.

Repair and rehabilitation options include concrete patch repair using polymer modified cementitious repair materials, use of penetrating sealers such as silanes, use of acrylic or methacrylate based coatings, or cathodic protection. Impressed current cathodic protection systems have been used where that remedial option has been adopted because of a higher level of confidence in their ability to protect affected structures than for galvanic systems and because of the ability to monitor their performance through the measurement of applied voltages and currents and the use of

reference electrodes. Results from corrosion investigations assist in the selection and design of the remedial measures.

Where replacement is the adopted option, the corrosion investigation and ongoing monitoring assist in determining the time of replacement.

Early corrosion investigations were carried out by specialist corrosion consultants. With the significant number of affected structures within the State, the majority of subsequent investigations were carried out by the Department's Materials and Research Division with the framework for the investigations and the interpretation of data established by the author.

The scope of corrosion investigations included:

- review of existing drawings and records
- visual inspection to record the overall condition of a structure and map defects including cracking, staining and spalling
- delamination surveys to ascertain the extent of incipient spalling of the concrete
- cover surveys to evaluate the depth to reinforcement and its variability
- coring of concrete and analysis for strength, density, cement (binder) content, water cement ratio, chloride profiles, sulphates and carbonation depth
- measurement of volume of permeable voids and Young's modulus for some samples
- petrographic examination of concrete samples for evidence of alkali aggregate reactivity, delayed ettringite formation or thaumasite attack
- a small number of samples were also examined with an electron microscope
- half cell potential surveys to indicate the probability of corrosion through interpretation of absolute values of half cell potentials and potential gradients
- resistivity surveys to provide an indication of likely corrosion rates.

Test methods are described in Chapter 2 of the Appendix.

Results of the corrosion investigations are then considered together with reviews of the structural, geometric and hydraulic adequacy of a structure to evaluate a range of options that include:

- monitoring, with an eventual need for some remedial measures
- patch repairs

- protective coatings
- penetrating sealers
- cathodic protection
- chloride extraction
- realkalisation
- concrete jacketing or encasement
- waterproofing membranes
- replacement of affected elements or the entire structure.

The corrosion investigations and sampling from a number of other bridges provided the data on concrete performance and some of the cover data that have been used as the basis of this thesis. Additional sampling of concrete generally resulted from a need for specific investigations, such as structural capacity, or from sampling of demolished bridges. The nature of the more extensive cover surveys is described in Chapter 8. Locations of the 58 structures for which investigations were undertaken are shown in figure 4.14. The figure shows that many of the investigated structures were located close to the coast, but that a number were inland, reflecting the range of deterioration mechanisms which are evident in the Tasmanian bridge stock. It is consistent with figures 4.8 and 4.9. Cover data were drawn from a total of 143 bridges and major culverts throughout the State.

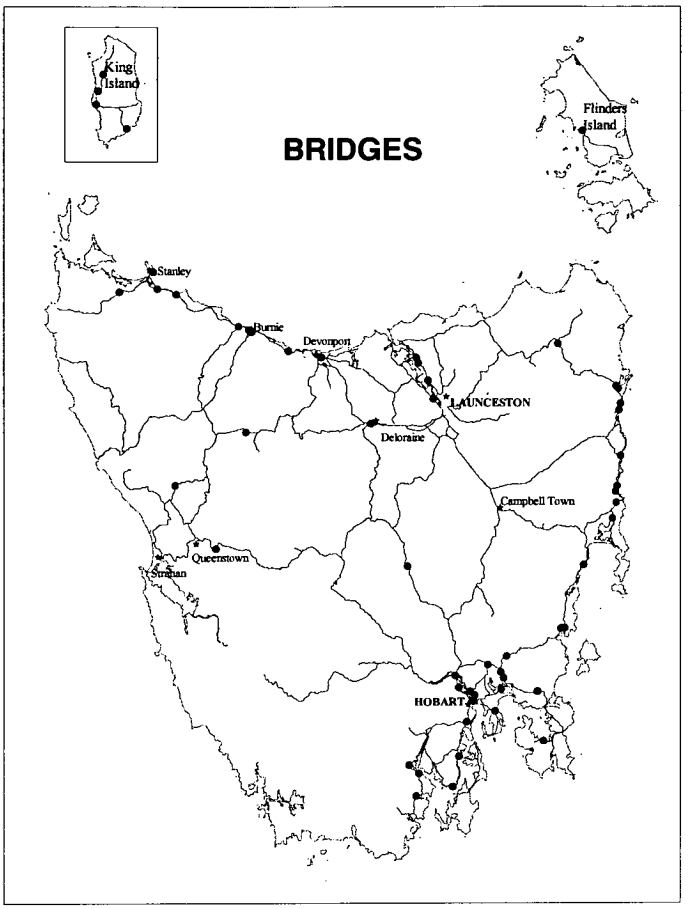

Figure 4.14 – Bridge and culvert locations

4.7 SUMMARY

DIER is responsible for the management of a substantial bridge stock, with concrete being the dominant material of construction. Because Tasmania is an island state, with much of its population close to the coast, more than 50% by value of the asset is in direct contact with salt water. With a temperate climate, there is only limited variability in mean temperatures and relative humidities between bridge sites from a macroclimatic perspective. Average annual rainfall however ranges from 530mm to 2340mm.

Analysis of condition data contained in this study shows a significant proportion of structures affected to some degree by one or more of the various forms of concrete deterioration. The likelihood is greater for older structures or those close to the coast, but inland and younger bridges and culverts are also affected. The analysis has also

indicated that the significance of deterioration of concrete will continue to increase as a management issue for the Department of Infrastructure, Energy and Resources.

A series of corrosion investigations on corrosion affected structures and sampling of others have provided the data which are the basis of this thesis.

5 CONCRETE PERFORMANCE

5.1 GENERAL

The purpose of this chapter is to examine the strength and compositional characteristics of the various concretes for subsequent investigation of possible correlations with chloride ingress and carbonation and ultimately for developing models for service life modelling and specifications, rather than being a detailed analysis of the long term performance of concrete.

Briefly, the basic materials in concrete are:

- coarse aggregate
- fine aggregate
- cement
- water.

Contemporary concretes also incorporate chemical admixtures, such as water reducers and air entraining agents, and may further include mineral admixtures, particularly silica fume, fly ash and ground granulated blast furnace slag. The use of chemical admixtures in the concretes which are the subject of this study is unknown but is nevertheless expected to be low, particularly with the older concretes, because of their age, the use of direct labour and site batching for many of the bridges. Any use is likely to be limited to water reducing and air entraining agents. It is unlikely that supplementary cementitious materials were present in any of the concretes involved in the study.

The use of calcium chloride as a set accelerator has generally been precluded in Departmental structures; it may however have been present in a small number of bridges, such as those built by contract.

Concrete has generally been specified in terms of its characteristic compressive strength because it directly affects the structural design of members. Composition has been used to a lesser extent. Where strength is specified, it is the objective of the mix designer to achieve a composition which will be the most economical for the supplier by having a target mean compressive strength as close as possible to the characteristic strength whilst achieving 95% of test results equal to or exceeding the characteristic

strength. Economy will be achieved by minimising the cement content of the concrete mix. Because of changed cement compositions and grinding practices, the cementitious content for a given compressive strength has progressively reduced, particularly in recent decades.

The strength of concrete has long been regarded as an indicator of its durability, and this principle is indeed embodied in the Australian standards for concrete structures and bridge design.

Other research has established correlations between the durability related performance of concrete and its composition, particularly in terms of cement content and water cement ratio. This principle has been incorporated in current DIER specifications, which include minimum cement contents and maximum water cement ratios in addition to compressive strength requirements for the various concrete grades.

The author has been responsible for the extraction of data from Departmental files, literature review and analysis.

5.2 STATISTICAL METHODS

Statistical techniques are used in this and the subsequent chapters on carbonation, chloride ingress and cover to reinforcement to examine possible correlations with a range of factors and to develop statistical distributions of variables for the service life modelling.

Statistical analysis was principally undertaken with the SPSS statistical analysis software package, with some use of Microsoft Excel.

For probabilistic modelling of service life, it was necessary to develop statistical models for variables describing chloride ingress and carbonation and any environmental or concrete compositional variables for which a correlation might be found. Numerical hypothesis testing, particularly for normal distributions, typically uses the Kolmogorov-Smirnov test or modifications such as the Lilliefors test. Assessment of normality may also use graphical techniques, with the method in fact recommended by some authors (McPherson 1990, Moore and M^{c}Cabe 1989, SPSS 1998). Graphical techniques use either a normal quantile plot or a normal probability plot. A normal quantile or quantile-quantile plot compares two distributions by

plotting their quantiles (or percentiles) against each other. If the distributions are similar, their quantiles will be similar and the quantile-quantile plot will be close to the line x=y. If not, the deviation from the line will indicate how the distributions differ. The technique is enhanced by using detrended plots which plot the difference between the measured and expected quantiles to characterise how the values differ from the distribution being used for comparison. The normal probability plot is similar and plots each observation against its expected z-score for a normal distribution. Graphical techniques were generally used for the assessment of the fit of the data with various probability distributions.

The statistical analysis was undertaken to develop models of parameters for subsequent service life modelling and to enable comparisons to be made with published data. Normal and longnormal probability distributions are commonly reported for the various parameters and these were readily available with the softwarer used in the analysis. Gamma, extreme value and similar distribution types could possibly have provided enhanced probabilistic but at the expense of the ability to compare with published data.

5.3 SPECIFICATIONS

The majority of structures from which samples were taken were built by direct labour without job specific specifications. In most cases, drawings simply stated the volume of concrete required without reference to its strength or composition. Specific requirements have been included in specifications for new bridges since the late 1980's as DIER increasingly built structures by contract.

Additionally, the majority of structures would have used site batched concrete with its inherent variability. Site batching was in fact used for bridges remote from the main centres of population until the mid 1970's.

Table 5.1 shows a diverse range of specified strengths and compositions for structures where there was in fact a specification, including differences in composition for the same specified compressive strength. Specifications for Tasman Bridge concretes are specific to the bridge, with the design and documentation having been prepared in the United Kingdom. Data are only included in more than one column of the table where the specifications or drawings define more than one aspect of the concrete.

Class	Strength	Composition
GENERAL		
	1500 psi (10.4 MPa)	
	2000 psi (13.8 MPa)	
	2000 psi (13.8 MPa)	1:2:4
	2200 psi (15.2 MPa)	1:6
	2500 psi (17.3 MPa)	
	2500 psi (17.3 MPa)	1:2:4
	3000 psi (20.7 MPa)	
	3000 psi (20.7 MPa)	1:2:4
	3000 psi (20.7 MPa)	1:1.5:3
	4000 psi (27.6 MPa)	
	4500 psi (31.1 MPa)	
	5000 psi (34.6 MPa)	
	20 MPa	
	30 MPa	
	38 MPa	
	40 MPa	
Class AA		
Class A		
Class B		
Class C		
Class D		
Class E		
TASMAN BRIDGE		
A	6500 psi (44.9 MPa)	
B	4500 psi (31.1 MPa)	
C	3000 psi (20.7 MPa)	
D		1:3:6
E		1:10

Table 5.1 - Concrete specifications
(Composition is cement:fine aggregate:coarse aggregate)

Figure 5.1 shows 3000psi/20 MPa concrete to have been the most commonly specified concrete for insitu elements, although the number of samples for which strength was specified is small compared to the overall number of samples.

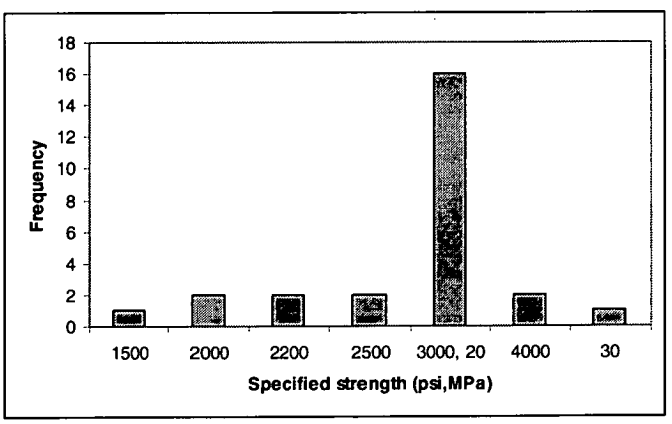

Figure 5.1 – Concrete strength specification frequencies (N=26)

While 3000psi/20MPa was commonly specified, figure 5.2 highlights the range in and the lack of a correlation between specified compressive strengths and the year in

which a structure was built, although there is a trend of the specified strength increasing.

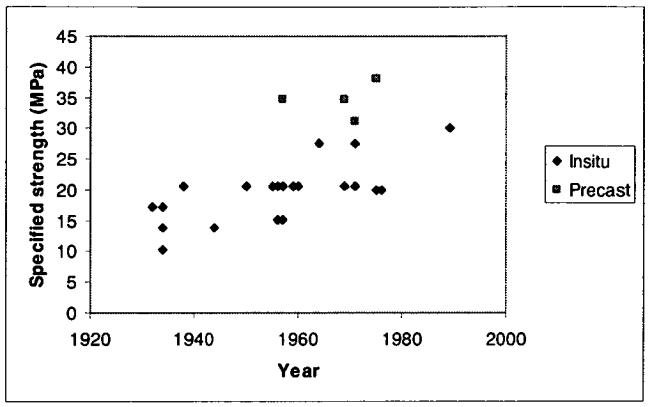

Figure 5.2 – Concrete specification trends

It is noted that compressive strengths of concrete for older bridges, which were typically 3000 psi or less, are significantly lower than those used in contemporary structures. Specified characteristic strengths were increased in the 1980's as a measure to enhance durability. The selection of concrete grade for new structures by DIER and its consultants is currently in accordance with the requirements of the AUSTROADS Bridge Design Code. For members in tidal or splash zones (exposure classification C), the minimum required characteristic strength of concrete is 50 MPa. In coastal zones, the minimum required strength is 40 MPa with a further reduction to 32 MPa for locations further inland. The strength requirements may be modified for particular soil or water exposures. Once a concrete grade is selected, DIER's standard specifications prescribe the minimum binder content and maximum water binder ratio. Minimum specified cementitious contents for 32 MPa, 40 MPa and 50 MPa concretes are 400 kg/m^3, 440 kg/m^3 and 500 kg/m^3 respectively while the respective maximum water binder ratios are 0.5, 0.45 and 0.4.

5.4 LONG TERM STRENGTH GAIN

5.4.1 Review of Relationships

Examination of the long term performance of concrete in the various structures includes consideration of the likely strength of the concrete at an age of 28 days for comparative purposes.

The primary objective of assessing 28 day strengths was to examine whether a relationship could be established between strength and durability performance for subsequent analysis and to assist with a review of specifications. Researching of Departmental records only located construction records of concrete strength for a few of the structures subsequently assessed. In many cases, compressive test cylinders would not have been made and tested because of the remoteness of the structures, the use of site batching and the limited availability of test facilities at the time of construction. The lack of test results for other structures may reflect record keeping practices and the implications of organisational change.

The relationship between the strength of cores and the 28 day strength of cylinders will be influenced by factors including the effects of site curing and ongoing exposure, variability of properties within structural elements, the location and orientation of cores, the influence of diameter given that the majority of cores are of 75mm diameter compared to the standard test cylinder diameters of 100mm or 150mm, the effect of length/diameter ratio, and differences between the strength of insitu concrete and that of standard cylinders. Malhotra (1977) discusses the complexity of the latter factor. Bartlett and M^{ac}Gregor (1996) analysed the relationship between the insitu compressive strength of concrete in structures and the specified concrete strength. Using 3756 cylinder tests representing 108 concrete mixes produced in Canada between 1988 and 1993, they found that the relationship could be represented as the product between two independent factors F_1 and F_2. Factor F_1 is the ratio of the average strength of standard cylinder specimens to specified strength f'_c, and had a mean value of 1.25 and standard deviation of 0.13 for concretes produced for insitu construction, or a mean value of 1.19 and a standard deviation of 0.06 for concretes produced for precast construction. F_2 is the ratio of the average insitu strength to the average strength of 28 day standard cylinder specimens, and depends on the age and height of the element and the quality of curing provided. At 28 days, the average value of F_2 was 0.95 for elements less than 450mm high or 1.03 for elements at least 450mm high. The average insitu strength increased by about 25% between 28 days and 1 year. The value of F_2 was independent of concrete strength and was represented by a lognormal distribution with a coefficient of variation of 14%.

Taylor (1977) presents relationships between compressive strength of 150mm diameter by 300mm cylinders and water cement ratio for ordinary portland cement and varying ages, as shown in Figure 5.3.

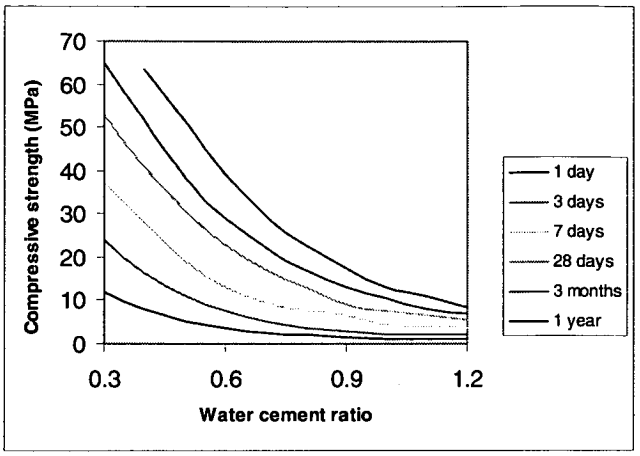

Figure 5.3 – Compressive strength ~ water cement ratio relationships

The figure can be transposed to provide a relationship between compressive strength and age for varying water cement ratios.

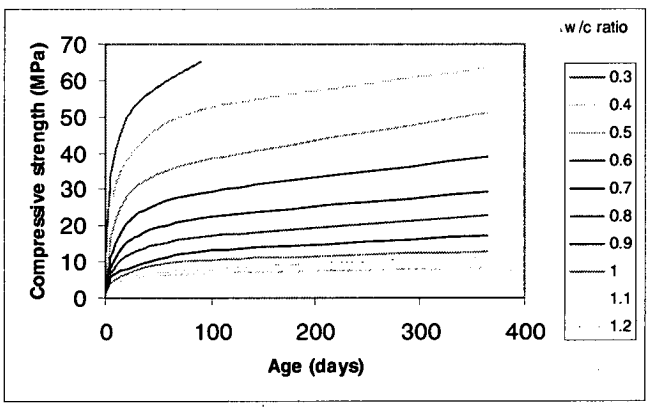

Figure 5.4 – Compressive strength ~ age relationship

Water cement ratios measured on the cores from Tasmanian bridges involved in this study ranged from 0.32 to 1.06 with a mean of 0.57. Ages of the cores ranged from 5 to 65 years with a mean of 27 years. While there is a degree of uncertainty about extrapolating the relationships beyond the one year time frame, a logarithmic curve fit for a water cement ratio of 0.5 nevertheless provides a basis for estimating the 28 day strengths of the different concretes using Taylor's relationships. Excel curve fitting gives a relationship of:

$$f_t = 7.86 \ln(t) + 3.77;\ R^2\ 0.996$$

where f_t = strength in MPa at age t; and

t = age in days

For a water cement ratio of 0.6, the comparable relationship is

$$f_t = 6.15 \ln(t) + 1.96; R^2\ 0.994$$

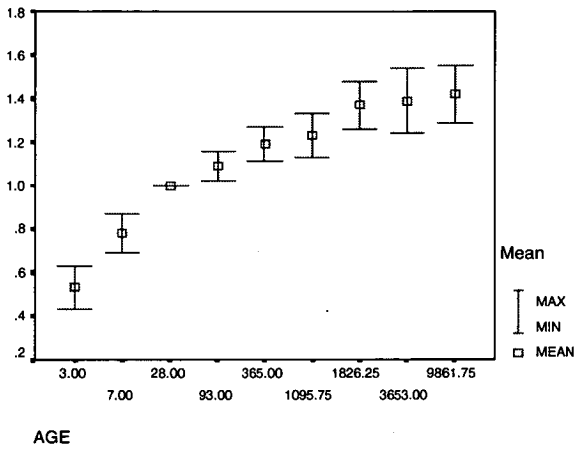

Figure 5.5 – Long term strength gain of concrete after Wood (Age in days, normalised compressive strength – reference strength at 28 days)

Figure 5.5 shows the long term strength gain of concretes up to 34 years as reported by Wood (1991). Ranges shown in the figure are ± 1 standard deviation from the mean. Excel curve fitting gives a line of best fit of

$$f_t = 0.102 \ln(t) + 0.560; R^2\ 0.936$$

where f_t = normalised strength; and

t = age in days

Washa et al (1975, 1989) have reported on three long term concrete test programs started at the University of Wisconsin-Madison in 1910. Large numbers of test cylinders and prisms were cast and tested periodically for compressive strength, transverse strength, volume changes, secant and dynamic modulii, and unit weight changes. Series A specimens were made in 1910 and moist cured for 14 days prior to storage in indoor, outdoor and underwater storage conditions. Series B (1923) and Series C (1937) were moist cured for 28 days prior to placement in indoor and outdoor storage conditions for Series B and outdoors for Series C. Compressive strengths at various ages are shown in Figure 5.6; additional detail is included in the Appendix.

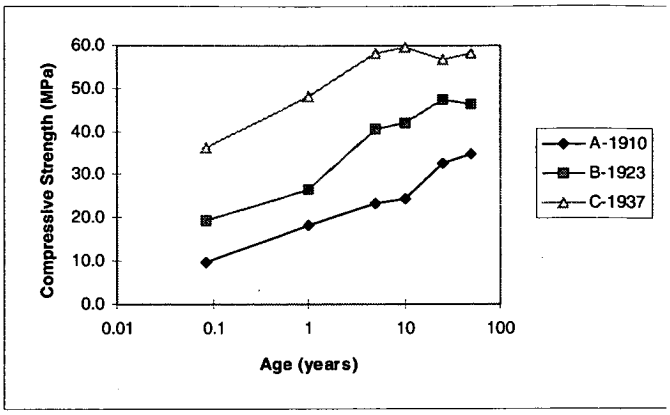

Figure 5.6 - Concrete strength-age relation (Washa et al)

Curve fitting similarly gives the relationships:

Series A:

$$f_t = 13.7 \ln(t) + 8.85; \; R^2 \; 0.956$$

where f_t = strength in MPa at age t; and

t = age in days

Series B:

$$f_t = 16.8 \ln(t) + 18.7; \; R^2 \; 0.946$$

where f_t = strength in MPa at age t; and

t = age in days

Series C:

$$f_t = 12.7 \ln(t) + 39.0; \; R^2 \; 0.849$$

where f_t = strength in MPa at age t; and

t = age in days

5.4.2 Tasmanian Bridges

Results of cylinder compression tests for a limited number of structures were available from DIER records for comparison with strengths measured on cores taken during corrosion investigations on a number of structures and from the Deloraine Rail Underpass, which was demolished during a highway realignment.

Bridges for which data were available are described in Table 5.4.

Bridge		Mix design	Year of completion
Symons Creek	– abutments	5:1	1938
- beams, deck			
Orielton Rivulet		4:2:1	1938
Mountain Creek		5:1	1943
Surges Creek		4:2:1	1944
Higgins Creek		4:2:1	1944
Rileys Creek		4:2:1	1944
Carlton Bridge		4:2:1	1945
Carlton Culvert		4:2:1	1946
Deloraine Rail	– abutments, deck	30 MPa, 400 kg/m^3 cement, 0.45 wc ratio	1989
- beams		40 MPa, 480 kg/m^3 cement, 0.45 wc ratio	

Table 5. 4 – Bridge details for compressive strength data

Short and long term strength gain data, normalised to proportions of 28 day compressive strength are summarised in figures 5.8 and 5.9.

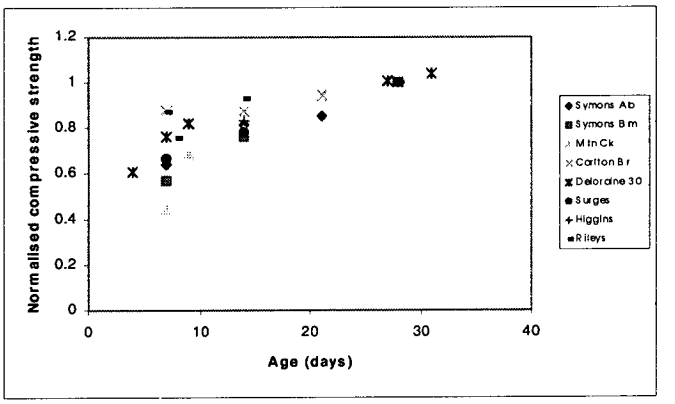

Figure 5.8 – Normalised short term strength gain data

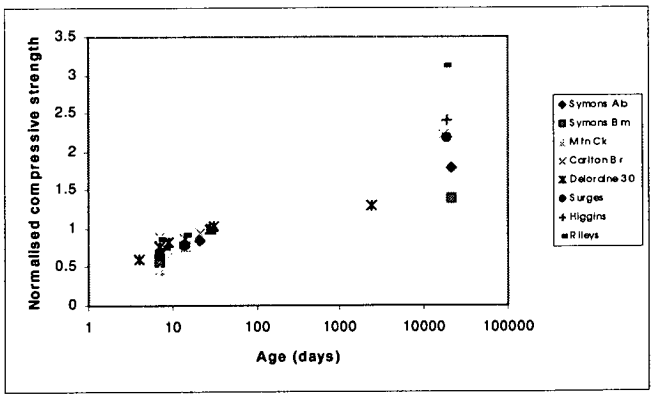

Figure 5.9 – Normalised long term strength gain data

5.4.3 Aggregated Data

Data from Washa et al, Wood, Taylor and the Tasmanian bridges represent a range of concretes manufactured over a long period (1910 to 1989). It includes a wide range of mix proportions, as well as a wide range of cement compositions and grinding practices. The aggregated data are shown in Figure 5.10.

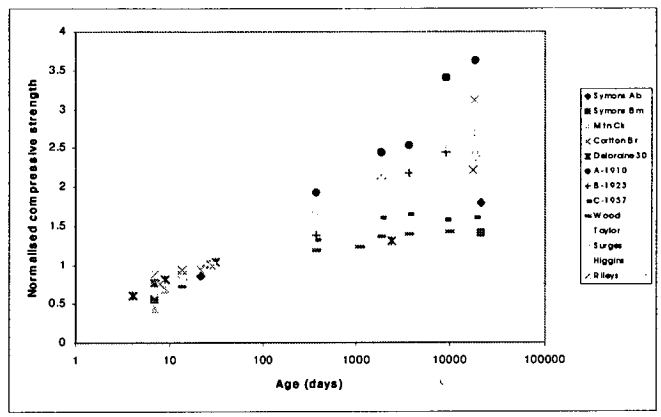

Figure 5.10 – Aggregated strength gain data

To provide a model for estimating 28 day concrete strengths from core strengths, a logarithmic curve was fitted to the aggregated data, as shown in figure 5.11.

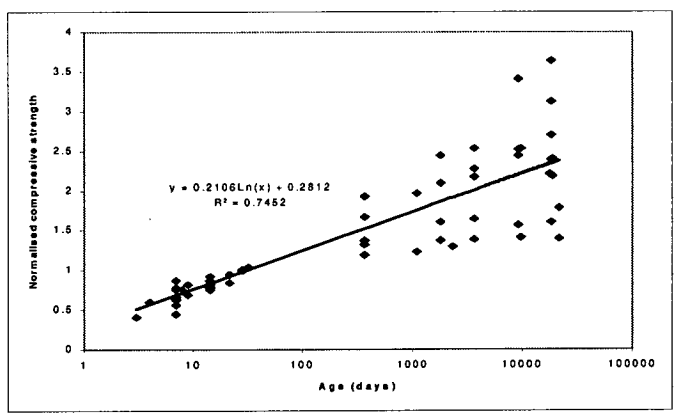

Figure 5.11 – Normalised strength gains

For concrete ages of at least 25 years, which excludes the relatively short term results from the Deloraine Underpass, results from the Tasmanian bridges and from the literature show a high variability in the ratio of long term strength to 28 day strength. For Tasmanian bridges, the ratio varies between 1.40 and 3.13 with a mean of 2.19, standard deviation of 0.58 and coefficient of variation 26.7%. Adding the results from

the literature increases the range to between 1.40 and 3.64, the mean to 2.34, the standard deviation to 0.68 and the coefficient of variation to 29.0%. The variability is reflected in the R^2 value of 0.745.

5.4.4 Estimated 28 Day Strengths for Tasmanian Bridges

The long term strength gain relationship developed in the previous section is used in this section to examine concrete strength characteristics for the sampled bridges.

Classes of concrete previously used by the Australian Government Department of Housing and Construction, and possibly in Tasmanian bridges, are described in Table 5.5 (Taylor, 1977).

Class	Water/cement ratio by mass	Cylinder Compressive Strength (MPa)	
		7 days	28 days
A	0.5	18.5	30.0
B	0.6	14.0	22.0
C	0.7	9.7	16.5

Table 5.5 – Properties of concrete classes

Concrete has typically been specified in terms of its characteristic compressive strength f'_c, which is defined as the value of strength, as determined by standard tests, that is exceeded by at least 95% of the individual test results (Symons, 1992). A mix designer establishes a target strength f_{cm}, which is the mean strength of test cylinders. Based on a normal distribution of test results, the relationship between target strength and mean strength is given by:

$$f_{cm} = f'_c + k.\sigma$$

where k = statistical factor used to calculate 95% confidence limit

= 1.65 for a normal distribution

σ = standard deviation

Where no test data are available, assumed standard deviations included in DIER specifications are as shown in Table 5.6.

Characteristic strength, f'c (MPa)	Assumed standard deviation, σ (MPa)
20	4.5
25	4.8
32	5.3
40	5.9
50	6.2

Table 5.6 – Assumed standard deviations for concrete mix design

Based upon the assumed standard deviations in Table 5.6 and the classes of concrete described by Taylor, characteristic strength of the three classes of concrete would be as detailed in Table 5.7.

Class	Water/cement ratio	Concrete compressive strengths at 28 days (MPa)	
		Characteristic	Mean
A	0.5	22.3	30.0
B	0.6	15.0	22.0
C	0.7	10.0	16.5

Table 5.7 – Concrete strengths

Examination of construction test results from Rileys Creek Bridge (1945), Higgins Creek Bridge (1944), Surges Creek Bridge (1944) and Carlton River Bridges (1945/46) shows a mean compressive strength of 21.5 MPa, for a specified 1:2:4 mix. Standard deviation is 5.8 MPa (N=12), giving a characteristic strength of 11.9 MPa. On the basis of the standard deviations from Table 5.6, the characteristic strength would be 14.5 MPa. Table 5.1 shows that the characteristic strength of a 1:2:4 was variously expected to be 13.8 MPa, 17.3 MPa or most commonly 20.7 MPa. While the bridges are all in the south eastern part of Tasmania and were built at approximately the same time, the variability is higher than would be indicated by the literature. This may be explained in part by the small number of samples from separate locations using different aggregates and possibly different workers, but may be characteristic of the variability in materials properties found in other aspects of this study.

Figure 5.12 is a scatterplot of estimated 28 day compressive strength of cores, using the relationship in figure 5.11 for long term strength gain, against the specified characteristic strengths, for bridges where 28 day strength was specified. The line is mean compressive strength against characteristic strength, using the standard deviations from table 5.6. Given that 95% of results should exceed the characteristic strength, the figure indicates that the compressive strengths at 28 days may not have

complied with the specified strength, although the validity of this interpretation is uncertain given the high variability in long term strength gain data.

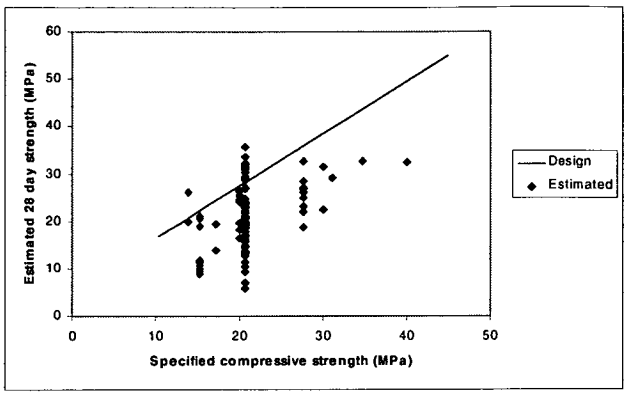

Figure 5.12 – Specified concrete strength ~ estimated 28 day strength

By comparison, comparisons of core compressive strengths at the time of investigation and the specified compressive strength in figure 5.13 indicate that there will be adequate long term structural compressive strength, notwithstanding the possible of low initial strengths. The line plots characteristic strengths equal to the specified compressive strength.

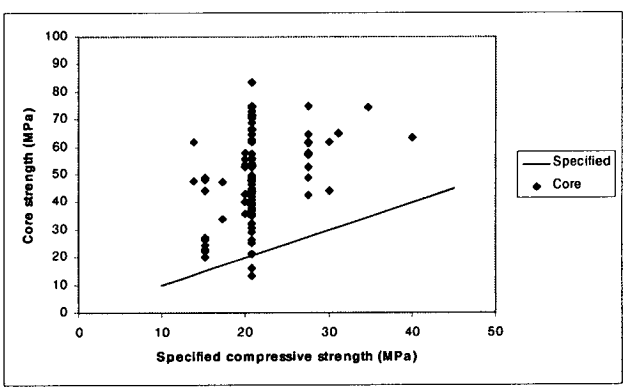

Figure 5.13 – Core strength ~ specified strength

Figures 5.14 examines estimated 28 day compressive strengths for concretes where a value of 20.7 MPa (3000 psi) was specified. The linearity of the normal probability plot indicates that it is reasonable to assume a normal distribution, with the histogram indicating a mean value of 19.9 MPa and a characteristic value of 9.8 MPa, for compressive strength. The results are consistent with the mean and characteristic strengths of 21.5 MPa and 11.9 MPa from the Rileys Creek, Higgins Creek, Surges Creek and Carlton River Bridges discussed previously, although this again needs to be

considered in the context of the variability in the long term strength gain data. In many cases, concrete was specified in terms of both strength (3000 psi) and composition (1:2:4); given the age of the bridges, it is likely that the composition would have been used on site for batching leading to lower compressive strengths.

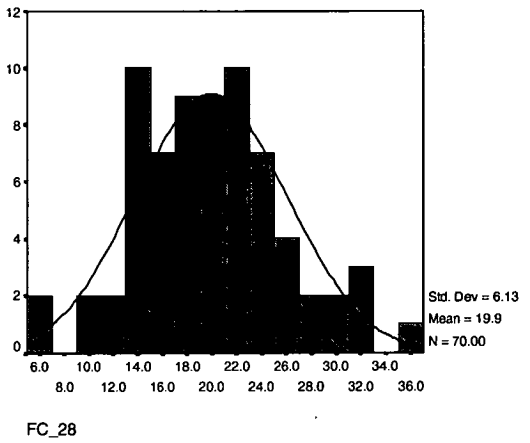

Figure 5.14 – Distribution of estimated 28 day strengths for specified strength of 3000psi/20 MPa

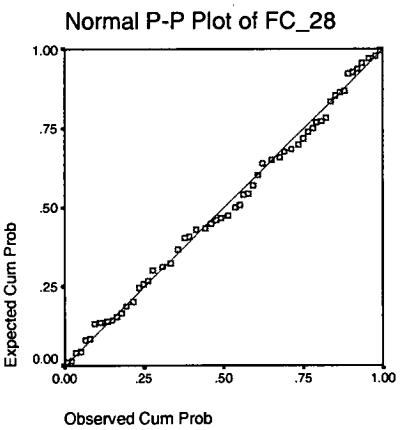

Figure 5.15 – Normal probability distribution of estimated 28 day strengths for specified strength of 3000psi/20 MPa

5.5 CEMENT AND WATER CONTENTS

In 1918, Abrams stated that for given materials, the strength of concrete was dependent only upon the water cement ratio (Symons, 1992). While this is likely to understate the situation, particularly with contemporary concretes, it nevertheless highlights the significance of water and cement contents in determining concrete strengths.

For given types of constituent materials, the chloride diffusivity of concrete is mainly influenced by the capillary porosity of the cement matrix and its chloride binding capacity, and compaction of the concrete (Nilsson et al, 1996). Primary influencing factors from the literature are the water cement ratio, binder content and properties influencing the workability of the fresh concrete, including the grading of aggregates and the slump of the concrete. Carbonation is similarly influenced by the composition and compaction of the concrete.

Concrete compositions, in terms of cement contents and water cement ratios, were analysed as part of this study to assess likely mix designs and to provide the basis for subsequent examinations of possible correlations between composition, strength, chloride ingress and carbonation. Cement contents were measured in accordance with Australian Standard AS1012 Part 15. Taylor (1977) states that the order of accuracy for the test is of the order of $\pm 10\%$, and is likely to be more accurate for rich mixes than for lean ones. The original water content of cores was determined by dehydrating a saturated sample at 593^0C for 2 hours, correcting for aggregate absorption and calculating from the previously determined cement content.

Minimum cement contents have only been specified by DIER since the late 1980's as a strategy to address deficiencies in the durability performance of concrete structures. Table 5.1 however showed that composition was commonly specified for structures, with a 1:2:4 mix being the most common. For a concrete density of 2500 kg/m^3 and water content of 180 l/m^3, the cement content equates to (2500-180)/(1+2+4) = 330 kg/m^3. The dominance of the 1:2:4 mix as the specified concrete composition for the sampled cores, where composition was specified, is highlighted in figure 5.16. The figure also reflects the small numbers of samples from recent bridges in the sample.

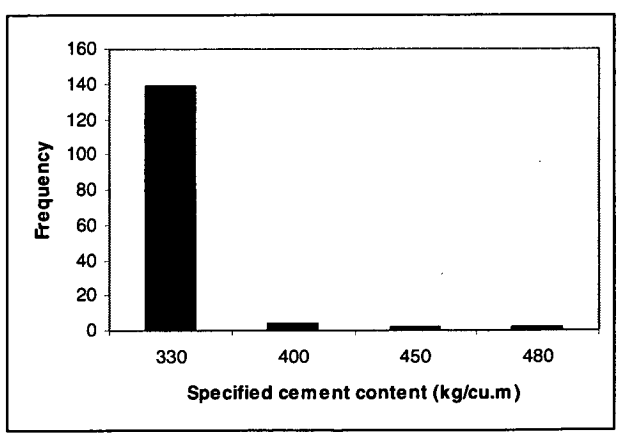

Figure 5.16 – Distribution of specified cement contents

Figure 5.17 shows the correlation between specified and measured cement contents. The plot indicates that cement contents for the higher specified levels are lower than specified, although the sample size is too small to draw reliable conclusions. DIER specifications which have specified a minimum cement content have typically resulted in characteristic strengths which would satisfy the strength requirements of the next highest grade. It is likely however that some concrete has been supplied to Departmental bridges on the basis of strength alone resulting in a lower cement content than required by the specification.

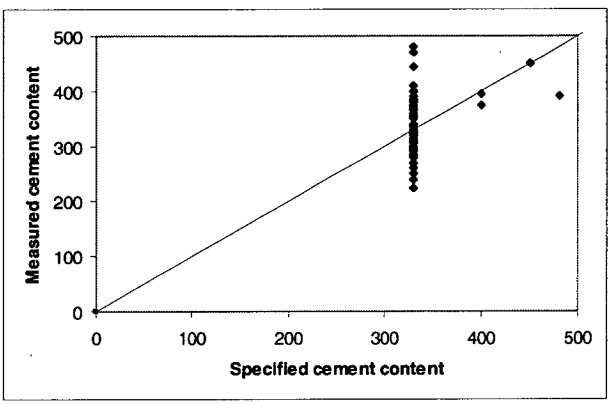

Figure 5.17 – Measured and specified cement contents

The distribution of measured cement contents for all samples and for the 1:2:4 mix is examined in figure 5.18. Normal distribution curves are plotted with the histograms. The difference in numbers of samples from the two histograms arises from the large number of structures for which the concrete composition was not specified. The distribution in figure 5.18 is influenced by the small number of samples with high cement contents, which partly arise from the samples from recent bridges with high specified cement levels. It nevertheless indicates that a 1:2:4 mix was likely to be common in the sampled bridges. The coefficient of variation of 20% indicates variability both within and between structures, which will be discussed in more detail later.

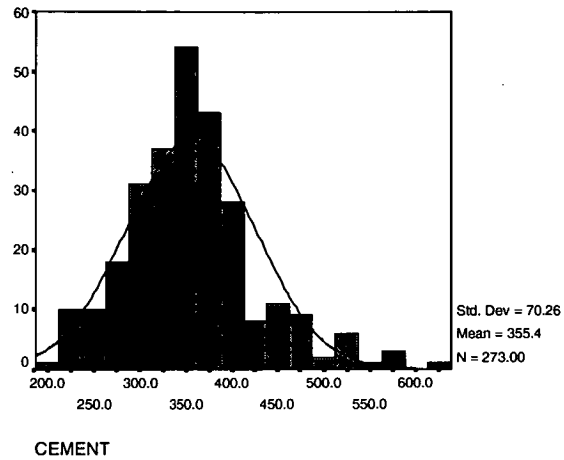

Figure 5.18 – Measured cement contents; all samples

The variability in measured cement contents for individual structures where a 1:2:4 mix was specified is shown in Table 5.8.

Bridge	No. cores	Minimum	Maximum	Range	Mean	St. dev	COV (%)
Faggs Gully Creek	1	350	350	0	350	-	-
Symons Creek	2	270	300	30	285	21.2	7.4
Surges Creek	2	295	350	55	323	38.9	12.1
Higgins Creek	3	270	380	110	342	62.1	18.2
Rileys Creek	7	315	385	70	351	22.6	6.5
Tasman Hwy Culverts	6	240	365	125	312	43.9	14.1
East Arm Creek Culvert	4	295	480	185	355	84.3	23.8
Argent Creek	5	225	290	65	269	27.2	10.1
Ralphs Bay Canal	3	340	470	130	387	72.3	18.7
Ringarooma River	7	250	410	160	343	47.9	14.0
Cormiston Creek	4	305	370	65	330	29.7	9.0
Camp Creek widening	3	340	445	105	382	55.7	14.6
Wrinklers	9	280	410	130	337	38.3	11.4
Reedy Creek	6	250	400	150	346	56.6	16.4
Boggy Creek	4	320	380	60	350	25.8	7.4

Table 5.8 – Cement contents for specified 1:2:4 mix

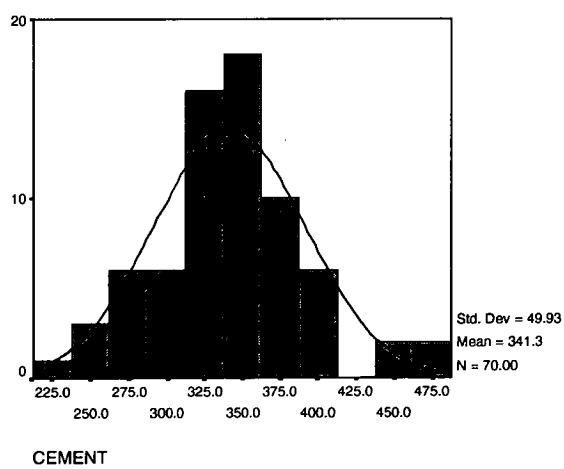

Figure 5.19 – Measured cement contents for 1:2:4 mix

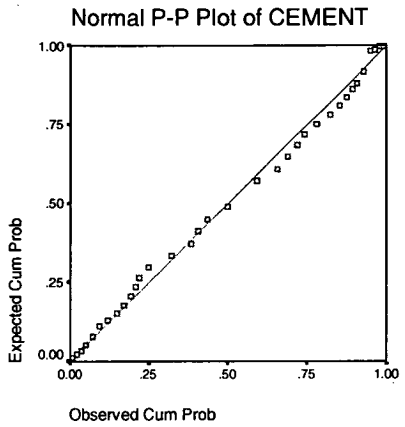

Figure 5.20 – Normal probability plot for cement contents, 1:2:4 mix

The linearity of 5.20 indicates that the distribution of cement contents for the 1:2:4 mix can reasonably be described by a normal distribution.

Water contents do not vary greatly across the range of concrete strengths and compositions used commonly in practice. Symons (1992) presents approximate free water contents for various levels of workability after Teychenne et al in the 1988 'Design of Normal Concrete Mixes' from the United Kingdom, as detailed in Table 5.9.

Maximum size of aggregate (mm)	Type of aggregate	Slump (mm)			
		0-10	10-30	30-60	60-180
10	Uncrushed	150	180	205	225
	Crushed	180	205	230	220
20	Uncrushed	135	160	180	195
	Crushed	170	190	210	225
40	Uncrushed	115	140	160	175
	Crushed	155	175	190	205

Table 5.9 – Approximate free water contents (kg/m^3) for various levels of workability

Bridge concretes would commonly have had slumps of 50 to 120 mm and maximum aggregate sizes of 10 to 20mm, although the use of larger aggregate pieces ('plums') did occur with older bridges, especially with mass concrete. Both river and alluvial gravels and crushed aggregates have been used, indicating likely water contents in the range of 180 to 230 kg/m^3. The current Departmental specification requires a slump of 60±15mm.

Figure 5.21 and the normal probability plot in figure 5.22 show that the water contents of the analysed cores can reasonably be described by a normal distribution with a

mean of 195 kg/m^3 and a standard deviation of 26.2 kg/m^3. The outlier of 350 kg/m^3 of water is from the base slab of the Risdon Cove Causeway Culvert, which would have been poured under water as part of an accelerated construction program following the Tasman Bridge disaster of 5 January 1975, and had a core compressive strength of 11.8 MPa at an age of 17 years. It is regarded as uncharacteristic of bridge concretes.

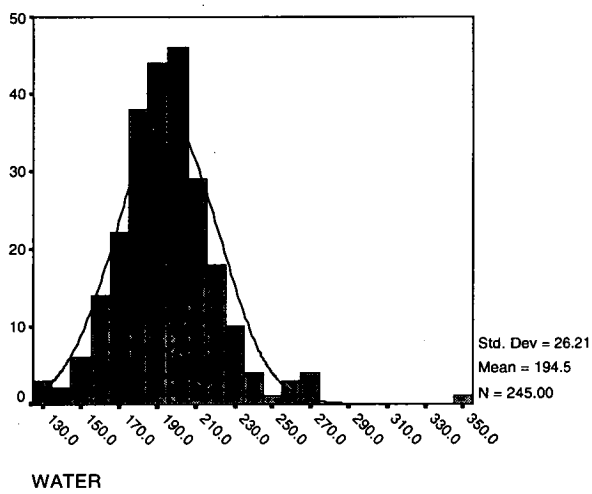

Figure 5.21 – Water contents of analysed cores

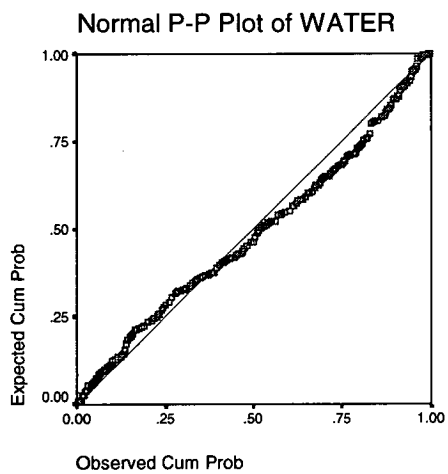

Figure 5.22 – Normal probability plot of water contents of analysed cores

Figure 5.23 shows the relationship between water content and cement content for the analysed cores. While there is a small increasing trend, the R^2 statistic for linear, logarithmic or exponential curve fits ranges from 0.178 to 0.189 indicating a poor correlation. For a typical range of cement contents between 300 and 450 kg/m^3, the fitted trendline has a slope of 6% with the correlation again poor (R^2 0.011). It is thus considered reasonable to assume a constant water content, with a normal distribution,

for the bridge concretes which are the subject of this study. This is consistent with contemporary Tasmanian premixed concretes having a water content of the order of 180 l/m^3, with the decrease from 195 l/m^3 attributable to the use of admixtures including water reducers.

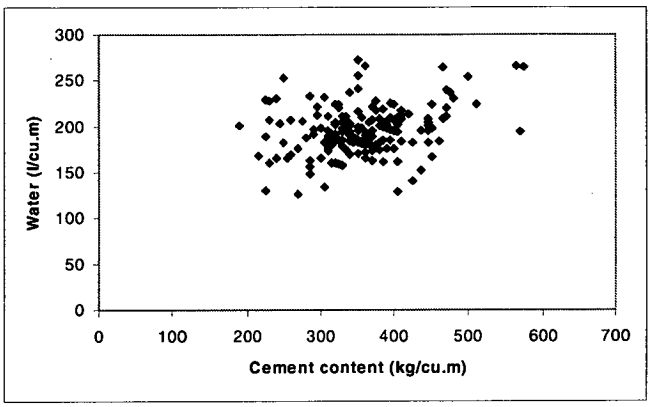

Figure 5.23 – Cement and water contents of cores

With a nominally constant water content and a normally distributed cement content, it would be expected that water cement ratios would be normally distributed. Fitting a straight line to a plot of water cement ratio against cement content (figure 5.24) gives an R^2 statistic of 0.53. Figures 5.25, 5.26 and 5.27 indicate that the assumption of a normal distribution for water cement ratio is reasonable, particularly for the nominal 1:2:4 mixes.

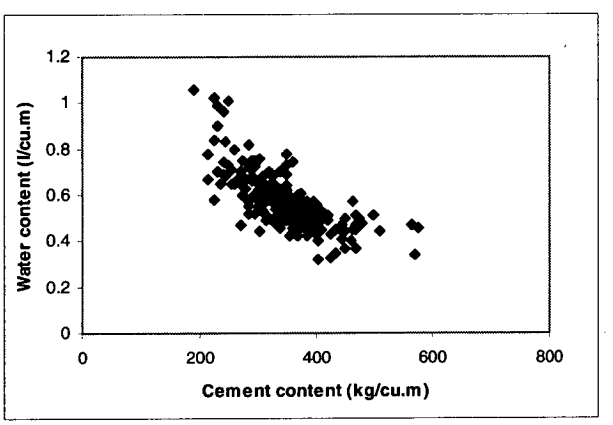

Figure 5.24 – Water cement ratio ~ cement content

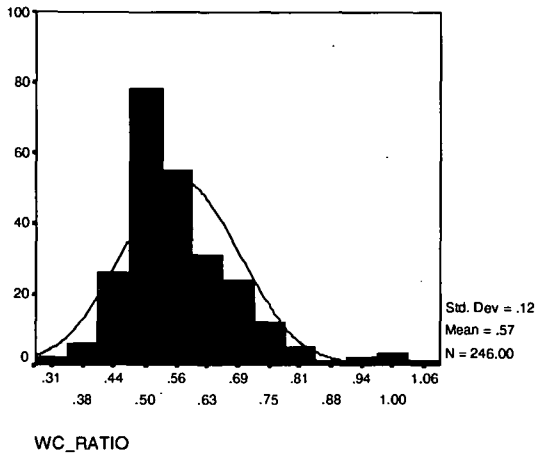

Figure 5.25 – Frequency distribution for water cement ratio, all samples

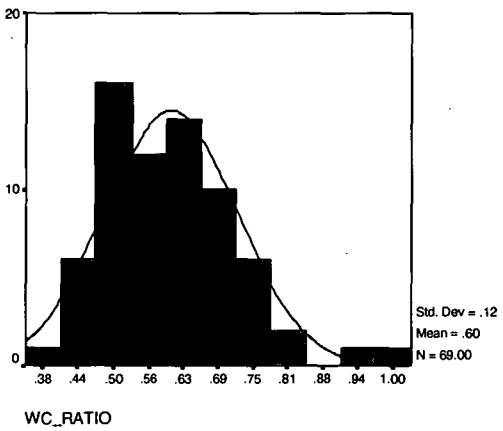

Figure 5.26 – Frequency distribution for water cement ratio, 1:2:4 mix

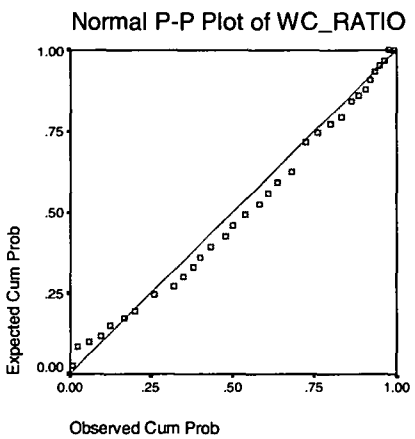

Figure 5.27 – Normal probability plot for water cement ratio, 1:2:4 mix

5.6 STRENGTH AND COMPOSITION RELATIONSHIPS

This section examines the relationship between concrete strengths and the cement and water contents of the cores. The initial discussion is drawn from Taylor (1977).

The quality of concrete is controlled to a high degree by the quantity of water used in the mix. For adequate hydration, portland cement must combine with about 20% of its own mass of water. At least twice this amount of water is normally needed to ensure workability. For water cement ratios of less than about 0.4 by mass, the cement does not fully hydrate.

As excess water evaporates or segregates from a mix, it forms capillaries and small voids which reduce the quality of the cement matrix in the hardened concrete. The resulting voids cement ratio is a critical factor which governs the strength and the durability of the concrete. From this concept arises Duff Abrams' water cement ratio law, which states that fundamentally 'the strength of concrete is governed by the ratio of the volume (or weight) of water to the volume (or weight) of cement in a mix, provided that it is plastic and workable, fully compacted, and adequately cured.' The relationship is shown in Figure 5.28, modified for the changes in concrete properties which had occurred between the publication of Abrams' law and Taylor's book. The figure also shows the need for high compaction effort and particular techniques at lower water cement ratios.

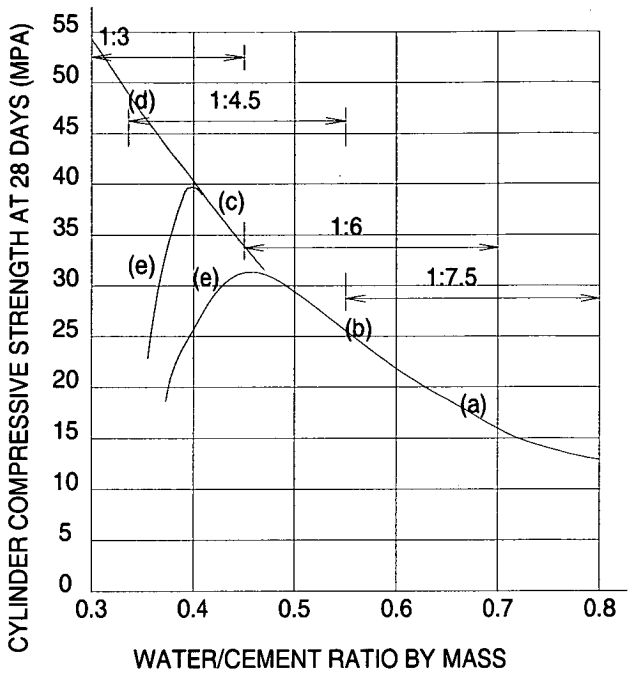

Figure 5.28 - Concrete compressive strength by water/cement ratio for ordinary portland cement. Proportions signify cement and combined aggregate. (a) Sloppy mix. (b) Manual compaction. (c) Vibratory compaction (d) Vibropressure compaction. (e) Partial compaction

Figure 5.29 plots Abrams' relationship, design strengths from Taylor as in Table 5.5, and the measured water cement ratios and estimated 28 day strengths from the concrete cores. Abrams' and Taylor's curves correspond closely and are not readily distinguishable in the figure. A regression analysis for the measured water cement ratios showed an inverse relationship as providing the best fit, with the following equation:

$$f_{c\_28} = -14.62 + \frac{17.65}{wcratio}$$

The R^2 statistic for the fitted curve, which is also shown in figure 5.29 is 0.602.

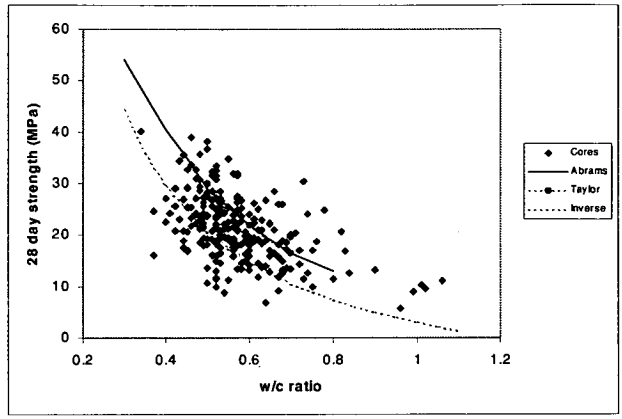

Figure 5.29 - Estimated 28 day compressive strength ~ water cement ratio

Differences between Abrams' data and the fitted curve are tabulated in Table 5.10.

wc ratio	Concrete compressive strength (MPa)		Difference	
	Abrams	Fitted curve	MPa	%
0.4	40.5	29.5	11	27
0.5	29	20.7	8.3	29
0.6	22	14.8	7.2	33
0.7	16.5	10.6	5.9	36
0.8	13	7.4	5.6	43

Table 5.10 – Compressive strength differences

The lower expected values from the cores may be attributable to a number of factors including:

- different cement compositions and coarser cement grinds for the concretes, given that the mean year of casting of the concrete cores was 1954 and the oldest concrete was manufactured in 1929
- aggregate shape and size
- differences between the properties of insitu concrete and test cylinders
- the influence of construction practices, including site batching, the level of compaction and the effectiveness of curing
- the accuracy and validity of the relationship used to estimate the 28 day strengths.

As discussed, Taylor and Abrams developed relationships between concrete compressive strength and water cement ratio. Factor analysis of cores from this study with SPSS however suggested a stronger correlation with cement content than water cement ratio (correlation coefficients 0.803 and –0.676 respectively). The strength~water cement ratio relationship is shown in figure 5.29, with the strength~cement content in figure 5.30.

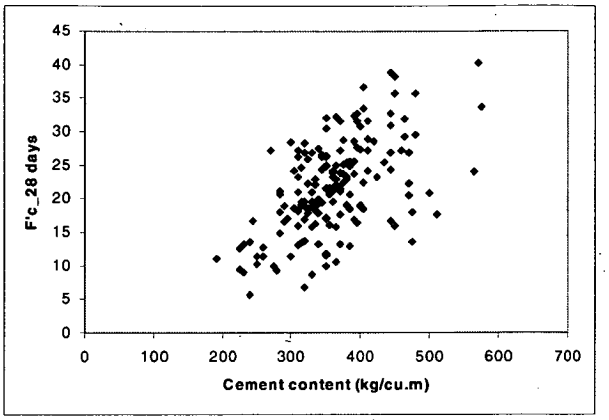

Figure 5.30 – Strength ~ cement content

5.7 SUMMARY

The analysis of the composition of concrete samples and their performance with respect to physical properties, particularly strength, has shown that the various properties can reasonably be described by normal distributions with relatively high coefficients of variation.

A wide range of specifications has been used for Tasmanian bridge concretes, describing them in terms of class, strength or composition. The most commonly specified requirements for concrete in the bridges involved in the study were for a characteristic strength of 3000 psi (20.7 MPa) and/or a composition of 1:2:4 cement:fine aggregate:coarse aggregate. There is a trend of increasing specified strength with more recent concretes, associated with increasing loads, the use of prestressing, changing design methods and endeavours to enhance durability. It is not however possible to assume a particular concrete specification on the basis of the age of a structure.

A range of sources were used to provide a basis on which to estimate the 28 day strength of concretes to facilitate comparisons, given that core ages ranged up to 62 years. There was a wide divergence in the strength gain of concretes from both the literature and for Tasmanian bridges where construction test data were available. For concretes of ages at least 25 years, the coefficient of variation in the range of the ratio of long term compressive strength to 28 day strength was 26.7% for the Tasmanian bridges, increasing to 29% when published data are included. A logarithmic curve fitted to the aggregated data indicated that 28 day compressive strengths for concrete

in the bridges would have been lower than specified, although adequate strength was developed as the concretes aged. Estimated 28 day compressive strengths for Tasmanian bridges can reasonably be described by a normal distribution. Because of the high coefficient of variation, caution is needed in drawing any conclusion that concrete strengths were inadequate. The subsequent analysis of water contents and their variability does however give some credence to such a conclusion. It is likely that many of the structures were built with uncoated timber formwork, curing compounds may not have been available, and continuous moist curing may have been difficult at night and weekends, and insitu concrete strengths may consequently have been lower than those that would have been measured with standard test cyclinders.

Cores from bridges with the most commonly specified cement content of approximately 330 kg/m^3 (nominal 1:2:4 mix) showed a mean cement content of 341 kg/ m^3, a standard deviation of 49.9 kg/m^3, a range from 225 to 480 kg/m^3 and a coefficient of variation of 14.6%. Water contents can similarly be described by a normal distribution with a mean of 195 l/m^3 and a standard deviation of 26.2 l/m^3, giving a coefficient of variation of 13.5%.

Factor analysis indicates a degree of correlation between composition and strength. A stronger correlation is indicated between strength and cement content than between strength and water cement ratio.

AS 1012.14 states that 'for a group of three cored specimens secured from the same location, cured in similar conditions and tested at age 28 days or more, the accuracy expressed as a percentage of the mean of the strengths obtained, is +7% at the 95% probability level, subject to a length/diameter ratio of 2:1. As this ratio decreases, the repeatability of the test also increases in value." The standard also notes that the compressive strength of cores is affected chiefly by:

- physical properties relating to the securing of the core itself
- properties of the concrete supplied
- factors related to the compaction and the curing of the concrete provided.

Coring for corrosion investigations typically involves the taking of 2 or 3 closely spaced cores from a number of locations, with different tests performed on the cores from each location to provide an overall picture of the structure. Accuracy is thus likely to be lower than the value stated in the Standard. The variability shown in the

analysis will also overshadow the accuracy of the compressive strengths indicated in the Standard.

The analysis here has shown a high variability in the physical and compositional properties of the hardened concrete in structures. This is expected to be attributable to a number of factors, including:

- variability in the concrete manufactured for each structure, particularly with site batching likely to have been used for the majority of structures involved in the structure, with variability both within and between batches
- variations in cement compositions and grinding practices
- aggregate shape and size
- effects of placing and compacting the concrete
- effects of differences in finishing and curing, including weather differences on days of concrete placement
- environmental differences between structures
- effects of securing of cores
- the use of different cores for the various tests, with cores taken from throughout structures
- the accuracies of the various test methods.

6 CHLORIDE INGRESS

6.1 GENERAL

In this chapter, the penetration of chlorides into concrete and chloride induced corrosion of reinforcing steel are discussed. Data from Tasmanian bridges are then analysed and possible correlations with a number of concrete and environmental factors examined. Models are developed for subsequent service life modelling.

As noted in the chapter on bridge exposures and conditions, approximately one-quarter by number and two-thirds by replacement cost of the State's bridges are located within one kilometre of the coast. There is consequently a high exposure of the asset to chlorides. Many of those bridges have suffered damage from chloride induced corrosion.

Remedial measures for affected structures that have been implemented to date have commonly involved the installation of cathodic protection systems. Current installations are at Grassy Wharf, Tasman Bridge, Kelvedon Creek Bridge, Newmans Creek Bridge, Sorell Causeway Bridge, Pats River Bridge, Bridgewater Bridge, Golden Fleece Bridge and Cam River Bridge, with additional systems proposed for the future. In a number of cases, such as Mountain Creek Bridge and Sorell Causeway Bridge, replacement has been required. Further bridge replacements due to chloride induced corrosion damage are also proposed. Installation costs for cathodic protection systems are high and implementation of remedial measures for a significant number of other bridges is dependent upon the availability of funds. Additionally, cathodic protection systems require active monitoring and control with the associated ongoing demand on resources, rather than the more passive management regime typically associated with bridges.

For other bridges at risk, there is a potential to undertake early preventative work such as the application of silane penetrating sealers. Again, funding constrains the rate at which such works can be undertaken and necessitates that preventative measures only be undertaken on structures for which a benefit can be demonstrated and derived.

6.2 CHLORIDE PENETRATION

6.2.1 Chloride Transport Process

The discussion in the early part of this chapter is to establish the context for the subsequent analysis and draws from a number of sources, including Nilsson et al (1996).

The penetration of chlorides into concrete is the result of a number of transport and binding processes, with concentrations at various depths a time-dependent function of the environmental conditions, the design of the structure and its material properties. This chapter considers only chlorides derived from environmental exposures and not those derived from processes such as the application of deicing salts for frost and snow because of the absence of such practices in Tasmania. It is also unlikely or rare that chlorides, in the form of calcium chloride, have been cast into concrete in Tasmanian bridges to act as a set accelerator because of the early recognition of the potential problems, and the use of direct labour for the majority of construction until about 1990.

Below low water level for structures located in salt water, environmental chloride concentrations are essentially uniform giving constant boundary conditions and thus the penetration of chlorides can be considered as a "pure diffusion" process. There may be some initial uptake of chlorides when the concrete is first exposed to saline water.

In tidal and splash zones, boundary conditions change. In splash zones, salt water is sucked into the concrete surface. Rain water washes the surface free from chlorides and may remove some from near the surface of the concrete. Evaporation increases their concentration. Chlorides, near the surface particularly, move inwards and outwards due to moisture flow and ion diffusion. Conditions vary at different heights. Closer to water level, the concrete is almost continuously saturated by water, by comparison with the alternate wetting and drying at higher locations.

Chlorides may also be present in the concrete mix from the aggregates, mixing water, admixtures or salt deposits on reinforcement.

6.2.2 Chloride Binding

Corrosion and transport processes in concrete are affected by the binding of chloride ions from the concrete pore solution into the solid hydrate binder phase.

Chloride binding may help to prevent or delay the activation of chloride induced reinforcement corrosion in two different ways:

- reducing the concentration of chloride ions in the pore solution available for transportation, hence reducing the rate of chloride ingress. At low concentrations, nearly all the free chlorides may be removed.
- only mobile chloride ions are believed to initiate reinforcement corrosion. If this assumption was correct, a higher total chloride concentration (free + bound) could be tolerated at the level of the reinforcement. Bound chlorides may however be released after corrosion initiation and contribute to the corrosion reactions (Glass et al, 2000); accepting higher chloride concentrations is thus likely to be unconservative.

The mechanisms of chloride binding are not well understood. Historically it was claimed that the formation of chloro-aluminate sulphates was the only means of chloride binding. It is now however considered that chloride binding is the result of several different mechanisms, with chemisorption and ion exchange theories more likely to describe chloride binding processes in concrete.

Chloride binding capacity is significantly affected by the means by which the chlorides enter the concrete. Chlorides added to the fresh concrete mix will alter the hydration process by comparison with a chloride free mix. Chlorides also alter the pore size distribution of the hydrated binder, and thus are likely to affect its absorption capacity.

For the purposes of this study, no distinction is made between bound and unbound chlorides, with concentrations being expressed in terms of total chlorides by mass of concrete determined through the analytical procedures described in the chapter on test methods.

6.2.3 Effects of Cement Composition

Records are not available to indicate the source of cement for particular structures or elements of those structures, including structures where precast elements have been manufactured remote from the site.

It is however likely that Goliath cement has been used in many, if not most of the structures involved in this study. There have nevertheless been periods, such as during industrial disputation, when cement was imported from sources including Geelong. On the Bass Strait islands, shipping arrangements may have led to the use of Victorian cements. In recent years, the usage of Blue Circle cement in Tasmania has also become commonplace because of corporate changes within the resource, cement and concrete industries.

Additionally, cement compositions and physical characteristics such as fineness of grind have changed due to economic and environmental pressures and changes in plants, particularly moves from wet to dry manufacturing processes.

Because of the variables and the inability to relate them to particular elements and structures, the factor analysis for chloride ingress and carbonation has not attempted to consider cement composition.

6.2.4 Chloride Penetration and Transport

The diffusion of ions in a solution results from differences in the concentration of the ions and is widely believed to follow Fick's First Law. In one dimension, Fick's First Law is

$$F = -D\frac{\partial c}{\partial x}$$

where F is the flow of ions in [kg/(m^{2}s)]
D is the diffusion coefficient [m^2/s]
c is the ion concentration [kg/m^3]
x is the distance [m]

In concrete, this situation only applies in laboratory situations such as diffusion cells where there are constant chloride concentrations in the solutions at the two sides of the specimen.

The movement of chloride ions in structural concrete is more complex, and is not a pure diffusion process. The Na^+ and Cl^- ions from the salt diffuse inward at different rates, and must be balanced by the movement of other ions, particularly Ca^{2+} and OH^-.

Other ions may also be involved, potentially changing the composition of the pore solution and chloride binding capacity.

Although the penetration of chlorides into concrete is complex, numerous studies have found that the process is best represented by a diffusion process if the concrete is assumed to be relatively moist (Stewart and Rosowsky, 1997). In this case the penetration of chlorides is given empirically by Fick's 2nd law of diffusion if the diffusion is considered as one-dimensional in a semi-infinite solid. The law is expressed as:

$$\frac{\partial c}{\partial t} = D\frac{\partial^2 c}{\partial x^2}$$

D is the apparent diffusion coefficient, and is assumed to be time invariant. There is however increasing evidence that the diffusion coefficient in concrete is time dependent, particularly in the early part of a structure's life. As the determination of c_s and D is a curve fitting process, it may however be that there is a compensating effect and that the use of a fixed value of diffusion coefficient is reasonable in many situations.

For the 'penetration' of chloride ions into a solution, with the left hand boundary at a constant concentration, $c(x=0, t) = c_s$, and the concentration in the body of the solution zero at the beginning, $c(x, t=0) = 0$, the chloride profiles are given by the common error function solution to Fick's 2nd law with these boundary and initial conditions:

$$c(x, t) = c_s\,[1 - \mathrm{erf}(\frac{x}{2\sqrt{D.t}})]$$

The error function and its numerical expansion are given by

$$\mathrm{erf}(x) = \frac{2}{\sqrt{\pi}}\int_0^x \exp(-x^2)dx$$

$$= \frac{2}{\sqrt{\pi}}(\frac{1.x}{0!.1} - \frac{1.x^3}{1!.3} + \frac{1.x^5}{2!.5} - \frac{1.x^7}{3!.7} + ...)$$

The error function can be solved numerically by iteration.

6.3 SKIN EFFECT

The skin, defined as the concrete closest to the surface, usually has different properties and composition from the concrete in the remainder of an element. Reasons for the differences include:

- the border or wall effect which causes more paste or mortar to accumulate near the surface
- carbonation of the concrete
- the precipitation of brucite ($Mg(OH)_2$) formed during contact with sea water
- coating of the concrete with overlays, paints or sealers.

The different composition and environmental actions, which induce a gradient of moisture through the depth of cover to reinforcement, sometimes produce an irregular chloride profile that may either exhibit a maximum chloride content some millimetres inside the outer surface or an anomalously high concentration at the surface (Andrade et al, 1997). The first phenomenon was observed in a number of cores (figure 6.1). The second was not observed in the study, possibly because of the relative coarseness of slices (typically 20mm for the two closest to the surface) compared to those typically used in laboratory studies.

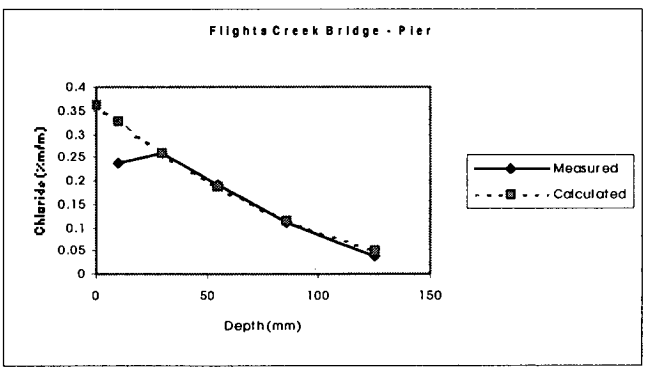

Figure 6.1 – Chloride profile

Andrade et al (1997) propose the use of a two layer model, illustrated in figure 6.2, to account for the differing properties. A resistance, R, may also exist between the two layers.

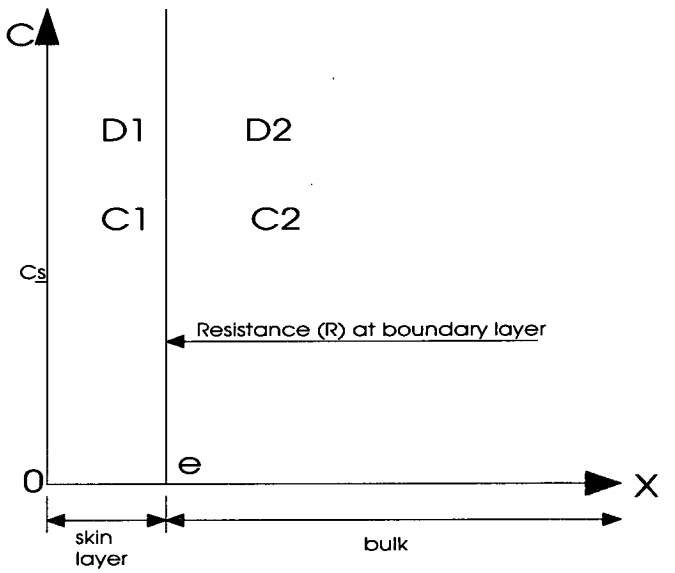

Figure 6.2 – Two layer concrete model

They have solved Fick's second law for the two layer model by assuming the following conditions:

Initial	$C_1(x,0)$	=	0	$0 < x < e$
	$C_2(x,0)$	=	0	$x > e$
Boundary	$C_1(e,t)$	=	$C_2(e,t)$	$t \geq 0$
	$C_1(0,t)$	=	C_s	$t \geq 0$

The resulting solution is:

$$C_1(x,t) = C_s \sum_{n=0}^{\infty} \alpha^n \left\{ erfc\left[\frac{2ne+x}{2\sqrt{D_1 t}}\right] - \alpha erfc\left[\frac{(2n+2)e-x}{2\sqrt{D_1 t}}\right]\right\}$$

$$C_2(x,t) = \frac{2kC_s}{k+1} \sum_{n=0}^{\infty} \alpha^n erfc\left[\frac{(2n+1)e+k(x-e)}{2\sqrt{D_1 t}}\right]$$

$$k = \sqrt{D_1 / D_2}$$

$$\alpha = \frac{1-k}{1+k}$$

For a resistance, R, between the two layers, the boundary conditions become:

$$C_1(0,t) = C_s \qquad t \geq 0$$

$$C_1(e,t) = RC_2(e,t) \qquad t \geq 0$$

and the new solution for C_2 becomes:

$$C_2(x,t) = \frac{2kC_sR}{k+1}\sum_{n=0}^{\infty}\alpha^n erfc\left[\frac{(2n+1)e+k(x-e)}{2\sqrt{D_1 t}}\right]$$

Weyers (1998) showed that the increase in surface chloride concentration mainly occurred in the 0 to 13mmm zone in an average period of 5 years, then it became constant. It was suggested that surface chloride concentration should be taken as constant to a depth of 13mm for older structures.

Chloride profiles for the cores which are the subject of this study have been described in terms of an apparent surface chloride concentration and an effective diffusion coefficient. While a number of cores exhibited a decrease in concentration for the slice closest to the surface, it did not necessarily occur with others from similar exposures or within the same structure. As the objective of fitting curves to the measured chloride profiles was to develop a model for subsequent service life modelling, rather than to examine the skin effect or the time dependence of the diffusion coefficient, the parameters for the modelling were determined by excluding the skin effect and assuming that they were constant with time.

6.4 RESULTS FROM OTHER RESEARCHERS

Bamforth (1996) reports published data of surface chloride concentrations from laboratory tests, from natural exposure trials and from structures up to 60 years old. The results are reproduced in Table 6.1.

Location	Age (years)	No. of results	Surface Chloride (%m/m concrete)	
			Range	Mean
Structures				
Bridge deck, US	13	4	0.56 - 0.65	0.60
Tidal/splash zone, Singapore	24	5	0.18 - 0.43	0.29
Submerged, tidal and splash zones, Australia	14	9	0.08 - 0.36	0.24
Tidal, splash and spray zones, Denmark				
Langeland bridge	15	12	0.01 - 0.37	0.22
Stignaes harbour	11	1	0.24	0.24
	16	2	0.65 - 0.77	0.71
Holsskov harbour	20	4	0.20 - 0.46	0.32
	16	2	0.15 - 0.17	0.16
Seawall, UK	30	1	0.11	0.11
Marine fort, UK, tidal and splash zones	34	5	0.18 - 0.71	0.41
Coastal bridge piers, Norway, splash zone, leeward surfaces	15	24	0.18 - 0.61	0.32
Coastal structures in Japan, splash zone	7.5	1	0.76	0.76
	17	6	0.08 - 0.25	0.15
	23	10	0.31 - 0.80	0.44
	24	1	0.15	0.15
	32	4	0.23 - 0.52	0.28
	32	4	0.21 - 0.27	0.24
	55	1	0.58	0.58
	58	5	0.13 - 0.37	0.26
	58	3	0.70 - 0.98	0.82
Marine discharge structure, Japan, splash and tidal	30	10	0.04 - 0.6	0.19
	30	10	0.03 - 0.74	0.31
Coastal structures in Japan			0.20 - 1.00	0.51
Natural exposure trials				
Splash zone, UK	6	54	0.20 - 0.67	0.42
Tidal zone, UK	2	1	0.44	0.44
Coastal exposure, Norway	2	7	0.39 - 1.06	0.62
Tidal exposure, Japan	4	3	0.56 - 0.76	0.64
Tropical, tidal, splash and atmospheric zone	1.5	6	0.20 - 0.50	0.39
Tidal exposure, UK	5	7	0.17 - 0.96	0.54
Marine exposure, Japan	6		0.15 - 0.82	0.42
Laboratory trials using seawater				
UK laboratory	2	6	0.39 - 0.68	0.53
Australian laboratory	21 day	12	0.23 - 0.67	0.42
	1	12	0.35 - 0.65	0.44

Table 6.1 – Surface chloride concentrations

While there is a wide scatter in the results, they show that the splash zone is the most severe with regard to the accumulation of surface chlorides. The accumulation is also affected by the orientation of a particular surface, the direction of prevailing winds and the degree of exposure to rainfall. Using a characteristic value approach (95% confidence limit), Bamforth proposes the values of surface chloride levels for design purposes shown in Table 10.2 for normal portland cement. He also suggests the use of effective diffusion coefficients in the range of 5×10^{-12} m^2/s to 1×10^{-13} m^2/s.

Exposure	Surface chloride level (%m/m)
Extreme	>0.75
Severe	0.5 to 0.75
Moderate	0.25 to 0.5
Mild	<0.25

Table 6.2 – Design surface chloride levels

Berke, Hicks and Tourney (unknown date) suggest typical values for surface concentrations of chlorides for severe marine environments in the splash and tidal zone of 18 kg/m^3. This equates to 0.73% m/m for a typical density of concrete from the cores involved in this study of 2450 kg/m^3.

6.5 TEMPERATURE EFFECTS

The temperature dependence of the effective diffusion coefficient D_{eff} can be described in terms of the Nernst-Einstein equation (Berke and Hicks,1993):

$$\frac{D\mu}{T} = \text{constant}$$

where T is the absolute temperature and μ is the viscosity of the solution. Mean temperatures at the various bridge and culvert sites vary only from 8°C to 14°C (281 to 285K), with the majority of structures in the range 11°C to 13°C (284K to 286K), variations of less than 1.5. With the small variation in mean temperature, the accuracy of chloride measurement, and the use of least squares curve fitting for the chloride profiles, it was considered that there would be little benefit from correcting apparent diffusion coefficients for temperature, except possibly in the use of temperatures for concrete maturities in factor analysis.

6.6 THRESHOLD CHLORIDE CONCENTRATIONS

Reinforcing steel in concrete is normally protected from corrosion by the formation of a passive oxide layer in the alkaline environment created by the pore water solution. The state of passivation is maintained until the concrete in contact with the steel becomes carbonated or until a sufficient concentration of water soluble aggressive ions has reached the steel surface. The aggressive ions, such as chloride ions, then locally penetrate the iron oxide layer and subsequently trigger the dissolution of the iron oxide layer and thence the steel.

The chloride threshold level can be defined as the minimum chloride level at the level of the reinforcement which results in active pitting corrosion of the reinforcement. This corresponds to the point in Tuutti's model when the initiation period ends and the propagation period starts. Tuutti's model is shown diagrammatically in Figure 6.3.

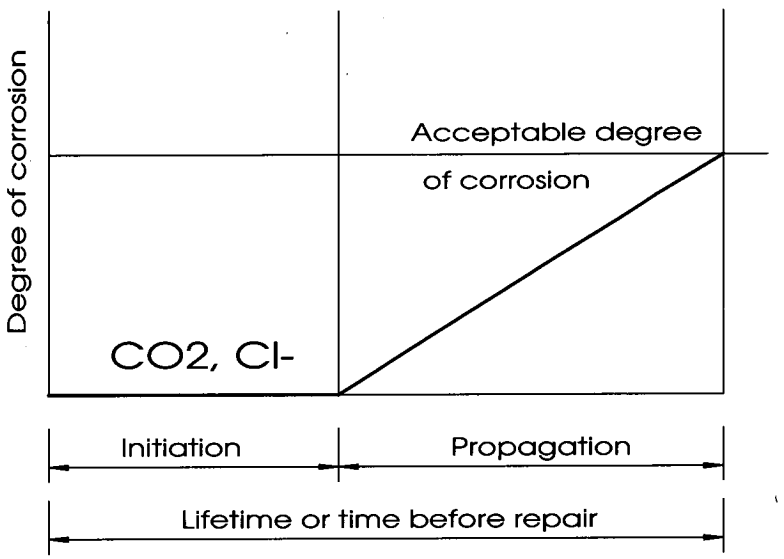

Figure 6.3 – Tuutti's corrosion model

Another possible definition is the critical chloride content at the steel surface at the time when deterioration of or damage to the structure starts. This definition corresponds to a less well-defined point in the propagation curve, where the chloride concentration is likely to be higher than at corrosion initiation, and depends itself on the definition of deterioration and damage. It is particularly difficult to define in the context of actual structures where the detection of damage will be influenced by a number of factors including:

- the frequency of inspections
- the range of ages of structures
- skills of inspectors
- access to relevant parts of the structure to detect damage, with the majority of structures affected by chlorides in the context of this investigation located over water
- obscuring of damage by marine growth
- the definition of damage, such as staining or cracking.

While the initiation of corrosion may be easy to detect in well defined laboratory experiments, with corrosion rates and currents increasing by orders of magnitude after

initiation, the threshold level is often less clear in the field due to a number of factors, including:

- neither the passive oxide layer nor the steel is uniform. As water, oxygen and ions move across the concrete to steel interface, small and very localised corrosion pits develop and repassivate on the steel surface. Sound concrete has a strong ability to restore passivity due to its buffer of calcium and alkali hydroxides.
- corrosion rates may vary due to microclimatic effects, including temperature and humidity
- the area of corroding steel is difficult to define
- measured corrosion rates are usually an average of contributions from passive regions and from localised corrosion pits.

The chloride threshold level can be presented in a number of ways:

- a total chloride content by mass of concrete
- a total mass of acid soluble chloride by mass of concrete
- a total chloride content by mass of binder
- a free (water soluble) chloride concentration in the pore solution
- a ratio between the free chloride and the free hydroxide concentration.

Reporting from the investigations which have provided the basis for this study has been expressed in terms of the total mass of acid soluble chloride by mass of concrete. Determination of cement content of mature concrete involves a number of assumptions because of the lack of information on the nature and amount of cement used in the concrete, and the determination of chloride content by mass of binder is thus considered less accurate than the determination of the chloride concrete by mass of concrete.

In laboratory tests with calcium hydroxide solution, the chloride threshold has been measured in terms of the chloride/hydroxyl ratio. Corrosion was found by Hausmann to occur when the chloride concentration exceeded 0.6 of the hydroxyl concentration (Broomfield, 1997). This approximates to a concentration of 0.4% by mass of concrete if chlorides are cast into the concrete and 0.2% if they diffuse in, with differences arising from alteration of the hydration process. The determination of chloride concentrations in the pore solution and the ratio of free chloride to free hydroxide concentration is complex and beyond the scope of this study.

The threshold concentration does not consider corrosion rates and thus the deterioration of the structure. In extremely dry environments, corrosion rates are low due to the high resistivity of the concrete. For totally saturated concrete, depassivation of the steel will not cause high corrosion rates because oxygen is excluded from the steel surface.

There is a wide range of parameters which are likely to affect the chloride threshold level in concrete. There is some evidence (HETEK, 1996) that the parameters described below are important in controlling the threshold level.

6.6.1 Passive steel potential and concrete alkalinity

By analogy with stainless steel, it is believed that a critical pitting potential exists for passivated mild steel in alkaline concrete. The critical pitting potential depends on the alkalinity of the pore solution in contact with the steel, as indicated in Figure 6.4.

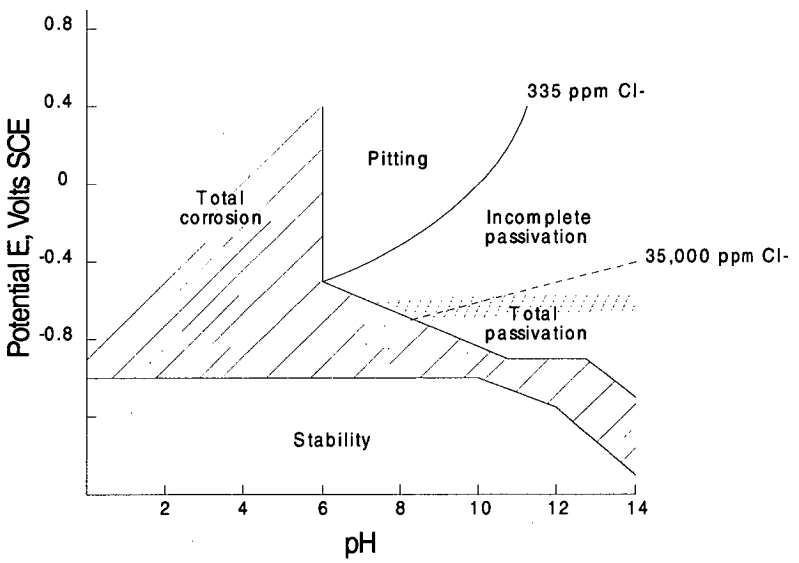

Figure 6.4 - Potential-pH diagram for corrosion of iron in solutions with chloride

Below the critical pitting potential, pitting corrosion cannot be established as the steel potential is too low to become anodic. In the absence of pitting corrosion, low potential conditions in high quality concrete are usually harmless because of low corrosion rates, provided that the reinforcement is properly embedded in the concrete.

6.6.2 Carbonation

Carbonation of the concrete to the depth of the reinforcement reduces the chloride threshold level to zero because:

- the carbonation of the binder leads to a reduction in alkalinity from pH>12.5 in uncarbonated concrete to pH<8 in carbonated concrete at which level the steel is not passive and pitting corrosion is easily promoted when chloride is present
- the binder loses most of its chloride binding capacity when carbonated, resulting in an increase in concentration of free chlorides in the pore solution.

6.6.3 Moisture and oxygen state at the reinforcement

Both the passivating formation of an oxide layer on the steel surface and the chloride initiated corrosion process can be divided into two sub-processes:

- the anodic dissolution in steel; in the presence of chloride ions, the process is boosted by the formation of soluble corrosion processes
- the cathodic reduction of oxygen.

The anodic reaction tends to decrease the steel potential and the cathodic reaction tends to increase it. This implies that the steel potential goes down as the availability of oxygen is restricted. As a result, the steel potential in concrete is closely related to the availability of free oxygen in the concrete. The transport of oxygen through concrete is in turn dependent upon the relative humidity of the concrete. Oxygen diffusion in gas is orders of magnitude faster than in water filled pores. The oxygen transport rate in concrete therefore drops dramatically when the pores become water saturated at high relative humidity. The steel potential in concrete is thus also closely related to the moisture state. The practical implications are that the chloride threshold level is higher in water saturated concrete than in concrete which is subject to wetting and drying. This correlates with the higher observed frequency of damage to reinforced concrete subject to wetting and drying.

6.6.4 Bonding at the steel-concrete interface

Steel in concrete normally has a much higher chloride resistance than when the same steel is exposed to a solution of the same composition as the concrete pore solution. The reasons for the improved resistance are not fully understood. Likely factors include physical adhesion between the cement hydrates and iron oxides on the steel surface, formation of voids at the steel-mortar interface, and precipitation of calcium hydroxide at the steel surface.

6.6.5 Cracks

Macrocracks at the concrete surface generally accelerate the chloride transport rate by modifying the transport processes, depressing the threshold level. The effects of

macrocracks on the chloride threshold level depend on crack size, exposure conditions and the cover thickness. As discussed previously however, no definitive relationship has been found between crack width and corrosion. This applies to cracks both parallel and normal to reinforcement.

6.6.6 Cast-in chlorides

Incorporation of chlorides in plastic concrete has a number of effects:

- the hydration process differs
- increased chloride binding occurs when the aluminate phase is hydrated in the presence of chlorides
- the pore size distribution is altered, potentially leading to increased permeability
- the sodium chloride increases alkalinity due to the formation of sodium hydroxide
- the formation of passivating oxides on the steel surface is less efficient at higher chloride concentrations.

It can thus be expected that chloride threshold levels would differ in concrete where the chloride is cast in from cases where the chlorides subsequently enter the concrete. There are insufficient data to assess the quantum of any differences. Once initiated however, the corrosion rate would be expected to be accelerated by the release of cast in chlorides (Glass et al, 2000).

Chloride profiles from the investigated structures indicate that, in most cases, the majority of chlorides are derived from external sources.

6.6.7 Cover thickness

In addition to providing a physical barrier to external chlorides, the cover also assists with stabilising the microenvironment at the level of the reinforcement. In other fields, it has been shown that variations in moisture, oxygen, salinity and other factors promote corrosion by comparison with a stable exposure condition. It is thus expected that a thicker cover would increase the chloride threshold level by reducing moisture and oxygen variations at the reinforcement. This compares with the high frequency of corrosion damage in concrete exposed to cyclic wetting and drying in a saline environment.

A thicker cover also results in a longer time for a carbonation front to reach the level of the reinforcement, with the associated reduction in alkalinity, and helps prevent the leaching of alkali hydroxides in the vicinity of the steel.

6.6.8 Water to binder ratio

A lower water to binder ratio helps to stabilise the microenvironment at the level of the reinforcement and has similar effects to increased cover. It may also have the following beneficial effects:

- a higher concrete resistivity and denser steel-concrete interface, reducing the area available for corrosion cells to develop
- lower chloride mobility
- a reduced leaching rate for alkalis and a buffer of unreacted cement to help maintain a high concrete alkalinity
- a higher cement content.

Experimental results from Pettersson (1992, 1993, 1994) and Schieβl and Breit (1995) indicate a higher chloride threshold level for concrete with a lower water to binder ratio.

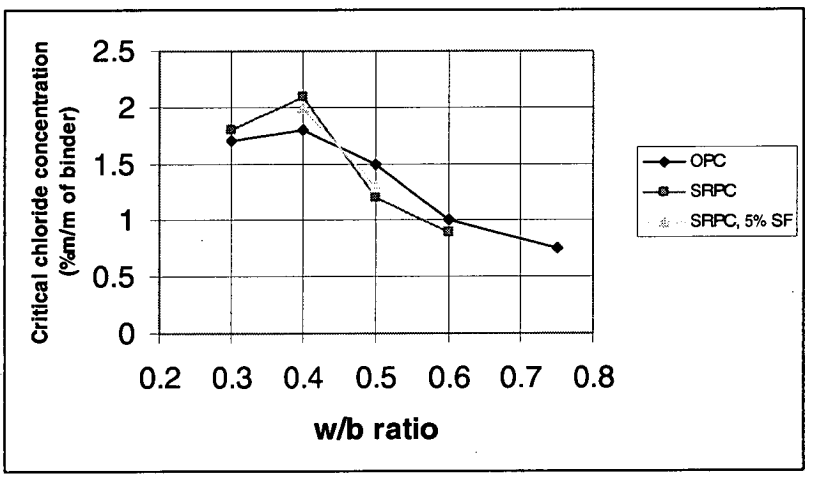

Figure 6.5 – Effect of w/b ratio on chloride threshold levels (Submerged concrete or mortar, Pettersson)

6.6.9 Binder type

Reported results on the effects of pozzolanic and supplementary cementitious materials (silica fume, flyash or ground granulated blast furnace slag) on the chloride threshold level are somewhat conflicting.

The use of supplementary cementitious materials results in a higher concrete resistivity and denser steel-concrete interface, reducing the area available for corrosion cells to develop. They also reduce chloride mobility.

Ground granulated blast furnace slag however usually contains sulphide ions, which have corrosive properties similar to chloride ions. Flyash properties may vary between and within sources. It may also contain chlorides. Pozzolanic materials also consume calcium and alkali hydroxides during the hydration process reducing the alkalinity of the concrete and reducing some of its repassivating capacity.

The chloride binding capacity of concrete will vary with the proportions of the various phases. Its binding capacity increases with the amount of the aluminate phase (C_3A). The low chloride binding capacity of some sulphate resisting cements, which are low in C_3A, has been shown to shorten the initiation time and increase the active corrosion rate compared with cements which are high in C_3A. However, the opposite effects have also been found for a sulphate resisting portland cement high in the ferrite phase (C_4AF). The uniformity and microstructure of the cast concrete, both in terms of concrete impermeability and bonding at the steel-concrete interface, are likely to be more important than the cement composition. These are controlled by the mix design, including the mixture proportions and the choice of aggregates, and the standard of execution of the works.

The chloride binding capacity of the binder appears to have little effect on the chloride threshold level.

Construction records from the structures which are the subject of this investigation do not include details of the source of the cement used or the mix design, with cement contents being determined analytically. The use of supplementary cementitious materials in bridges in Tasmania until recently has been rare if at all, given that ground granulated blast furnace slag and flyash must be imported into the State. Silica fume was available during part of the 1970's and 1980's as a byproduct of ferrosilicon production in the north of the State. While the use of supplementary cementitious materials was precluded in Departmental specifications at that time, this not necessarily mean that silica fume was not used because of its common usage across the construction industry to reduce total cementitious content, with a consequent reduction in costs for the premixed concrete supplier, while continuing to meet compressive strength specification requirements.

The effect of binder type is thus not included within the scope of this investigation.

6.6.10 Exposure time

Glass and Buenfeld (1995) have suggested that the slow redistribution of chloride ions in concrete as well as the stochastic nature of passive film breakdown may explain the apparent decrease in chloride threshold with time reported by Yonezawa et al and Schieβl and Breit.

6.6.11 Temperature

The corrosion resistance of stainless steels in chloride solutions is known to be affected by temperature. By analogy, it would be expected that the chloride threshold level would decrease as the temperature increases, but direct experimental evidence is lacking. The review of climate earlier in this study has shown that temperature variations are small and are thus unlikely to be significant.

6.6.12 Threshold levels

The literature on chloride threshold levels for the initiation of corrosion in concrete is conflicting, with levels of 0.17% to 2.5% by mass of binder having been reported.

Thresholds are approximations for a number of reasons, including:

- concrete pH varies with the type of cement and concrete mix. A tiny pH change represents a massive change in hydroxyl ion (OH^-) concentration and therefore theoretically the threshold moves dramatically with pH.
- chlorides can be bound chemically and physically, by adsorption, in concrete removing them temporarily or permanently from the corrosion reaction.
- corrosion reactions require the presence of water and oxygen and thus may not occur in dry or saturated concrete.

Clear (1974) discusses threshold levels in the context of the repair of concrete bridge decks. His studies suggested a level of 0.20% Cl^- by mass of cement. For a typical bridge deck with 6 no. 94lb bags of cement per cubic yard of concrete of density 145 pcf, this equated to 0.028% by mass of concrete. For a 7 bag mix, the corresponding proportion is 0.033%. For practical purposes in determining an appropriate strategy for a concrete bridge deck, the following guidelines were given:

Less than 1.0 lbs Cl^-/yd^3	- leave concrete intact
Greater that 2.0 lbs Cl^-/yd^3	- remove concrete below top reinforcement mat or entire deck
1.0 to 2.0 lbs Cl^-/yd^3	- questionable area subject to assessment of risks

Pettersson (1992) discusses threshold levels and corrosion rates for concrete. She notes that the chloride threshold value is dependent on several factors, with the primary factors being:

- pH
- levels of C_3A and C_4AF
- admixtures
- curing time
- carbonation.

She also reports results of a number of researchers, described in Table 6.3.

Researcher	Critical Cl- concentration % of cement	Remarks
Hauseman, 1967	0.06-1	pH= 12.5 – 13.2
Cady, 1978	0.2 - 0.4	Concentration varied with pH
Matsushita, 1980	0.8	Submarine tunnel
Brown, 1981	0.4	Varied with cement type
Hansson & Sørensen, 1989	0.6 – 1.4	Varied with cement type, curing, water/binder ratio, admixtures, etc
Schieβl & Raupach, 1990	0.48 – 2.02	Varied with cement type and admixtures

Table 6.3 – Chloride threshold levels

Pettersson's research was undertaken using mortar prisms with a cement/sand ratio of 1:2, with a range of cement types, water binder ratios and mineral admixtures, and used differing curing and exposure regimes. Chloride threshold levels varied from 0.5% to 1.8% by weight of cement, with the critical chloride concentration increasing with decreasing water/binder ratio.

Frederiksen (2000) reports on a review of chloride threshold levels undertaken by Glass and Buenfeld in 1995 and shown in Table 6.4.

Total chloride (% by wt cement)	Free chloride (mole/l)	[Cl]/[OH]	Exposure type	Reference
0.17-1.4			Field	Stratful et al. (1975)
0.2-1.5			Field	Vassie (1984)
0.25			Field	West & Hime (1985)
0.25-0.5			Laboratory	Elsener & Böhni (1986)
0.3-0.7			Field	Henriksen (1993)
0.4			Outdoors	Bamforth & Chapman-Andrews (1994)
0.4-1.6			Laboratory	Hansson & Sørensen (1990)
0.5-2			Laboratory	Schießl & Raupach (1990)
0.5			Outdoors	Thomas et al. (1990)
0.5 – 1.4			Laboratory	Tuutti (1993)
0.6			Laboratory	Locke & Siman (1980)
1.6 – 2.5		3-20	Laboratory	Lambert et al. (1991)
1.8 – 2.2			Field	Lukas (1985)
	0.14 – 1.8	2.5 – 6	Laboratory	Pettersson (1993)
		0.26 – 0.8	Laboratory	Goni & Andrade (1990)
		0.3	Laboratory	Diamond (1986)
		0.6	Laboratory	Hausmann (1967)
		1-40	Laboratory	Yonezawa et al. (1988)

Table 6.4 – Measured ranges of chloride threshold levels (black steel) in macro crack free concrete in various exposure regimes after Glass & Buenfeld (Frederiksen, 2000)

Henriksen and Stoltzner (1993) found that 0.05% chloride of dry concrete weight was the minimum level for initiation of corrosion in reinforcement. Their work was based on corrosion in columns of damaged and undamaged road underpasses in Denmark subject to chloride exposure from deicing salts. Results are detailed in Table 6.5.

	Chloride content at reinforcement at ground level (%w/w)						
	<0.04	0.05	0.06	0.07	0.08	0.09	0.10
No. of corrosion cases	21	8	2	3	3	0	11
Proportion of cases	0%	40%	100%	33%	67%	0%	92%

Table 6.5 – Chloride levels at reinforcement in bridge columns

6.7 ANALYSIS

6.7.1 General

The cores used in this analysis were originally taken as part of a broader investigation into the causes and extent of deterioration in a number of concrete structures for the purpose of determining appropriate management strategies. Those investigations involved a number of surveys and tests, with the extent of testing being a balance between accuracy and cost. The thickness of the slices used for chloride analysis were typically, in order from the surface, 20mm, 20mm, 30mm, 30mm and then 40mm or 50mm increments to reflect likely ranges of cover to reinforcement and limit

investigation costs. It is noted that laboratory investigations would commonly use thinner slices.

Chloride profiles for each of the analysed cores were described with an apparent surface concentration, c_s, and effective diffusion coefficient, D, in Fick's second law of diffusion with the parameters determined using a numerical expansion of the error function and a least squares analysis with a programmable calculator. In the equation, x is taken as the mid-depth of each slice and t is the age of the core.

$$c(x, t) = c_s [1 - \text{erf}(\frac{x}{2\sqrt{D.t}})]$$

Figure 6.6 shows a fitted chloride profile with the associated parameters.

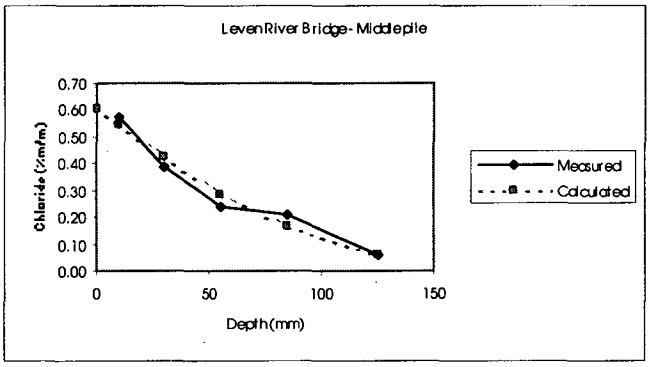

Parameters		Chloride concentration (%m/m) at depth (mm)						
Age (years)	60	Depth	0	10	30	55	85	125
C_s	0.60	Measured		0.57	0.39	0.24	0.21	0.06
D	1.56E-12	Calculated	0.604	0.542	0.421	0.286	0.162	0.063

Figure 6.6 – Fitted chloride profile

The two parameters, c_s and D, are examined for possible correlations with the following factors, both individually and as multiple factors:

- height above mean water level (MWL)
- distance from the coast
- age
- concrete maturity
- concrete density
- cement content

- water cement ratio
- concrete strength
- Young's modulus
- permeable voids ratio
- annual rainfall at bridge site
- mean temperature at bridge site
- site humidity
- chloride concentration in water at bridge site.

The first two parameters relate to the exposure of the concrete. The next group are properties of the concrete itself, while the remainder relate to broader environmental conditions. On the basis of the literature, it was considered that some relationship may have been found with the following concrete properties: cement content, water cement ratio, concrete strength and permeable voids ratio.

Scatterplots are used for the preliminary assessment of possible correlations.

6.7.2 Surface Chloride Concentration

Section 4.2.1 of the Appendix includes plots of apparent surface chloride concentration against the various factors. No correlations are apparent with the exception of height above mean water level and distance from the coast. Correlations with the latter two factors would be expected, with the surface chloride concentrations reducing rapidly as the exposure of the concrete surface changes from direct contact with salt water through splash to aerosol. The lack of correlation is confirmed with the SPSS statistical analysis software.

A scatterplot of the relationship between surface chloride concentration and height above mean water level is shown in Figure 6.7, while the envelope of surface chloride concentration against distance from salt water is shown in Figure 6.8.

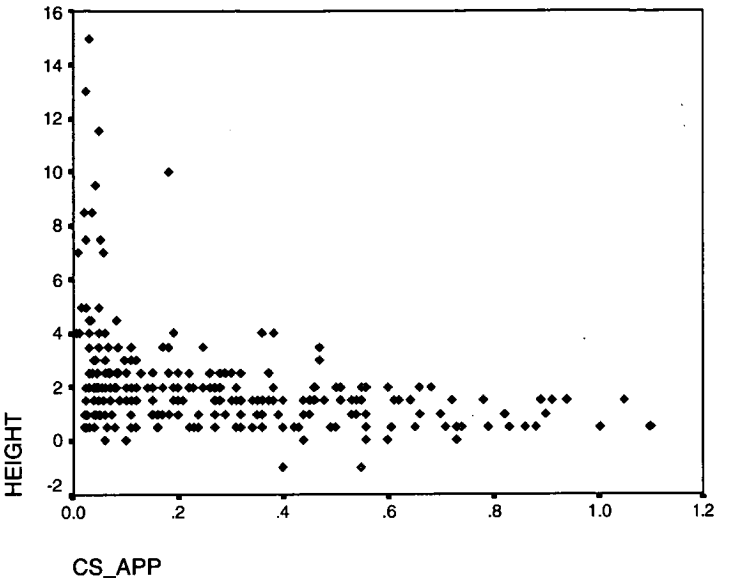

Figure 6.7– Apparent surface chloride concentration ~ height above MWL for all data

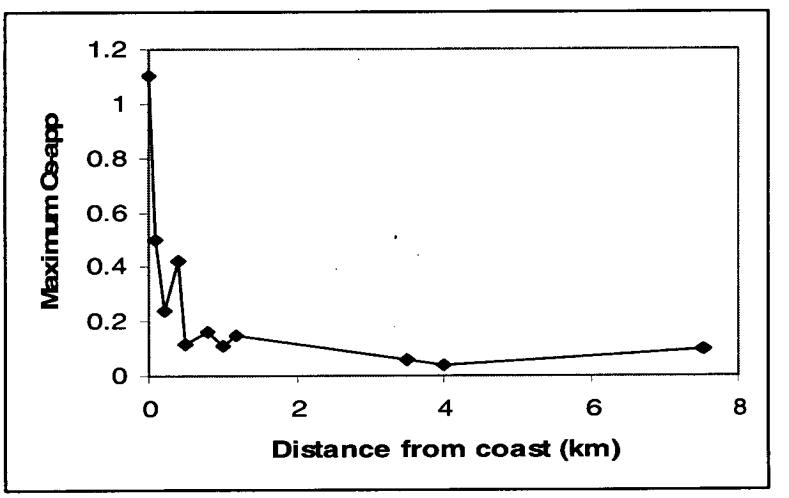

Figure 6.8 – Envelope of surface chloride concentration and distance from coast

6.7.3 Diffusion Coefficient

Scatterplots are similarly used in section 4.2.2 of the Appendix to examine possible correlations between diffusion coefficients and the various parameters.

Again no relationship is apparent. This was confirmed with low correlation coefficients from the statistical analysis software. Possible reasons are identified in the following section.

6.7.4 Analysis with Reduced Data Set

While values of surface chloride concentration and diffusion coefficient were calculated for all cores, a number of samples showed anomalous profiles as indicated in Figure 6.9. The irregular profiles may result from effects such as cracking of the concrete.

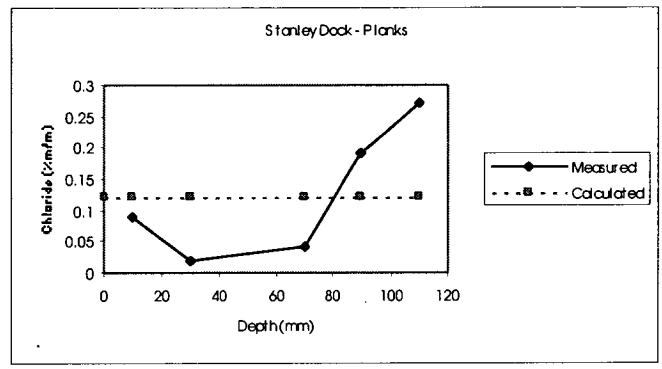

Figure 6.9 - Chloride profile (Stanley Dock)

Further analysis was undertaken with a reduced data set which omitted cores with anomalous chloride profiles such as those in the figure. Poor correlations were again found. The lack of correlation is consistent with the variability found in the examination of the physical and compositional properties of hardened concrete, and is likely to be attributable to a number of factors, including:

- variability in the concrete manufactured for each structure, particularly with site batching likely to have been used for the majority of structures involved in the investigation, with variability both within and between batches
- variations in cement compositions and grinding practices
- effects of placing and compacting the concrete
- effects of differences in finishing and curing, including weather differences on days of concrete placement
- environmental differences between structures
- effects of securing of cores
- cracking or other damage to the cores
- the use of different cores for the various tests, with cores taken from throughout structures
- the accuracy of the various test methods
- the curve fitting process used to calculate apparent surface chloride concentrations and diffusion coefficients

- the frequency of use of a nominal 3000psi or 1:2:4 mix in the surveyed bridges
- the use of lumped data, rather than subsets of the data obtained through processes such as dividing structures into comparatively small zones for analysis.

Use of the same deterioration variables for a complete structure may result in unrealistic uncertainty levels being considered (Sterritt and Chryssanthopoulos, 1999). The analysis has however examined possible correlations with a range of factors, including those relating to different microclimates for different structural elements.

It had been expected that some form of correlation between chloride ingress parameters and cement content or water cement ratio would have been identified, with a number of models having been developed to consider the influence of mix proportions on chloride diffusion coefficients (Vu and Stewart, 2000). The models all exhibit similar trends and, for water cement ratios of 0.35 to 0.5 typical for reinforced concrete structures, differences between models are not significant. Additionally, the gradient of the chloride diffusion coefficient ~ water-cement ratio relationship is relatively flat for values of the latter parameter less than about 0.55, which comprises the majority of samples involved in the study.

The next section examines the form of distributions of the apparent surface chloride concentration and effective diffusion coefficient to develop models for service life analysis.

6.8 PARAMETERS FOR SERVICE LIFE MODELLING

6.8.1 General

With no correlations identified between surface chloride concentration, diffusion coefficient and the range of factors examined (with the exception of height above water level and distance from salt water for the surface concentration), this section examines probability distributions for subsequent service life modelling.

6.8.2 Surface Chloride Concentration

A histogram of all values of apparent surface chloride concentration is skewed towards the lower values as shown in Figure 6.10 and is consistent with the scatterplot showing its relationship with height above mean water level in Figure 6.7. The figure also includes values from cores with irregular chloride profiles.

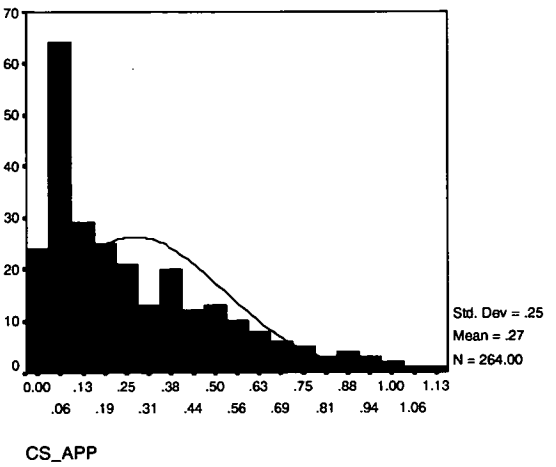

Figure 6.10 –Surface chloride concentrations, all cores

It would be expected that the surface chloride concentration would be dependent upon the exposure of the concrete surface, with the highest concentrations occurring for elements within the tidal and splash zones and the concentration reducing with height above mean water level and distance from the coast.

Subsets of the data were examined using histograms and normal probability plots to establish parameters for service life modelling. Selected plots are included in section 4.3.1 of the Appendix. The largest subset is for cores taken from a height not more than 2m from structures in contact with salt water reflecting the sample of bridges involved in the investigations and the relatively high incidence of corrosion in tidal and splash zones. Table 4.2 highlights the limited range of tidal zone for many of the structures involved in the study, although there is a higher range for the north of the State. Subsets of the data and parameters for modelling have adopted a height above Mean Water Level for cores, rather than a more common submerged/tidal/atmospheric zone classsification, because of reduced subjectivity and possible easier application to design and specification. Few, if any, cores were taken from the submerged zone because of more difficult access for sampling and the lesser degree of visible damage to concrete.

Examination of the plots and reference to statistical analysis from the SPSS software package indicated that subsets of the data could reasonably be described by normal probability distributions as summarised in Table 6.6.

Data set	Mean	Standard deviation	COV (%)	Range	No. cores
All cores	0.273	0.251	91.9	0.01-1.10	264
Limited data set					
Overall	0.380	0.248	65.3	0.05-1.05	102
Distance from coast 0km, height ≤ 2m	0.464	0.253	54.5	0.08-1.10	62
Distance from coast 0km, 2m<height ≤ 4m	0.207	0.148	71.5	0.05-0.42	16
Distance from coast 0km, height > 4m					
Distance from coast 0.1km	0.287	0.136	47.4	0.10-0.50	12
Distance from coast > 0.5km (0.6-0.8km)	0.135	0.024	17.8	0.11-0.16	4

Note: Number of cores is greater than for diffusion coefficients because some values of diffusion coefficient were taken to be constant; mean and standard deviation %m/m concrete.

Table 6.6 – Apparent surface chloride concentration

Values of the apparent surface chloride concentration for greater distances from the coast are consistently small and are detailed in Table 6.7. They are at or below the threshold concentrations meaning little or no probability of corrosion except where chlorides have been cast into a structure.

Distance from coast (km)	Apparent surface chloride concentration (% m/m concrete)
3	0.04, 0.04, 0.04
3.5	0.06
4	0.04
7.5	0.1, 0.06, 0.03
32	0.011, 0.006
Mean	0.043

Table 6.7 – Apparent surface chloride concentration

Figure 6.11 fits a logarithmic curve to the variation in apparent surface chloride concentration with distance from the coast, taking the values for 0.1km and 0.7km (0.6 – 0.8km) from Table 6.6 and a value of 0.04 for a distance of 3km from Table 6.7.

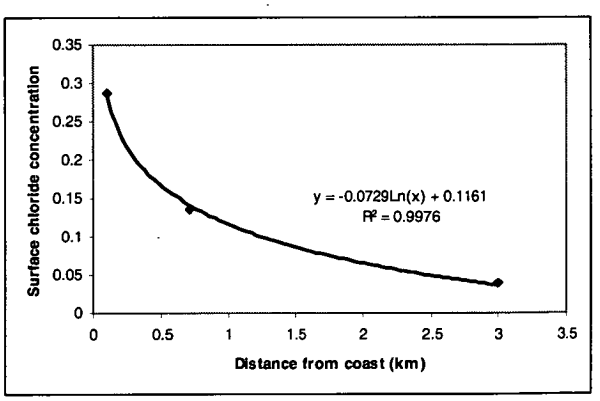

Figure 6.11 - Mean surface chloride concentration ~ distance from coast

Coefficients of variation differ for the various structure locations; using a weighted average of the coefficients for distances from the coast of 0.1km, 0.6 to 0.8km, and 3 to 32 km gives a value of 48.7%. Parameters for surface chloride concentration adopted for service life modelling are given in Table 6.8. Normal distributions apply.

Distance from coast,d (km)	Height (m)	Apparent surface chloride concentration (%m/m)	COV (%)
0	≤2	0.380	65.3
0	>2, ≤4	0.148	71.5
0	>4	0.116	79.0
0.1 to 2.84	All	-0.0729ln(d)+0.1161	48.7
>2.84	All	0.04	48.7

Table 6.8 – Parameters for modelling

6.8.3 Diffusion Coefficient

In this section, probability distributions for values of the diffusion coefficient are examined using logarithmic transformations to base 10. Figures 6.12 and 6.13 show a histogram and normal probability plot of the values of the coefficient and indicate that a normal distribution can be applied to the transformed values.

Subsets of the data, based on the analysis for the surface chloride concentration, are included in section 4.3.2 of the Appendix.

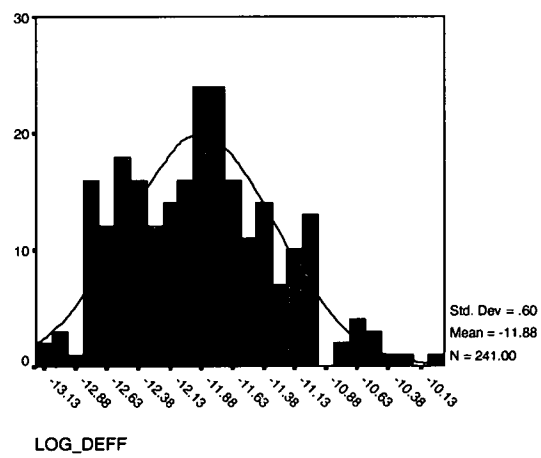

Figure 6.12 – Distribution of diffusion coefficients, all cores (log_{10} transform)

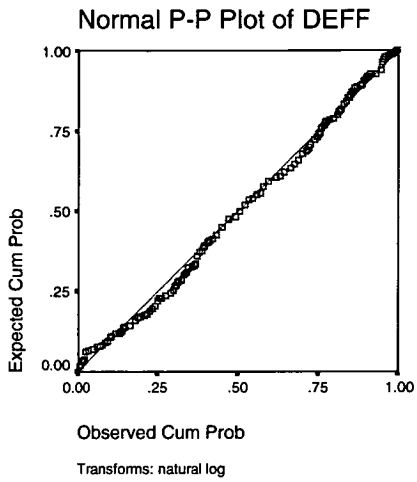

Figure 6.13 - Normal probability plot of diffusion coefficients, all cores (log_{10} transform)

Table 6.9 summarises values for the chloride diffusion coefficient for all cores and for the subsets of the data. Examination of the histograms and normal probability plots indicated that lognormal distributions could be used.

Data set	Mean*	COV (%)	Range*	No. cores
All cores	-11.88	5.1	-13.2 to -10.0	241
Limited data set				
Overall	-12.00	4.0	-13.0 to -11.0	102
Distance from coast 0km, height ≤ 2m	-11.89	3.9	-12.8 to -11.0	62
Distance from coast 0km, 2m<height ≤ 4m	-12.18	3.5	-12.7 to -11.3	16
Distance from coast 0.1km	-12.24	3.8	-13.0 to -11.5	12
Distance from coast > 0.5km	-12.16	3.4	-12.6 to -11.8	4

* log_{10} transform

Table 6.9 – Chloride diffusion coefficients

Table 6.9 shows little variation in the mean value of the transformed diffusion coefficient between the various data sets. The higher variability for all cores, shown by the value of the standard deviation, reflects the inclusion of results from cores with irregular chloride profiles, and the values derived from the limited data set are considered to be more reliable for subsequent analysis

The model to be used for subsequent analysis is thus for the distribution of diffusion coefficients to be lognormal, with a mean of –12.0 and a standard deviation of 0.48 for the transformed values. The mean value equates to a diffusion coefficient of 1.00×10^{-12} m^2/s.

6.9 SUMMARY

The penetration of chlorides into concrete is the result of a number of transport and binding processes, with concentrations at various depths a time-dependent function of the environmental conditions, the design of the structure and its material properties. While the processes are complex, they are commonly modelled with Fick's 2nd Law of Diffusion allowing the chloride concentration at time t and depth x to be described in terms of an apparent surface chloride concentration c_s and effective diffusion coefficient D. Comparisons can be made with published data based on Fickian diffusion modelling.

There are a number of influences on the threshold concentration of chlorides for the initiation of reinforcement corrosion, with levels of 0.17% to 2.5% by mass of binder having been reported. A concentration of 0.05% chloride by dry concrete weight (Henriksen and Stoltzner, 1993) was adopted as the basis for subsequent service life modelling as a value that was likely to have some conservation; a sensitivity analysis for higher threshold values was also used.

The diffusion parameters derived by curve fitting for the cores involved in the study were examined for possible correlations with a range of environmental and materials factors. A number of influences are likely to contribute to the lack of any identified correlations.

Probability distributions were derived for the apparent surface chloride concentration and effective diffusion coefficient for subsequent service life modelling. Normal and lognormal distributions, characterised by high variability, were adopted.

High variability in diffusion parameters is commonly observed in actual structures and exterior environments. Large scatter and variation has been observed in concrete blocks exposed to deicing salts adjacent to a Swedish highway (Nilsson et al, 2000). Large scatter has also been observed between what should be comparable bridges and also on individual bridges in measurements on road bridges in Denmark and Sweden (Lindvall et al, 2000). Minimum coefficients of variation of 65% for diffusion coefficients and values of 45% to 90% in coefficients of variation for surface chloride concentrations were observed in elements of the Maracaibo bridge in Venezuela (Izquierdo et al, 2000).

The variability in the concretes involved in the study is consistent with the variability reported by others, particularly in light of the range of ages, structure types and exposures involved.

7 CARBONATION

7.1 INTRODUCTION

As discussed in the chapter on corrosion mechanisms, carbonation of concrete occurs when carbon dioxide from the atmosphere reacts with calcium hydroxide produced from the cement hydration reactions. As a result, the pH of the pore solution decreases potentially affecting the passive oxide layer on the reinforcing steel and possibly leading to corrosion. The rate of corrosion will depend on the availability of both oxygen and water. In an arid environment or saturated conditions, corrosion rates due to carbonation may be so low that the service life of a structure is unaffected. Reinforcement may corrode at intermediate levels of humidity leading to cracking and spalling of the cover concrete.

The following discussion is based on a paper by Browne (1988).

In solution, the reaction between calcium hydroxide and carbon dioxide is rapid, and thus the carbon dioxide in solution is unlikely to penetrate beyond pores in the cement paste which contain calcium hydroxide. A distinct boundary, known as the 'carbonation front', between reacted and unreacted calcium hydroxide thus forms. The distinct boundary facilitates accurate measurement of the depth of carbonation, typically with phenolpthalein solution, and there is thus a considerable amount of data available on the subject. Phenolpthalein solution has been used for the measurements of carbonation depth in this study.

Figure 7.1 – Measurement of carbonation depth
(Note: Freshly fractured surfaces generally used for measurement)

The rate of carbonation is affected by the degree of saturation of the concrete. If all pores are filled with water, the rate of carbonation will be decreased by orders of

magnitude due to the slower diffusion rate of carbon dioxide gas into water filled capillary pores. Conversely, in very dry environments (less than 25% relative humidity), there is insufficient water in the pores for the gas to dissolve and the carbonation process ceases. Carbonation occurs most rapidly at relative humidities between 50% and 70%.

As early as 1965 it was identified that the depth of carbonation was related to the square root of the age of the concrete.

Smolczyk used data from an eight year study in Germany to develop the following expression:

$$x = 8.46\left[\frac{10w/c}{\sqrt{f_c}} - 0.193 - 0.076w/c\right]\sqrt{t_m} + 0.95$$

where x = depth of carbonation (mm)
w/c = water/cement ratio
f_c = compressive strength at 7 days (kg/cm^2)
t_m = time of exposure (months)

The expression was however considered to only be valid for the prevailing exposure conditions of temperature, relative humidity and atmospheric pollution.

Klopfer developed the following more general expression for the depth of carbonation:

$$x = \sqrt{2\overline{D}t}$$

where x = depth of carbonation (mm)
$\overline{D}$ = carbonation coefficient (mm^2/year)
t = time of exposure (year)

The carbonation coefficient is dependent upon the properties of the carbonating concrete and is thus a unique value for a particular concrete exposed to the specific carbonating environment.

Figure 7.2 shows the relationships developed by Klopfer in 1972 for different grades of concrete in dry conditions in the open air.

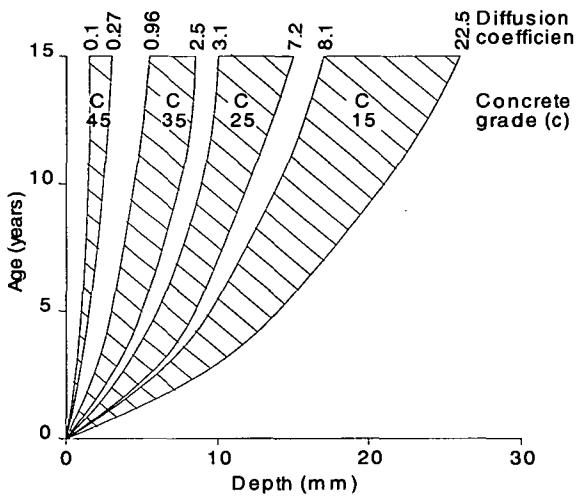

Figure 7.2 - Depth of carbonation with time as affected by concrete grade (Klopfer)

Tuutti showed that carbonation rates in urban environments with high levels of carbon dioxide in the atmosphere (0.1%) were of the order of 3 to 4 times faster than at the more typical concentration at that time of 0.03%. The value of 0.03% may have increased because of greenhouse gas effects. He also showed that increasing the cement content, but maintaining the same permeability, decreased the carbonation rate because of the increased free calcium hydroxide. The two relationships are shown in Figures 7.3 and 7.4.

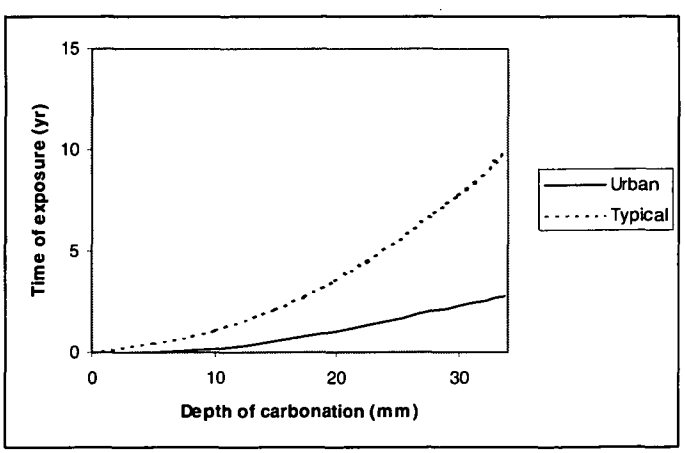

Figure 7.3 - Effect of CO_2 concentration on carbonation rate

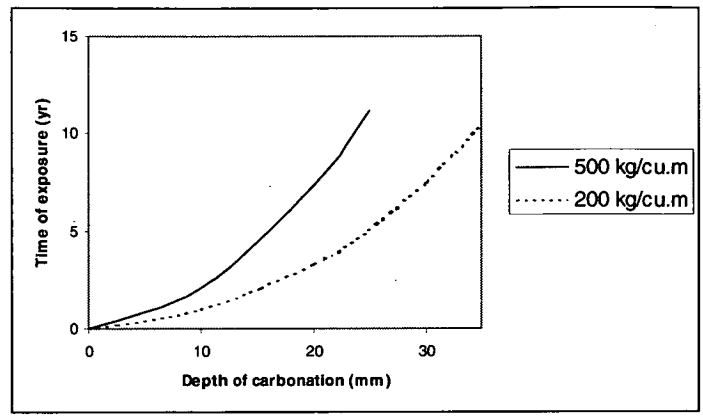

Figure 7.4 - Effect of cement content on carbonation rate

The structures which form the basis of this study are predominantly located in rural environments. Additionally, Tasmania does not have the heavy industrialisation and high traffic volumes that would be expected to lead to carbon dioxide concentrations approaching the 0.1% level. No data were readily accessible on carbon dioxide concentrations in the vicinity of the various structures, and the possibility of a correlation was not investigated.

Decreasing the permeability of the concrete also has a marked effect on the rate of carbonation of concrete as shown in Figure 7.5.

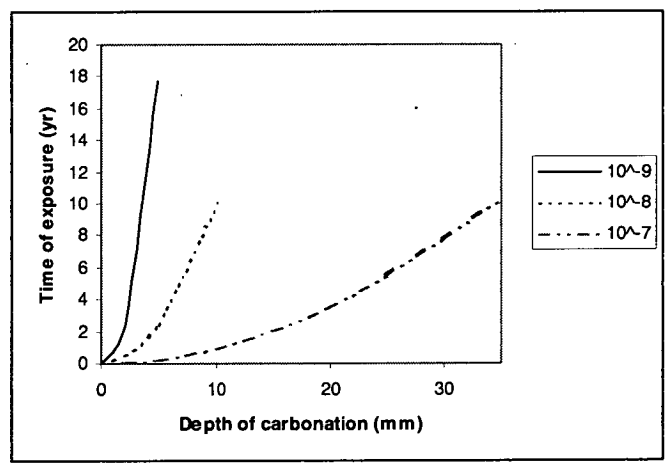

Figure 7.5 - Effect of permeability on carbonation rate

Ho and Lewis (1981) have reported on the effects of PFA and water reducing admixtures on carbonation. They confirmed that, for different exposures, a diffusion relationship was appropriate and that carbonation depth was proportional to $\sqrt{\frac{1}{f_c}}$.

Perrott (1994) proposed that the initiation period corresponded to the time in years when the carbonation depth, d (mm) equalled the minimum cover, D (mm). His examination of the literature suggested that D could be related to the initiation period by the equation

$$D = d = ak^{1.4}t^{n} / c^{0.5}$$

where k (in units of 10^{-16} m^2) is the air permeability of cover concrete and depends on the relative humidity, r%, in the cover concrete. If k is unknown, it can be estimated from the permeability of a test specimen dried at 60% relative humidity, k_{60}, using the equations

$$k = m\,k_{60}$$
$$m = 1.6 - 0.00115r - 0.0001475\,r^2 \text{ or}$$
$$m = 1.0 \text{ if } r<60$$

n is a power exponent that is close to 0.5 for indoor exposure but decreases as the relative humidity rises above 70% to account for the slower rates of carbonation observed under wetter conditions

$$n = 0.02536 + 0.01785\,r - 0.0001623\,r^2$$

c is the calcium oxide content in the hydrated cement matrix of the cover concrete (in kg/m^3 of cement matrix) that can react with and effectively retard the rate of carbon dioxide penetration; it depends on the cement composition, exposure condition and the proportion of cement reacted

a is a coefficient that can be assigned a value of 64 on the basis of available published data.

7.2 FACTOR ANALYSIS

As with chloride ingress, carbonation data were examined for possible correlations with the following concrete properties and environmental factors using scatterplots.

- age
- maturity
- density
- cement content
- water cement ratio
- compressive strength
- Young's modulus
- volume of permeable voids
- distance from coast
- annual rainfall at bridge site
- temperature at bridge site
- humidity at bridge site
- frost days
- site water chloride concentration
- site water sulphate concentration
- site water pH
- height above mean water level (MWL).

Scatterplots used for the preliminary assessment are included in Chapter 5 of the Appendix. The scatterplots do not indicate any correlation between carbonation depth and the various factors examined. The lack of correlation was confirmed with the statistical analysis software.

On the basis of the literature, it was considered possible that some correlation may have been found with properties such as cement content, water cement ratio, compressive strength, volume of permeable voids and humidity at the bridge site. The lack of correlation may be attributable to factors such as:

- variability in concrete properties, particularly with site batching likely to have been used for the majority of structures involved in the study, and variability both within and between batches
- variations in cement compositions and grinding practices
- aggregate shape and size

- effects of placing and compacting concrete
- effects of differences in finishing and curing, including weather differences on days of concrete placement
- environmental differences between structures
- effects of securing cores
- the accuracy of measuring carbonation depth given its variability across the width of a core
- the use of different cores for the various tests, with cores taken from throughout structures
- the frequency of use of a nominal 3000 psi or 1:2:4 mix in the surveyed structures
- the use of lumped data.

7.3 PARAMETERS FOR SERVICE LIFE MODELLING

Probability distributions of subsets of carbonation data, based on groupings of ages of structures, are examined in section 5.2 of the Appendix. Examination of subsets of the data in 10 year age groups indicates that normal or lognormal distributions can be fitted to those subsets, although the fits are variable. Results are summarised in Table 7.1 and Figure 7.6.

Age	Carbonation depth			No. of cores
	Mean (mm)	Standard deviation (mm)	COV (%)	
15 to 24	14.3	7.66	53.6	20
25 to 34	11.0	6.60	60.0	48
35 to 44	12.8	6.86	53.6	87
45 to 54	11.3	7.81	69.1	60
55 to 64	14.3	9.24	64.6	40

Table 7.1 – Carbonation depths at various ages

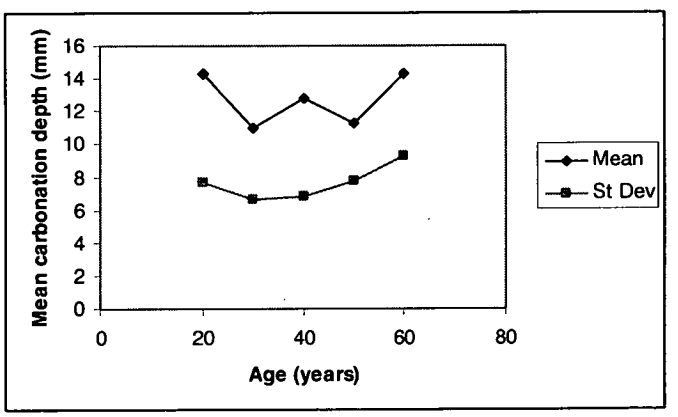

Figure 7.6 – Carbonation depths at various ages

It would be expected, based upon the literature, that the mean carbonation depth would increase with age with a parabolic or similar relationship consistent with that of Klopfer.

$$x = \sqrt{2\overline{D}t}$$

The lack of an increasing trend may be attributable to a range of factors, including:

- the influence of humidity on carbonation rates, with the majority of structures having been investigated for chloride induced damage and thus subject to locally high relative humidities
- the age distribution of samples, with a bias towards older bridges so that the sample size for younger bridges was relatively small
- the variability of concrete as described previously
- the variability in durability related properties as discussed in section 6.9.

With the lack of an observable trend, carbonation data were aggregated and the histogram and probability plots in Figures 7.7 to 7.9 used to examine the distribution of k, where

$$k = \sqrt{2\overline{D}}$$

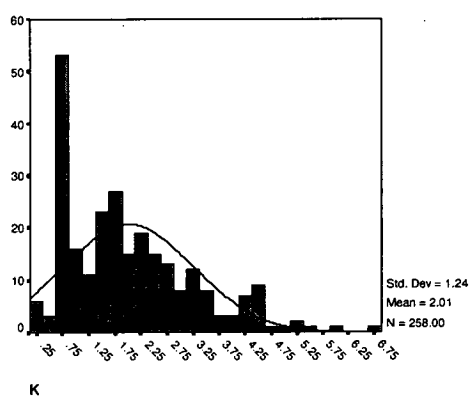

Figure 7.7 – Distribution of k

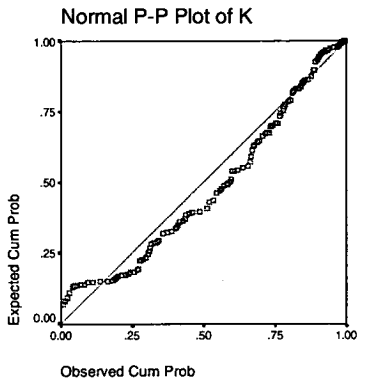

Figure 7.8 – Normal probability plot of k

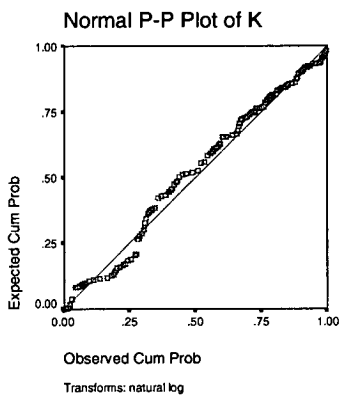

Figure 7.9 – Lognormal probability plot of k

The plots indicate that k can be described by a normal distribution with a mean of 2.01 and standard deviation of 1.24 or a lognormal distribution, with the mean and standard deviation of the transformed (ln) values being –1.353 and 0.7723 respectively. Units for k are mm/yr$^{1/2}$.

7.4 DISCUSSION

While the frequency and severity of carbonation damage in Tasmanian bridges is less than for chloride induced deterioration, there is nevertheless a number of cases where damage has occurred. The damage commonly occurs in concrete bridge railings where low and variable covers to reinforcement are common.

Figure 7.10 – Carbonation induced corrosion damage to structure

While other researchers have found relationships between the rate of carbonation and factors including water cement ratio and concrete compressive strength, no correlations were identified in the analysed cores.

As with concrete properties and chloride penetration, the lack of correlation is likely to be due to a number of factors including:

- variability in the concrete used in each structure, particularly with site batching likely to have been used for the majority of structures involved in the study, and variability both within and between batches
- variations in cement compositions and grinding practices
- aggregate shape and size
- effects of placing and compacting the concrete
- effects of differences in finishing and curing, including weather differences on days of concrete placement
- environmental differences between structures
- effects of securing cores
- the use of different cores for the various tests.

There is additionally the inherent variability that has been observed in chloride related durability related properties of concrete that could similarly be expected to apply to carbonation.

Carbonation in the analysed cores can be described in terms of a carbonation parameter, k, with a normal or lognormal distribution in the equation:

$$x = k\sqrt{t}$$

k can be described by a normal distribution with a mean of 2.01 and standard deviation of 1.24 or a lognormal distribution, with the mean and standard deviation of the transformed (ln) values being –1.353 and 0.7723 respectively. Units for k are mm/yr$^{1/2}$.

The use of subsets of the data has been examined, particularly in terms of age groupings. Aggregate data will however be used in the service life modelling aspects of the thesis because of the objective of developing service life models and the lesser significance of carbonation as a bridge management issue with its lower aggressiveness by comparison with chloride induced corrosion of reinforcing and prestressing steel.

7.5 SUMMARY

Carbonation occurs when carbon dioxide from the atmosphere reacts with calcium hydroxide from the cement hydration reactions, reducing the alkalinity of the pore solution and potentially affecting the passive oxide layer on the reinforcing steel allowing corrosion to occur once the carbonation front reaches the level of the reinforcement

Other researchers have identified relationships between carbonation rate and factors such as concrete strength and water cement ratio. No correlations between carbonation rate and a range of material and environmental factors were however identified in this study.

Normal and lognormal probability distributions have been derived for service life modelling.

8 COVER TO REINFORCEMENT

8.1 INTRODUCTION

This chapter describes the background to and investigations of the variability of cover to reinforcement in concrete by others and the research undertaken on Tasmanian bridges.

The literature relating to variability in cover and a range of codes and specification requirements are examined. Data from Tasmanian bridges are analysed to assess changes in accuracy of reinforcement placement over six decades of bridge building to determine tolerances which are likely to be achievable in both insitu and precast construction, to assist with a review of specifications and to determine parameters for use in service life modelling.

8.2 GENERAL

Interest by the author in the variability of cover to reinforcement in structures was initially generated by Marrosszeky and Chew in their 1989 paper in the journal of the Concrete Institute of Australia, CIA News. The implications of low cover, in respect of both low specified cover and in variability, were highlighted as the Department of Infrastructure, Energy and Resources established a systematic bridge inspection and maintenance program and the significant number of structures with visible evidence of corrosion became apparent. In a number of cases, reinforcement was visible either where there had been no cover or where cover concrete had spalled.

The variability in cover from the nominal value highlighted by Marrosszeky and Chew was confirmed in a cover survey which was part of a comprehensive program of testing of the Princess River Bridge on Tasmania's west coast undertaken in August 1991 prior to the bridge's inundation by the King River Power Development (M^{c}Gee, 1993). The bridge was a reinforced concrete T-beam structure with insitu reinforced concrete slab deck. Figures 8.1 and 8.2 show cover distributions for the Princess River Bridge; figure 8.2 includes a comparison with the work of Marrosszeky and Chew and shows the comparability of results.

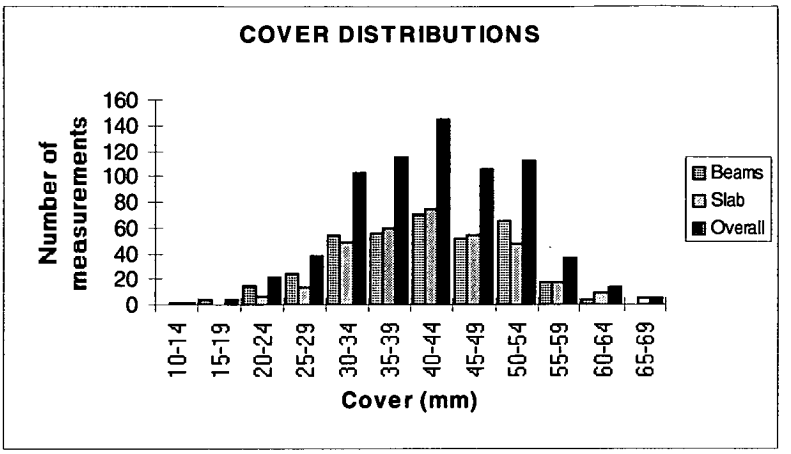

Figure 8.1 - Princess River Bridge cover distributions

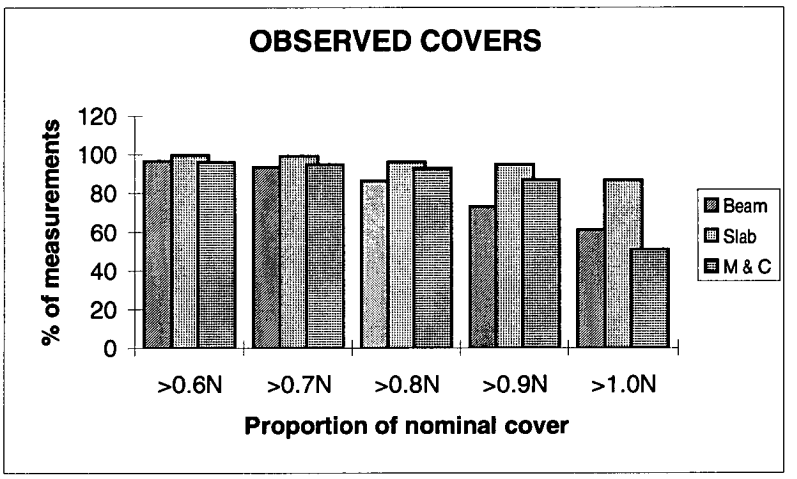

Figure 8.2 - Comparisons of Princess River cover distributions
(M&C – Marrosszeky and Chew)

A program of cover surveys covering a range of Tasmanian bridges was consequently established. That program provided the basis for this part of the thesis.

8.3 OBJECTIVES

Objectives of the cover survey program were to:

- review available information on the variability of cover to reinforcement
- examine the variability of cover to reinforcement in Tasmanian bridges
- determine tolerances which are likely to be achieved in practice for both insitu and precast concrete to assist with a review of specifications and for code development
- develop models of cover to reinforcement for use in deterioration models
- develop models of cover to reinforcement for use in corrosion reliability analysis

- publish results to raise awareness of cover variability within industry with a view to improving performance.

8.4 OTHER RESEARCH

A number of researchers have investigated the variability of cover to reinforcement in structures, and their work is discussed below.

Morgan et al (1982) presented the results of an investigation into the pre-pour placement precision of reinforcement in office building rectangular slabs. They found that the tolerances at the time (-0+5mm) were not achieved by a wide margin on any of the sites investigated. Variations in reinforcement placement were found to be normally distributed.

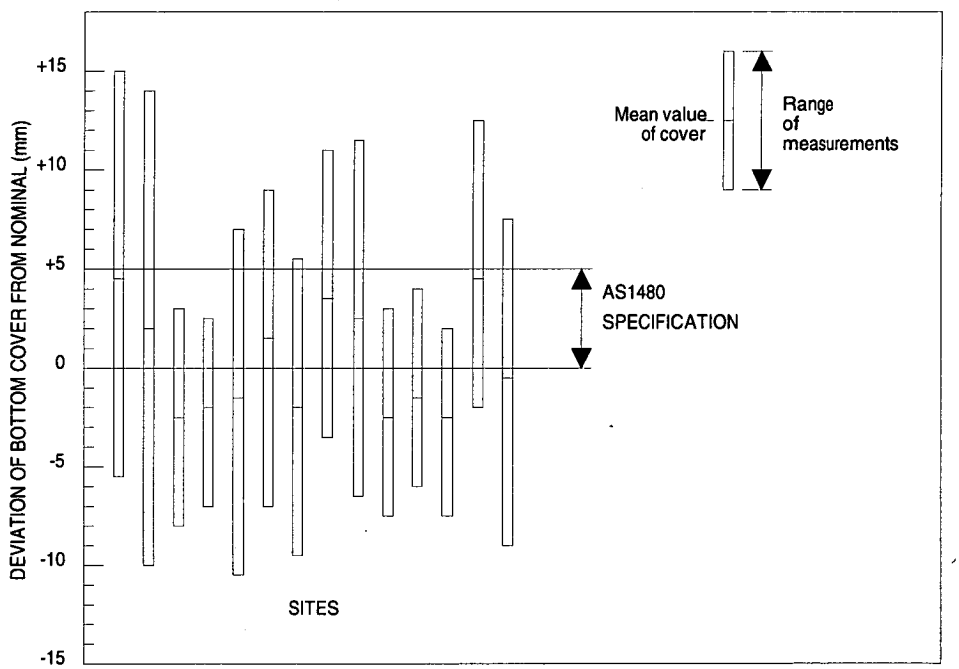

Figure 8.3 - Reinforcement placement in rectangular concrete slabs (Morgan et al)

Morgan et al (1986) also reviewed the provisions of the interacting Australian Codes controlling concrete slab tolerances, and concluded that current Australian practice could not satisfactorily achieve both depth to steel and cover requirements specified directly or indirectly in the Australian Concrete Structures Code (AS1480 - 1974). Proposals were made for code changes to permit a better match between specification, codes and practice.

Marrosszeky and Chew (1989, 1990) reported on the cover aspects of a three-part research project undertaken at the Building Research Centre at the University of New South Wales which investigated factors causing corrosion-induced durability faults in buildings.

Objectives of their work were:

- to measure the accuracy of reinforcement placement on site
- to identify the most common areas where there is a lack of adequate cover
- to analyse the cause of the problem in each case
- to assess which parties in the design and construction process are best placed to prevent problems from occurring for each problem area
- to assess the life cycle benefit achieved due to improved quality management during construction.

More than 10,000 measurements were taken on the buildings studied, with a similar set of readings being taken on bridges. The results are illustrated in Figure 8.4, which shows the percentages of measurements exceeding various proportions of the specified cover, *N*. The figure shows significantly better performance on bridges.

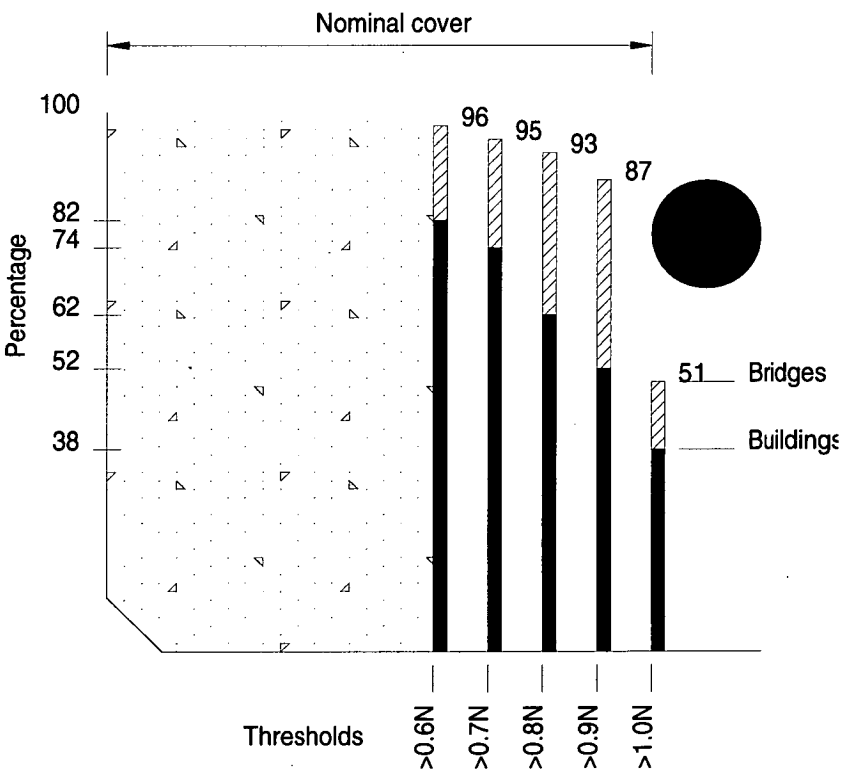

Figure 8.4 - Percentages of covers exceeding various thresholds

Factors leading to problems were analysed, with the results as tabulated in Table 8.1.

Category	Problem	Cause	Frequency	Consequence
Reinforcement chairs and ties	Reinforcement Incorrectly shaped or sized	Inadequate engineering design and documentation	Frequent	Major
		Incorrect scheduling	Infrequent	Major
		Incorrect fabrication on and off site		Major
		Damage during handling and after placement		Minor
	Reinforcement in incorrect position	Deformed bar chair	Infrequent	Major
		Inadequate reference lines	Frequent	Major
		Bar chairs missing or out of place	Frequent	Major
		Inappropriate bar chairs - shape, size, material	Frequent	Major
		Clashing reinforcement	Frequent	Major
		Reinforcement cage too heavy to adjust	Infrequent	Major
		Inaccessible location	Frequent	Major
		Negligent placement and fixing	Frequent	Major
		Ties missing and loose	Frequent	Major
		Reinforcement position altered after placement due to heavy treatment of other trades	Infrequent	Minor
	Bar chairs too close to edge	Placed over critical areas such as drip drains	Frequent	Major
		Displaced due to inappropriate bar chair	Frequent	Minor
		Displaced due to rough treatment	Infrequent	Minor
	Ties too close to edge	Ties bent out towards edge	Frequent	Major
Conduits and Inclusions Clashing with Reinforcement	Due to off-site problems	Lack of coordination of services and structure	Frequent	Major
		Position not documented	Frequent	Major
		Lack of communication between consultants	Frequent	Major
	Due to on-site problems	Inadequate information on site of correct position	Frequent	Major
		Careless placement of conduits	Frequent	Major
		Inadequate fixing of conduits in correct position	Frequent	Major
Formwork	Formwork incorrectly Positioned	Incorrect setting out	Infrequent	Major
		Negligent positioning	Infrequent	Major
		Incorrect or inadequate drawings	Infrequent	Major
		Inadequate tolerances	Infrequent	Major
	Contamination	Inadequate cleaning out	Frequent	Major
	Movement during placement of concrete	Inadequate form thickness	Infrequent	Major
		Inadequate bracing	Infrequent	Major

Table 8.1 - Factors leading to cover problems

They concluded that a complex interaction of human factors in design and construction, and priority being given to short construction times and low initial cost, often led to a product of insufficient quality to meet long term requirements. While improved quality attracts increased labour and supervision costs, careless construction of reinforced concrete structures attracts a disproportionate penalty in unnecessary maintenance and repair costs during the life of the building. They note that defining realistic quality standards which can be achieved in the workplace is a major task.

Sirivivatnanon and Cao (1991) analysed cover data from a large number of buildings in Australia and Japan. They found that the levels of confidence (LOC) for achieving minimum concrete cover for durability were poor, with less than 50% of structures achieving a 90% LOC. It was suggested that, with improvements in design detailing, selection of suitable spacers and good installation practice, an LOC of 90% could be achieved and should be specified.

Cover data were assumed to have a normal distribution, with the validity of the assumption having been validated by Morgan et al (1982). The mean of the cover was related to the specified cover and its tolerance by the following equations, which relate the different parameters of a normal distribution curve.

$$C_m = (C_s + t) + k \times SD$$

$$k = 1/SD \times [(C_m - C_s) - t]$$

$$\text{ie } k = 1/SD \times [M - t]$$

where C_s =specified cover (mm)

C_m =mean cover (mm)

M =difference between mean cover and specified cover ($C_m - C_s$)

SD =standard deviation of cover (mm)

t =tolerance for cover (mm) - negative tolerance is specified for minimum cover

k =a statistical constant

n =number of cover measurements

The Level of Compliance (LOC) was defined as the percentage of cover measurements which are at least equal to the absolute minimum cover (specified cover plus the negative tolerance). LOC can be determined from the statistical constant k and normal distribution tables.

Matta (1993) reviewed data from condition surveys of about 100 reinforced concrete structures in the United Arab Emirates. The work showed widespread low covers, with the results presented in Figure 8.5. Reasons for the low covers were considered to include failure to specify a minimum or average depth of cover, poor control during construction, poor or insufficient use of spacers and chairs, poor formwork fixing procedures, and poor reinforcement cutting and bending procedures.

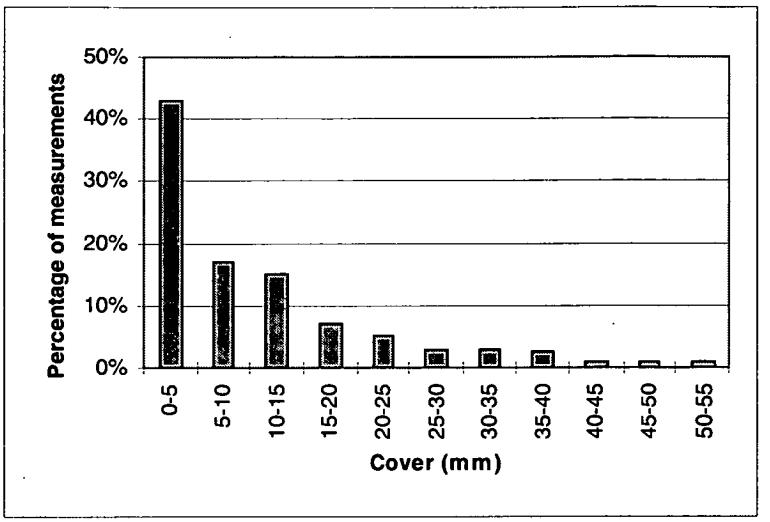

Figure 8.5 - Cover surveys after Matta

Ohta et al (1992) presented the results of a series of investigations on a deteriorated and rehabilitated prestressed concrete bridge. While the design cover thickness was 27.5mm in the web of the beam, a cover survey showed an average cover of 21.7mm with some reinforcing bars exposed. The distribution is shown in Figure 8.6.

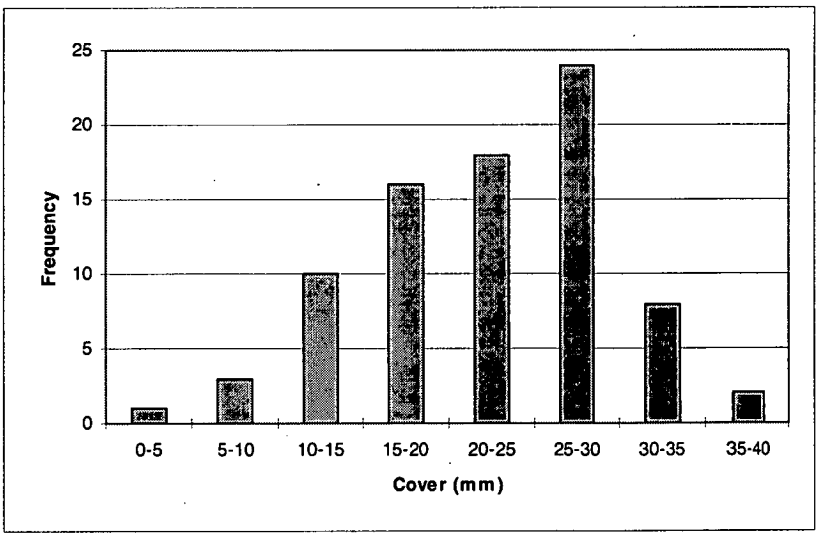

Figure 8.6 - Cover survey after Ohta

Kompen (1997) describes the background to the Norwegian Public Roads Administration specification for reinforcement cover. His paper includes data from cover surveys on:

- Gimsøystraumen bridge, a free cantilever bridge in a maritime climate in northern Norway built between 1978 and 1981

- a Japanese investigation of T-beams of a bridge built in 1957 (J)
- surveys of a hundred concrete structures in the United Arab Emirates (UAE)
- a British investigation from 1985 of cover in bridge piers (GB)
- a Norwegian condominium project built in the early 1980's (N).

Figures 8.7 and 8.8 show a high variability in reinforcement placement in all surveys, with mean cover substantially less than specified in all cases. Variability in the Gimsøystraumen bridge was however less than that in other cases.

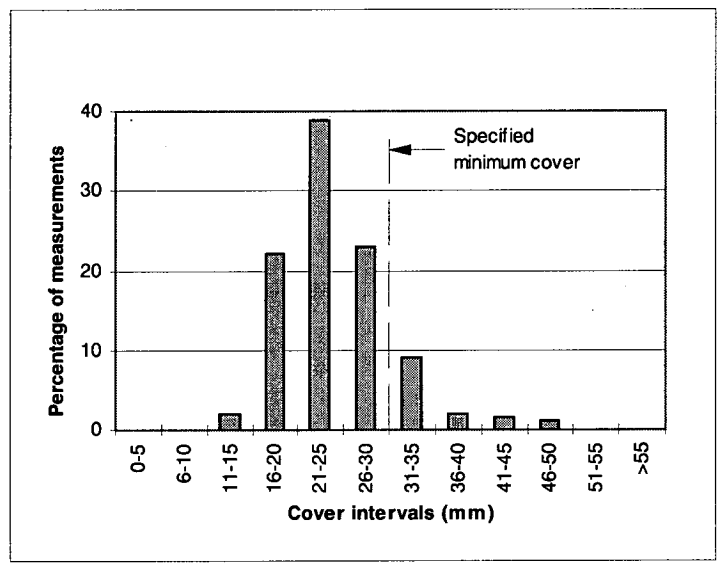

Figure 8.7 - Distribution of reinforcement cover, Gimsøystraumen bridge span 1

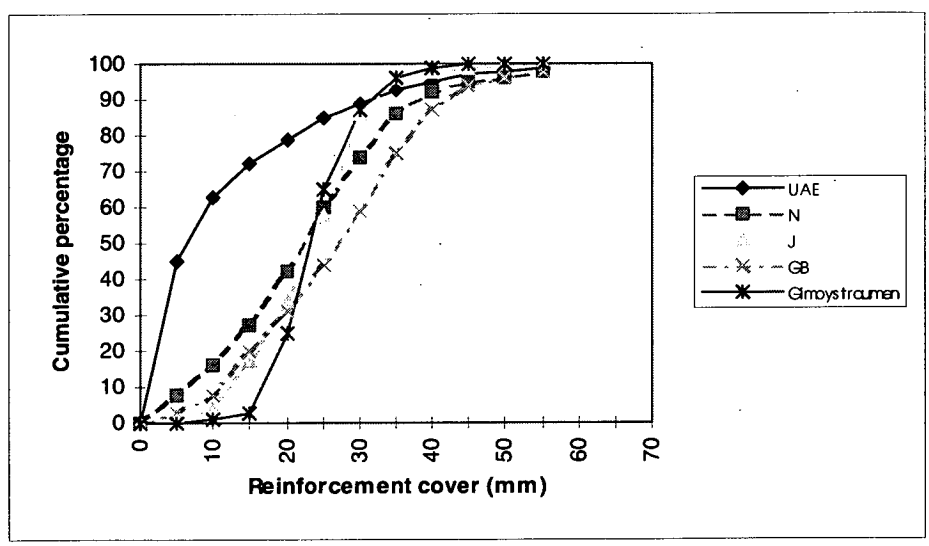

Figure 8.8 - Cumulative distributions of reinforcement cover

The review noted that specified cover had generally increased over the years, with the exception of the period between 1973 and 1989.

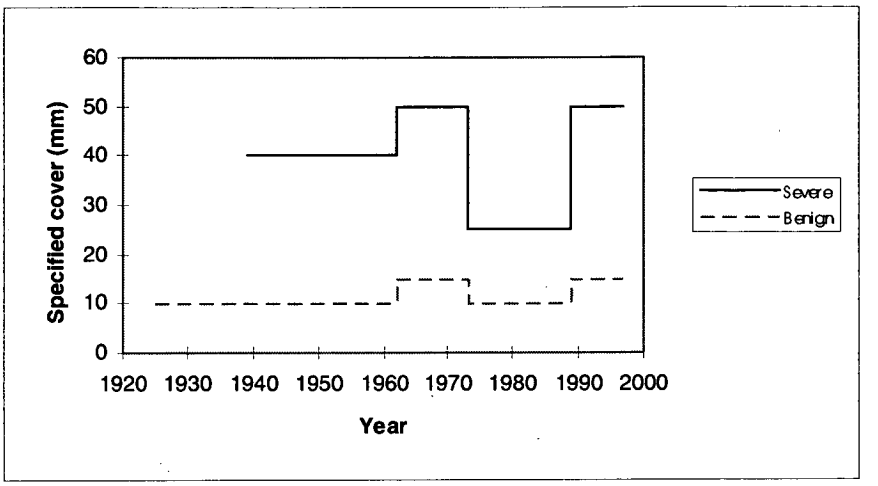

Figure 8.9 - Required cover to Norwegian Standards for different exposures

To reduce the number of variants in site construction, the specifications for cover shown in Table 8.2 have been adopted. 100mm cover is specified for underwater concreting and in the tidal zone, up to 6m height in mild coastal areas, and at least 12m in harsh marine climates. For surfaces frequently exposed to salt spray from traffic and for structural elements exposed to salt and moisture, but with limited accessibility for inspection and maintenance, 60mm or more is required. 40mm cover is the normal minimum elsewhere, except for dry and accessible structures where the cover may be reduced to 30mm.

Minimum cover C_o for design (mm)	40	60	100
Margin, ΔC (mm)	15	15	20
Design cover for structural reinforcement (mm)	55	75	120
Size of spacers (mm)	40	60	100

Table 8.2 - Specified covers, Norwegian standards

Sharp (1997) discusses the divergence of views between designers and builders and those who have subsequently measured covers in the field. He draws from a number of documents which show that the location of reinforcing bars after concreting follows a Gaussian distribution.

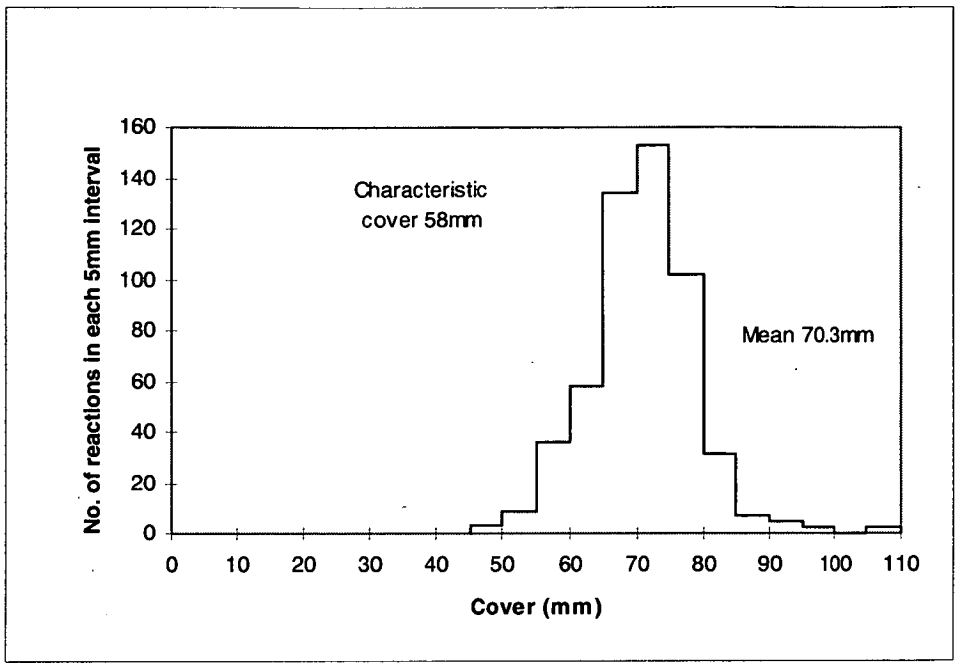

Figure 8.10 - Distribution of retaining wall cover measurements after Sharp

It was suggested that there needs to be a substantial margin (about 17mm) between nominal cover and the required minimum to ensure a 95% compliance or a 23mm margin for 99% compliance.

Weyers (1998) has used a standard deviation of 9.5mm in the modelling of service life for concrete bridge decks.

Izquierdo et al (2000) report on more than 80 cover measurements on the Maracaibo Bridge in Venezuela. The mean cover was 48mm, with a standard deviation of 24.3mm. A shifted log-normal distribution was considered to provide the best fit.

8.5 COVER SPECIFICATIONS

Prior to 1953, each of the Australian state road authorities developed and used its own design specifications for highway bridges. In 1953 a uniform highway bridge design specification was published by the Conference of State Road Authorities of Australia. The specification was based upon that of the American Association of State Highway Officials (AASHO). The specification stated that 'the minimum covering from the surface of the concrete to the face of any reinforcing steel shall be not less than 1 ¼ inches except in slabs, where the minimum cover shall be 1 inch. In work exposed to the action of sea water, the minimum covering shall be 3 inches except in precast

piles, where a minimum of 2 inches may be used. In no case shall the minimum covering measured from the surface of the concrete to the face of any reinforcing steel be less than one and one half (1½) times the diameter of the steel. Where slabs as in the case of box culvert floors are cast directly onto the ground the minimum cover shall be not less than 1 ½ inches. These minimum dimensions are only to be used where conditions are favourable and good workmanship is assured.'

The 1965 NAASRA Highway Bridge Design Specification required that 'the minimum cover from the surface of any concrete normally in contact only with air to the face of any reinforcing steel shall be not less than 1 ¼ inches except in slabs, where the minimum cover shall be one inch. In the footings of abutments and retaining walls and in piers and other concrete generally in contact with earth filling or fresh water, the minimum cover shall be 2 inches. In work exposed to the action of sea water, the minimum cover shall be 3 inches except in precast piles, where the minimum cover shall be 2 ½ inches. In no case shall the minimum cover, measured from the surface of the concrete to the face of any reinforcing steel, be less than 1 ½ times the diameter of the steel.' The requirements were restated in the 1970 edition of the Specification.

In the 1973 metric addendum, the values were substituted as follows:

25mm for 1 in.
50mm for 2 in
75mm for 3 in
65mm for 2 ½ in.

Reinforcement cover is selected with the objectives of ensuring that the concrete can be placed and is protected against corrosion of the reinforcing or prestressing steel.

The 1976 NAASRA Bridge Design Specification included the following cover requirements where conditions were favourable and good workmanship was assured:

(a) Normal exposure

i. 30mm except in slabs where it may be reduced to 25mm
ii. 1.5 times the normal diameter of the reinforcing bar
iii. 1.5 times the nominal maximum size of the aggregate
iv. the nominal size of aggregate for the top of slabs.

For concrete cast against the ground the cover shall be increased by 15mm minimum.

(b) Severe exposure. Cover shall be increased for more severe exposures as follows:

i. Formed or screeded surfaces in contact with fresh water or earth filling - 20mm

ii. Formed or screeded surfaces exposed to the action of sea water - 45mm

Where slabs, as in the case of box culvert floors, are cast directly on to the ground, the minimum cover shall be not less than 40mm.

While cover was specified for early bridges, tolerances on reinforcement placement were not usually explicitly specified. Prior to about 1989, the majority of the Tasmanian bridges were built by day labour without detailed specifications. Some larger bridges were however built by contract. Specifications for Tasman Bridge (1959) required the 'steel reinforcement to be bent accurately to the form and dimensions shown in the bending schedule and fixed exactly in the positions shown on the Drawings so that the specified cover is everywhere maintained' implying a zero negative tolerance. For Paterson Bridge (1971) in the north of the State, the specification stated that 'the concrete cover to steel reinforcement shown on the Drawings is clear cover to all the reinforcement and shall be adhered to during construction work within a tolerance of ¼ inch.'

The 1992 AUSTROADS Bridge Design Code specifies that the cover for concrete placement shall be not less than the greater of the following:

- 1.5 times the maximum nominal size of the aggregate
- the diameter of the reinforcing bar being protected
- twice the diameter of pretensioning tendons, except that this value does not have to be greater than 40mm
- 50mm from the surface of any post-tensioning duct in the soffit of members and 40mm elsewhere
- 50mm to post-tensioning anchorages.

For durability, the Code then specifies minimum cover in accordance with the exposure classification and concrete grade, with increases if the concrete is cast

against the ground. Relatively benign environments are exposure classification A. Classification B1 includes atmospheric exposures more than 1km from the coastline, while B2 includes above-ground exterior environments up to 1 km from the coast. Exposure classification C applies to tidal and splash zones. Values are shown in Tables 8.3 and 8.4.

Exposure Classification	Nominal cover (mm) for concrete of characteristic strength (f'_c) not less than:			
	25 MPa	32 MPa	40 MPa	50 MPa
A	35	30	25	25
B1	-	45	40	35
B2	-	-	55	45
C	-	-	-	70

Table 8.3 - Nominal cover where standard formwork and compaction are used

Exposure Classification	Nominal cover (mm) for concrete of characteristic strength (f'_c) not less than:			
	25 MPa	32 MPa	40 MPa	50 MPa
A	25	25	25	25
B1	-	35	30	25
B2	-	-	45	35
C	-	-	-	50

Table 8.4 - Nominal cover where rigid formwork and intense compaction are used

Permitted tolerances in the Code are as follows:

- for formed slabs, beams, walls and columns -5+10mm
- for slabs on ground -10+20mm
- for footings cast in ground and cast-in-place piles without permanent steel casing -20+40mm

Required covers in AS3600 are lower than those in the AUSTROADS Bridge Design Code, reflecting the shorter design lives of structures covered by that Code. Covers are shown in Tables 8.5 and 8.6, with those for 20 MPa concrete excluded.

Exposure Classification	AS3600 required cover (mm) for characteristic strength (f'_c)			
	25 MPa	32 MPa	40 MPa	50 MPa
A1	20	20	20	20
A2	30	25	30	20
B1	-	40	30	25
B2	-	-	45	35
C	-	-	-	50

Table 8.5 - Nominal cover where standard formwork and compaction are used

Exposure Classification	AS3600 required cover (mm) for characteristic strength (f'_c)			
	25 MPa	32 MPa	40 MPa	50 MPa
A1	15	15	15	15
A2	20	15	15	15
B1	-	30	25	20
B2	-	-	35	25
C	-	-	-	40

Table 8.6 - Nominal cover where rigid formwork and intense compaction are used

Specified covers for most elements from the codes used in bridge design in Tasmania are summarised in Table 8.7.

Year	Specified cover	
	Normal exposure	Severe exposure
1953	32mm (1.25")	76 mm (3")
1976	30mm	75mm
1992	45mm	70mm

Table 8.7 – Code specified cover

Mean specified covers from the cover surveys of Tasmanian bridges are tabulated in Table 8.8 and shown diagrammatically in Figure 8.11. The slight downward trend since the 1950's reflects the increasing use of precast components in bridge construction. The mean specified covers correspond more closely to those for normal exposure than for severe exposure notwithstanding the nature of the environment for most of the bridges involved in this study.

Decade	Mean specified cover (mm)				
	Insitu	Precast	Insitu+precast	Culverts	Overall
1930's	26.9	-	26.9	-	26.9
1940's	23.5	-	23.5	-	23.5
1950's	37.5	45.4	39.0	-	39.0
1960's	42.6	48.6	44.5	23.3	37.5
1970's	47.5	37.3	45.3	23.2	35.6
1980's	47.5	27.8	42.8	25.0	32.1
1990's	48.9	38.7	44.0	27.0	34.4

Table 8.8 – Mean specified cover from surveys

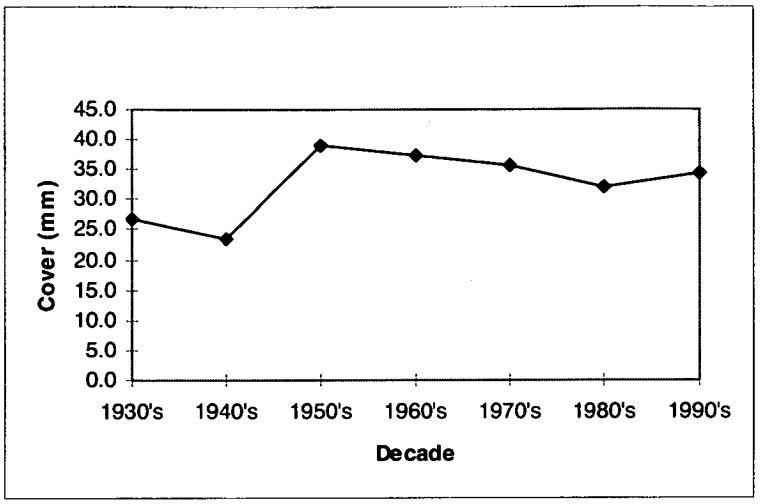

Figure 8.11 – Mean specified cover by decade

The first Departmental specification identified permitted a tolerance of ±5mm for the placing of reinforcement from the position shown on the drawings. In September 1994, permitted tolerances for insitu elements changed to -0+5mm measured at reinforcement supports and -5+10mm elsewhere. The –5+10mm remains in the current version of the specification.

8.6 COVER SURVEYS

Cover surveys were undertaken on Tasmanian bridges for the following reasons:

- as part of corrosion investigations for deteriorated structures
- during audits of completed structures as part of the process of issuing a Certificate of Practical Completion to the contractor
- as part of a program of investigation of the reasons for poor durability performance of precast box culverts
- as part of the broader program initiated with the Princess River Bridge to provide sufficient samples for a comprehensive analysis of cover, which included the ability to examine time based trends.

Measurements for corrosion investigations were generally taken by officers from the then Department of Transport's Materials and Research Branch, with a small number by consultants. Technical officer W Whenn took some of the measurements associated with audits of completed structures and the precast culvert investigation. The remainder of the measurements were taken by the author. Profometer 3 electromagnetic covermeters manufactured by the Proceq company of Switzerland were used for measurements by Departmental personnel and the author. The accuracy

of the covermeters is discussed in section 6.3 of the Appendix and shown to be marginal in the analysis of the data.

Cover data from the surveys do not differentiate between the tops, sides or soffits of elements, although this has occurred in some surveys.

A sufficiency of samples to allow for longitudinal analysis was considered to be a minimum of 1,000 insitu measurements on at least 10 structures for all decades in which a number of reinforced or prestressed concrete structures exist. Precast elements have been separately identified to facilitate comparisons between insitu and precast concrete. Precast culverts have also been separately identified because of particular durability issues with the type of structure and the specific processes used for their manufacture. Numbers of structures and measurements are detailed in Table 8.9.

Cover surveys undertaken as part of corrosion investigations generally comprised comprehensive measurements over a limited number of focussed areas. Surveys of other bridges generally encompassed randomly located measurements over broader areas.

Appendix 6 includes details of the surveyed structures. The details are summarised in Table 8.9 and Figure 8.12, which show that the structures are distributed throughout the State.

Description	Decade							Overall
	1930's	1940's	1950's	1960's	1970's	1980's	1990's	
Insitu concrete								
Structures	10	12	18	10	10	10	13	83
Measurements	2,084	2,729	3,084	1,574	1,244	1,119	1,063	12,897
Precast elements								
Structures	-	-	4	6	8	7	12	37
Measurements	-	-	741	736	355	488	1,165	3485
Precast + insitu								
Structures	10	12	18	11	10	10	16	87
Measurements	2,084	2,729	3,825	2,310	1,599	1,607	2,228	16,382
Precast culverts								
Structures	-	-	-	7	7	18	24	56
Measurements				1,126	1,250	2,355	2,942	7,673
Overall								
Structures	10	12	18	18	17	28	40	143
Measurements	2,084	2,729	3,825	3,436	2,849	3,962	5,170	24,055

Table 8.9 – Cover data
(Note: Structures for different categories not mutually exclusive)

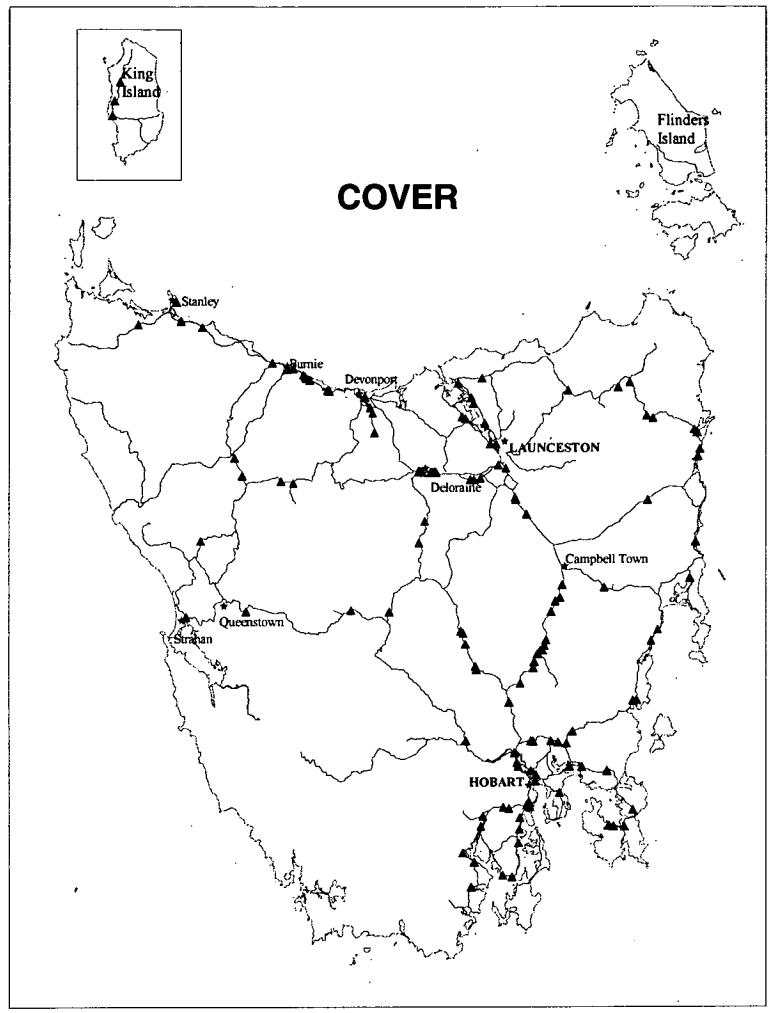

Figure 8.12 – Locations of surveyed structures

8.7 OVERVIEW OF DATA

The measurements encompass specified covers ranging from ½" (12.7mm) to 100mm. Specified covers vary between structures and between elements within individual structures. For preliminary comparisons and analysis, all measurements were normalised to proportions of specified cover and aggregated.

Figures 8.13 and 8.14 provide an initial overview of all cover measurements. Figure 8.13 compares the percentages of cover measurements exceeding 60%, 70%, 80%, 90% and 100% of specified cover with the results reported by Marrosszeky and Chew

(1989). Figure 8.14 shows the influence of construction period on the same data. It indicates a declining performance until a reversal in the 1960's. Any inferences however need to be considered in the context of the increasing mean specified cover shown in Figure 8.11 and the significant proportion of measurements of cover on precast bridge elements and box culvert crown units from the 1960's.

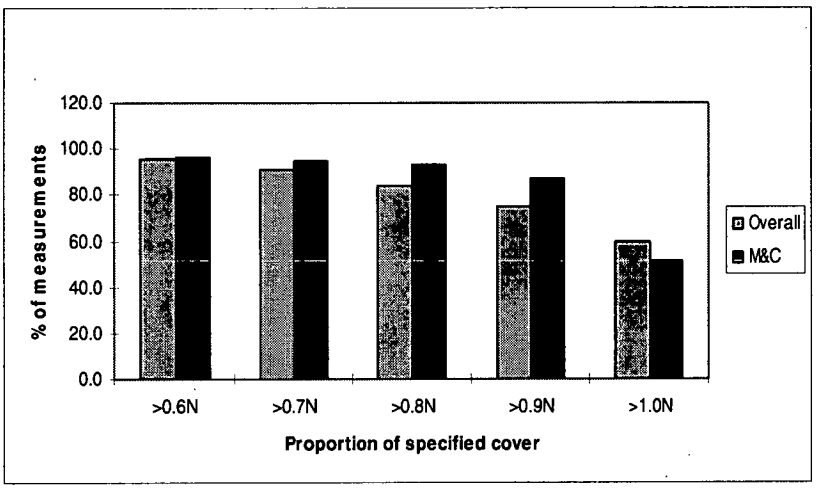

Figure 8.13 – Percentage of measurements exceeding proportions of specified cover

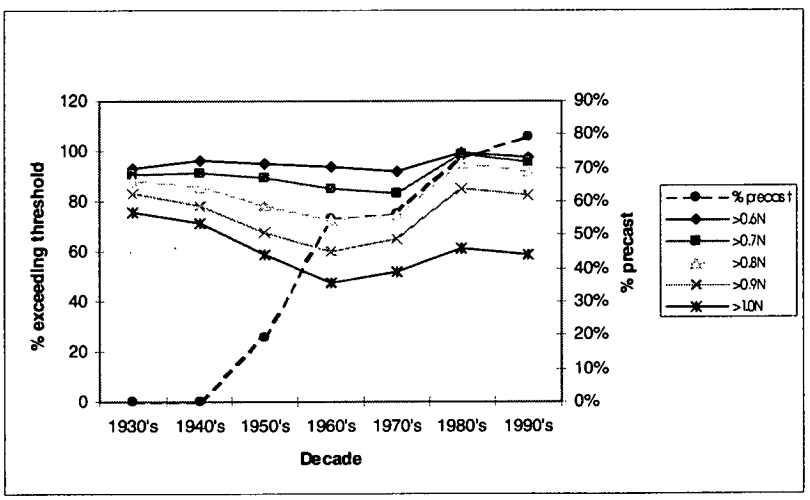

Figure 8.14 – Percentages exceeding proportions of specified cover by decade

Figures 8.15 to 8.17 present the data for insitu, precast and culvert elements separately. For insitu elements, a declining performance in achieving specified cover is indicated. For precast elements, the improvement in performance for the lower proportions is contrasted with the reduced compliance for the higher proportions of

specified cover. Compliance for the precast culvert units increases markedly for those built more recently.

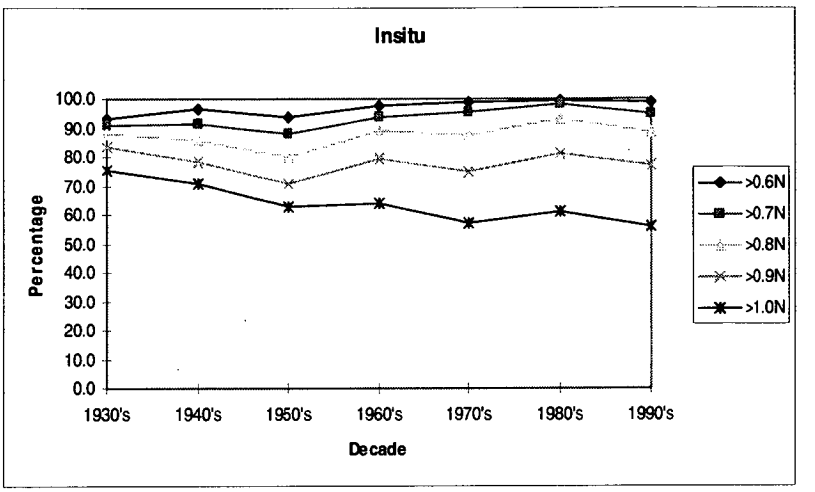

Figure 8.15 – Percentages exceeding proportions of specified cover by decade – insitu elements

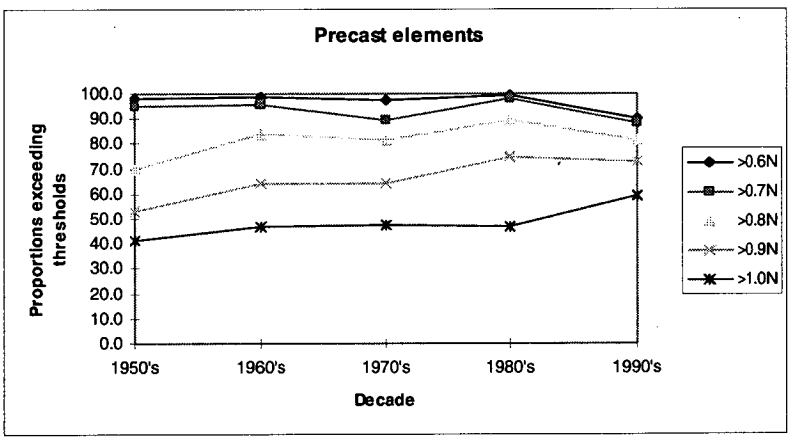

Figure 8.16 – Percentages exceeding proportions of specified cover by decade – precast elements

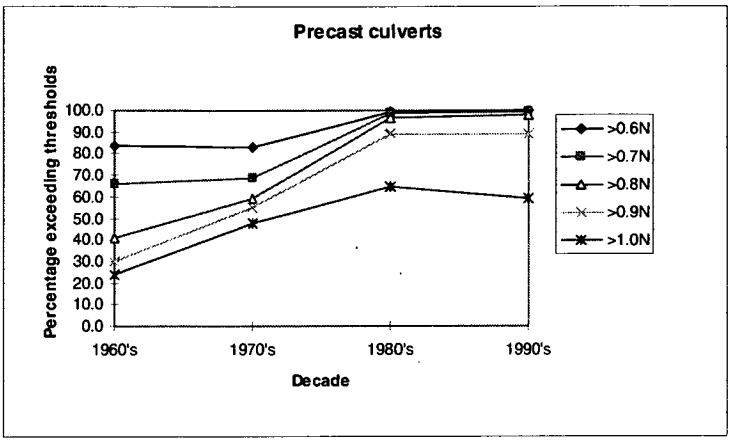

Figure 8.17 – Percentages exceeding proportions of specified cover by decade – precast culverts

Figure 8.18 provides some indication of the accuracy and variability of reinforcement placement by plotting means and standard deviations of normalised measurements in each decade. The results again need to be considered in the context of the lower mean specified cover for older bridges, the increasing proportion of measurements on precast elements in newer structures and the proportion of measurements in the sample on precast box culvert units.

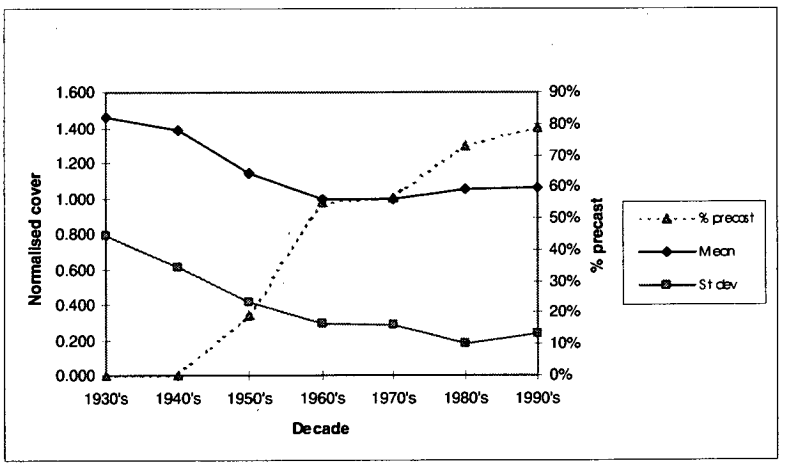

Figure 8.18 – Overall cover as a mean and standard deviation from specified cover

Accuracy of reinforcement placement is described in Figure 8.19 , which plots:

- the proportion of measurements with covers less less than the specified cover minus 5mm

- the proportion of measurements complying with the earlier tolerance of ± 5mm of specified cover
- the proportion of measurements complying with the contemporary tolerance of −5+10mm of specified cover
- the percentage of measurements on precast elements in the sample.

Results again need to be considered in the context of specified covers and the proportion of measurements from precast concrete elements.

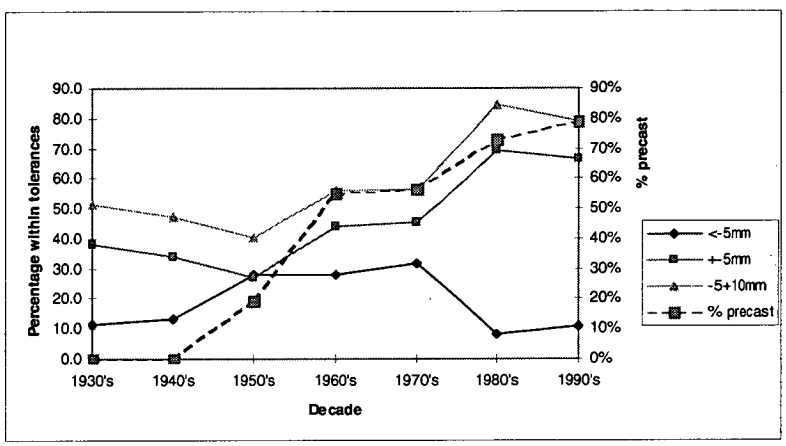

Figure 8.19 – Overall cover as percentages within tolerances

The data are also plotted separately for insitu, precast and culvert elements in Figures 8.20 to 8.22. For insitu elements, a trend of improving performance is indicated with a reversal in the 1990's. Data for precast elements also indicate improving performance, with a reversal of the trend in the 1990's. By contrast, performance for precast culvert units improves markedly in the 1980's and 1990's.

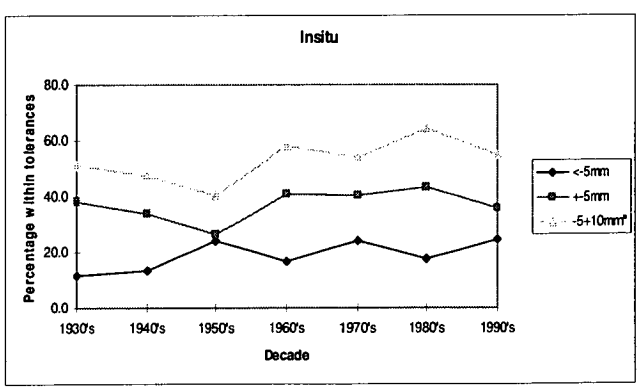

Figure 8.20 – Overall cover as percentages within tolerances, insitu elements

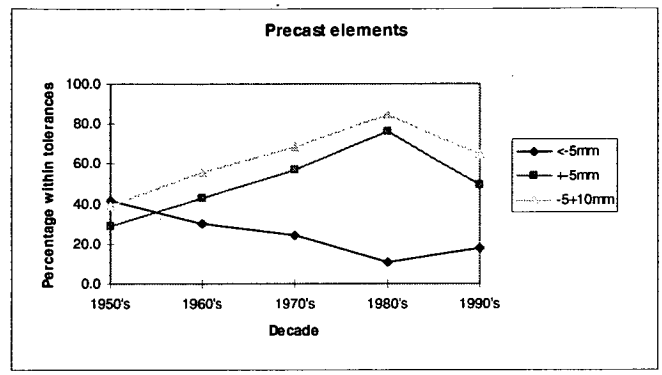

Figure 8.21 – Overall cover as percentages within tolerances, precast elements

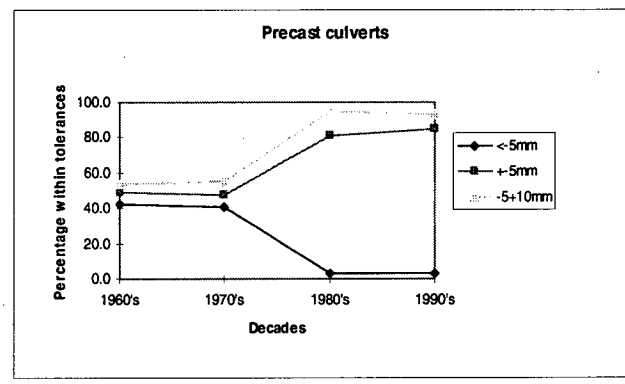

Figure 8.22 – Overall cover as percentages within tolerances, culvert elements

8.8 ANALYSIS

Analysis of the cover data to develop parameters for service life modelling and assess achievable construction tolerances again used a graphical approach with normal probability and quantile plots.

The data were examined

- as aggregate data
- subdivided into insitu and precast concrete elements and precast culvert units
- grouped into subsets of nominal specified cover of 19mm, 25mm, 38mm and 50 mm
- grouped by age
- normalised as proportions of specified cover.

Details of the analysis are included in Chapter 6 of the Appendix.

8.9 MODELS

The analysis showed absolute values of tolerance for cover to reinforcement to be reasonably constant for a range of specified covers.

Achievable tolerances for 90% compliance, using normal distributions, can thus be described in terms of the mean cover $\pm$ 1.65 standard deviations.

For the subsequent service life modelling, cover is specified in terms of its mean value and standard deviation.

Results of the analysis are summarised in Table 8.10.

Element type	Mean cover	σ	1.65 σ
Insitu	Specified + 6mm	11.5 mm	19 mm
Precast	Specified + 3mm	9.7 mm	16 mm
Culvert	Specified	3.6 mm	6 mm

Table 8.10 – Cover models for analysis

8.10 DISCUSSION

Histograms and normal quantile plots for the individual cases of nominal cover generally indicate that the measurements of cover follow a normal distribution. In a small number of cases, there is an improvement in fit when a log transformation is used. The evidence is not however sufficient reject an hypothesis that a normal distribution can be used to describe the variability in cover to reinforcement. It does however demonstrate that the mean will differ slightly from the specified cover. The assumption of a normal distribution is consistent with the findings of Morgan et al (1982) and Sharp (1997). Normal distributions have consequently been adopted for subsequent analysis.

The plots of cover compliance for the different nominal covers indicate that the variability in cover is independent of the nominal cover, and that there is only a small difference between insitu and precast elements. Compliance for precast culvert units is however substantially better. Proposed tolerances to achieve 90% compliance are – 15+25mm for insitu elements, -15+20mm for precast elements and $\pm$6mm for precast culverts. The distributions presented in Table 8.10 will be used for analysis.

Time based performance was assessed using plots of the proportions of measurements exceeding various proportions of specified cover, the proportions of measurements complying with various tolerances and the cover range for a 90% compliance of measurements. While it might be expected that performance would improve due to factors such as specialisation of steel fixing and the introduction of quality assurance from the late 1980's and early 1990's, the assessment indicates that this is not in fact the case with a declining performance for both insitu and precast elements in the 1990's. Quality assurance systems were introduced as a requirement for contractors undertaking road and bridge works for DIER in the late 1980's. The exception is the improved cover compliance for more recent precast culvert units.

8.11 SUMMARY

Cover to reinforcement is a fundamental factor in determining the durability of concrete. A balance is required between minimising cover for structural efficiency and crack control and providing an appropriate amount for durability and service life reasons. Cover provides the resistance component of a load and resistance factor design approach to the durability of concrete structures.

Tolerances on cover to reinforcement in hardened concrete in codes and specifications appear to have been based on intuition rather than a sound analytical approach. Values ranging from –0+5mm to –5+10mm have been typical for 30 years or more.

The literature from 1982 however consistently shows that specified tolerances on cover have not been achieved. The degree of variability is consistent with that measured in Tasmanian bridges, although mean covers are more commonly lower than specified compared with the higher mean found in this analysis.

The variability of cover is consistent since 1931 when the first surveyed structure was built indicating that there is a realistically achievable tolerance on cover which is independent of technology and systems such as quality assurance.

Models have been developed for use in service life modelling and as a basis for changing tolerances in codes and specifications.

9 SERVICE LIFE MODELLING

9.1 GENERAL

This chapter provides the synthesis of the parameters for chloride ingress, carbonation and cover to reinforcement developed in the earlier part of this study to develop deterministic and probabilistic service life models for Tasmanian bridges.

A number of definitions for service life are considered, and a definition adopted for the purposes of this study. Reliability concepts and the literature on service life modelling are discussed.

Results of the service life modelling are compared with the observed performance of Tasmanian bridges and implications for the asset, specifications and codes are discussed.

9.2 DEFINITIONS

The service life of a concrete structure can be defined by a number of technical criteria including:

- initiation of corrosion
- corrosion products becoming visible on the surface of the concrete
- cracking and/or spalling due to concrete corrosion
- loss of capacity of structure from corrosion compromising safety.

Further to the technical criteria, a number of subjective criteria may be used for service life:

- adverse aesthetic impacts of rust staining
- public perceptions of reduced safety arising from staining, cracking and spalling
- compromising of public safety because of spalled concrete falling from the structure.

Two official definitions have been identified:

- *Eurocare:* "The service life is the period of time after installation during which all essential properties meet or exceed minimum acceptable values, when routinely maintained."
- *ISO TC59/SC3:* "The design life is the designer's intended durability for the building and its parts as specified by the client."

Somerville (1986) proposes a definition of service life as "the minimum period for which the structure can be expected to perform its intended function, without significant loss of utility, and not requiring too much maintenance."

Service life in the context of chloride or carbonation induced corrosion is commonly described by the Tuutti (1982) corrosion model, shown schematically in Figure 9.1. During the initiation period, the principal processes are the ingress of chloride ions through the cover concrete and/or the progress of the carbonation front. In this phase, the corrosion rate of the reinforcement is very low as the chloride concentration is below the threshold value and the pH value of the pore solution is high enough to maintain passivity of the reinforcement.

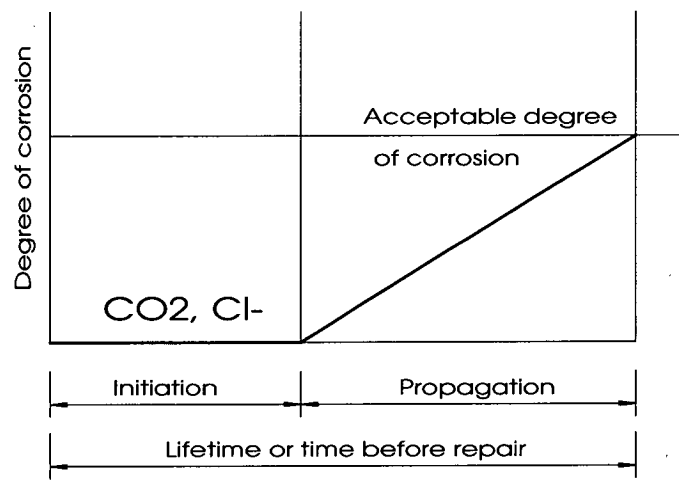

Figure 9.1 – Tuutti corrosion model

Once initiated, the corrosion rate during the propagation period is controlled by the rate of oxygen diffusion to the cathode, resistivity of the pore solution and temperature. The corrosion rate may vary with time as the cover concrete cracks or spalls, as corrosion product accumulates or is removed from the surface of the steel, or

as the availability of oxygen and water changes. Corrosion rates in chloride exposures may be high, resulting in a relatively short time between corrosion initiation and the appearance of visible damage.

Amongst a substantial bridge stock, there will be many structures that are readily accessible to members of the public and have pedestrians, vehicles or vessels passing beneath them. The subjective criteria of adverse effects of rust staining, public perceptions of reduced safety and compromised safety associated with spalling thus become a significant consideration.

De Sitter's Law of Fives (AUSTROADS,1997) states that:

> "$1 spent in getting the structure designed and built correctly is as effective as $5 spent in subsequent preventative maintenance in the pre-corrosion phase while carbonation and chlorides are penetrating towards the steel reinforcement. In addition, this $1 is as effective as $25 spent in repair and maintenance when local active corrosion is taking place, and as effective as $125 spent where generalised corrosion is taking place, and where major repairs are necessary and possibly including replacement of complete members".

The transition from the initiation phase to the propagation phase is consistent with a substantial increase in costs in accordance with de Sitter's Law and marks a point at which lower cost preventative measures, such as coatings and penetrating sealers, are likely to become unviable and patch repair, electrochemical techniques or replacement are required, especially with chloride induced corrosion.

The data available for this research are limited to estimation of times to initiation. Analysis and prediction of the propagation phase would require:

- models of deterioration processes, including corrosion of steel and cracking and spalling of concrete accounting for micro and macro climatic influences
- estimation or determination of corrosion rates
- effects of deterioration on structural properties including flexure, shear, bond and anchorage.

With the range of economic, technical and subjective factors to be considered, a conservative approach is indicated and, for the purpose of this thesis, service life is defined as the time to initiation of corrosion.

9.3 LITERATURE REVIEW

Methods that have been used for predicting the service lives of construction materials include:

- estimates based on experience
- deductions from performance of similar materials
- accelerated testing
- mathematical modelling based on the chemistry and physics of degradation processes
- applications of reliability and stochastic concepts (Clifton,1993).

The various approaches are often used in combination.

Estimates based on experience do not form a reliable basis for service life prediction because of the long lives of concrete structures and changes in environments and materials. Comparisons between old and new concretes are similarly complicated by variations in cement and concrete properties, the use of admixtures and the effects of microclimates. Accelerated test methods require the development of a correlation between the rates of degradation in the accelerated ageing tests and long term in-service performance. Mathematical models are generally based on Tuutti's model and Fick's 2nd law of diffusion for chloride ingress. Service life models using stochastic methods are based on the premise that service lives cannot be accurately predicted because of a variety of factors including adherence to design specifications, variability in the properties of hardened concrete, randomness of the in-service environment, and material response to microclimates.

The corrosion of steel in concrete involves many factors, including uncertainties relating to the material itself and to the environment. There is a lack of theoretical models able to adequately reproduce the chemical changes in concrete with time, depth and variations in exposure. Prezzi et al (1996) proposed that the diffusion coefficient of a concrete specimen could be estimated through model inversion of a particular solution of Fick's second law at each point for which there is a measurement of chloride content. The realisations of the diffusion coefficients so obtained are used to determine its probability density function (PDF), which is then used to perform a reliability analysis to assess the probability of corrosion under a given set of conditions. The reinforced concrete was considered to have reached its limit state when corrosion initiated at a certain depth through the chloride concentration at that

depth exceeding the threshold level. They noted that Fick's law still provided the only way to model chloride diffusion into concrete although many of the assumptions in its derivation are not valid. These assumptions include the facts that the concrete is generally only partially saturated, that it is not homogeneous, that the medium is reactive and adsorptive, and that the diffusion coefficient varies with time, solution type and concentration. They use a threshold chloride concentration of 0.4% acid soluble chloride by mass of cement based on the Norwegian code NS3420. For their research, where only the diffusion coefficient D was considered to be random, the limit state function $g(D)$ was written as:

$$g(D) = C_T - C(D)$$

where C_T is the threshold chloride concentration and $C(D)$ is the chloride concentration at a distance x from the exposed concrete surface at time t. The function $g(D)$ is positive only if the concrete element is in a "safe" state, ie the chloride concentration at the reinforcement at a distance x from the concrete surface is less than the threshold concentration. The limit state function $g(D)$ can also be seen as a safety margin against the exceedance of C_T. The probability that the threshold concentration is exceeded at a given time t and location x can be expressed as

$$P_f = P(C>C_T) = 1 - F_C(C_T)$$

where $F_C(.)$ is the cumulative distribution function of C

For a one-to-one relationship between C and D, the exceedance failure probability can be rewritten as

$$P_f = P(C>C_T) = P(D>D_T) = 1 - F_D(D_T)$$

where $F_D(.)$ is the cumulative distribution function of D, and D_T is the threshold diffusion coefficient obtained by the inversion of Fick's second law ($D_T = f^{-1}[C_T]$). Assuming a lognormal distribution for the diffusion coefficient, the exceedance probability is obtained as follows

$$P_f = P(C>C_T)$$

$$= 1 - \Phi\left[\frac{\ln(D_T) - \lambda_D}{\xi_D}\right]$$

$$= \Phi\left[-\frac{\ln(D_T) - \lambda_D}{\xi_D}\right]$$

where λ_D and ξ_D are the parameters of the lognormal distribution and $\Phi(.)$ is the standard normal CDF. The parameters λ_D and ξ_D are estimated from the diffusion values obtained through model inversion of the solution of Fick's second law for each given chloride concentration profile and the value of D_T is found by Newton-Raphson iteration. The failure probability P_f is computed using the above equation or reliability software. Testing was undertaken on ten high strength lightweight concrete mixes, and results are not necessarily transferrable to the normal weight concrete which is the subject of this study. Reported mean diffusion coefficients nevertheless ranged from 1.49 x 10^{-11} to 5.6 x 10^{-11} m^2/s and standard deviations from 0.38_{10}^{-13} to 1.72 x 10^{-13} m^2/s.

Maage et al (1996) present a model for service life prediction of existing structures based on Fick's second law of diffusion combined with empirical data from existing structures and laboratory tests. Figure 9.2 shows the relationship between chloride diffusion coefficient and concrete maturity derived from laboratory tests. Work by three of the authors and from Japan and the United Kingdom had fitted a similar relationship for results from existing structures, although only a few test results had been identified from the literature.

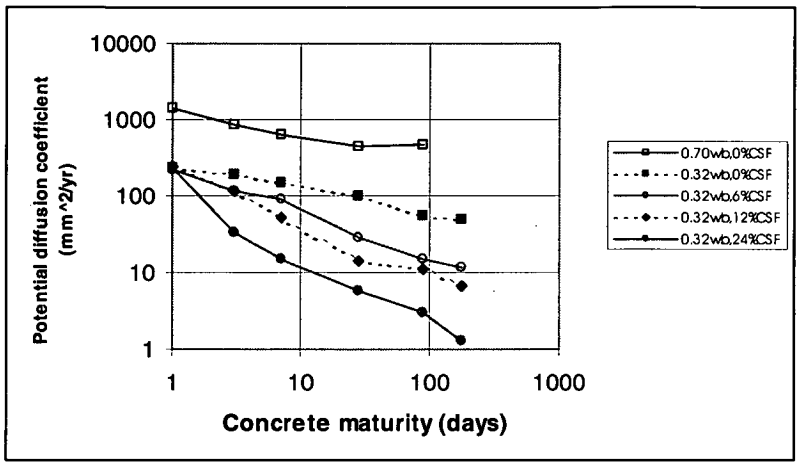

Figure 9.2 – Chloride diffusion coefficient ~ concrete maturity

For structures with plain cement mixes, diffusion coefficients did not vary substantially and the rate of change decreased. Additionally, the data were for periods up to six months compared to the substantially greater ages for concretes involved in this study.

Relationships were also derived between the potential and achieved chloride diffusion coefficients. The service life was again defined as the age of the concrete when the chloride concentration at the reinforcing bars reached the 'critical (threshold) concentration level. Service life estimation used an algorithm which was based on measurements of chloride concentration from drilling of a structure and measurement of cover using a parameter α which is calculated as:

$$\alpha = \frac{\ln(D_{ac} / D_{p0})}{\ln(t_0 / t_c)}$$

where D_{ac} = achieved chloride diffusion coefficient at time t_c

D_{p0} = potential diffusion coefficient

t_0 = time of initial exposure to chlorides.

Weyers (1998) presents a model which is based on measurements of cover and chloride penetration in concrete bridge decks exposed to deicing salts, with some corrosion rate measurements. He proposes that the time to first maintenance can be estimated by using the 2.5 percentile lowest cover to reinforcement and a time to

cracking of 5 years from initiation, although time to cracking may be less for covers less than 76mm and high corrosion rates. Estimated time from cracking initiation to first cracking of concrete cover may be 2 to 5 years for north American bridge decks (Liu and Weyers, 1998)

Amey et al (1998) present a methodology for service life calculation that incorporates surface environment, chloride transport, temperature of the surrounding medium, seasonal effects and construction variability. They draw on work by other researchers including Berke, Cady and Weyers. A suggested failure criterion is when 30 percent of reinforcement is corroding.

To date, there has been extensive research effort directed at the computation of probabilities of structural collapse. Little research has however been directed at the computation of probabilities of serviceability failure, although it is likely that these failures constitute the greatest source of economic loss (Stewart, 1997). Monte Carlo analysis was used to assess the effects of poor, fair and good levels of compaction and curing performance of serviceability reliabilities, namely deflection criteria. It was found that poor concreting workmanship increased the probability of serviceability failure by more than an order of magnitude and had a greater influence than variations in element dimensions and cover to reinforcement.

Frangopol et al (1997) use a reliability approach to examine the influence of a range of dimensional, structural and corrosion variables on the reliability of concrete structures over their lifetime with the objective of minimising lifetime costs. They report that, according to West and Hime in 1985, corrosion initiation occurs at a chloride concentration at the reinforcing bar of about 0.83 kg/m^3. For typical Tasmanian concretes with a density of the order of 2450 kg/m^3, this equates to a proportion of 0.034% by mass of concrete.

Stewart and Rosowsky (1997) developed a structural deterioration reliability model to calculate probabilities of flexural structural failure in a typical continuous reinforced concrete slab bridge. The analysis includes the random variability of chloride and carbon dioxide diffusion, critical threshold chloride concentration, crack width, corrosion rates, concrete material properties, element dimensions, reinforcement placement, environmental conditions and loads. A sensitivity analysis was undertaken to investigate the influence of parameter uncertainties on the final results. The analysis showed that failure probabilities were significantly increased and structural

safety reduced by exposure to chlorides from deicing salts or marine exposure and reductions in cover from that specified. Exposure to atmospheric carbon dioxide resulted in a negligible decrease in structural reliability.

9.4 MODELS FOR ANALYSIS

The models used for service life modelling have been derived previously and are described below.

9.4.1 Chloride models

It was determined that a lognormal distribution would be used for the diffusion coefficient, with a mean of −12.0 and a standard deviation of 0.48 for the transformed values ($\log_{10}$). The mean value equates to a diffusion coefficient of 1.00×10^{-12} m^2/s.

Parameters adopted for the modelling of apparent surface chloride concentration are given in Table 9.1, with the concentration normally distributed.

Distance from coast,d (km)	Height (m)	Apparent surface chloride concentration (%m/m)	COV (%)
0	≤2	0.380	65.3
0	>2, ≤4	0.148	71.5
0	>4	0.116	79.0
0.1 to 2.84	All	-0.0729ln(d)+0.1161	48.7
>2.84	All	0.04	48.7

Table 9.1 – Parameters for chloride modelling

9.4.2 Chloride threshold concentrations

As discussed, the literature on chloride threshold concentrations for the initiation of corrosion in concrete is conflicting, with levels from 0.06% to 2.5% by mass of binder having been reported. Threshold concentrations of 0.03% to 0.05% by mass of concrete are typically used.

Chloride concentrations in this study have been reported as a proportion of the mass of concrete, with measured cement contents ranging from 190 kg/m^3 to 615 kg/m^3, with a mean of 355 kg/m^3. The range of possible chloride concentration concentrations by mass of concrete is described in Table 9.2, with the assumed concrete density being 2500 kg/m^3.

Chloride concentration by mass of cement (%)	Chloride concentration (%) by mass of concrete for cement content (kg/m³)		
	190	355	615
0.06	0.005	0.009	0.015
0.2	0.015	0.028	0.049
0.4	0.030	0.057	0.098
0.6	0.046	0.085	0.145
0.8	0.061	0.114	0.197
1.0	0.076	0.142	0.246
1.2	0.091	0.170	0.295
1.4	0.106	0.199	0.344
1.6	0.122	0.227	0.394
1.8	0.137	0.256	0.443
2.0	0.152	0.284	0.492

Table 9.2 – Range of possible chloride threshold concentrations

The analysis assesses the sensitivity of the corrosion initiation to threshold levels ranging from 0.05% to 0.3%. Chloride corrosion threshold concentration has not been considered as a random variable because of the range of reported levels and the lack of definitive data.

9.4.3 Carbonation models

The depth of carbonation x at time t is described by the equation:

$$x = k\sqrt{t}$$

where the coefficient k is distributed either normally with a mean 2.01 and standard deviation 1.24 or lognormally with the mean and standard deviation of the transformed (ln) values being –1.353 and 0.7723 respectively. Units for k are mm/yr$^{1/2}$.

9.4.4 Cover models

Cover to reinforcement is described by a normal distribution in accordance with Table 9.3.

Element Type	Mean cover	Standard deviation
Insitu	Specified + 6mm	11.5mm
Precast	Specified + 3mm	9.7mm
Precast culvert	Specified	3.6mm

Table 9.3 – Cover models

Cover to reinforcement is truncated at a zero value equating to the point at which the reinforcement begins to protrude from the concrete surface.

9.5 MODELLING

9.5.1 Deterministic modelling

9.5.1.1 Chloride ingress

Deterministic modelling uses the mean values of the various parameters to determine the expected time to initiation of corrosion for structures at differing heights, various distances from the sea and with differing specified covers.

The chloride concentration at depth x and time t is calculated using the error function solution to Fick's 2nd law of diffusion, with the appropriate distribution functions used for the surface chloride concentration c_s, the diffusion coefficient D and the nominal cover x.

$$c(x, t) = c_s [1 - \text{erf}(\frac{x}{2\sqrt{D.t}})]$$

The time to initiation is the time at which the expected value of the chloride concentration reaches the threshold concentration.

A trial and error process using an Excel model was used to determine the time to initiation for the range of locations (using the relevant values of apparent surface concentrations and effective diffusion coefficients) and specified covers.

Figure 9.3 shows the effect of differing chloride threshold concentrations on the time to initiation for nominal covers from 10mm to 75mm for insitu elements of structures directly in contact with salt water (distance from coast 0, height $\leq$ 2m).

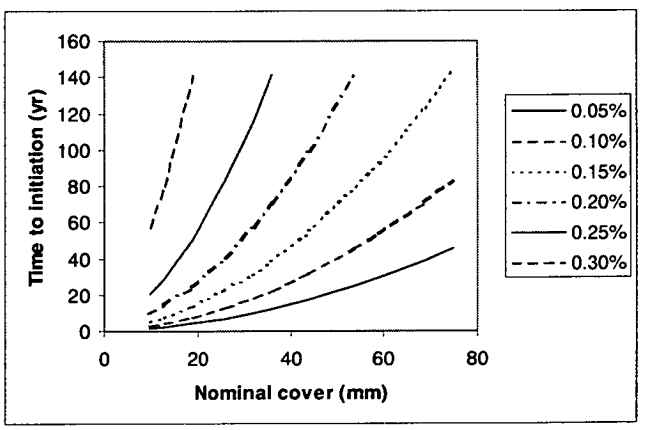

Figure 9.3– Effect of threshold concentration on time to initiation Insitu elements, distance from salt water 0km, height $\leq$ 2m

Nominal covers for a time to initiation of 100 years for the various corrosion thresholds are summarised in Table 9.4. It shows that a 100 year service life will not be achieved with the lower values of corrosion threshold.

Corrosion Threshold	Nominal cover
0.05%	-
0.10%	-
0.15%	62mm
0.20%	44mm
0.25%	29mm
0.30%	15mm

Table 9.4 – Nominal covers for varying corrosion thresholds Insitu elements, distance from salt water 0km, height ≤ 2m

Figures 9.4 to 9.6 show the effect of the distance of the structure from the coast on the time to initiation for threshold chloride concentrations of 0.05%, 0.10% and 0.15%, using apparent surface chloride concentrations from Table 9.1. For structures more than 2m above water level or more than 0.63km from salt water, the surface chloride concentration is less than 0.15% m/m concrete and corrosion does not initiate for higher threshold concentrations using the deterministic model. For structures in the figures in contact with salt water, the height above mean water level is less than or equal to 2m.

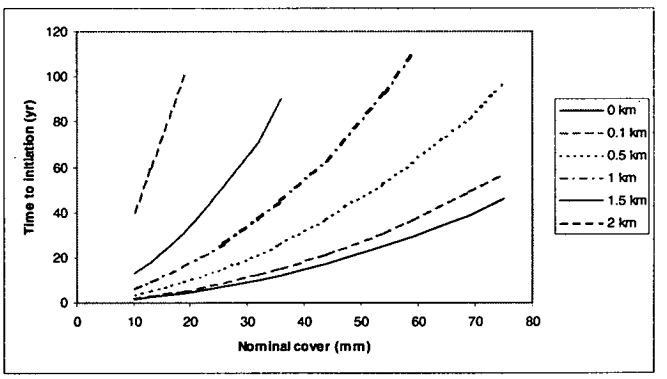

Figure 9.4 - Effect of distance from coast on time to initiation, threshold chloride concentration 0.05%

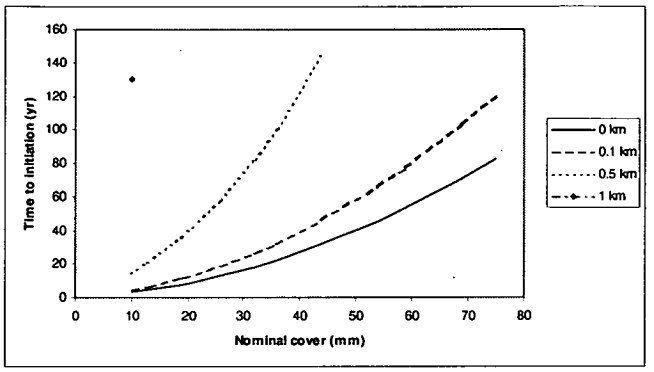

Figure 9.5 - Effect of distance from coast on time to initiation, threshold chloride concentration 0.10%

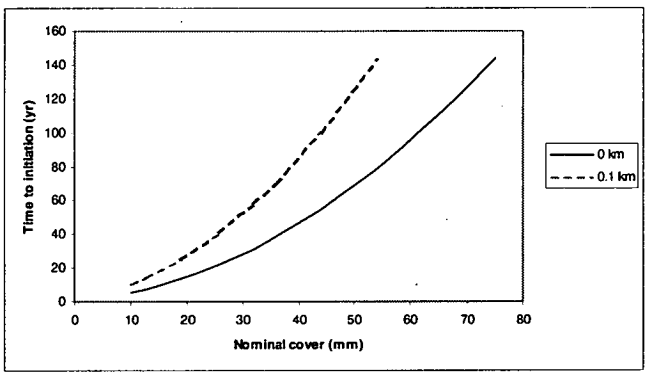

Figure 9.6 - Effect of distance from coast on time to initiation, threshold chloride concentration 0.15%

Deterministic models give shorter times to initiation for precast and culvert elements, equating to specified covers 3mm and 6mm less than for insitu elements, because the mean values of cover are closer to the specified values. Deterministic modelling with mean values does not consider the reduced variability in reinforcement location.

The expected value of the time to initiation can either be interpreted as the time when 50% of structures are affected or when 50% of reinforcement with the nominal cover in the exposure condition has started to corrode. Both interpretations are non-conservative from a bridge management perspective.

As an alternative to calculating the expected time of corrosion initiation, characteristic values of the various parameters can be used to better indicate the age of a structure when lower cost options, such as penetrating sealers, may become not viable and active and/or more expensive options, such as cathodic protection and replacement, need to be considered. Characteristic values have been taken to be at the 95% level, 1.65 standard deviations from the mean with a normal distribution. The values

adopted for chloride ingress and cover are detailed in Tables 9.5 and 9.6. Lower characteristic values are used for cover, while upper characteristic values are used for chloride ingress and carbonation parameters. A logarithmic curve is fitted to characteristic values for distances from the coast between 0.1 km and 3 km. Expected times to initiation would be at a percentile less than 5, and are thus conservative.

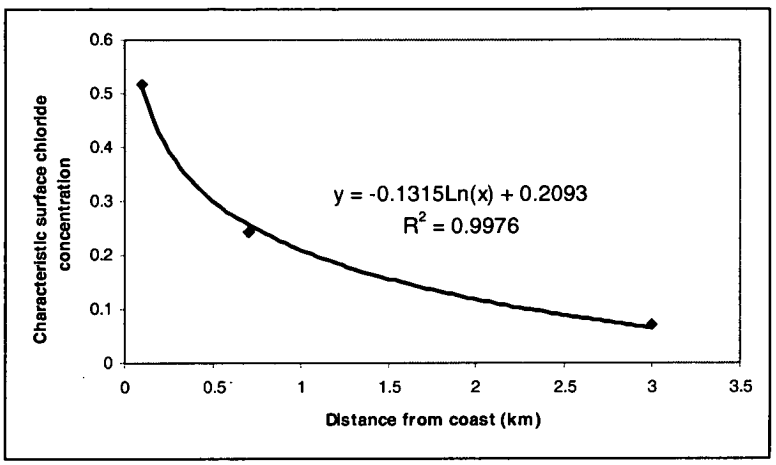

Figure 9.7 – Characteristic surface chloride concentration ~ distance from coast

Distance from coast,d (km)	Height (m)	Apparent surface chloride concentration (%m/m)
0	≤2	0.789
0	>2, ≤4	0.254
0	>4	0.267
0.1 to 2.84	All	-0.1315ln(d) + 0.2093
>2.84	All	0.072

Table 9.5 – Characteristic values of surface chloride concentration

Element Type	Characteristic cover
Insitu	Specified – 13.0mm
Precast	Specified – 13.0mm
Precast culvert	Specified – 5.9mm

Table 9.6 – Characteristic cover parameters

The mean value and standard deviation of the transformed ($\log_{10}$) of the diffusion coefficient for modelling are –12.0 and 0.48, giving a characteristic transformed value of –11.2 and a characteristic value of 6.19×10^{-12}.

Figure 9.8 shows the effect of threshold chloride concentrations on the time to initiation for structures in contact with salt water. Figures 9.9 and 9.10 show the effect of distance from the coast on time to initiation for chloride threshold concentrations of

0.05% and 0.10% by mass of concrete. Times are significantly reduced from those calculated using mean values in all cases due to the variability in the parameters.

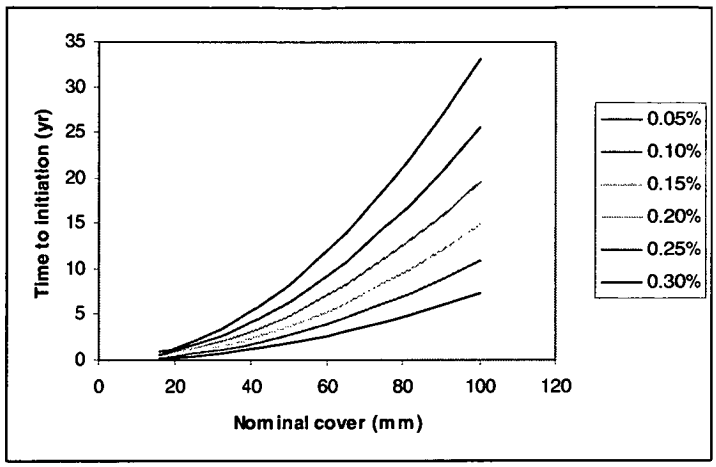

Figure 9.8 – Effect of corrosion threshold on time to initiation, characteristic values

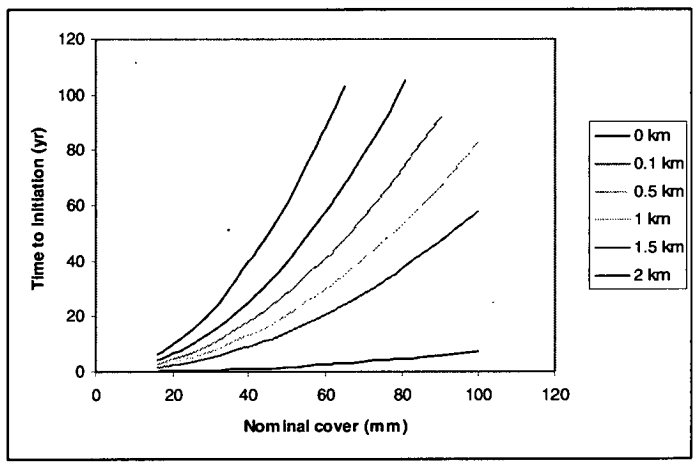

Figure 9.9 - Effect of distance from coast on time to initiation, corrosion threshold 0.05%, characteristic values

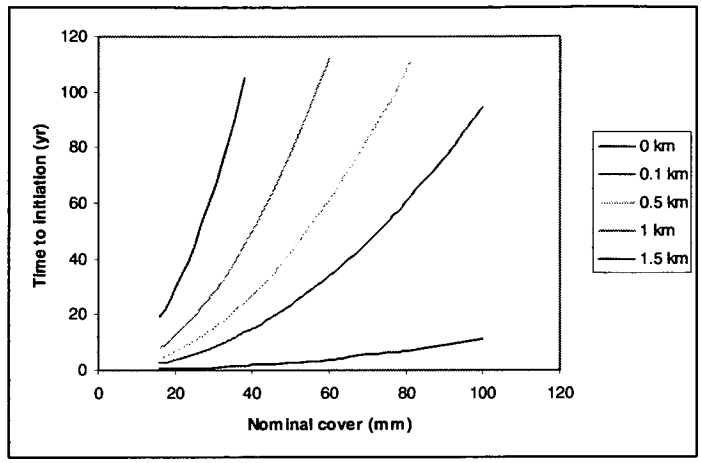

Figure 9.10 - Effect of distance from coast on time to initiation, corrosion threshold 0.10%, characteristic values

9.5.1.2 Carbonation

For carbonation damage, the only variables to be considered are the cover to reinforcement and the age of the concrete. Transforming the previously defined relationship gives

$$t = \left(\frac{Cover}{k} \right)^2$$

where t = time to initiation (years)

$Cover$ = expected value of cover

k = carbonation parameter

= 2.01, normal distribution

= -1.353, lognormal distribution, ln transformation

Figures 9.11 and 9.12 show the expected time to initiation of corrosion due to carbonation for specified covers up to 75mm and 20mm respectively, based on the mean values of parameters for the normal distribution. The second figure is a subset of the first. Times to initiation are higher for insitu concrete because the mean is 6mm higher than specified, compared to 3mm higher for precast concrete and equal to the specified value for precast culverts.

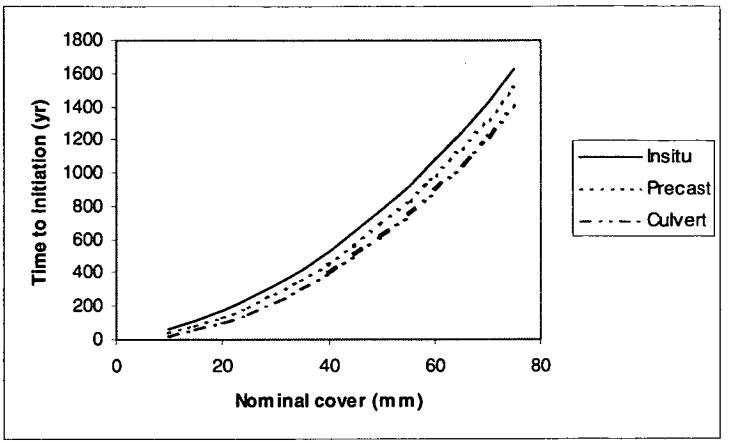

Figure 9.11 – Time to initiation due to carbonation

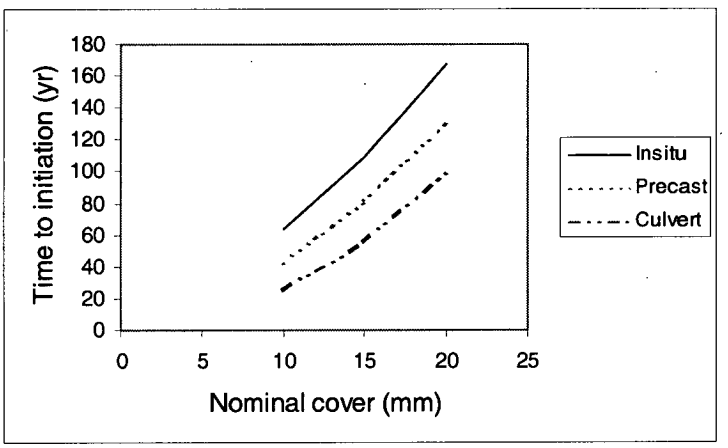

Figure 9.12 – Time to initiation due to carbonation

Specified covers for a 100 year time to initiation are listed in Table 9.7.

Specified cover (mm)		
Insitu	Precast	Culvert
14.1	17.1	20.1

Table 9.7 –Specified covers for 100 year time to initiation due to carbonation

As with chloride ingress, characteristic values are used to better assess the time at which there is a transition between lower and higher cost management options for affected structures.

Carbonation is described in terms of the parameter k, which has a characteristic value of 4.06 for a normal distribution and –0.079 for the transformed (ln) value. It is noted that the probability distribution is significantly influenced by the number of samples with a value of approximately 0.75 (see figure 7.7).

Figure 9.13 shows times to initiation for different elements using characteristic values of cover and the carbonation parameter using a normal distribution. Values for insitu and precast bridge elements are the same as they have the same characteristic values for cover although the mean values differ. For 100 years to initiation, specified cover would be 53.6 mm for insitu and precast bridge elements and 46.5mm for precast culvert units.

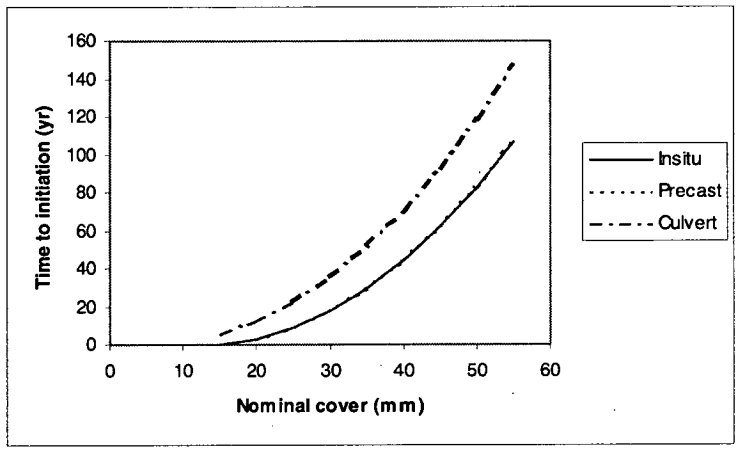

Figure 9.13 – Time to initiation, characteristic values, normal distribution

Figure 9.14 similarly shows times to initiation for different elements using characteristic values of cover and the carbonation parameter using a lognormal distribution. For 100 years to initiation, specified cover would be 22.4 mm for insitu and precast bridge elements and 15.1mm for precast culvert units.

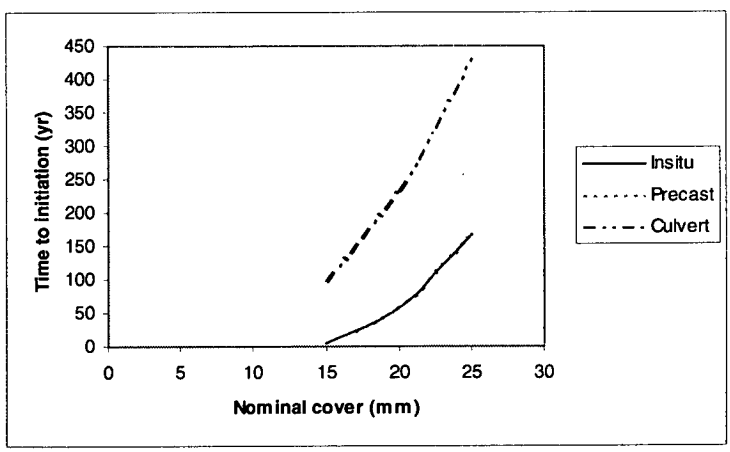

Figure 9.14 – Time to initiation, characteristic values, lognormal distribution

As with chloride ingress, times to initiation are reduced substantially from those calculated using mean values because of the variability in the parameters.

9.5.2 Probabilistic modelling

This analysis uses the principles of limit states and structural reliability. In structural terms, failure of an element occurs when the load effect (S) exceeds the resistance (R) (Stewart, 1998). Reliability can then be expressed as a probability of failure (p_f) or 'reliability index' (β), defined as:

$$\begin{aligned} p_f &= \Phi(-\beta) \\ &= \Pr(R \leq S) \\ &= \Pr(R\text{-}S \leq 0) \\ &= \Pr(G(R,S) \leq 0) \\ &= \int_0^{\infty} F_R(r) f_s(r) dr \end{aligned}$$

where Φ is the standard normal distribution function, $G()$ is the 'limit state function' [which is equal to R-S in this case], $f_s(R)$ is the probability density function of the load and $F_R(R)$ is the cumulative probability density function of the resistance, as shown in Figure 9.15. Structural reliability theory is easily extended to include the reliability analysis of structural systems. It follows that the probability of failure is the probability of exceeding the limit state function and so the limit state defines "failure".

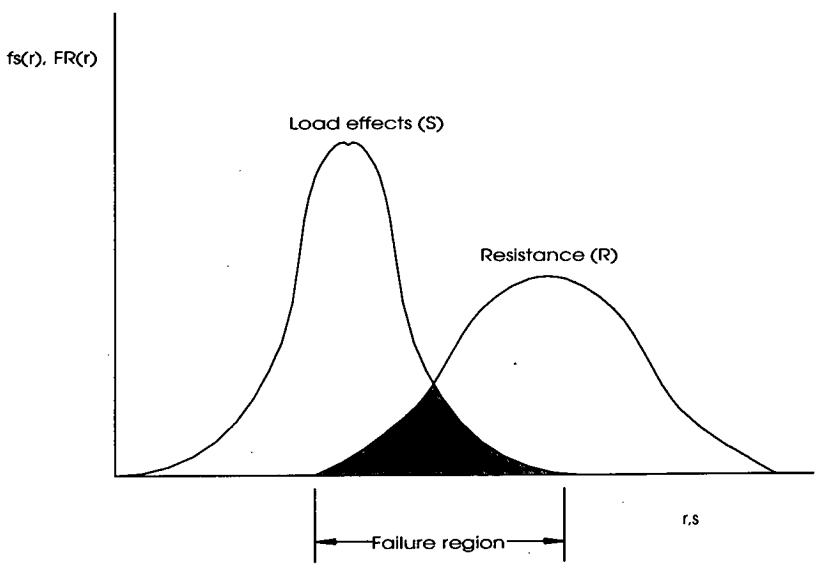

Figure 9.15 – Distributions of load effects and structural resistance

Figure 9.15 shows resistance as time invariant, with the load being the peak effect over a period such as design life. In reality, both variables are likely to be time dependent and the probability of failure is likely to increase with time or load applications as shown in Figure 9.16 (Schuëller, 1985).

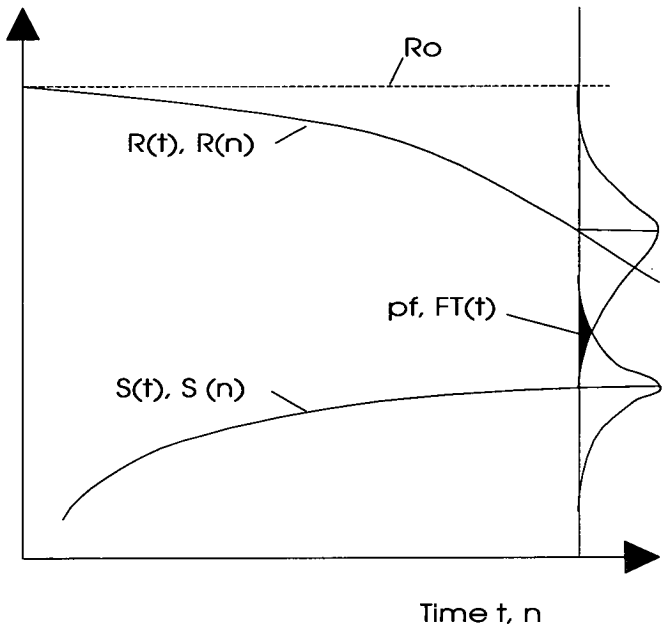

Figure 9.16 - Reliability concept for two time dependent random variables

The concept can be further developed to model the probability distribution function for service life of reinforced concrete structures subject to chloride ingress or carbonation as shown in Figure 9.17 (Rostam, 1999).

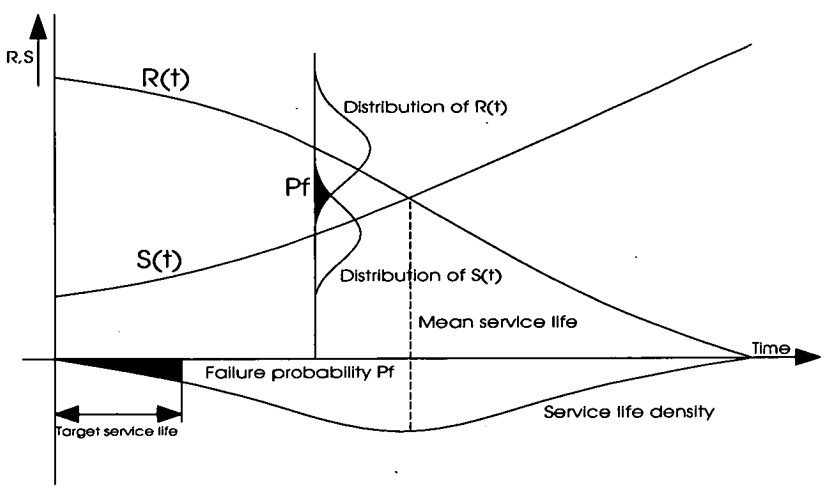

Figure 9.17 – Reliability concept applied to service life modelling of concrete structures

For the purposes of this analysis, the load effects are those of chloride ingresss or carbon dioxide penetration and the resistance effect is the cover to reinforcement so that the failure region is the proportion of reinforcement for which corrosion has initiated, ie where chloride concentrations are above the threshold or where the carbonation front has reached the reinforcement. Both chloride and carbon dioxide penetration are time dependent, while reinforcement location is fixed, and the reliability relationship is thus expressed as

$$p_f = \Pr(R<S(t))$$

For modelling that included the propagation phase and considered the effects of corrosion on structural capacity, the resistance would also be time dependent.

If it is assumed that chloride penetration and carbonation are independent events, then the probability of failure is

$$p_f = \Pr[R < S_1(t) \cap R < S_2(t)]$$

where $S_1(t)$ is the effect due to chloride and $S_2(t)$ is the effect due to carbon dioxide.

The assumption of independence is considered reasonable in the context of this study given that correlations could not be found in the earlier analysis.

Monte Carlo sampling has traditionally been used for random or pseudo-random sampling from probability distributions. The techniques are entirely random so that a given sample may fall anywhere within the range of the input distribution. Samples are consequently more likely to be drawn from areas of the distribution with high probabilities of occurrence. With enough iterations, Monte Carlo sampling will recreate the input distribution. When a small number of iterations are performed, it is possible that values in the outer range of a distribution are not represented in the sample. The implications are especially significant when the values in the outer ranges have a significant effect on the simulation outcomes. The Latin hypercube technique has been developed to ensure that there is sufficient sampling over the full range of input distributions. The technique involves stratified sampling of the input probability distributions. Stratification divides the cumulative curve into equal intervals on the cumulative probability scale. A sample is then taken from each interval to stratify the input distribution, thus forcing the sampling to represent values

in each interval and recreate the input probability distribution (Palisade Corporation, 1997).

Modelling was undertaken using @RISK software, which is an add-on to Microsoft Excel. The Latin hypercube technique was used, although the software does have Monte Carlo simulation as an option. For chloride ingress, a simulation using 500 iterations was undertaken for each case at ages 2, 5, 10, 15, 20, 25, 30, 35, 40, 45, 50, 55, 60, 65, 70, 75, 80, 85, 90, 95 and 100 years and for nominal covers of 10, 13, 19, 26, 32, 36, 44, 54, 59, 69 and 75 mm. Specified covers for analysis were selected to correspond to values for particular service lives from the deterministic modelling. A lesser range of covers was used for carbonation as probabilities of corrosion initiation became sufficiently small at the higher specified covers.

The chloride concentration $c(x,t)$ at depth x and time t is calculated using the error function solution to Fick's 2nd Law of Diffusion, with the appropriate probability distributions used for the surface chloride concentration c_s, the diffusion coefficient D and the nominal cover x. The threshold chloride concentration c_0 is subtracted from $c(x,t)$ and the distribution function for $c(x,t)$-c_0 obtained using @RISK. A typical distribution is shown in Figure 9.18.

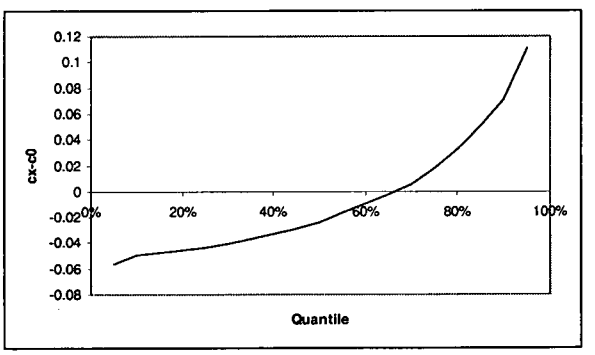

Figure 9.18 – Distribution of c_x-c_0 for 54 mm nominal cover, distance from coast 0 km, 2m < height ≤ 4m, threshold chloride concentration 0.05%, age 35 years.

The software provides results at five percentile intervals. The intercept is obtained using a parabolic interpolation with a programmable calculator. The probability of corrosion initiation is the proportion of positive values and is the complement of the value obtained from the interpolation. Curves are truncated at earlier ages because of a lack of convergence of the simulations, due possibly in part to characteristics of the numerical expansion of the error function or insufficient simulations.

9.5.2.1 Chloride ingress

Results of the simulations are presented as graphs of probability of corrosion initiation against age for nominal covers between 10mm and 75mm. A series of graphs are presented in section 7.2 of the Appendix and examine the effect of height above mean water level, distance from the coast, threshold chloride concentration for corrosion initiation, element type, truncation of cover negative tolerance and reduced coefficients of variation on the probabilities of corrosion initiation.

Figure 9.19 shows the probability of corrosion initiation for insitu concrete elements in the tidal zone in contact with salt water. The irregularities in the curves are likely to be attributable to the number of iterations used for the simulation, the variability in modelling parameters and the linear expansion of the error function. They would be expected to reduce with increased numbers of iterations but with a penalty of calculation time.

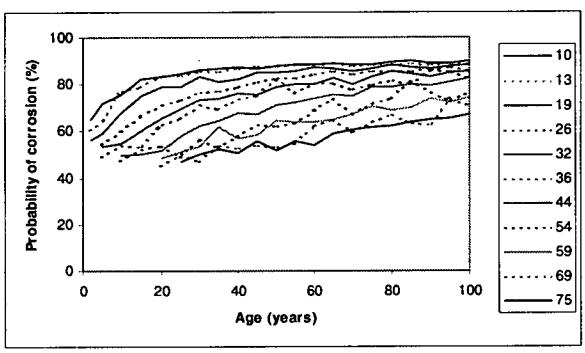

Figure 9.19 – Probability of corrosion for distance from coast 0 km, height ≤ 2m, insitu, threshold concentration 0.05 %

Probabilities of corrosion initiation can be transformed to reliability or safety indices using a complementary standard normal table (Melchers, 1987). Figure 9.20 shows the transformation of figure 9.19 for structure ages of 50 and 100 years.

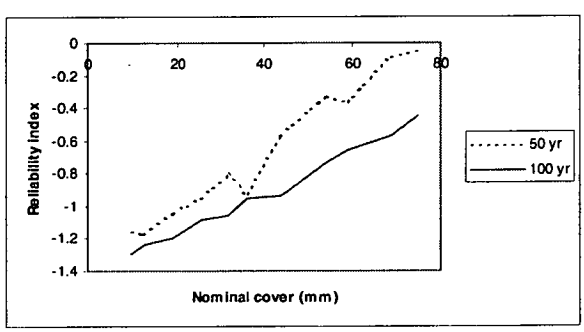

Figure 9.20 – Reliability indices for distance from coast 0 km, height ≤ 2m, insitu, threshold concentration 0.05 %

Figure 9.21 summarises the effect of corrosion threshold and nominal cover on probability of corrosion initiation from a structure in the tidal zone at age 100 years.

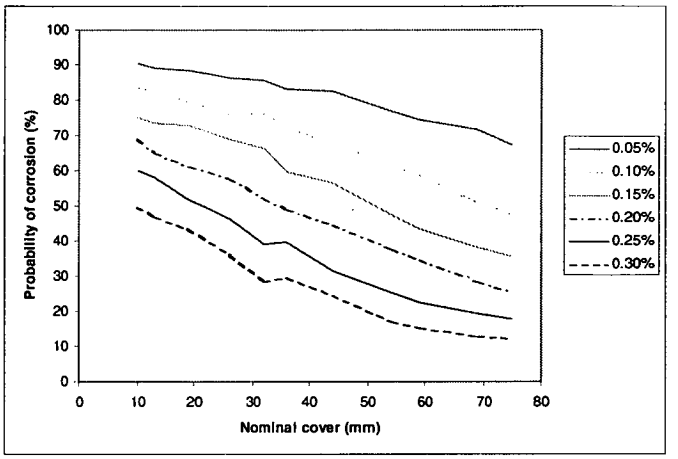

Figure 9.21 – Effect of corrosion threshold and nominal cover on probability of corrosion initiation, insitu element, 0<height≤2m, distance from coast 0km, age 100 years

The shape of the curves can be compared with those using lower coefficients of variation shown in the Appendix and a time dependent diffusion coefficient calculated in accordance with the following equation:

$$D(t) = D_0\left(\frac{t_0}{t}\right)^{\alpha}$$

The exponent reflects the rate of reduction of diffusion coefficient with time. The value of α for laboratory specimens varies from 0.4 to 0.8 depending on binder type, water binder ratio, curing time and interactions between the concrete and the exposure environment (Shayan, 2001).

Figure 9.22 presents a curve using the following parameters (Markeset, 2000) where N( ) indicates a normal distribution, LN( ) a lognormal distribution and X the nominal cover:

c_s = N(0.4%m/m concrete, 60%)

D_0 = N(7.0 x 10^{-12} m^2/s, 15%)

α = N(0.4, 15%)

X = LN(x mm, 10)

c_t = 0.05%, 0.10%

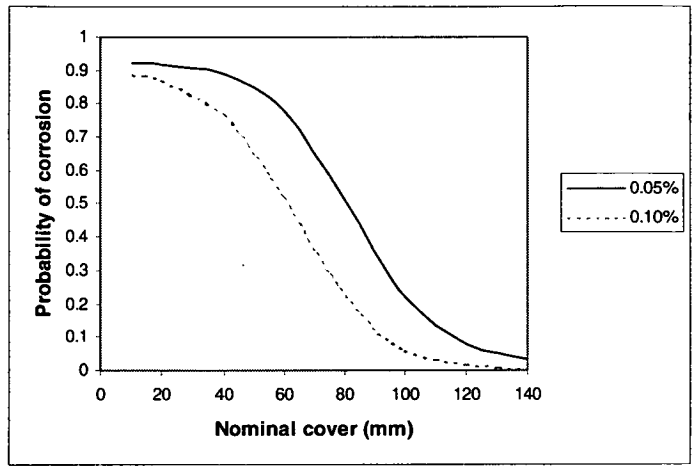

Figure 9.22 – Probability distribution for 100 year service life for two corrosion thresholds (Markeset, 2000)

The gradient of the steeper central section of the curves is increased by the reduced variability of the parameters by comparison with those used for modelling Tasmanian bridges and by the effects of the coefficient α whereby the diffusivity of the concrete reduces with time.

9.5.2.2 Carbonation

For probabilistic modelling of carbonation, the following previously defined relationship is used to determine the probability that the depth of carbonation x is greater than the depth of reinforcement, with k and the depth of reinforcement being the random variables.

$$x = k\sqrt{t}$$

Only three cases are involved because of the absence of an identified correlation between carbonation and the various factors examined.

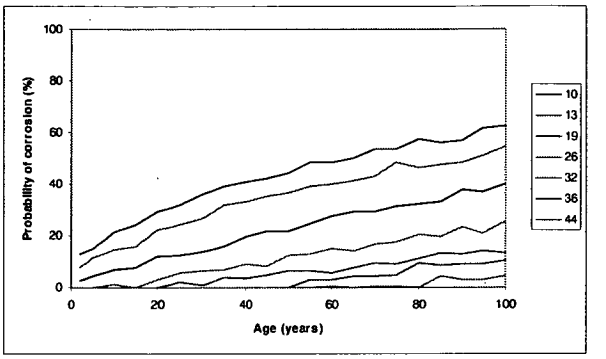

Figure 9.23 – Probability of corrosion for insitu elements, normal distribution of k

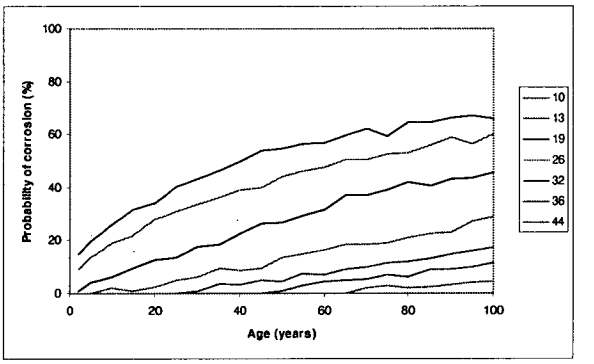

Figure 9.24 – Probability of corrosion for precast elements, normal distribution of k

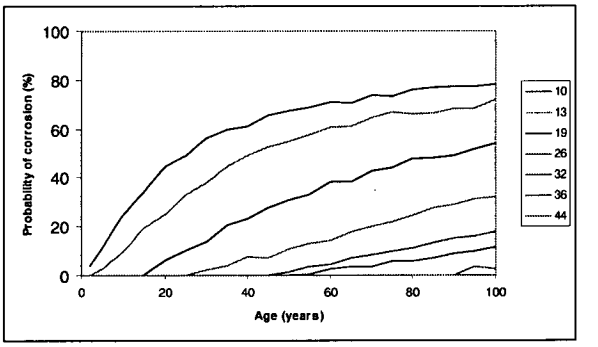

Figure 9.25– Probability of corrosion for precast culvert elements, normal distribution of k

Reliability indices are again determined using a complementary standard normal table.

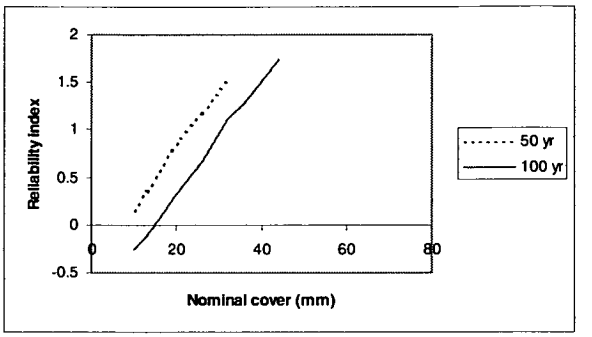

Figure 9.26 – Reliability indices for insitu elements, normal distribution of k

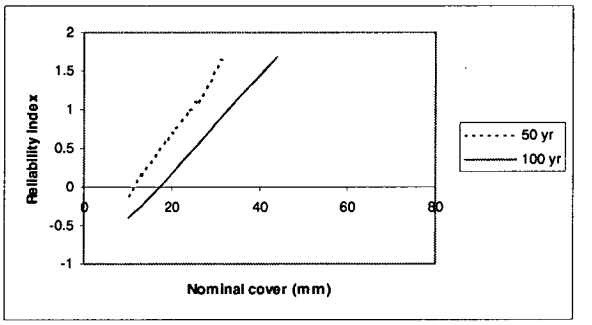

Figure 9.27 – Reliability indices for precast elements, normal distribution of k

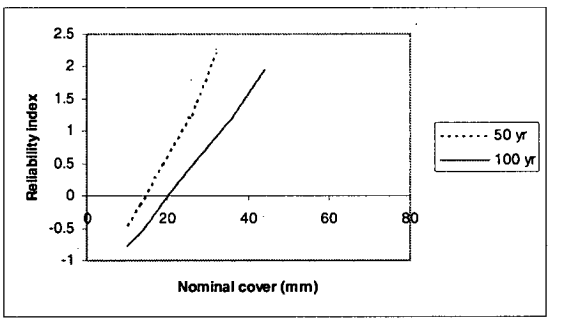

Figure 9.28 – Reliability indices for precast culvert elements, normal distribution of k

9.6 TASMANIAN BRIDGES

This section examines the performance of the bridges that are part of this study to seek to indentify any relationship between predicted and observed performance. Because of the age of the bridge stock, it relies on records of bridge inspections. Records are however incomplete for a number of reasons, including:

- the lack of a comprehensive and systematic statewide inspection process prior to 1990, associated with higher funding levels and a focus on new construction
- records of inspections prior to 1990 generally having been held in regional offices without copies being forwarded to head office

- the loss of records from regional offices during government restructuring during the late 1980's and early 1990's.

Details of the structures are included in section 7.3 of the Appendix.

The ages to reported distress and repair or replacement are plotted in figures 9.29 and 9.30. The times provide an upper bound because of the lack of a systematic inspection and reporting system prior to the 1990's. Both figures show that distress, and the consequent need for repair or replacement of a structure, can occur relatively quickly after construction notwithstanding the magnitude of the specified cover. The minimum time to visible distress is 8 years with a design cover of 50mm, while for times to repair the corresponding values are 12 years and 127mm. It is noted that visible distress requires the corrosion process to have initiated and propagated to the extent that there is enough corrosion product generated on the reinforcement to create tensile stresses sufficient to crack the cover concrete. The limited number of structures which have been repaired or replaced due to corrosion is likely to be attributable to a number of factors including the historic inspection and maintenance regime and the limited number of effective remedial options, especially for chloride induced corrosion, prior to the 1990's. Some cases of epoxy repairs exist but these have proven to be generally ineffective principally because physical and electrochemical properties differ substantially from those of the parent concrete

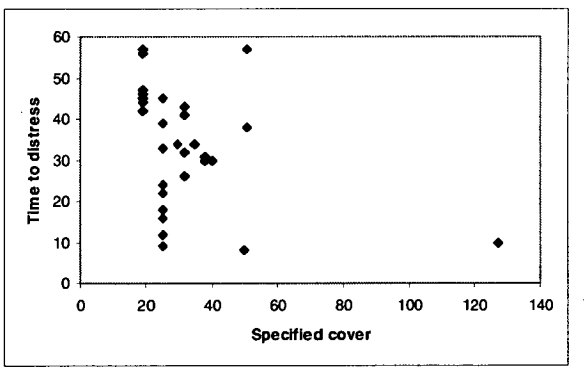

Figure 9.29 – Times to reported visible distress (N=36)

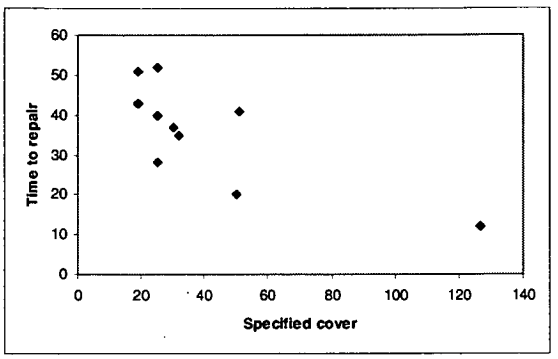

Figure 9.30 – Times to repair or replacement (N=10)

9.7 DISCUSSION

There is a wide range of definitions used for the service life of a structure, ranging from the time to initiation of corrosion, through time to visible evidence or significant maintenance, to the time at which there is a loss of structural capacity compromising safety.

From an asset management perspective, the time to initiation provides a conservative estimate of service life, although it can also indicate the age before which preventative maintenance should be undertaken. Research on rates of corrosion during the propagation phase by others is continuing, but the collection of relevant data was outside the scope and budget of the investigations which have formed the basis of this study. Experience with structures such as Grassy Wharf and the western interchange of Tasman Bridge indicates that times from initiation of corrosion to significant distress, and a consequent need for remedial action, may be short. This is consistent with Weyers' proposal that the time to maintenance be 5 years from the time of initiation for the 2.5 percentile lowest cover to reinforcement.

The time at which there is a loss of structural capacity compromising safety would relate more closely to the economic life of a structure, when replacement is likely to be the only available option.

For chloride induced corrosion, preventative maintenance may involve the application of a silane penetrating sealer at comparatively low cost. The installation of impressed current cathodic protection systems has been the Department of Infrastructure, Energy and Resources' favoured option for structures with significant distress but adequate structural capacity. Replacement of structures involves substantial cost to the Department and the community generally because of the costs associated with

building a new structure to contemporary loadings and geometric standards, demolition of the existing structure and delays to road users during the replacement works. Both options are beyond the scope of routine maintenance activity, with reference to the definitions of service life described at the start of this chapter.

The time to initiation has consequently been adopted as the definition of service life as it maximises the options that are available to the asset owner and because of the rapid propagation of chloride induced corrosion after initiation possible with bridge structures.

Deterministic modelling using mean values of parameters showed that, for structures exposed to chlorides, service lives of 100 years would be achievable with a combination of high cover to reinforcement and high chloride threshold concentrations. For nominal covers of 20mm to 50mm and a threshold concentration of 0.05% by mass of concrete, expected times to initiation of corrosion for elements on the coastline and less than 2m above mean water level range from 4 to 15 years respectively. This is consistent with the lower bound values of 4 to 5 years using the results from Table 12.6 and subtracting 4 years on the basis of Weyers' proposition.

The use of characteristic values for the parameters however suggests that 100 year service lives will not be achieved for structures in contact with or close to salt water even with large specified covers and high corrosion thresholds; the target service life becomes achievable for structures more than about 0.5km from the coast.

The results of the probabilistic analysis reinforce those of the deterministic modelling, showing probabilities of initiation of corrosion ranging from about 10% to 90% for a range of exposures, ages, chloride threshold concentrations and chloride diffusion parameters. The corresponding reliability indices range from 1.4 to -1.6.

By comparison, both deterministic and probabilistic modelling show that the risk of initiation of corrosion due to carbonation can be reduced to an acceptably low level with adequate cover; deterministic modelling indicates a specified cover of the order of 10 to 15 mm using mean values of parameters and 45mm to 55mm with characteristic values, while probabilistic modelling indicates a specified cover of around 50 to 55mm for a reliability index of 2.3. A reliability index of 1.5 is achieved for insitu, precast and culvert elements at a specified cover of the order of 40mm.

There was a high degree of consistency between the deterministic and probabilistic modelling for carbonation, with differences between the expected value of time to initiation from the deterministic modelling and the 50% probability of initiation from the probabilistic modelling within about 1 year. While there were greater differences with the modelling of chloride ingress, results were comparable. The greater differences in the chloride modelling may have been attributable to the use of two probabilistic parameters (c_s and D) rather than one (k), and the use of a linear expansion for the error function, given that coefficients of variation for the three parameters are of a similar order of magnitude.

It might have been expected that the probability of corrosion for chloride induced corrosion could be reduced to sufficiently low values by a number of mechanisms relating to reinforcement cover, diffusion parameters and chloride threshold concentration.

The analysis of cover to reinforcement has shown that variability has been consistently high in structures built over six decades. It is consequently considered unlikely that any significant changes can be made to that variability, although Norwegian developments in reinforcement spacers may assist in truncating the negative tolerances (Kompen, 1997).

Comparing figure A7.16 with figure A7.1 shows that reducing the effective diffusion coefficient by an order of magnitude, through mechanisms such as the use of supplementary cementitious materials, is unlikely to reduce the probability of initiation of corrosion to an acceptably low value. It is likely that a diffusion coefficient of $1x10^{-13}$ m^2/s is unachievable in practice, particularly if considered as a mean value that would need to be achieved consistently during the construction of a bridge. Achievable lower bound values may be closer to $4x10^{-13}$ m^2/s. Figure A7.17 shows early beneficial effects of reducing variability in properties in an element, but these benefits are reduced substantially as the structure ages. The degree to which variability can be reduced is limited by the effects of placement, compaction and curing through the concrete elements which are typical of bridges and highlighted by the concepts of 'covercrete', 'heartcrete', 'realcrete' and 'labcrete'.

The chloride corrosion threshold may be increased through techniques such as the incorporation of corrosion inhibitors in the concrete mix or applying them to the

surface of the concrete and allowing them to migrate to the level of the reinforcement. Commercially based inhibitors are based either on calcium nitrite or amines.

Table 9.8 shows the effects of incorporating calcium nitrite corrosion inhibitor in concrete mixes up to the maximum recommended dosage of 30l/m^3 as advised by the manufacturer (Grace, 1994). It shows that the maximum achievable chloride corrosion threshold is the same as the mean value of the chloride surface concentration used for modelling of service life. A similar upper limit is likely for the amine based inhibitors.

Calcium Nitrite (DCI) Dosage (l/m^3)	Chloride Protection (kg/m^3)	Chloride (%m/m concrete)
9.89	3.56	0.14
14.83	5.87	0.24
19.78	7.72	0.31
24.72	8.90	0.36
29.66	9.50	0.38

Notes: Assumed concrete density 2500 kg/m^3

Table 9.8 – Effects of calcium nitrite corrosion inhibitor on corrosion threshold

Figures A7.2 to A7.6 show the beneficial effects on probability of corrosion initiation of increasing the chloride threshold concentration by techniques such as the incorporation of corrosion inhibitors. The effects do not reduce the probability of corrosion to an acceptably low level, even at high inhibitor dosage rates. Recent experience on the duplication of the Blythe River Bridge has shown that careful control is required to manage concrete with high dosage rates of calcium nitrite corrosion inhibitor because of the set accelerating effect, even when a set modified admixture is used. Occupational health, safety and welfare issues associated with the use of inhibitors also need to be considered.

Stainless steel thus becomes an option for reinforcement in aggressive environments, ie for structures close to the coastline. Stainless steel has a chloride threshold concentration substantially higher that that of black steel, thus reducing the probability of corrosion to an acceptably low level. Additionally, the corrosion rate of stainless steel would be less than that of black steel even if corrosion initiated. Extensive research at the UK Building Research Establishment showed that austenitic stainless steels were virtually immune to corrosion in chloride contaminated concretes. Studies at the Politechnico di Milano, Italy showed decreasing chloride-induced corrosion with increasing alkalinity and critical chloride threshold levels exceeding 10% by weight of cement in highly alkaline solutions. The Italian results are shown diagrammatically in figures 9.31 and 9.32 (The Concrete Society, 1998). For a

cement content of 350 kg/m^3 and a concrete density of 2500 kg/m^3, the 10% by weight of cement corresponds to a threshold concentration of 1.4% by mass of concrete, or 28 times the 0.05% used as the base concentration in the analysis. By comparison, the maximum apparent surface chloride concentration for any core from this study was 1.1%.

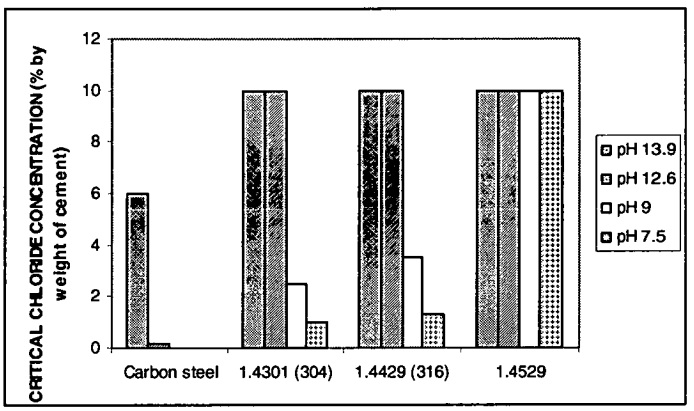

Figure 9.31 – Critical chloride concentrations for different steel types in solutions simulating the pore solution (20^{0}C)

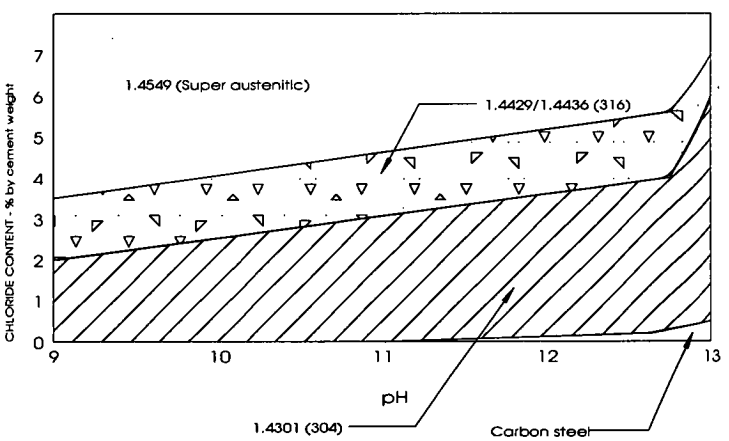

Figure 9.32 – Schematic representation of fields of applicability of different stainless steels in chloride containing environments (20^{0}C)

The majority of contemporary bridges structures are prestressed and thus contain both black steel and prestressing steel. A particular consideration is the possibility of pitting and brittleness in high tensile steels arising from exposure to chlorides. Stainless steel is more noble in the galvanic table than mild or high tensile steel resulting in a risk of galvanic corrosion. Testing in Denmark, Italy and the USA has shown that the use of stainless steel lapped with carbon steel does not lead to a significant increase in the corrosion rate of carbon steel compared with carbon steel used alone. In environments where both are passive, carbon steel may be slightly

more noble than stainless steel. Research at the Politechnico di Milano has shown that the increase in carbonation rate of corroding carbon steel embedded in chloride contaminated or carbonated concrete, due to galvanic coupling with stainless steel, is significantly lower than the increase brought about by coupling with passive carbon steel (The Concrete Society, 1998).

While the use of stainless steel in aggressive environments essentially eliminates the likelihood of reinforcement corrosion, including galvanic corrosion, the majority of contemporary structures are prestressed. The requirement for low penetrability concrete is thus not negated, especially in pretensioned elements where the prestressing strand is not contained in a sheath and the strand is comparatively close to the surface.

Using 3km from the coastline as the limit of chloride exposure, 453 of a total of 1158 or 39% by number and $779m of a total replacement cost of $1077m or 72% by value of the bridge stock is at risk of chloride induced corrosion. With mean specified covers of insitu elements only approaching 50mm since the 1970's, and those for precast elements and culverts typically being between 20 and 40mm, there is also a significant risk of carbonation in a substantial proportion of structures unlikely to be affected by chlorides. It can thus be expected that replacement of the majority of the State's bridges will result from corrosion rather than from structural inadequacy, notwithstanding progressive increases in permissible vehicle masses.

Chapter 8 discusses the selection of cover to reinforcement and concrete for new structures using a series a tables based on qualitative assessments of exposure. Four exposure categories are shown, with a further category U, requiring specific design considerations. Approaches are similar for both AS3600 and the AUSTROADS bridge code.

By comparison, structural aspects of design involve comprehensive analysis typically using computer software to implicitly achieve low probabilities of serviceability or structural failure in accordance with load and resistance factor design principles.

Differences between durability and structural design aspects are highlighted when the differences in reliability indices are considered.

An objective of code calibration in load and resistance factor design is to achieve a degree of consistency of the safety index, β, between various failure mechanisms although higher indices would typically be adopted where consequences of failure were greater or brittle failure mechanisms were involved. This would imply that safety indices for materials aspects should be comparable with those for structural aspects.

There will however generally be visible distress, and a consequent opportunity to undertake remedial works or initiate replacement of a structure, well before there is significant loss of structural capacity and before serious safety implications arise. A higher probability of failure is therefore likely to be acceptable for durability failure than for structural failure.

For the ultimate limit state, the structural reliability index, β, is typically about 4. Eurocode 1 is based on a risk of 7×10^{-5} [$\beta = 3.8$] (Bamforth, 1999). For existing structures, this may be overconservative and a target lifetime reliability index of 3 may be more appropriate (Frangopol et al, 1999).

In developing repair strategies using a system reliability approach, a minimum allowable reliability index as low as 2.0 may be used (Estes and Frangopol, 1999). Such an approach is however predicated upon undertaking repairs ahen system reliability reduces to that level. For asset owners with large bridge stocks and constrained funding, it may not be possible to undertake repairs at that time and continued deterioration may reduce system reliability to below that level.

Bamforth suggests that a probability of corrosion initiation of 10^{-2} ($\beta = 2.3$) may be more appropriate. On the Western Scheldt Tunnel, Gehlen and Schieβl (1999) adopted a target reliability index within the range of 1.5 to 1.8; this is however likely to be associated with higher levels of quality control and assurance and supervision than for the majority of bridge structures.

This analysis has shown reliability indices ranging from –1.6 to 1.4, with values of –1.3 to –0.5 at age 100 years for elements in the most severe exposures, based on a chloride threshold concentration of 0.05% by mass of concrete. The materials reliabilities for severe environments in particular are thus substantially lower than structural reliabilities and the values proposed by Bamforth, Gehlen and Schieβl.

While the approach to durability in current Australian codes made a significant step in highlighting concrete durability as an issue, the simplistic approach has not necessarily resulted in enhancing the durability of structures sufficiently to reduce the probability of corrosion to an acceptable level, particularly in aggressive environments. It is thus proposed that improving the durability of structures to appropriate levels requires an approach which reflects and parallels the structural design process so that environmental loads and mechanisms by which materials resist them are properly considered by designers.

While still qualitative, European Standard prEN206 (ISO, 1997) progresses the load and resistance factor approach to the durability design of structures by using the following series of exposure classes as the basis for the selection of a concrete mix and its placement.

Class designation	Description of the environment
No risk of corrosion or attack	
X0	Very dry
Corrosion induced by carbonation	
XC1	Dry
XC2	Wet, rarely dry
XC3	Moderate humidity
XC4	Cyclic wet and dry
Corrosion induced by chlorides	(Sources other than sea water)
XD1	Moderate humidity
XD2	Wet, rarely dry
XD3	Cyclic wet and dry
Corrosion induced by chlorides	(Derived from sea water)
XS1	Exposed to airborne salt
XS2	Submerged
XS3	Tidal, splash and spray zones
Freeze thaw attack	
XF1	Moderate water saturation without de-icing agent
XF2	Moderate water saturation with deicing agent
XF3	High water saturation without de-icing agent
XF4	High water saturation with deicing agent
Chemical attack	
XA1	Slightly aggressive environment
XA2	Moderately aggressive environment
XA3	Highly aggressive environment

Table 9.9 - prEN206 exposure classifications

Reference concretes, specified in terms of compressive strength, minimum cement content and maximum water/cementitious content ratios, are recommended to provide adequate resistance for each of the exposure classifications. The previous analysis has

indicated that specification in terms of the three basic parameters may be insufficient in more aggressive environments.

Andrade and Alonso (1997) have proposed a simplified method for carbonation depth which is summarised as follows:

$$P_{CO2} = V_{CO2} \cdot \delta_q \cdot \delta_{exp} \cdot \delta_g \cdot \sqrt{t}$$

where P_{CO2} = penetration of carbonation front at time t (mm)

V_{CO2} = carbonation rate (mm/year$^{0.5}$)

δ_q = partial ponderation factor, quality of concrete

δ_{exp} = partial ponderation factor, exposure

δ_g = partial ponderation factor, geometry

A similar approach is proposed for chloride penetration.

Incorporating an allowance for the variability in reinforcement cover, the following expression is obtained:

$$V_{CO2} \cdot \delta_q \cdot \delta_{exp} \cdot \delta_g \cdot \sqrt{t} \quad < \quad \varphi \cdot c$$

where φ = factor for accuracy of reinforcement placement

c = specified cover

The approach is similar to that for load and resistance factor design and would be likely to enhance durability related design as part of a process involving consideration of all feasible deterioration mechanisms. The analysis in this study has not found correlations sufficient to derive partial ponderation factors for either carbonation or chlorides. For carbonation, the value of φ can be determined by fitting a curve to the probabilities of corrosion initiation for the range of specified covers, as shown in figure 9.33.

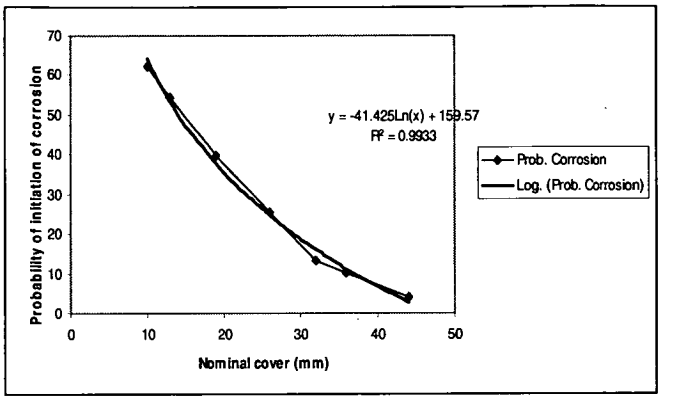

Figure 9.33 – Probabilities of corrosion for insitu concrete

Using partial ponderation factors of 1.0,

$$V_{CO2} = 2.01 \text{ mm/yr}^{0.5}$$

$$c = 46 \text{ mm (from curve fitting for probability of 1\%)}$$

$$\therefore \; 2.01\sqrt{100} = \varphi 46$$

$$\varphi = 0.44$$

Values of φ for precast elements and precast culvert units are similarly calculated at 0.42 and 0.44 respectively. The values are significantly lower than those typically used as capacity reduction factors for bending and shear in structural design, reflecting the variability in cover.

Because of the high probabilities determined for chloride induced corrosion and the expected associated low numbers, and the more complex diffusion model, values of φ have not been calculated for chloride ingress. Calculations for this approach would be simplified if curve fitting using a power relationship, rather than Fick's diffusion model, was used to describe profiles.

The calculations do however indicate the potential for the model, with additional research required to correlate parameters derived from laboratory specimens and field samples with insitu concrete throughout structural elements. A sound statistical base would be required for such a design process.

This thesis has only considered concrete deterioration due to chloride ingress and carbonation, and not mechanisms which affect the concrete matrix. Enhancements to design processes would need to consider the full range of deterioration mechanisms.

9.8 IMPLICATIONS FOR BRIDGE STOCK

Deterministic modelling indicates that service lives of 100 years for structures exposed to chlorides (up to approximately 3km from direct contact with salt water) can only be achieved with a combination of high specified cover and relatively high chloride threshold concentration. For structures in contact with salt water, using a value of 0.05% for the threshold concentration, and with mean specified covers from the cover surveys of the order of 25 mm for older insitu and precast culvert elements and 40 to 45 mm for newer insitu and precast elements, times to initiation of the order of 7 years and 15 to 18 years respectively are indicated. Using characteristic values of the parameters, times to initiation are reduced to about 1 to 2 years.

Probabilistic modelling shows high probabilities of initiation of corrosion, and consequently low reliability indices, for all cases where there is an exposure to chlorides due to the high variability in the cover, apparent surface concentration and effective diffusion coefficient parameters. There are some beneficial effects from reducing the variability of each of the parameters or increasing the threshold concentration, but these are relatively small at greater ages and insufficient to reduce probabilities of corrosion initiation to an acceptably low level.

By comparison, both deterministic and probabilistic modelling show that the risk of initiation of corrosion due to carbonation can be reduced to an acceptably low level with adequate cover; deterministic modelling using mean values of parameters indicates a specified cover of the order of 10 to 15 mm, while deterministic modelling using characteristic values of parameters and probabilistic modelling indicate a specified cover of around 50 mm.

The low values of times to initiation, particularly for chloride exposures, are consistent with the observed performance of the bridge stock where visible distress has occurred in as little as 8 years.

Detailed assessment of implications for the overall bridge asset would involve a review of specified covers and exposures for at least a statistically significant sample of the more than 1100 structures that comprise the bridge stock and is beyond the scope of the study. A representative bridge could however be taken as one from the 1960's given that the average age of the bridge asset in 1998 was 32 years and there were a large number and high value of bridges built during that decade.

Figures 9.34 and 9.35 show additionally that mean specified cover for insitu elements has not increased significantly since the 1960's; for precast elements there may however be increased risk for the more recent structures from the reduced mean covers.

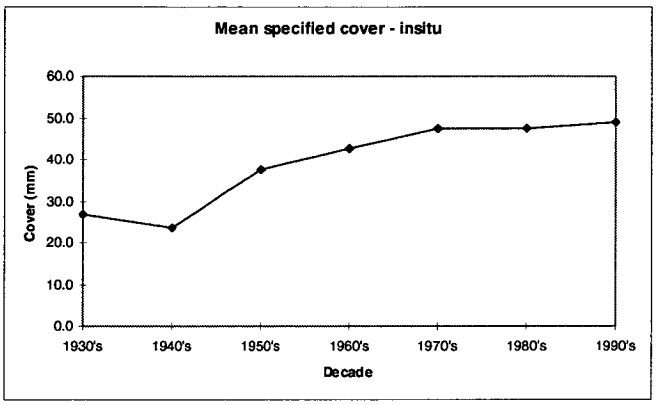

Figure 9.34 – Mean specified cover, insitu elements

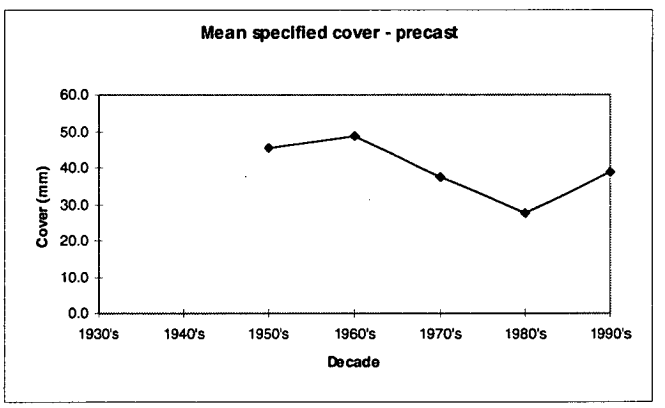

Figure 9.35 – Mean specified cover, precast elements

The representative bridge is then used with the exposures from table 4.1 to provide an indication of the implications for the bridge stock.

Weyers service life model used the 2.5 percentile lowest cover to reinforcement which corresponds to 1.96 standard deviations for a normal probability distribution. For the cover models used in this thesis, the corresponding covers are 17mm, 16mm and 7mm less than the specified cover for insitu, precast and precast culvert units respectively.

Based on the mean specified cover of 48.6mm for surveyed insitu elements built during the 1960's and the 17mm less than specified cover from Weyers model, 30mm

is used as a representative value of cover for an indicative assessment of the implications for the State's bridge stock.

Figures 9.36 to 9.38 show chloride profiles for structures 0.5km, 1km and 2km from the coast using the characteristic value of the surface chloride concentration and diffusion coefficients representing upper, mean and lower characteristic values.

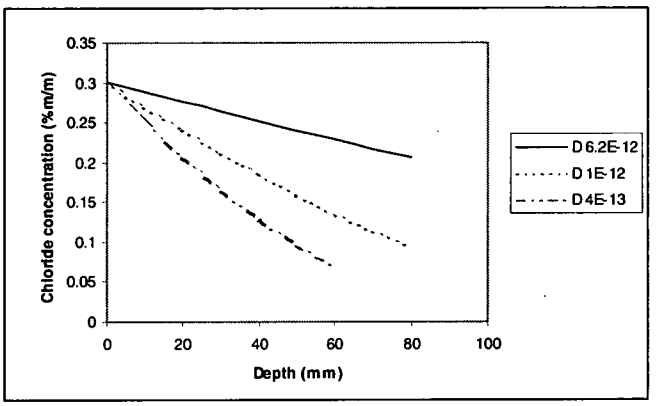

Figure 9.36 – Chloride profiles, distance from coast 0.5km

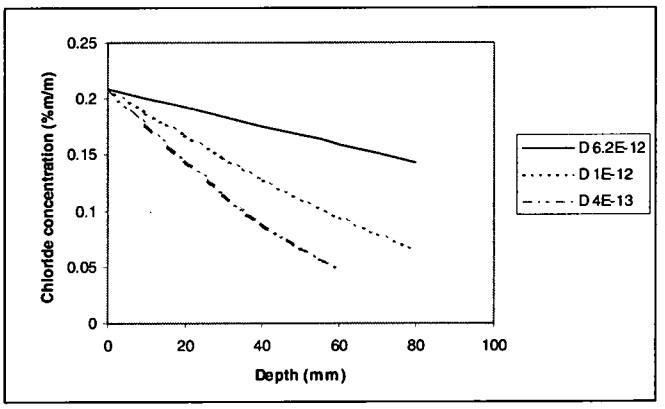

Figure 9.37 – Chloride profiles, distance from coast 1km

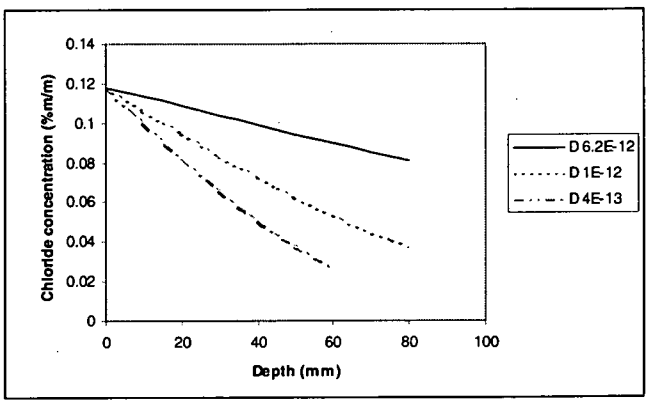

Figure 9.38 – Chloride profiles, distance from coast 2km

Consideration of probabilities of and reliabilities for chloride induced corrosion from seawater (figures A7.12 and A7.29), figures 9.36 to 9.38 for a depth of 30mm, the mean and characteristic values of surface chloride concentration from tables 9.1 and 9.5, and a threshold chloride concentration of 0.05%m/m concrete suggests that the limit of chloride exposure is approximately 3km from direct contact with salt water. This corresponds to some 38% of the number of structures and 72% of their value or 440 structures with a replacement cost of $770m.

Use of mean values of parameters suggests that there is little risk of carbonation damage where specified covers exceed 20mm. The use of characteristic values and probabilistic modelling indicates that the likelihood of carbonation damage is higher than the value adopted in defining service life where specific covers are less than about 50mm. Based on mean specified covers, insitu elements built before the 1950's and precast elements built after the 1960's are particularly at risk. Precast culvert units are also at risk, with virtually all having a specified cover of 25mm, although their life may be controlled by other deterioration mechanisms.

As specified covers more than 50mm are typically limited to chloride exposures, the analysis suggests that virtually all the existing bridge stock will be subject to chloride or carbonation induced corrosion of reinforcement within the 100 year design life.

Risks are likely to have been reduced since the inclusion of minimum cement contents and maximum water cement ratios in DIER specifications in the late 1980's and the consequent reduction in the possibility of high penetrability concretes being used. Table 9.10 shows AUSTROADS Bridge Design Code requirements for minimum characteristic strength for the various exposure classifications with the corresponding minimum cementitious content and maximum water binder ratio from the current DIER specification for supply of concrete. For structures subject to carbonation damage in exposure classification B1, the minimum cementitious content of 400 kg/m^3 corresponds to an increase of about 60 kg/m^3 over the mean value of existing concretes determined in this study. The reduced risk however only applies to about 10% of the number of structures and less in terms of value.

Exposure classification	Minimum characteristic strength f'c (MPa)	Minimum cementitious content (kg/m³)	Maximum water/binder ratio
A	25	350	0.55
B1	32	400	0.5
B2	40	440	0.45
C	50	500	0.4

Table 9.10 – Concrete characteristic strengths (AUSTROADS) and compositions (DIER)

The analysis thus indicates a high continuing demand for remedial measures and early replacements of bridges. Because of the high probabilities of chloride induced corrosion initiation even at early ages, there will be few opportunities for preventative measures such as the application of silanes except perhaps for distances between about 2 and 3 km from direct contact with seawater.

Greater opportunities however exist for structures subject to carbonation only, ie more than 3km from direct contact with salt water. Using figures 9.23 and 9.24 for probabilistic modelling and the values of mean specified cover in figures 9.34 and 9.35, indicative maximum ages for preventative measures are of the order of 50 years for insitu elements and 30 years for precast elements respectively. Preventative measures may take the form of anti-carbonation coatings or cementitious renders with their beneficial effects on alkalinity. There is also a greater ability to implement remedial measures, such as patch repair, for structures affected by carbonation damage because of its lower aggressivity by comparison with chloride induced corrosion.

9.9 IMPLICATIONS FOR SPECIFICATIONS AND CODES

The approaches developed in this section draw from both the analysis undertaken in this study and from the author's experience in bridge design, construction, maintenance and management.

The analysis has shown that the probability of chloride induced corrosion initiation for structures in contact with or in close proximity to salt water cannot be reduced to appropriate levels by reducing the diffusion coefficient, decreasing the variability of the parameters or increasing the cover to reinforcement to levels that are likely to be achievable for actual structures because of the magnitudes of improvement in performance required (refer Appendix figures A7.15 to A7.17 particularly). Significant increases in specified cover are additionally likely to be counterproductive

because of reduced effectiveness in crack control and added cost of structures associated with increased concrete volumes and masses.

Because of its high corrosion threshold, stainless steel reinforcement thus becomes the preferred option for structures close to direct contact with salt water. Corrosion inhibitors do not increase the corrosion threshold sufficiently for structures in close proximity to salt water but become an option at intermediate distances and it is a matter of determining transition points.

While stainless steel reinforcement is itself approximately 6 times more expensive than carbon steel bars, there is little or no effect on other costs of bridge design and construction, including steel fixing, formwork, falsework, concrete supply and placement, foundations, joints, bearings, roadways surfacings, parapets and supervision, and the increase in the cost of building a new structure may be of the order of 10% (Markeset, 2000) for full replacement and less for selective use. This is balanced by the expected substantial reduction in future costs associated with maintenance and premature replacement, including both costs associated directly with the bridge and those resulting from disruption to traffic. The level of replacement of black steel with stainless steel needs to consider the level of specialist materials design input and supervision standards, and may be reduced where those inputs are at a high level.

With new structures incorporating supplementary cementitious materials in the binder that are properly cured, it is likely that the diffusion coefficient can be reduced from the values determined in this study, with further time dependent reductions, although it is not possible to quantify the magnitude of such reductions. Figures 9.36 to 9.38 showed the effect of diffusion coefficient on chloride profiles for structures 0.5km, 1km and 2km from the coast. Figure 9.39 shows the effect of increasing dosages of calcium nitrite corrosion inhibitor on the chloride corrosion threshold concentration from the values in Table 9.8.

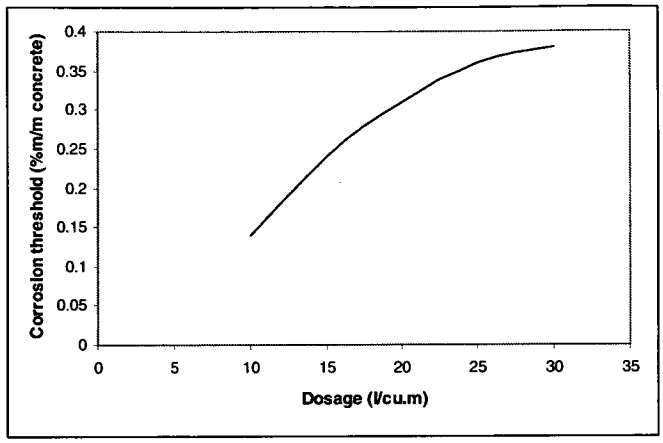

Figure 9.39 – Effect of cacium nitrite corrosion inhibitor on chloride threshold

A maximum dosage of calcium nitrite corrosion inhibitor of the order of $20l/m^3$ is likely to achieve a beneficial increase in corrosion threshold while limiting the effects on concrete set modification and cost. Appropriate precautions in its use will nevertheless be required. The rate of increase in corrosion threshold is also reduced as the dosage increases beyond 20 l/m^3. This dosage corresponds to a chloride threshold concentration of approximately 0.3%m/m concrete which is the characteristic surface chloride concentration 0.5km from the coast. A distance of 0.5km is thus indicated as the transition point between stainless steel reinforcement and the use of corrosion inhibitors with black steel because of the flatness of the chloride profile corresponding to the upper characteristic value of diffusion coefficient.

A further transition point, in terms of required dosage of corrosion inhibitor or increased corrosion threshold, at a distance of 2km from the coast is similarly indicated.

Requirements for chloride exposure are summarised in Table 9.11.

Distance from coast (km)	Durability requirements
0-0.5	Stainless steel reinforcement
0.5 – 2	Corrosion inhibitor, threshold 0.3kg/m³ m/m concrete
2-3	Corrosion inhibitor, threshold 0.12kg/m³ m/m concrete
>3	No requirements

Table 9.11 – Chloride based durability requirements

As codes and specifications do not currently explicitly address stainless steel reinforcement and corrosion inhibitors, there is a need to enhance them to include specific provisions.

A minimum cover of 40mm for stainless steel reinforcement has been recommended (Markeset, 2000) and is considered appropriate. Specifications need to include requirements for particular care in the use of stainless steel, particularly the avoidance of contamination with black steel and pickling and passivation of damaged areas.

For distances between 0.5km and 3km from the coast, the current requirements of the AUSTROADS Bridge Design Code for cover detailed in Table 8.3 could be adopted on the basis of the incorporation of corrosion inhibitors. With the variability in properties of concrete and the need to protect prestressing steel in many members, the 35mm cover for exposure classification B1 and 45mm for classification B2 for 50 MPa concrete may however be inadequate and it is likely to be advantageous to rationalise the minimum cover to 50mm. This study has provided no evidence to suggest that the 10mm to 20mm reduction in the Code of specified cover for rigid formwork and intense compaction is appropriate particularly with characteristic covers being the same.

For carbonation damage, the AUSTROADS Bridge Design Code specifies a minimum cover of 45mm for exposure classification B1 with a characteristic concrete strength of 32 MPa. The 32 MPa corresponds to a minimum binder content of 400 kg/m^3 and maximum water binder ratio of 0.5 in the current DIER specification. For a 100 year design life and moderate humidities and/or cyclic wet/dry environments proposed British requirements associated with the European Standard prEN206 for carbonation were a minimum cover of 30mm, maximum water cement ratio of 0.45 and concrete strength of 40 MPa, with no reduction in cover for higher strength grades (Hobbs, 1998). No distinction is made for elements with rigid formwork and intense compaction. With the characteristic cover from this study for insitu elements being 17mm less than the nominal cover, the 30mm minimum cover corresponds to a specified cover of 50mm.

Probabilistic modelling indicated that a specified cover of 50mm to 55mm would be required to achieve a service life of 100 years for a reliability index of 2.3 while the deterministic modelling indicated a specified cover of 45mm to 55mm. Higher cement contents would be expected to reduce the rate of carbonation because of the increased amount of alkali available to react with the carbon dioxide. Other effects to be considered include a reduction in alkalinity from the incorporation of

supplementary cementitious materials and pore refinement associated with higher cement contents, proper curing and supplementary cementitious materials.

Climatic data detailed in the Appendix shows that for much of the State, relative humidities are between the 50% and 70% corresponding to the highest rates of carbonation for at least part of the year and a degree of conservatism is required in the provisions of a standard specification that applies throughout Tasmania. It is noted that the focus of the corrosion investigations on which this study has been based was primarily on chloride induced damage and the carbonation models are consequently less reliable.

On the basis of the above discussion, the 45mm nominal cover from the AUSTROADS Bridge Design Code is retained, but the minimum binder content is increased to 440 kg/m^3 with a maximum water binder ratio of 0.45 corresponding to the 40 MPa strength grade. The 440 kg/m^3 binder content is less than the minimum 500kg/m^3 currently required for grade 50 concrete in the DIER specification, and can thus assist with reducing risks of plastic shrinkage cracking during placement and the magnitude of the shrinkage strain in hardened concrete. As discussed in section 5.5, water contents of Tasmanian concretes are relatively uniform and, for the concretes typically used in bridge construction, lower water cement ratios to potentially achieve reductions in chloride penetrability would be accompanied by higher binder contents and the consequent issues. Occasions when a lower binder content and water binder ratio could be achieved concurrently are likely to be unusual, and restricted to specific projects involving high levels of materials design input and construction supervision.

The above provisions can readily be incorporated into specifications and, with some of the additional work described in the next section, provide the basis for code enhancements.

10 SUMMARY AND CONCLUSIONS

10.1 GENERAL

Mortars and pozzolanic cements have been used by humans for buildings since Egyptian, Greek and Roman times. Portland cement was not discovered until early in the 19th century, but it now provides the basis for concrete which has become the most commonly used construction material with worldwide consumption having grown to approximately eight billion tonnes per annum.

The predominance of concrete as a construction material has arisen from its ability to be formed into a wide range of shapes and the development of reinforced concrete in the 1850's and prestressed concrete in the 1950's.

While concrete structures continue to perform well in many situations, lack of durability in others has emerged over the last two to three decades as a mjor issue for asset owners throughout the world. Chloride induced corrosion of reinforcing and prestressing steel is perhaps the most significant mechanism economically. Other mechanisms include carbonation induced damage of reinforcement, alkali aggregate reaction, delayed ettringitre formation, sulfate attack, thaumasite attack, acid attack, freeze thaw damage, abrasion and impact.

Chloride induced corrosion of reinforcing and prestressing steel is a significant management issue for the Tasmanian Department of Infrastructure, Energy and Resources because of the large proportion of the value of its bridge asset located in close proximity to salt water. The corrosion has led to a need to install cathodic protection systems on a number of structures and replace others. Carbonation damage to bridges has also necessitated repairs and been a factor in replacement of others. Rehabilitation and replacement of affected structures continue as funds permit.

Data collected as part of corrosion assessments of damaged structures and surveys of others have been collated and analysed to assist with the management of the existing bridge asset and to provide a basis for improving the performance of new structures through enhancements to codes, specifications and practice.

10.2 CONCRETE DETERIORATION MECHANISMS

While concrete often performs well from a durability perspective, it can deteriorate through a number of mechanisms, with the primary mechanisms summarised in Table 10.1.

Mechanism	Causes
Reinforcement corrosion	Chloride ingress Carbonation
Disintegration of matrix	Alkali aggregate reaction (AAR) Sulphate attack Thaumasite Delayed ettringite formation (DEF) Acid attack Freeze-thaw
Physical damage	Overloading Impact Abrasion

Table 10.1 – Concrete Deterioration Mechanisms

The reinforcing or prestressing steel in contemporary structures is normally protected from corrosion by a passive oxide layer created by the highly alkaline pore water solution. In the first two cases, that protection is lost as a result of the ingress of chloride ions or the reduction in pH from the reaction of carbon dioxide with the alkaline pore water solution and, in the presence of oxygen and water, the steel can corrode leading to staining, cracking and spalling of the cover concrete and progressive loss of strength.

With alkali aggregate reaction, sulfate attack, thaumasite, delayed ettringite formation, acid attack and freeze-thaw, the concrete matrix itself is damaged and may crack and disintegrate exposing more of the concrete matrix to damage and/or facilitating corrosion of the reinforcing or prestressing steel.

Physical damage to concrete may result from structural effects such as overloading, impact or abrasion.

Cracking due to construction effects, loading or the various deterioration mechanisms may facilitate the ingress of aggressive agents. There is however a lack of a clear relationship between cracking and corrosion of reinforcing and prestressing steel.

The thesis has only considered chloride ingress and carbonation leading to the corrosion of reinforcement.

10.3 TASMANIAN BRIDGE STOCK

The Tasmanian Department of Infrastructure, Energy and Resources is responsible for a substantial bridge asset comprising over 1100 bridges and major culverts with an estimated replacement cost exceeding A$1b. Concrete is the dominant material of construction. A major construction period in the 1960's, which included the building of the Tasman Bridge, means that a significant proportion of the bridge asset has an age of 30 to 40 years.

As an island state with much of its population living near the coastline, much of the bridge asset is exposed to chlorides. About ¼ by number and 2/3 by value of the asset is located within 1km of direct contact with salt water.

Many structures are affected by one or more of the various forms of concrete deterioration, necessitating significant expenditures on repair, rehabilitation and replacement.

A number of corrosion investigations have been undertaken to understand the nature and cause of the deterioration, determine management strategies for affected structures and provide the basis for the design of cathodic protection systems where they are selected as the appropriate option. Data from the corrosion investigations and cover surveys of other structures have provided the basis for this thesis.

10.4 CONCRETE PERFORMANCE

Strength and compositional data from cores taken for the corrosion investigations were analysed to provide the basis for subsequent investigation of possible correlations with chloride ingress and carbonation and potentially to assist with the enhancement of specification and code provisions.

The majority of structures involved in the study were built by direct labour, probably with site batching, and without the use of job specific specifications. Where specifications were provided, a characteristic strength of 3000 psi (20.7 MPa) and/or 1:2:4 cement:fine aggregate: coarse aggregate were most commonly used. The range of specified strengths varied from 1500 psi (10.4 MPa) to 6500 psi (44.9 MPa).

Published data and Departmental records were used to develop a relationship to estimate 28 day compressive strength from core test results. The relationship

indicated that 28 day compressive strengths in the structures may have been lower than specified although high coefficients of variation mean that caution is required in drawing any firm conclusions.

Cement and water contents from the analysed cores could be described with normal probability distributions with a mean cement content of 341 kg/m^3 and water content of 195 l/m^3. Coefficients of variation were 14.6% and 13.5% respectively.

Factor analysis indicates a degree of correlation between composition and strength, although this was not as strong as may have been expected from the literature due perhaps to the age and variability of the concrete and the use of different cores for different tests.

10.5 CHLORIDE INGRESS

The penetration of chlorides into concrete is the result of a number of transport and binding processes, with concentrations at various depths a function of environmental conditions, the design and detailing of structures and materials properties. While the processes are complex, they are commonly modelled using Fick's 2nd Law of Diffusion whereby the chloride penetration can be described in terms of a surface chloride concentration and a diffusion coefficient.

Diffusion parameters derived for analysed cores were examined for possible correlations with a range of materials and environmental factors. A number of factors, and particularly the high variability in properties, are likely to contribute to the lack of identified correlations. The values of the derived parameters and their variability were nevertheless consistent with those reported in the literature. A lognormal distribution was used to describe the diffusion coefficient, with a normal distribution for the chloride surface concentration.

A number of influences and a range of values of threshold chloride concentrations for the initiation of corrosion have been reported. A value of 0.05% by mass of concrete was adopted as the basis for subsequent service life modelling, with some investigation of the sensitivity of corrosion initiation probabilities to higher values.

10.6 CARBONATION

Carbonation in the analysed cores was described in terms of a relationship consistent with that of Klopfer. As with chlorides, no correlation between carbonation and a range of environmental and materials factors was identified.

Normal and lognormal probability distributions were derived for subsequent service life modelling.

10.7 COVER TO REINFORCEMENT

While the variability in cover to reinforcement has been described in the literature for some 20 years, narrow tolerances have continued to be included in codes and specifications.

Analysis of measurements of cover to reinforcement on structures built in Tasmania since 1931, and the literature, have indicated that there is a realistically achievable tolerance in the hardened concrete that is higher than that suggested by codes and specifications.

Models using normal probability distributions were developed for service life modelling.

10.8 SERVICE LIFE MODELLING

Models for chloride ingress, carbonation and cover to reinforcement were used to assess expected service lives and probabilities of durability related failure of reinforced concrete in Tasmanian bridges. Time to initiation of corrosion was adopted as the service life criterion.

The modelling indicates that for structures in close proximity to salt water, 100 year service lives are not possible even with high covers to reinforcement and high corrosion thresholds through mechanisms such as corrosion inhibitors, because of the high variability in the properties of aged concrete.

By comparison, 100 year service lives for structures subject to carbonation are achievable with specified covers of the order of 50mm.

10.9 IMPLICATIONS FOR BRIDGE ASSET

The analysis has shown high probabilities of corrosion initiation for structures subject to the ingress of chlorides, with the limit of exposure being approximately 3km from direct contact with salt water. This equates to some 38% by number of structures and 72% of the value of the asset or 440 structures with a replacement cost of $770m. The continuing use of cathodic protection systems or early replacements for affected structures is indicated because of the aggressive nature of the corrosion process.

Structures that are clear of chloride exposures may be subject to carbonation damage. Greater opportunities however exist for the use of preventative or remedial measures, such as anti-carbonation coatings and patch repairs.

While the risk to structures built in the last decade has reduced because of the inclusion of minimum cementitious contents and maximum water binder ratios, this only equates to about 10% by number and less by value of the asset and does not substantially reduce the future demand for maintenance, rehabilitation and replacement of corrosion affected structures.

10.10 IMPLICATIONS FOR CODES AND SPECIFICATIONS

The research has provided the basis for enhancements to standard specifications and, with some additional research, to codes.

An approach using stainless steel reinforcement for structures in close proximity to salt water and corrosion inhibitors at intermediate distances to address chloride induced corrosion has been proposed.

10.11 FUTURE WORK/FURTHER RESEARCH

The analysis has identified a number of areas which would benefit from further research, including:

- relationships between properties of laboratory specimens, test samples and insitu concrete both through structural element sections for a range of strength grades and binder types

- relationships between properties from accelerated tests and insitu exposures for both chloride ingress and carbonation for a range of strength grades and binder types
- development of design processes for concrete to parallel structural design processes, including the development of partial factors for load and resistance and quantification of durability related properties of concrete structures
- investigation of the performance of concretes manufactured over the last 10 to 20 years to investigate whether of not the variability has reduced
- quantification of the beneficial effects of SCM's on chloride ingress and possible adverse effects on carbonation resistance
- mechanisms by which the variability in cover to reinforcement might be reduced, including improvements in quality control and assurance
- mechanisms by which the variability in insitu properties of aged concrete might be reduced
- research on developing models for prediction of damage through other mechanisms (eg AAR, DEF, freeze thaw, sulphate, etc)
- collection and analysis of additional carbonation data across Tasmania.

For carbonation, a combination of minimum specified cover to reinforcement, minimum binder content and maximum water binder ratio is proposed.

11 REFERENCES

Amey S L, Johnson D A, Miltenberger M A and Farzam H, (1998), *Predicting the Service Life of Concrete Marine Structures*, ACI Structural Journal, March-April 1998, American Concrete Institute, USA

Andrade C, Díez J M and Alonso C, (1997;6), *Mathematical Modeling of a Concrete Surface "Skin Effect" on Diffusion in Chloride Contaminated Media*, Advanced Cement Based Materials, Elsevier Science Ltd, USA

AUSTROADS, (1992), *Bridge Design Code, Section 5: Concrete*, Sydney

AUSTROADS, (1997), *Concrete Structures – Durability, Inspection and Maintenance Procedures – Position Paper*, Austroads, Sydney

Bamforth P B, (1996), *Definition of Exposure Classes and Concrete Mix Requirements for Chloride Contaminated Environments*, SCI 4th International Symposium on Corrosion of Reinforcement in Concrete Construction, Cambridge, UK

Bamforth P, (1999), *Double Standards in Design* in 'Concrete', The Concrete Society, Slough, UK

Bartlett F M and M^{ac}Gregor J G, (1996), *Statistical Analysis of the Compressive Strength of Concrete in Structures*, ACI Materials Journal, March-April, ACI, USA

Beeby A W, (1983), *Cracking, Cover and Corrosion of Reinforcement*, Concrete International, February 1983

Berke N S and Hicks M C, (1993), '*Predicting Chloride Profiles in Concrete*, Proceedings of Corrosion '93 Conference, March 1993, New Orleans

Berke N S, Hicks M C and Tourney P G, (unknown date), *100 Year Service Lives in Marine Environments Using Belts and Braces Approach with Calcium Nitrite*, W R Grace and Co., Cambridge, MA, USA

Broomfield J P, (1997), *Corrosion of Steel in Concrete – Understanding, investigation and repair*, E & FN Spon, London, UK

Bureau of Meteorology, (1993), *Climate of Tasmania*, Commonwealth of Australia, Canberra

Beeby A W, (1983), *Cracking, Cover, and Corrosion of Reinforcement*, Concrete International

Browne R D, (1988), *Carbonation* in 'Manual for Life Cycle Aspects of Concrete in Buildings and Structures', Taywood Engineering, Perth, Western Australia

Clear K C, (1974), *Evaluation of Portland Cement Concrete for Permanent Bridge Deck Repair*, Federal Highway Administration, USA

Clifton J R, (1993), *Predicting the Service Life of Concrete*, ACI Materials Journal, Nov-Dec 1993, American Concrete Institute, USA

The Concrete Society, (1996), *Discussion Document – Developments in Durability Design and Performance-Based Specification of Concrete*, The Concrete Society, Slough, UK

The Concrete Society, (1998), *Technical Report No.51 - Guidance on the use of stainless steel reinforcement*, The Concrete Society, Slough, UK

Conference of State Road Authorities of Australia, (1953), *Highway Bridge Design Specification*, Sydney

Estes A C and Frangopol D M, (1999), *Repair Optimization of Highway Bridges Using System Reliability Approach*, Journal of Structural Engineering July 1999, American Society of Civil Engineers, USA

Frangopol D M, Lin K-Y and Estes A C, (1997), *Reliability of Reinforced Concrete Girders under Corrosion Attack*, Journal of Structural Engineering March 1997, American Society of Civil Engineers, USA

Frangopol D M, Enright M P and Estes A C, (1999*),Integration of Maintenance, Repair and Replacement Decisions in Bridge Management Based on Reliability, Optimization and Life-Cycle Cost,* Transportation Research Circular 498, Transportation Research Board, USA

Frederiksen J M, (2000), *Chloride Threshold Values for Service Life Design*, Proceedings of the 2nd International RILEM Workshop on Testing and Modelling the Chloride Ingress into Concrete, RILEM, Paris, France

Gehlen C and Schieβl P, (1999*), Probability-based durability for the Western Scheldt Tunnel*, Structural Concrete, V1, No.2, 1-7

Glass G K, Reddy B and Buenfeld N R, (2000), *The participation of bound chloride in passive film breakdown on steel in concrete*, Corrosion Science 42, Elsevier, United Kingdom

Grace W R & Co., (1994), *Engineering Bulletin – DCI Corrosion Inhibitor/No.2,* W R Grace & Co, USA

Griffiths D, Marrosszeky M and Sade D, (1987*), Site Study of Factors Leading to a Reduction in Durability of Reinforced Concrete*, Concrete Durability - Katharine and Bryant Mather International Conference ACI SP-100, American Concrete Institute

Harrison S R and Tamaschke H U, (1984), *Applied Statistical Analysis*, Prentice-Hall, Sydney

Henriksen C F and Stoltzner E, (1993*), Chloride Corrosion in Danish Road Bridge Columns*, Concrete International, American Concrete Institute, USA, August 1993

Ho D W S and Lewis R K, (1981), *The Effects of Fly Ash and Water Reducing Agents on the Durability of Concrete*, CSIRO Division of Building Research, Australia

Hobbs D W ed, (1998), *Minimum requirements for durable concrete*, British Cement Association, United Kingdom

International Organisation for Standardisation, (1997), *prEN206 Draft European Standard; Concrete – Performance, production and conformity*, ISO, Norway

Izquierdo D, Andrade C and de Rincón O, (2000), *Statistical Analysis of the Diffusion Coefficients Measured in the Piles of Maracaibo's Bridge*, Proceedings of the 2nd RILEM International Workshop on Chloride Ingress Into Concrete, RILEM, Paris, France

Kompen R, (1997), *How to Achieve Proper Reinforcement Cover in Concrete Bridges - New Specifications*, Road Research Laboratory, Public Roads Administration, Norway

Lindvall A, Andersen A and Nilsson L-O, (2000*), Chloride Ingress Data from Danish and Swedish Road Bridges exposed to Splash from De-icing Salt*, Proceedings of the 2nd International RILEM Workshop on Testing and Modelling the Chloride Ingress into Concrete, RILEM, Paris, France

Liu Y and Weyers R E, (1998*), Modeling the Time-To-Corrosion Cracking in Chloride Contaminated Reinforced Concrete Structures,* ACI Materials Journal, November-December 1998, American Concrete Institute, USA

Maage M, Helland S, Poulsen E, Vennesland Ø and Carlsen, (1996), *Service Life Prediction of Existing Concrete Structures Exposed to Marine Environment*, ACI Materials Journal, American Concrete Institute, November-December 1996, USA

Malhotra V M, (1977*), Contract Strength Requirements – Cores Versus In Situ Evaluation*, ACI Journal, American Concrete Institute, USA

Markeset G, (2000), *Cost Optimal Design, Construction and Maintenance of Concrete Quays and Jetties*, Concrete Remediation, Design and Long Life Solutions Seminars, Australian Stainless Steel Development Association, Brisbane

Marrosszeky M and Chew M, (1990*), Site Investigation of Reinforcement Placement on Buildings and Bridges*, Concrete International, American Concrete Institute, USA

Marrosszeky M and Chew M, (1989*), Site Investigation of Reinforcement Placement on Buildings and Bridges*, CIA News, Concrete Institute of Australia, Sydney

Maunsell G and Partners, (1959), *New Hobart Bridge,* Tender documents, Public Works Department, Hobart

Maunsell G and Partners, (1971), *The New Gorge Bridge, Launceston,* Contract documents, Public Works Department, Hobart

M^{c}Gee R W, (1993), *Princess River Bridge - Testing to Destruction,* Proceedings of the Concrete Institute of Australia Biennial Conference, Concrete Institute of Australia, Sydney

Mehta P K, (1997), *Durability – Critical Issues for the Future' in 'Concrete International,* American Concrete Institute, USA

Melchers R E, (1987), *Structural Reliability – Analysis and Prediction,* Ellis Horwood, Chichester, UK

Moore D S and M^{c}Cabe G P, (1989), *Introduction to the Practice of Statistics,* W H Freeman and Company, USA

Morgan P R, Ng T E, Smith N H M and Base G D, (1982*), Reinforcement Placement in Rectangular Concrete Slabs in Australia,* Civil Engineering Transactions CE24 No.1, The Institution of Engineers Australia, Canberra

Morgan P R, Ng T E, Smith N H M and Base G D, (1982), *How Accurately Can Reinforcing Steel Be Placed? Field Tolerance Measurement Compared to Codes,* Concrete International, Vol.4 No.10, American Concrete Institute, USA

Morgan P R, Smith N M H and Zyhajlo E, (1986*), Slab Reinforcement Location Versus Code Specification,* Civil Engineering Transactions, The Institution of Engineers, Australia, Canberra

National Association of Australian State Road Authorities (NAASRA), (1965), *Highway Bridge Design Specification,* NAASRA, Sydney

National Association of Australian State Road Authorities (NAASRA), (1970), *Highway Bridge Design Specification,* NAASRA, Sydney

National Association of Australian State Road Authorities (NAASRA), (1970), *Highway Bridge Design Specification- 1970 (Metric Addendum),* NAASRA, Sydney

National Association of Australian State Road Authorities (NAASRA), (1976), *Highway Bridge Design Specification- 1976* , NAASRA, Sydney

Nilsson L-O, Poulsen E, Sandberg P, Sørensen H E and Klinghoffer O, (1996), *HETEK, Chloride penetration into concrete, State of the art, Transport processes, corrosion initiation, test methods and prediction models*, The Road Directorate, Copenhagen, Denmark

Nilsson L-O, Andersen A, Luping T and Utgenannt, (2000*), Chloride Ingress Data from Field Exposure in a Swedish Road Environment,* Proceedings of the 2nd International RILEM Workshop on Testing and Modelling the Chloride Ingress into Concrete, RILEM, Paris, France

Ohta T, Sakai K, Obi M and Ono S, (1992*), Deterioration in a Rehabilitated Prestressed Concrete Bridge*, American Concrete Institute Materials Journal Vol. 89 No.4, USA

Palisade Corporation, (1997), *@Risk – Advanced Risk Analysis for Spreadsheets*, Palisade Corporation, Newfield, NY, USA

Parrott P J, (1994), *Design for Avoiding Damage Due to Carbonation-Induced Corrosion* in Proceedings of 3rd Canmet-ACI International Conference on Durability of Concrete, American Concrete Institute Publication ACI SP145, USA

Pettersson K, (1992*), Corrosion threshold value and corrosion rates in reinforced concrete*, Swedish Cement and Concrete Research Institute, Stockholm

Prezzi M, Geyskens and Montiero, (1996), *Reliability Approach to Service Life Prediction of Concrete Exposed to Marine Environments*, ACI Materials Journal, Nov-Dec 1996, American Concrete Institute, USA

Port Authorities of Hobart, Burnie, Devonport and Launceston, (1997*), Tasmania Tides*, Tasmania

Proceq, (1986), *Operating Instructions – Rebar Locator PROFOMETER 3*, Proceq SA, Zurich, Switzerland

Rostam S R, (1999), CEB Design Guide and the DuraCrete Design Manual, DuraNet/CEN TC 104 Workshop – Design of Durable Structures, Berlin

Schieβl P and Raupach M, (1997), *Laboratory Studies and Calculations on the Influence of Crack Width on Chloride-Induced Corrosion of Steel in Concrete*, ACI Materials Journal Jan-Feb 1997 , American Concrete Institute, USA

Schuëller G I, (1985*), Approaches to Service Life Prediction of Metals in the Nuclear Industry*, in 'Problems in Service Life Prediction of Building and Construction Materials', Martinus Nijhoff Publishers, Dordrecht, Netherlands

Shayan A, (2001*), Management of Concrete Structures to Extend their Service Life*, AUSTROADS, Sydney

Sharp B, (1997), *Criteria for cover - a "black hole"*, Concrete Vol.31 No.6, The Concrete Society, Slough, United Kingdom

Sirivivatnanon V and Cao H T, (1991*), Quality Assurance of Concrete Structures - Analysis of In-Situ Concrete Cover*, Civil Engineering Transactions Vol. CE33 No.2, The Institution of Engineers, Australia, Canberra

Snedecor G W and Cochran W G, (1980), *Statistical Methods*, The Iowa State University Press, Iowa, USA

Somerville G, (1986), *The design life of concrete structures*, The Structural Engineer, Vol 64A, No.2, p60, Institution of Structural Engineers, UK

SPSS, (1998), *SPSS Base 8.0 - User's Guide*, SPSS, Chicago, USA

SPSS, (1998), *SPSS Base 8.0 - Applications Guide*, SPSS, Chicago, USA

Standards Australia, (1979), *AS1012.15-1979, Methods of testing concrete, Part 15: Method for the estimation of portland cement content of hardened concrete*, Standards Australia, Sydney

Standards Australia, (1991), *Methods of testing concrete, Method 14: Method for securing and testing cores from hardened concrete for compressive strength*, Standards Australia, Sydney

Standards Australia, (1994), *AS3600 - Concrete Structures*, Standards Australia, Sydney

Sterritt G and Chryssanthopoulos M K, (1999), *Probabilistic Limit State Modelling of Deteriorating R C Bridges Using a Spatial Approach*, Proceedings of current and future trends in bridge design construction and maintenance October 1999, Thomas Telford, UK

Stewart M G and Rosowsky D V, (1998), *Time-Dependent Reliability of Deteriorating Reinforced Concrete Bridge Decks*, Structural Safety, Vol.20, No.1, pp 99-109

Stewart M G, (1997), *Concreting Workmanship at Its Influence on Serviceability Reliability*, ACI Materials Journal, November-December 1997, American Concrete Institute, USA

Stewart M G, (1998), *Risk-based Approaches to the Assessment of Existing Bridges*, Research Report No.168.10.1998, The University of Newcastle

Symons M G, (1992), *Mix Design* in Ryan W G and Samarin A, 'Australian Concrete Technology', Longman Cheshire, Melbourne

Taylor W H, (1977), *Concrete Technology and Practice*, McGraw-Hill Book Company, Sydney

Tuutti K, (1982), *Corrosion of Steel in Concrete*, Cement och Betong Institutet, Stockholm, Sweden

Vu K A T and Stewart M G, (2000), *Structural reliability of concrete bridges including improved chloride-induced corrosion models*, Structural Safety Vol 22 No 4, Elsevier Science Ltd, United Kingdom

Walpole R E and Myers R H, (1978), *Probability and Statistics for Engineers and Scientists*, Macmillan Publishing, New York, USA

Warner R F, Rangan B V and Hall A S, (1982), *Reinforced Concrete*, Pitman Publishing, Carlton, Victoria

Washa G W and Wendt K F, *Fifty Year Properties of Concrete*, (January 1975), ACI Journal, USA

Washa G W, Saemann J C and Cramer S M, *Fifty Year Properties of Concrete Made in 1937*, (July-August 1989), ACI Materials Journal, USA

Weyers R E, (1998), *Service Life Model for Concrete Structures in Chloride Laden Environments*, ACI Materials Journal, American Concrete Institute Jul-Aug 1998, USA

Wood S L, (1991), *Evaluation of the Long-Term Properties of Concrete*, ACI Materials Journal 88 (6), American Concrete Institute, USA

ON THE

SERVICE LIFE MODELLING

OF

TASMANIAN CONCRETE BRIDGES

APPENDIX

by

Rodney W. M^{c}Gee ESM FIEAust CPEng

BE(Hons), ME, GDipBusProfMan, ADEM, BSocSc(EmMan)

University of Tasmania

November 2001

1 INTRODUCTION

1.1 GENERAL

This appendix includes detailed data on climate, environment, concrete performance and cover measurements, and the use of parameters derived from that data to develop service life models for concrete structures.

2 TEST METHODS

2.1 GENERAL

This section provides an overview of the investigation processes and test methods that were used for the analysis of water and concrete samples and the measurement of cover to reinforcement.

2.2 WATER SAMPLES

All samples were analysed by the Tasmanian Government Analytical and Forensic Laboratory with methods accredited by NATA.

2.2.1 PH DETERMINATION

Measurement was based on Standard Methods for the Examination of Water and Wastewater 19th Edition 1995. 4500H. pH Value.

The basic principle of electrometric pH measurement is the determination of the activity of hydrogen ions, generally using an indicating (glass) electrode and a reference electrode or a variation of this combination. The pH measuring instrument is calibrated potentiometrically with standard buffer solutions.

2.2.2 CHLORIDE AND SULPHATE DETERMINATION

Measurement was based on Standard Methods for the Examination of Water and Wastewater, 19th Edition 1995. 4110C. Single-Column Ion Chromatography with electronic suppression of Eluent Conductivity and Conductivity Detection (Proposed) and instrument manufacturers' recommendations.

A small portion of a filtered homogeneous aqueous sample or a sample containing no particles larger than 0.45μ is injected into an ion chromatograph. The sample merges with the eluent stream and is pumped through the chromatographic system. Anions are separated on the basis of their affinity for the active sites of the column packing material. Conductivity detector readings are used to compute concentrations.

2.2.3 CHLORIDE DETERMINATIONS; HIGH LEVELS (SALINE SAMPLES)

Measurement is based on an electrometric titration method for the determination of chloride in water.

The chloride is determined by electrometrically titrating a sample of water with silver nitrate of a known concentration to a given end-point.

2.3 CONCRETE SAMPLES

2.3.1 MASS PER UNIT VOLUME

Test portions from each specimen were initially oven dried at 105°C. The specimens were then tested for Mass per Unit Volume in accordance with AS1012 Part 12-1986, Section 1, Method 1.

2.3.2 CEMENT CONTENT

Prepared samples were tested for determination of cement content in accordance with AS1012 Part 15-1979 EDTA titrimetric method (acid extractable calcium). It was assumed that cement of 64.5% calcium oxide content was the sole source of extractable calcium. Loss upon ignition of prepared samples was determined and the values used to correct cement contents to a dry ingredients basis. This procedure yields the cement content in % of total sample. This figure was then converted to kg/m^3 by using the previously determined mass per unit volume of the core that had been oven dried to constant mass. The Standard notes that, where constituent aggregate samples are available and the determined calcium oxide content of the constituent aggregate is less than 5 percent, an analytical accuracy within $\pm$ 1 percent can be expected. Where constituent aggregate samples are not available, as is the case with the majority of analysed cores, results will be influenced by the presence of calcium oxide in sand, aggregate and any chemical and mineral admixtures and the accuracy will be reduced.

Taylor (1977) states that the order of accuracy for the test is of the order of $\pm$10%, and is likely to be more accurate for rich mixes than for lean ones.

2.3.3 WATER/CEMENT RATIO

The water/cement ratio was calculated by determining the original water content of the concrete at the time of hardening, ascertained by immersing the sample of hardened concrete in water for 24 hours and then dehydration at 593°C for 2 hours. The resulting % total moulding water was converted to kg/m^3 using the mass per unit volume of the concrete and then corrected for aggregate absorption. The water/cement ratio was then calculated using the previously determined cement content.

2.3.4 CHLORIDE CONTENT

Total chloride contents were determined on samples, after extraction of chloride with 1M nitric acid, using mercury thiocyanate spectrophotometric method.

2.3.5 SULPHUR TRIOXIDE

Total sulphur trioxide contents were determined on samples after extraction with 1M hydrochloric acid, using the classical gravimetric procedure of precipitation with barium chloride solution, filtration, washing and ignition of the barium sulphate precipitate.

2.3.6 CARBONATION DEPTH

Each test specimen was initially split axially to expose a fresh uncarbonated surface. This fresh surface was then sprayed with phenolpthalein solution to enable determination of the depth of carbonated concrete by direct measurement.

Phenolpthalein is a pH indicator which turns a bright red/violet colour at a pH of 10 but is colourless at a pH of 8. It is commonly used to indicate the extent of carbonated concrete as uncarbonated concrete assumes a bright red/violet colour when treated with phenolpthalein.

2.3.7 PERMEABLE VOIDS

The test method consists of drying the specimens at 100 to 110°C to constant weight (for a minimum of 48 hours), immersion of the specimens in water at 21°C until uptake of water is minimised (for a minimum of 48 hours), then boiling the specimens for 5 hours and subsequently obtaining weights in air and immersed in water. In this method, the volume of permeable voids is defined as that void volume which is emptied during the specified drying and filled with water during the subsequent

immersion and boiling. Any voids which do not empty during drying or which do not fill with water during wetting are not included in the interconnected pore space determined by this method.

2.4 COVER TO REINFORCEMENT

Cover to reinforcement was measured using Profometer 3 covermeters manufactured by the Proceq company of Switzerland. The machines have probes for cover, cover at significant depths and reinforcement diameter, and a test block for calibration.

The procedure for measuring cover with the instrument is as follows:

- Hold the probe in the air; if "0" does not appear automatically, press the switch
- Set the reinforcement diameter on the switch; the diameter is generally available from drawings but, if not, is obtained using the diameter probe or a default value of "16mm" used
- The probe is moved over the surface of the concrete until the minimum value, indicated by a 'beep' of the machine, is obtained
- Raw values are then recorded for later analysis.

In the subsequent analysis, a calibration factor of 1.1 is applied to the raw data based on measurements of a number of exposures of reinforcement of a range of diameters and covers from a number of structures.

3 TASMANIAN BRIDGE STOCK

3.1 INTRODUCTION

This section provides a description of each bridge for which an investigation was undertaken, an overview of that bridge's condition and climatic and environmental data for each structure.

3.2 BRIDGE DESCRIPTIONS

Camp Creek Bridge

Camp Creek Bridge is a reinforced concrete slab bridge located near Currie on King Island, with length of 4.1m and width of 12.8m. The structure was built in 1934 and widened in 1957.

A corrosion investigation was undertaken in 1996 because of spalling, cracking and exposed reinforcement in the abutments and deck.

Leven River Bridge

Leven River Bridge is a seven span bridge with an overall length of 130.2m and width of 9.5m, including a footpath on the upstream side. The superstructure comprises steel beams with a concrete deck. Piers are supported on reinforced concrete piles, with infill walls between the piles above water level. It was built in 1934, and is located on Hobbs Parade in Ulverstone.

A corrosion investigation was undertaken in 1995 because of extensive staining and cracking in the piers. Some localised spalling was evident in the deck, with cracking and spalling also of the concrete fence.

Porky Creek Bridge

Porky Creek Bridge is a single span bridge comprising a reinforced concrete deck supported on steel beams and reinforced concrete abutments. It is located approximately 7km north of Currie on King Island. It has a length of 10.1m and width of 6.1m, and was built in 1935.

A corrosion investigation was undertaken in 1996 because of significant cracking, delamination, spalling and exposure of reinforcement on the deck soffit.

Peggs Creek Bridge

Peggs Creek Bridge is a three span reinforced concrete T-beam structure located on the Bass Highway near Smithton. It has an overall length of 10.3m, with 2.1m cantilever end spans and was built in 1938.

A corrosion investigation was undertaken in 1995 because of extensive staining, cracking and spalling in both superstructure and substructures.

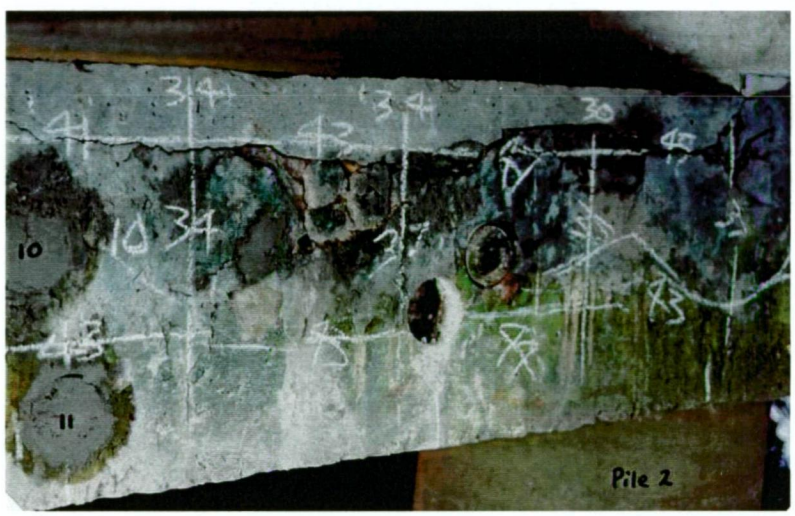

Figure A3.1 – Cracking of Peggs Creek Bridge pier crosshead

Replacement of the bridge is programmed.

Orielton Rivulet Bridge

Orielton Rivulet Bridge was a single span reinforced concrete T-beam bridge located on the Tasman Highway north of Sorell. It was built in 1938 and had an overall length of 9.6m and width of 7.1m.

The bridge was demolished as part of a road upgrading in 1996 and concrete samples taken to assess durability performance.

Saltwater Creek Bridge

Saltwater Creek Bridge was a single span reinforced concrete T-beam bridge located on the Tasman Highway north of Sorell. It was built in 1939 and had an overall length of 11.9m and width of 7.7m.

The bridge was demolished as part of a road upgrading in 1996 and concrete samples taken to assess durability performance.

Emu River Bridge

Emu River Bridge is a reinforced concrete bowstring arch bridge located on the Bass Highway at Burnie. It was built in 1939, and has an overall length of 43m and width of 14.8m.

A corrosion investigation was undertaken in 1995 because of spalling and reinforcement corrosion in substructures, beams, slabs and columns.

The installation of a cathodic protection system and the application of sealers and coatings are programmed.

Detention River Bridge

Detention River Bridge is a five span reinforced concrete T-beam bridge located on the Bass Highway approximately 20km west of Boat Harbour. It was built in 1940 and has an overall length of 70m and width of 7.6m.

A corrosion investigation was undertaken in 1996 because of cracking, staining, delamination and spalling of the pier columns and infills, particularly in the tidal region. Lesser amounts of corrosion were evident in the abutments and beams. A number of previous patch repairs, likely to be epoxy based, had failed.

Planning for replacement of the bridge has been initiated.

Mountain Creek Bridge

Mountain Creek Bridge is a reinforced concrete slab bridge on the Channel Highway. It was built in 1942/43 and has an overall length of 5.2m and width of 8.4m.

The deck was replaced in 1994 because of severe corrosion of the deck slab. The original mass concrete abutments were retained, notwithstanding the significant chloride ingress, because of the absence of reinforcing steel.

Faggs Gully Creek Culvert

Faggs Gully Creek Culvert is a twin cell box culvert located on the East Derwent Highway in Lindisfarne. It has an overall length of 45m and width of 4.7m. The original section of insitu reinforced concrete culvert was built in 1943. The culvert was extended with the same form of construction in 1951, and again with precast crown units in 1975.

A corrosion investigation was undertaken in 1994 to assist with a residual life assessment prior to a proposed further widening.

Surges Creek Bridge

Surges Creek Bridge is a three span reinforced concrete T-beam bridge located on the Huon Highway approximately 9km south of Geeveston. It has an overall length of 21.3m and width of 7.7m and was built in 1944.

A corrosion investigation was undertaken in 1995 because of spalling in the beams and fences.

Higgins Creek Bridge

Higgins Creek Bridge is a single span reinforced concrete stiffened kerb slab bridge with a length of 4.6m and overall width of 8m. It was built in 1944 and is located on the Huon Highway just north of Raminea. It is subject to tidal activity.

A corrosion investigation was undertaken in 1996 because of spalled concrete and exposed reinforcement at the edge of the deck.

Carlton River Culvert

The structure is a five cell insitu reinforced concrete box culvert of length along the culvert centreline of 7.5m and width of 21.6m. It was built in 1945 and is located on the Arthur Highway near Copping.

A corrosion investigation of the culvert and nearby bridge was undertaken in 1994 because of spalling and exposed and corroded reinforcement in the kerbs and fences.

Carlton River Bridge

Carlton River Bridge is a three span reinforced concrete stiffened kerb structure located on the Arthur Highway near Copping. It was built in 1945 and has an overall length of 29.6m and width of 7.8m.

A corrosion investigation was undertaken in 1994 because of significant corrosion and spalling in the kerbs and fence.

Rileys Creek Bridge

Rileys Creek Bridge is a three span reinforced concrete stiffened kerb bridge located on the Huon Highway south of Geeveston. It was built in 1945 and has an overall length of 18.6 and width of 7.7m.

A corrosion investigation was undertaken in 1995 because of corrosion induced spalling of the deck soffit and fences.

Scopus Creek Bridge

Scopus Creek Bridge was a single span reinforced concrete T-beam bridge located on the Montagu Main Road near Smithton. It was built in 1947 and had an overall length of 9.4m and width between kerbs of 5.5m. The T-beams were built into reinforced concrete cantilever abutments.

The bridge was demolished and replaced with a pipe culvert in 1992 because of severe near vertical cracking in the beams adjacent to the abutments, which may have been attributable principally to restrained shrinkage.

Concrete samples and cover measurements were taken prior to demolition to assess durability performance.

Bridgewater Bridge

Bridgewater Bridge carries the Midland Highway across the Derwent River approximately 15km north of Hobart. It is in an estuarine environment, subject to tidal activity. The salinity of the river is variable, depending on seasonal runoff, but may at times be that that of seawater. The salinity also varies through the water column because of the wedge associated with the mixing of salt and fresh water.

The bridge comprises a lift span and two flanking spans of steel truss construction, with approach spans comprising steel girders with non-composite reinforced concrete deck. A railway is carried on the northern side of the bridge. Approach span piers are reinforced concrete columns and walls supported on timber piles. The lift and flanking spans are supported on circular reinforced concrete caissons. The bridge was completed in 1947, with the construction period having been extended by material shortages during the Second World War. It has an overall length of 338m.

A corrosion investigation was undertaken in 1996 because of extensive cracking, staining and spalling of the approach span piers and delamination of parts of the deck soffit.

Remedial works, involving cathodic protection, concrete repair and coating, were completed in 1998.

Lilla Villa Bridge

Lilla Villa Bridge is a 12 span reinforced concrete T-beam bridge of overall length 147m and width 7.6m located on the Tasman Highway near Bicheno on Tasmania's east coast. It was completed in 1947. A corrosion investigation was undertaken in 1992 as a result of spalling of concrete railing, kerbs, beams and piers.

Maclaines Creek Bridge

Maclaines Creek Bridge is located on the Tasman Highway at Triabunna. It was built in 1948 and is a 21 span reinforced concrete T-beam bridge with an overall length of 262m and width of 8.4m. The river span is of 18.2m, including a suspended span, with 16.8m flanking spans. Approach spans have a span of 12m.

A corrosion investigation was undertaken in 1997, principally because of corrosion of the stepped joints in the river span. There was additionally some localised spalling associated with low covers to reinforcement.

Stanley Dock

Stanley Dock provides berthing and unloading facilities for fishing vessels in the harbour at Stanley in the State's north west. Part of the dock also supports a fish processing factory. It is consequently exposed to chlorides from direct exposure to sea water in submerged and tidal zones, in the splash zone and from runoff from the unloading, storage and processing of fish.

Figure A3.2 - Stanley Dock beam and slab

The original dock was built prior to 1950, and incorporates precast piles and beams supporting an insitu concrete deck and fish holding tanks. The 1964 extension is of similar construction. Both sections are in poor condition, with extensive cracking, spalling and staining. There was no distress evident in the subsequent 1993 extension at the time of the investigation.

Because of the poor condition of the structure, a corrosion investigation was undertaken in 1995.

Tasman Highway Culverts

The three culverts were built circa 1950, and are located approximately 7km north of Bicheno on the Tasman Highway. They have a width between kerbs of 7.5m and a clear span of 2.8m. They consist of insitu reinforced concrete stiffened kerb deck slabs supported on mass concrete abutments with spread footings.

A corrosion investigation was undertaken in 1994 because of spalling and reinforcement corrosion in the soffits of deck slabs.

Wardlaws Creek Bridge

Wardlaws Creek Bridge is a three span reinforced concrete bridge of overall length 33.5m and width 7.7m. It was built in 1951. The central span comprises reinforced concrete T-beams, with shorter end spans of reinforced concrete slabs having drop panels at the piers to match the central span structural depth.

A corrosion investigation was undertaken in 1992 because of extensive spalling of the southern drop panel and corrosion defects in a number of other locations. Repairs with polymer modified cementitious repair mortars and coatings have subsequently been undertaken.

Flights Creek Bridge

Flights Creek Bridge is a three span reinforced concrete bridge located on the Channel Highway south of Kettering. It has an overall length of 17.3m and width of 7.8m, and was built in 1951. It is located adjacent to a beach and exposed to tidal flows and salt spray.

The bridge has corrosion induced spalling of the beams and deck, together with honeycombing and flexural cracking. A corrosion investigation was undertaken in 1995.

King Island Main Road Bridge

The King Island Main Road Bridge is a single cell reinforced concrete box culvert located approximately 17km north of Currie on King Island. It was built in 1953 and has a length of 1.8m along the road centreline and width of 7.4m.

A corrosion investigation was undertaken in 1996 because of cracking, delamination, spalling and exposed reinforced of a number of the deck units.

East Arm Creek Culvert

East Arm Creek Culvert is a single span reinforced concrete box culvert located on the East Tamar Highway approximately 27km north of Launceston. It was built in 1956 and widened shortly after construction and again on 1993. A corrosion investigation was undertaken in 1996 as part of an assessment for further modifications.

Ralphs Bay Canal Bridge

The bridge is a single span reinforced concrete slab with stiffened kerb of span 8.2m and width between kerbs of 6.7m. It is supported on precast concrete piles with abutment fill retained by precast reinforced concrete panels supported by the piles. The bridge is located at Lauderdale at the mouth of the Ralphs Bay Canal.

The bridge was built in 1956. A corrosion investigation was undertaken in 1994 because of cracking, spalling and staining of the substructures.

Argent River Bridge

Argent River Bridge is a single span reinforced concrete slab of overall length of 9.8m and width 7.9m completed in 1957.

A corrosion investigation was undertaken in 1995 because of corrosion damage, including one localised area of severe damage.

Figure A3.3 – Argent River Bridge

Egg Island Creek Bridge

Egg Island Creek Bridge is a three span reinforced concrete slab bridge with an overall length of 10.3m and overall width of 9.4m. It was built in 1956 and is located on the East Tamar Highway approximately 25km north of Launceston.

A corrosion investigation was undertaken in 1996 because of spalling and reinforcement corrosion, generally associated with low reinforcement covers on the edges of the deck.

Sorell Causeway Bridge

Sorell Causeway bridge was completed in 1957 and is the first prestressed concrete bridge on the classified road network and the second in the State. It comprises 34 spans of approximately 13.5m, with an overall length of 457m and width of 8.8m. The superstructure comprises 14 post-tensioned concrete bulb-T beams transversely prestressed without insitu concrete topping but with asphalt wearing surface. The bridge is supported on trestled piers using prestressed concrete piles. Ducts for prestressing of the beams are likely to have been formed by using an inflated rubber tube during casting of the concrete, with the tube subsequently being deflated and withdrawn.

A corrosion investigation was undertaken in 1994 because of cracking, staining and spalling of the substructures and beam ends. Longitudinal cracking of the beams, attributable to corrosion of the prestressing strands, has subsequently been identified with the number of beams affected increasing annually.

Figure A3.4 – Cracking of Sorell Causeway prestressed concrete beam

Replacement of the bridge has been initiated.

Ringarooma River Bridge

Ringarooma River Bridge is a three span reinforced concrete T-beam bridge, including a central suspended span, located on the Tasman Highway at Moorina, approximately 10km east of Derby. It has an overall length of 35.5m and width of 7.9m and was built in 1957.

A corrosion investigation was undertaken in 1995 because of distress in the stepped joints of the suspended span.

Pats River Bridge

Pats River Bridge is a three span bridge of overall length 23.3m and width 7.7 completed in 1957. The superstructure comprises steel girders with a reinforced concrete deck. It is located near the west coast of King Island.

A corrosion investigation was undertaken in 1992 because of corrosion damage, particularly to the pier columns.

Repairs, comprising cathodic protection and coatings, have subsequently been undertaken.

Cormiston Creek Bridge

Cormiston Creek Bridge is a single span reinforced concrete slab bridge located on the West Tamar Highway approximately 10km north of Launceston. It was built in 1958 and has an overall length of 9.2m and width of 12.2m.

A corrosion investigation was undertaken in 1996 because of spalling of abutments and the bridge's exposure to tidal activity.

Golden Fleece Bridge

Golden Fleece Bridge is a six span reinforced concrete slab bridge located on the Tasman Highway at St Helens. It is supported on reinforced concrete piles, and has an overall length of 61m and width of 9.9m including a downstream footway. It was built in 1958.

Figure A3.5 – Cracking of Golden Fleece Bridge pile

A corrosion investigation was undertaken in 1995 because of corrosion induced distress throughout most of the structure, including longitudinal cracking of piles and crossheads. Previous repairs, likely to have been epoxy based and often associated with distress, were evident. A cathodic protection system was installed during 1999.

Wrinklers Bridge

Wrinklers Bridge is a two span reinforced concrete stiffened kerb bridge with an overall length of 18m and width of 7.8m, built in 1959. It is located on the Tasman Highway, approximately 1km north of Scamander.

A corrosion investigation was undertaken in 1995 because of extensive corrosion induced spalling, cracking and staining throughout the structure, particularly the deck soffit, edge beams, piles and bridge fences.

Figure A3.6 – Corrosion of Wrinklers Bridge superstructure

Reedy Creek Bridge

Reedy Creek Bridge is a single span reinforced concrete slab bridge located on the Tasman Highway approximately 10 km south of St Helens. It has an overall length of 8.5m and width between kerbs of 6.7m. It was built in 1959.

A corrosion investigation was undertaken in 1994 because of spalling due to corroding reinforcement, particularly in the sides of the deck.

Princess River Bridge

Princess River Bridge was a reinforced concrete T-beam bridge with two 10.5m spans and a width of 6.7m between kerbs. The abutments and pier were supported on square reinforced concrete piles.

It was located on a section of the Lyell Highway, about 20km from Queenstown, which was inundated by the King River power development. A comprehensive test program, including structural, construction and durability aspects, was undertaken immediately prior to flooding.

Symons Creek Bridge

Symons Creek Bridge is a single span reinforced concrete T-beam structure located on the East Tamar Highway approximately 18km north of Launceston. Its length and width are both 9.7m and the bridge was completed in 1959.

A corrosion investigation was undertaken in 1996 because of spalling and exposure of reinforcement on the eastern edge of the deck.

Denison River Bridge

Denison River Bridge is a four span reinforced concrete stiffened kerb structure with equal span lengths of 8.3m and an overall width of 7.8m. Piers are frame structures comprising a reinforced concrete crosshead supported on a single row of five precast reinforced concrete piles. Abutments are of similar construction. The bridge is located on the Tasman Highway approximately 10km north of Bicheno and was built in 1960.

A corrosion investigation was undertaken in 1995 because of corrosion induced spalling and cracking of the piers, deck and fences.

Boggy Creek Bridge

Boggy Creek Bridge was built in 1960 and is located on the Tasman Highway at St Helens. It is a single span reinforced concrete slab bridge with a length of 9.4m and width between kerbs of 7.2m. The abutments are supported on precast reinforced concrete piles.

The bridge is exposed to salt spray and a corrosion investigation was undertaken in 1994 because of corrosion induced spalling and cracking, particularly in the eastern face of the deck and the northern abutment crosshead.

Tasman Bridge

Tasman Bridge is the largest bridge in Tasmania. It was opened to traffic in 1964 and completed in 1965. It has an overall length of 1.5km and carries 5 lanes of traffic, after widening from 4 lanes as part of the restoration after the *1975 s.s. Lake Illawarra* collision.

While the bridge is generally performing well, durability related distress had become evident in the western interchange columns by the early 1970's. Epoxy based repairs undertaken as part of the restoration proved ineffective, and a corrosion investigation was undertaken in 1992/93 to determine an appropriate management strategy. Although the investigation focussed on the western interchange, it included limited sampling of the main viaduct.

Repairs to the western interchange columns have involved the installation of a cathodic protection system.

Cam River Bridge

Cam River Bridge is a seven span post-tensioned I-girder bridge of overall length 129m and overall width of 11.0m. It is supported on both piled and spread footing substructures, with piles being precast octagonal reinforced concrete.

It was built in 1964 and is located at Somerset in the State's north west.

A corrosion investigation was undertaken in 1996 because of spalling, cracking and staining in a number of piles. A cathodic protection system has subsequently been installed.

Newmans Creek Bridge

Newmans Creek Bridge is a 2 span reinforced concrete U-beam bridge, supported on reinforced concrete piles. It has an overall length of 18.9m and width of 7.9m. It was built in 1969.

A corrosion investigation was undertaken in 1995 because of cracking, spalling and corrosion staining in the pier piles.

Remedial works have involved the installation of a cathodic protection system to the piers and a coating to exposed concrete surfaces.

Huon Highway Stock Underpass

The structure is a single cell box culvert type structure which is now used as a pedestrian underpass. It was built in 1969, has an overall length of 20.8m and incorporates 17 precast crown units of nominal dimensions 2.4m by 2.4m. 15 of the crown units were spalled due to corrosion and sampling was undertaken as part of a broader investigation into the performance of precast concrete box culverts.

Figure A3.7 - Spalling of Huon Highway Underpass crown units

Hunterston Culvert

Two reinforced concrete box culverts incorporating precast crown units are located on the Lake Highway at Hunterston. Culvert No. 1979 is a 2 cell culvert of overall length 9.8m incorporating 16 precast crown units of nominal dimensions 1.8m wide by 1.8m high. It was built in 1969. There is spalling and cracking of the crown units from corrosion and sampling was undertaken as part of the precast box culvert investigation.

Victoria Bridge

The Victoria Bridge carries the Bass Highway over the Mersey River at Devonport. It was built in 1970 and has an overall length of 185.9m and width of 12.2m. The superstructure comprises 5 spans of steel girders with an insitu concrete deck.

Concrete testing to assist with the durability design of the new structure immediately upstream indicated significant chloride ingress in some locations. A more comprehensive corrosion investigation was undertaken in 1995 to better understand the condition of the structure.

Coal River Bridge abutments

The original Coal River bridge was a timber structure with concrete abutments which was replaced in 1993 by a prestressed concrete bridge. A durability investigation of the abutments was undertaken during the design phase to determine whether or not they could be incorporated in the new structure; the investigation indicated that their expected life was commensurate with that of the new structure and they were thus incorporated with the application of coatings to enhance durability.

Grassy Wharf

Grassy Harbour was built between May 1970 and May 1972. It includes a marginal wharf, originally 85m long and 15m wide, built from reinforced concrete precast deck slabs and insitu deck supported on octagonal steel piles.

Deterioration of the superstructure became evident in 1980, when spalling concrete from the soffit of the deck slabs at the inner end of the wharf was observed, along with slight longitudinal cracking in the lower sides of the supporting concrete beams.

A comprehensive visual inspection was undertaken in 1984, followed by a diagnostic investigation in 1988. As a result of the investigations, an expanded mixed metal oxide mesh anode cathodic protection system was installed, with commissioning in September 1992.

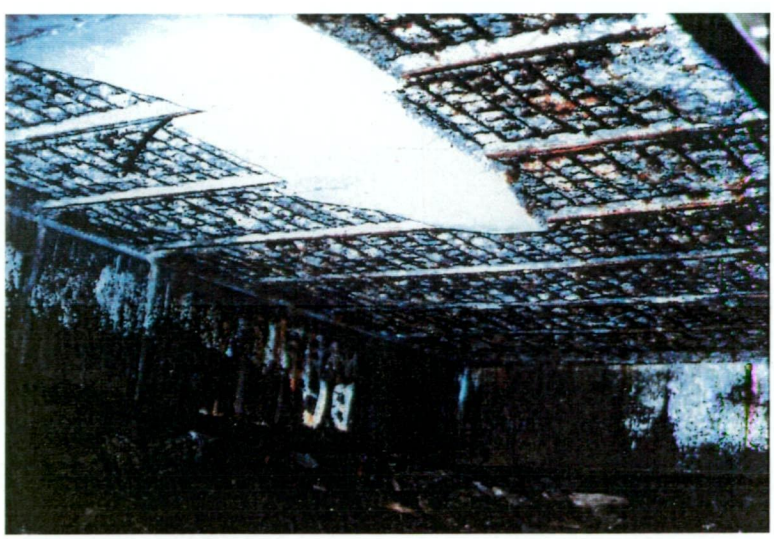

Figure A3.8 - Soffit of Grassy Wharf

Freestone Point Developmental Road Culvert

Freestone Point Developmental Road Culvert is located near Triabunna. It is a 2 cell precast box culvert, with each cell comprising 7 units of nominal width 2.7m and height 1.35m. It was built in 1975 and has an overall length of 8.6m. 12 of the 14 precast units have spalled, exposing reinforcement. Samples were taken as part of the investigation of the performance of precast box culverts.

Faulkners Rivulet Culvert

Faulkers Rivulet Culvert is located on the Brooker Highway at Claremont. It comprises an insitu central section, with ends of precast culvert crown units. It has 2 cells, an overall length of 113.9m, and was built in 1976. Precast crown units have a nominal width of 2.7m and height of 2.4m.

79 of the 105 precast units are spalled due to corrosion, with 89 honeycombed from construction. The insitu section is performing well. Samples were taken as part of the investigation into the performance of precast box culvert units.

Cusicks Creek Culvert

Cusicks Creek Culvert is a 3 cell reinforced concrete box culvert located on the Coles Bay Tourist Road. It was built in 1982, has an overall length of 9.7m and comprises 24 precast crown units of nominal height 0.9m and span 1.2m. There is extensive spalling of the units due to corrosion and sampling was undertaken as part of the precast culvert investigation.

Figure A3.9 – Spalling of Cusicks Creek Culvert crown units

Runnymede Culvert

Runnymede Culvert is a twin cell box culvert incorporating precast crown units. It has an overall length of 12.2m and comprises 20 crown units of nominal dimensions 1.8m high and 4m wide. It was completed in 1992. It is generally in good condition, but with cracking of 4 precast units.

Samples were taken as part of an investigation into the durability performance of precast crown units.

Burnie Port Access Bridge

The Burnie Port Access Bridge is a single span prestressed concrete bridge of overall length 9.3m and width 27.3m. It was built in 1975. A collision in January 1993 involving an overheight vehicle extensively damaged two of the beams, necessitating their replacement. The repairs provided an opportunity to take samples for analysis.

Vale River Culvert

Vale River Culvert is a 3 cell culvert located near Cradle Mountain in the State's north west. Outer cells are of precast concrete crown units with the centre cell formed by a precast link slab supported on the outer units. Cells are nominally 3.4m wide and 1.5m high, with the culvert having an overall length of approximately 23m. It was built circa 1986.

A corrosion investigation was undertaken in 1996 because of significant cracking and lime leaching and deposition, particularly in the south eastern corner.

Deloraine Rail Underpass

Deloraine Rail Underpass was a single span bridge of overall length 9m and width 12.5m located on the Bass Highway near Deloraine built in 1989. The superstructure comprised pretensioned concrete planks with an insitu reinforced concrete deck. Abutments were of Reinforced Earth.

The bridge was demolished as part of the upgrading of the Bass Highway. Samples were taken for analysis during the demolition.

3.3 CLIMATIC CONDITIONS

In this section, climatic data sourced from *Climate of Tasmania* (Bureau of Meteorology, 1993) for a number of locations around Tasmania are presented. The locations provide a basis for subsequent interpolation to estimate macroscopic climatic conditions at the various bridge sites.

Rainfall is described in terms of nine meteorological districts as shown in Figure A3.10.

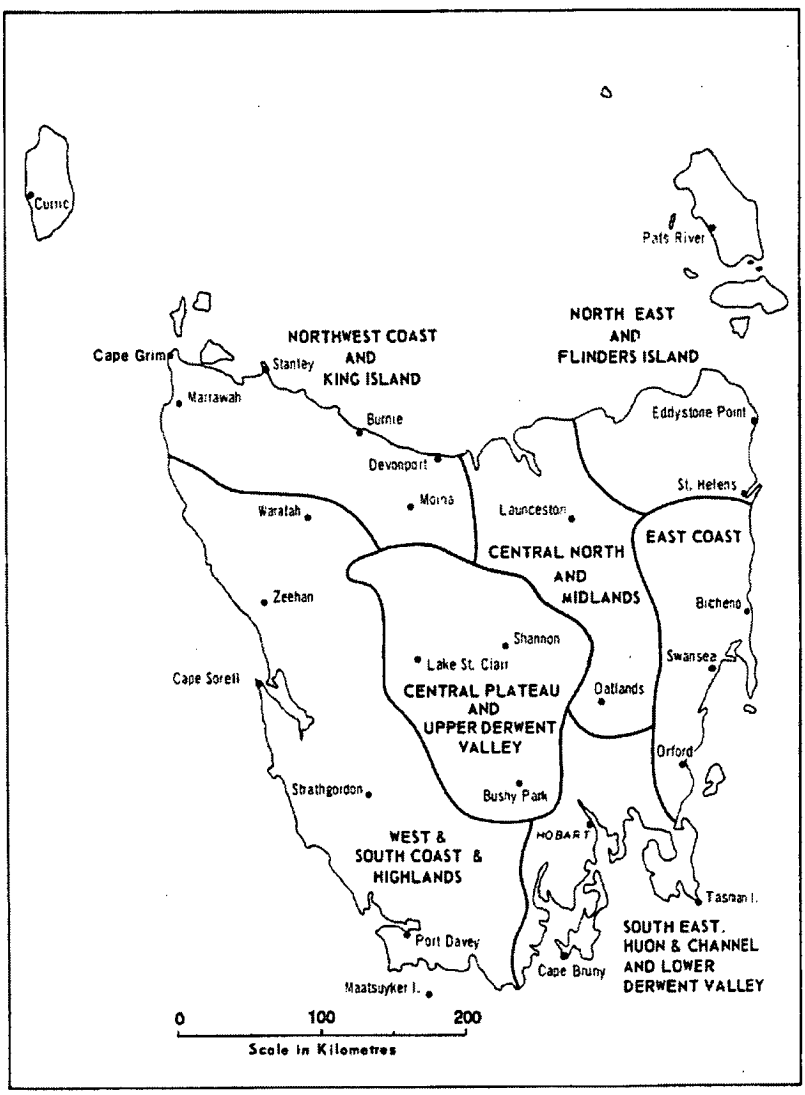

Figure A3.10 - Tasmanian meteorological districts

District	District Name	1st decile	Median	9th decile
91	Northern	748	956	1255
92	East Coast	573	772	1073
93	Midlands	390	529	711
94	Southeast	565	758	949
95	Derwent Valley	525	697	881
96	Central Plateau	713	988	1304
97	West Coast	1910	2336	2803
98	King Island	706	904	1178
99	Flinders Island	574	707	951

Table A3.1- Rainfall data (mm/yr)

The publication includes mean daily maximum and mean daily minimum temperatures. The likelihood of frosts is indicated by the average number of days per year with temperatures at or below 2.2°C.

No.	Station	Jan	Feb	Mar	Apr	May	Jun	Jul	Aug	Sep	Oct	Nov	Dec	Ann
91009	Burnie	20.9	21.0	19.8	17.6	15.2	13.3	12.5	13.0	14.2	15.8	17.6	19.3	16.7
91022	Cressy	23.6	23.6	21.4	17.5	14.1	11.5	10.9	12.2	14.3	16.6	18.9	21.5	17.2
91057	Low Head	20.2	20.8	19.5	17.1	14.6	12.4	11.8	12.3	13.4	14.9	16.8	18.7	14.9
91080	Quoiba	21.8	21.9	20.6	17.9	15.2	13.1	12.4	13.2	14.6	16.3	18.1	20.0	17.1
91092	Smithton	21.0	21.6	20.2	17.8	15.4	13.5	12.8	13.4	14.5	16.2	17.9	19.4	17.0
91104	Launceston Airport	23.1	23.1	21.0	17.3	13.9	11.3	10.7	11.9	14.1	16.3	18.7	21.1	16.9
91112	Wynyard East	21.4	21.7	20.4	18.1	15.5	13.4	12.8	13.3	14.7	16.4	18.4	19.8	17.2
91119	Erriba	18.4	18.9	16.8	13.7	10.8	8.6	7.7	8.6	10.2	12.4	14.5	16.2	13.1
91186	Forthside	20.7	21.3	19.8	16.9	14.3	12.1	11.4	12.1	13.3	15.4	17.2	18.8	16.1
92003	Bicheno	20.9	21.3	20.3	19.1	16.3	14.4	13.8	14.3	16.0	17.4	18.3	19.5	17.6
92033	St Helens	22.6	22.9	21.5	19.0	16.3	14.2	13.6	14.3	15.9	18.0	19.4	21.0	18.6
92038	Swansea	22.2	22.1	20.8	18.6	15.8	13.8	13.1	13.9	15.7	17.5	19.0	20.3	17.7
92045	Eddystone Point	20.5	20.9	20.0	17.9	15.5	13.5	12.8	13.2	14.5	16.1	17.6	18.9	16.8
92094	Scamander	21.8	21.9	20.6	18.8	16.6	14.3	13.7	14.7	16.2	17.5	18.9	20.0	17.9
93014	Oatlands	21.8	22.0	19.4	15.9	12.4	10.0	9.4	10.6	12.8	15.2	17.5	19.6	15.5
93027	Palmerston	23.8	24.5	21.8	17.9	14.3	11.5	11.1	12.4	14.4	17.0	19.3	21.7	17.5
94010	Cape Bruny	18.1	18.4	17.5	15.4	13.3	11.5	11.1	11.7	13.2	14.3	15.5	16.9	14.7
94029	Hobart R.O.	21.5	21.6	20.1	17.2	14.3	11.8	11.5	12.9	15.0	16.9	18.6	20.2	16.8
94041	Maatsuyker Island	17.1	17.2	16.4	14.5	12.7	11.4	10.9	11.2	12.2	13.3	14.4	15.8	13.9
94069	Grove	22.2	22.2	20.3	17.5	14.2	11.8	11.4	12.7	14.6	16.8	18.3	20.0	16.8
95003	Bushy Park	23.6	23.7	21.7	17.8	14.1	11.0	10.8	12.8	15.4	17.5	19.7	21.8	17.5
95011	Maydena	21.6	21.8	19.4	15.8	12.5	9.9	9.6	11.0	13.1	15.3	17.3	19.3	15.5
96003	Butlers Gorge	18.8	18.7	16.4	13.0	9.9	7.5	6.9	7.9	10.1	12.4	14.4	16.5	12.7
96015	Lake St Clair	18.5	18.8	16.3	12.9	9.7	7.5	6.6	7.7	9.7	12.1	14.1	16.1	12.5
96021	Shannon	17.7	17.6	15.2	11.6	8.4	6.2	5.3	6.2	8.6	11.1	13.1	15.4	11.4
97034	Queenstown	21.1	22.0	19.7	16.6	14.5	12.3	11.6	12.5	13.6	15.9	17.6	19.3	16.4
97047	Savage River	19.1	20.1	17.6	14.6	12.2	10.1	9.3	9.9	11.1	13.5	15.4	17.2	14.2
97053	Strathgordon	19.2	19.6	17.5	14.4	11.7	9.4	8.9	9.8	11.5	13.4	15.8	17.2	14.0
97067	Strahan	20.7	21.4	19.5	17.0	14.8	12.5	12.1	12.8	14.2	16.0	17.9	19.1	16.5
98001	King Is (Currie)	20.3	20.6	19.6	17.2	15.1	13.5	12.9	13.2	14.3	15.6	17.0	18.7	16.5
99005	Flinders Is Airport	21.9	22.6	21.3	18.7	16.2	14.0	13.2	13.6	15.0	16.8	18.4	19.9	17.6

Table A3.2 - Mean daily maximum temperatures (°C)

No.	Station	Jan	Feb	Mar	Apr	May	Jun	Jul	Aug	Sep	Oct	Nov	Dec	Ann
91009	Burnie	12.3	12.9	11.8	9.7	8.1	6.4	5.5	5.8	6.5	7.7	9.5	10.7	8.9
91022	Cressy	9.1	9.3	8.0	5.3	3.3	1.4	0.9	2.0	3.4	4.7	6.5	7.9	5.1
91057	Low Head	12.8	13.2	12.2	10.3	8.3	6.5	5.9	6.3	7.4	8.6	10.1	11.6	9.4
91080	Quoiba	10.8	11.1	9.8	7.2	5.2	3.3	2.6	3.6	4.4	6.4	7.9	9.5	6.8
91092	Smithton	11.1	11.5	10.4	8.7	7.2	5.2	4.5	5.2	6.2	7.2	8.7	9.9	8.0
91104	Launceston Airport	10.0	10.2	9.0	6.7	4.7	2.8	2.2	3.0	4.2	5.5	7.2	8.7	5.9
91112	Wynyard East	11.9	12.3	11.0	8.8	6.8	4.6	3.9	4.5	5.7	6.9	9.0	10.4	8.0
91119	Erriba	7.7	8.2	7.4	5.5	3.9	2.1	1.5	1.8	2.6	3.7	5.2	6.5	4.7
91186	Forthside	11.0	11.7	10.5	8.2	6.3	4.0	3.4	4.2	4.9	6.2	8.3	9.4	7.3
92003	Bicheno	12.4	12.8	12.0	10.5	8.5	6.6	6.0	6.2	7.5	8.4	10.1	11.4	9.4
92033	St Helens	11.7	11.9	10.7	7.8	5.7	3.8	2.5	3.7	5.1	6.9	8.9	10.5	7.4
92038	Swansea	11.3	11.5	10.3	8.2	6.1	4.3	3.4	4.2	5.6	7.0	8.9	10.3	7.6
92045	Eddystone Point	13.4	14.1	13.5	11.5	9.6	7.9	6.9	7.1	8.0	9.2	10.7	12.2	10.3
92094	Scamander	12.3	12.5	11.9	9.4	7.6	5.3	4.2	4.3	6.6	8.1	10.2	11.3	8.6
93014	Oatlands	8.7	8.6	7.5	5.7	3.5	1.7	1.0	1.7	3.1	4.5	6.1	7.6	5.0
93027	Palmerston	8.6	9.1	8.0	5.2	3.2	1.1	0.7	2.1	3.5	4.7	6.6	7.8	5.1
94010	Cape Bruny	11.2	11.5	11.0	9.6	8.2	6.6	6.0	6.2	6.9	7.8	8.9	10.2	8.7
94029	Hobart R.O.	11.7	11.9	10.7	8.9	6.9	5.1	4.4	5.1	6.3	7.7	9.2	10.7	8.2
94041	Maatsuyker Island	10.6	11.0	10.6	9.5	8.4	7.2	6.5	6.4	6.8	7.4	8.4	9.5	8.5
94069	Grove	9.3	9.4	8.1	6.4	4.2	2.4	1.9	2.6	4.0	5.6	7.0	8.7	5.8
95003	Bushy Park	10.0	10.1	8.7	6.5	4.3	2.3	1.5	2.5	4.0	5.9	7.7	9.2	6.1
95011	Maydena	8.2	8.5	7.0	5.5	3.6	1.9	1.2	1.5	2.8	4.0	5.9	7.4	4.8
96003	Butlers Gorge	6.3	6.3	5.2	3.3	1.7	0.2	-0.5	0.0	0.9	2.4	3.9	5.5	2.9
96015	Lake St Clair	7.2	7.4	6.1	4.5	2.8	1.2	0.4	0.8	1.6	3.2	4.5	6.1	3.8
96021	Shannon	5.8	6.0	4.8	2.8	1.3	-0.4	-1.1	-0.8	0.2	1.7	3.0	4.7	2.3
97034	Queenstown	8.3	8.5	7.7	6.4	4.4	2.6	2.3	3.1	4.2	5.0	6.4	7.8	5.6
97047	Savage River	9.2	9.9	8.5	7.3	5.8	4.1	3.5	3.6	4.2	5.3	6.7	7.9	6.3
97053	Strathgordon	9.4	9.5	8.6	7.1	5.3	3.8	2.9	3.4	4.4	5.5	7.0	8.3	6.3
97067	Strahan	10.6	10.6	9.8	8.8	7.4	5.4	4.8	5.3	6.4	7.2	8.3	9.6	7.9
98001	King Is (Currie)	12.5	13.1	12.6	11.2	9.8	8.5	7.7	7.8	8.2	9.0	9.9	11.4	10.1
99005	Flinders Is Airport	13.0	13.4	12.6	10.9	9.1	6.9	5.9	6.4	7.5	8.5	10.1	11.7	9.7

Table A3.3 - Mean daily minimum temperatures (°C)

No.	Station	Jan	Feb	Mar	Apr	May	Jun	Jul	Aug	Sep	Oct	Nov	Dec	Ann
91009	Burnie	0	0	0	0	1	2	3	3	2	1	0	0	12
91022	Cressy	1	1	2	7	12	18	20	15	10	8	3	2	99
91057	Low Head	0	0	0	0	0	2	4	2	0	0	0	0	8
91080	Quoiba	0	0	0	3	7	13	15	11	9	3	1	0	62
91092	Smithton	0	0	1	1	3	7	9	6	4	2	1	0	34
91104	Launceston Airport	0	0	1	3	8	13	16	13	8	5	2	1	70
91112	Wynyard East	0	0	0	1	3	9	11	7	5	2	1	0	39
91119	Erriba	1	1	2	5	10	15	19	18	13	10	6	3	103
91186	Forthside	0	0	0	1	3	9	11	8	6	3	1	0	42
92003	Bicheno	0	0	0	0	0	1	2	1	0	0	0	0	4
92033	St Helens	0	0	0	2	6	11	17	12	7	3	1	0	59
92038	Swansea	0	0	0	1	5	9	12	9	6	2	1	0	45
92045	Eddystone Point	0	0	0	0	0	1	1	1	0	0	0	0	3
92094	Scamander	0	0	0	0	1	3	7	4	1	0	0	0	16
93014	Oatlands	1	1	2	5	9	14	16	15	10	7	3	1	84
93027	Palmerston	1	1	3	8	13	19	20	17	12	9	4	3	110
94010	Cape Bruny	0	0	0	0	0	1	0	1	0	0	0	0	2
94029	Hobart R.O.	0	0	0	0	1	4	6	4	1	0	0	0	16
94041	Maatsuyker Island	0	0	0	0	0	0	1	0	0	0	0	0	1
94069	Grove	0	1	2	5	10	16	18	15	10	6	2	1	86
95003	Bushy Park	0	0	1	3	9	16	20	15	8	4	1	0	77
95011	Maydena	1	1	2	4	10	14	18	17	12	8	3	2	92
96003	Butlers Gorge	3	4	6	12	18	22	26	25	21	15	9	5	166
96015	Lake St Clair	2	2	4	8	14	19	24	22	18	13	7	4	137
96021	Shannon	5	4	8	14	19	22	26	25	22	17	13	8	183
97034	Queenstown	1	1	1	3	9	14	15	12	9	7	4	2	78
97047	Savage River	0	0	0	1	4	7	9	8	6	3	1	0	39
97053	Strathgordon	0	0	0	1	4	8	12	10	6	3	1	0	45
97067	Strahan	0	0	0	0	2	6	7	5	3	1	1	0	25
98001	King Is (Currie)	0	0	0	0	0	0	0	0	0	0	0	0	0
99005	Flinders Is Airport	0	0	0	0	1	4	6	5	3	2	0	0	21

Table A3.4 - Average number of days per year with temperatures at or below 2.2°C

No.	Station	Jan	Feb	Mar	Apr	May	Jun	Jul	Aug	Sep	Oct	Nov	Dec	Ann
91009	Burnie	68	69	70	74	80	80	81	79	74	70	69	67	73
91022	Cressy	63	67	72	78	85	87	87	83	76	70	67	65	75
91057	Low Head	72	75	78	82	85	86	87	86	83	79	76	74	80
91080	Quoiba	65	68	71	77	83	84	85	82	76	71	68	67	75
91092	Smithton	73	77	78	84	89	90	90	88	81	75	73	73	81
91104	Launceston Airport	64	68	73	81	88	90	90	87	79	72	68	65	77
91112	Wynyard East	71	74	75	81	87	89	90	86	78	72	72	71	79
91119	Erriba	75	78	80	84	87	86	87	86	82	77	76	76	81
91186	Forthside	67	70	73	78	83	85	85	82	75	72	72	69	76
92003	Bicheno	70	70	69	69	75	73	73	72	66	68	68	70	70
92033	St Helens	66	70	73	76	81	83	83	79	70	66	65	67	73
92038	Swansea	64	68	68	73	78	79	79	76	68	64	67	66	71
92045	Eddystone Point	79	78	78	79	84	85	85	83	80	76	78	78	80
92094	Scamander	70	72	73	74	79	81	80	77	70	66	69	69	73
93014	Oatlands	64	69	72	78	84	86	87	83	75	69	68	65	75
93027	Palmerston	64	68	71	78	85	87	87	83	76	69	68	67	75
94010	Cape Bruny	76	78	79	81	84	85	85	82	79	77	77	76	80
94029	Hobart R.O.	59	63	66	70	76	79	78	74	66	62	60	59	68
94041	Maatsuyker Island	82	82	83	84	86	86	86	86	84	83	83	82	84
94069	Grove	65	70	74	77	83	85	85	82	73	68	67	66	75
95003	Bushy Park	64	68	74	80	86	88	88	85	76	70	66	64	76
95011	Maydena	72	77	79	86	91	93	93	89	80	75	73	71	82
96003	Butlers Gorge	72	80	84	87	89	91	91	89	82	77	75	73	83
96015	Lake St Clair	69	73	76	78	80	80	81	79	76	71	69	69	75
96021	Shannon	68	73	77	81	86	88	88	86	79	73	70	68	78
97034	Queenstown	76	82	82	88	90	91	91	88	82	75	76	74	83
97047	Savage River	79	81	82	88	90	91	92	90	87	81	80	79	85
97053	Strathgordon	77	81	81	86	88	89	89	88	82	78	76	76	83
97067	Strahan	77	81	83	85	87	89	87	87	82	76	77	77	82
98001	King Is (Currie)	73	77	77	80	83	84	84	82	80	78	76	75	79
99005	Flinders Is Airport	70	73	72	75	82	84	83	80	75	72	72	72	76

Table A3.5 - Mean 9am relative humidity (%)

No.	Station	Jan	Feb	Mar	Apr	May	Jun	Jul	Aug	Sep	Oct	Nov	Dec	Ann
91009	Burnie	61	63	65	67	72	71	72	70	68	64	64	60	66
91022	Cressy	42	42	49	56	66	72	69	64	59	55	51	47	56
91057	Low Head	67	68	68	70	75	77	78	76	76	74	71	69	72
91080	Quoiba	59	60	62	66	71	72	71	69	67	65	64	62	66
91092	Smithton	59	60	64	69	75	76	77	73	68	64	62	62	67
91104	Launceston Airport	44	45	50	57	67	72	71	66	60	57	53	49	58
91112	Wynyard East													
91119	Erriba	61	61	67	73	78	79	79	75	73	68	66	66	71
91186	Forthside													
92003	Bicheno	67	67	67	65	69	67	66	67	63	68	66	68	67
92033	St Helens	57	57	60	61	64	66	64	61	60	59	58	60	61
92038	Swansea	57	59	60	61	65	65	64	62	59	59	60	61	61
92045	Eddystone Point	70	72	71	71	75	77	76	75	73	72	71	72	73
92094	Scamander	61	63	66	63	67	68	65	63	61	63	63	63	64
93014	Oatlands	44	45	51	59	69	73	72	66	61	56	54	49	58
93027	Palmerston	42	42	48	58	67	71	70	63	60	55	53	50	57
94010	Cape Bruny	73	72	72	74	77	77	77	75	73	74	73	73	74
94029	Hobart R.O.	53	54	55	59	63	67	65	60	56	56	55	58	58
94041	Maatsuyker Island	77	77	78	80	83	83	82	81	80	79	78	77	80
94069	Grove	52	52	55	59	66	69	68	62	58	56	56	55	59
95003	Bushy Park	45	46	50	59	70	75	73	64	59	54	52	50	58
95011	Maydena	49	50	56	67	76	79	78	72	63	58	54	54	63
96003	Butlers Gorge	52	56	59	66	74	77	77	72	65	60	60	55	64
96015	Lake St Clair	49	52	65	67	68	67	66	65	55	57	58	56	60
96021	Shannon	50	53	57	64	73	76	75	71	64	61	57	54	63
97034	Queenstown	58	57	62	70	74	75	76	71	69	63	61	59	66
97047	Savage River	60	58	68	75	81	84	84	80	77	71	66	64	72
97053	Strathgordon	56	56	61	69	77	80	78	73	67	61	58	58	66
97067	Strahan	60	61	65	69	77	78	75	73	68	67	64	64	68
98001	King Is (Currie)	66	68	70	74	79	80	79	77	75	74	72	69	74
99005	Flinders Is Airport	62	63	65	69	74	76	75	72	71	69	67	66	69

Table A3.6 - Mean 3pm relative humidity (%)

No.	Station	Median Rainfall (mm)	Mean Temperature (°C)	'Frost' Days	Humidity (%)		
					Mean	Minimum	Maximum
91009	Burnie	956	12.8	12	70	60	81
91022	Cressy	956	11.2	99	66	42	87
91057	Low Head	956	12.7	8	76	67	87
91080	Quoiba	956	12.0	62	70	59	85
91092	Smithton	956	12.5	34	74	59	90
91104	Launceston Airport	956	11.5	70	67	44	90
91112	Wynyard East	956	12.6	39	-	-	90
91119	Erriba	956	8.9	103	76	61	87
91186	Forthside	956	11.7	42	-	-	85
92003	Bicheno	772	13.5	4	69	63	75
92033	St Helens	772	12.9	59	67	57	83
92038	Swansea	772	12.7	45	66	57	79
92045	Eddystone Point	772	13.6	3	77	70	85
92094	Scamander	772	13.3	16	69	61	81
93014	Oatlands	529	10.3	84	67	44	87
93027	Palmerston	529	11.3	110	66	42	87
94010	Cape Bruny	758	11.7	2	77	72	85
94029	Hobart R.O.	758	12.5	16	63	53	79
94041	Maatsuyker Island	758	11.2	1	82	77	86
94069	Grove	758	11.3	86	67	52	85
95003	Bushy Park	697	11.8	77	67	45	88
95011	Maydena	697	10.2	92	73	49	93
96003	Butlers Gorge	988	7.8	166	74	52	91
96015	Lake St Clair	988	8.2	137	68	49	81
96021	Shannon	988	6.9	183	71	50	88
97034	Queenstown	2336	11.0	78	75	57	91
97047	Savage River	2336	10.3	39	79	58	92
97053	Strathgordon	2336	10.2	45	74	56	89
97067	Strahan	2336	12.2	25	75	60	89
98001	King Is (Currie)	904	13.3	0	76	66	84
99005	Flinders Is Airport	707	13.7	21	72	62	84

Notes:
1. Median rainfall is that for the meteorological district.
2. Mean temperature is taken to be mean of average minimum and maximum temperatures.
3. 'Frost' days are taken to be those below 2.2°C.
4. Mean humidity is taken to be average of 9am and 3pm humidities.

Table A3.7 - Summary climatic data

3.4 CLIMATIC DATA

By interpolating and extrapolating the Tasmanian climatic data, climatic conditions at each of the bridge sites are estimated. Exposure classifications are those of the *AUSTROADS Bridge Design Code* (AUSTROADS, 1992), which states that the requirements apply to plain, reinforced and prestressed concrete structures with a design life of 100 years.

In terms of the Code, Tasmania falls entirely within the temperate climatic zone. The exposure classification is taken to be the most severe exposure of any of the bridge elements.

Bridge		Distance from coast (km)	AUSTROADS Classification	Median Rainfall (mm)	Mean Temperature (°C)	'Frost' Days	Humidity (%)		
							Mean	Minimum	Maximum
15	Bridgewater Bridge	0	C	760	12	40	65	50	85
33	Pats River Bridge	1.2	B1, U	700	14	21	72	62	84
44	Faggs Gully Creek Culvert	0.5	B2, U	760	13	16	63	53	79
65	Leven River Bridge	0	C	960	13	12	70	60	81
119	Ralphs Bay Canal Bridge	0	C	760	13	16	63	53	79
147	Wrinklers Bridge	0	C	770	13	16	69	61	81
163	Maclaines Creek Bridge	0.1	B2, U	770	13	45	66	57	79
165	Argent River	25	B1, U	2340	11	70	75	57	91
169	Kelvedon Creek Bridge	0.1	B2, U	770	13	45	66	57	79
173	Vale River Culvert	75	B1, U	2340	11	100	75	60	90
187	Huon Highway Stock Underpass	2.5	B1	760	12	30	65	53	80
190	Coal River Bridge	2	B1	600	12	50	65	50	80
219	Detention River Bridge	0	C	960	13	30	72	60	85
225	Mersey River (Victoria) Bridge	0	C	960	13	40	70	60	85
243	Cam River Bridge	0	C	960	13	12	70	60	81
279	Porky Creek Bridge	0.8	B2, U	900	13	0	76	66	84
284	Camp Creek Bridge	0.8	B2, U	900	13	0	76	66	84
298	Surges Creek Bridge	0.2	B2, U	760	11	50	65	52	80
333	Lilla Villa Bridge	3	B1, U	770	13	4	70	63	75
509	Sorell Causeway Bridge	0	C	760	13	10	70	60	85
605	Saltwater Creek Bridge	3	B1, U	760	13	20	65	53	80
796	King Island Main Road Culvert	4	B1, U	900	13	0	76	66	84
864	Ringarooma River Bridge	27	B1, U	800	12	70	70	60	85
877	Golden Fleece Bridge	0	C	770	13	59	67	57	83
879	Boggy Creek Bridge	0	C	770	13	59	67	57	83
884	Reedy Creek Bridge	0.1	B2, U	770	13	40	68	60	82
911	Cormiston Creek Bridge	0.4	B2,U	960	12	50	70	50	90
935	Wardlaws Creek Bridge	0.4	B2, U	770	13	20	70	60	82
940	Denison River Bridge	0.1	B2,U	770	13	10	69	62	80
953	Symons Creek Bridge	1.4	B1,U	960	12	50	70	50	90
1099	Stanley Fishing Dock	0	C	960	13	30	74	59	90
1185	Emu River Bridge	0	C	960	13	12	70	60	81
1330	Runnymede Culvert	15	B1, U	760	13	20	65	53	80
1336	Orielton Rivulet Bridge	6.5	B1, U	760	13	20	65	53	80
1465	Peggs Creek Bridge	0.6	B1,U	960	13	35	74	59	90
1805	Princess River Bridge	32	B1,U	2340	11	70	75	57	90
1979	Hunterston Culvert	88	B1,U	800	9	120	70	50	90
2039	Higgins Creek Bridge	0	C	760	11	50	65	52	80
2326	Mountain Creek Bridge	0	C	760	11	50	65	52	80
2469	Tasman Highway Culverts	1.0	B1, U	770	13	4	69	63	75
2658	Newmans Creek Bridge	0	C	760	12	20	70	60	80
2777	Cusicks Creek Culvert	1.4	B1,U	770	13	5	70	63	75
2795	Carlton River Bridge	7.5	B1,U	760	13	20	65	53	80
2796	Rileys Creek Bridge	3.5	B1,U	760	11	50	65	52	80
2889	Flights Creek Bridge	0	C	760	11	50	65	52	80
3178	Carlton River Bridge	7.5	B1,U	760	13	20	65	53	80
3194	Scopus Creek Bridge	0.8	B2,U	960	13	34	74	59	90
3782	East Arm Creek Culvert	1.0	B2,U	960	12	50	70	50	90
3786	Egg Island Creek Bridge	1.8	B1,U	960	12	50	70	50	90
5067	Freestone Point Road Culvert	0.7	B2,U	770	13	50	67	60	80
5512	Tasman Bridge	0	C	760	13	16	63	53	79
5566	Burnie Port Access Bridge	0.1	B1	960	13	12	70	60	81
5569	Faulkners Rivulet Culvert	0.7	B2, U	760	13	16	63	53	79
5602	Risdon Cove Causeway Culvert	0	C	760	13	16	63	53	79
5694	Deloraine Rail Underpass	42	B1	960	11	80	70	60	90
5749	Grassy Wharf	0	C	900	13	0	76	66	84

Table A3.8 - Indicative climatic data for bridges

Bridge		Distance from coast (km)	AUSTROADS Classification	Median Rainfall (mm)	Mean Temperature (°C)	'Frost' Days	Humidity (%)		
							Mean	Minimum	Maximum
100	Inverquharity Creek Culvert	9	B1, U	760	13	20	65	53	80
173	Vale River Culvert	75	B1, U	2340	11	100	75	60	90
187	Huon Highway Stock Underpass	2.5	B1	760	12	30	65	53	80
536	Stock Underpass	50	B1	530	10	84	67	44	87
547	Chiswick Stock Underpass	50	B1	530	10	84	67	44	87
550	Cameron Stock Underpass South	50	B1	530	10	84	67	44	87
554	St Peters Stock Underpass North	50	B1	530	10	84	67	44	87
555	St Peters Stock Underpass South	50	B1	530	10	84	67	44	87
556	Somercotes Stock Underpass	50	B1	530	10	84	67	44	87
593	Lake Highway Culvert	70	B1, U	990	8	110	70	50	87
755	Hortons Creek Bridge	30	B1, U	600	11	70	67	50	85
892	Fingal Rivulet Culvert	26	B1, U	600	12	70	67	50	85
1237	Strathallan Rivulet Culvert	25	B1, U	760	13	20	65	53	80
1301	Wilcox Creek Culvert	0.1	B1, U	760	11	80	67	52	85
1330	Runnymede Culvert	15	B1, U	760	13	20	65	53	80
1979	Hunterston Rivulet Culvert	88	B1, U	800	9	120	70	50	90
2299	Strathallen Rivulet Culvert	25	B1, U	760	13	20	65	53	80
2390	Hunterston Culvert	88	B1, U	800	9	120	70	50	90
2533	Iris River Culvert	76	B1, U	2340	11	100	75	60	90
2870	Tatnells Creek Bridge	0.3	B1, U	760	12	20	70	60	80
3771	Four Mile Creek Bridge	0.3	B2,U	960	13	8	76	67	87
5258	Broken Leg Creek Culvert	85	B1,U	990	8	150	70	50	85
5291	Lake Highway Culvert	75	B1, U	800	9	120	70	50	90
5292	Weasel Plains Creek Culvert	90	B1, U	800	9	120	70	50	90
5293	Lake Highway Culvert	90	B1, U	800	9	120	70	50	90
5569	Faulkners Rivulet Culvert	0.7	B1, U	760	13	16	63	53	79
5602	Risdon Cove Causeway Culvert	0	C	760	13	16	63	53	79
5646	Little Quoin Creek Culvert	45	B1,U	530	10	84	67	44	87
5647	Oakmore Stock Underpass	45	B1	530	10	84	67	44	87
5655	Midland Highway Stock	53	B1	530	10	84	67	44	87
5666	Midland Highway Stock	55	B1	530	10	84	67	44	87
5679	Lemon Springs Stock Underpass	53	B1	530	10	84	67	44	87
5716	Boles Street Stock Underpass	53	B1	530	10	84	67	44	87
5717	Trafalgar Street Stock Underpass	53	B1	530	10	84	67	44	87
5718	Weedington Stock Underpass	53	B1	530	10	84	67	44	87
5726	Parremore Stock Underpass	7	B1	760	11	50	65	53	80
5767	Burnside Culvert	9	B1, U	760	13	20	65	53	80
5806	Fairfield Stock Underpass	40	B1	960	11	80	67	44	87
5809	Elsdon Stock Underpass	40	B1	960	11	80	67	44	87
5817	Forton Stock Underpass	40	B1	960	11	80	67	44	87
5820	Belmont Rivulet Culvert	40	B1, U	700	11	80	70	47	90
5832	Hatherley Stock Underpass	40	B1	960	11	80	67	43	88
5834	Ashburn Stock Underpass	40	B1	960	11	80	67	43	88
5875	Best Stock Underpass	45	B1	960	11	80	70	60	90
5877	Thompson Stock Underpass	42	B1	960	11	80	70	60	90
5878	Bonnies Creek Culvert	45	B1, U	960	11	80	70	60	90
5880	Atkins Stock Underpass	45	B1	960	11	80	70	60	90
5881	Hill Stock Underpass	45	B1	960	11	80	70	60	90
5882	Faulkner Stock Underpass	45	B1	960	11	80	70	60	90
5883	Gibsons Stock Underpass	45	B1	960	11	80	70	60	90

Table A3.9 - Indicative climatic data for precast culverts

3.5 ENVIRONMENTAL DATA

Water samples were collected from each of the bridge sites, other than overpasses and underpasses, and analysed for chloride and sulphate contents and pH. Results of the analyses are presented below.

Bridge		Date of sampling	Stream flow	Chloride	Sulphate	pH
15	Bridgewater Bridge	8/1/98	Low tide	910 mg/l	127 mg/l	7.8
33	Pats River Bridge – 5m upstream	26/2/98	Low flow	400 mg/l	770 mg/l	7.4
	- near weir	26/2/98	Low flow	7700 mg/l	1,600 mg/l	7.2
44	Faggs Gully Creek Culvert	3/11/97	Low flow	81 mg/l	53 mg/l	7.4
65	Leven River Bridge	21/1/98	High tide	19,000 mg/l	2,600 mg/l	7.8
119	Ralphs Bay Canal Bridge	9/1/98	Low tide	18,000 mg/l	2,400 mg/l	7.6
147	Wrinklers Bridge – lagoon	19/2/98	Barway closed	16,500 mg/l	2,400 mg/l	7.5
	- sea	19/2/98	High tide	20,000 mg/l	2,800 mg/l	8.1
163	Maclaines Creek Bridge	2/11/97	Low, after rain	13,000 mg/l	1,800 mg/l	7.5
165	Argent River	12/3/98	Low flow	7.1 mg/l	16 mg/l	5.5
169	Kelvedon Creek Bridge	2/11/97	Lagoon, after rain	2,900 mg/l	420 mg/l	8.6
			Sea	20,000 mg/l	2,700 mg/l	8.0
173	Vale River Culvert	12/3/98	Low flow	5.7 mg/l	1.6 mg/l	7.8
187	Huon Highway Stock Underpass	N/A	N/A	N/A	N/A	N/A
190	Coal River Bridge	15/2/98	Low flow	120 mg/l	9.1 mg/l	7.5
219	Detention River Bridge	21/1/98	Low tide	14,000 mg/l	1,900 mg/l	7.2
225	Mersey River (Victoria) Bridge	21/1/98	Low tide	18,000 mg/l	2,500 mg/l	7.7
243	Cam River Bridge	21/1/98	Low flood tide	19,000 mg/l	2,600 mg/l	7.9
279	Porky Creek Bridge	10/2/98	Low flow	410 mg/l	150 mg/l	7.4
284	Camp Creek Bridge	10/2/98	No flow	240 mg/l	58 mg/l	8.0
298	Surges Creek Bridge	15/1/98	Low flow	47 mg/l	7.7 mg/l	8.4
333	Lilla Villa Bridge	13/1/98	No flow	130 mg/l	15 mg/l	7.6
509	Sorell Causeway Bridge	23/10/97	Dry weather	19,000 mg/l	2,600 mg/l	8.0
605	Saltwater Creek Bridge	2/11/97	Low, after rain	2300 mg/l	140 mg/l	8.0
796	King Island Main Road Culvert	-	No water	N/A	N/A	
864	Ringarooma River Bridge	19/2/98	Low flow	12 mg/l	0.6 mg/l	7.5
877	Golden Fleece Bridge	19/2/98	High tide	19,500 mg/l	3,000 mg/l	7.6
879	Boggy Creek Bridge – lagoon	19/2/98	No flow	17,500 mg/l	3,100 mg/l	6.2
	- Georges Bay	19/2/98	High tide	19,000 mg/l	2,700 mg/l	8.2
884	Reedy Creek Bridge	19/2/98	No flow	460 mg/l	420 mg/l	5.7
911	Cormiston Creek Bridge	23/1/98	Low flow	490 mg/l	65 mg/l	8.5
935	Wardlaws Creek Bridge	19/2/98	Low flow	55 mg/l	7.8 mg/l	8.2
940	Denison River Bridge (lagoon)	19/2/98	Barway closed	140 mg/l	19 mg/l	7.4
953	Symons Creek Bridge	18/2/98	Low flow	160 mg/l	4.3 mg/l	8.3
1099	Stanley Fishing Dock	21/1/98	Mid tide	20,000 mg/l	2,600 mg/l	7.7
1185	Emu River Bridge	21/1/98	Low flow, high	440 mg/l	61 mg/l	8.0
1330	Runnymede Culvert	2/11/97	Low, after rain	460 mg/l	13 mg/l	7.5
1336	Orielton Rivulet Bridge	2/11/97	Low, after rain	170 mg/l	6.3 mg/l	8.3
1465	Peggs Creek Bridge	21/1/98	Low flow	20,000 mg/l	2,800 mg/l	7.7
1805	Princess River Bridge	8/1991	Winter	9.9 mg/l	8.5 mg/l	6.9
1979	Hunterston Culvert	15/12/97	Low flow	79 mg/l	28 mg/l	7.8
2039	Higgins Creek Bridge	15/1/98	Low flow	17,000 mg/l	2,200 mg/l	6.7
		15/1/98	Esperance River	10,000 mg/l	1,400 mg/l	6.9
2326	Mountain Creek Bridge	11/11/97	Low, after rain	140 mg/l	25 mg/l	7.8
2469	Tasman Highway Culverts	19/2/98	No flow	43mg/l	3.4 mg/l	6.9
2658	Newmans Creek Bridge	23/10/97	Dry weather	2,800 mg/l	320 mg/l	7.5
2777	Cusicks Creek Culvert	19/2/98	Low flow	59 mg/l	6.5 mg/l	6.7
2795	Carlton River Bridge	23/10/97	Dry weather	190 mg/l	15 mg/l	7.7
2796	Rileys Creek Bridge	15/1/98	Low flow	60 mg/l	9.0 mg/l	8.2
2889	Flights Creek Bridge	8/11/97	Flood tide	12,000 mg/l	1,600 mg/l	7.6
3178	Carlton River Bridge	23/10/97	Dry weather	190 mg/l	15 mg/l	7.7
3194	Scopus Creek Bridge	21/1/98	Low flow	61 mg/l	100 mg/l	8.1
3782	East Arm Creek Culvert	18/2/98	Low flow	940 mg/l	32 mg/l	7.0
3786	Egg Island Creek Bridge	22/1/98	No flow	840 mg/l	17 mg/l	7.6
5067	Freestone Point Road Culvert	2/11/97	No flow, after rain	2100 mg/l	220 mg/l	7.7
5512	Tasman Bridge – eastern abutment	23/10/97	Dry weather	640 mg/l	900 mg/l	7.7
	- span 12	26/2/98	High ebb tide	11,000 mg/l	1,100 mg/l	7.3

Bridge		Date of sampling	Stream flow	Chloride	Sulphate	pH
5602	Risdon Cove Causeway Culvert	3/11/97	Low tide	10,000 mg/l	1,300 mg/l	7.7
5566	Burnie Port Access Bridge	N/A	N/A	N/A	N/A	N/A
5569	Faulkners Rivulet Culvert	23/10/97	Dry weather	110 mg/l	25 mg/l	7.8
5694	Deloraine Rail Underpass	N/A	N/A	N/A	N/A	N/A
5749	Grassy Wharf	22/1/98	2hrs before low	20,000 mg/l	3,000 mg/l	8.1

Table A3.10 - Indicative environmental data for bridges

Bridge		Date of sampling	Stream flow	Chloride	Sulphate	PH
100	Inverquharity Creek Culvert	15/2/98	Low flow	630 mg/l	36 mg/l	8.1
173	Vale River Culvert	12/3/98	Low flow	5.7 mg/l	1.6 mg/l	7.8
187	Huon Highway Stock Underpass	N/A	N/A	N/A	N/A	N/A
536	Stock Underpass	N/A	N/A	N/A	N/A	N/A
547	Chiswick Stock Underpass	N/A	N/A	N/A	N/A	N/A
550	Cameron Stock Underpass South	N/A	N/A	N/A	N/A	N/A
554	St Peters Stock Underpass North	N/A	N/A	N/A	N/A	N/A
555	St Peters Stock Underpass South	N/A	N/A	N/A	N/A	N/A
556	Somercotes Stock Underpass	N/A	N/A	N/A	N/A	N/A
593	Lake Highway Culvert	30/1/98	Low flow	4.2 mg/l	1.1 mg/l	8.7
755	Hortons Creek Bridge	29/5/98	No flow	16 mg/l	1.7 mg/l	6.7
892	Fingal Rivulet Culvert	19/2/98	Low flow	12 mg/l	1.9 mg/l	7.4
1237	Strathallan Rivulet Culvert	14/3/98	Low flow	560 mg/l	75 mg/l	8.4
1261	Windfall Culvert	N/A	Dry bed	N/A	N/A	N/A
1262	Windfall Culvert	N/A	Dry bed	N/A	N/A	N/A
1301	Wilcox Creek Culvert	15/1/98	Low flow	460 mg/l	110 mg/l	7.9
1330	Runnymede Culvert	2/11/97	Dry weather	460 mg/l	13 mg/l	7.5
1979	Hunterston Rivulet Culvert	15/12/97	Low flow	79 mg/l	28 mg/l	7.8
2299	Strathallen Rivulet Culvert	14/3/98	Low flow	340 mg/l	54 mg/l	8.3
2390	Hunterston Culvert	15/12/97	Low flow	11 mg/l	2.1 mg/l	7.9
2533	Iris River Culvert	12/3/98	Low flow	5.4 mg/l	1.1 mg/l	8.2
2870	Tatnells Creek Bridge	23/10/97	Dry weather	120 mg/l	12 mg/l	7.4
3771	Four Mile Creek Bridge	18/2/98	Low flow	220 mg/l	15 mg/l	7.7
5258	Broken Leg Creek Culvert	12/3/98	Low flow	9.2 mg/l	1.0 mg/l	8.2
5291	Lake Highway Culvert	15/12/97	Low flow	74 mg/l	4.0 mg/l	7.2
5292	Weasel Plains Creek Culvert	15/12/97	Low flow	500 mg/l	99 mg/l	7.6
5293	Lake Highway Culvert	Refer 5292	No sample	500 mg/l	99 mg/l	7.6
5602	Risdon Cove Causeway Culvert	3/11/97	Low tide	10,000 mg/l	1,300 mg/l	7.7
5646	Little Quoin Creek Culvert	29/5/98	No flow	36 mg/l	3.8 mg/l	6.8
5647	Oakmore Stock Underpass	N/A	N/A	N/A	N/A	N/A
5655	Midland Highway Stock Underpass	N/A	N/A	N/A	N/A	N/A
5666	Midland Highway Stock Underpass	N/A	N/A	N/A	N/A	N/A
5679	Lemon Springs Stock Underpass	N/A	N/A	N/A	N/A	N/A
5716	Boles Street Stock Underpass	N/A	N/A	N/A	N/A	N/A
5717	Trafalgar Street Stock Underpass	N/A	N/A	N/A	N/A	N/A
5718	Weedington Stock Underpass	N/A	N/A	N/A	N/A	N/A
5726	Parremore Stock Underpass	N/A	N/A	N/A	N/A	N/A
5767	Burnside Culvert	2/11/97	No flow,	36 mg/l	3.0 mg/l	7.6
5806	Fairfield Stock Underpass	N/A	N/A	N/A	N/A	N/A
5809	Elsdon Stock Underpass	N/A	N/A	N/A	N/A	N/A
5817	Forton Stock Underpass	N/A	N/A	N/A	N/A	N/A
5820	Belmont Rivulet Culvert	12/3/98	Low flow	29 mg/l	13 mg/l	8.0
5832	Hatherley Stock Underpass	N/A	N/A	N/A	N/A	N/A
5834	Ashburn Stock Underpass	N/A	N/A	N/A	N/A	N/A
5875	Best Stock Underpass	N/A	N/A	N/A	N/A	N/A
5877	Thompson Stock Underpass	N/A	N/A	N/A	N/A	N/A
5878	Bonnies Creek Culvert	15/5/98	No flow	26 mg/l	14 mg/l	6.5
5880	Atkins Stock Underpass	N/A	N/A	N/A	N/A	N/A
5881	Hill Stock Underpass	N/A	N/A	N/A	N/A	N/A
5882	Faulkner Stock Underpass	N/A	N/A	N/A	N/A	N/A
5883	Gibsons Stock Underpass	N/A	N/A	N/A	N/A	N/A

Table A3.11 - Indicative environmental data for precast culverts

4 CHLORIDE INGRESS

4.1 CHLORIDE PROFILE DATA

This section tabulates the measured and fitted chloride profiles for all the cores analysed for the study. Graphs of the profiles are included except where chloride concentrations are below the values likely to initiate corrosion, especially at the level of the reinforcement.

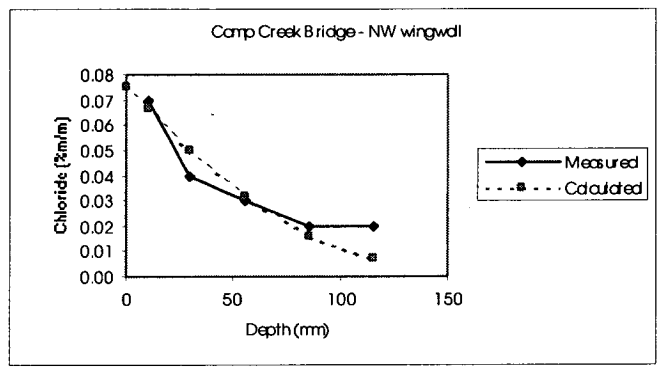

Parameters		Chloride concentration (%m/m) at depth (mm)						
Age (years)	62	Depth	0	10	30	55	85	115
C_s	0.075	Measured		0.07	0.04	0.03	0.02	0.02
D	1.20E-12	Calculated	0.075	0.066	0.050	0.032	0.016	0.007

Camp Creek Bridge – North west wingwall

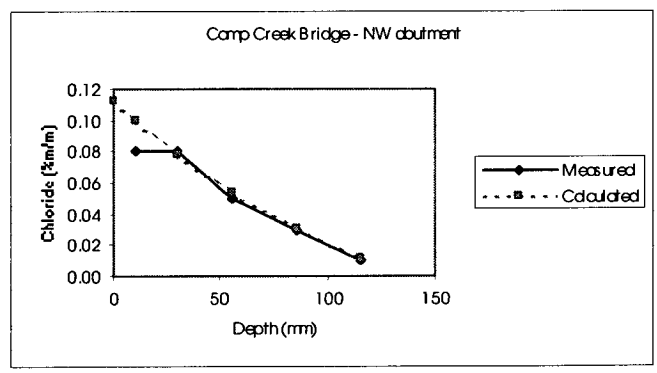

Parameters		Chloride concentration (%m/m) at depth (mm)						
Age (years)	62	Depth	0	10	30	55	85	115
C_s	0.11	Measured		0.08	0.08	0.05	0.03	0.01
D	1.50E-12	Calculated	0.112	0.100	0.078	0.053	0.030	0.012

Camp Creek Bridge – North west abutment

Parameters		Chloride concentration (%m/m) at depth (mm)				
Age (years)	62	Depth	0	10	30	55
C_s	0.042	Measured		0.03	0.01	0.00
D	1.85E-13	Calculated	0.042	0.030	0.011	0.002

Camp Creek Bridge - Deck

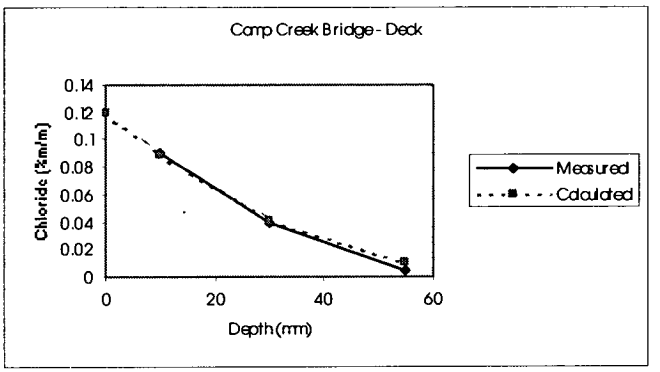

Parameters		Chloride concentration (%m/m) at depth (mm)				
Age (years)	62	Depth	0	10	30	55
C_s	0.12	Measured		0.09	0.04	0.005
D	2.54E-13	Calculated	0.119	0.090	0.041	0.010

Camp Creek Bridge - Deck

Parameters		Chloride concentration (%m/m) at depth (mm)						
Age (years)	60	Depth	0	10	30	55	85	125
C_s	0.048	Measured		0.04	0.04	0.02	0.02	0.01
D	2.00E-12	Calculated	0.048	0.044	0.035	0.025	0.016	0.007

Leven River Bridge – Abutment crosshead

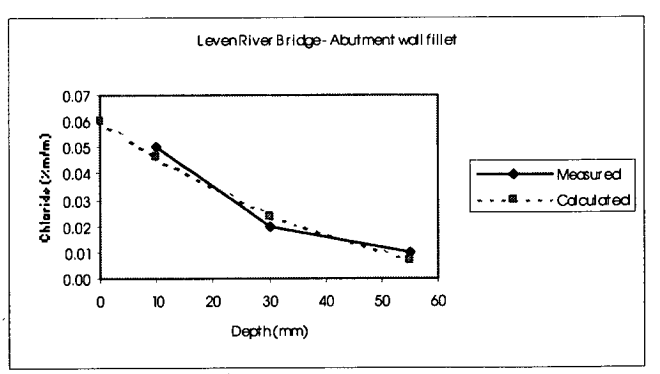

Parameters		Chloride concentration (%m/m) at depth (mm)				
Age (years)	60	Depth	0	10	30	55
C_s	0.06	Measured		0.05	0.02	0.01
D	3.30E-13	Calculated	0.060	0.046	0.023	0.007

Leven River Bridge – Abutment wall fillet

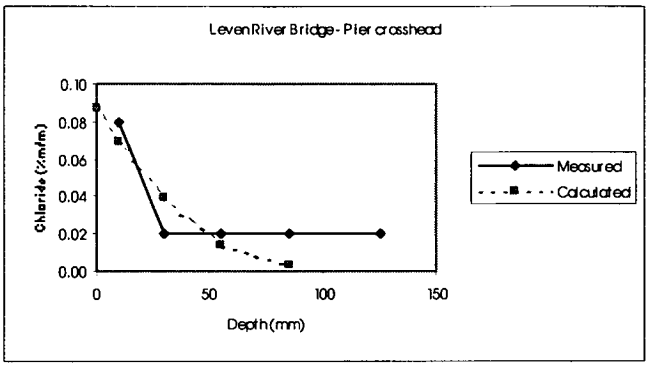

Parameters		Chloride concentration (%m/m) at depth (mm)						
Age (years)	60	Depth	0	10	30	55	85	125
C_s	0.087	Measured		0.08	0.02	0.02	0.02	0.02
D	4.13E-13	Calculated	0.087	0.070	0.039	0.014	0.003	

Leven River Bridge – Pier crosshead

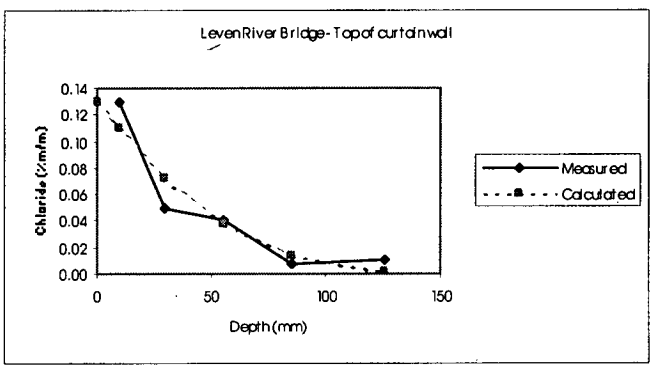

Parameters		Chloride concentration (%m/m) at depth (mm)						
Age (years)	60	Depth	0	10	30	55	85	125
C_s	0.13	Measured		0.13	0.05	0.04	0.01	0.01
D	7.00E-13	Calculated	0.130	0.110	0.073	0.037	0.013	0.002

Leven River Bridge – Top of curtain wall

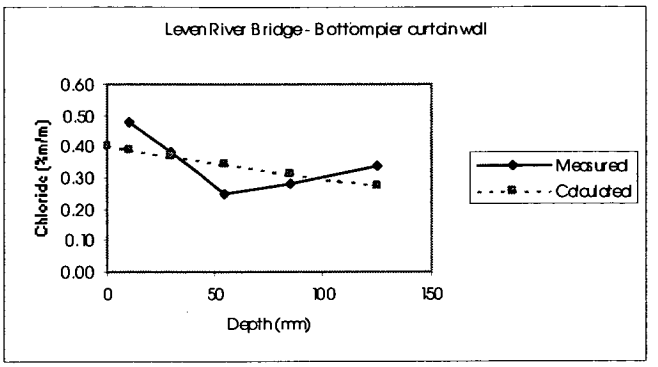

Parameters		Chloride concentration (%m/m) at depth (mm)						
Age (years)	60	Depth	0	10	30	55	85	125
C_s	0.40	Measured		0.48	0.38	0.25	0.28	0.34
D	2.40E-11	Calculated	0.400	0.389	0.368	0.342	0.311	0.271

Leven River Bridge – Bottom of pier curtain wall

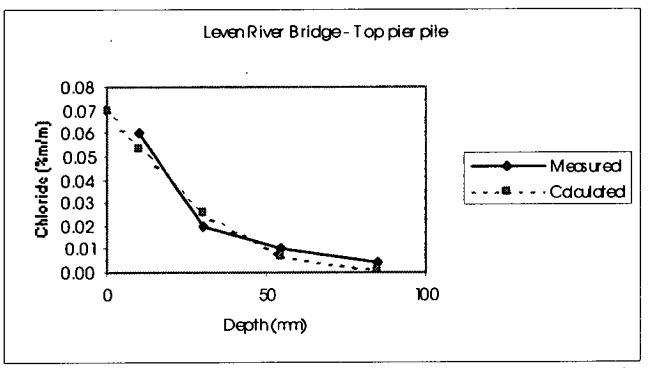

Parameters		Chloride concentration (%m/m) at depth (mm)					
Age (years)	60	Depth	0	10	30	55	85
C_s	0.07	Measured		0.06	0.02	0.01	0.005
D	3.00E-13	Calculated	0.070	0.054	0.026	0.007	0.001

Leven River Bridge – Top of pier pile

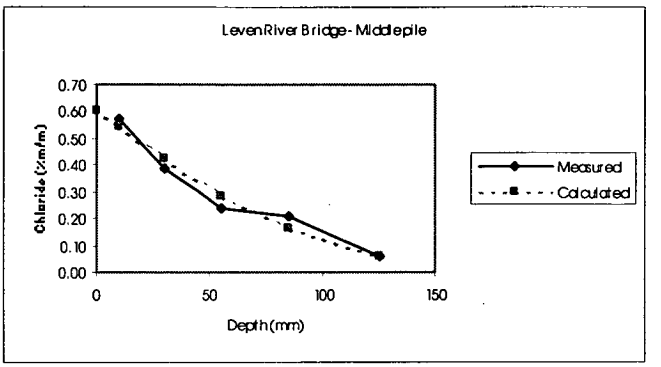

Parameters		Chloride concentration (%m/m) at depth (mm)						
Age (years)	60	Depth	0	10	30	55	85	125
C_s	0.60	Measured		0.57	0.39	0.24	0.21	0.06
D	1.56E-12	Calculated	0.604	0.542	0.421	0.286	0.162	0.063

Leven River Bridge – Middle pile

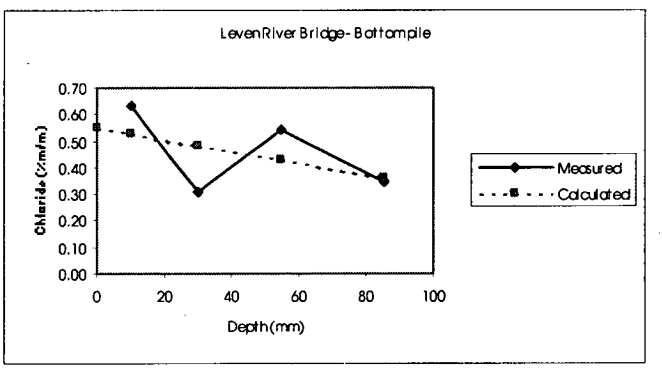

Parameters		Chloride concentration (%m/m) at depth (mm)					
Age (years)	60	Depth	0	10	30	55	85
C_s	0.55	Measured		0.63	0.31	0.54	0.35
D	1.00E-11	Calculated	0.550	0.527	0.483	0.428	0.364

Leven River Bridge – Bottom pile

Parameters		Chloride concentration (%m/m) at depth (mm)					
Age (years)	61	Depth	0	10	30	55	85
C_s	0.05	Measured		0.03	0.04	0.03	0.02
D	2.55E-12	Calculated	0.052	0.048	0.040	0.030	0.020

Porky Creek Bridge – Abutment wall

Parameters		Chloride concentration (%m/m) at depth (mm)					
Age (years)	61	Depth	0	10	30	55	85
C_s	0.05	Measured		0.04	0.04	0.02	0.03
D	2.50E-12	Calculated	0.048	0.044	0.037	0.028	0.019

Porky Creek Bridge – South east wingwall

Parameters		Chloride concentration (%m/m) at depth (mm)				
Age (years)	61	Depth	0	10	30	60
C_s	0.06	Measured		0.05	0.01	0.01
D	2.80E-13	Calculated	0.060	0.046	0.022	0.004

Porky Creek Bridge – South east wingwall

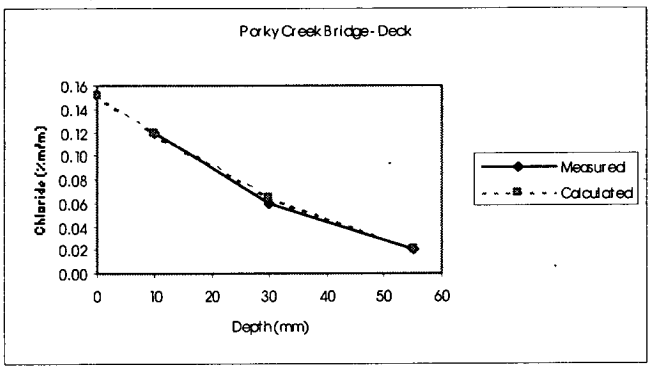

Parameters		Chloride concentration (%m/m) at depth (mm)				
Age (years)	61	Depth	0	10	30	55
C_s	0.15	Measured		0.12	0.06	0.02
D	3.60E-13	Calculated	0.152	0.120	0.064	0.021

Porky Creek Bridge - Deck

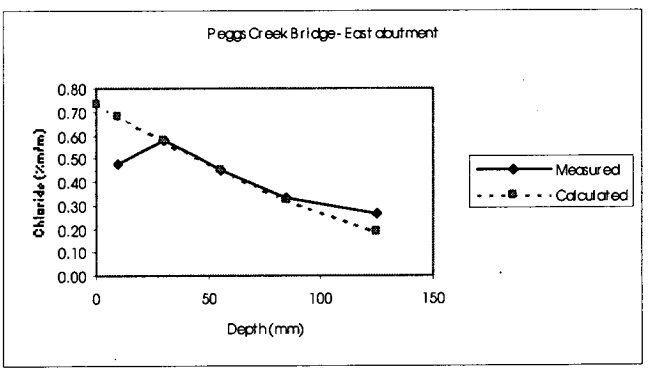

Parameters		Chloride concentration (%m/m) at depth (mm)						
Age (years)	56	Depth	0	10	30	55	85	125
C_s	0.73	Measured		0.48	0.58	0.45	0.33	0.26
D	3.50E-12	Calculated	0.730	0.678	0.575	0.453	0.325	0.191

Peggs Creek Bridge – East abutment

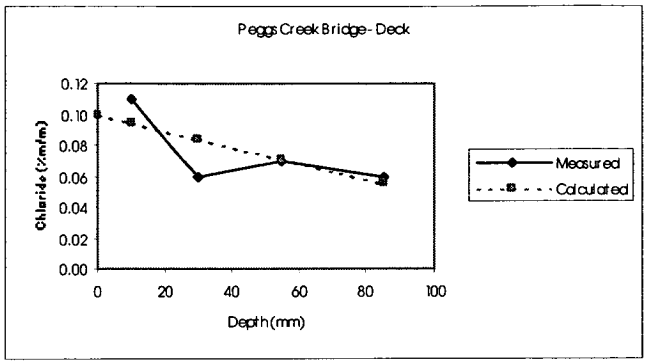

Parameters		Chloride concentration (%m/m) at depth (mm)					
Age (years)	56	Depth	0	10	30	55	85
C_s	0.10	Measured		0.11	0.06	0.07	0.06
D	6.00E-12	Calculated	0.100	0.095	0.084	0.071	0.056

Peggs Creek Bridge - Deck

Parameters		Chloride concentration (%m/m) at depth (mm)					
Age (years)	56	Depth	0	10	30	55	85
C_s	0.05	Measured		0.06	0.04	0.05	0.06
D	Constant	Calculated	0.050	0.050	0.050	0.050	0.050

Peggs Creek Bridge - Deck

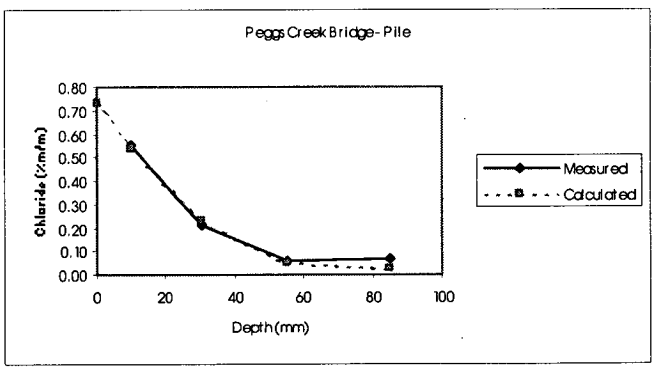

Parameters		Chloride concentration (%m/m) at depth (mm)					
Age (years)	56	Depth	0	10	30	55	85
C_s	0.73	Measured		0.55	0.21	0.06	0.07
D	2.50E-13	Calculated	0.730	0.538	0.228	0.047	0.024

Peggs Creek Bridge - Pile

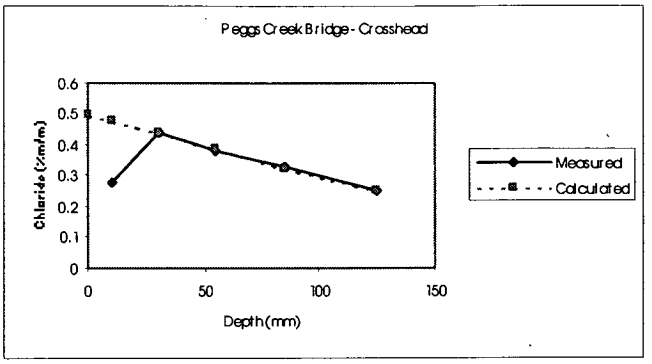

Parameters		Chloride concentration (%m/m) at depth (mm)						
Age (years)	56	Depth	0	10	30	55	85	125
C_s	0.50	Measured		0.28	0.44	0.38	0.33	0.25
D	1.00E-11	Calculated	0.500	0.479	0.437	0.385	0.326	0.253

Peggs Creek Bridge – Crosshead

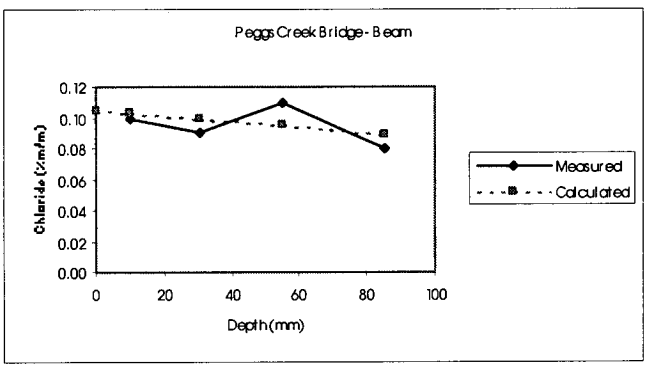

Parameters		Chloride concentration (%m/m) at depth (mm)					
Age (years)	56	Depth	0	10	30	55	85
C_s	0.11	Measured		0.10	0.09	0.11	0.08
D	6.00E-11	Calculated	0.105	0.103	0.100	0.095	0.090

Peggs Creek Bridge – Beam

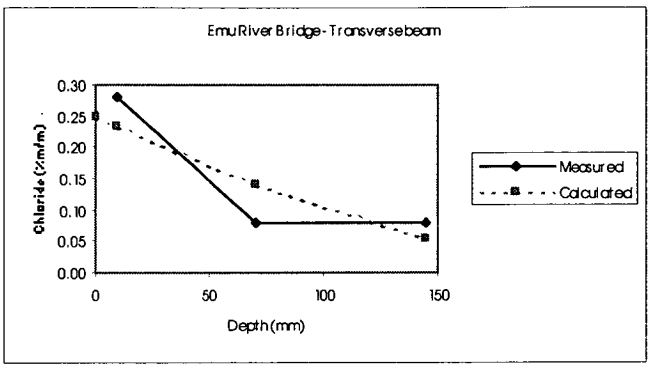

Parameters		Chloride concentration (%m/m) at depth (mm)				
Age (years)	56	Depth	0	10	70	145
C_s	0.25	Measured		0.28	0.08	0.08
D	4.00E-12	Calculated	0.250	0.233	0.139	0.056

Emu River Bridge – Transverse beam

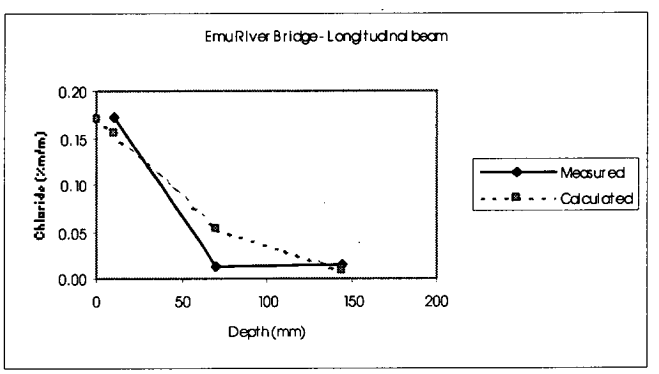

Parameters		Chloride concentration (%m/m) at depth (mm)				
Age (years)	56	Depth	0	10	70	145
C_s	0.17	Measured		0.17	0.01	0.02
D	2.20E-12	Calculated	0.170	0.155	0.052	0.008

Emu River Bridge – Longitudinal beam

Parameters		Chloride concentration (%m/m) at depth (mm)				
Age (years)	56	Depth	0	10	70	145
C_s	0.05	Measured		0.04	0.01	0.01
D	4.80E-13	Calculated	0.047	0.038	0.016	0.004

Emu River Bridge – Longitudinal beam

Parameters		Chloride concentration (%m/m) at depth (mm)				
Age (years)	56	Depth	0	10	70	145
C_s	0.01	Measured		0.01	0.009	0.011
D	Constant	Calculated	0.010	0.010	0.010	0.010

Emu River Bridge - Column

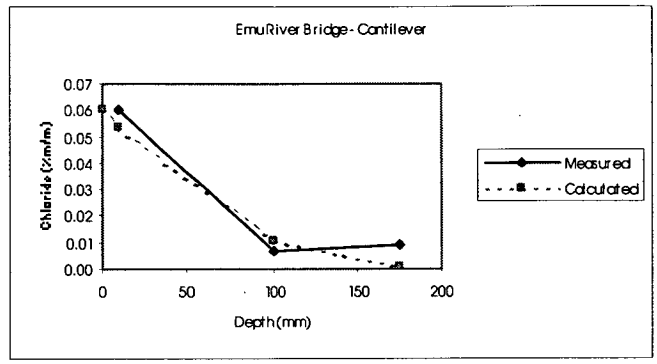

Parameters		Chloride concentration (%m/m) at depth (mm)				
Age (years)	56	Depth	0	10	100	175
C_s	0.06	Measured		0.06	0.01	0.01
D	1.50E-12	Calculated	0.060	0.053	0.010	0.001

Emu River Bridge - Cantilever

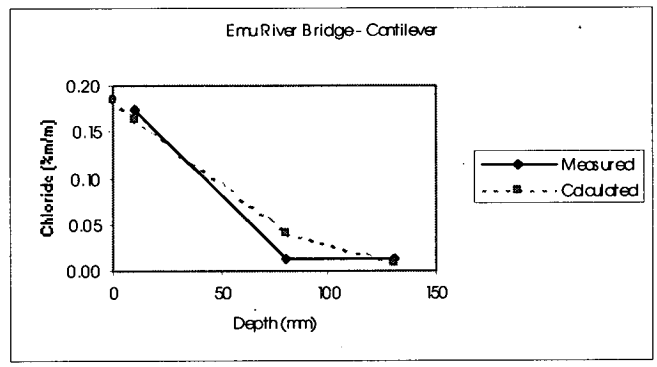

Parameters		Chloride concentration (%m/m) at depth (mm)				
Age (years)	56	Depth	0	10	80	130
C_s	0.19	Measured		0.17	0.01	0.01
D	1.20E-12	Calculated	0.185	0.162	0.041	0.009

Emu River Bridge - Cantilever

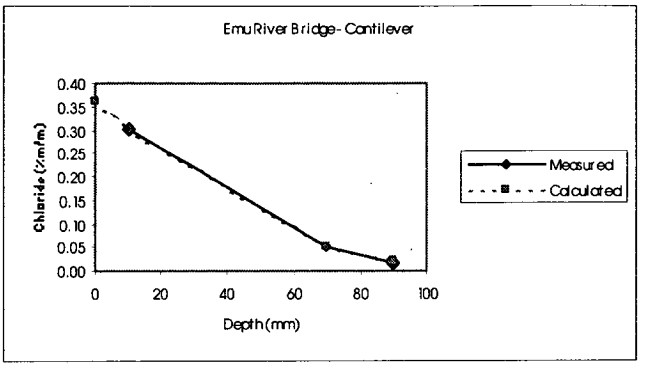

Parameters		Chloride concentration (%m/m) at depth (mm)				
Age (years)	56	Depth	0	10	70	90
C_s	0.36	Measured		0.30	0.05	0.02
D	6.60E-13	Calculated	0.360	0.301	0.053	0.023

Emu River Bridge - Cantilever

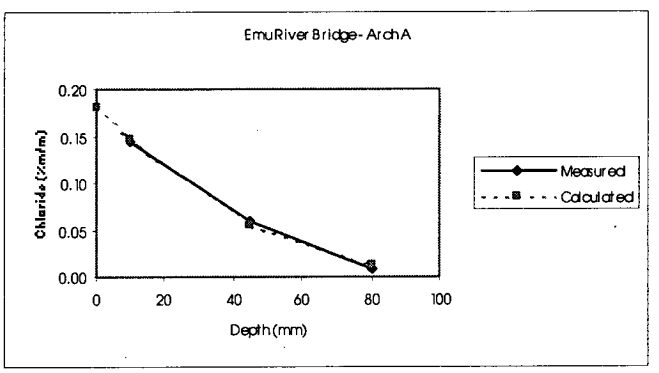

Parameters		Chloride concentration (%m/m) at depth (mm)				
Age (years)	56	Depth	0	10	45	80
C_s	0.18	Measured		0.15	0.06	0.01
D	5.50E-13	Calculated	0.180	0.148	0.055	0.013

Emu River Bridge – Arch A

Parameters		Chloride concentration (%m/m) at depth (mm)				
Age (years)	56	Depth	0	10	80	175
C_s	0.03	Measured		0.03	0.01	0.00
D	3.10E-12	Calculated	0.031	0.029	0.014	0.003

Emu River Bridge - Deck

Parameters		Chloride concentration (%m/m) at depth (mm)					
Age (years)	55	Depth	0	10	30	55	85	125
C_s	0.06	Measured		0.05	0.04	0.02	0.008	0.003
D	8.80E-13	Calculated	0.063	0.054	0.037	0.020	0.008	0.002

Detention River Bridge – East abutment

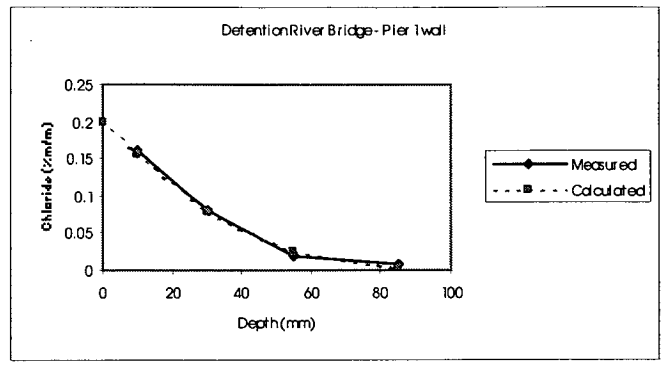

Parameters		Chloride concentration (%m/m) at depth (mm)					
Age (years)	55	Depth	0	10	30	55	85
C_s	0.20	Measured		0.16	0.08	0.02	0.008
D	3.50E-13	Calculated	0.200	0.155	0.078	0.023	0.003

Detention River Bridge – Pier 1 wall

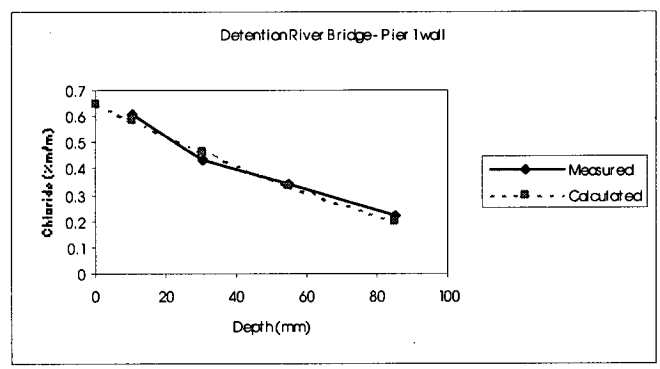

Parameters		Chloride concentration (%m/m) at depth (mm)					
Age (years)	55	Depth	0	10	30	55	85
C_s	0.65	Measured		0.61	0.43	0.34	0.22
D	2.00E-12	Calculated	0.650	0.588	0.467	0.331	0.200

Detention River Bridge – Pier 1 wall

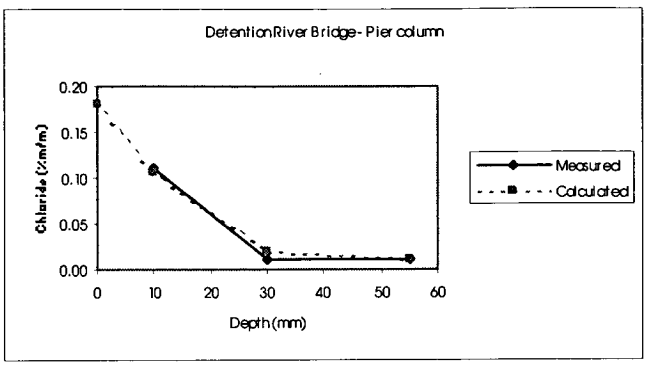

Parameters		Chloride concentration (%m/m) at depth (mm)				
Age (years)	55	Depth	0	10	30	55
C_s	0.18	Measured		0.11	0.01	0.01
D	1.00E-13	Calculated	0.180	0.107	0.019	0.011

Detention River Bridge – Pier column

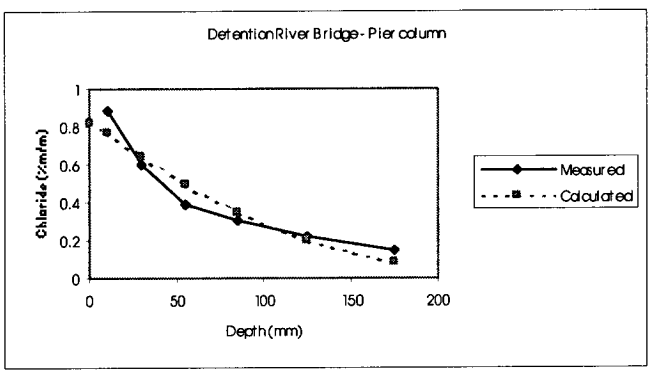

Parameters		Chloride concentration (%m/m) at depth (mm)							
Age (years)	55	Depth	0	10	30	55	85	125	175
C_s	0.83	Measured		0.88	0.60	0.39	0.31	0.22	0.15
D	3.25E-12	Calculated	0.826	0.764	0.643	0.500	0.350	0.198	0.082

Detention River Bridge - Pier column

Parameters		Chloride concentration (%m/m) at depth (mm)				
Age (years)'	55	Depth	0	10	30	55
C_s	0.05	Measured		0.04	0.02	0.01
D	4.66E-13	Calculated	0.048	0.039	0.022	0.008

Detention River Bridge - Beam

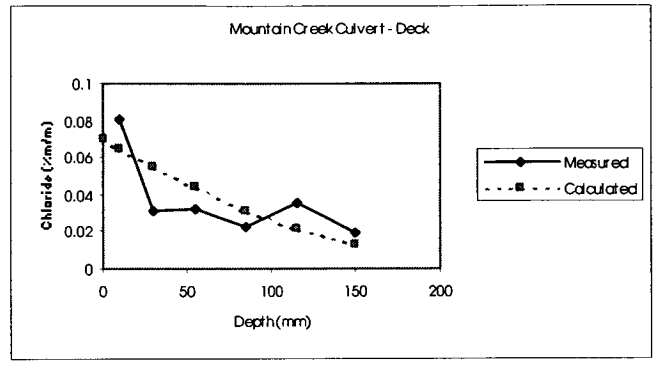

Parameters		Chloride concentration (%m/m) at depth (mm)							
Age (years)	50	Depth	0	10	30	55	85	115	150
C_s	0.07	Measured		0.08	0.03	0.03	0.023	0.036	0.019
D	4.00E-12	Calculated	0.070	0.065	0.055	0.044	0.032	0.021	0.013

Mountain Creek Culvert - Deck

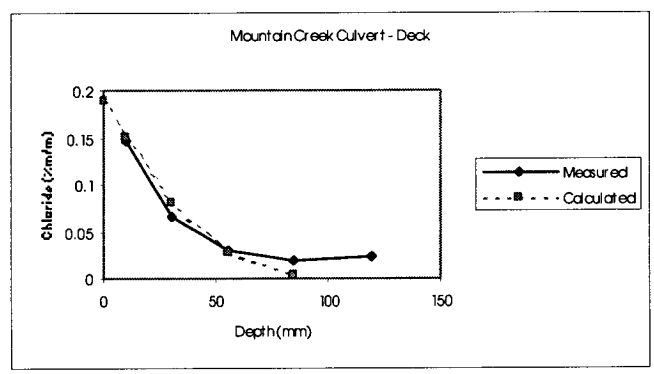

Parameters		Chloride concentration (%m/m) at depth (mm)						
Age (years)	50	Depth	0	10	30	55	85	120
C_s	0.19	Measured		0.15	0.07	0.03	0.02	0.023
D	4.50E-13	Calculated	0.190	0.150	0.081	0.027	0.005	

Mountain Creek Culvert - Deck

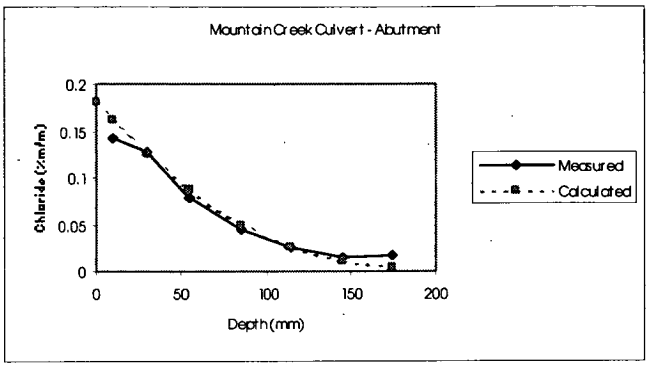

Parameters		Chloride concentration (%m/m) at depth (mm)								
Age (years)	50	Depth	0	10	30	55	85	115	145	175
C_s	0.18	Measured		0.14	0.13	0.08	0.044	0.025	0.015	0.016
D	1.93E-12	Calculated	0.180	0.162	0.126	0.087	0.050	0.025	0.011	0.005

Mountain Creek Culvert - Abutment

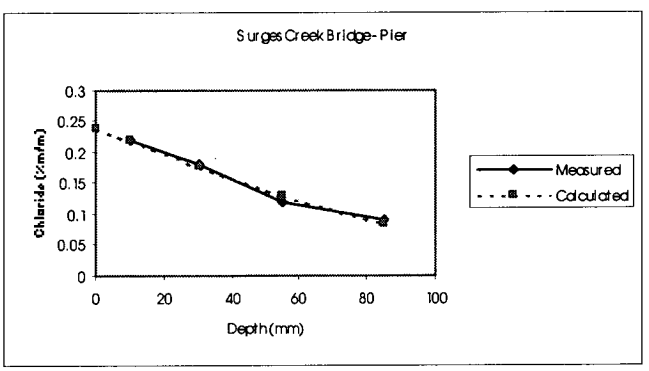

Parameters		Chloride concentration (%m/m) at depth (mm)					
Age (years)	51	Depth	0	10	30	55	85
C_s	0.24	Measured		0.22	0.18	0.12	0.09
D	2.50E-12	Calculated	0.240	0.219	0.177	0.130	0.082

Surges Creek Bridge - Pier

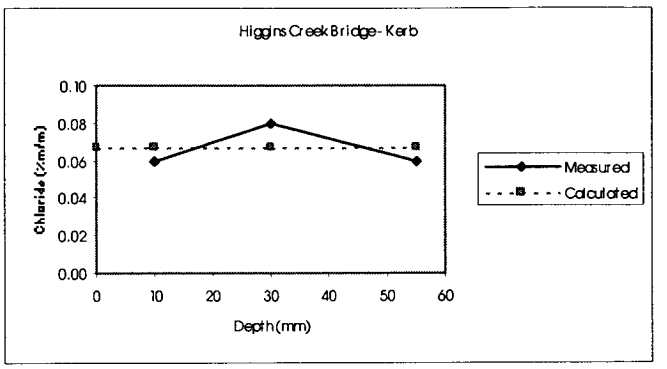

Parameters		Chloride concentration (%m/m) at depth (mm)				
Age (years)	51	Depth	0	10	30	55
C_s	0.07	Measured		0.06	0.08	0.06
D	Constant	Calculated	0.067	0.067	0.067	0.067

Higgins Creek Bridge - Kerb

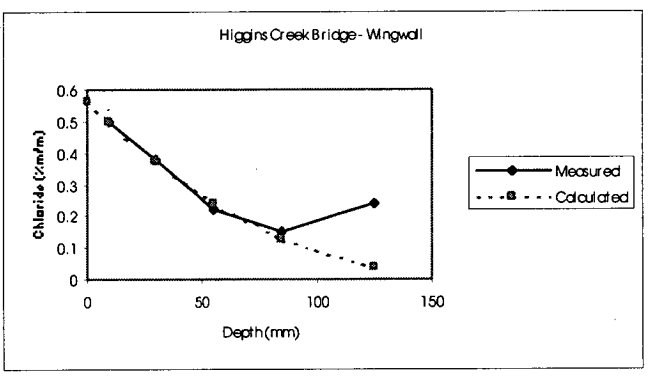

Parameters		Chloride concentration (%m/m) at depth (mm)						
Age (years)	51	Depth	0	10	30	55	85	125
C_s	0.56	Measured		0.50	0.38	0.22	0.15	0.24
D	1.50E-12	Calculated	0.560	0.496	0.373	0.240	0.124	0.040

Higgins Creek Bridge - Wingwall

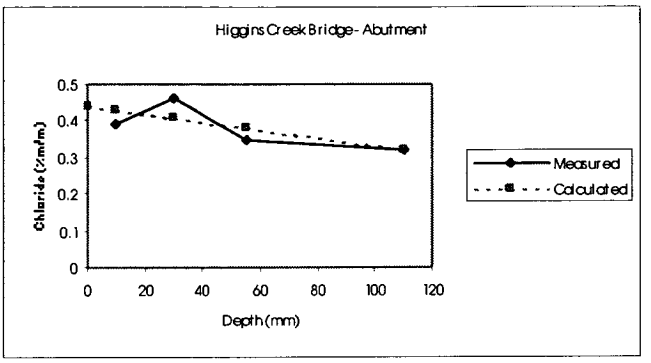

Parameters		Chloride concentration (%m/m) at depth (mm)					
Age (years)	51	Depth	0	10	30	55	110
C_s	0.44	Measured		0.39	0.46	0.35	0.32
D	3.00E-11	Calculated	0.440	0.429	0.406	0.378	0.318

Higgins Creek Bridge - Abutment

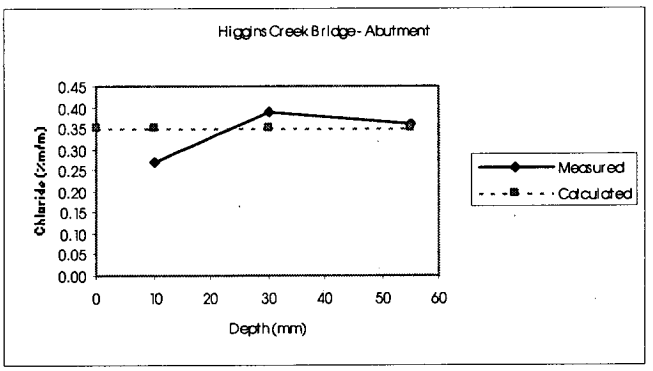

Parameters		Chloride concentration (%m/m) at depth (mm)				
Age (years)	51	Depth	0	10	30	55
C_s	0.35	Measured		0.27	0.39	0.36
D	Constant	Calculated	0.350	0.350	0.350	0.350

Higgins Creek Bridge - Abutment

Parameters		Chloride concentration (%m/m) at depth (mm)				
Age (years)	48	Depth	0	10	30	55
C_s	0.05	Measured		0.04	0.03	0.01
D	6.00E-13	Calculated	0.051	0.042	0.025	0.010

Carlton River Bridge - Abutment

Parameters		Chloride concentration (%m/m) at depth (mm)					
Age (years)	48	Depth	0	10	30	55	85
C_s	0.04	Measured		0.04	0.03	0.02	0.021
D	3.00E-12	Calculated	0.036	0.033	0.027	0.020	0.013

Carlton River Bridge – Cell walls

Parameters		Chloride concentration (%m/m) at depth (mm)						
Age (years)	48	Depth	0	10	30	55	85	125
C_s	0.06	Measured		0.06	0.05	0.03	0.024	0.035
D	4.00E-12	Calculated	0.058	0.054	0.046	0.036	0.026	0.015

Carlton River Bridge - Floor

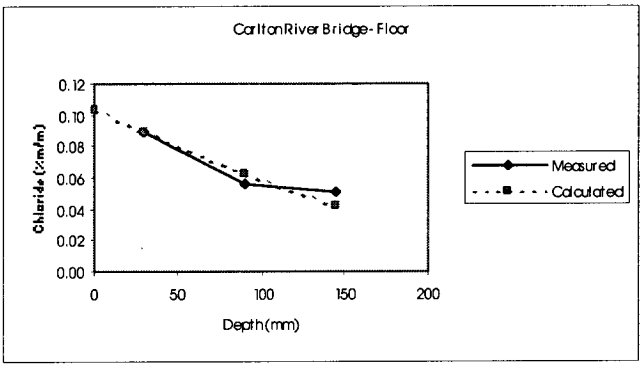

Parameters		Chloride concentration (%m/m) at depth (mm)				
Age (years)	48	Depth	0	30	90	145
C_s	0.10	Measured		0.09	0.06	0.05
D	1.00E-11	Calculated	0.104	0.090	0.063	0.042

Carlton River Bridge - Floor

Parameters		Chloride concentration (%m/m) at depth (mm)					
Age (years)	48	Depth	0	10	30	50	85
C_s	0.04	Measured		0.04	0.03	0.04	0.033
D	Constant	Calculated	0.035	0.035	0.035	0.035	0.035

Carlton River Bridge - Deck

Parameters		Chloride concentration (%m/m) at depth (mm)				
Age (years)	48	Depth	0	10	30	60
C_s	0.04	Measured		0.04	0.04	0.04
D	Constant	Calculated	0.039	0.039	0.039	0.039

Carlton River Bridge - Deck

Parameters		Chloride concentration (%m/m) at depth (mm)						
Age (years)	49	Depth	0	10	30	55	85	125
C_s	0.06	Measured		0.04	0.01	0.01	0.004	0.001
D	2.00E-13	Calculated	0.055	0.038	0.013	0.002		

Carlton River Bridge – Pier footing

Parameters		Chloride concentration (%m/m) at depth (mm)						
Age (years)	46	Depth	0	10	30	55	85	115
C_s	0.07	Measured		0.05	0.02	0.03	0.022	0.022
D	3.50E-13	Calculated	0.069	0.052	0.024	0.006	0.001	

Scopus Creek Bridge - Deck

Parameters		Chloride concentration (%m/m) at depth (mm)					
Age (years)	46	Depth	0	10	30	55	85
C_s	0.06	Measured		0.06	0.04	0.02	0.02
D	2.00E-12	Calculated	0.058	0.052	0.040	0.027	0.015

Scopus Creek Bridge - Deck

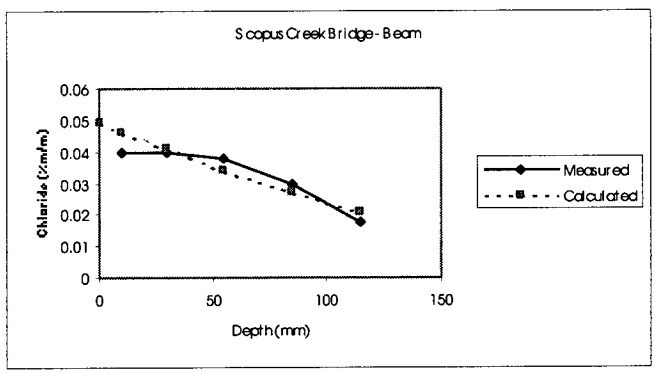

Parameters		Chloride concentration (%m/m) at depth (mm)						
Age (years)	46	Depth	0	10	30	55	85	115
C_s	0.05	Measured		0.04	0.04	0.04	0.03	0.018
D	7.00E-12	Calculated	0.049	0.046	0.041	0.034	0.027	0.021

Scopus Creek Bridge - Beam

Parameters		Chloride concentration (%m/m) at depth (mm)					
Age (years)	46	Depth	0	10	30	55	85
C_s	0.04	Measured		0.05	0.03	0.05	0.03
D	Constant	Calculated	0.040	0.040	0.040	0.040	0.040

Scopus Creek Bridge - Deck

Parameters		Chloride concentration (%m/m) at depth (mm)					
Age (years)	46	Depth	0	10	30	55	85
C_s	0.03	Measured		0.02	0.03	0.02	0.02
D	2.50E-11	Calculated	0.025	0.024	0.023	0.021	0.019

Scopus Creek Bridge - Deck

Parameters		Chloride concentration (%m/m) at depth (mm)					
Age (years)	46	Depth	0	10	30	55	85
C_s	0.06	Measured		0.06	0.04	0.02	0.04
D	5.00E-12	Calculated	0.055	0.051	0.044	0.036	0.026

Scopus Creek Bridge - Beam

Parameters		Chloride concentration (%m/m) at depth (mm)					
Age (years)	46	Depth	0	10	30	55	85
C_s	0.04	Measured		0.03	0.05	0.02	0.04
D	1.00E-11	Calculated	0.042	0.040	0.036	0.031	0.026

Scopus Creek Bridge - Abutment

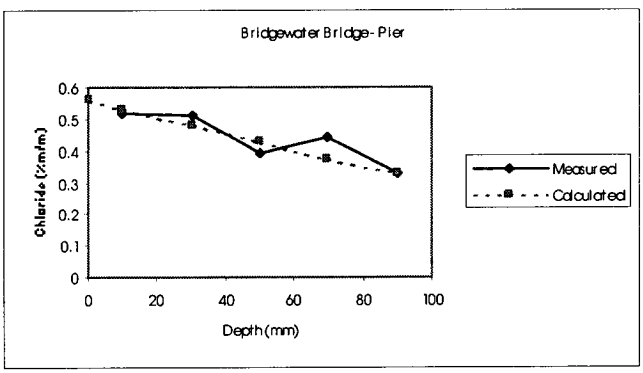

Parameters		Chloride concentration (%m/m) at depth (mm)						
Age (years)	43	Depth	0	10	30	50	70	90
C_s	0.56	Measured		0.52	0.51	0.39	0.44	0.33
D	1.00E-11	Calculated	0.560	0.533	0.479	0.426	0.376	0.328

Bridgewater Bridge - Pier

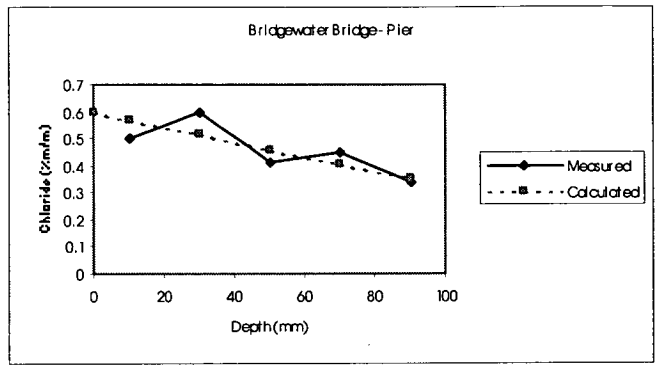

Parameters		Chloride concentration (%m/m) at depth (mm)						
Age (years)	43	Depth	0	10	30	50	70	90
C_s	0.60	Measured		0.5	0.6	0.41	0.45	0.34
D	1.00E-11	Calculated	0.600	0.571	0.513	0.457	0.403	0.351

Bridgewater Bridge - Pier

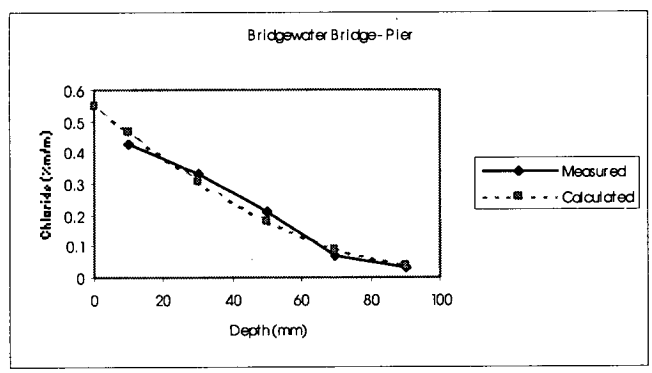

Parameters		Chloride concentration (%m/m) at depth (mm)						
Age (years)	43	Depth	0	10	30	50	70	90
C_s	0.55	Measured		0.43	0.33	0.21	0.07	0.03
D	9.40E-13	Calculated	0.550	0.464	0.304	0.177	0.091	0.041

Bridgewater Bridge - Pier

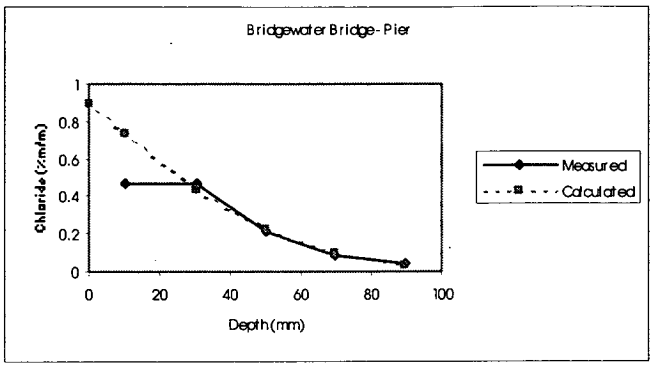

Parameters		Chloride concentration (%m/m) at depth (mm)						
Age (years)	43	Depth	0	10	30	50	70	90
C_s	0.89	Measured		0.47	0.47	0.2	0.09	0.04
D	7.14E-13	Calculated	0.890	0.730	0.441	0.228	0.100	0.036

Bridgewater Bridge - Pier

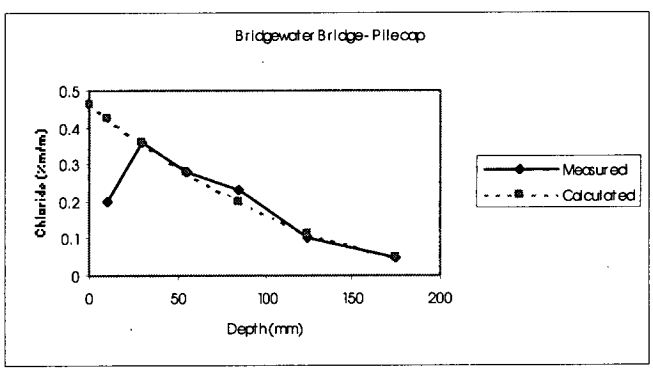

Parameters		Chloride concentration (%m/m) at depth (mm)							
Age (years)	49	Depth	0	10	30	55	85	125	175
C_s	0.46	Measured		0.2	0.36	0.28	0.23	0.1	0.05
D	3.79E-12	Calculated	0.460	0.426	0.360	0.281	0.199	0.114	0.049

Bridgewater Bridge – Pile cap

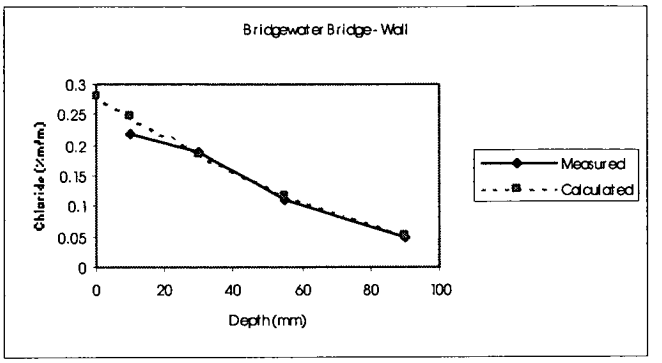

Parameters		Chloride concentration (%m/m) at depth (mm)					
Age (years)	49	Depth	0	10	30	55	90
C_s	0.28	Measured		0.22	0.19	0.11	0.05
D	1.49E-12	Calculated	0.280	0.247	0.185	0.117	0.052

Bridgewater Bridge – Wall

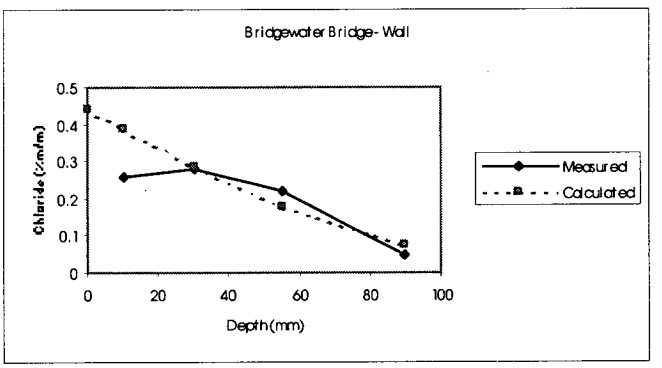

Parameters		Chloride concentration (%m/m) at depth (mm)					
Age (years)	49	Depth	0	10	30	55	90
C_s	0.44	Measured		0.26	0.28	0.22	0.05
D	1.40E-12	Calculated	0.440	0.387	0.285	0.177	0.075

Bridgewater Bridge - Wall

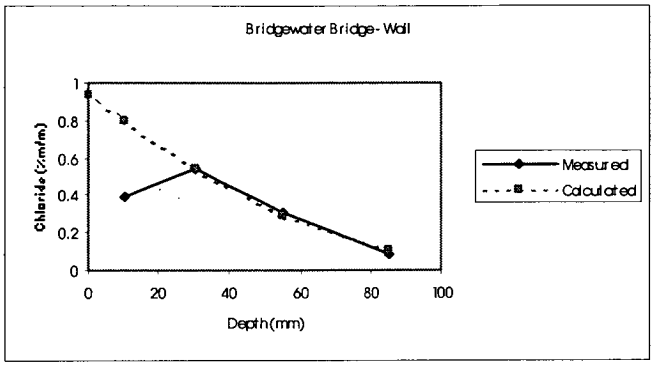

Parameters		Chloride concentration (%m/m) at depth (mm)					
Age (years)	49	Depth	0	10	30	55	85
C_s	0.94	Measured		0.39	0.54	0.31	0.08
D	9.50E-13	Calculated	0.940	0.802	0.545	0.292	0.110

Bridgewater Bridge - Wall

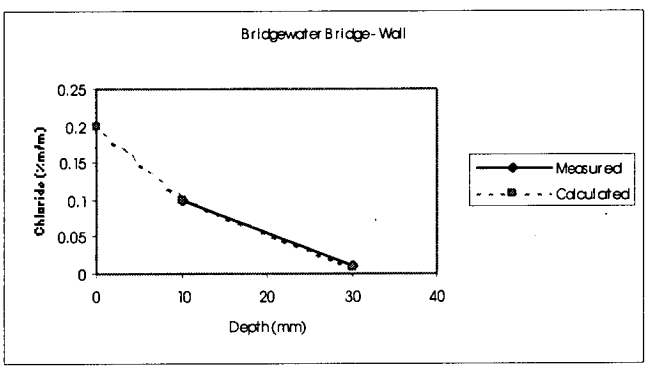

Parameters		Chloride concentration (%m/m) at depth (mm)			
Age (years)	49	Depth	0	10	30
C_s	0.20	Measured		0.1	0.01
D	7.20E-14	Calculated	0.200	0.101	0.009

Bridgewater Bridge - Wall

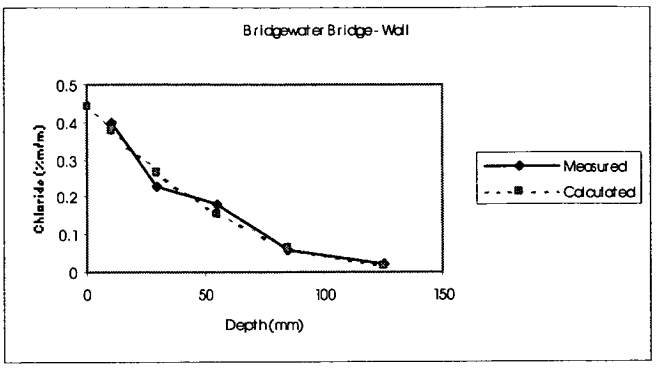

Parameters		Chloride concentration (%m/m) at depth (mm)						
Age (years)	49	Depth	0	10	30	55	85	125
C_s	0.44	Measured		0.4	0.23	0.18	0.06	0.02
D	1.10E-12	Calculated	0.440	0.380	0.267	0.152	0.064	0.014

Bridgewater Bridge - Wall

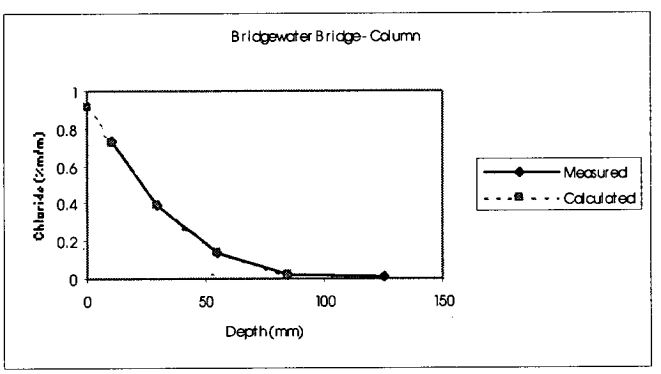

Parameters		Chloride concentration (%m/m) at depth (mm)						
Age (years)	49	Depth	0	10	30	55	85	125
C_s	0.91	Measured		0.73	0.39	0.14	0.02	0.007
D	4.80E-13	Calculated	0.910	0.724	0.397	0.140	0.025	

Bridgewater Bridge - Column

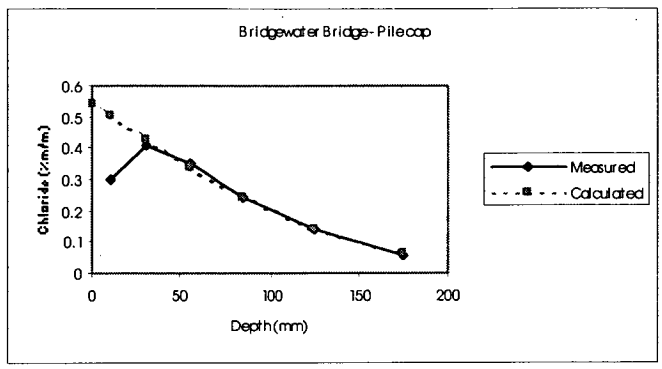

Parameters		Chloride concentration (%m/m) at depth (mm)							
Age (years)	49	Depth	0	10	30	55	85	125	175
C_s	0.54	Measured		0.3	0.41	0.35	0.24	0.14	0.06
D	4.00E-12	Calculated	0.540	0.501	0.425	0.335	0.240	0.141	0.062

Bridgewater Bridge – Pile cap

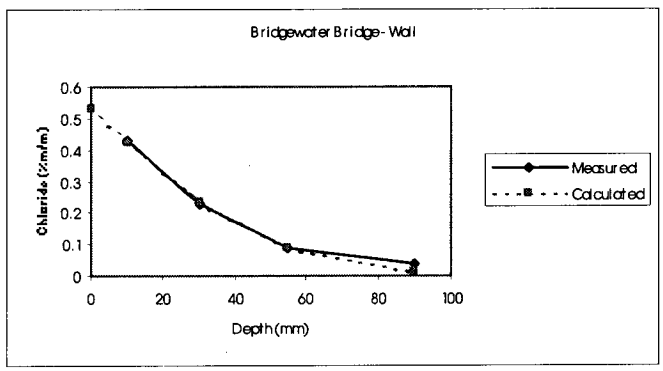

Parameters		Chloride concentration (%m/m) at depth (mm)					
Age (years)	49	Depth	0	10	30	55	90
C_s	0.53	Measured		0.43	0.23	0.09	0.04
D	5.00E-13	Calculated	0.530	0.424	0.236	0.086	0.012

Bridgewater Bridge - Wall

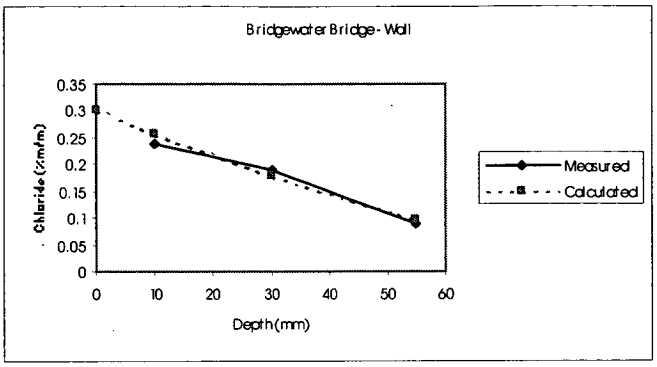

Parameters		Chloride concentration (%m/m) at depth (mm)				
Age (years)	49	Depth	0	10	30	55
C_s	0.30	Measured		0.24	0.19	0.09
D	1.00E-12	Calculated	0.300	0.257	0.177	0.097

Bridgewater Bridge - Wall

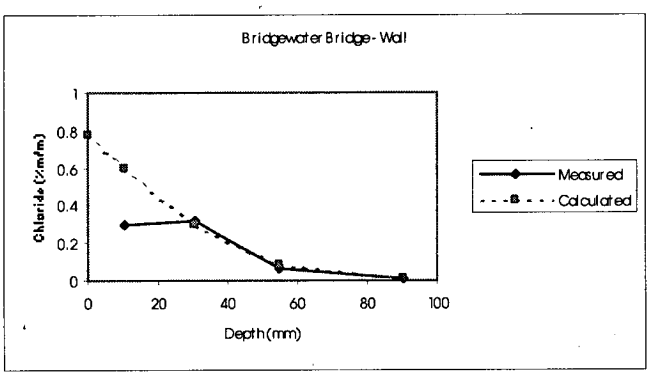

Parameters		Chloride concentration (%m/m) at depth (mm)					
Age (years)	49	Depth	0	10	30	55	90
C_s	0.78	Measured		0.3	0.32	0.06	0.008
D	3.80E-13	Calculated	0.780	0.601	0.298	0.085	0.011

Bridgewater Bridge - Wall

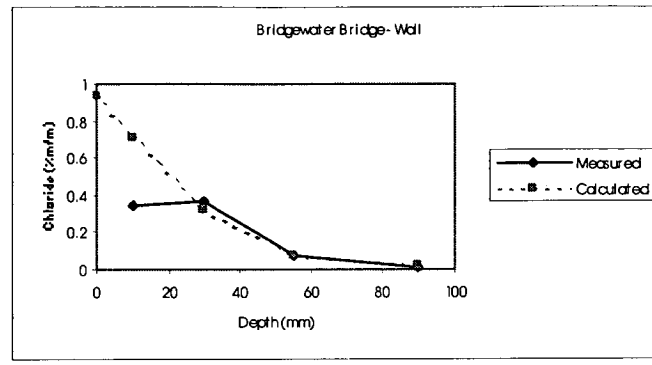

Parameters		Chloride concentration (%m/m) at depth (mm)					
Age (years)	49	Depth	0	10	30	55	90
C_s	0.94	Measured		0.34	0.37	0.07	0.008
D	3.30E-13	Calculated	0.940	0.709	0.327	0.080	0.025

Bridgewater Bridge - Wall

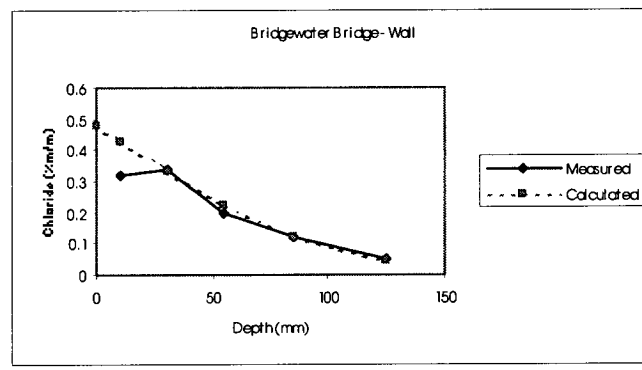

Parameters		Chloride concentration (%m/m) at depth (mm)						
Age (years)	49	Depth	0	10	30	55	85	125
C_s	0.48	Measured		0.32	0.34	0.2	0.12	0.05
D	1.80E-12	Calculated	0.480	0.429	0.330	0.221	0.122	0.045

Bridgewater Bridge - Wall

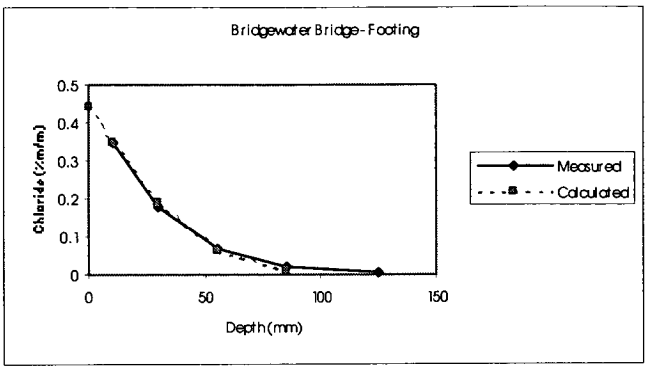

Parameters		Chloride concentration (%m/m) at depth (mm)						
Age (years)	49	Depth	0	10	30	55	85	125
C_s	0.44	Measured		0.35	0.18	0.07	0.02	0.005
D	4.70E-13	Calculated	0.440	0.349	0.190	0.066	0.011	

Bridgewater Bridge - Footing

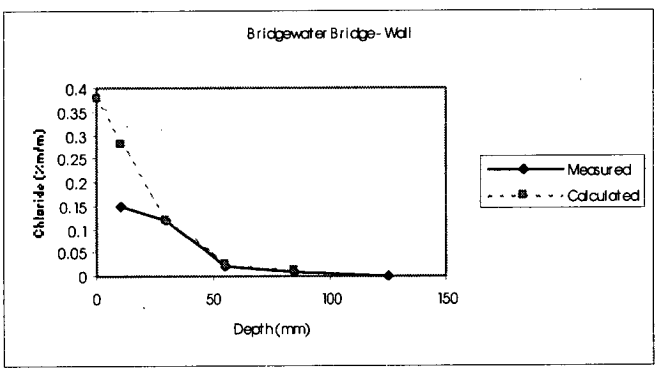

Parameters		Chloride concentration (%m/m) at depth (mm)						
Age (years)	49	Depth	0	10	30	55	85	125
C_s	0.38	Measured		0.15	0.12	0.02	0.007	0.002
D	2.90E-13	Calculated	0.380	0.281	0.120	0.025	0.011	

Bridgewater Bridge - Wall

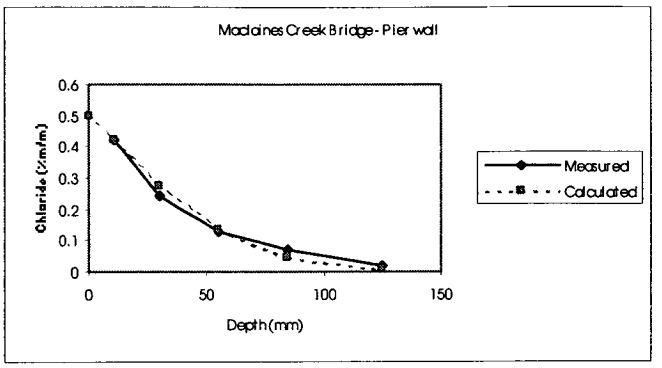

Parameters		Chloride concentration (%m/m) at depth (mm)						
Age (years)	47	Depth	0	10	30	55	85	125
C_s	0.50	Measured		0.42	0.24	0.13	0.07	0.02
D	8.50E-13	Calculated	0.500	0.421	0.275	0.137	0.045	0.007

Maclaines Creek Bridge – Pier wall

Parameters		Chloride concentration (%m/m) at depth (mm)					
Age (years)	47	Depth	0	10	30	55	85
C_s	0.041	Measured		0.03	0.008	0.003	0.001
D	2.00E-13	Calculated	0.041	0.028	0.009	0.001	

Maclaines Creek Bridge – Pier wall

Parameters		Chloride concentration (%m/m) at depth (mm)				
Age (years)	47	Depth	0	10	30	55
C_s	0.025	Measured		0.02	0.01	0.004
D	5.00E-13	Calculated	0.025	0.020	0.011	0.004

Maclaines Creek Bridge - Diaphragm

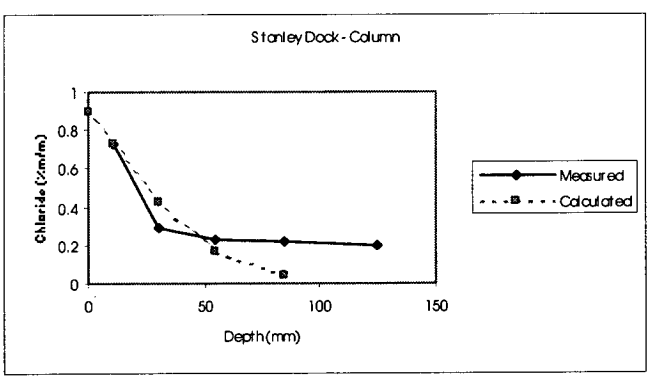

Parameters		Chloride concentration (%m/m) at depth (mm)						
Age (years)	46	Depth	0	10	30	55	85	125
C_s	0.900	Measured		0.73	0.29	0.23	0.22	0.2
D	6.00E-13	Calculated	0.900	0.730	0.425	0.169	0.038	

Stanley Dock – Column

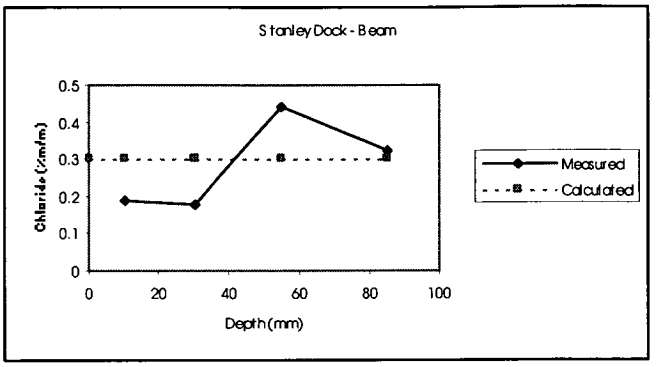

Parameters		Chloride concentration (%m/m) at depth (mm)					
Age (years)	46	Depth	0	10	30	55	85
C_s	0.300	Measured		0.19	0.18	0.44	0.32
D	Constant	Calculated	0.300	0.300	0.300	0.300	0.300

Stanley Dock - Beam

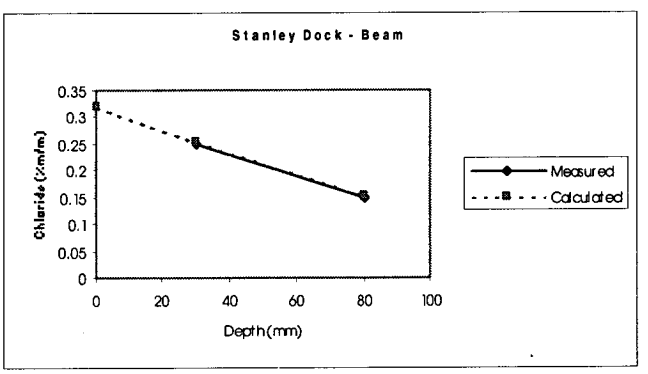

Parameters		Chloride concentration (%m/m) at depth (mm)			
Age (years)	46	Depth	0	30	80
C_s	0.320	Measured		0.25	0.15
D	4.40E-12	Calculated	0.320	0.253	0.153

Stanley Dock - Beam

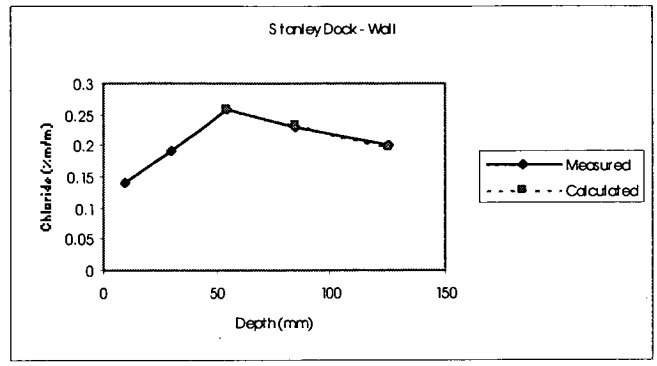

Parameters		Chloride concentration (%m/m) at depth (mm)						
Age (years)	46	Depth	0	10	20	55	85	125
C_s	0.260	Measured		0.14	0.19	0.26	0.23	0.2
D	1.90E-11	Calculated				0.260	0.234	0.199

NB: Skin effect (55mm) excluded

Stanley Dock - Wall

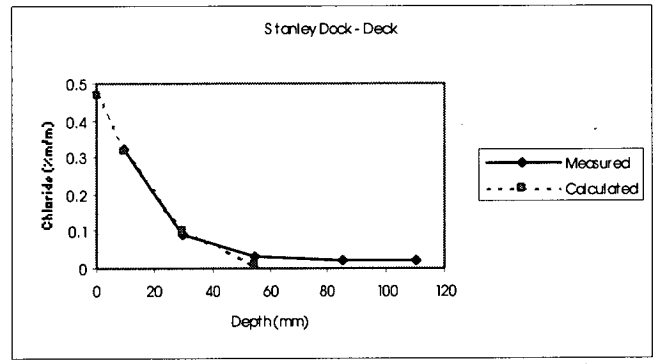

Parameters		Chloride concentration (%m/m) at depth (mm)						
Age (years)	31	Depth	0	10	30	55	85	110
C_s	0.470	Measured		0.32	0.09	0.03	0.02	0.02
D	3.00E-13	Calculated	0.470	0.320	0.101	0.011		

Stanley Dock - Deck

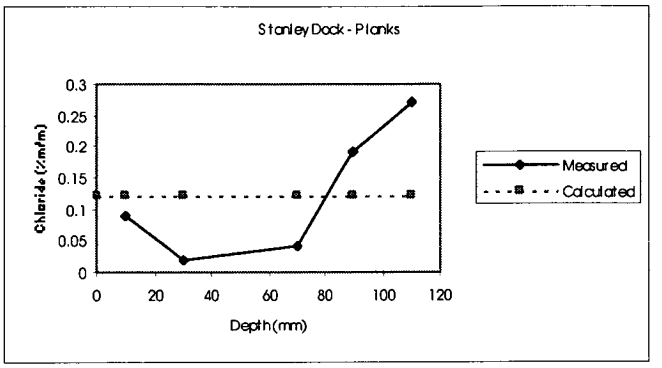

Parameters		Chloride concentration (%m/m) at depth (mm)						
Age (years)	31	Depth	0	10	30	70	90	110
C_s	0.120	Measured		0.09	0.02	0.04	0.19	0.27
D	Constant	Calculated	0.120	0.120	0.120	0.120	0.120	0.120

Stanley Dock - Planks

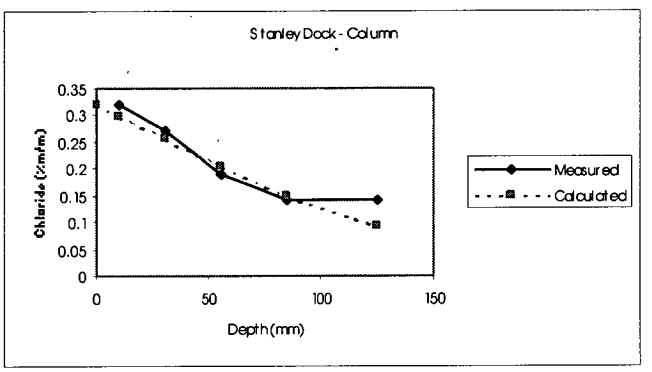

Parameters		Chloride concentration (%m/m) at depth (mm)						
Age (years)	31	Depth	0	10	30	55	85	125
C_s	0.320	Measured		0.32	0.27	0.19	0.14	0.14
D	7.00E-12	Calculated	0.320	0.298	0.255	0.204	0.150	0.091

Stanley Dock - Column

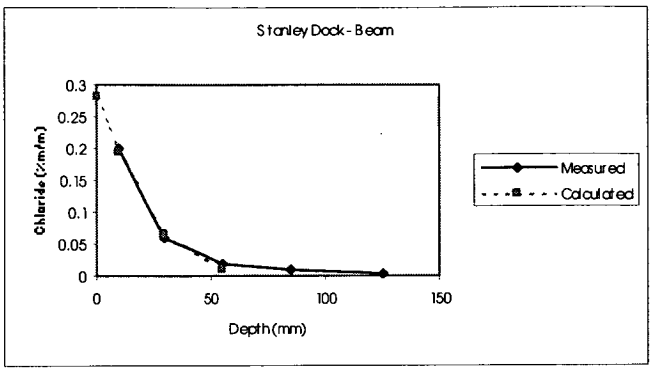

Parameters		Chloride concentration (%m/m) at depth (mm)						
Age (years)	31	Depth	0	10	30	55	85	125
C_s	0.280	Measured		0.2	0.06	0.02	0.01	0.003
D	3.30E-13	Calculated	0.280	0.194	0.067	0.009		

Stanley Dock - Beam

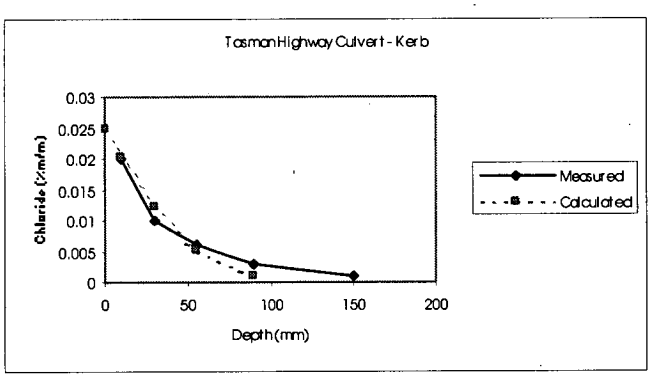

Parameters		Chloride concentration (%m/m) at depth (mm)						
Age (years)	44	Depth	0	10	30	55	90	150
C_s	0.025	Measured		0.02	0.01	0.006	0.003	0.001
D	7.00E-13	Calculated	0.025	0.020	0.012	0.005	0.001	

Tasman Highway Culvert - Kerb

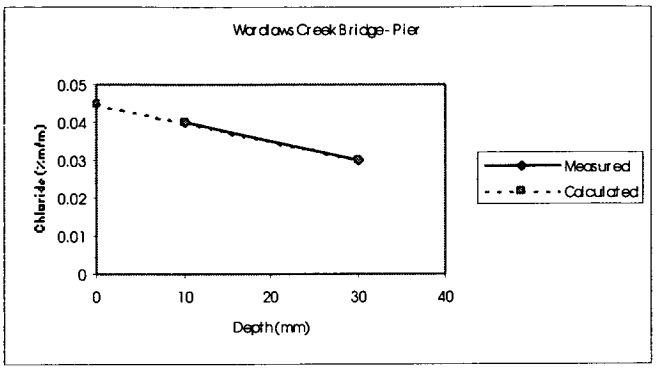

Parameters		Chloride concentration (%m/m) at depth (mm)			
Age (years)	41	Depth	0	10	30
C_s	0.045	Measured		0.04	0.03
D	1.90E-12	Calculated	0.045	0.040	0.030

Wardlaws Creek Bridge - Pier

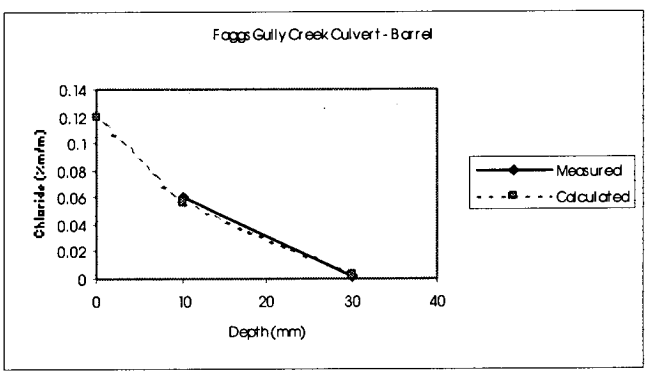

Parameters		Chloride concentration (%m/m) at depth (mm)			
Age (years)	44	Depth	0	10	30
C_s	0.120	Measured		0.06	0.001
D	7.00E-14	Calculated	0.120	0.056	0.004

Faggs Gully Creek Culvert - Barrel

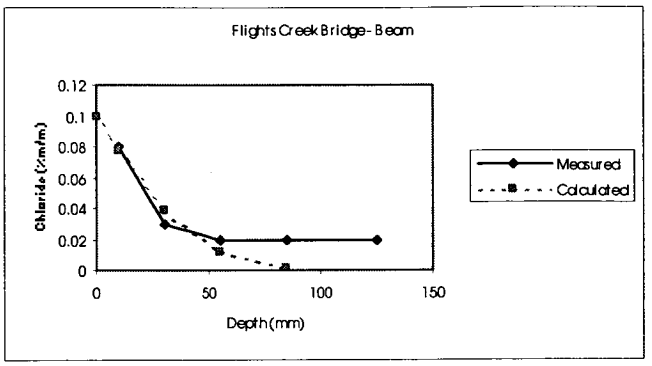

Parameters		Chloride concentration (%m/m) at depth (mm)						
Age (years)	43	Depth	0	10	30	55	85	125
C_s	0.100	Measured		0.08	0.03	0.02	0.02	0.02
D	4.50E-13	Calculated	0.100	0.078	0.039	0.012	0.002	

Flights Creek Bridge - Beam

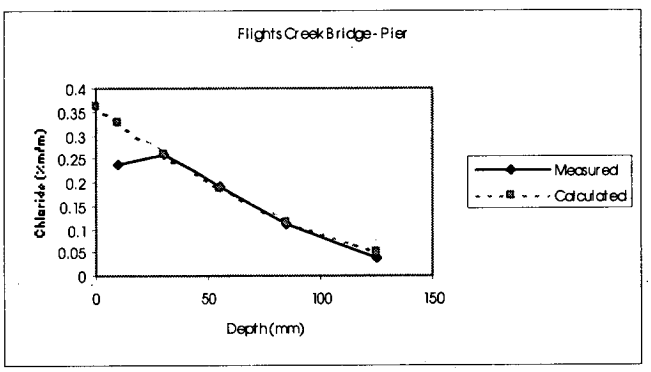

Parameters		Chloride concentration (%m/m) at depth (mm)						
Age (years)	43	Depth	0	10	30	55	85	125
C_s	0.360	Measured		0.24	0.26	0.19	0.11	0.04
D	2.70E-12	Calculated	0.360	0.327	0.261	0.187	0.115	0.052

Flights Creek Bridge - Pier

Parameters		Chloride concentration (%m/m) at depth (mm)					
Age (years)	43	Depth	0	10	30	55	85
C_s	0.041	Measured		0.03	0.01	0.004	0.001
D	2.60E-13	Calculated	0.041	0.029	0.011	0.002	

Flights Creek Bridge - Deck

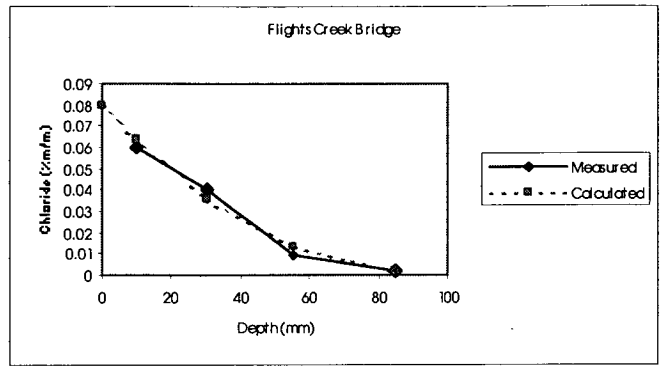

Parameters		Chloride concentration (%m/m) at depth (mm)					
Age (years)	43	Depth	0	10	30	55	85
C_s	0.080	Measured		0.06	0.04	0.009	0.002
D	5.60E-13	Calculated	0.080	0.064	0.035	0.013	0.002

Flights Creek Bridge

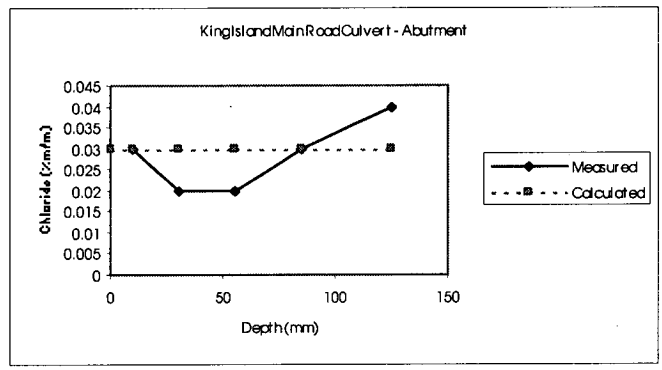

Parameters		Chloride concentration (%m/m) at depth (mm)						
Age (years)	43	Depth	0	10	30	55	85	125
C_s	0.030	Measured		0.03	0.02	0.02	0.03	0.04
D	Constant	Calculated	0.030	0.030	0.030	0.030	0.030	0.030

King Island Main Road Culvert - Abutment

Parameters		Chloride concentration (%m/m) at depth (mm)						
Age (years)	43	Depth	0	10	30	55	85	125
C_s	0.020	Measured		0.02	0.02	0.02	0.02	0.02
D	Constant	Calculated	0.02	0.02	0.02	0.02	0.02	0.02

King Island Main Road Culvert - Abutment

Parameters		Chloride concentration (%m/m) at depth (mm)					
Age (years)	43	Depth	0	10	30	50	90
C_s	0.040	Measured		0.03	0.03	0.04	0.02
D	1.30E-12	Calculated				0.04	0.02

Note: Skin effect (50mm) excluded

King Island Main Road Culvert – Deck plank

Parameters		Chloride concentration (%m/m) at depth (mm)					
Age (years)	41	Depth	0	10	30	55	85
C_s	0.026	Measured		0.02	0.01	0.004	0.001
D	4.80E-13	Calculated	0.026	0.020	0.010	0.003	0.000

East Arm Culvert - Wingwall

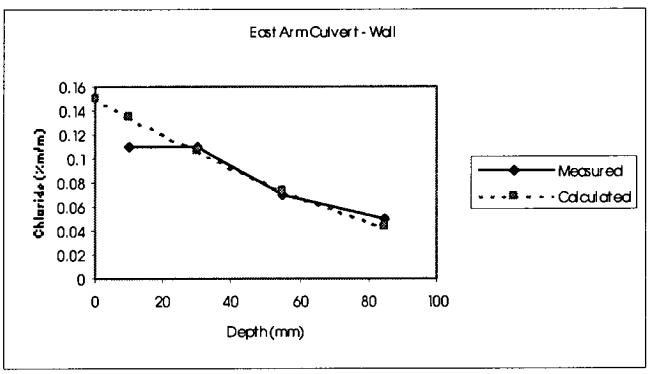

Parameters		Chloride concentration (%m/m) at depth (mm)					
Age (years)	41	Depth	0	10	30	55	85
C_s	0.150	Measured		0.11	0.11	0.07	0.05
D	2.50E-12	Calculated	0.150	0.135	0.106	0.074	0.044

East Arm Culvert - Wall

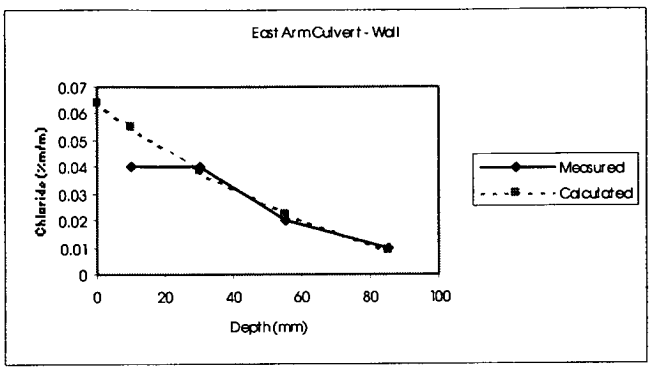

Parameters		Chloride concentration (%m/m) at depth (mm)					
Age (years)	41	Depth	0	10	30	55	85
C_s	0.064	Measured		0.04	0.04	0.02	0.01
D	1.30E-12	Calculated	0.064	0.055	0.039	0.022	0.009

East Arm Culvert - Wall

Parameters		Chloride concentration (%m/m) at depth (mm)				
Age (years)	37	Depth	0	10	30	55
C_s	0.026	Measured		0.02	0.01	0.01
D	5.00E-13	Calculated	0.026	0.020	0.010	0.003

Ralphs Bay Canal Bridge - Crosshead

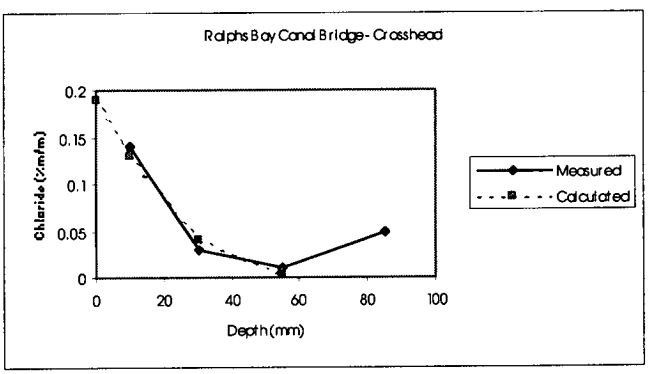

Parameters		Chloride concentration (%m/m) at depth (mm)					
Age (years)	37	Depth	0	10	30	55	85
C_s	0.190	Measured		0.14	0.03	0.01	0.05
D	2.50E-13	Calculated	0.190	0.129	0.041	0.004	

Ralphs Bay Canal Bridge - Crosshead

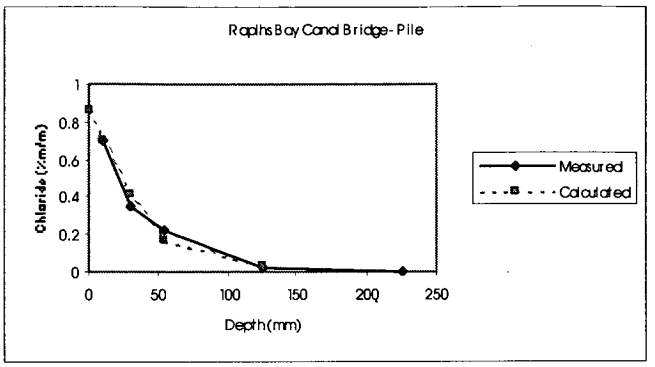

Parameters		Chloride concentration (%m/m) at depth (mm)						
Age (years)	37	Depth	0	10	30	55	125	225
C_s	0.860	Measured		0.7	0.35	0.22	0.02	0.001
D	8.00E-13	Calculated	0.860	0.703	0.419	0.175	0.035	

Ralphs Bay Canal Bridge - Pile

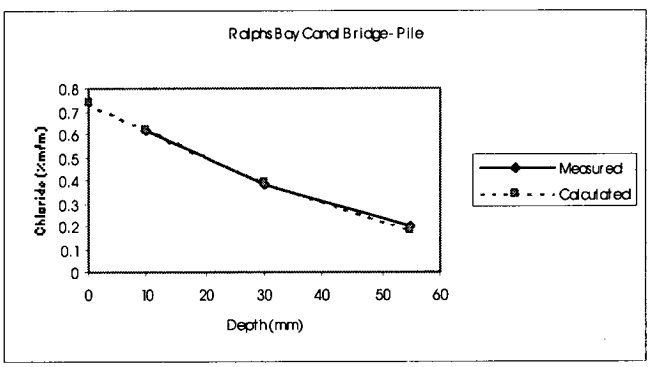

Parameters		Chloride concentration (%m/m) at depth (mm)				
Age (years)	37	Depth	0	10	30	55
C_s	0.740	Measured		0.62	0.38	0.2
D	9.60E-13	Calculated	0.740	0.616	0.390	0.182

Ralphs Bay Canal Bridge - Pile

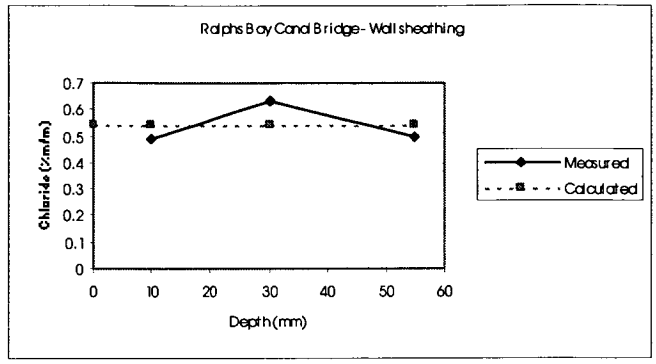

Parameters		Chloride concentration (%m/m) at depth (mm)				
Age (years)	37	Depth	0	10	30	55
C_s	0.540	Measured		0.49	0.63	0.5
D	Constant	Calculated	0.540	0.540	0.540	0.540

Ralphs Bay Canal Bridge – Wall sheathing

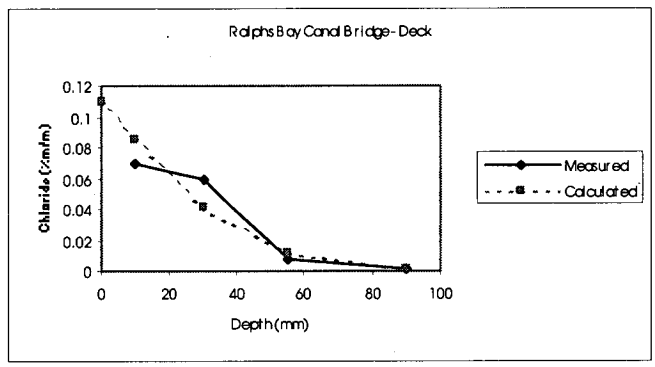

Parameters		Chloride concentration (%m/m) at depth (mm)					
Age (years)	37	Depth	0	10	30	55	90
C_s	0.110	Measured		0.07	0.06	0.008	0.001
D	5.00E-13	Calculated	0.110	0.085	0.042	0.012	0.002

Ralphs Bay Canal Bridge - Deck

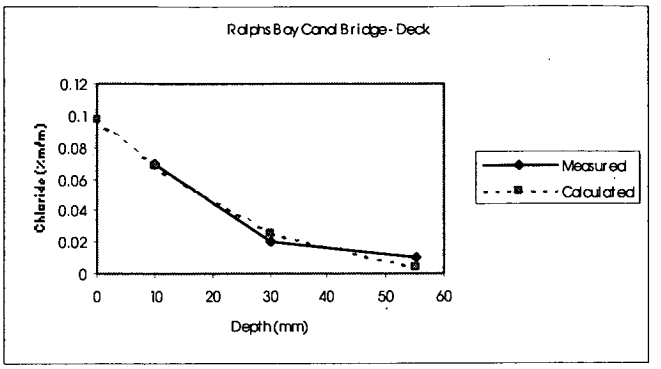

Parameters		Chloride concentration (%m/m) at depth (mm)				
Age (years)	37	Depth	0	10	30	55
C_s	0.097	Measured		0.07	0.02	0.01
D	3.00E-13	Calculated	0.097	0.068	0.025	0.004

Ralphs Bay Canal Bridge - Deck

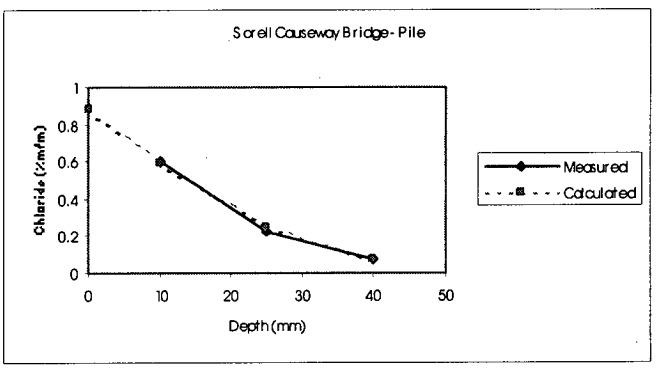

Parameters		Chloride concentration (%m/m) at depth (mm)				
Age (years)	37	Depth	0	10	25	40
C_s	0.880	Measured		0.6	0.23	0.08
D	2.30E-13	Calculated	0.880	0.596	0.247	0.074

Sorell Causeway Bridge - Pile

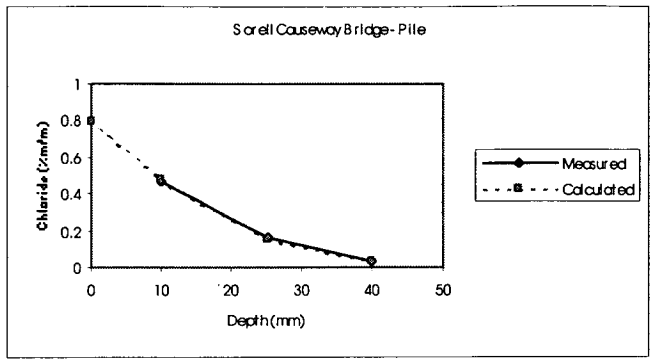

Parameters		Chloride concentration (%m/m) at depth (mm)				
Age (years)	37	Depth	0	10	25	40
C_s	0.790	Measured		0.47	0.16	0.03
D	1.60E-13	Calculated	0.790	0.478	0.155	0.031

Sorell Causeway Bridge - Pile

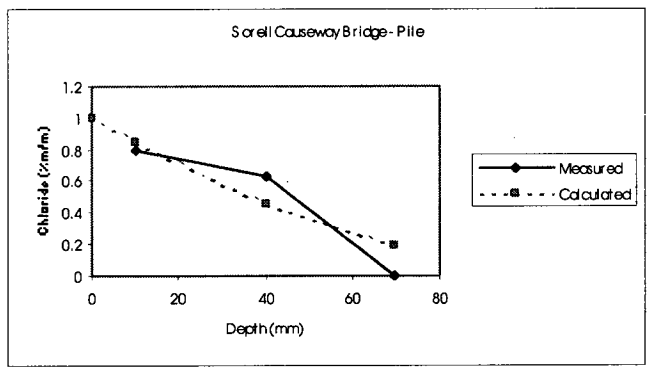

Parameters		Chloride concentration (%m/m) at depth (mm)				
Age (years)	37	Depth	0	10	40	70
C_s	1.000	Measured		0.79	0.63	0.004
D	1.23E-12	Calculated	1.000	0.852	0.456	0.192

Sorell Causeway Bridge - Pile

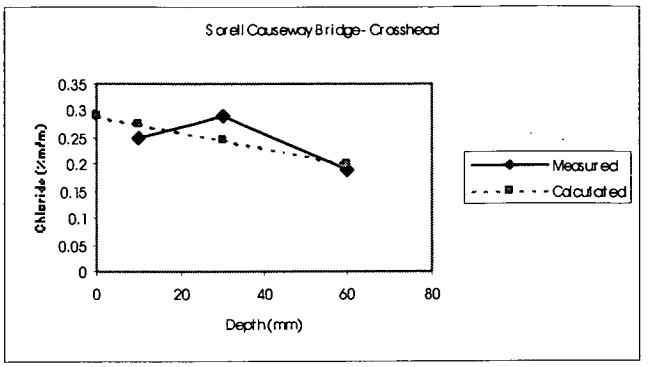

Parameters		Chloride concentration (%m/m) at depth (mm)				
Age (years)	37	Depth	0	10	30	60
C_s	0.290	Measured		0.25	0.29	0.19
D	1.00E-11	Calculated	0.290	0.275	0.245	0.201

Sorell Causeway Bridge - Crosshead

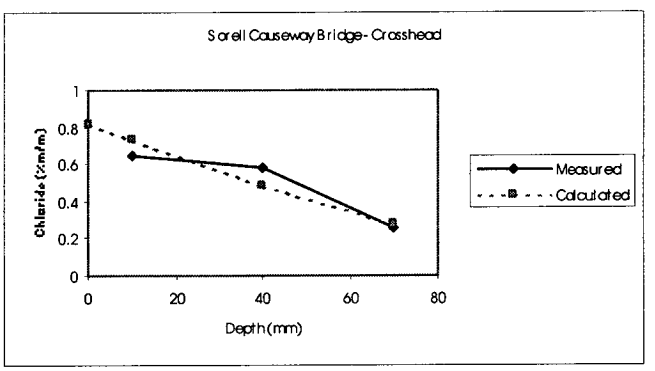

Parameters		Chloride concentration (%m/m) at depth (mm)				
Age (years)	37	Depth	0	10	40	70
C_s	0.820	Measured		0.64	0.58	0.26
D	2.30E-12	Calculated	0.820	0.731	0.480	0.278

Sorell Causeway Bridge - Crosshead

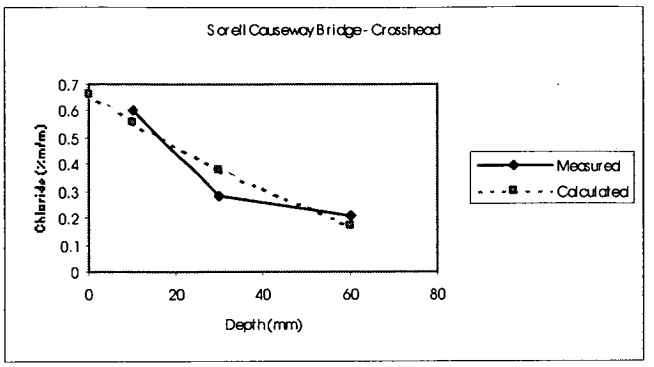

Parameters		Chloride concentration (%m/m) at depth (mm)				
Age (years)	37	Depth	0	10	30	60
C_s	0.660	Measured		0.6	0.28	0.21
D	1.20E-12	Calculated	0.660	0.561	0.377	0.170

Sorell Causeway Bridge - Crosshead

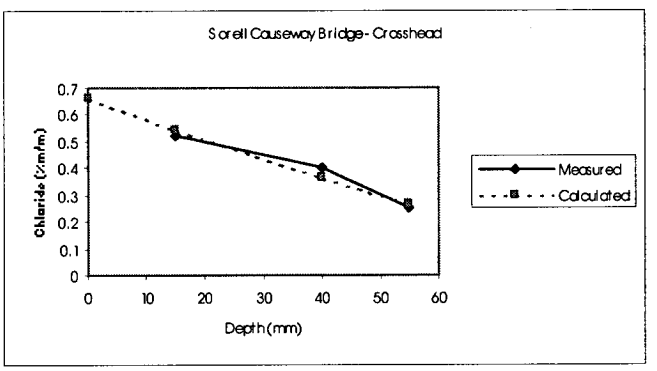

Parameters		Chloride concentration (%m/m) at depth (mm)				
Age (years)	37	Depth	0	15	40	55
C_s	0.660	Measured		0.52	0.4	0.25
D	1.90E-12	Calculated	0.660	0.542	0.362	0.270

Sorell Causeway Bridge - Crosshead

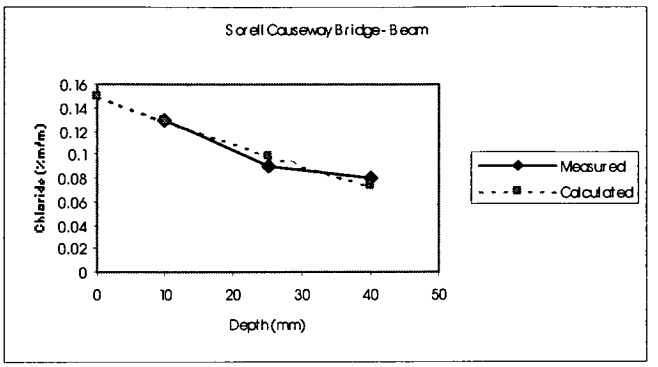

Parameters		Chloride concentration (%m/m) at depth (mm)				
Age (years)	37	Depth	0	10	25	40
C_s	0.150	Measured		0.13	0.09	0.08
D	1.40E-12	Calculated	0.150	0.129	0.099	0.073

Sorell Causeway Bridge - Beam

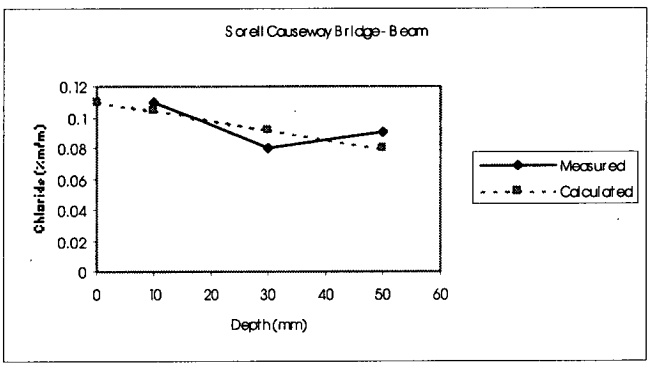

Parameters		Chloride concentration (%m/m) at depth (mm)				
Age (years)	37	Depth	0	10	30	50
C_s	0.110	Measured		0.11	0.08	0.09
D	9.00E-12	Calculated	0.110	0.104	0.092	0.080

Sorell Causeway Bridge - Beam

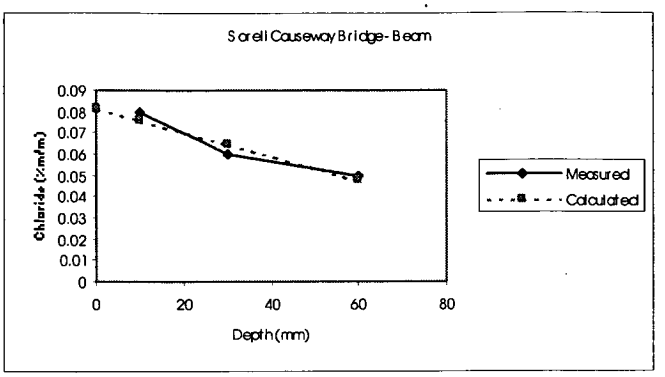

Parameters		Chloride concentration (%m/m) at depth (mm)				
Age (years)	37	Depth	0	10	30	60
C_s	0.082	Measured		0.08	0.06	0.05
D	5.20E-12	Calculated	0.082	0.076	0.064	0.048

Sorell Causeway Bridge - Beam

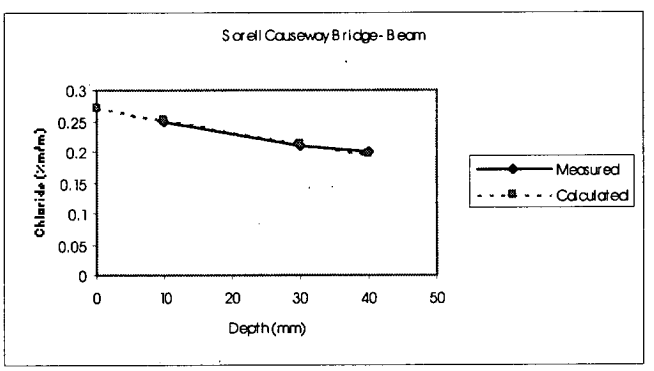

Parameters		Chloride concentration (%m/m) at depth (mm)				
Age (years)	37	Depth	0	10	30	40
C_s	0.270	Measured		0.25	0.21	0.2
D	5.60E-12	Calculated	0.270	0.251	0.214	0.196

Sorell Causeway Bridge - Beam

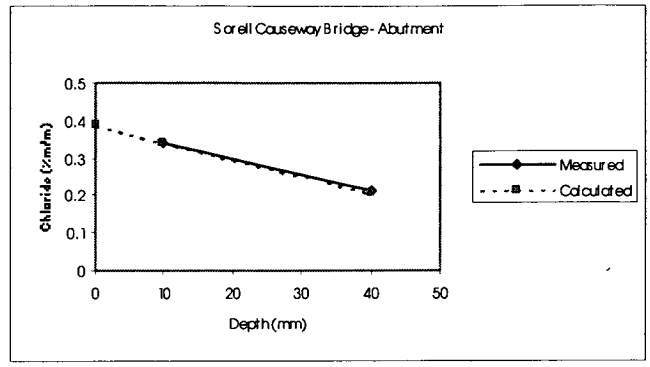

Parameters		Chloride concentration (%m/m) at depth (mm)			
Age (years)	35	Depth	0	10	40
C_s	0.390	Measured		0.34	0.212
D	1.90E-12	Calculated	0.390	0.342	0.209

Sorell Causeway Bridge - Abutment

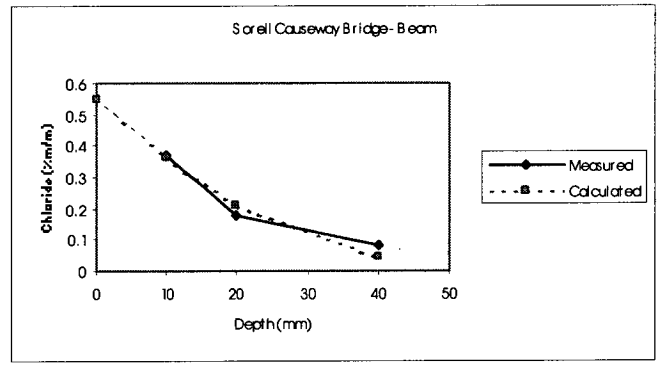

Parameters		Chloride concentration (%m/m) at depth (mm)				
Age (years)	40	Depth	0	10	20	40
C_s	0.550	Measured		0.37	0.18	0.08
D	2.10E-13	Calculated	0.550	0.365	0.212	0.045

Sorell Causeway Bridge - Beam

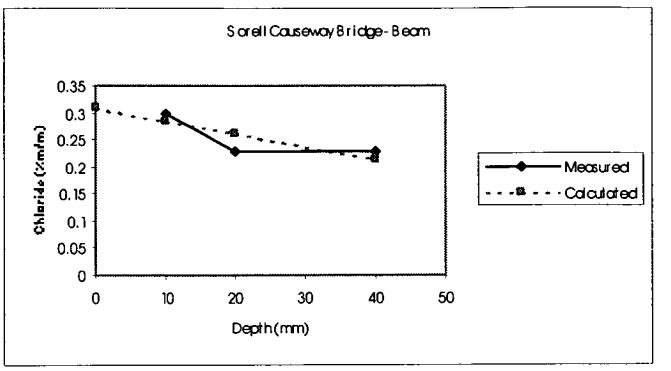

Parameters		Chloride concentration (%m/m) at depth (mm)				
Age (years)	40	Depth	0	10	20	40
C_s	0.310	Measured		0.3	0.23	0.23
D	4.00E-12	Calculated	0.310	0.285	0.261	0.214

Sorell Causeway Bridge - Beam

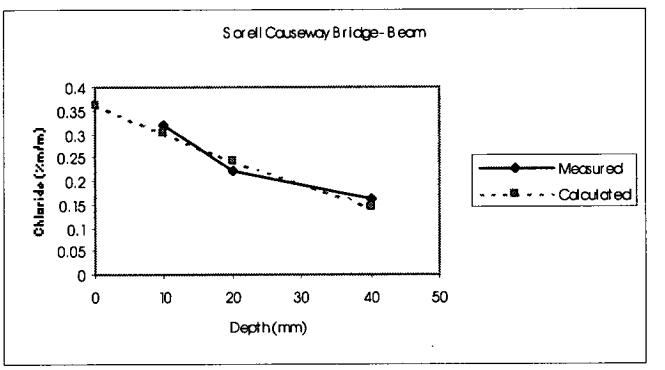

Parameters		Chloride concentration (%m/m) at depth (mm)				
Age (years)	40	Depth	0	10	20	40
C_s	0.360	Measured		0.32	0.22	0.16
D	9.20E-13	Calculated	0.360	0.301	0.244	0.146

Sorell Causeway Bridge - Beam

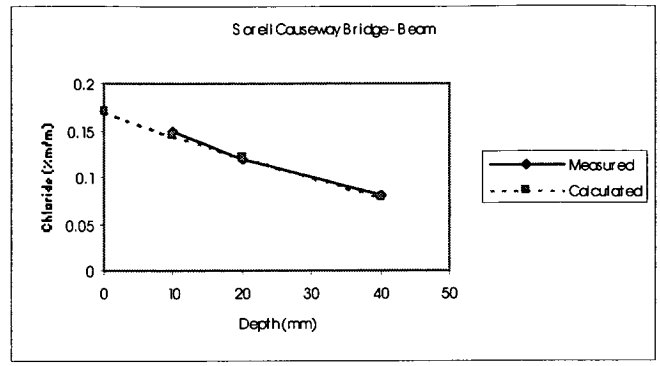

Parameters		Chloride concentration (%m/m) at depth (mm)				
Age (years)	40	Depth	0	10	20	40
C_s	0.170	Measured		0.15	0.12	0.08
D	1.20E-12	Calculated	0.170	0.146	0.122	0.080

Sorell Causeway Bridge - Beam

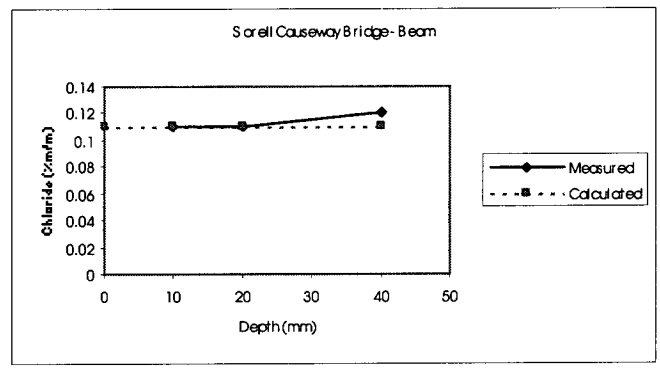

Parameters		Chloride concentration (%m/m) at depth (mm)				
Age (years)	40	Depth	0	10	20	40
C_s	0.110	Measured		0.11	0.11	0.12
D	Constant	Calculated	0.110	0.110	0.110	0.110

Sorell Causeway Bridge - Beam

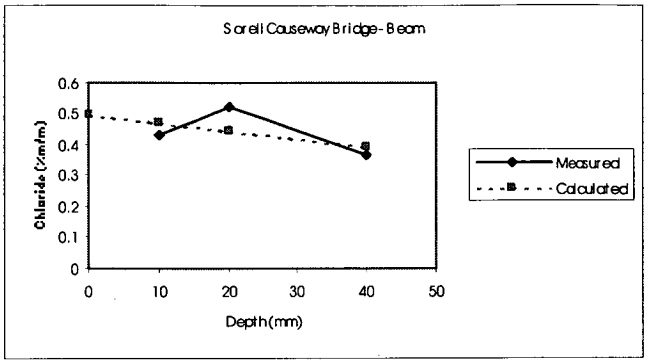

Parameters		Chloride concentration (%m/m) at depth (mm)				
Age (years)	40	Depth	0	10	20	40
C_s	0.500	Measured		0.43	0.52	0.37
D	8.50E-12	Calculated	0.500	0.473	0.446	0.392

Sorell Causeway Bridge - Beam

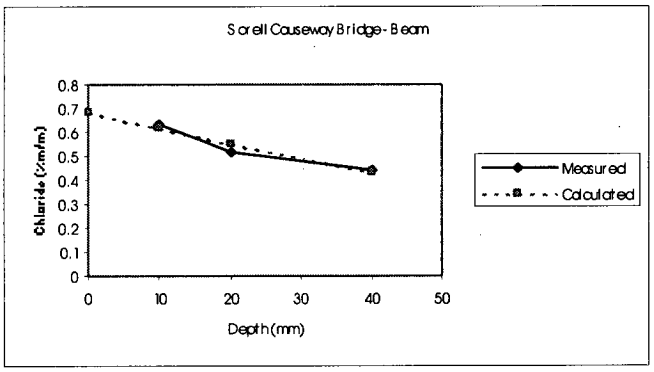

Parameters		Chloride concentration (%m/m) at depth (mm)				
Age (years)	40	Depth	0	10	20	40
C_s	0.680	Measured		0.63	0.52	0.44
D	2.80E-12	Calculated	0.680	0.616	0.552	0.431

Sorell Causeway Bridge - Beam

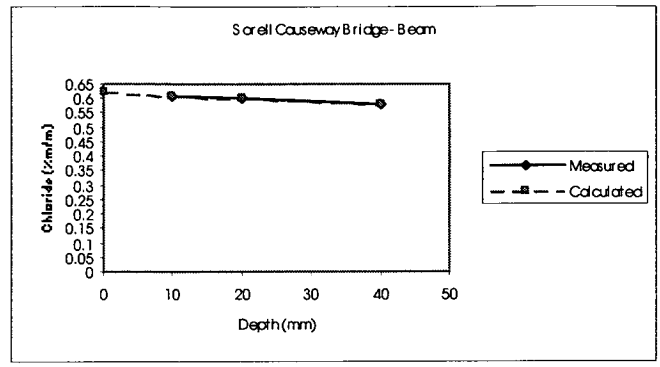

Parameters		Chloride concentration (%m/m) at depth (mm)				
Age (years)	40	Depth	0	10	20	40
C_s	0.620	Measured		0.61	0.6	0.58
D	9.70E-11	Calculated	0.620	0.610	0.600	0.580

Sorell Causeway Bridge - Beam

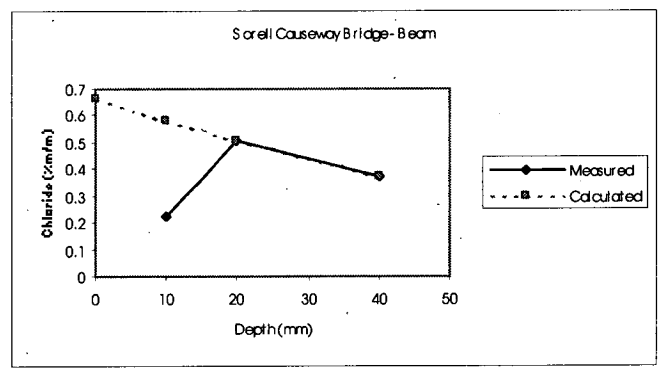

Parameters		Chloride concentration (%m/m) at depth (mm)				
Age (years)	40	Depth	0	10	20	40
C_s	0.660	Measured		0.22	0.51	0.37
D	1.90E-12	Calculated	0.660	0.584	0.510	0.372

Sorell Causeway Bridge - Beam

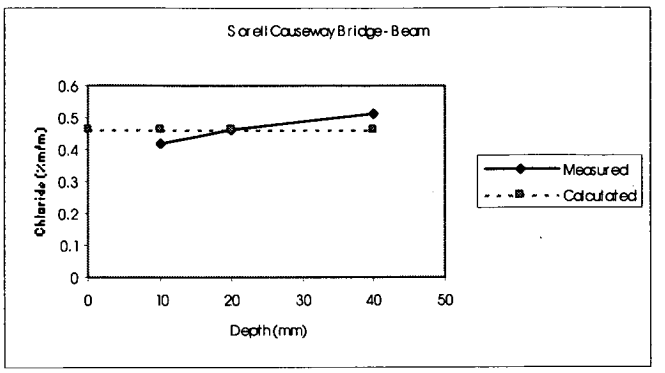

Parameters		Chloride concentration (%m/m) at depth (mm)				
Age (years)	40	Depth	0	10	20	40
C_s	0.460	Measured		0.42	0.46	0.51
D	Constant	Calculated	0.460	0.460	0.460	0.460

Sorell Causeway Bridge - Beam

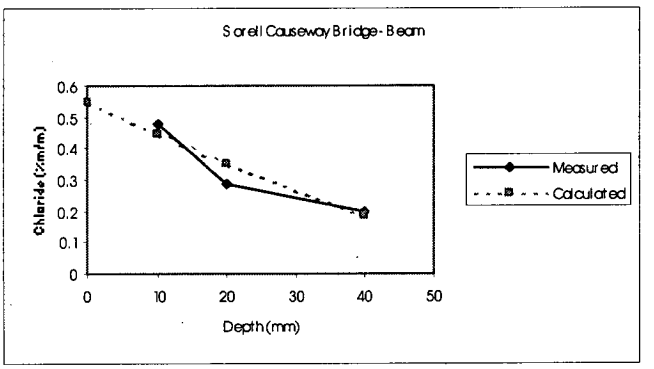

Parameters		Chloride concentration (%m/m) at depth (mm)				
Age (years)	40	Depth	0	10	20	40
C_s	0.550	Measured		0.48	0.29	0.2
D	7.00E-13	Calculated	0.550	0.447	0.349	0.188

Sorell Causeway Bridge - Beam

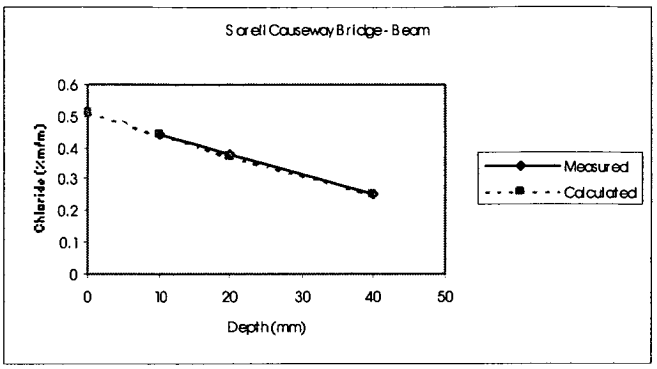

Parameters		Chloride concentration (%m/m) at depth (mm)				
Age (years)	40	Depth	0	10	20	40
C_s	0.510	Measured		0.44	0.38	0.25
D	1.40E-12	Calculated	0.510	0.442	0.376	0.256

Sorell Causeway Bridge - Beam

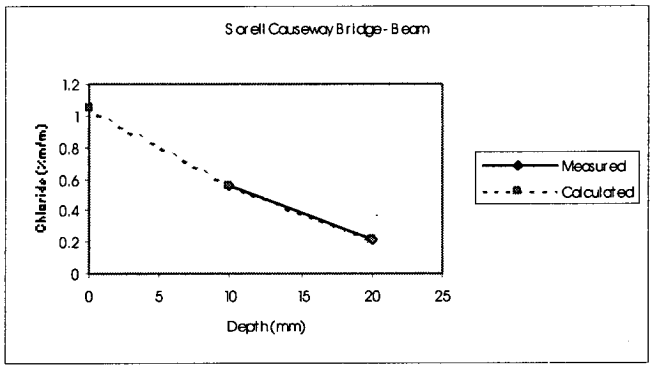

Parameters		Chloride concentration (%m/m) at depth (mm)			
Age (years)	40	Depth	0	10	20
C_s	1.050	Measured		0.56	0.21
D	9.90E-14	Calculated	1.050	0.553	0.216

Sorell Causeway Bridge - Beam

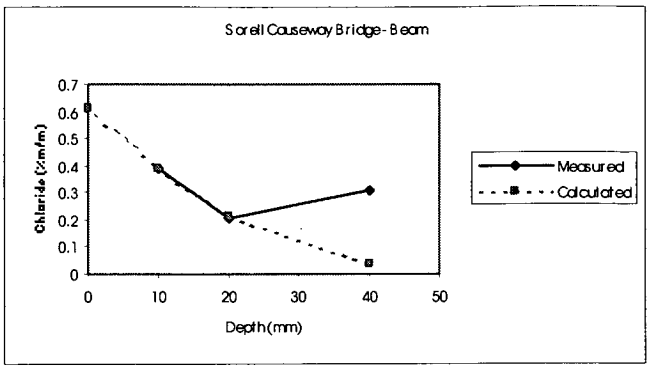

Parameters		Chloride concentration (%m/m) at depth (mm)				
Age (years)	40	Depth	0	10	20	40
C_s	0.610	Measured		0.39	0.21	0.31
D	1.80E-13	Calculated	0.610	0.390	0.212	0.037

Sorell Causeway Bridge - Beam

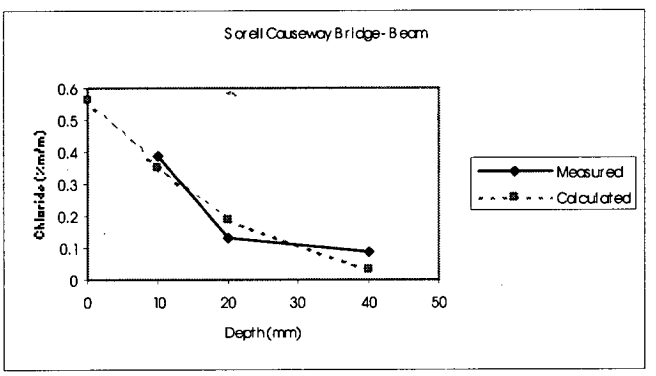

Parameters		Chloride concentration (%m/m) at depth (mm)				
Age (years)	40	Depth	0	10	20	40
C_s	0.560	Measured		0.39	0.13	0.09
D	1.70E-13	Calculated	0.560	0.352	0.187	0.030

Sorell Causeway Bridge - Beam

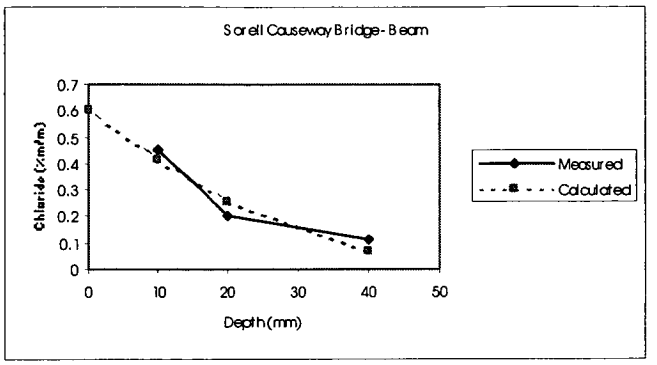

Parameters		Chloride concentration (%m/m) at depth (mm)				
Age (years)	40	Depth	0	10	20	40
C_s	0.600	Measured		0.45	0.2	0.11
D	2.50E-13	Calculated	0.600	0.414	0.256	0.067

Sorell Causeway Bridge - Beam

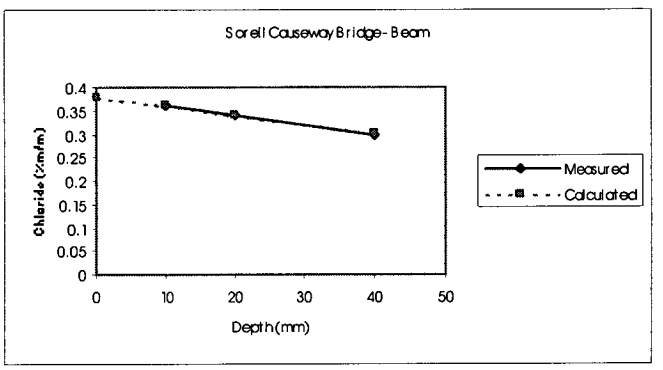

Parameters		Chloride concentration (%m/m) at depth (mm)				
Age (years)	40	Depth	0	10	20	40
C_s	0.380	Measured		0.36	0.34	0.3
D	9.10E-12	Calculated	0.380	0.360	0.340	0.301

Sorell Causeway Bridge - Beam

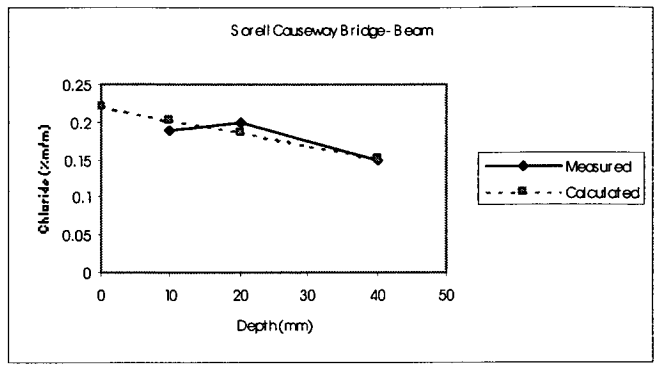

Parameters		Chloride concentration (%m/m) at depth (mm)				
Age (years)	40	Depth	0	10	20	40
C_s	0.220	Measured		0.19	0.2	0.15
D	3.90E-12	Calculated	0.220	0.202	0.185	0.151

Sorell Causeway Bridge - Beam

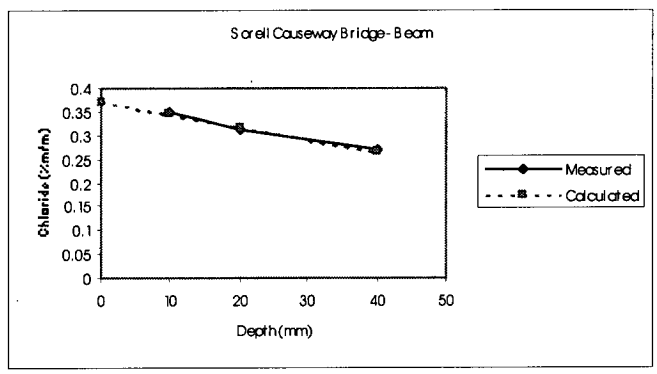

Parameters		Chloride concentration (%m/m) at depth (mm)				
Age (years)	40	Depth	0	10	20	40
C_s	0.370	Measured		0.35	0.31	0.27
D	5.00E-12	Calculated	0.370	0.344	0.318	0.267

Sorell Causeway Bridge - Beam

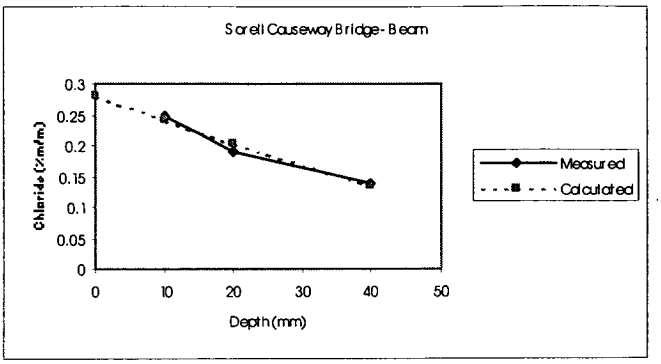

Parameters		Chloride concentration (%m/m) at depth (mm)				
Age (years)	40	Depth	0	10	20	40
C_s	0.280	Measured		0.25	0.19	0.14
D	1.30E-12	Calculated	0.280	0.241	0.204	0.136

Sorell Causeway Bridge - Beam

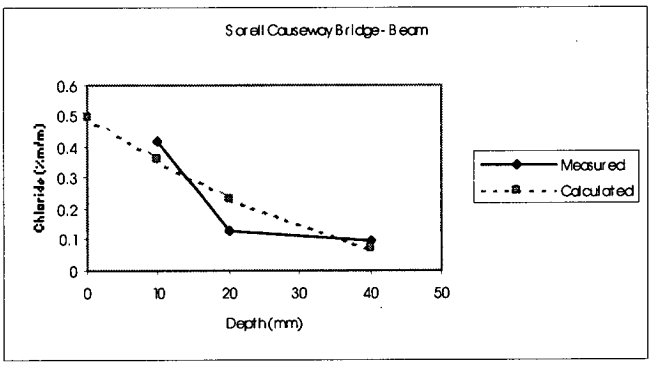

Parameters		Chloride concentration (%m/m) at depth (mm)				
Age (years)	40	Depth	0	10	20	40
C_s	0.500	Measured		0.42	0.13	0.1
D	3.00E-13	Calculated	0.500	0.358	0.234	0.073

Sorell Causeway Bridge - Beam

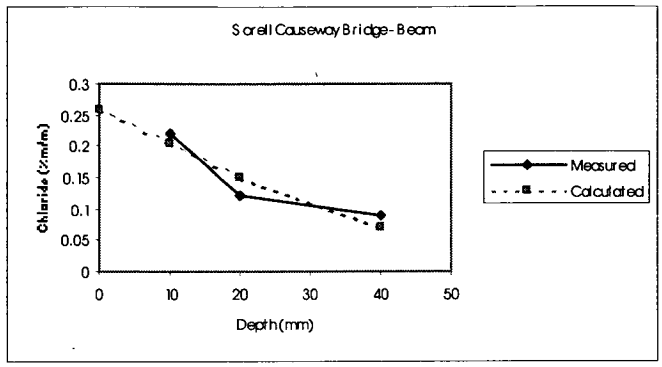

Parameters		Chloride concentration (%m/m) at depth (mm)				
Age (years)	40	Depth	0	10	20	40
C_s	0.260	Measured		0.22	0.12	0.09
D	5.20E-13	Calculated	0.260	0.204	0.151	0.070

Sorell Causeway Bridge - Beam

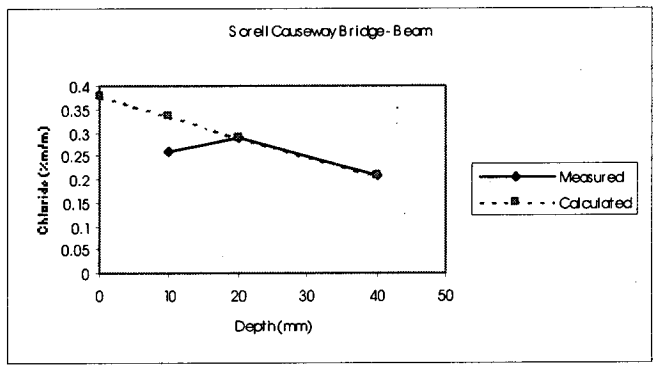

Parameters		Chloride concentration (%m/m) at depth (mm)				
Age (years)	40	Depth	0	10	20	40
C_s	0.380	Measured		0.26	0.29	0.21
D	1.80E-12	Calculated	0.380	0.335	0.291	0.210

Sorell Causeway Bridge - Beam

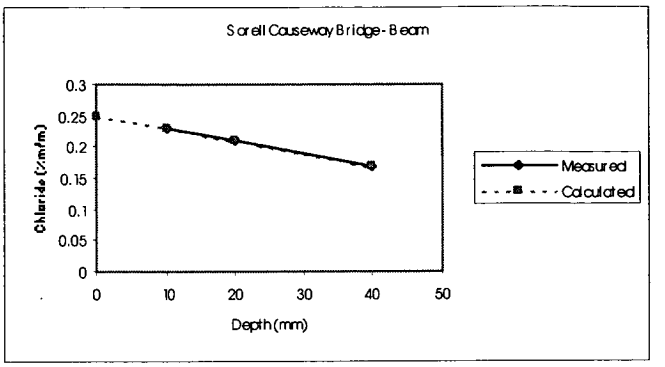

Parameters		Chloride concentration (%m/m) at depth (mm)				
Age (years)	40	Depth	0	10	20	40
C_s	0.250	Measured		0.23	0.21	0.17
D	3.80E-12	Calculated	0.250	0.230	0.210	0.171

Sorell Causeway Bridge - Beam

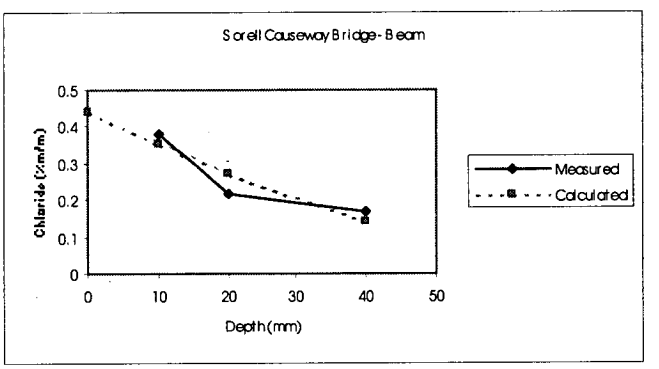

Parameters		Chloride concentration (%m/m) at depth (mm)				
Age (years)	40	Depth	0	10	20	40
C_s	0.440	Measured		0.38	0.22	0.17
D	6.40E-13	Calculated	0.440	0.354	0.272	0.141

Sorell Causeway Bridge - Beam

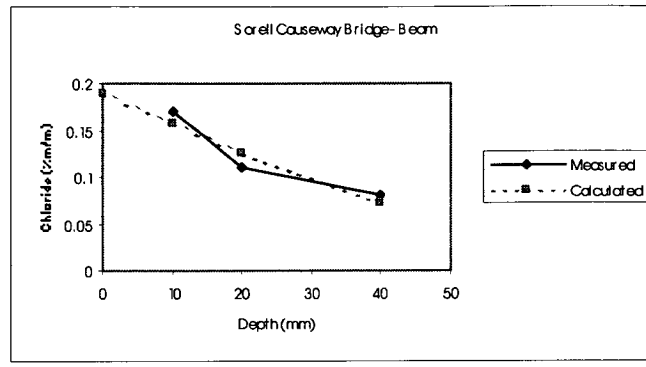

Parameters		Chloride concentration (%m/m) at depth (mm)				
Age (years)	40	Depth	0	10	20	40
C_s	0.190	Measured		0.17	0.11	0.08
D	8.30E-13	Calculated	0.190	0.157	0.126	0.073

Sorell Causeway Bridge - Beam

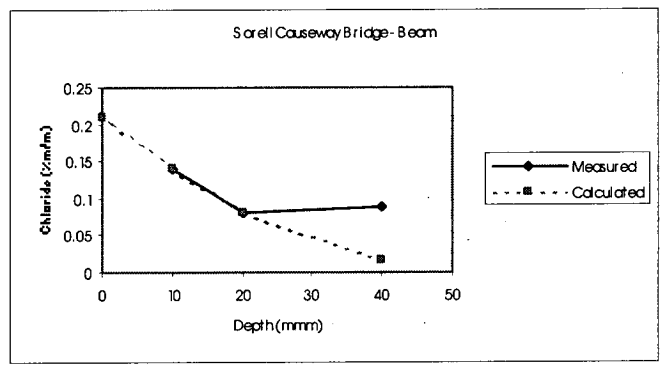

Parameters		Chloride concentration (%m/m) at depth (mm)				
Age (years)	40	Depth	0	10	20	40
C_s	0.210	Measured		0.14	0.08	0.09
D	2.10E-13	Calculated	0.210	0.140	0.081	0.017

Sorell Causeway Bridge - Beam

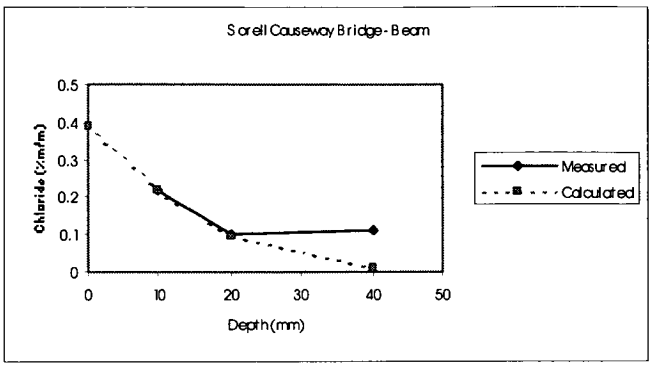

Parameters		Chloride concentration (%m/m) at depth (mm)				
Age (years)	40	Depth	0	10	20	40
C_s	0.390	Measured		0.22	0.1	0.11
D	1.20E-13	Calculated	0.390	0.221	0.098	0.009

Sorell Causeway Bridge - Beam

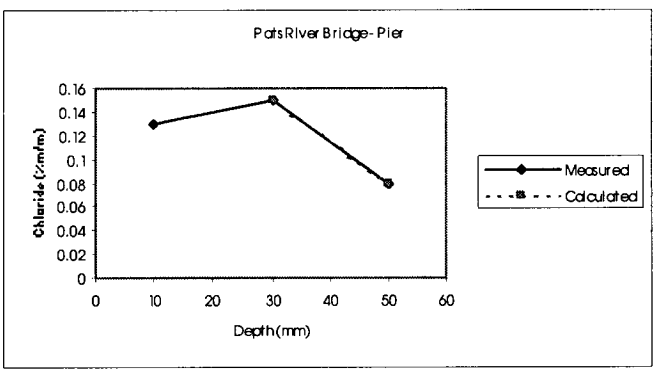

Parameters		Chloride concentration (%m/m) at depth (mm)				
Age (years)	35	Depth	0	10	30	50
C_s	0.150	Measured		0.13	0.15	0.08
D	4.67E-13	Calculated			0.150	0.080

Note: Skin effect (30mm) excluded

Pats River Bridge - Pier

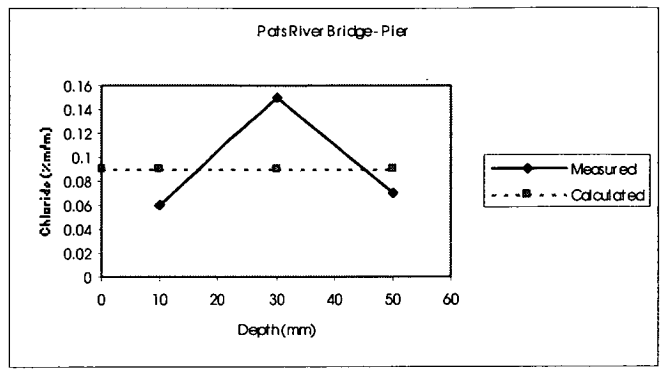

Parameters		Chloride concentration (%m/m) at depth (mm)				
Age (years)	35	Depth	0	10	30	50
C_s	0.090	Measured		0.06	0.15	0.07
D	Constant	Calculated	0.090	0.090	0.090	0.090

Pats River Bridge - Pier

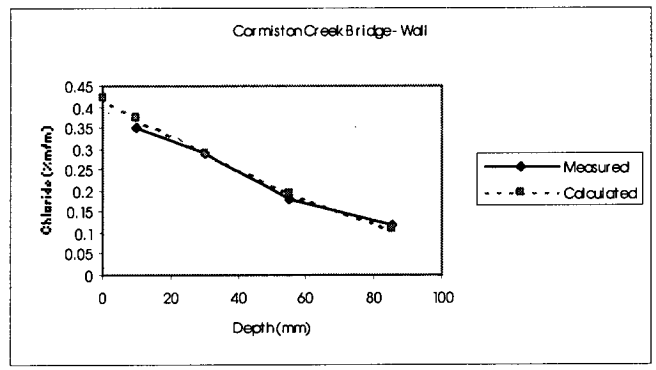

Parameters		Chloride concentration (%m/m) at depth (mm)					
Age (years)	39	Depth	0	10	30	55	85
C_s	0.420	Measured		0.35	0.29	0.18	0.12
D	2.30E-12	Calculated	0.420	0.376	0.290	0.195	0.109

Cormiston Creek Bridge - Wall

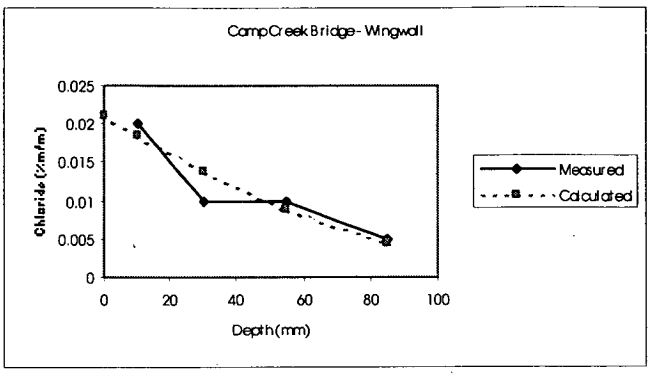

Parameters		Chloride concentration (%m/m) at depth (mm)					
Age (years)	39	Depth	0	10	30	55	85
C_s	0.021	Measured		0.02	0.01	0.01	0.005
D	1.90E-12	Calculated	0.021	0.019	0.014	0.009	0.005

Camp Creek Bridge - Wingwall

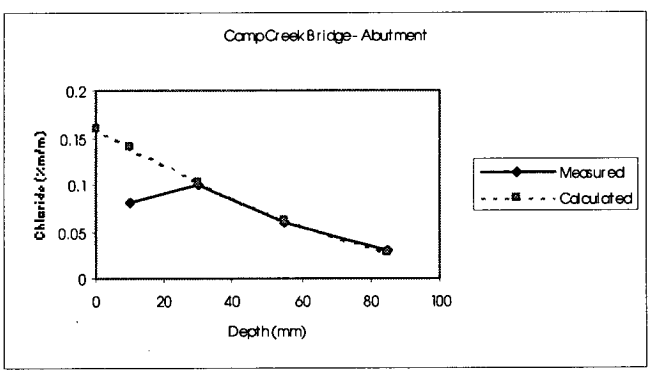

Parameters		Chloride concentration (%m/m) at depth (mm)					
Age (years)	39	Depth	0	10	30	55	85
C_s	0.160	Measured		0.08	0.1	0.06	0.03
D	1.60E-12	Calculated	0.160	0.140	0.101	0.061	0.028

Camp Creek Bridge - Abutment

Parameters		Chloride concentration (%m/m) at depth (mm)			
Age (years)	39	Depth	0	10	30
C_s	0.031	Measured		0.02	0.005
D	1.90E-13	Calculated	0.031	0.020	0.005

Camp Creek Bridge - Deck

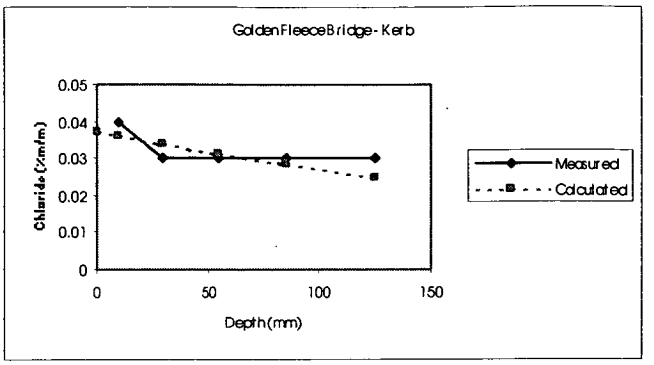

Parameters		Chloride concentration (%m/m) at depth (mm)						
Age (years)	36	Depth	0	10	30	55	85	125
C_s	0.037	Measured		0.04	0.03	0.03	0.03	0.03
D	3.70E-11	Calculated	0.037	0.036	0.034	0.031	0.029	0.025

Golden Fleece Bridge - Kerb

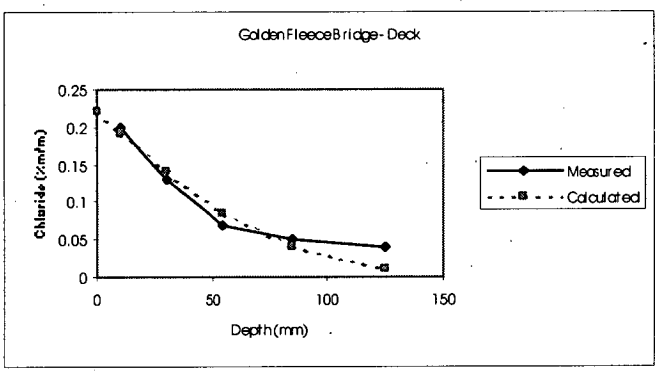

Parameters		Chloride concentration (%m/m) at depth (mm)						
Age (years)	36	Depth	0	10	30	55	85	125
C_s	0.220	Measured		0.2	0.13	0.07	0.05	0.04
D	1.80E-12	Calculated	0.220	0.193	0.141	0.086	0.040	0.011

Golden Fleece Bridge - Deck

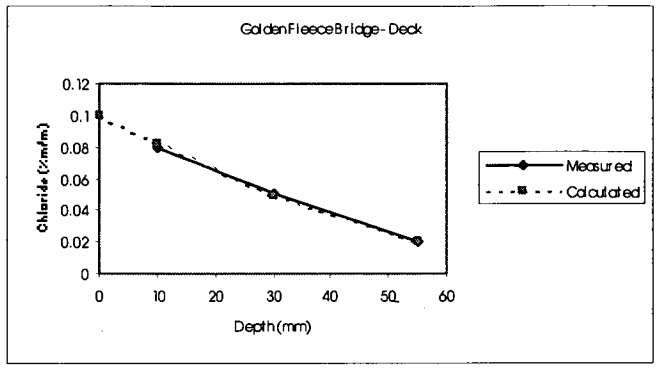

Parameters		Chloride concentration (%m/m) at depth (mm)				
Age (years)	36	Depth	0	10	30	55
C_s	0.100	Measured		0.08	0.05	0.02
D	8.30E-13	Calculated	0.100	0.082	0.049	0.021

Golden Fleece Bridge - Deck

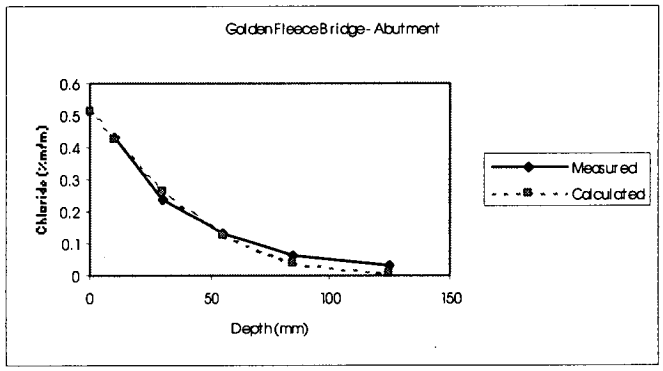

Parameters		Chloride concentration (%m/m) at depth (mm)						
Age (years)	36	Depth	0	10	30	55	85	125
C_s	0.510	Measured		0.43	0.24	0.13	0.06	0.03
D	9.60E-13	Calculated	0.510	0.424	0.266	0.122	0.035	0.008

Golden Fleece Bridge - Abutment

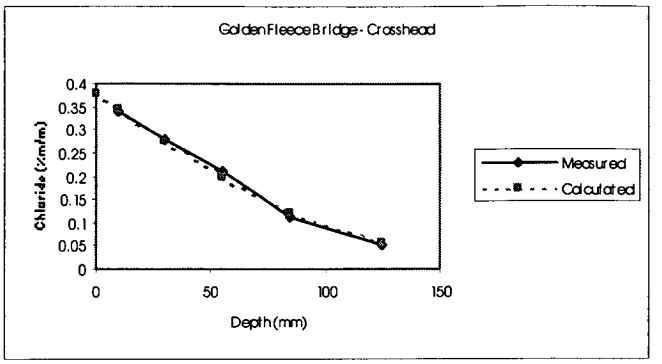

Parameters		Chloride concentration (%m/m) at depth (mm)						
Age (years)	36	Depth	0	10	30	55	85	125
C_s	0.380	Measured		0.34	0.28	0.21	0.11	0.05
D	3.20E-12	Calculated	0.380	0.345	0.276	0.197	0.121	0.054

Golden Fleece Bridge - Crosshead

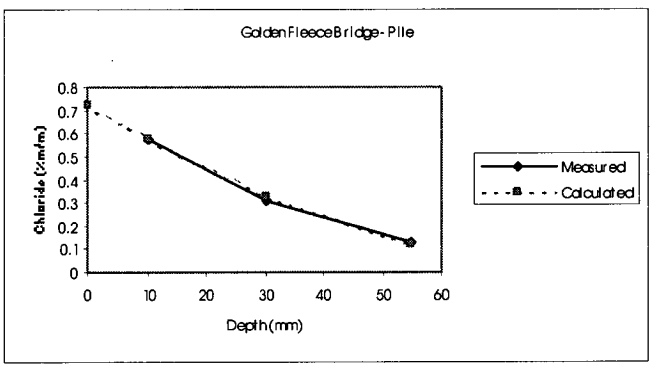

Parameters		Chloride concentration (%m/m) at depth (mm)				
Age (years)	36	Depth	0	10	30	55
C_s	0.720	Measured		0.58	0.31	0.13
D	6.90E-13	Calculated	0.720	0.576	0.323	0.119

Golden Fleece Bridge - Pile

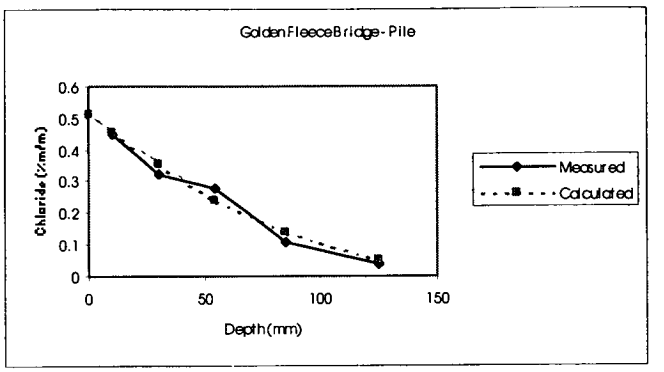

Parameters		Chloride concentration (%m/m) at depth (mm)						
Age (years)	36	Depth	0	10	30	55	85	125
C_s	0.510	Measured		0.45	0.32	0.28	0.11	0.04
D	2.50E-12	Calculated	0.510	0.457	0.355	0.242	0.137	0.053

Golden Fleece Bridge - Pile

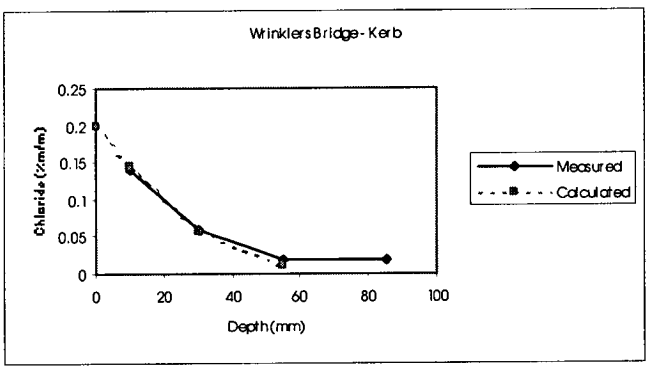

Parameters		Chloride concentration (%m/m) at depth (mm)					
Age (years)	35	Depth	0	10	30	55	85
C_s	0.200	Measured		0.14	0.06	0.02	0.02
D	3.60E-13	Calculated	0.200	0.145	0.058	0.010	

Wrinklers Bridge - Kerb

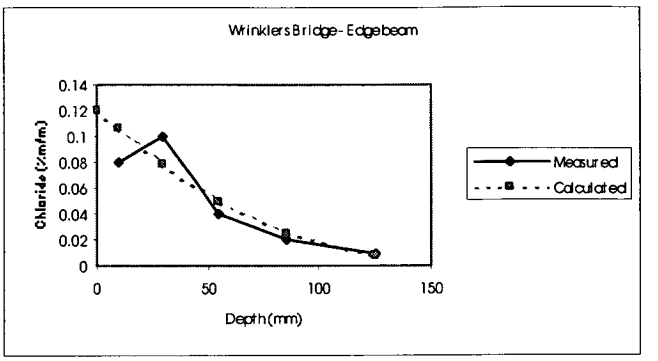

Parameters		Chloride concentration (%m/m) at depth (mm)						
Age (years)	35	Depth	0	10	30	55	85	125
C_s	0.120	Measured		0.08	0.1	0.04	0.02	0.01
D	2.00E-12	Calculated	0.120	0.106	0.078	0.049	0.024	0.007

Wrinklers Bridge – Edge beam

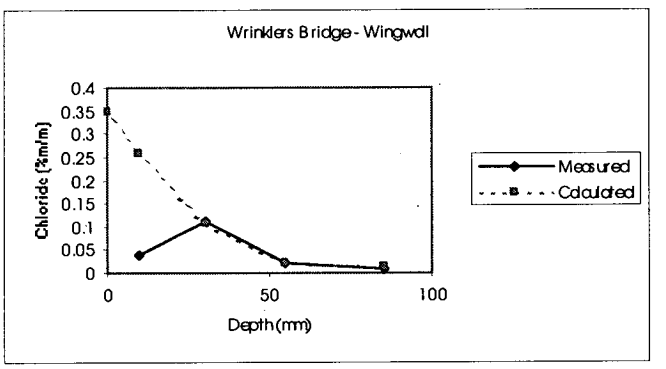

Parameters		Chloride concentration (%m/m) at depth (mm)					
Age (years)	35	Depth	0	10	30	55	85
C_s	0.350	Measured		0.04	0.11	0.02	0.01
D	4.00E-13	Calculated	0.350	0.258	0.110	0.023	0.012

Wrinklers Bridge - Wingwall

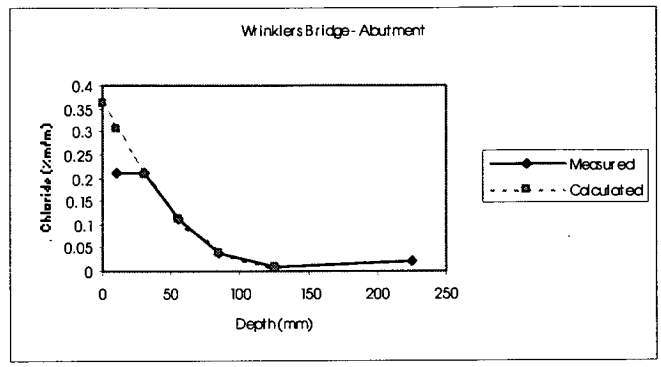

Parameters		Chloride concentration (%m/m) at depth (mm)							
Age (years)	35	Depth	0	10	30	55	85	125	225
C_s	0.360	Measured		0.21	0.21	0.11	0.04	0.01	0.02
D	1.30E-12	Calculated	0.360	0.307	0.207	0.110	0.041	0.007	

Wrinklers Bridge - Abutment

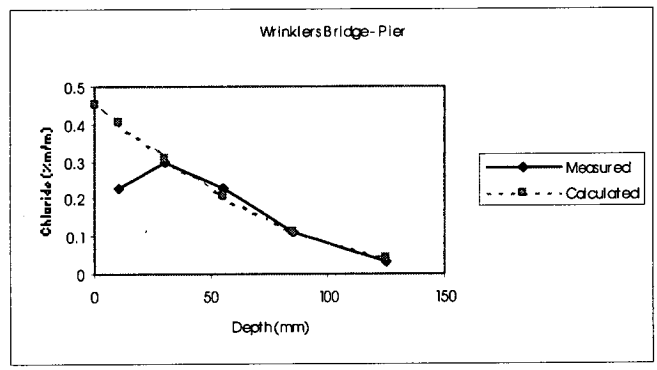

Parameters		Chloride concentration (%m/m) at depth (mm)						
Age (years)	35	Depth	0	10	30	55	85	125
C_s	0.450	Measured		0.23	0.3	0.23	0.11	0.03
D	2.50E-12	Calculated	0.450	0.402	0.309	0.207	0.114	0.042

Wrinklers Bridge - Pier

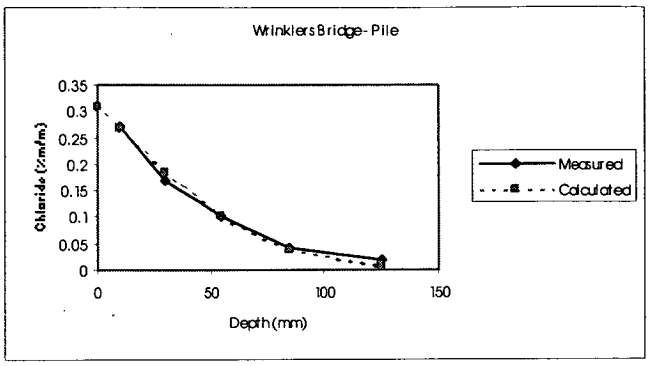

Parameters		Chloride concentration (%m/m) at depth (mm)						
Age (years)	35	Depth	0	10	30	55	85	125
C_s	0.310	Measured		0.27	0.17	0.1	0.04	0.02
D	1.40E-12	Calculated	0.310	0.266	0.183	0.100	0.039	0.008

Wrinklers Bridge - Pile

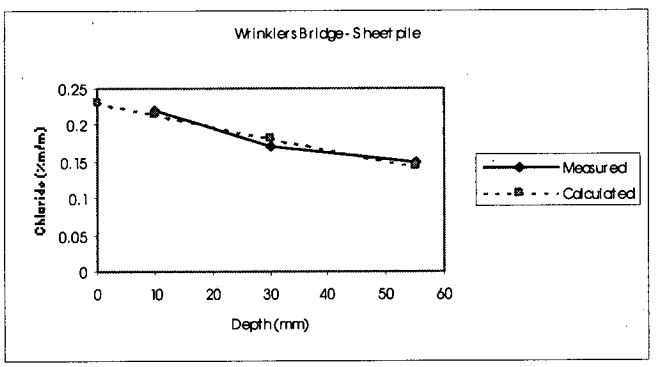

Parameters		Chloride concentration (%m/m) at depth (mm)				
Age (years)	35	Depth	0	10	30	55
C_s	0.230	Measured		0.22	0.17	0.15
D	5.70E-12	Calculated	0.230	0.214	0.182	0.144

Wrinklers Bridge – Sheet pile

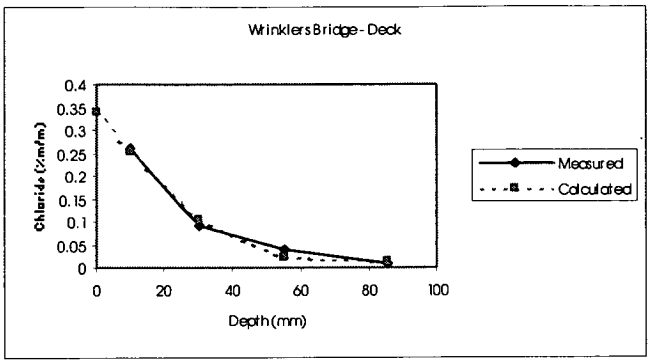

Parameters		Chloride concentration (%m/m) at depth (mm)					
Age (years)	35	Depth	0	10	30	55	85
C_s	0.340	Measured		0.26	0.09	0.04	0.01
D	4.00E-13	Calculated	0.340	0.250	0.106	0.022	0.011

Wrinklers Bridge - Deck

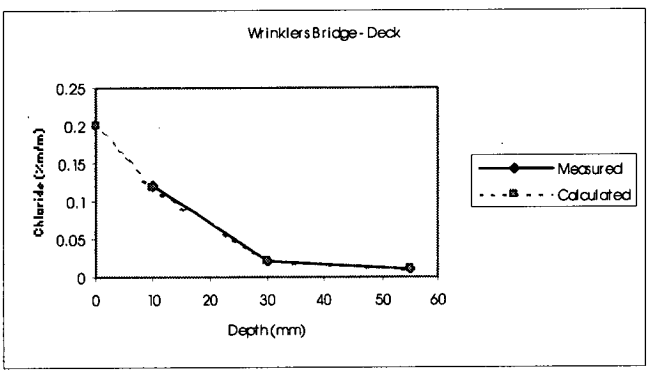

Parameters		Chloride concentration (%m/m) at depth (mm)				
Age (years)	35	Depth	0	10	30	55
C_s	0.200	Measured		0.12	0.02	0.01
D	1.60E-13	Calculated	0.200	0.119	0.022	0.010

Wrinklers Bridge - Deck

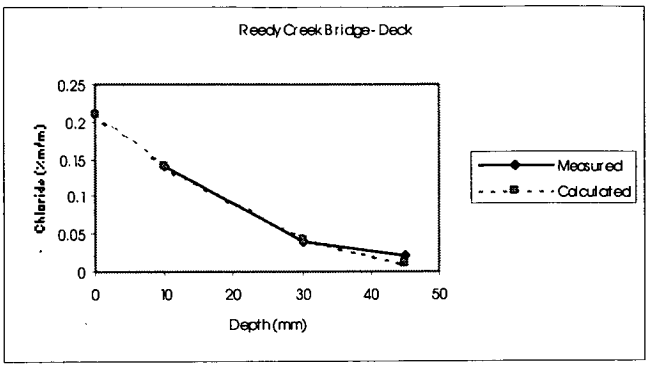

Parameters		Chloride concentration (%m/m) at depth (mm)				
Age (years)	35	Depth	0	10	30	45
C_s	0.210	Measured		0.14	0.04	0.02
D	2.50E-13	Calculated	0.210	0.141	0.042	0.012

Reedy Creek Bridge - Deck

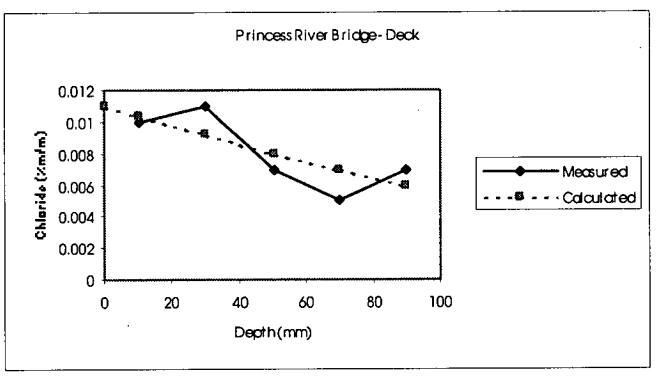

Parameters		Chloride concentration (%m/m) at depth (mm)						
Age (years)	33	Depth	0	10	30	50	70	90
C_s	0.011	Measured		0.01	0.011	0.007	0.005	0.007
D	1.00E-11	Calculated	0.011	0.010	0.009	0.008	0.007	0.006

Princess River Bridge – Deck

Parameters		Chloride concentration (%m/m) at depth (mm)						
Age (years)	33	Depth	0	15	40	60	80	100
C_s	0.006	Measured		0.004	0.005	0.005	0.007	0.01
D	Constant	Calculated	0.006	0.006	0.006	0.006	0.006	0.006

Princess River Bridge - Deck

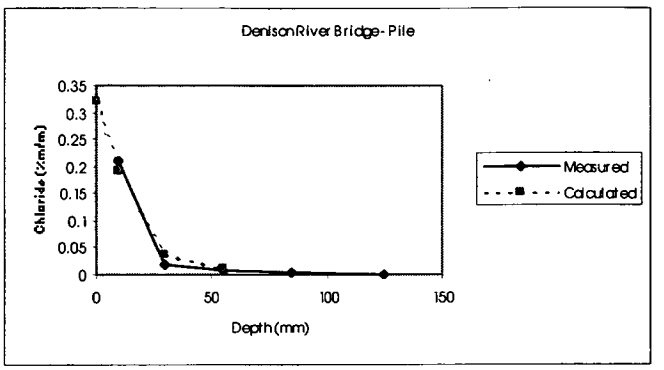

Parameters		Chloride concentration (%m/m) at depth (mm)						
Age (years)	34	Depth	0	10	30	55	85	125
C_s	0.320	Measured		0.21	0.02	0.008	0.005	0.001
D	1.70E-13	Calculated	0.320	0.192	0.037	0.012		

Denison River Bridge – Pile

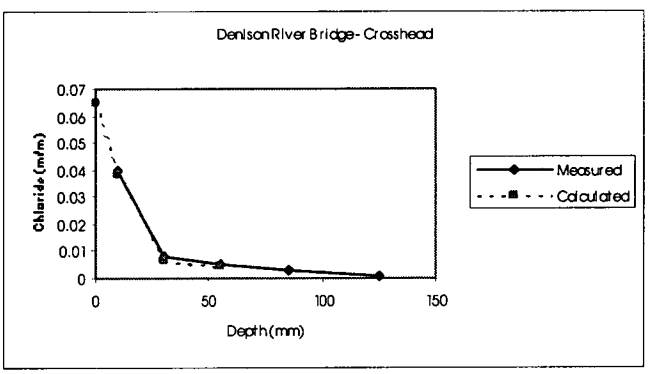

Parameters		Chloride concentration (%m/m) at depth (mm)						
Age (years)	34	Depth	0	10	30	55	85	125
C_s	0.065	Measured		0.04	0.008	0.005	0.003	0.001
D	1.60E-13	Calculated	0.065	0.038	0.007	0.004		

Denison River Bridge - Crosshead

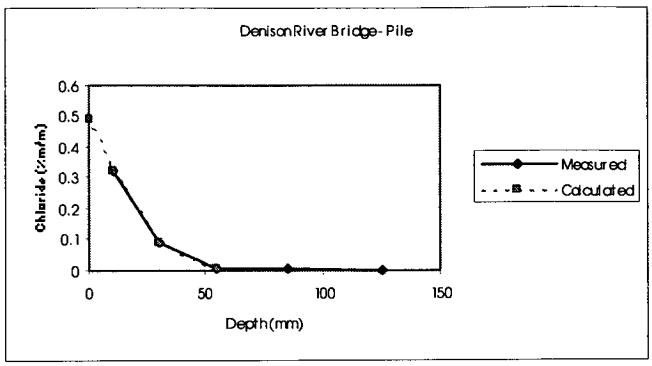

Parameters		Chloride concentration (%m/m) at depth (mm)						
Age (years)	34	Depth	0	10	30	55	85	125
C_s	0.490	Measured		0.32	0.09	0.008	0.005	0.001
D	2.40E-13	Calculated	0.490	0.323	0.091	0.008		

Denison River Bridge - Pile

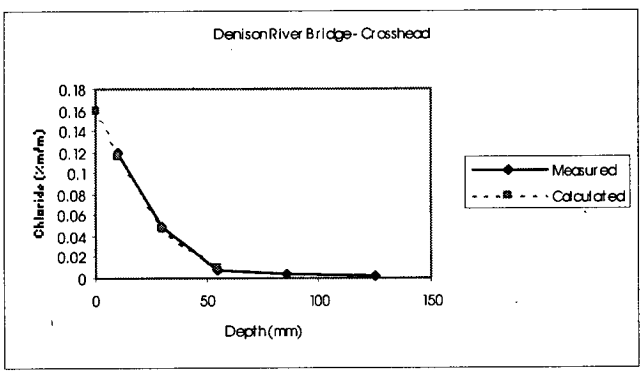

Parameters		Chloride concentration (%m/m) at depth (mm)						
Age (years)	34	Depth	0	10	30	55	85	125
C_s	0.160	Measured		0.12	0.05	0.008	0.003	0.001
D	3.80E-13	Calculated	0.160	0.116	0.047	0.009		

Denison Canal Bridge - Crosshead

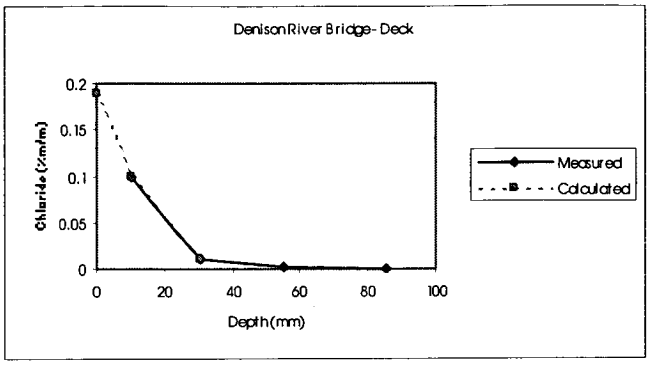

Parameters		Chloride concentration (%m/m) at depth (mm)					
Age (years)	34	Depth	0	10	30	55	85
C_s	0.190	Measured		0.1	0.01	0.002	0.001
D	1.10E-13	Calculated	0.190	0.098	0.010		

Denison River Bridge - Deck

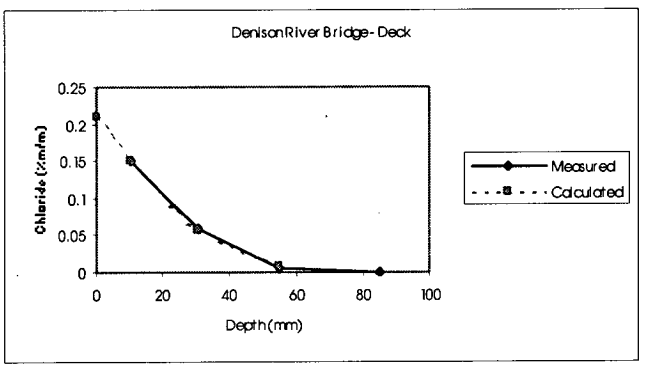

Parameters		Chloride concentration (%m/m) at depth (mm)					
Age (years)	34	Depth	0	10	30	55	85
C_s	0.210	Measured		0.15	0.06	0.005	0.001
D	3.50E-13	Calculated	0.210	0.150	0.058	0.009	

Denison River Bridge - Deck

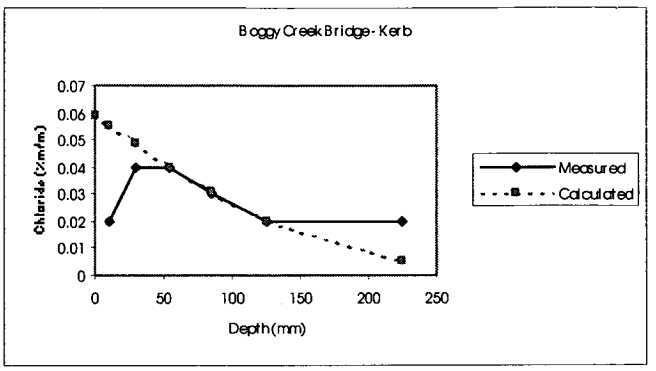

Parameters		Chloride concentration (%m/m) at depth (mm)							
Age (years)	34	Depth	0	10	30	55	85	125	225
C_s	0.059	Measured		0.02	0.04	0.04	0.03	0.02	0.02
D	8.10E-12	Calculated	0.059	0.055	0.048	0.040	0.031	0.020	0.005

Boggy Creek Bridge - Kerb

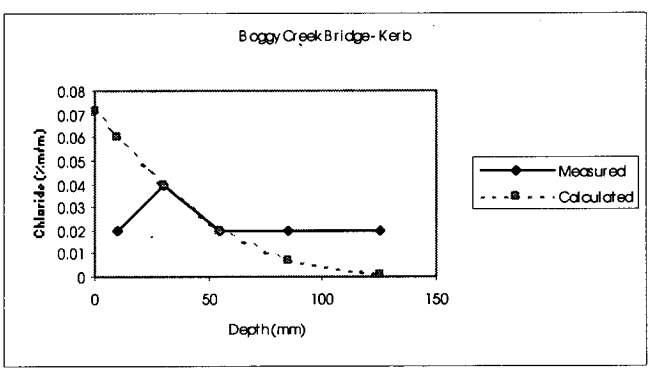

Parameters		Chloride concentration (%m/m) at depth (mm)						
Age (years)	34	Depth	0	10	30	55	85	125
C_s	0.071	Measured		0.02	0.04	0.02	0.02	0.02
D	1.20E-12	Calculated	0.071	0.060	0.039	0.020	0.007	0.001

Boggy Creek Bridge - Kerb

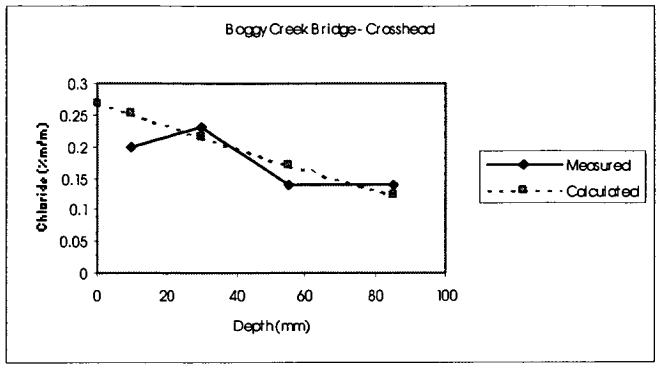

Parameters		Chloride concentration (%m/m) at depth (mm)					
Age (years)	34	Depth	0	10	30	55	85
C_s	0.270	Measured		0.2	0.23	0.14	0.14
D	6.20E-12	Calculated	0.270	0.251	0.215	0.171	0.125

Boggy Creek Bridge - Crosshead

Parameters		Chloride concentration (%m/m) at depth (mm)					
Age (years)	34	Depth	0	10	30	55	85
C_s	0.026	Measured		0.02	0.008	0.004	0.001
D	4.80E-13	Calculated	0.026	0.020	0.009	0.002	

Boggy Creek Bridge - Crosshead

Parameters		Chloride concentration (%m/m) at depth (mm)					
Age (years)	34	Depth	0	10	30	55	85
C_s	0.081	Measured		0.07	0.04	0.02	0.01
D	1.10E-12	Calculated	0.081	0.068	0.044	0.021	0.007

Boggy Creek Bridge - Abutment

Parameters		Chloride concentration (%m/m) at depth (mm)					
Age (years)	34	Depth	0	10	30	55	85
C_s	0.025	Measured		0.02	0.01	0.01	0.01
D	5.90E-13	Calculated	0.025	0.020	0.010	0.003	0.000

Boggy Creek Bridge - Abutment

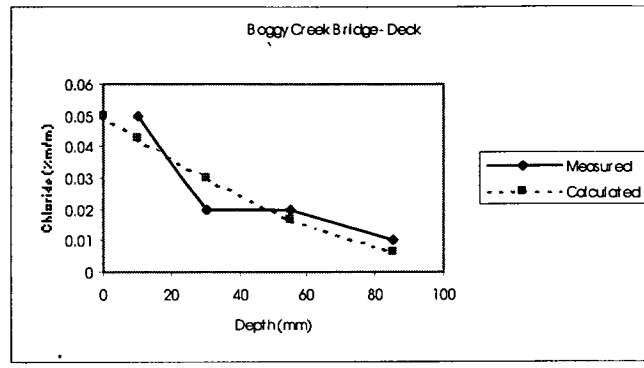

Parameters		Chloride concentration (%m/m) at depth (mm)					
Age (years)	34	Depth	0	10	30	55	85
C_s	0.050	Measured		0.05	0.02	0.02	0.01
D	1.50E-12	Calculated	0.050	0.043	0.030	0.017	0.007

Boggy Creek Bridge - Deck

Parameters		Chloride concentration (%m/m) at depth (mm)				
Age (years)	34	Depth	0	10	30	55
C_s	0.051	Measured		0.04	0.02	0.02
D	5.80E-13	Calculated	0.051	0.040	0.020	0.006

Boggy Creek Bridge - Deck

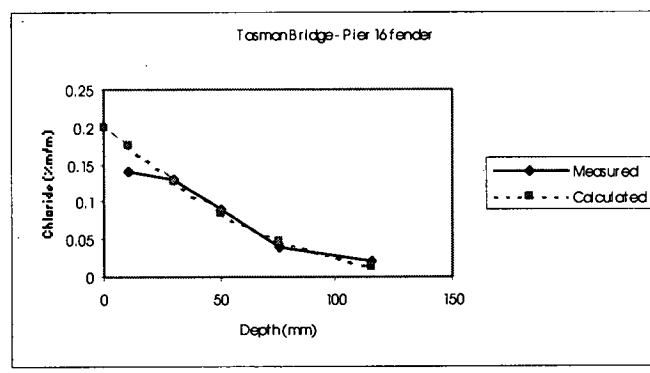

Parameters		Chloride concentration (%m/m) at depth (mm)						
Age (years)	29	Depth	0	10	30	50	75	115
C_s	0.200	Measured		0.14	0.13	0.09	0.04	0.02
D	2.20E-12	Calculated	0.200	0.175	0.127	0.086	0.047	0.014

Tasman Bridge – Pier 16 fender

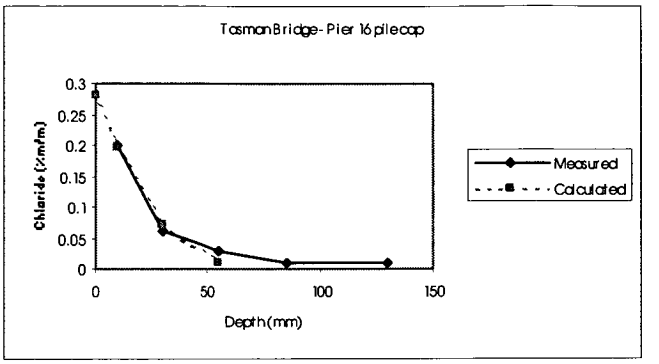

Parameters		Chloride concentration (%m/m) at depth (mm)						
Age (years)	29	Depth	0	10	30	55	85	130
C_s	0.280	Measured		0.2	0.06	0.03	0.01	0.01
D	3.70E-13	Calculated	0.280	0.196	0.070	0.010		

Tasman Bridge – Pier 16 pile cap

Parameters		Chloride concentration (%m/m) at depth (mm)						
Age (years)	29	Depth	0	10	30	55	85	110
C_s	0.025	Measured		0.02	0.01	0.01	0.01	0.01
D	6.90E-13	Calculated	0.025	0.020	0.010	0.003	0.000	

Tasman Bridge – Pier 15 column

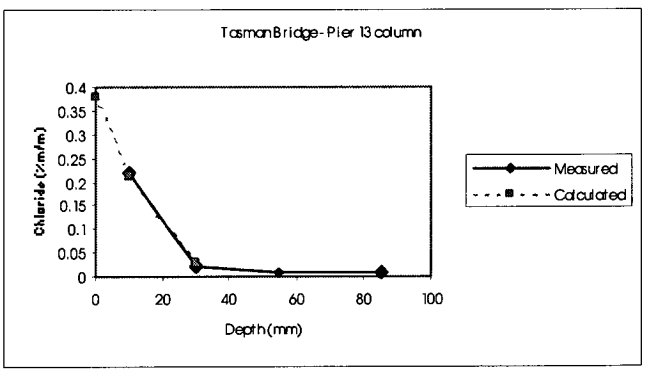

Parameters		Chloride concentration (%m/m) at depth (mm)					
Age (years)	29	Depth	0	10	30	55	85
C_s	0.380	Measured		0.22	0.02	0.01	0.01
D	1.60E-13	Calculated	0.380	0.212	0.030		

Tasman Bridge – Pier 13 column

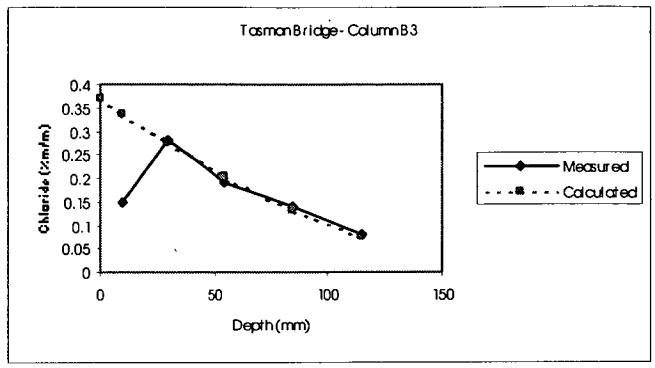

Parameters		Chloride concentration (%m/m) at depth (mm)						
Age (years)	29	Depth	0	10	30	55	85	115
C_s	0.370	Measured		0.15	0.28	0.19	0.14	0.08
D	4.60E-12	Calculated	0.370	0.338	0.275	0.203	0.131	0.078

Tasman Bridge – Column B3

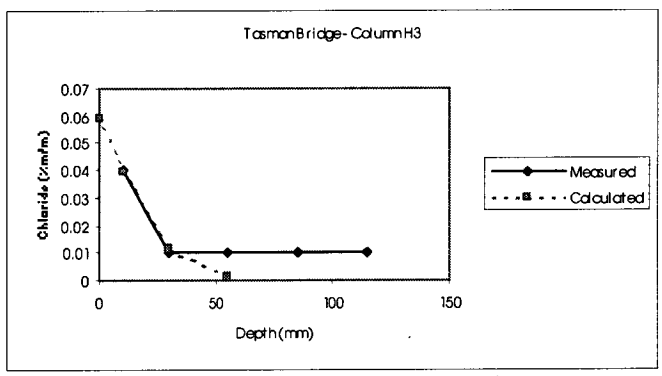

Parameters		Chloride concentration (%m/m) at depth (mm)						
Age (years)	29	Depth	0	10	30	55	85	115
C_s	0.59	Measured		0.04	0.01	0.01	0.01	0.01
D	3.00E-13	Calculated	0.059	0.040	0.012	0.001		

Tasman Bridge – Column H3

Parameters		Chloride concentration (%m/m) at depth (mm)						
Age (years)	29	Depth	0	10	30	55	85	110
C_s	0.035	Measured		0.03	0.02	0.01	0.01	0.01
D	1.50E-12	Calculated	0.035	0.030	0.020	0.010	0.004	0.001

Tasman Bridge – Column F3

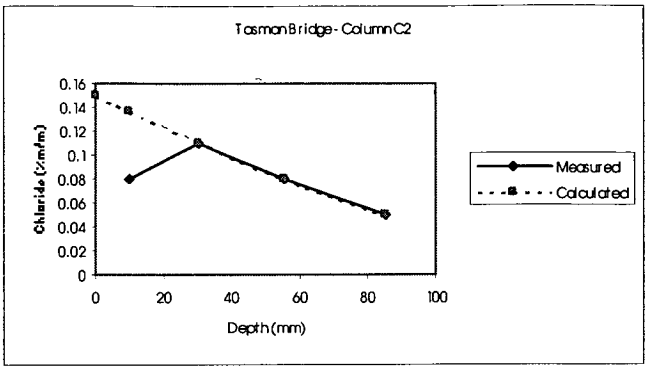

Parameters		Chloride concentration (%m/m) at depth (mm)					
Age (years)	29	Depth	0	10	30	55	85
C_s	0.150	Measured		0.08	0.11	0.08	0.05
D	4.20E-12	Calculated	0.150	0.136	0.110	0.080	0.050

Tasman Bridge – Column C2

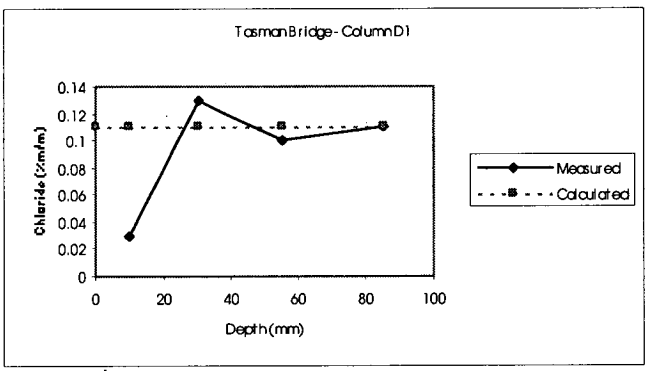

Parameters		Chloride concentration (%m/m) at depth (mm)					
Age (years)	29	Depth	0	10	30	55	85
C_s	0.110	Measured		0.03	0.13	0.1	0.11
D	Constant	Calculated	0.110	0.110	0.110	0.110	0.110

Tasman Bridge – Column D1

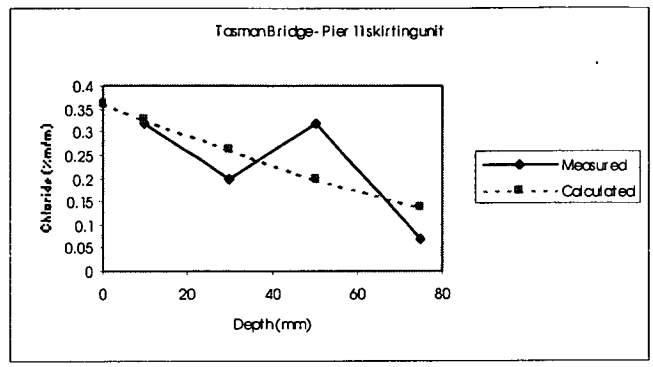

Parameters		Chloride concentration (%m/m) at depth (mm)					
Age (years)	30	Depth	0	10	30	50	75
C_s	0.360	Measured		0.32	0.2	0.32	0.07
D	3.80E-12	Calculated	0.360	0.326	0.261	0.200	0.136

Tasman Bridge – Pier 11 skirting unit

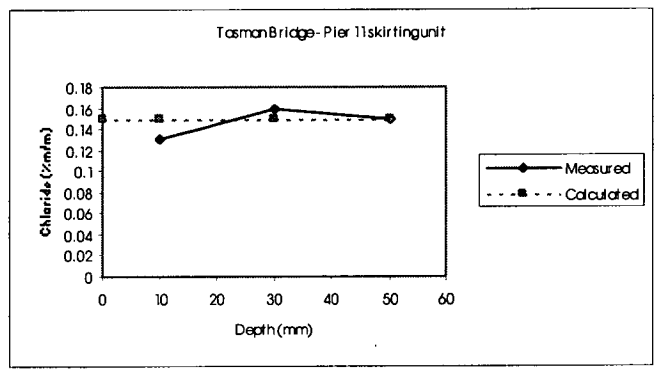

Parameters		Chloride concentration (%m/m) at depth (mm)				
Age (years)	30	Depth	0	10	30	50
C_s	0.150	Measured		0.13	0.16	0.15
D	Constant	Calculated	0.150	0.150	0.150	0.150

Tasman Bridge – Pier 11 skirting unit

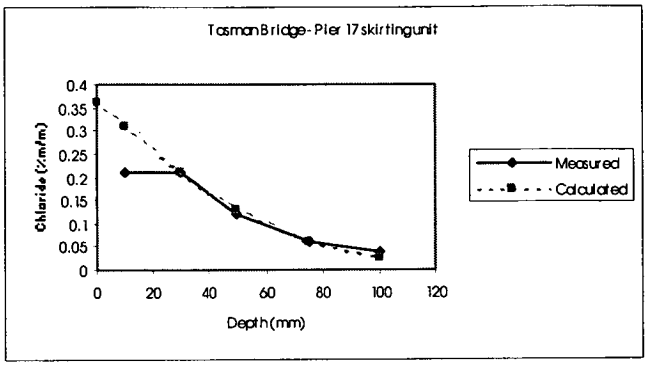

Parameters		Chloride concentration (%m/m) at depth (mm)						
Age (years)	30	Depth	0	10	30	50	75	100
C_s	0.360	Measured		0.21	0.21	0.12	0.06	0.04
D	1.60E-12	Calculated	0.360	0.308	0.211	0.131	0.062	0.025

Tasman Bridge – Pier 17 skirting unit

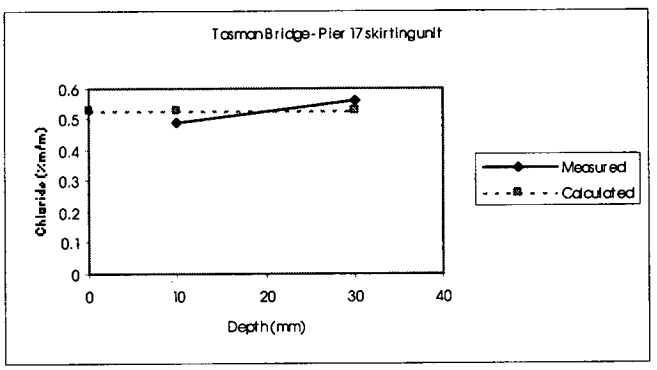

Parameters		Chloride concentration (%m/m) at depth (mm)			
Age (years)	30	Depth	0	10	30
C_s	0.530	Measured		0.49	0.56
D	Constant	Calculated	0.530	0.530	0.530

Tasman Bridge – Pier 17 skirting unit

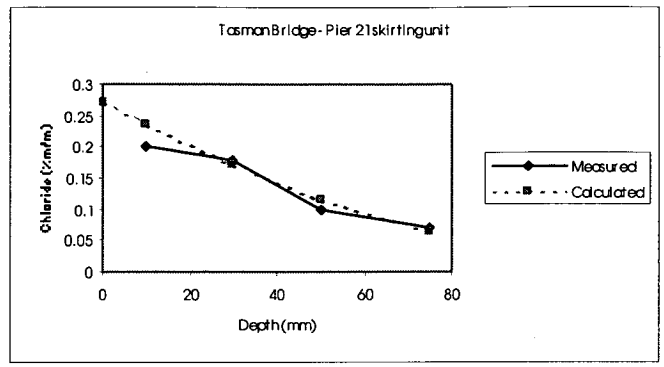

Parameters		Chloride concentration (%m/m) at depth (mm)					
Age (years)	30	Depth	0	10	30	50	75
C_s	0.270	Measured		0.2	0.18	0.1	0.07
D	2.10E-12	Calculated	0.270	0.236	0.171	0.116	0.063

Tasman Bridge – Pier 21 skirting unit

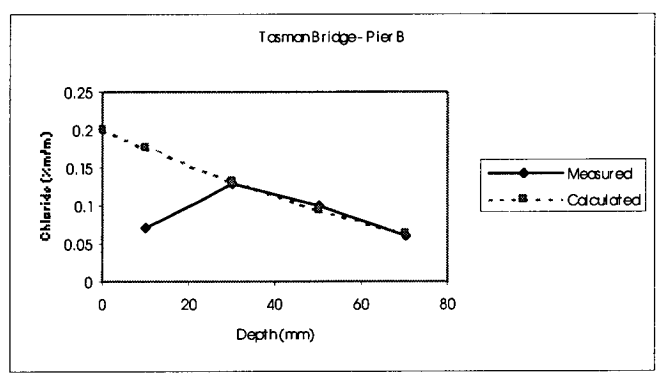

Parameters		Chloride concentration (%m/m) at depth (mm)					
Age (years)	29	Depth	0	10	30	50	70
C_s	0.200	Measured		0.07	0.13	0.1	0.06
D	2.60E-12	Calculated	0.200	0.177	0.133	0.094	0.062

Tasman Bridge – Pier B

Parameters		Chloride concentration (%m/m) at depth (mm)				
Age (years)	29	Depth	0	10	30	50
C_s	0.042	Measured		0.03	0.01	0.01
D	3.60E-13	Calculated	0.042	0.029	0.010	

Tasman Bridge – Pier B

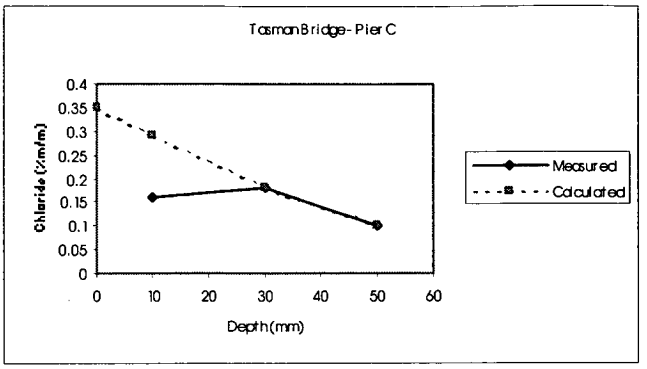

Parameters		Chloride concentration (%m/m) at depth (mm)				
Age (years)	29	Depth	0	10	30	50
C_s	0.350	Measured		0.16	0.18	0.1
D	1.20E-12	Calculated	0.350	0.291	0.183	0.100

Tasman Bridge – Pier C

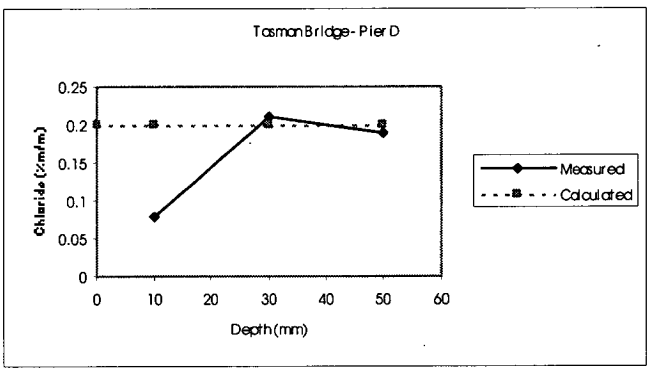

Parameters		Chloride concentration (%m/m) at depth (mm)				
Age (years)	29	Depth	0	10	30	50
C_s	0.200	Measured		0.08	0.21	0.19
D	Constant	Calculated	0.200	0.200	0.200	0.200

Tasman Bridge – Pier D

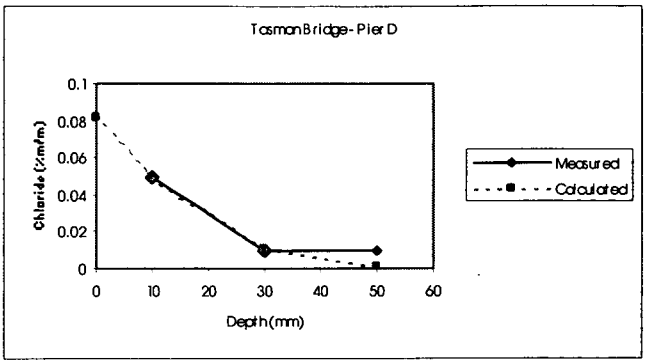

Parameters		Chloride concentration (%m/m) at depth (mm)				
Age (years)	29	Depth	0	10	30	50
C_s	0.082	Measured		0.05	0.01	0.01
D	2.10E-13	Calculated	0.082	0.050	0.010	0.001

Tasman Bridge – Pier D

Parameters		Chloride concentration (%m/m) at depth (mm)				
Age (years)	29	Depth	0	10	30	50
C_s	0.042	Measured		0.04	0.03	0.03
D	7.10E-12	Calculated	0.042	0.039	0.033	0.028

Tasman Bridge – Pier E

Parameters		Chloride concentration (%m/m) at depth (mm)				
Age (years)	29	Depth	0	10	30	50
C_s	0.015	Measured		0.01	0.02	0.01
D	Constant	Calculated	0.015	0.015	0.015	0.015

Tasman Bridge – Pier F

Parameters		Chloride concentration (%m/m) at depth (mm)				
Age (years)	29	Depth	0	10	30	50
C_s	0.026	Measured		0.02	0.01	0.01
D	6.50E-13	Calculated	0.026	0.020	0.010	0.004

Tasman Bridge – Pier F

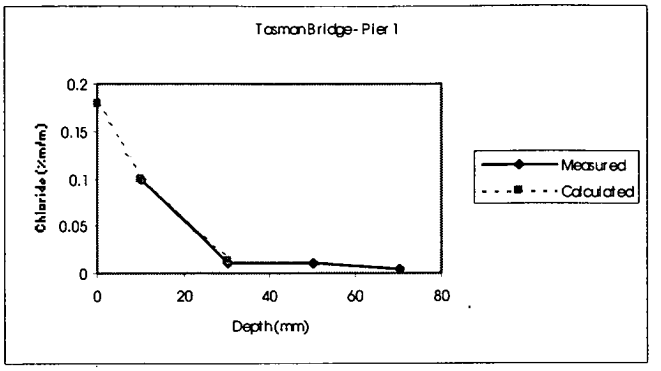

Parameters		Chloride concentration (%m/m) at depth (mm)					
Age (years)	29	Depth	0	10	30	50	70
C_s	0.180	Measured		0.1	0.01	0.01	0.005
D	1.50E-13	Calculated	0.180	0.098	0.013		

Tasman Bridge – Pier 1

Parameters		Chloride concentration (%m/m) at depth (mm)				
Age (years)	29	Depth	0	10	30	50
C_s	0.030	Measured		0.02	0.006	0.001
D	3.00E-13	Calculated	0.030	0.020	0.006	0.001

Tasman Bridge – Pier 1

Parameters		Chloride concentration (%m/m) at depth (mm)				
Age (years)	29	Depth	0	10	30	50
C_s	0.030	Measured		0.02	0.006	0.001
D	3.00E-13	Calculated	0.030	0.020	0.006	0.001

Tasman Bridge – Pier 1

Parameters		Chloride concentration (%m/m) at depth (mm)				
Age (years)	29	Depth	0	10	30	50
C_s	0.051	Measured		0.03	0.005	0.001
D	1.80E-13	Calculated	0.051	0.030	0.005	0.001

Tasman Bridge – Pier 15

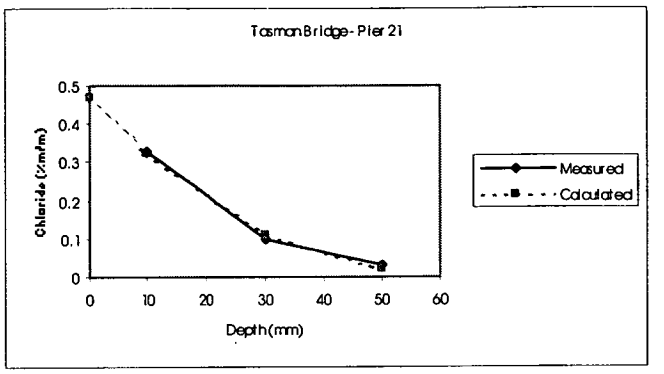

Parameters		Chloride concentration (%m/m) at depth (mm)				
Age (years)	29	Depth	0	10	30	50
C_s	0.470	Measured		0.33	0.1	0.03
D	3.40E-13	Calculated	0.470	0.324	0.108	0.021

Tasman Bridge – Pier 21

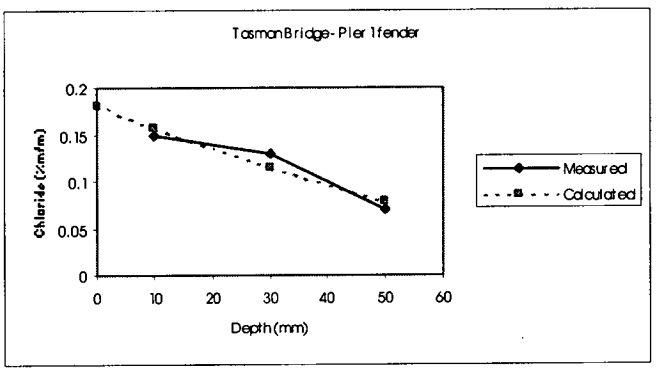

Parameters		Chloride concentration (%m/m) at depth (mm)				
Age (years)	29	Depth	0	10	30	50
C_s	0.180	Measured		0.15	0.13	0.07
D	2.30E-12	Calculated	0.180	0.158	0.116	0.079

Tasman Bridge – Pier 1 fender

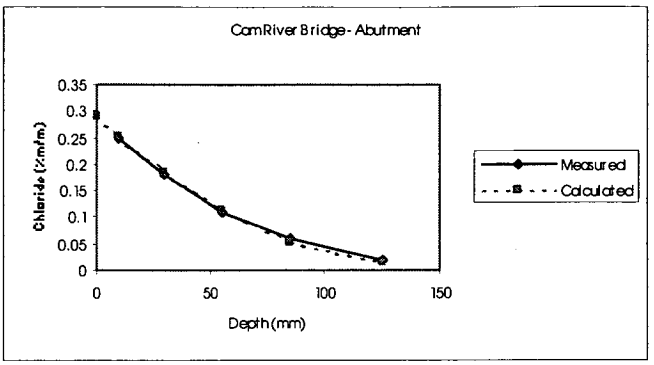

Parameters		Chloride concentration (%m/m) at depth (mm)					
Age (years)	31	Depth	0	10	30	55	85	125
C_s	0.290	Measured		0.25	0.18	0.11	0.06	0.02
D	2.10E-12	Calculated	0.290	0.254	0.186	0.113	0.054	0.015

Cam River Bridge - Abutment

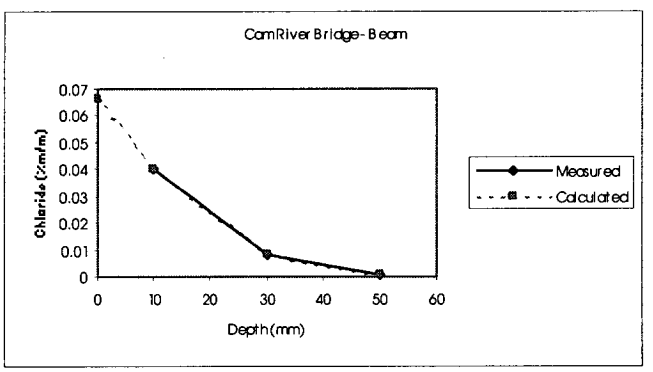

Parameters		Chloride concentration (%m/m) at depth (mm)				
Age (years)	31	Depth	0	10	30	50
C_s	0.066	Measured		0.04	0.008	0.001
D	1.90E-13	Calculated	0.066	0.040	0.008	0.001

Cam River Bridge - Beam

Parameters		Chloride concentration (%m/m) at depth (mm)				
Age (years)	31	Depth	0	10	30	50
C_s	0.050	Measured		0.03	0.006	0.001
D	1.90E-13	Calculated	0.050	0.030	0.006	0.001

Cam River Bridge - Beam

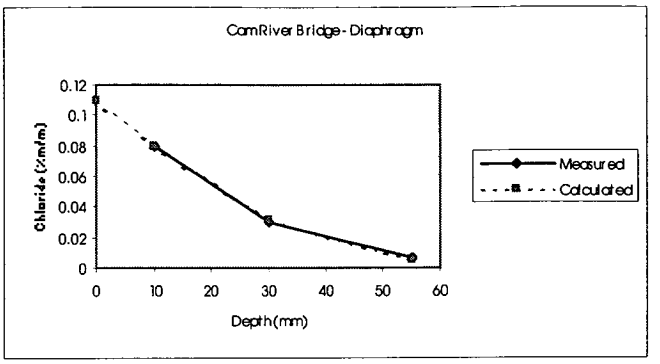

Parameters		Chloride concentration (%m/m) at depth (mm)				
Age (years)	31	Depth	0	10	30	55
C_s	0.110	Measured		0.08	0.03	0.007
D	4.00E-13	Calculated	0.110	0.079	0.031	0.005

Cam River Bridge - Diaphragm

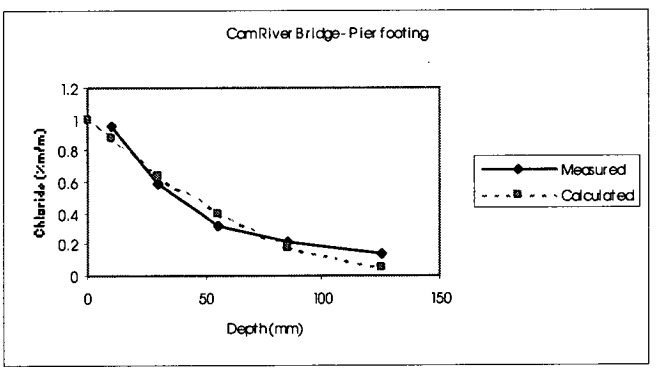

Parameters		Chloride concentration (%m/m) at depth (mm)						
Age (years)	31	Depth	0	10	30	55	85	125
C_s	1.000	Measured		0.96	0.59	0.32	0.22	0.14
D	2.10E-12	Calculated	1.000	0.876	0.640	0.391	0.185	0.051

Cam River Bridge – Pier footing

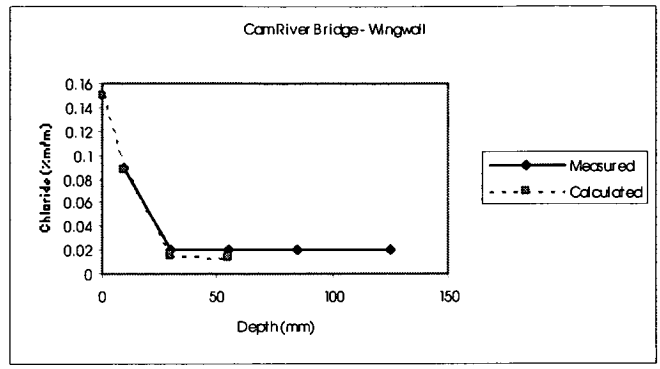

Parameters		Chloride concentration (%m/m) at depth (mm)						
Age (years)	31	Depth	0	10	30	55	85	125
C_s	0.150	Measured		0.09	0.02	0.02	0.02	0.02
D	1.70E-13	Calculated	0.150	0.088	0.015	0.013		

Cam River Bridge - Wingwall

Parameters		Chloride concentration (%m/m) at depth (mm)			
Age (years)	31	Depth	0	10	30
C_s	0.031	Measured		0.02	0.005
D	2.40E-13	Calculated	0.031	0.020	0.005

Cam River Bridge - Deck

Parameters		Chloride concentration (%m/m) at depth (mm)			
Age (years)	31	Depth	0	10	30
C_s	0.049	Measured		0.03	0.005
D	1.80E-13	Calculated	0.049	0.029	0.005

Cam River Bridge - Deck

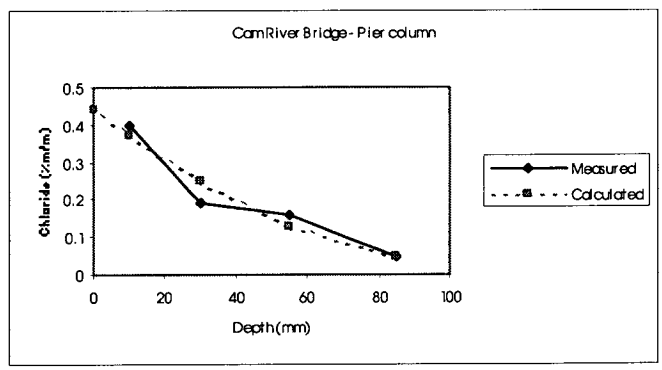

Parameters		Chloride concentration (%m/m) at depth (mm)					
Age (years)	31	Depth	0	10	30	55	85
C_s	0.440	Measured		0.4	0.19	0.16	0.05
D	1.40E-12	Calculated	0.440	0.373	0.249	0.129	0.046

Cam River Bridge – Pier column

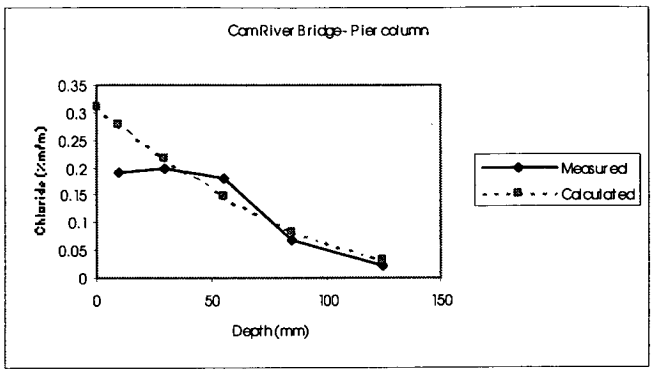

Parameters		Chloride concentration (%m/m) at depth (mm)						
Age (years)	31	Depth	0	10	30	55	85	125
C_s	0.310	Measured		0.19	0.2	0.18	0.07	0.02
D	3.00E-12	Calculated	0.310	0.278	0.216	0.147	0.083	0.032

Cam River Bridge – Pier column

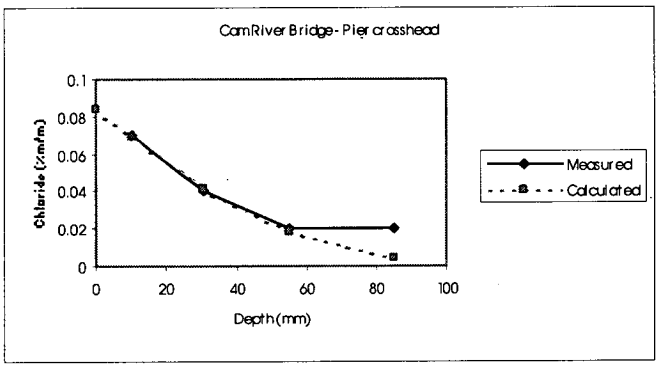

Parameters		Chloride concentration (%m/m) at depth (mm)					
Age (years)	31	Depth	0	10	30	55	85
C_s	0.084	Measured		0.07	0.04	0.02	0.02
D	1.00E-12	Calculated	0.084	0.069	0.042	0.018	0.005

Cam River Bridge – Pier crosshead

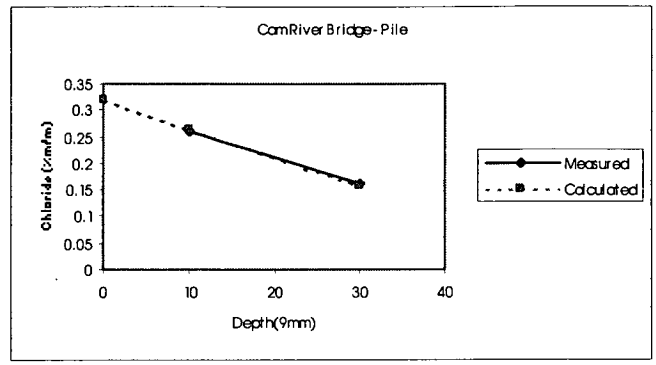

Parameters		Chloride concentration (%m/m) at depth (mm)			
Age (years)	32	Depth	0	10	30
C_s	0.320	Measured		0.26	0.16
D	1.00E-12	Calculated	0.320	0.263	0.159

Cam River Bridge - Pile

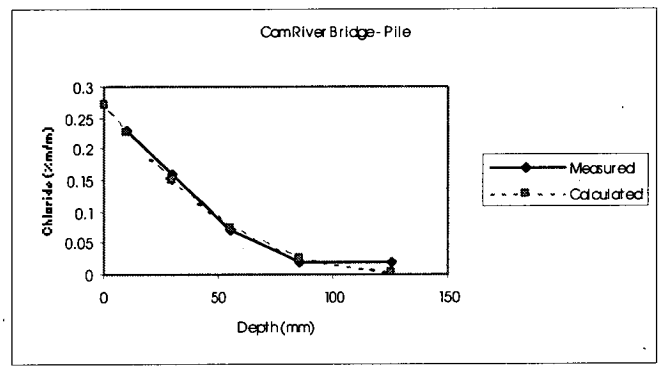

Parameters		Chloride concentration (%m/m) at depth (mm)						
Age (years)	31	Depth	0	10	30	55	85	125
C_s	0.270	Measured		0.23	0.16	0.07	0.02	0.02
D	1.30E-12	Calculated	0.270	0.228	0.149	0.074	0.025	0.004

Cam River Bridge - Pile

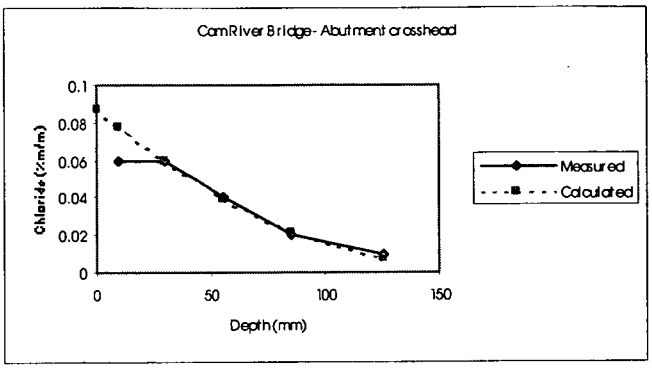

Parameters		Chloride concentration (%m/m) at depth (mm)						
Age (years)	31	Depth	0	10	30	55	85	125
C_s	0.087	Measured		0.06	0.06	0.04	0.02	0.01
D	2.80E-12	Calculated	0.087	0.078	0.060	0.040	0.022	0.008

Cam River Bridge – Abutment crosshead

Parameters		Chloride concentration (%m/m) at depth (mm)				
Age (years)	25	Depth	0	10	30	55
C_s	0.047	Measured		0.03	0.007	0.001
D	2.70E-13	Calculated	0.047	0.030	0.007	0.001

Newmans Creek Bridge – Crosshead

Parameters		Chloride concentration (%m/m) at depth (mm)					
Age (years)	25	Depth	0	10	30	55	85
C_s	0.045	Measured		0.04	0.03	0.03	0.01
D	4.60E-12	Calculated	0.045	0.041	0.033	0.023	0.014

Newmans Creek Bridge - Pile

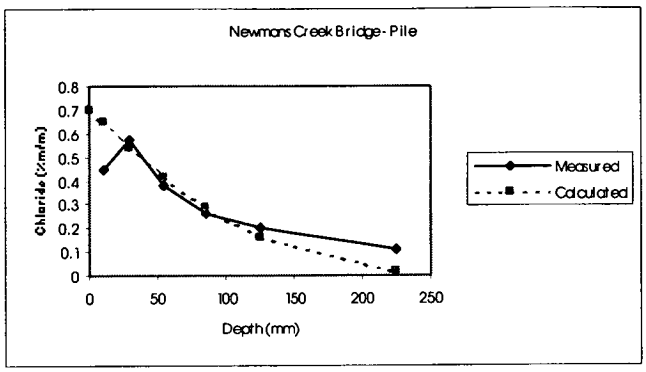

Parameters		Chloride concentration (%m/m) at depth (mm)						
Age (years)	25	Depth	0	10	30	55	85	125	225
C_s	0.700	Measured		0.45	0.57	0.38	0.26	0.2	0.11
D	6.80E-12	Calculated	0.700	0.646	0.541	0.417	0.288	0.159	0.021

Newmans Creek Bridge - Pile

Parameters		Chloride concentration (%m/m) at depth (mm)				
Age (years)	24	Depth	0	10	55	80
C_s	0.050	Measured		0.043	0.013	0.008
D	1.80E-12	Calculated	0.050	0.042	0.015	0.006

Victoria Bridge - Deck

Parameters		Chloride concentration (%m/m) at depth (mm)				
Age (years)	24	Depth	0	10	90	145
C_s	0.022	Measured		0.022	0.011	0.012
D	2.40E-11	Calculated	0.022	0.021	0.014	0.010

Victoria Bridge - Crosshead

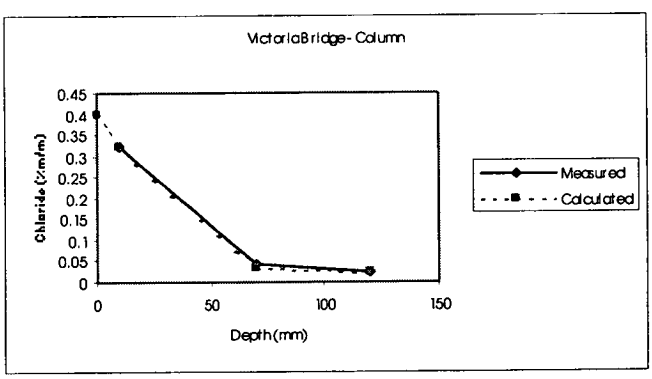

Parameters		Chloride concentration (%m/m) at depth (mm)				
Age (years)	24	Depth	0	10	70	120
C_s	0.400	Measured		0.32	0.045	0.022
D	1.10E-12	Calculated	0.400	0.323	0.035	0.022

Victoria Bridge - Column

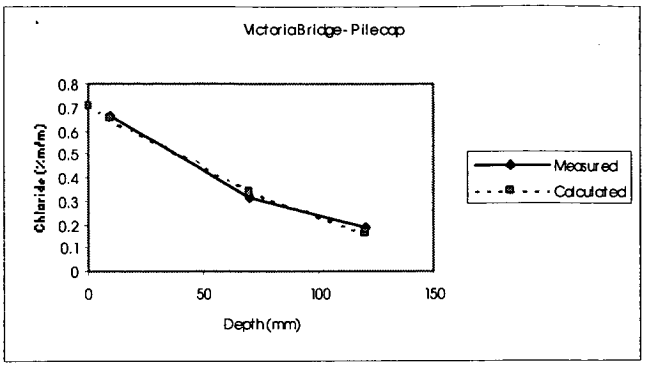

Parameters		Chloride concentration (%m/m) at depth (mm)				
Age (years)	24	Depth	0	10	70	120
C_s	0.710	Measured		0.661	0.312	0.186
D	6.50E-12	Calculated	0.710	0.653	0.341	0.161

Victoria Bridge – Pile Cap

Parameters		Chloride concentration (%m/m) at depth (mm)				
Age (years)	24	Depth	0	10	60	110
C_s	0.037	Measured		0.029	0.005	0.003
D	9.00E-13	Calculated	0.037	0.029	0.004	0.003

Victoria Bridge - Crosshead

Parameters		Chloride concentration (%m/m) at depth (mm)				
Age (years)	24	Depth	0	10	70	120
C_s	0.041	Measured		0.036	0.032	0.009
D	1.10E-11	Calculated	0.041	0.039	0.024	0.015

Victoria Bridge - Column

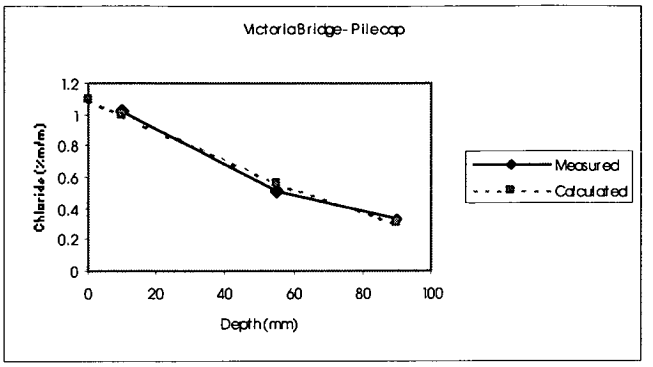

Parameters		Chloride concentration (%m/m) at depth (mm)				
Age (years)	24	Depth	0	10	55	90
C_s	1.100	Measured		1.016	0.512	0.332
D	4.50E-12	Calculated	1.100	0.994	0.556	0.303

Victoria Bridge – Pile cap

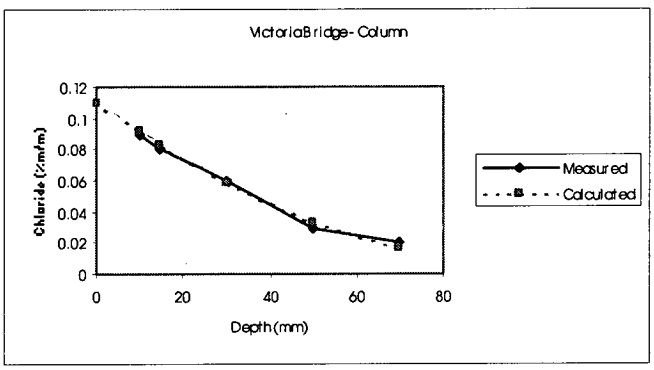

Parameters		Chloride concentration (%m/m) at depth (mm)						
Age (years)	22	Depth	0	10	15	30	50	70
C_s	0.110	Measured		0.09	0.08	0.06	0.03	0.02
D	1.70E-12	Calculated	0.110	0.092	0.083	0.059	0.033	0.017

Victoria Bridge - Column

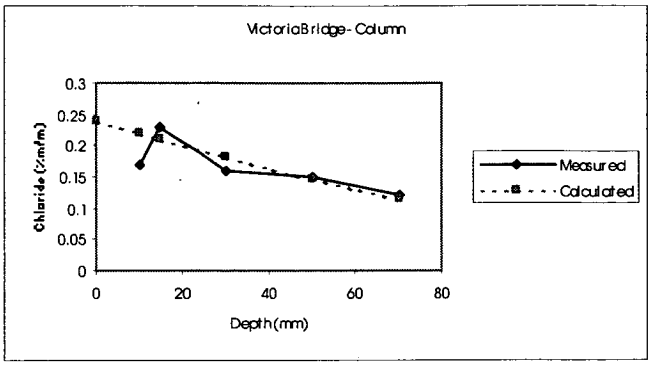

Parameters		Chloride concentration (%m/m) at depth (mm)						
Age (years)	22	Depth	0	10	15	30	50	70
C_s	0.240	Measured		0.17	0.23	0.16	0.15	0.12
D	7.10E-12	Calculated	0.240	0.221	0.211	0.183	0.148	0.115

Victoria Bridge - Column

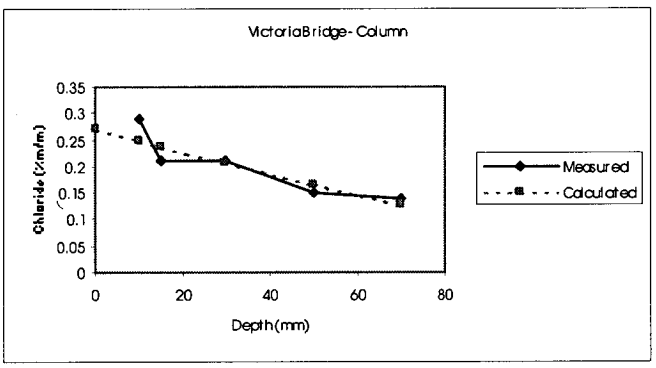

Parameters		Chloride concentration (%m/m) at depth (mm)						
Age (years)	22	Depth	0	10	15	30	50	70
C_s	0.270	Measured		0.29	0.21	0.21	0.15	0.14
D	7.00E-12	Calculated	0.270	0.248	0.237	0.205	0.165	0.129

Victoria Bridge - Column

Parameters		Chloride concentration (%m/m) at depth (mm)						
Age (years)	22	Depth	0	10	15	30	50	70
C_s	0.054	Measured		0.05	0.03	0.05	0.01	0.01
D	2.20E-12	Calculated	0.054	0.046	0.042	0.032	0.020	0.011

Victoria Bridge - Column

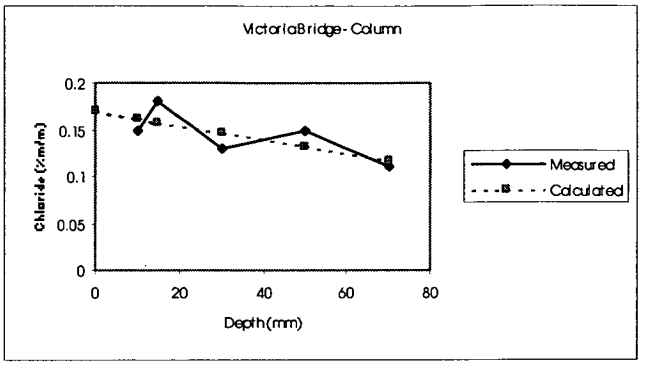

Parameters		Chloride concentration (%m/m) at depth (mm)						
Age (years)	22	Depth	0	10	15	30	50	70
C_s	0.170	Measured		0.15	0.18	0.13	0.15	0.11
D	2.20E-11	Calculated	0.170	0.162	0.158	0.147	0.132	0.117

Victoria Bridge - Column

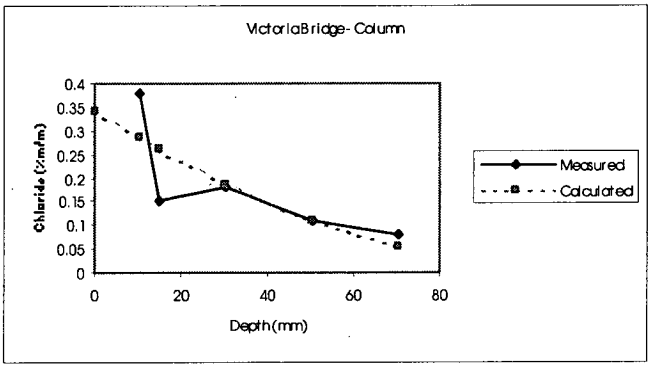

Parameters		Chloride concentration (%m/m) at depth (mm)						
Age (years)	22	Depth	0	10	15	30	50	70
C_s	0.340	Measured		0.38	0.15	0.18	0.11	0.08
D	1.80E-12	Calculated	0.340	0.286	0.260	0.187	0.108	0.055

Victoria Bridge - Column

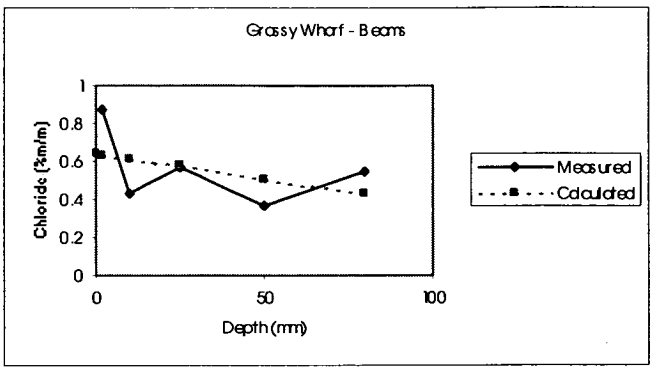

Parameters		Chloride concentration (%m/m) at depth (mm)						
Age (years)	18	Depth	0	2	10	25	50	80
C_s	0.640	Measured		0.87	0.43	0.57	0.37	0.55
D	3.30E-11	Calculated	0.640	0.635	0.614	0.574	0.510	0.435

Grassy Wharf - Beam

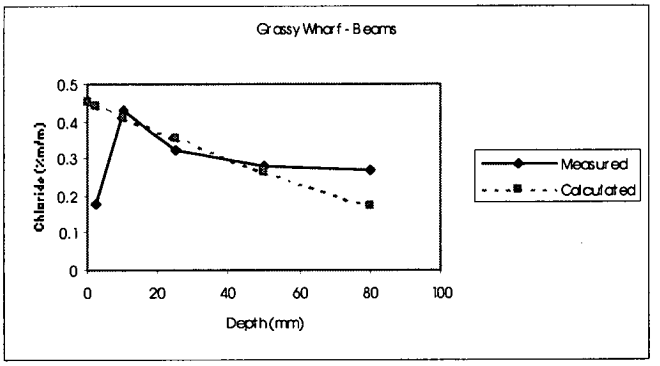

Parameters		Chloride concentration (%m/m) at depth (mm)						
Age (years)	18	Depth	0	2	10	25	50	80
C_s	0.450	Measured		0.18	0.43	0.32	0.28	0.27
D	7.50E-12	Calculated	0.450	0.442	0.411	0.354	0.265	0.174

Grassy Wharf - Beam

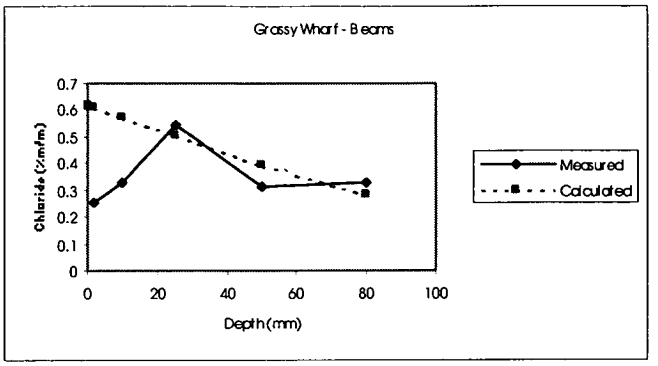

Parameters		Chloride concentration (%m/m) at depth (mm)						
Age (years)	18	Depth	0	2	10	25	50	80
C_s	0.620	Measured		0.25	0.33	0.54	0.31	0.33
D	9.90E-12	Calculated	0.620	0.611	0.573	0.505	0.395	0.279

Grassy Wharf - Beam

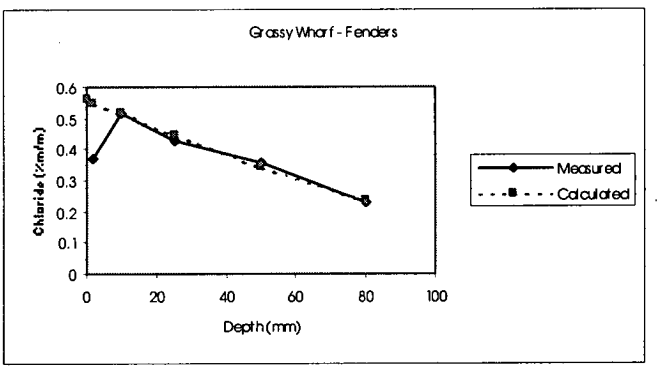

Parameters		Chloride concentration (%m/m) at depth (mm)						
Age (years)	18	Depth	0	2	10	25	50	80
C_s	0.560	Measured		0.37	0.52	0.43	0.36	0.23
D	8.70E-12	Calculated	0.560	0.551	0.515	0.449	0.344	0.236

Grassy Wharf - Fender

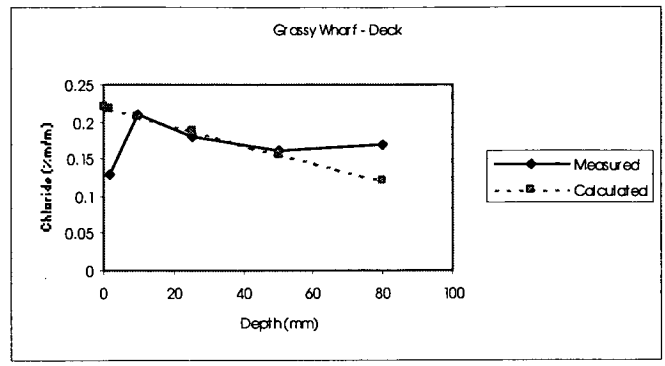

Parameters		Chloride concentration (%m/m) at depth (mm)						
Age (years)	18	Depth	0	2	10	25	50	80
C_s	0.220	Measured		0.13	0.21	0.18	0.16	0.17
D	1.60E-11	Calculated	0.220	0.217	0.207	0.188	0.156	0.122

Grassy Wharf - Deck

Parameters		Chloride concentration (%m/m) at depth (mm)						
Age (years)	18	Depth	0	10	30	55	85	115
C_s	0.034	Measured		0.04	0.02	0.03	0.02	0.02
D	3.20E-11	Calculated	0.034	0.033	0.030	0.026	0.022	0.019

Burnie Port Access Bridge - Kerb

Parameters		Chloride concentration (%m/m) at depth (mm)						
Age (years)	18	Depth	0	10	30	55	85	100
C_s	0.043	Measured		0.04	0.02	0.02	0.02	0.02
D	3.00E-12	Calculated	0.043	0.037	0.026	0.015	0.006	0.004

Burnie Port Access Bridge - Kerb

Parameters		Chloride concentration (%m/m) at depth (mm)				
Age (years)	17	Depth	0	10	30	50
C_s	0.028	Measured		0.027	0.012	0.015
D	3.60E-12	Calculated	0.028	0.024	0.018	0.012

Risdon Cove Causeway Culvert

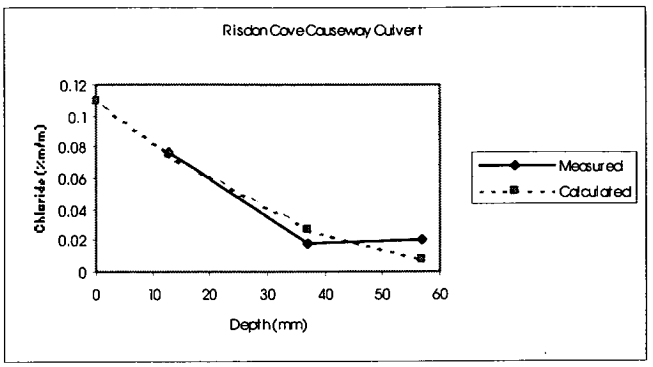

Parameters		Chloride concentration (%m/m) at depth (mm)				
Age (years)	17	Depth	0	13	37	57
C_s	0.110	Measured		0.076	0.018	0.021
D	9.50E-13	Calculated	0.110	0.075	0.027	0.008

Risdon Cove Causeway Culvert

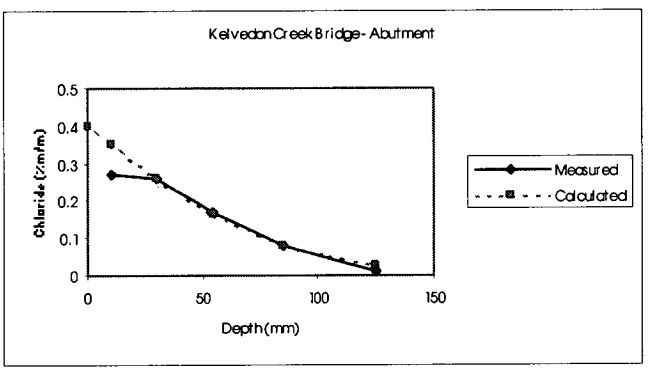

Parameters		Chloride concentration (%m/m) at depth (mm)						
Age (years)	20	Depth	0	10	30	55	85	125
C_s	0.400	Measured		0.27	0.26	0.17	0.08	0.01
D	3.50E-12	Calculated	0.400	0.352	0.261	0.163	0.080	0.024

Kelvedon Creek Bridge - Abutment

Parameters		Chloride concentration (%m/m) at depth (mm)				
Age (years)	20	Depth	0	10	30	55
C_s	0.049	Measured		0.04	0.03	0.01
D	1.90E-12	Calculated	0.049	0.041	0.027	0.013

Kelvedon Creek Bridge - Abutment

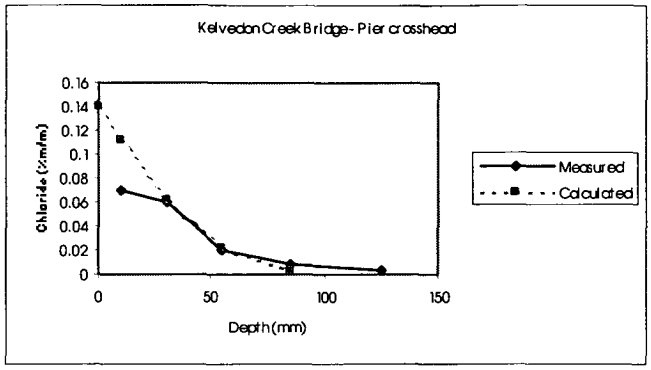

Parameters		Chloride concentration (%m/m) at depth (mm)						
Age (years)	20	Depth	0	10	30	55	85	125
C_s	0.140	Measured		0.07	0.06	0.02	0.008	0.003
D	1.20E-12	Calculated	0.140	0.112	0.062	0.022	0.004	

Kelvedon Creek Bridge – Pier crosshead

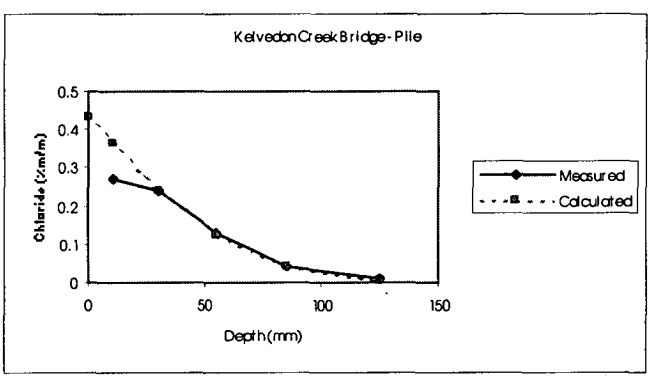

Parameters		Chloride concentration (%m/m) at depth (mm)						
Age (years)	20	Depth	0	10	30	55	85	125
C_s	0.430	Measured		0.27	0.24	0.13	0.04	0.008
D	2.10E-12	Calculated	0.430	0.364	0.241	0.123	0.043	0.007

Kelvedon Creek Bridge - Pile

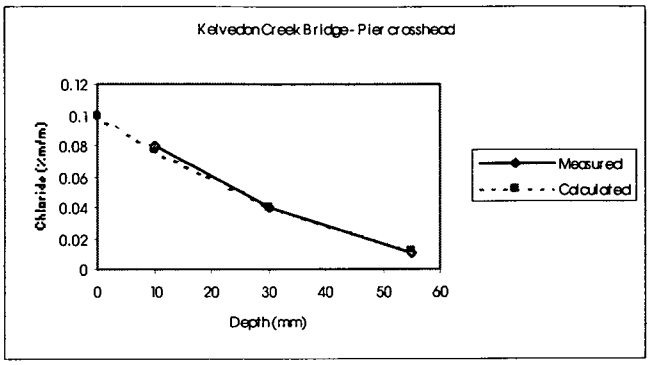

Parameters		Chloride concentration (%m/m) at depth (mm)				
Age (years)	20	Depth	0	10	30	55
C_s	0.100	Measured		0.08	0.04	0.01
D	1.00E-12	Calculated	0.100	0.078	0.040	0.012

Kelvedon Creek Bridge – Pier crosshead

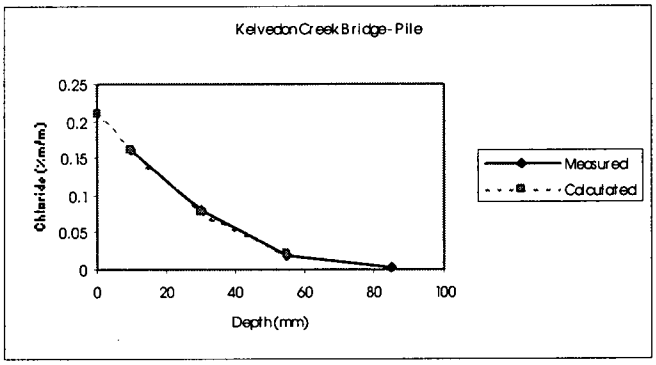

Parameters		Chloride concentration (%m/m) at depth (mm)					
Age (years)	20	Depth	0	10	30	55	85)
C_s	0.210	Measured		0.16	0.08	0.02	0.003
D	9.00E-13	Calculated	0.210	0.161	0.078	0.022	

Kelvedon Creek Bridge - Pile

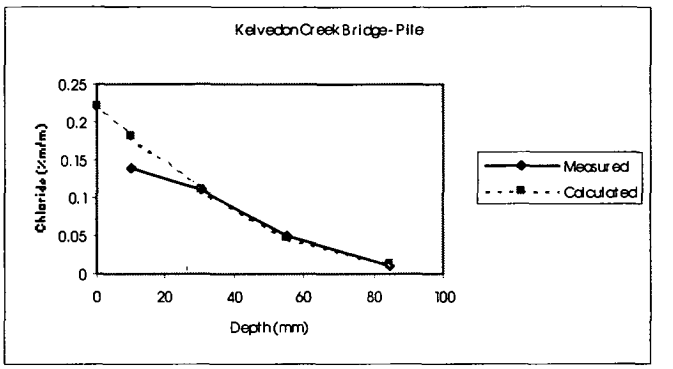

Parameters		Chloride concentration (%m/m) at depth (mm)					
Age (years)	20	Depth	0	10	30	55	85
C_s	0.220	Measured		0.14	0.11	0.05	0.01
D	1.60E-12	Calculated	0.220	0.181	0.111	0.049	0.013

Kelvedon Creek Bridge - Pile

Parameters		Chloride concentration (%m/m) at depth (mm)					
Age (years)	20	Depth	0	10	30	55	85
C_s	0.043	Measured		0.02	0.02	0.006	0.001
D	1.20E-12	Calculated	0.043	0.034	0.019	0.007	0.001

Kelvedon Creek Bridge - Kerb

4.2 CHLORIDE PROFILE ANALYSIS

4.2.1 SURFACE CHLORIDE CONCENTRATION

Figure A4.1 plots the apparent chloride surface concentration against the height of the core above mean water level. While the number of samples at greater heights is small, the plot nevertheless indicates a significant reduction in the apparent surface chloride concentration for heights above 4m.

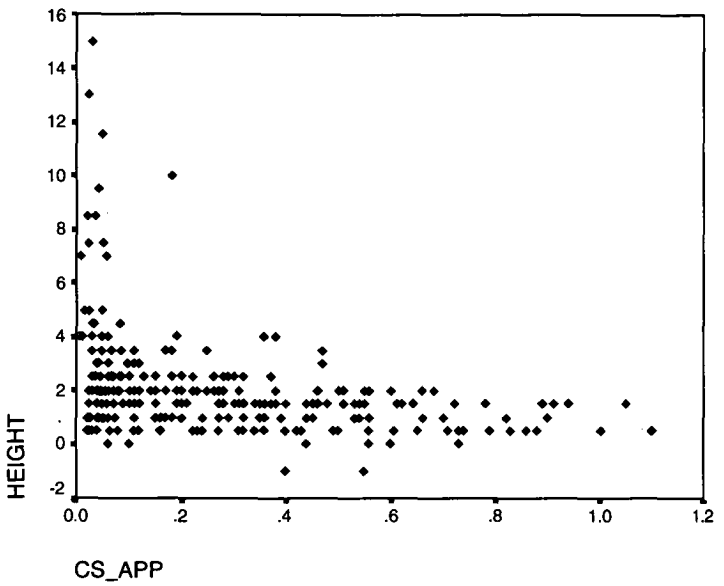

Figure A4.1– Apparent surface chloride concentration ~ height above MWL for all data

Tables A4.1 and A4.2 and figures A4.2 and A4.3 detail the maximum apparent surface concentration of chlorides against height above mean water level and against the distance of the structure from the coast.

Height above MWL (m)	Maximum $C_{s\text{-}app}$
-1	0.55
0	0.73
0.5	1.1
1	0.9
1.5	1.05
2	0.68
2.5	0.37
3	0.47
3.5	0.47
4	0.38
4.5	0.082
5	0.05
7	0.059
7.5	0.051
8.5	0.037
9.5	0.042
10	0.18
11.5	0.05
13	0.026
15	0.03

Table A4.1 – Surface chloride concentration and height above MWL

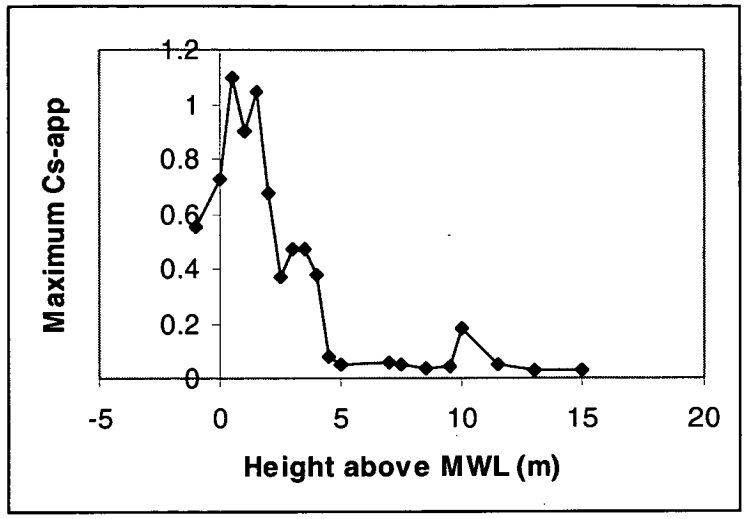

Figure A4.2 – Surface chloride concentration and height above MWL

The outlier for a height of 10m is from a single sample from the top of the bowstring arch of the Emu River Bridge.

Distance from coast (km)	Maximum $C_{s\text{-}app}$
0	1.1
0.1	0.5
0.2	0.24
0.4	0.42
0.5	0.12
0.8	0.16
1	0.11
1.2	0.15
3.5	0.06
4	0.04
7.5	0.1
32	0.011

Table A4.2 – Surface chloride concentration and distance from coast

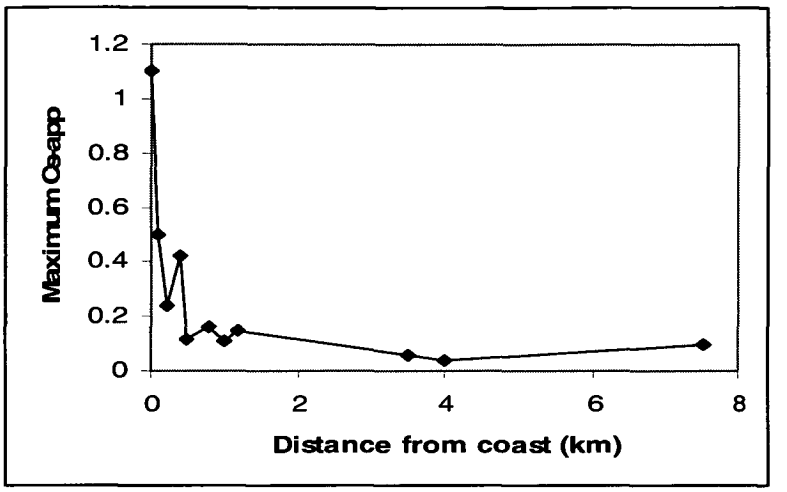

Figure A4.3 – Envelope of surface chloride concentration and distance from coast

The following charts plot the relationship between the apparent surface chloride concentration and the effective diffusion coefficient and the a range of parameters listed in section 6.7.1 of the thesis.

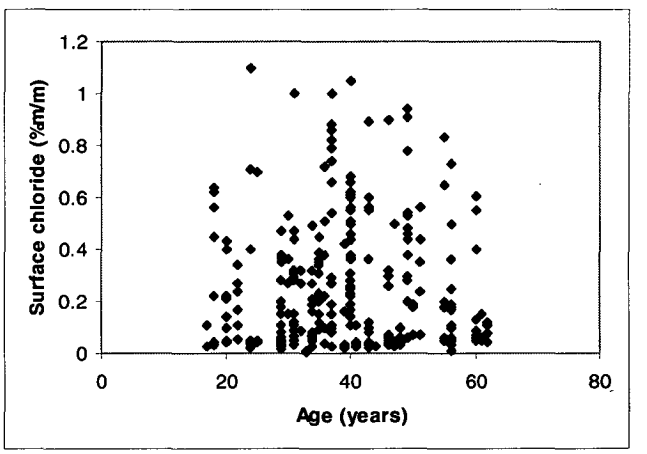

Figure A4.4 – Surface chloride concentration and age

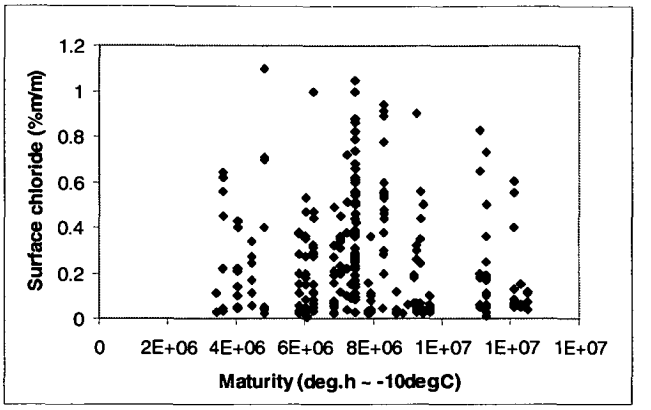

Figure A4.5 – Surface chloride concentration and concrete maturity

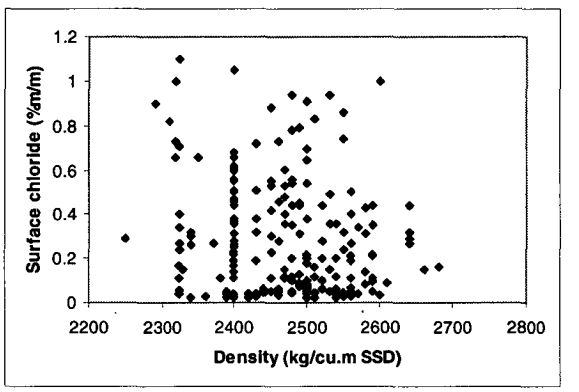

Figure A4.6 – Surface chloride concentration and density

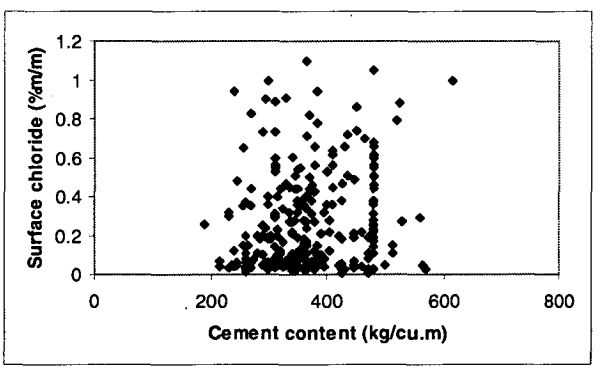

Figure A4.7 – Surface chloride concentration and cement content

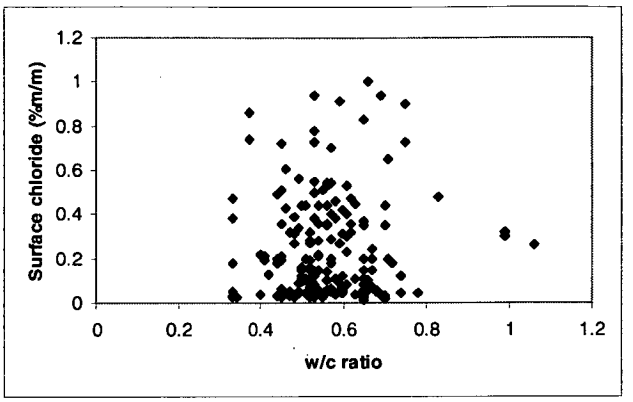

Figure A4.8 – Surface chloride concentration and water cement ratio

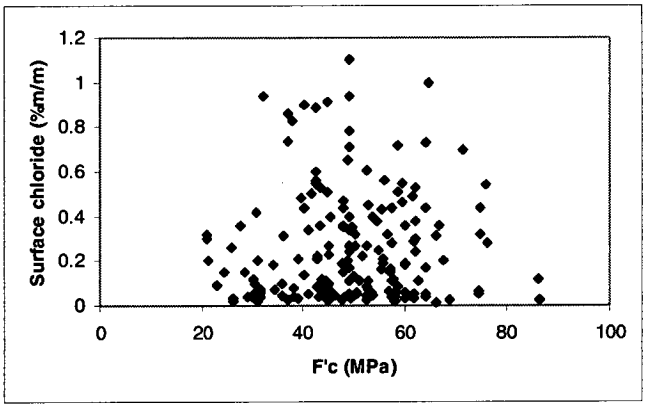

Figure A4.9 – Surface chloride concentration and concrete strength

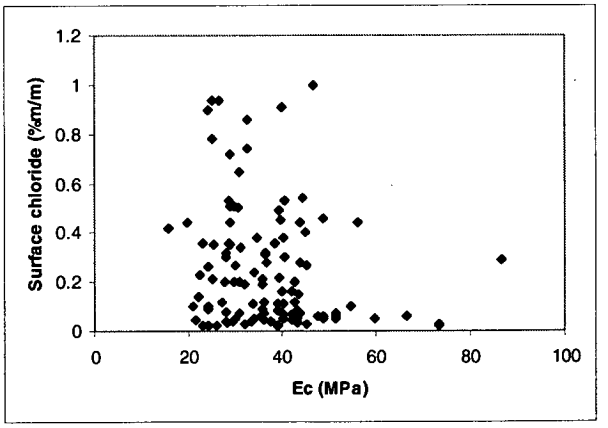

Figure A4.10 – Surface chloride concentration and Young's modulus

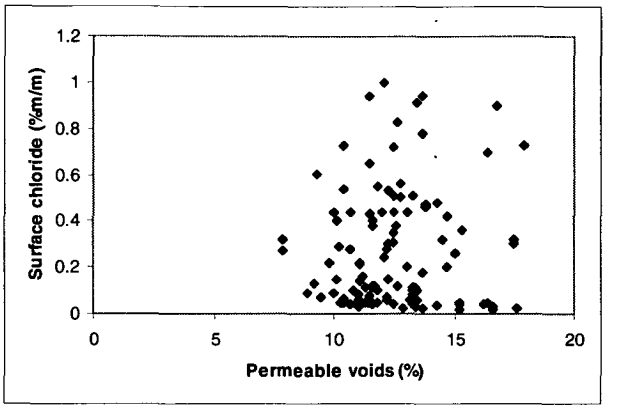

Figure A4.11 – Surface chloride concentration and permeable voids

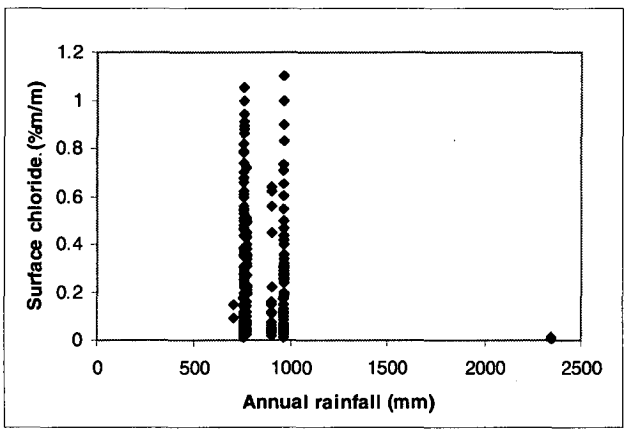

Figure A4.12 – Surface chloride concentration and rainfall

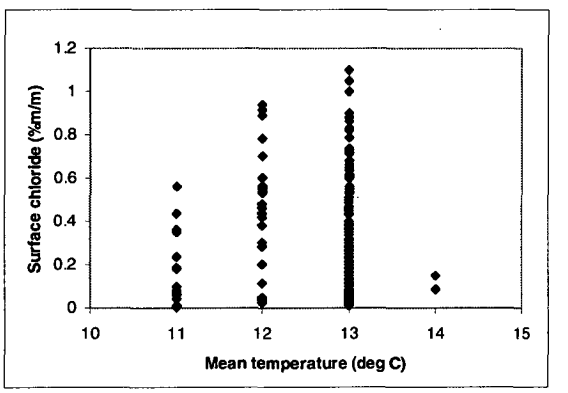

Figure A4.13 – Surface chloride concentration and temperature

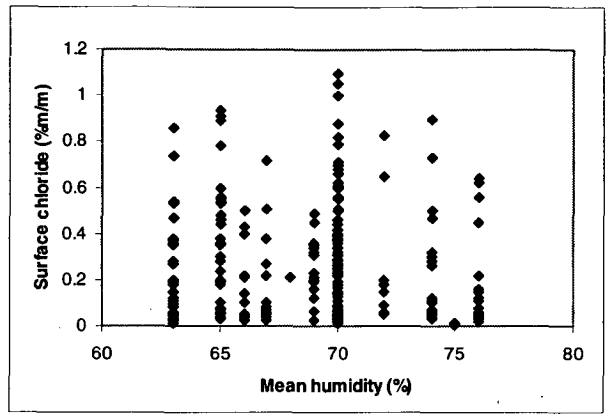

Figure A4.14 – Surface chloride concentration and humidity

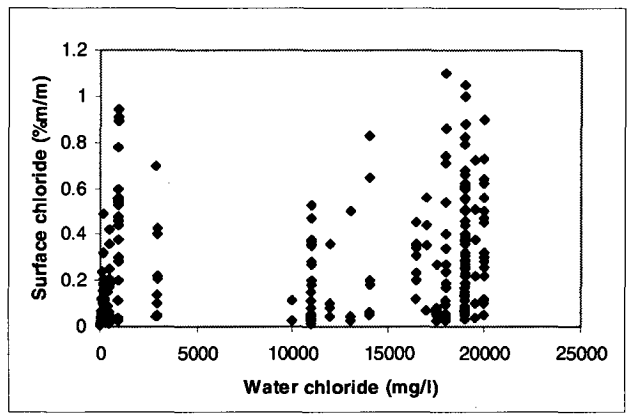

Figure A4.15 – Surface chloride concentration and water chloride

The scatterplots do not indicate any correlation between the apparent surface concentration of chlorides and the various factors.

4.2.2 CHLORIDE DIFFUSION COEFFICIENT

Scatterplots are again used to examine possible correlations between the effective chloride diffusion coefficient and a range of factors.

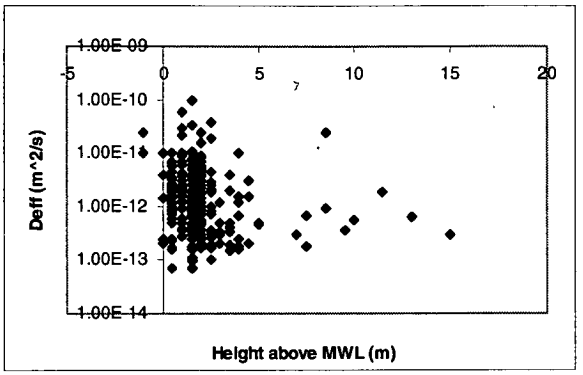

Figure A4.16 – Chloride diffusion coefficient and height above MWL

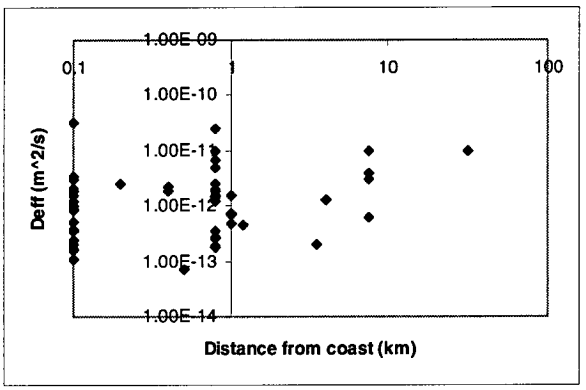

Figure A4.17 – Chloride diffusion coefficient and distance from coast

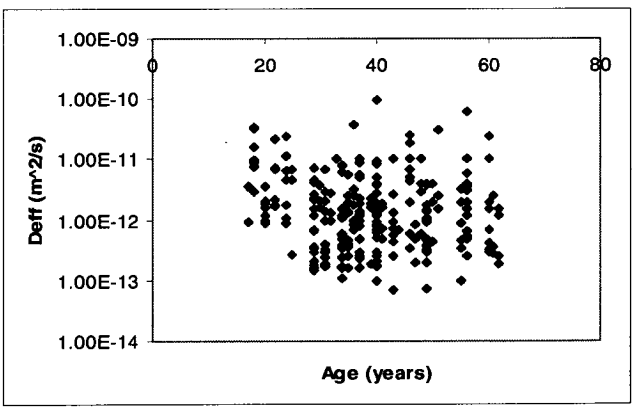

Figure A4.18 – Chloride diffusion coefficient and age

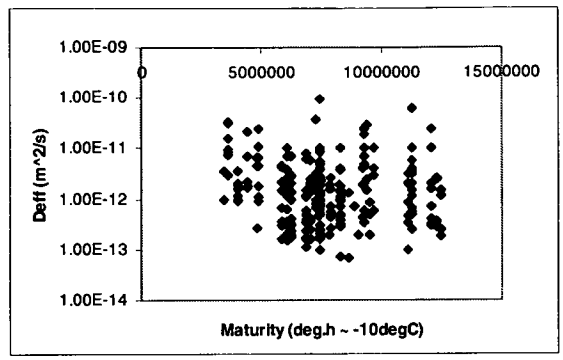

Figure A4.19 – Chloride diffusion coefficient and maturity

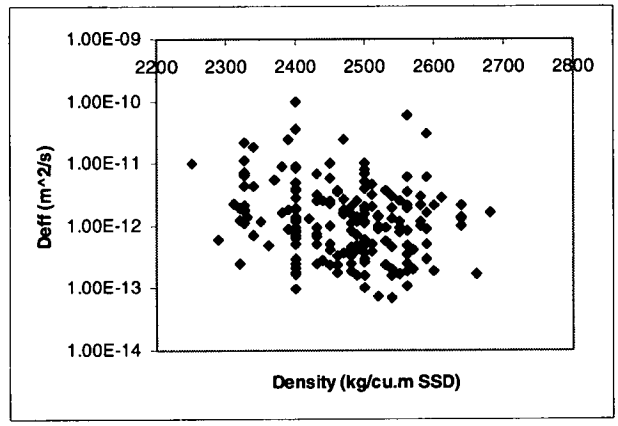

Figure A4.20 – Chloride diffusion coefficient and density

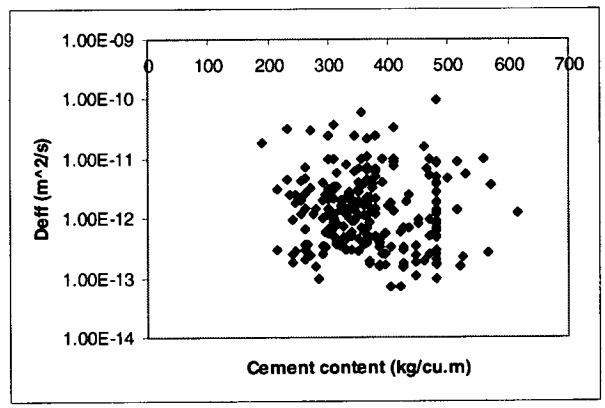

Figure A4.21 – Chloride diffusion coefficient and cement content

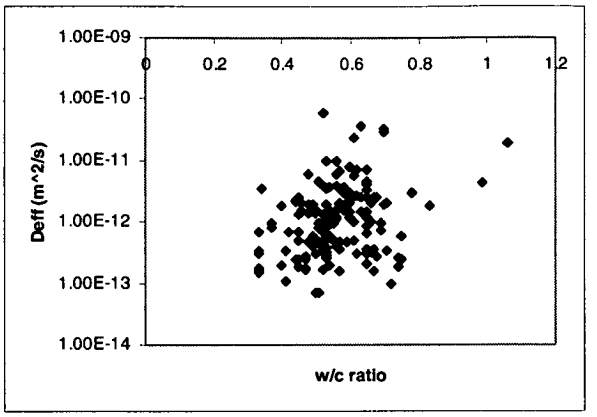

Figure A4.22 – Chloride diffusion coefficient and water cement ratio

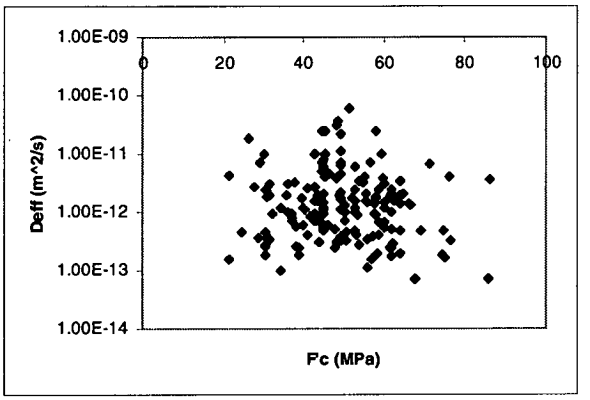

Figure A4.23 – Chloride diffusion coefficient and concrete strength

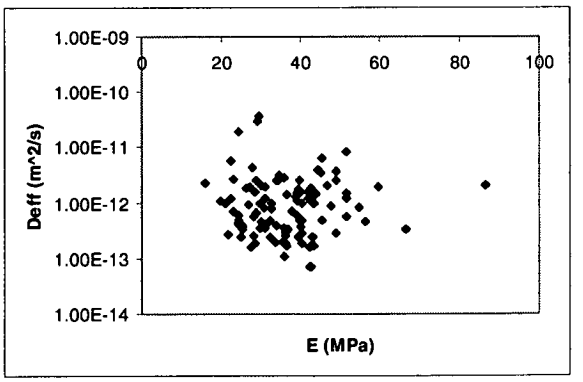

Figure A4.24 – Chloride diffusion coefficient and Youngs modulus

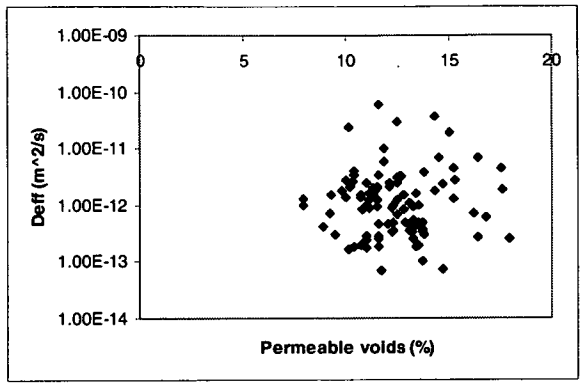

Figure A4.25 – Chloride diffusion coefficient and permeable voids

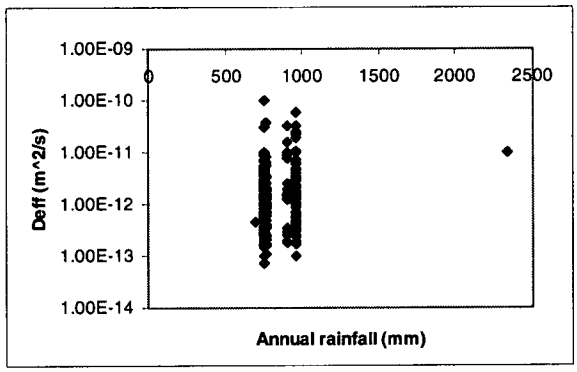

Figure A4.26 – Chloride diffusion coefficient and rainfall

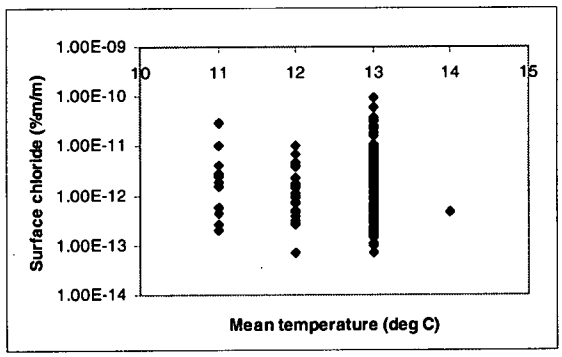

Figure A4.27 – Chloride diffusion coefficient and temperature

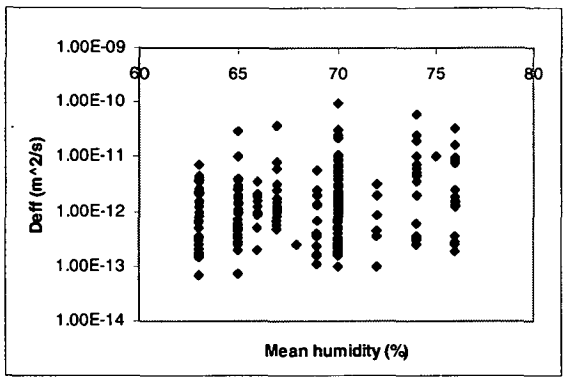

Figure A4.28 – Chloride diffusion coefficient and humidity

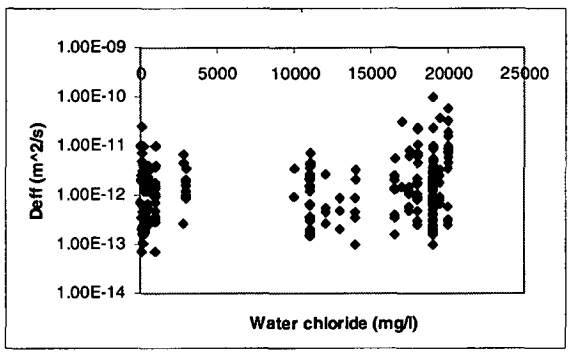

Figure A4.29 – Chloride diffusion coefficient and water chloride concentration

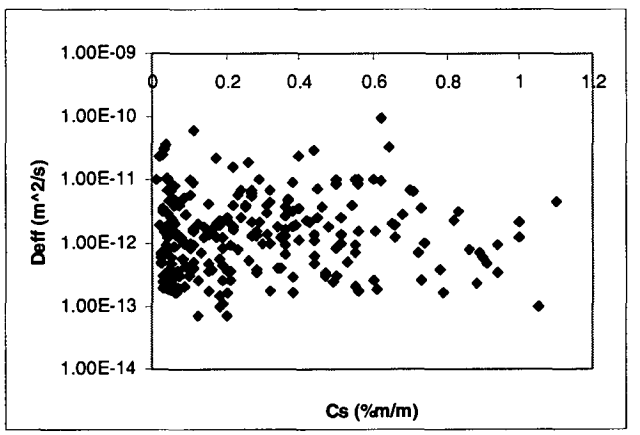

Figure A4.30 – Chloride diffusion coefficient and surface chloride concentration

As with the apparent surface chloride concentration, there is no apparent relationship between the effective diffusion coefficient and a range of factors.

4.3 PARAMETERS FOR SERVICE LIFE MODELLING

4.3.1 SURFACE CHLORIDE CONCENTRATION

The following figures examine probability distributions of surface chloride concentration data involving all cores and with subsets of the data where results from cores with irregular chloride profiles have been omitted and with limited values of height above mean water level and distance from salt water.

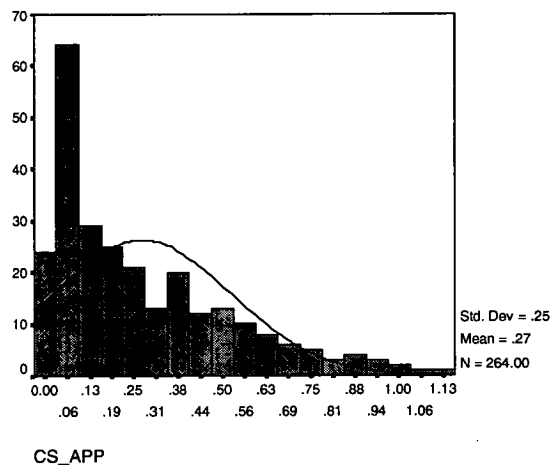

Figure A4.31 –Surface chloride concentrations, all cores

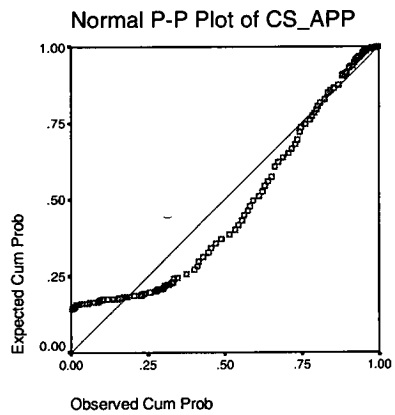

Figure A4.32 –Surface chloride concentrations, all cores

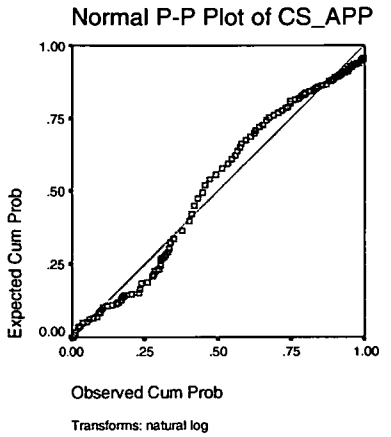

Figure A4.33 –Surface chloride concentrations, all cores, ln transformation

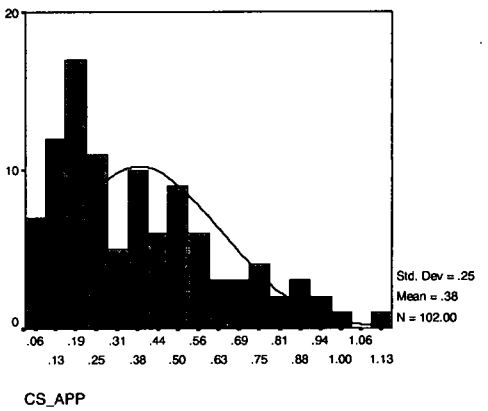

Figure A4.34 –Surface chloride concentrations, limited data set (irregular chloride profiles omitted)

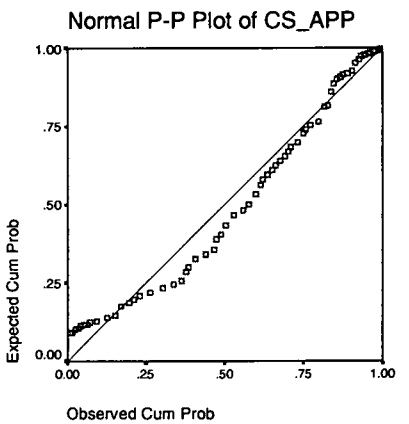

Figure A4.35 –Surface chloride concentrations, limited data set

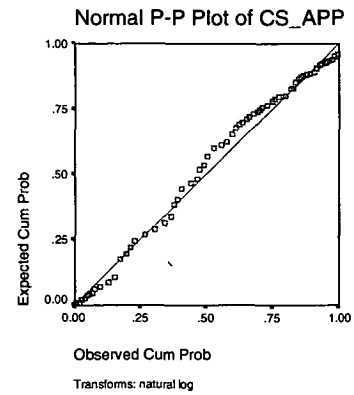

Figure A4.36 –Surface chloride concentrations, limited data set, ln transformation

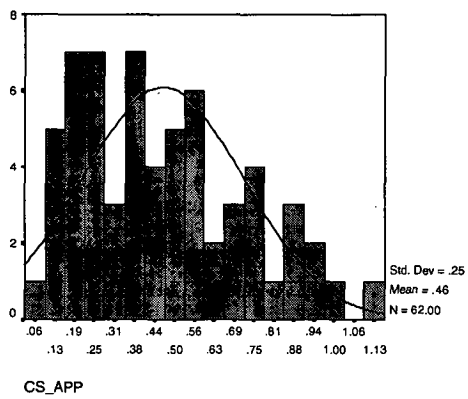

Figure A4.37 –Surface chloride concentrations, distance from coast 0km, height ≤ 2m

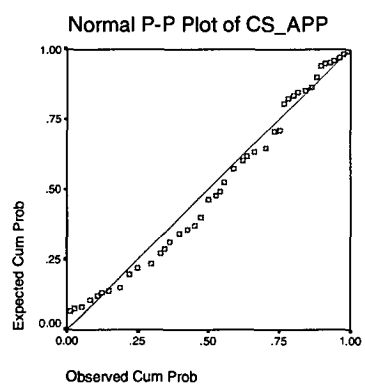

Figure A4.38 –Surface chloride concentrations, distance from coast 0km, height ≤ 2m

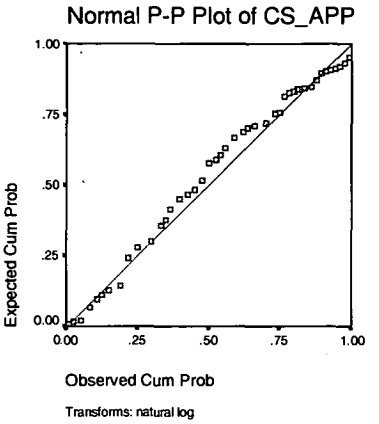

Figure A4.39 –Surface chloride concentrations, distance from coast 0km, height ≤ 2m, ln transformation

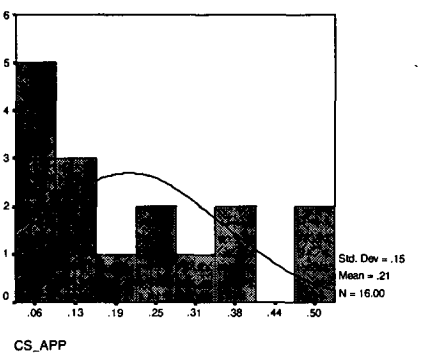

Figure A4.40 –Surface chloride concentrations, distance from coast 0km, 2m < height ≤ 4m

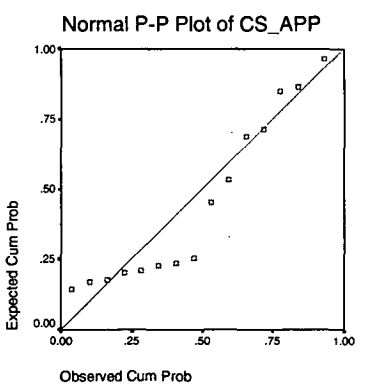

Figure A4.41 –Surface chloride concentrations, distance from coast 0km, 2m < height ≤ 4m

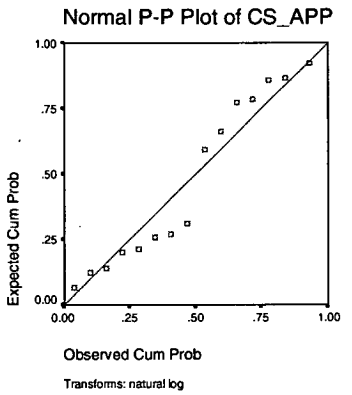

Figure A4.42 –Surface chloride concentrations, distance from coast 0km, 2m < height ≤ 4m, ln transformation

The histogram and normal probability plots for zero distance from the coast and heights greater than 4m are not plotted because of the small number of samples.

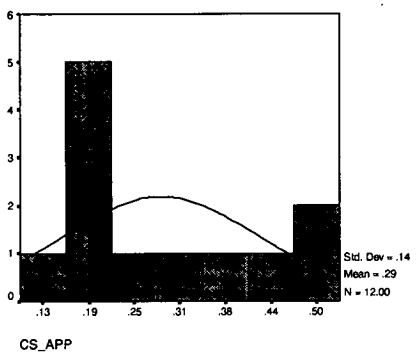

Figure A4.43 –Surface chloride concentrations, distance from coast 0.1 km

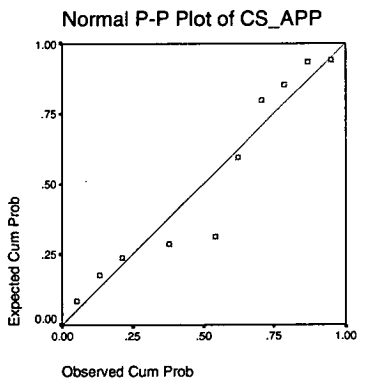

Figure A4.44 –Surface chloride concentrations, distance from coast 0.1 km

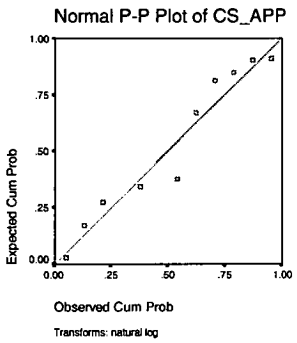

Figure A4.45 –Surface chloride concentrations, distance from coast 0.1 km, ln transformation

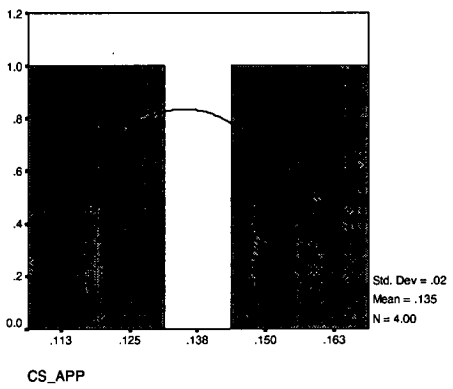

Figure A4.46 –Surface chloride concentrations, distance from coast 0.5 km

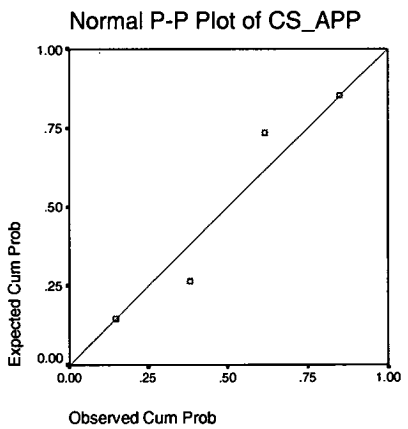

Figure A4.47 –Surface chloride concentrations, distance from coast 0.5 km

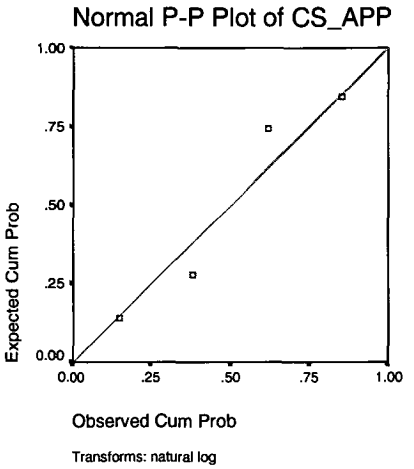

Figure A4.48 –Surface chloride concentrations, distance from coast 0.5 km, ln transformation

4.3.2 DIFFUSION COEFFICIENT

The following figures examine probability distributions of subsets of the data for chloride diffusion coefficient.

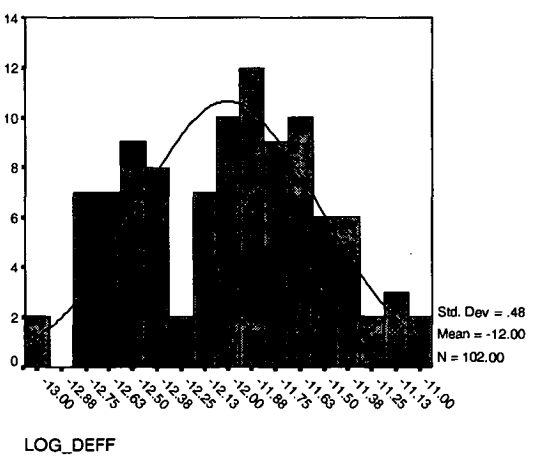

Figure A4.49 - Distribution of diffusion coefficients, limited set (log_{10} transform)

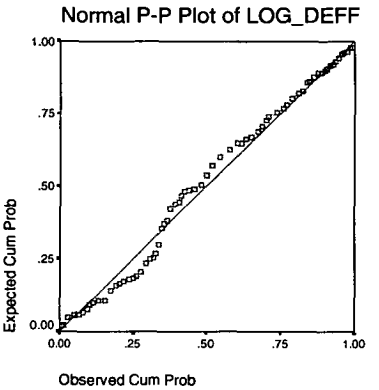

Figure A4.50 - Normal probability plot of diffusion coefficients, limited set (log_{10} transform)

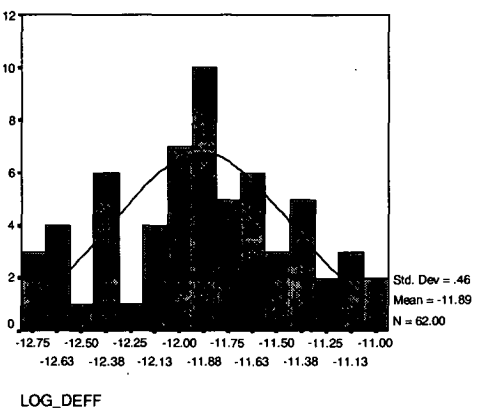

Figure A4.51 - Distribution of diffusion coefficients, limited set, distance from coast 0km, height ≤ 2m (log_{10} transform)

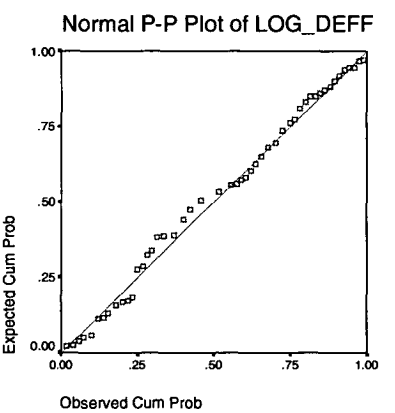

Figure A4.52 - Normal probability plot of diffusion coefficients, limited set, distance from coast 0km, height ≤ 2m (log_{10} transform)

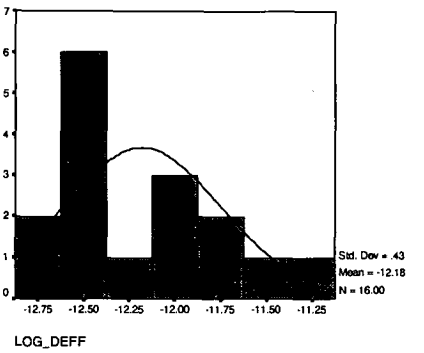

Figure A4.53 - Distribution of diffusion coefficients, limited set, distance from coast 0km, 2m<height≤ 4m (log_{10} transform)

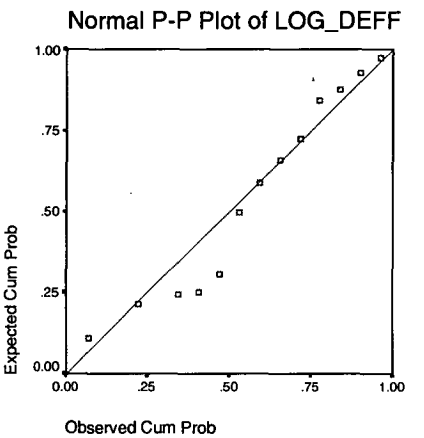

Figure A4.54 - Normal probability plot of diffusion coefficients, limited set, distance from coast 0km, 2m<height≤ 4m (log_{10} transform)

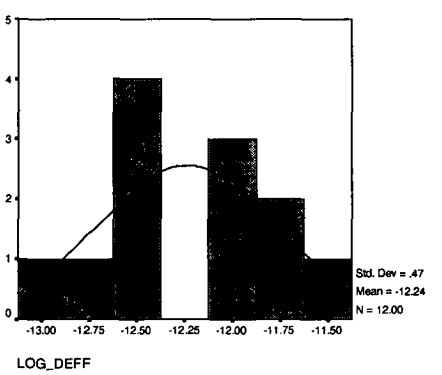

Figure A4.55 - Distribution of diffusion coefficients, limited set, distance from coast 0.1km, (log_{10} transform)

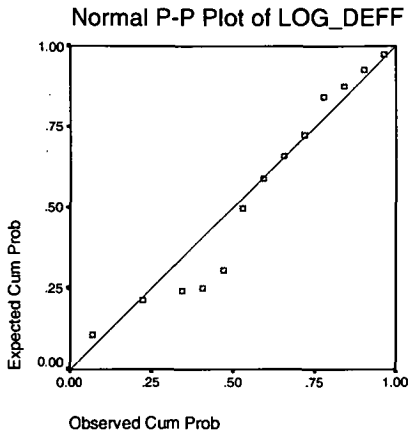

Figure A4.56 - Normal probability plot of diffusion coefficients, limited set, distance from coast 0.1km (log_{10} transform)

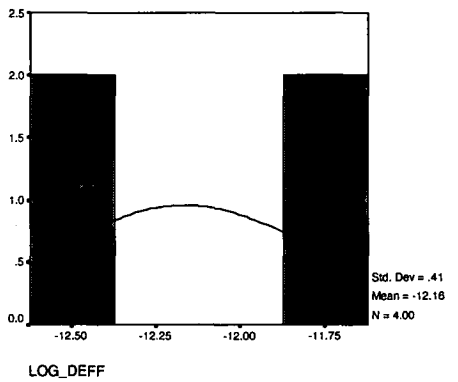

Figure A4.57 - Distribution of diffusion coefficients, limited set, distance from coast >0.5km, (log_{10} transform)

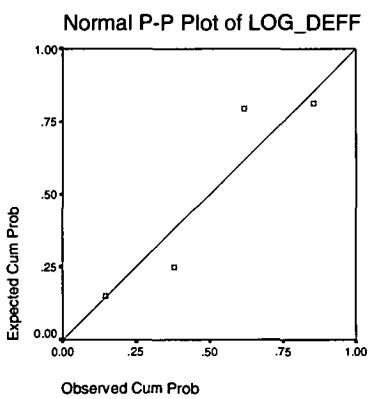

Figure A4.58 - Normal probability plot of diffusion coefficients, limited set, distance from coast >0.5km (log_{10} transform)

5 CARBONATION

5.1 PRELIMINARY ANALYSIS

Figures A5.1 to A5.21 are scatterplots used for a preliminary assessment of possible correlations between carbonation and a range of concrete properties and environmental factors.

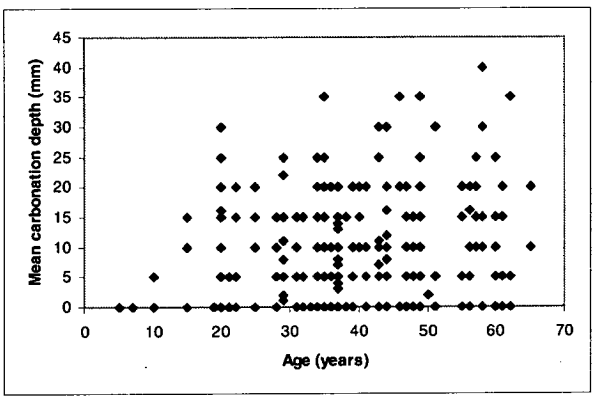

Figure A5.1 – Mean carbonation depth ~ age

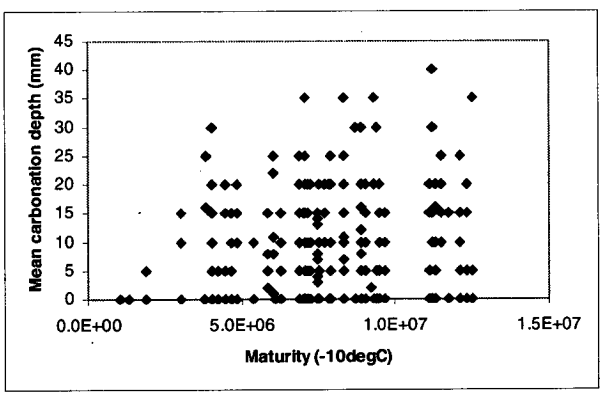

Figure A5.2 – Mean carbonation depth ~ maturity (-10°C datum)

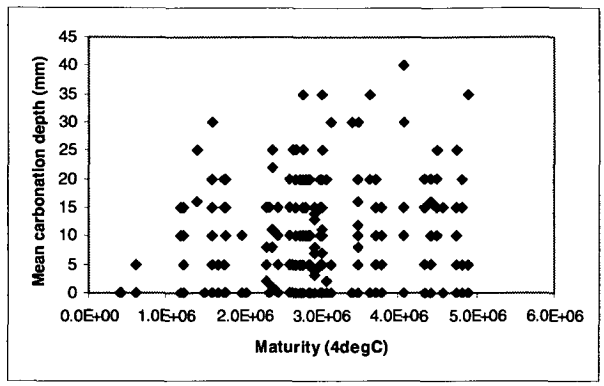

Figure A5.3 – Mean carbonation depth ~ maturity (4°C datum)

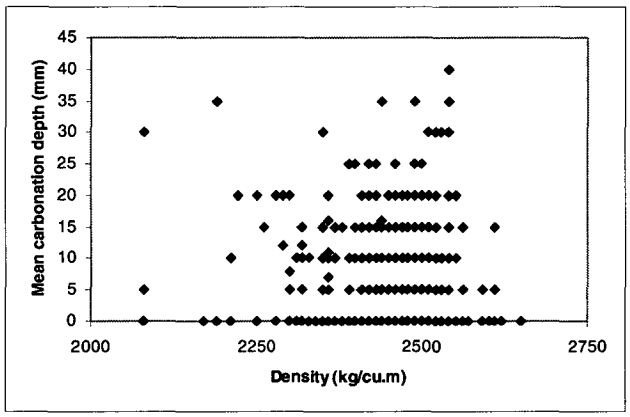

Figure A5.4 – Mean carbonation depth ~ density

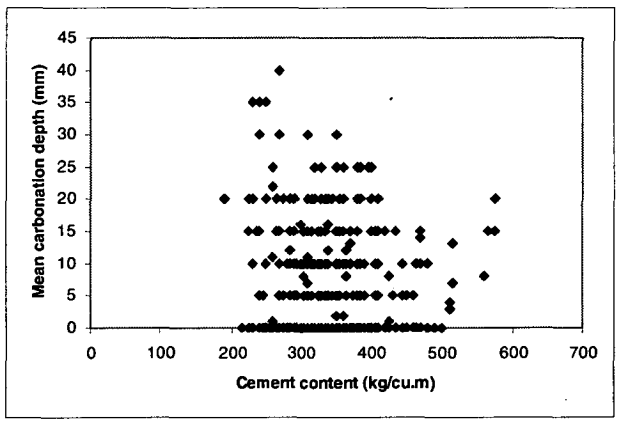

Figure A5.5 – Mean carbonation depth ~ cement content

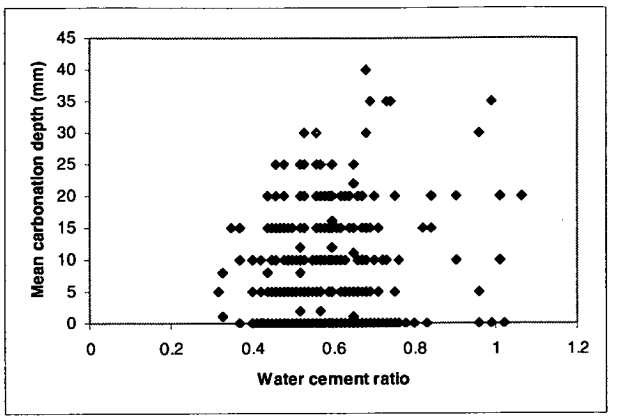

Figure A5.6 – Mean carbonation depth ~ water cement ratio

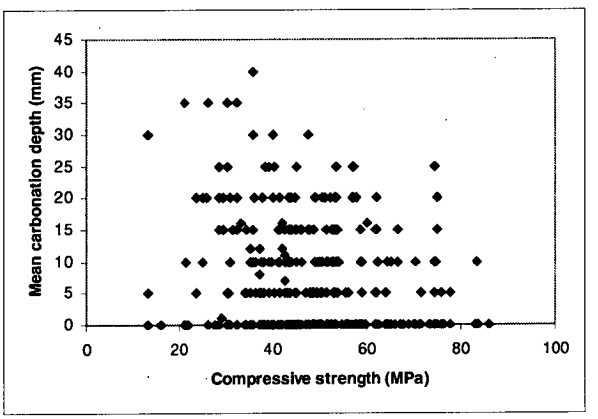

Figure A5.7 – Mean carbonation depth ~ compressive strength

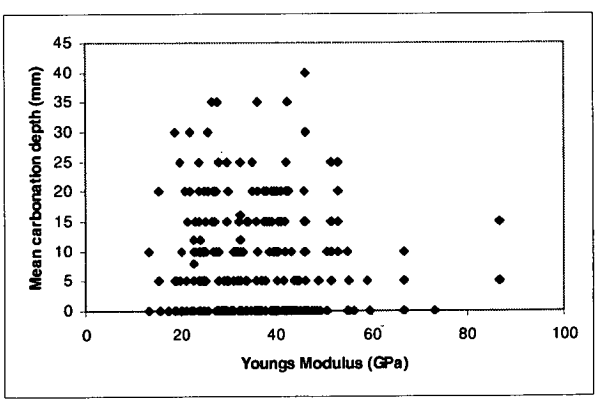

Figure A5.8 – Mean carbonation depth ~ Young's modulus

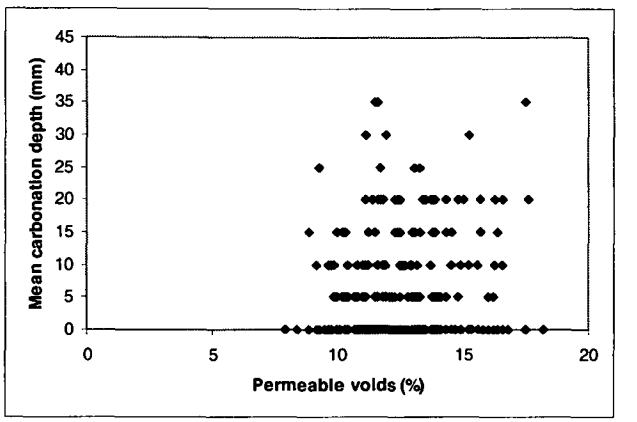

Figure A5.9 – Mean carbonation depth ~ volume of permeable voids

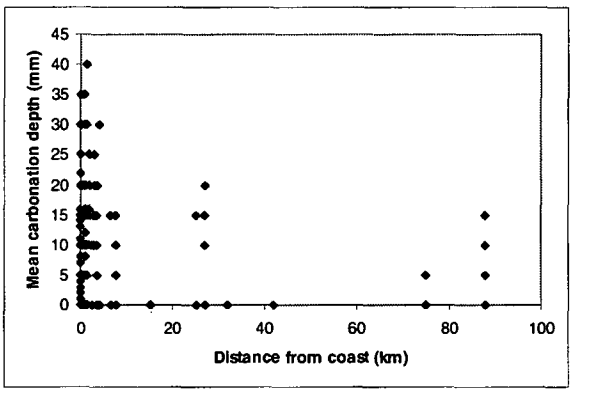

Figure A5.10 – Mean carbonation depth ~ distance from coast

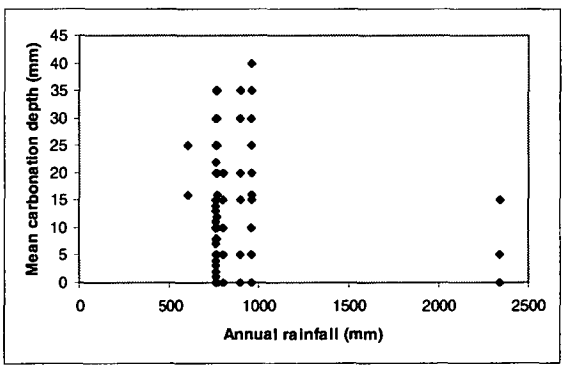

Figure A5.11 – Mean carbonation depth ~ annual rainfall

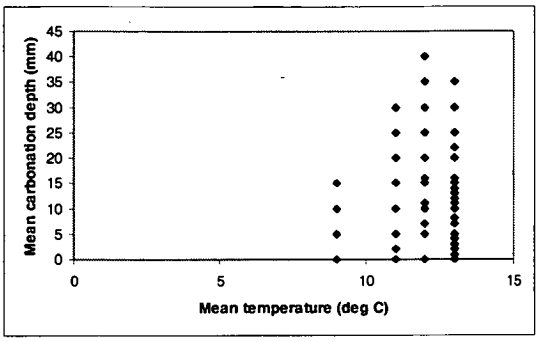

Figure A5.12 – Mean carbonation depth ~ mean temperature

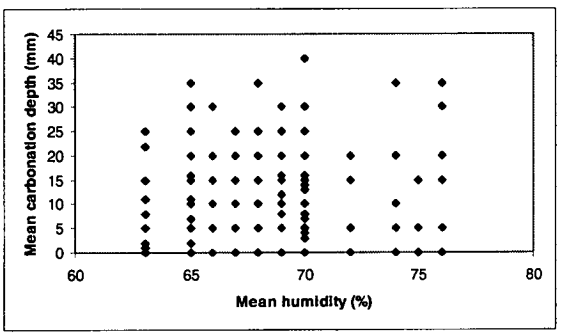

Figure A5.13 – Mean carbonation depth ~ mean humidity

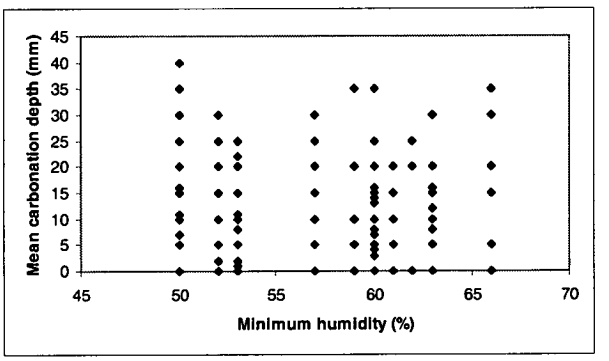

Figure A5.14 – Mean carbonation depth ~ minimum humidity

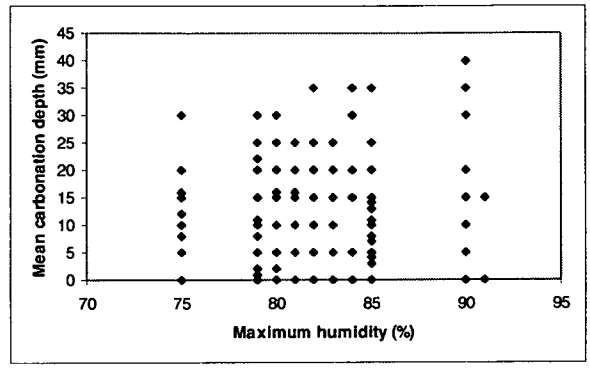

Figure A5.16 – Mean carbonation depth ~ maximum humidity

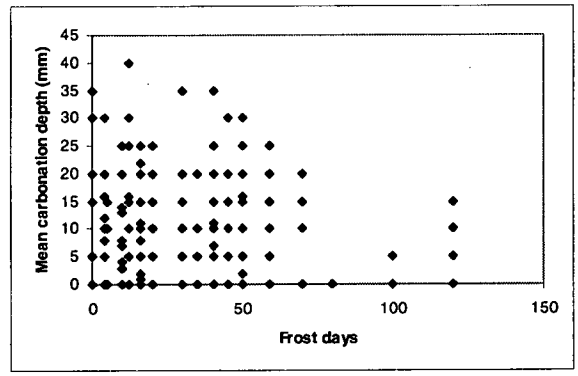

Figure A5.17 – Mean carbonation depth ~ frost days

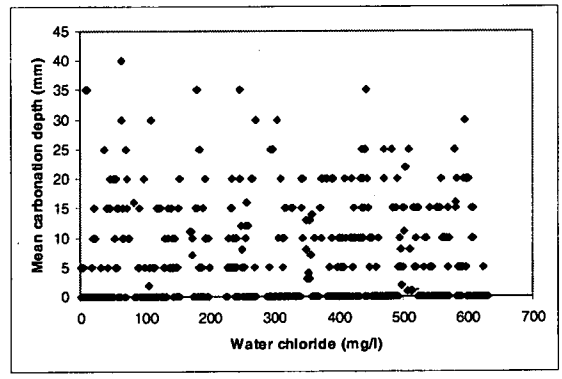

Figure A5.18 – Mean carbonation depth ~ water chloride concentration

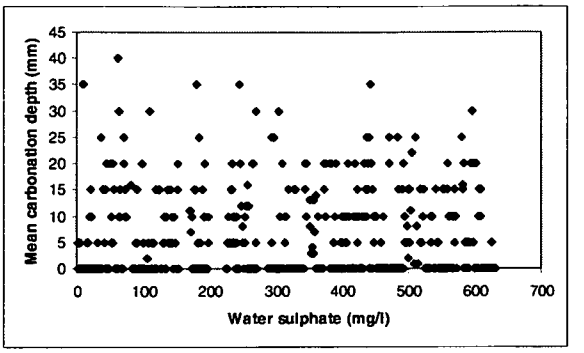

Figure A5.19 – Mean carbonation depth ~ water sulphate concentration

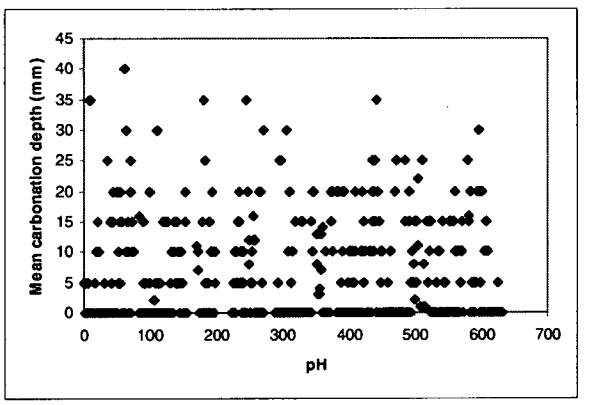

Figure A5.20 – Mean carbonation depth ~ water pH

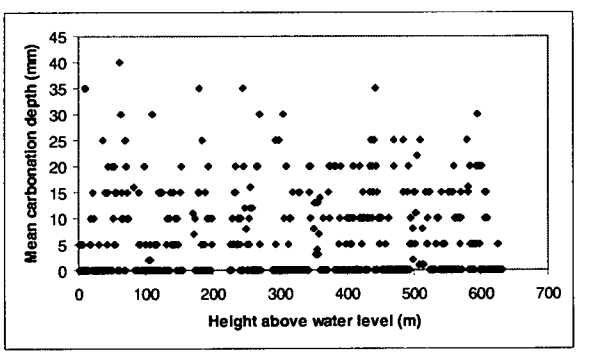

Figure A5.21 – Mean carbonation depth ~ height above MWL

The scatterplots do not indicate any correlation between carbonation depth and concrete properties or environmental factors. The lack of correlation was confirmed through a factor analysis using the SPSS statistical package.

The next series of histograms and normal probability plots examine distributions of mean carbonation depth with concrete age where there is a measurable depth of carbonation. Ages are expressed in years.

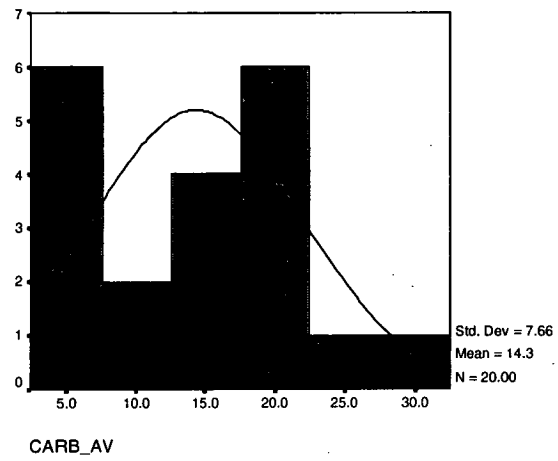

Figure A5.22– Carbonation depth, 15≤age<24

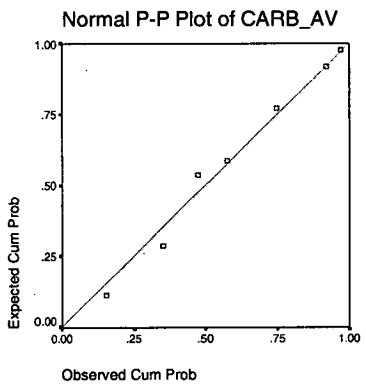

Figure A5.23 – Carbonation depth, 15≤age<24

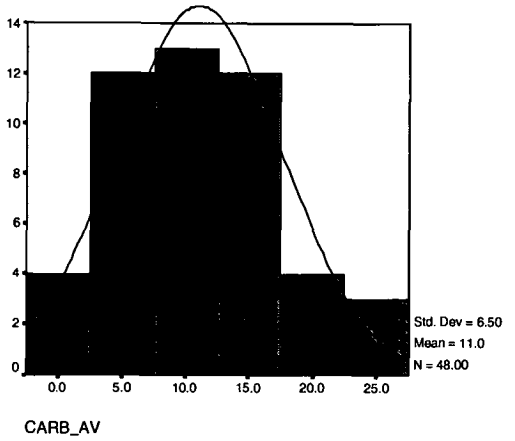

Figure A5.24 – Carbonation depth, 25≤age<34

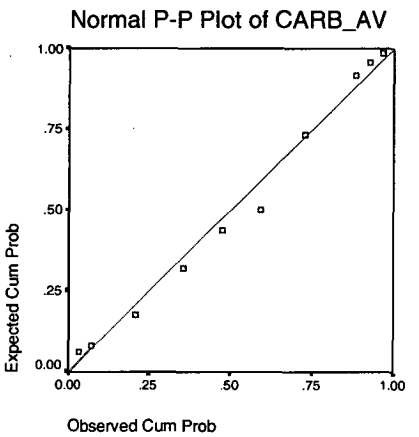

Figure A5.25 – Carbonation depth, 25≤age<34

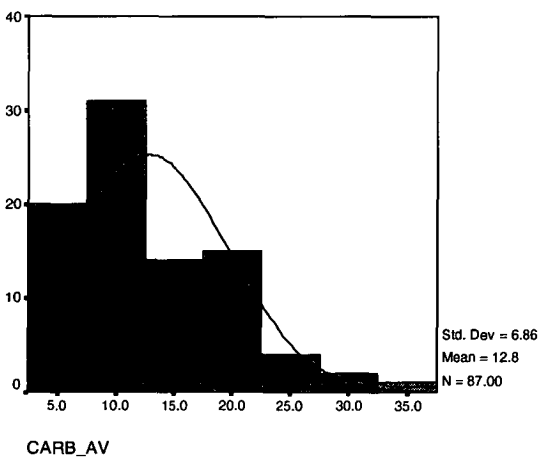

Figure A5.26 – Carbonation depth, 35≤age<44

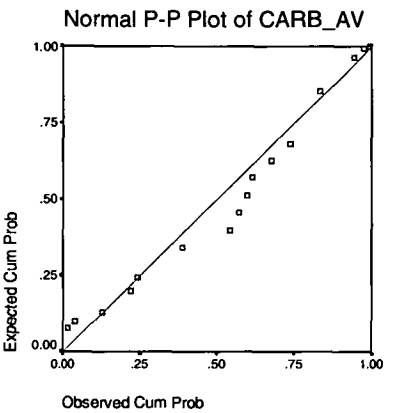

Figure A5.27 – Carbonation depth, 35≤age<44

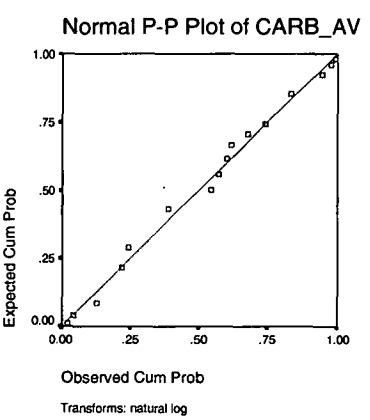

Figure A5.28 – Carbonation depth, 35≤age<44

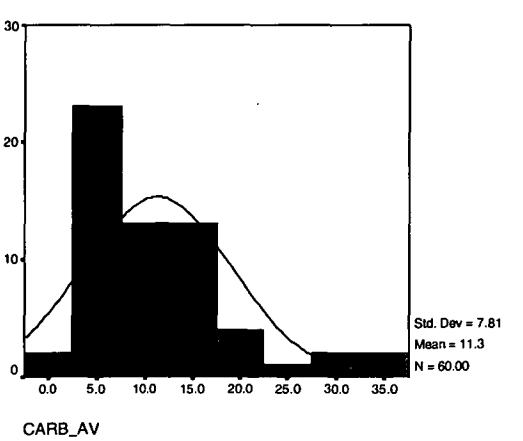

Figure A5.29 – Carbonation depth, 45≤age<54

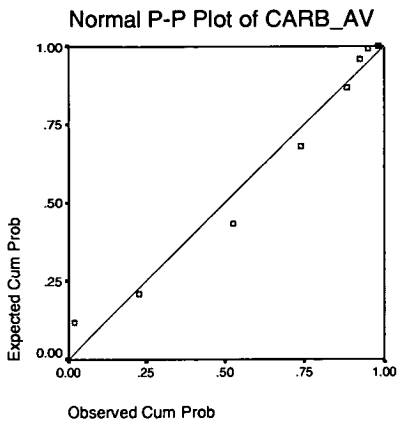

Figure A5.30 – Carbonation depth, 45≤age<54

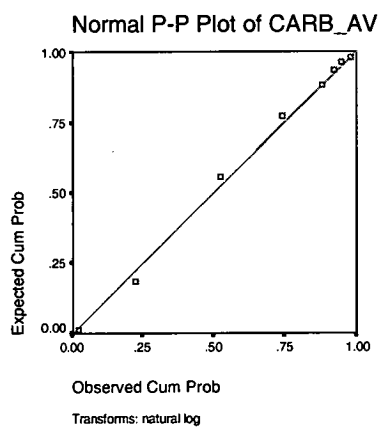

Figure A5.31 – Carbonation depth, 45≤age<54

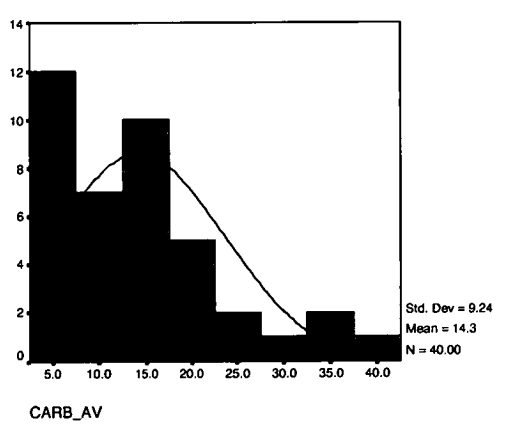

Figure A5.32 – Carbonation depth, 55≤age<64

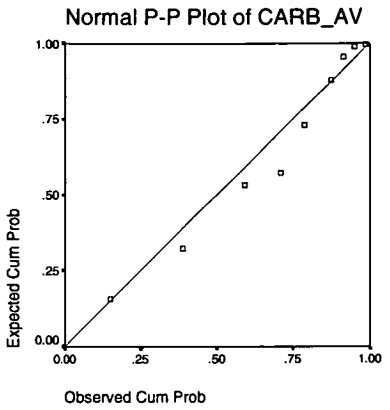

Figure A5.33 – Carbonation depth, 55≤age<64

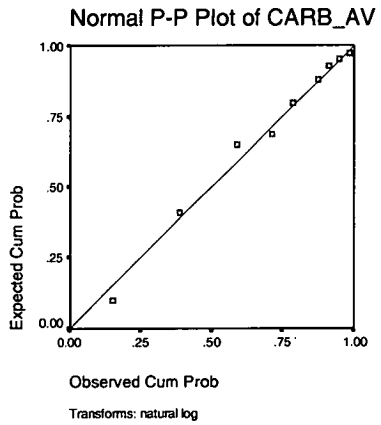

Figure A5.34 – Carbonation depth, 55≤age<64

The plots indicate that carbonation depths for the various age groups can reasonably be described by a normal distribution, with results summarised in Table A5.1.

Age	Carbonation depth			No. of cores
	Mean (mm)	Standard deviation (mm)	COV (%)	
15 to 24	14.3	7.66	53.6	20
25 to 34	11.0	6.60	60.0	48
35 to 44	12.8	6.86	53.6	87
45 to 54	11.3	7.81	69.1	60
55 to 64	14.3	9.24	64.6	40

Table A5.1 – Carbonation depths at various ages

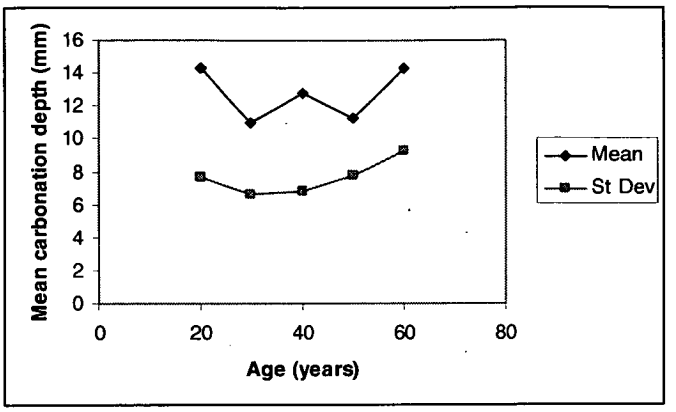

Figure A5.35 – Carbonation depths at various ages

Figure A5.35 does not indicate a trend of increasing depth with age as found by other researchers. This may be attributable to the relatively small number of samples, the variability in carbonation and the range of environments. In particular, investigations were focussed on bridges with chloride induced corrosion damage meaning that relative humidities may have been higher than for bridges in which carbonation damage was the primary mechanism.

6 COVER TO REINFORCEMENT

6.1 SURVEYED STRUCTURES

Table A6.1 provides details and descriptions of the structures that were surveyed for measurements of cover to reinforcement. Locations of surveyed bridges are shown in Figure 8.12 in the thesis.

Bridge		YOC	Length (m)	Width (m)	Spans	Description
1	North West Bay River	1931	24.4	6.1	2	Reinforced concrete T-beam
44	Faggs Gully Creek	1932/51/	11.4	4.7	2	Insitu and precast culvert
51	Vincents Rivulet	1933	10.4	3.7	1	Composite steel girder
65	Leven River	1934	130.2	9.5	7	Steel girder
284	Camp Creek	1934	4.1	12.8	1	Insitu culvert
279	Porky Creek	1935	10.1	6.1	1	Steel girder
953	Symons Creek	1959	9.7	8.5	1	Reinforced concrete T-beam
1220	Browns River	1937	31.1	7.9	3	Reinforced concrete T-beam
853	Doctors Creek	1938	29.5	2.5	1	Insitu culvert
1465	Peggs Creek	1938	10.7	7.7	3	Reinforced concrete T-beam
1185	Emu River	1939	43	14.8	3	Reinforced concrete arch
1466	Margate Rivulet	1940	17.4	10.4	3	Reinforced concrete T-beam
219	Detention River	1940	69.5	7.6	5	Reinforced concrete T-beam
2326	Mountain Creek	1942	5.2	8.4	1	Reinforced concrete slab
2039	Higgins Creek	1944	4.6	7.9	1	Reinforced concrete slab
298	Surges Creek	1944	21.3	7.7	3	Reinforced concrete T-beam
2796	Rileys Creek	1945	18.6	7.7	3	Reinforced concrete slab
2795	Carlton Rivulet	1945	29.6	7.8	3	Reinforced concrete slab
3178	Carlton Rivulet	1946	21.6	7.5	5	Insitu culvert
3194	Scopus Creek	1947	9.5	5.5	1	Reinforced concrete T-beam
15	Bridgewater	1947	338	15.5	14	Steel truss and girder
1099	Stanley Dock	1949/64	-	-	-	Concrete wharf
163	Maclaines Creek	1948	262	8.4	21	Reinforced concrete T-beam
802	Caroline Creek	1949	11	7.7	1	Reinforced concrete slab
917	Supply River	1950	4.3	7.3	1	Reinforced concrete T-beam
2889	Flights Creek	1951	17.4	7.6	1	Reinforced concrete T-beam
796	King Island Main Road	1953	7.4	1.8	1	Insitu culvert
3782	East Arm	1955	34.6	2.4	1	Insitu culvert
165	Argent Creek	1956	9.8	7.9	1	Reinforced concrete slab
119	Ralphs Bay Canal	1956	7.6	9.3	1	Reinforced concrete slab
3786	Egg Island Creek	1956	10.3	9.5	3	Reinforced concrete slab
579	Sorell Causeway	1957	19.7	13.5	5	Insitu culvert
284	Camp Creek	1957	4.1	12.8	1	Insitu culvert
911	Cormiston Creek	1957	9.1	12.2	1	Reinforced concrete slab
864	Ringarooma River	1957	35.5	7.9	3	Reinforced concrete T-beam
147	Wrinklers Lagoon	1958	19.4	7.9	2	Reinforced concrete slab
877	Golden Fleece	1958	58.9	9.9	6	Reinforced concrete slab
1805	Princess River	1959	22	7.7	2	Reinforced concrete T-beam
884	Reedy Creek	1959	12.2	7.8	1	Reinforced concrete slab
914	Stoney Brook	1959	11.7	12.8	1	Reinforced concrete T-beam
1999	Mersey River	1960	59.7	9.8	7	Reinforced concrete slab
940	Denison River	1960	34.8	7.8	4	Reinforced concrete slab
4836	Hatfield River	1962	30.2	7.9	3	Steel girder
4837	Fossey River	1962	26.5	7.9	3	Reinforced concrete slab
879	Boggy Creek	1961	13.5	8.3	1	Reinforced concrete slab
243	Cam River	1964	128.6	11	7	Prestressed girder
1678	Flinders Creek	1964	11.3	7.9	1	Insitu stiffened kerb slab
5128	Eddie Creek	1968	6.5	9	2	Insitu culvert
5258	Broken Leg Creek	1968	12.2	4	2	Precast crown unit culvert
2658	Newmans Creek	1969	19.5	7.9	2	Reinforced concrete U-beam

	Bridge	YOC	Length (m)	Width (m)	Spans	Description
187	Huon Highway Stock	1969	21	2.4	1	Precast crown unit culvert
1969	Hunterston Culvert	1969	9.1	8.5	1	Precast crown unit culvert
1979	Hunterston Culvert	1969	9.9	4.3	2	Precast crown unit culvert
5291	Lake Highway Culvert	1969	10	4	2	Precast crown unit culvert
5292	Lake Highway Culvert	1969	8.6	6.4	3	Precast crown unit culvert
5293	Lake Highway Culvert	1969	8.6	6.4	3	Precast crown unit culvert
5330	Tacky Creek	1970	16	6.9	2	Insitu culvert
225	Mersey River	1971	185.9	12.2	5	Steel girder
7	Mersey River	1972	144.3	8.6	6	Prestressed concrete I-beam
596	Cascade River	1972	31.6	8.5	2	Prestressed girder
1696	Sandy Creek	1974	9.6	9	1	Reinforced concrete U-beam
2647	Parsons Bay Creek	1974	19	9.8	2	Reinforced concrete U-beam
5067	Freestone Point Road	1975	8.5	5.1	2	Precast crown unit culvert
169	Kelvedon Creek	1976	39.1	8.6	3	Prestressed concrete girder
521	Taranna Creek	1976	12.6	9	2	Reinforced concrete U-beam
5602	Risdon Cove Culvert	1976	13.5	7.9	3	Precast crown unit culvert
5646	Little Quoin Creek Culvert	1977	22	5.2	1	Precast crown unit culvert
868	North George River	1978	37.7	9.8	3	Prestressed plank
5647	Oakmore Stock Underpass	1978	17.1	5.4	1	Precast crown unit culvert
5631	Lovett Street	1979	52.3	15.8	3	Prestressed girder
5655	Midland Highway Stock	1979	22.1	1.8	1	Precast crown unit culvert
5666	Midland Highway Stock	1980	18.4	2.8	1	Precast crown unit culvert
5683	Arthur Highway Culvert	1980	25.2	5.0	2	Precast crown unit culvert
5698	Round Hill	1981	45.0	-	-	Cantilever retaining wall
323	Brandum Creek	1982	13	9	3	Insitu culvert
1301	Wilcox Creek Culvert	1982	13.3	8	2	Precast crown unit culvert
1944	Mountain River Bridge	1982	46.1	10.0	3	Prestressed girder
2777	Cusicks Creek Culvert	1982	9.9	4.3	3	Precast crown unit culvert
5679	Lemon Springs Stock	1982	23.2	2.5	1	Precast crown unit culvert
560	Clyde River	1983	152.4	9.8	7	Prestressed girder
5672	Emu River	1983	65.4	12.2	3	Prestressed girder
5716	Boles Street Underpass	1983	18.5	2	1	Precast crown unit culvert
5717	Trafalgar Underpass	1983	14	3	1	Precast crown unit culvert
5718	Weedings Underpass	1983	17	2	1	Precast crown unit culvert
5726	Parremore Stock Underpass	1984	19.7	2.8	1	Precast crown unit culvert
2089	Manuka Creek	1984	18.0	8.0	2	U-beam
5691	Jinglers Creek	1985	48	6.9	2	Insitu culvert
755	Hortons Creek Culvert	1985	11	11.5	3	Precast crown unit culvert
173	Vale River	1986	23.3	10.4	3	Precast crown unit culvert
3771	Four Mile Creek Culvert	1986	19.2	6.1	2	Precast crown unit culvert
5767	Burnside Culvert	1986	16	2.7	1	Precast crown unit culvert
5806	Fairfield Stock Underpass	1986	14.8	2.7	1	Precast crown unit culvert
5775	Snug Creek	1987	12.8	10.2	1	Prestressed plank
866	North George River	1987	43.1	8.7	2	Prestressed girder
593	Lake Highway Culvert	1987	16.6	3	1	Precast crown unit culvert
2462	Serpentine Creek Flood	1987	7.2	4	1	Precast crown unit culvert
5820	Belmont Culvert	1987	17.2	5.4	2	Precast crown unit culvert
2870	Tatnells Creek Culvert	1988	18.4	4	1	Precast crown unit culvert
5694	Deloraine Rail	1989	10.2	12.2	1	Prestressed plank
5614	Roseneath Pedestrian	1990	16.7	2.9	1	Insitu culvert
5739	Cormiston Creek	1990	27.6	10.2	3	Prestressed plank
5832	Hatherley Stock Underpass	1990	18.4	3	1	Precast crown unit culvert
5822	Bracknell Main Road	1991	44.4	10.4		Prestressed plank
2533	Iris River Culvert	1991	18.4	11.4	3	Precast crown unit culvert
5809	Elsdon Stock Underpass	1991	14.8	5.4	2	Precast crown unit culvert
5817	Forton Stock Underpass	1991	19.7	2.7	1	Precast crown unit culvert
5834	Forton Stock Underpass	1991	20.9	2.7	1	Precast crown unit culvert
272	Prospect Interchange	1992	67.1	12.8	2	Prestressed concrete girder
1330	Runnymede Culvert	1992	4.9	8.6	2	Precast crown unit culvert
5567	Newnham Creek Culvert	1992	70.8	9.9	3	Precast crown unit culvert
190	Coal River Bridge	1993	100.3	9.0	7	Prestressed plank
547	Chiswick Stock Underpass	1993	3.0	14.6	1	Precast crown unit culvert
554	St Peters Stock Underpass	1993	3.0	14.6	1	Precast crown unit culvert
555	St Peters Stock Underpass	1993	3.0	14.6	1	Precast crown unit culvert
892	Fingal Rivulet	1993	11.7	12.2	3	Precast crown unit culvert
5864	Mersey River	1994	238	9.4	7	Prestressed concrete box
558	Tarleton Street	1994	30.9	12.0	3	Reinforced concrete slab

Bridge		YOC	Length (m)	Width (m)	Spans	Description
5873	Formby Road	1994	51.5	11.0	2	Prestressed concrete girder
5239	Devonport Rail Underpass	1994	170.7	19.2	9	Steel girder
100	Inverquharity Creek	1994	4.0	12.5	1	Precast crown unit culvert
536	Midland Highway Stock	1994	2.8	20.8	1	Precast crown unit culvert
550	Cameron Stock Underpass	1994	3.0	14.6	1	Precast crown unit culvert
556	Somercotes Stock	1994	2.7	16.0	1	Precast crown unit culvert
1237	Strathallen Rivulet Culvert	1994	10.7	7.3	2	Precast crown unit culvert
	Symmons Stock Underpass	1995	-	-	-	Precast culvert
2299	Strathallen Rivulet Culvert	1995	11.6	7.3	2	Precast crown unit culvert
5875	Best Stock Underpass	1995	4.0	20.9	1	Precast crown unit culvert
5877	Thompson Stock Underpass	1995	3.4	23.4	1	Precast crown unit culvert
5878	Bonnies Creek Culvert	1995	3.9	40.5	1	Precast crown unit culvert
5886	Beresfords Lane	1996	56.3	7.5	2	Prestressed concrete girder
5892	Pine Main Road	1996	24.4	22.6	1	Prestressed concrete trough
5880	Atkins Stock Underpass	1996	2.4	23.4	1	Precast crown unit culvert
5881	Hill Stock Underpass	1996	3.3	24.6	1	Precast crown unit culvert
5882	Faulkner Stock Underpass	1996	3.3	23.4	1	Precast crown unit culvert
5883	Gibsons Stock Underpass	1996	3.1	38.1	1	Precast crown unit culvert
5885	Violet Banks Rail Underpass	1996	7.9	17.2	1	Prestressed concrete girder
5895	Sulphur Creek	1997	2.4	93.6	1	Insitu culvert
5893	Gofton Stock Underpass	1997	3.7	30.0	1	Precast crown unit culvert

Table A6.1 – Surveyed bridges

6.2 PROBABILITY DISTRIBUTIONS

Probability distributions for subsets of the cover data are examined graphically in Figures A6.1 to A6.36 using boxplots, histograms and normal probability and quantile plots. The first group involves a nominal specified cover of 50mm. In the boxplot, the horizontal line within the box marks the median of the sample. The edges of the box mark the 25^{th} and 75^{th} percentiles. The length of the box is called the hspread, with the whiskers showing the range of values which fall within 1.5 hspreads of the edges of the box.

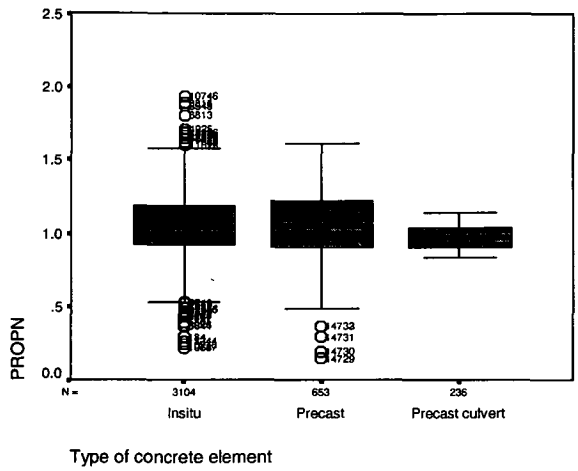

Figure A6.1 – Boxplot for 50mm nominal cover

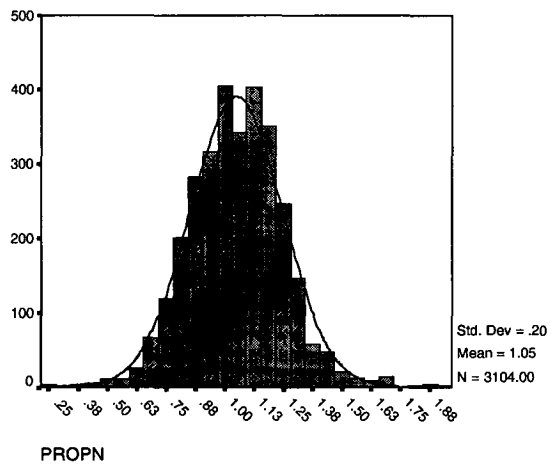

Figure A6.2 – Frequency distribution for 50mm nominal cover, insitu elements

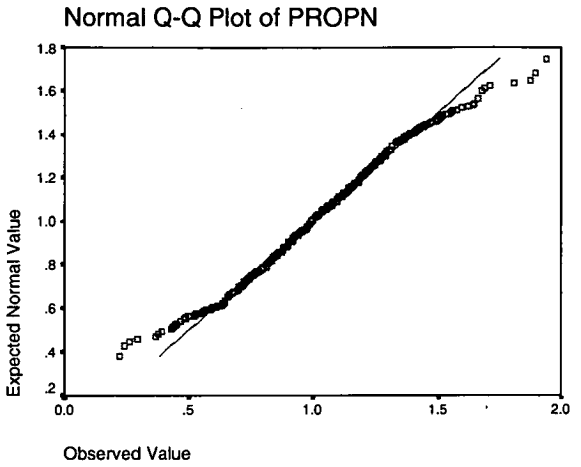

Figure A6.3 – Normal quantile plot for 50mm nominal cover, insitu elements

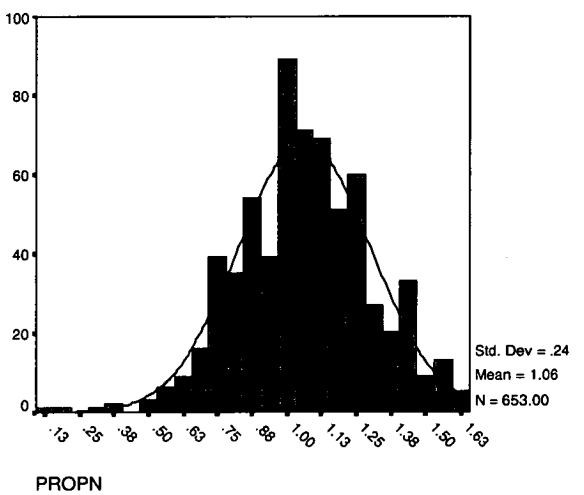

Figure A6.4 – Frequency distribution for 50mm nominal cover, precast elements

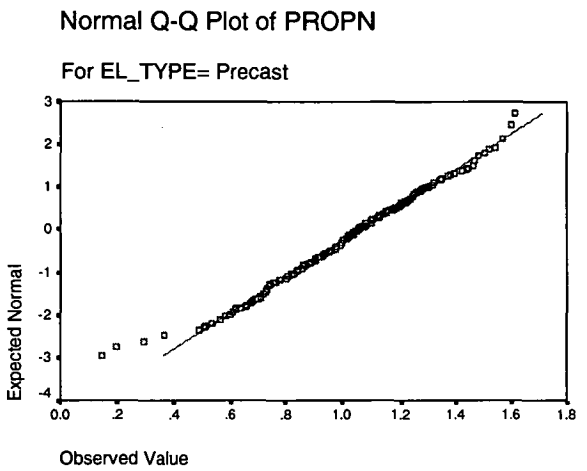

Figure A6.5 – Normal quantile plot for 50mm nominal cover, precast elements

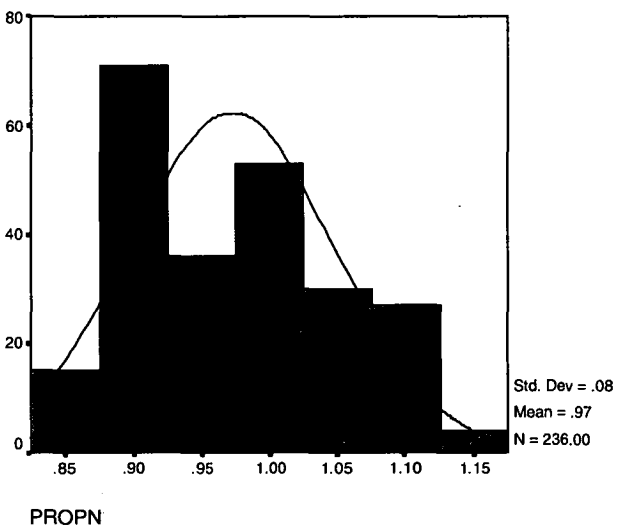

Figure A6.6 – Frequency distribution for 50mm nominal cover, precast culverts

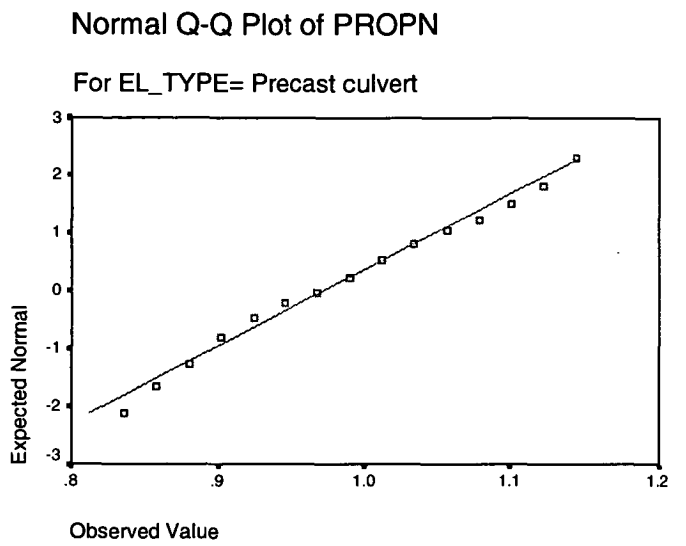

Figure A6.7 – Normal quantile plot for 50mm nominal cover, precast culverts

Figure A6.8 to A6.15 describe measurements with a nominal cover of 38mm. Figure 8.42 shows the age distribution of measurements within the range, and highlights the predominance of structures between 30 to 42 years old.

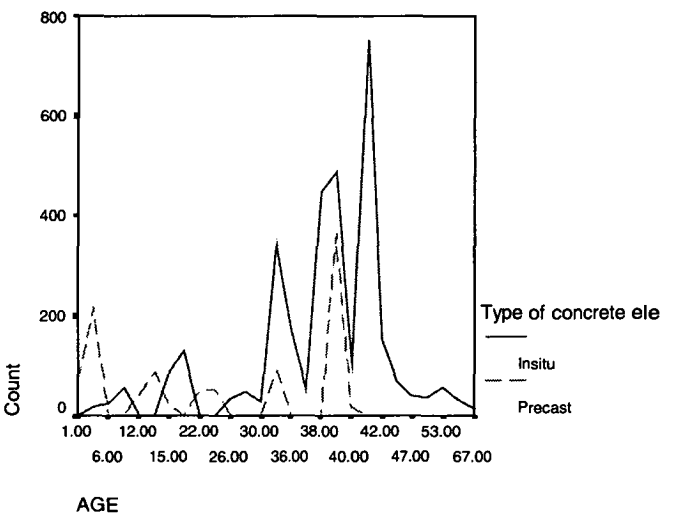

Figure A6.8 - Age distribution of measurements for 38mm nominal cover

The age distribution shows that few measurements for a nominal cover of 38mm fall outside ages of 30 to 47 years. Additionally, there are no measurements for precast culverts. Consequently, the analysis for 38mm nominal cover has used all measurements and not considered the effects of age.

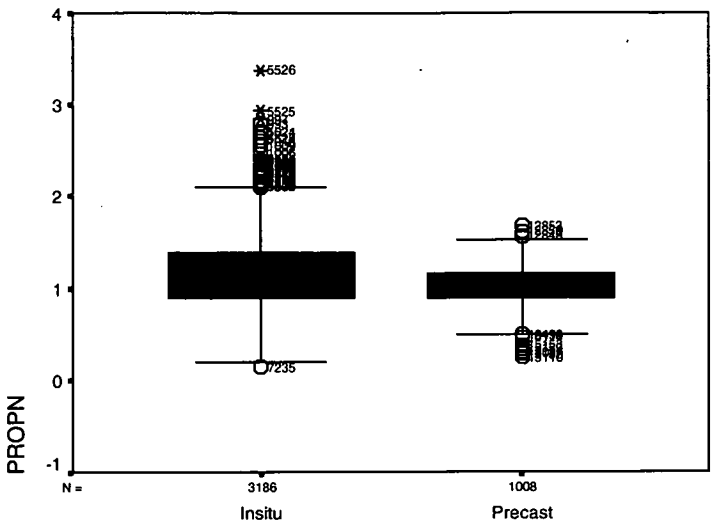

Figure A6.9 – Boxplot for 38mm nominal cover

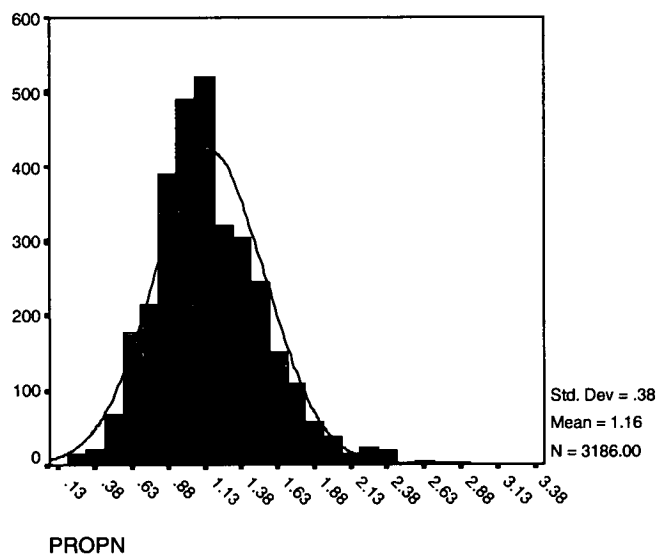

Figure A6.10 – Frequency distribution for 38 nominal cover, insitu elements

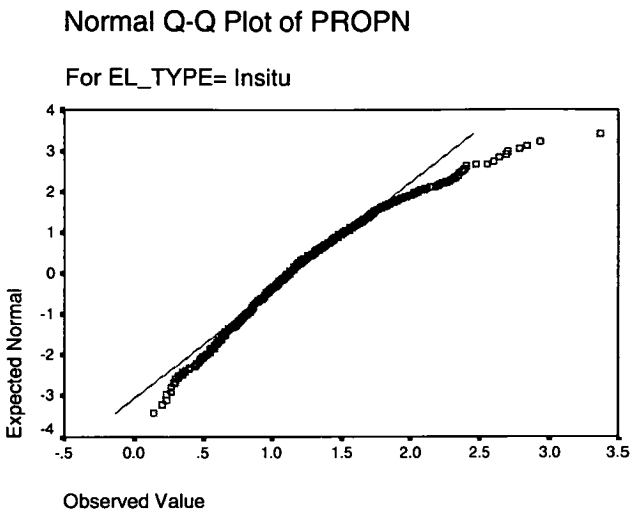

Figure A6.11 – Normal quantile plot for 38mm nominal cover, insitu elements

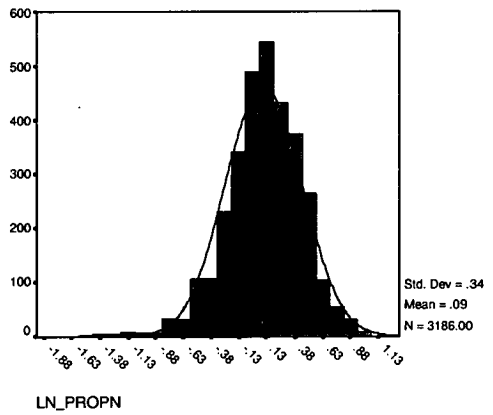

Figure A6.12 – Frequency distribution for 38mm nominal cover, insitu elements (ln transformation)

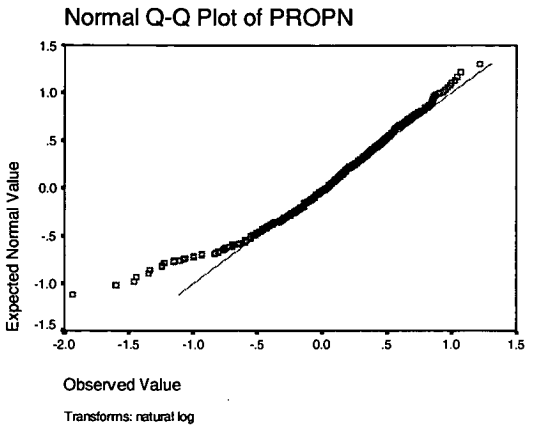

Figure A6.13 – Normal quantile plot for 38mm nominal cover, insitu elements (ln transformation)

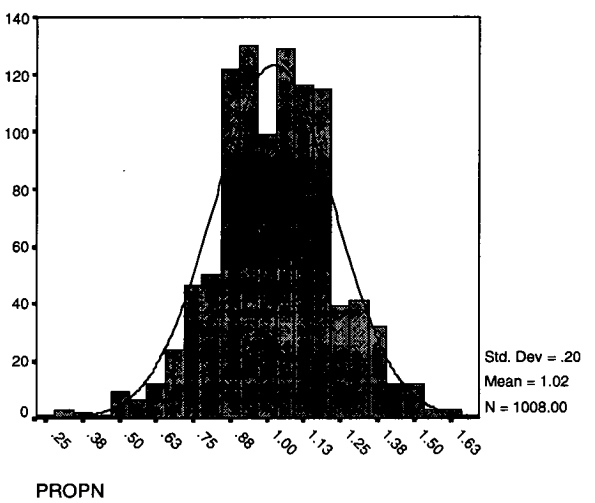

Figure A6.14 – Frequency distribution for 38 nominal cover, precast elements

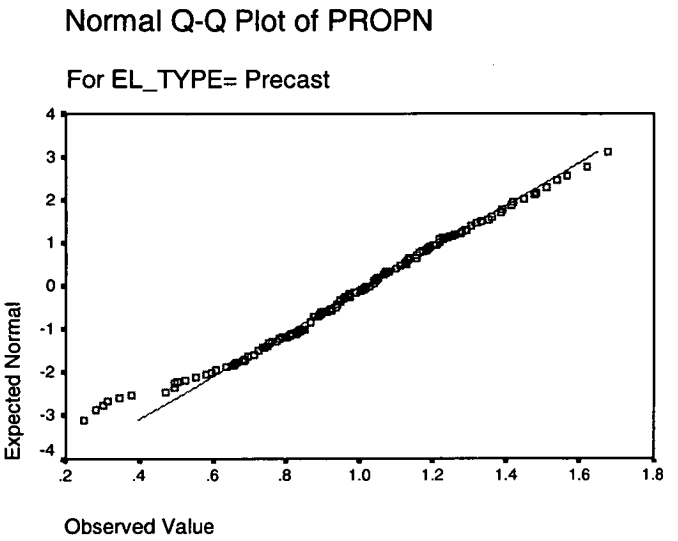

Figure A6.15 – Normal quantile plot for 38mm nominal cover, precast elements

Figures A6.16 to A6.29 describe distributions of measurements for a nominal cover of 25mm. The distribution is strongly influenced by the number of measurements for precast culvert crown units, with the majority having had a specified cover of 25mm over the approximately 30 years that they have been used by DIER. By comparison, the majority of insitu elements with specified nominal covers of 25mm are older than 30 years.

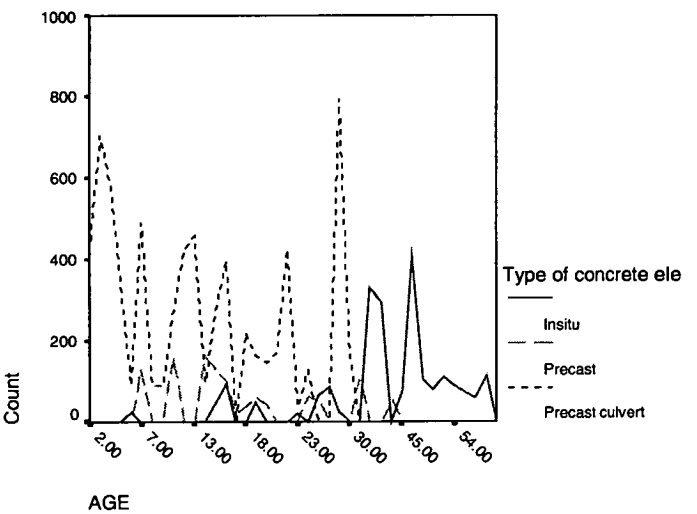

Figure A6.16 – Age distribution for 25 nominal cover

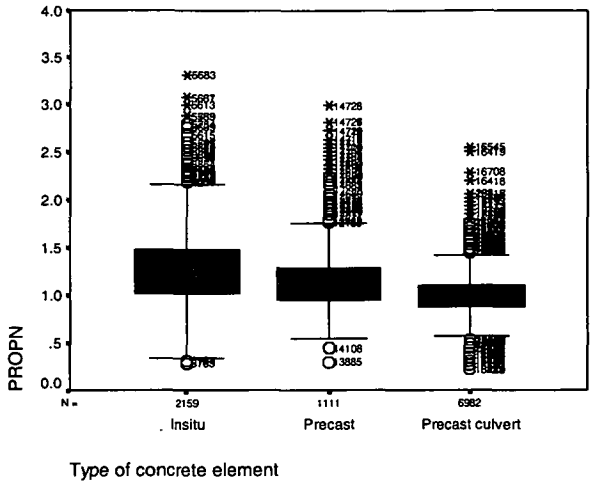

Figure A6.17 – Boxplot for 25 nominal cover

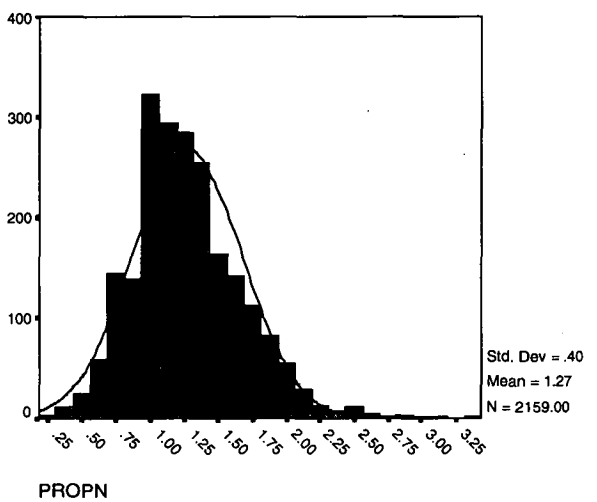

Figure A6.18 – Frequency distribution for 25 nominal cover, insitu elements

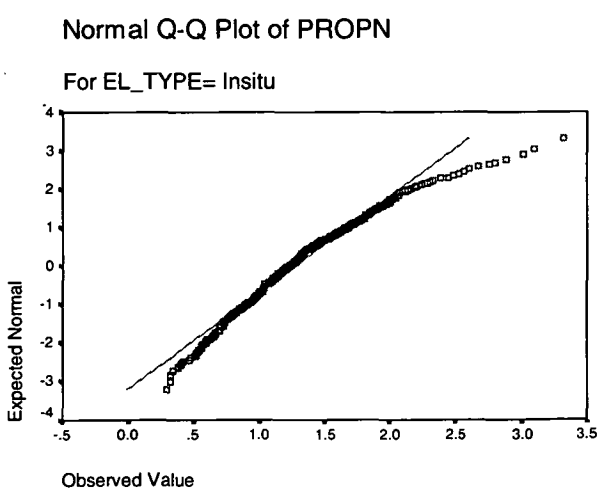

Figure A6.19 – Normal quantile plot for 25 nominal cover, insitu elements

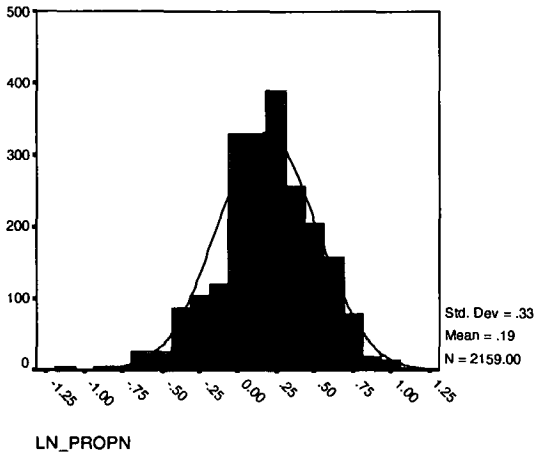

Figure A6.20 – Frequency distribution for 25mm nominal cover, insitu (ln transform)

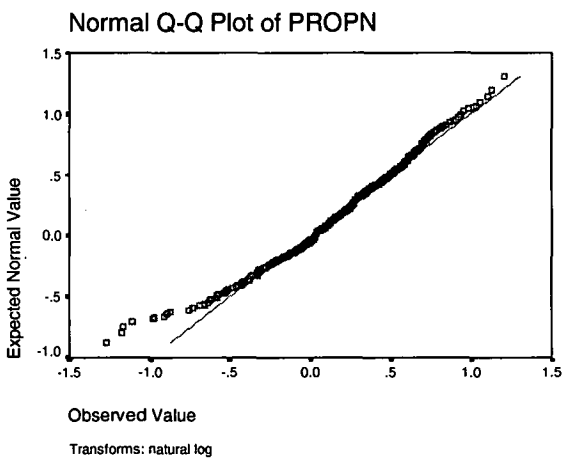

Figure A6.21 – Normal quantile plot for 25mm nominal cover, insitu (ln transform)

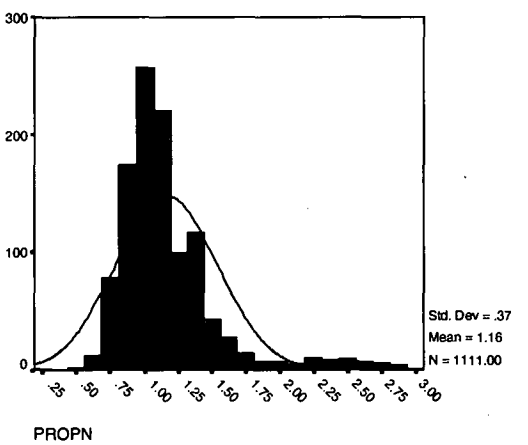

Figure A6.22 – Frequency distribution for 25mm nominal cover, precast elements

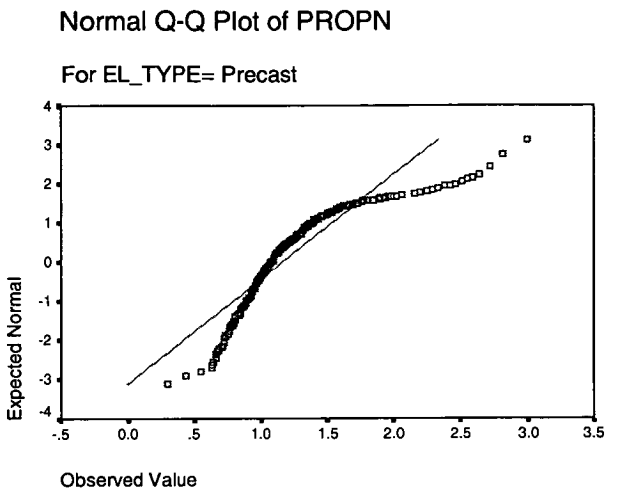

Figure A6.23 – Normal quantile plot for 25 nominal cover, precast elements

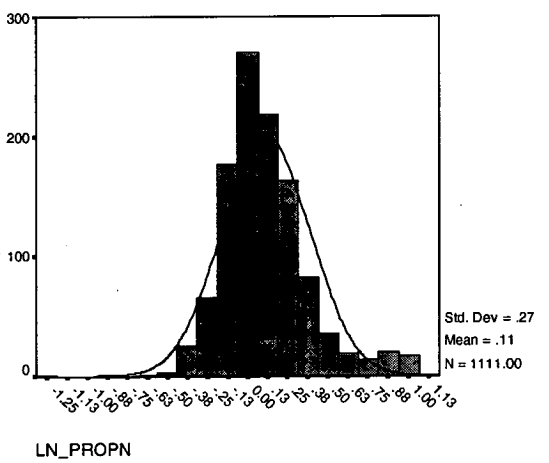

Figure A6.24 – Frequency distribution for 25mm nominal cover, precast elements (ln transform)

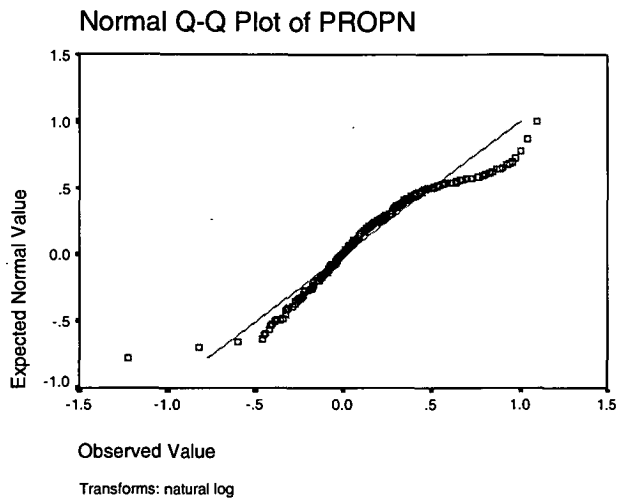

Figure A6.25 – Normal quantile plot for 25mm nominal cover, precast elements (ln transform)

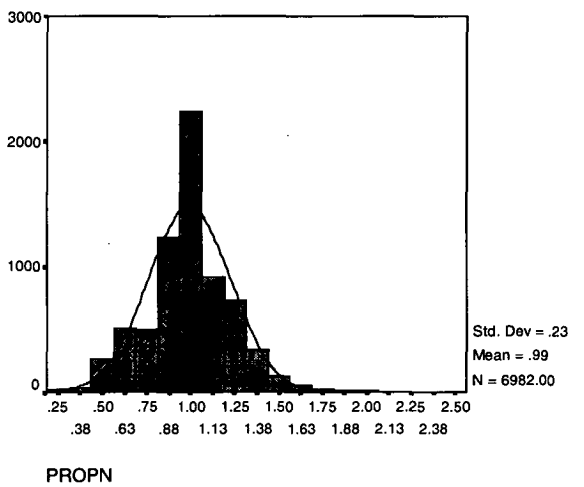

Figure A6.26 – Frequency distribution for 25mm nominal cover, precast culverts

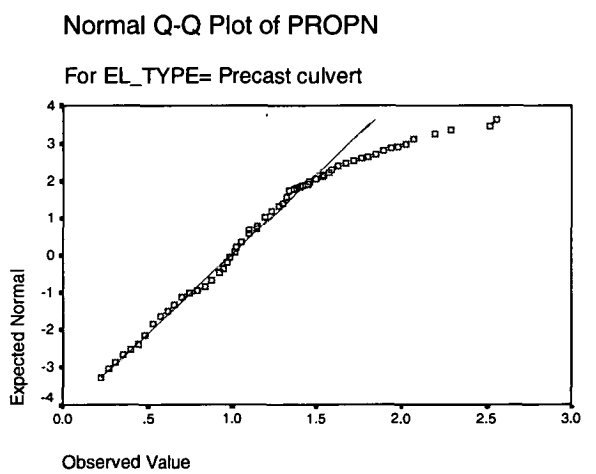

Figure A6.27 – Normal quantile plot for 25 nominal cover, precast culverts

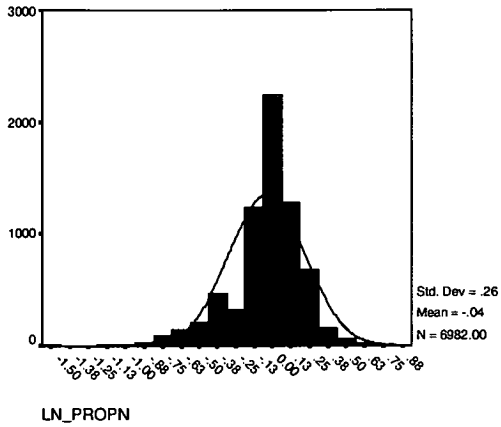

Figure A6.28 – Frequency distribution for 25mm nominal cover, precast culverts (ln transform)

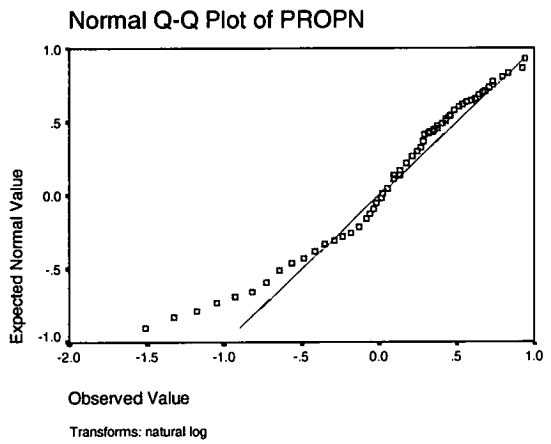

Figure A6.29 – Normal quantile plot for 25mm nominal cover, precast culverts (ln transform)

Figures A6.30 to A6.36 describe cover measurements for a nominal specified cover of 19mm. The age distribution shows that virtually all measurements are for structures at least 48 years old, with a small number of measurements from a precast culvert of age 12 years. The effects of age have consequently not been assessed.

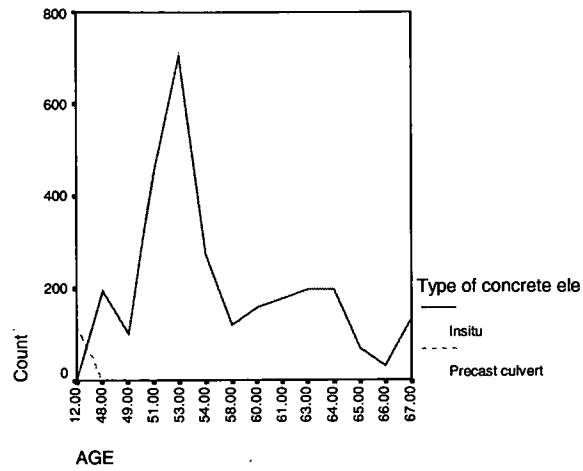

Figure A6.30 – Age distribution of measurements for 19mm nominal cover

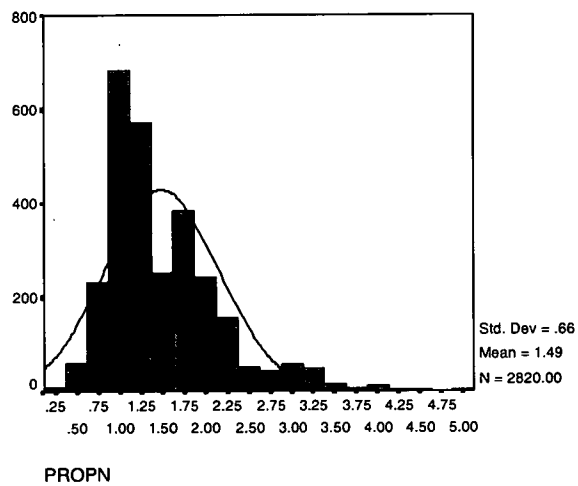

Figure A6.31 – Frequency distribution for 19 nominal cover, insitu elements

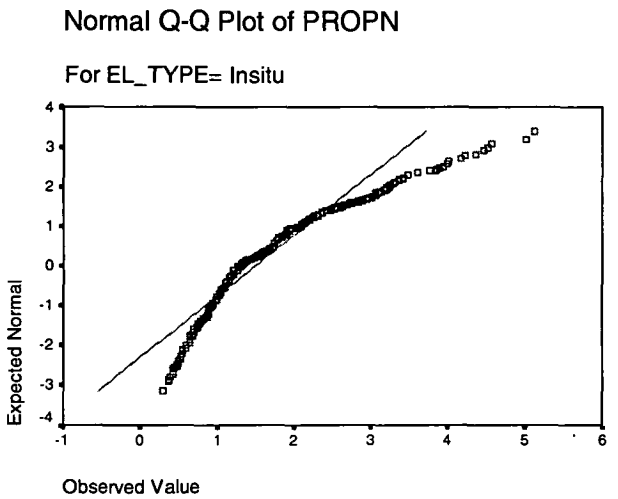

Figure A6.32 – Normal quantile plot 19mm nominal cover, insitu elements

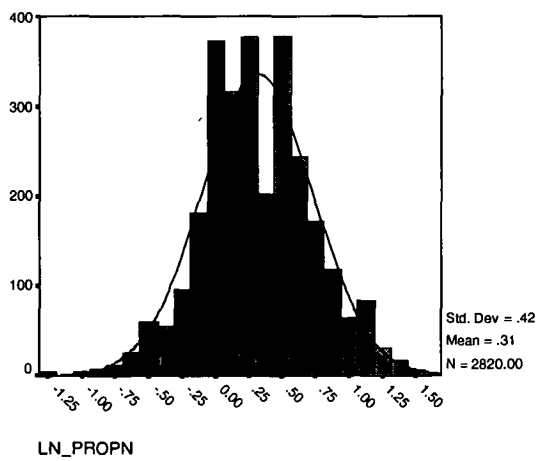

Figure A6.33 – Frequency distribution for 19 nominal cover, insitu elements (ln transform)

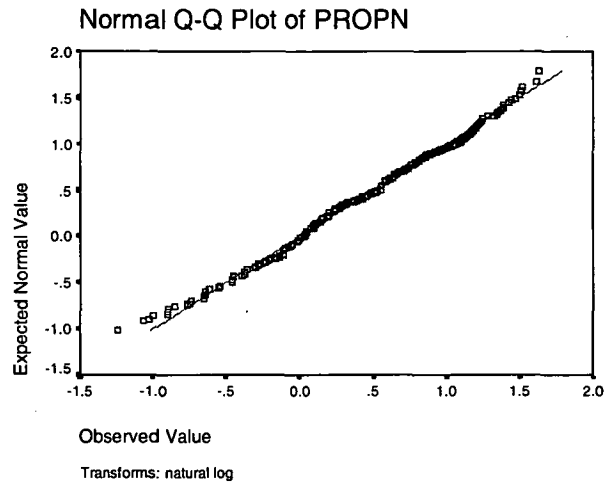

Figure A6.34 – Normal quantile plot 19mm nominal cover, insitu elements (ln transform)

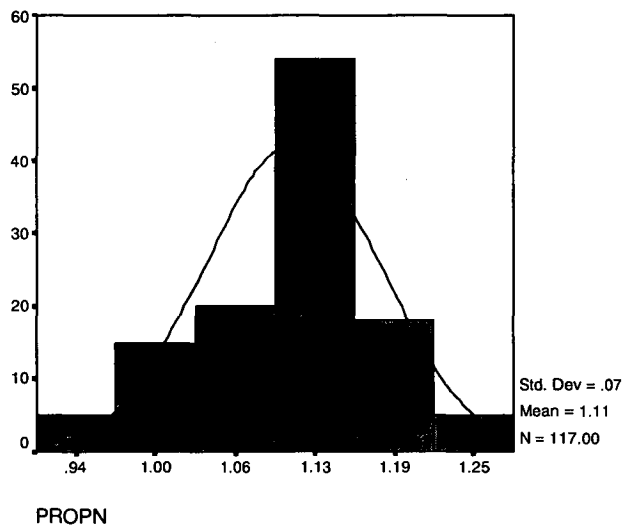

Figure A6.35 – Distribution of measurements for 19mm nominal cover, precast culverts

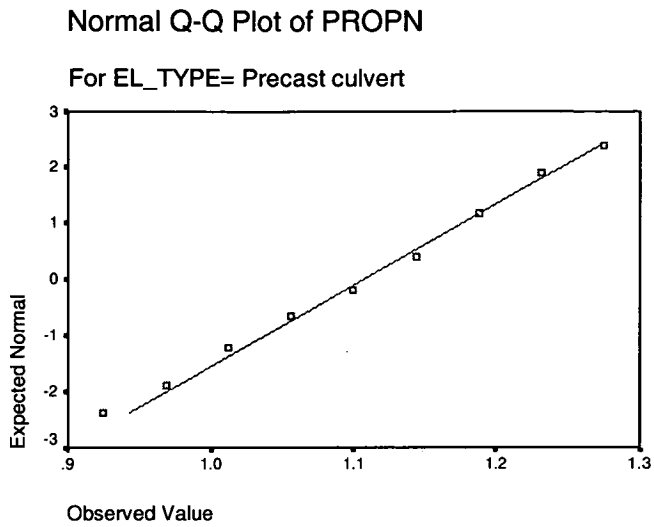

Figure A6.36 – Normal quantile plot, 19mm nominal cover, precast culverts

Examination of the histograms and normal probability and quantile plots indicates that the cover measurements can reasonably be described by normal probability distributions particularly when the measurements are grouped according to nominal specified cover and the larger samples are considered. The reasonableness of the assumption is confirmed with statistical analysis software.

Figures A6.39 and A6.40 show the overall distribution of measurements using differing class intervals. Figure A6.39 has an interval of 0.05 of specified cover, which corresponds to a range of about 1 to 2mm. Figure A6.40 uses an interval of 0.25 of specified cover and incorporates a normal curve; the distribution is affected by the long tails from surveys including Emu River Bridge.

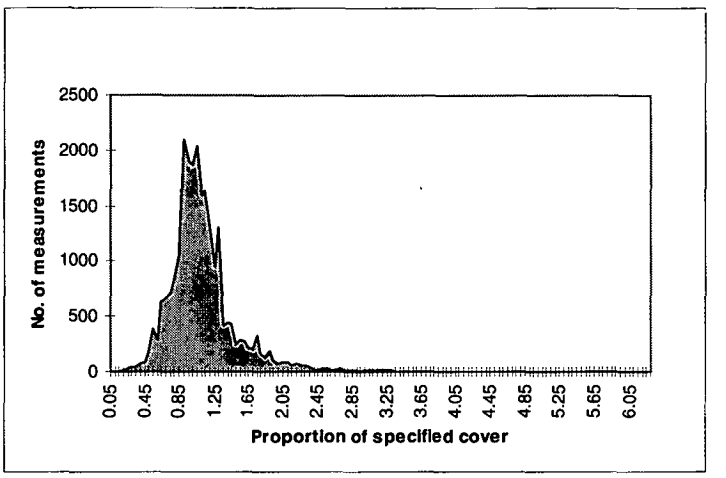

Figure A6.39 – Overall distribution as a proportion of specified cover

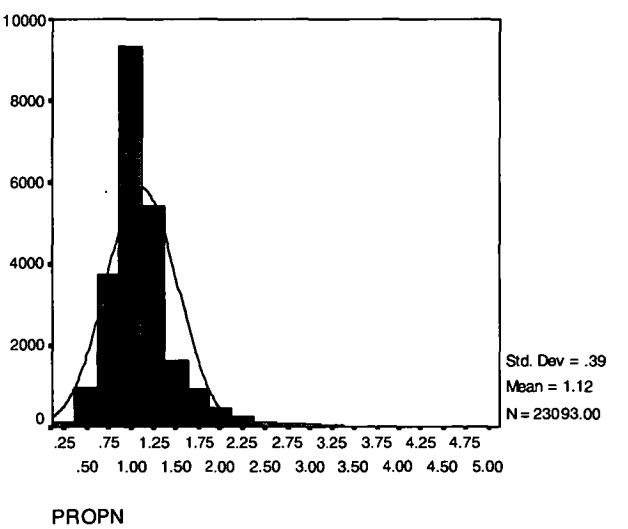

Figure A6.40 – Overall distribution as a proportion of specified cover

A normal quantile plot (figure A6.41) does not indicate a high degree of normality for the aggregated data; there is an improved fit using a natural log transform (figures A6.42 and A6.43). The fit is not improved with other types of distribution. The boxplot highlights the spread of measurements in the fourth quartile corresponding to the long tails in figures A6.42 and A6.43.

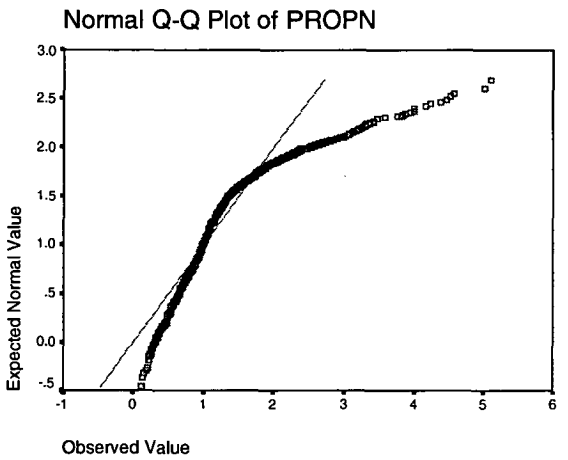

Figure A6.41 – Normal quantile plot for aggregate data

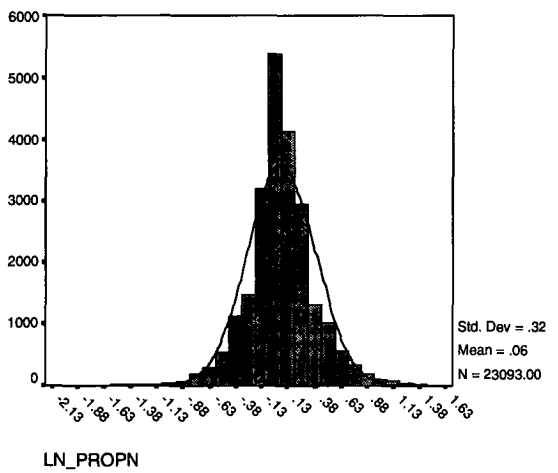

Figure A6.42 – Overall distribution (ln transformation) as a proportion of specified cover

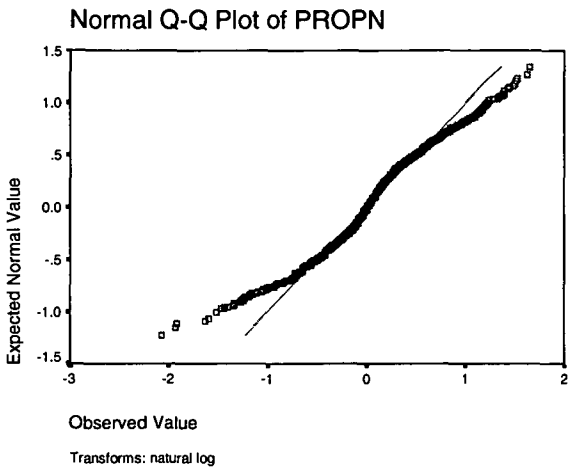

Figure A6.43 – Normal quantile plot (ln transformation) for aggregate data

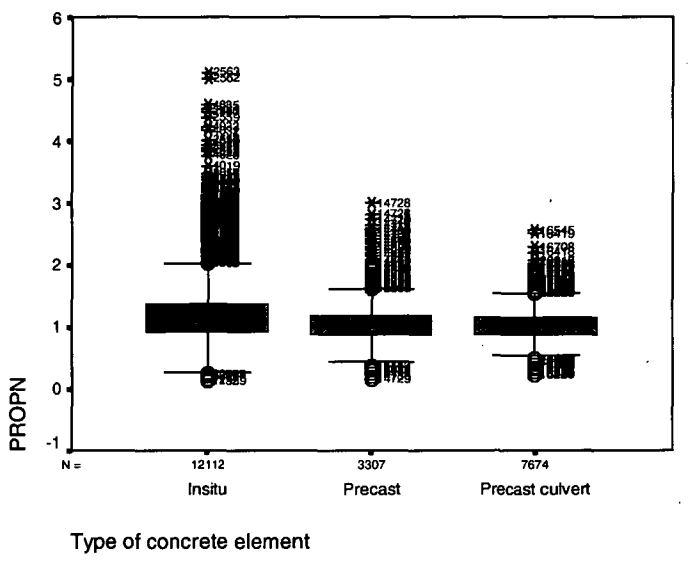

Figure A6.44 – Boxplot of overall cover distributions by element type

Figures 8.30 to 8.33 explore the distribution of specified covers. They show a substantial proportion of measured covers at nominal specified covers of 19mm (3/4"), 25mm (1"), 38mm (1.5") and 50mm (2") . The number of measurements for a specified cover of 25mm (1") is strongly influenced by approximately 7000 measurements for precast box culvert crown units.

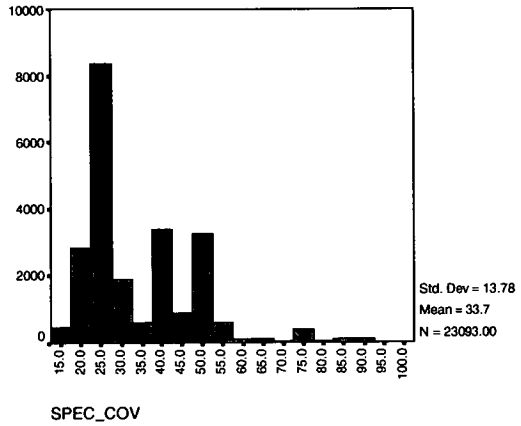

Figure A6.45 – Frequency distribution for specified cover (aggregate data)

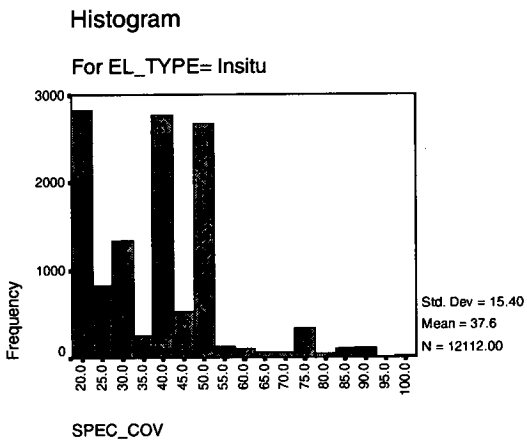

Figure A6.46 – Frequency distribution for specified cover of insitu elements

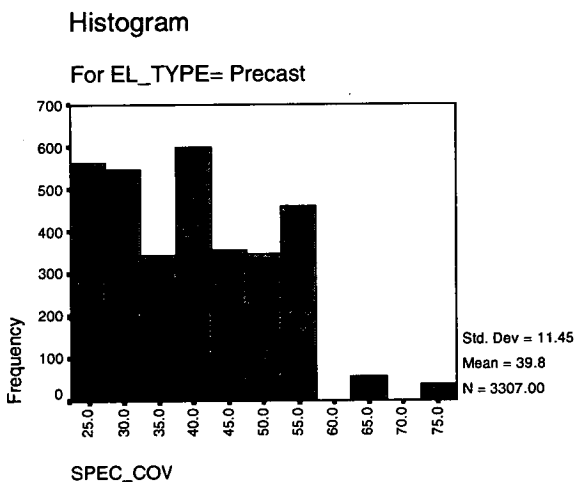

Figure A6.47 – Frequency distribution for specified cover of precast elements

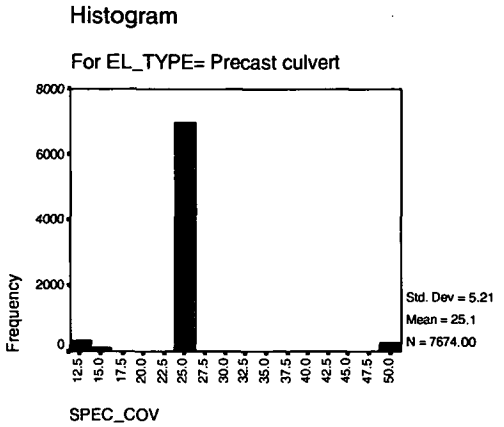

Figure A6.48 – Frequency distribution for specified cover of precast culvert units

It was considered likely that the overall distributions were influenced by measurements for specified covers other than the nominal covers for which the majority of measurements occur. In particular, the influence of measurements for higher specified covers was likely to be significant because of a reduced accuracy of measurement with the cover meters at higher ranges. For that reason, more detailed analysis has focussed on cover measurements over the ranges of specified covers where there are relatively large numbers of measurements.

The range of specified covers adopted for the nominal covers are detailed in Table A6.1

Nominal Cover (mm)	Range of specified covers (mm)	No. of measurements		
		Insitu	Precast	Culverts
19	15-22	2820	-	117
25	24-32	2159	1111	6982
38	35-44	3186	1008	-
50	45-55	3104	653	236

Table A6.1 – Cover ranges

More detailed analysis commenced for a nominal cover of 50mm. Figure 8.34 shows that measurements for both insitu and precast elements are distributed across structures of ages up to 64 years, facilitating trend analysis as well as comparisons between the different types of element.

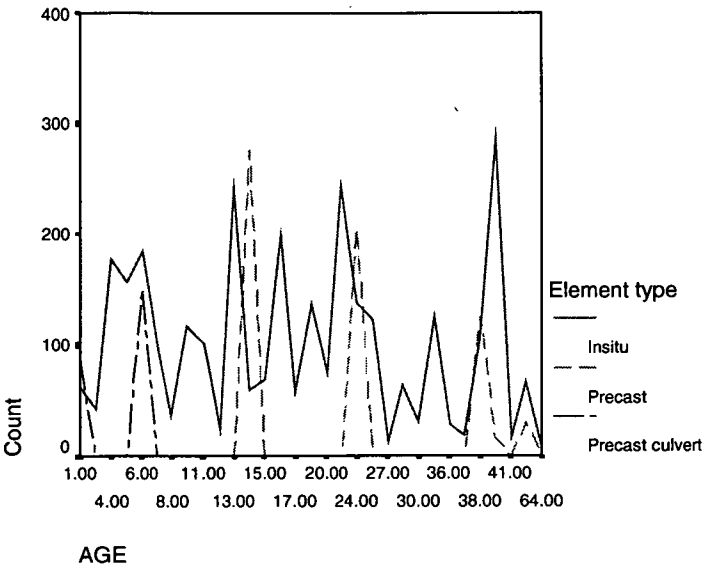

Figure A6.49 - Age distribution of measurements for 50mm nominal cover

Table 8.12 presents overall and disaggregated data in terms of measured and normalised distributions to provide a basis for developing models for service life assessment and tolerances for specifications and codes.

Description	No. of measurements	Normal distribution				Minimum cover (mm)		Cover tolerance from specified (mm)		Cover range (mm)	
		Normalised		Value (mm)		95% compliance[1]		90% compliance[1,2]		90% compliance[1,2]	
		μ	σ	μ	σ	Normal distribution	Measured	Normal distribution	Measured	Normal distribution	Measured
Overall[3]	23093	1.115	0.390	37.6	13.2	15.9	21.4	-17.8, +25.7	-12.3, +27.0	43.5	39.3
Insitu[3]	12112	1.206	0.464	45.3	17.4	16.5	24.5	-21.0, +36.5	-13.0,+39.6	57.5	52.6
Precast[3]	3307	1.046	0.294	41.7	11.7	22.4	27.2	-17.5, +21.2	-12.5, +19.9	38.7	32.4
Culvert[3]	7674	1.002	0.232	25.1	5.8	15.5	14.4	-9.6, +9.6	-10.7, +8.0	19.2	18.7
Nominal cover 50											
Overall											
Insitu	3104	1.048	0.198	52.4	9.9	36.1	36.7	-13.9, +18.7	-13.3, +17.8	32.6	31.1
Precast	653	1.062	0.237	53.1	11.9	33.6	34.5	-16.4, +22.6	-15.5, +23.3	39.0	38.8
Culvert	236	0.972	0.075	48.6	3.8	42.4	42.9	-7.6, +4.8	-7.1, +5.2	12.4	12.3
Age ≤ 12											
Insitu	1001	1.075	0.203	53.8	10.2	37.0	37.4	-13.0, +20.5	-12.6, +21.5	33.5	34.1
Precast	0										
Culvert	236	0.972	0.075	48.6	3.8	42.4	42.9	-7.6, +4.8	-7.1, +5.2	12.4	12.3
12<Age<27											
Insitu	1354	1.038	0.184	51.9	9.2	36.7	36.7	-13.3, +17.1	-13.3, +16.0	30.4	29.3
Precast	482	1.083	0.252	54.2	12.6	33.4	35.5	-16.6, +24.9	-14.5, +25.0	41.5	39.5
Culvert	0										
27<Age											
Insitu	749	1.032	0.210	51.6	10.5	34.3	34.0	-15.7, +18.9	-16.0, +17.6	34.6	33.6
Precast	171	1.004	0.176	50.2	8.8	35.7	33.3	-14.3, 14.7	-16.7, +11.7	29.0	28.4

Description	No. of measurements	Normal distribution				Minimum cover (mm)		Cover tolerance from specified (mm)		Cover range (mm)	
		Normalised		Value (mm)		95% compliance[1]		90% compliance[1,2]		90% compliance[1,2]	
		μ	σ	μ	σ	Normal distribution	Measured	Normal distribution	Measured	Normal distribution	Measured
Culvert	0										
Nominal cover 38											
Insitu	3186	1.160	0.377	44.1	14.3	20.4	23.0	-17.6, +29.7	-15.0, +31.1	47.3	46.1
Precast	1008	1.023	0.203	38.9	7.7	26.1	26.4	-11.9, +13.6	-11.6, +13.7	25.5	25.3
Nominal cover 25											
Overall											
Insitu	2159	1.269	0.400	31.7	10.0	15.2	17.2	-9.8, +23.2	-7.8, +25.0	33.0	32.8
Precast	1111	1.165	0.373	29.1	9.3	13.7	19.3	-11.3, +19.5	-5.7, +23.8	30.8	29.5
Culvert	6982	0.990	0.233	24.8	5.8	15.1	14.3	-9.9, +9.4	-10.7, +8.0	19.3	18.7
Age ≤ 18											
Insitu	170	1.220	0.327	30.5	8.2	17.0	18.3	-8.0, +19.0	-6.7, +20.3	27.0	27.0
Precast	736	1.158	0.423	29.0	10.6	11.5	19.0	-13.5, 21.4	-6.0, 32.2	34.9	38.2
Culvert	4945	1.055	0.161	26.4	4.0	19.7	20.9	-5.3, +8.0	-4.1, +8.0	13.3	12.1
18 < age ≤ 35											
Insitu	245	1.249	0.294	31.2	7.4	19.1	22.6	-5.9, 18.4	-2.4, +21.0	24.3	23.4
Precast	321	1.137	0.229	28.4	5.7	19.0	20.2	-6.0, 12.9	-4.8, +14.1	18.9	18.9
Culvert	2037	0.835	0.298	20.9	7.5	8.6	12.1	-16.4, +8.2	-12.9, +8.0	24.6	20.9
Age > 35											
Insitu	1744	1.277	0.418	31.9	10.5	14.7	17.0	-10.3, 24.2	-8.0, 25.2	34.5	33.2
Precast	54	1.414	0.217	35.4	5.4	26.4	27.5	+1.4, 19.3	+2.5, +22.5	20.7	25.0
Culvert	0										

Description	No. of measurements	Normal distribution				Minimum cover (mm)		Cover tolerance from specified (mm)		Cover range (mm)	
		Normalised		Value (mm)		95% compliance[1]		90% compliance[1,2]		90% compliance[1,2]	
		μ	σ	μ	σ	Normal distribution	Measured	Normal distribution	Measured	Normal distribution	Measured
Nominal cover 19											
Insitu	2820	1.489	0.656	28.3	12.5	15.8	13.0	-11.3, 29.9	-6.0, 35.9	41.2	41.9
Culvert	117	1.108	0.069	21.0	1.3	18.9	19.1	-0.1, 4.2	0.1, 3.7	4.3	3.8

Notes: 1. 90% compliance based on 5% less than minimum and 5% greater than maximum
2. Compliance based on $\mu \pm 1.65\sigma$
3. Mean specified covers for aggregated measurements are 33.7mm overall, 37.6mm insitu, 39.8mm precast and 25.1mm precast culverts.

Table A6.2 – Cover distribution parameters

6.3 ACCURACY OF COVERMETERS

Cover measurements taken by the author and by Materials and Research staff as part of corrosion investigations used Profometer 3 covermeters. Figure A6.37 shows the accuracy of the meters as given by the manufacturer Proceq in their operating instructions.

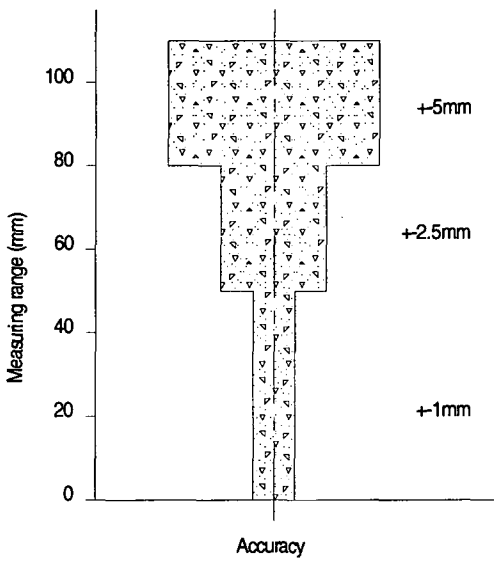

Figure A6.37 – Covermeter accuracy

Using the midpoints of the cover ranges, and extending to the capacity of 220mm, the accuracy is plotted in Figure A6.38 and shown in Table A6.3.

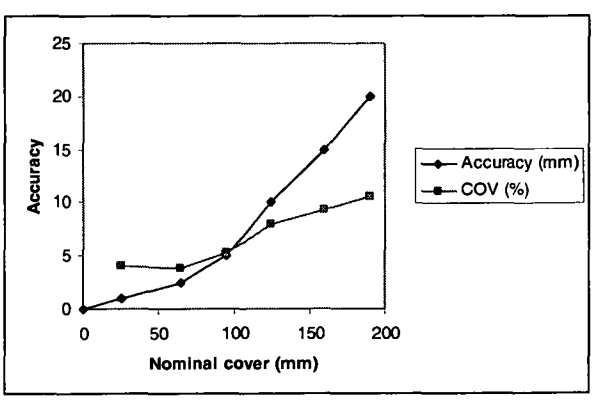

Figure A6.38 – Covermeter accuracy

Midpoint of range (mm)	Accuracy (mm)	COV (%)
0	0	
25	1	4.00
65	2.5	3.85
95	5	5.26
125	10	8.00
160	15	9.38
190	20	10.53

Table A6.3 – Covermeter accuracy

For the purposes of considering the effect of covermeter accuracy on the distribution of cover to reinforcement, a coefficient of variation of 4% has been adopted.

The variability in cover is a combination of the true variability and the variability due to sampling and measurement. The variability effects of covermeter accuracy can be discounted from the variability in reinforcement cover using the relationship:

$$COV(cover)^2 = COV(true+sampling)^2 + COV(covermeter)^2$$

From Table A6.3 and the above relationship, the range in coefficients of variation from the analysis and those adjusted for covermeter accuracy on the basis of a 4% coefficient of variation are detailed in Table A6.4.

Insitu		Precast		Culverts	
Analysis	Adjusted	Analysis	Adjusted	Analysis	Adjusted
18.9	18.5	22.4	22.0	7.8	6.7
19.0	18.6	23.2	22.9	7.8	6.7
17.7	17.2	17.5	17.0	23.4	23.1
20.3	19.9	19.8	19.4	15.2	14.7
32.4	32.2	32.0	31.7	35.9	35.7
31.5	31.2	50.7	20.3	6.2	4.7
26.9	26.6	20.1	19.7		
23.7	23.4	15.3	14.8		
32.9	32.7				
44.2	44.0				

Table A6.4 – Coefficients of variation for cover (%)

The effects of covermeter accuracy are marginal, with the only significant effects occurring for three of the precast culvert measurement ranges. Even with the precast culvert units however, coefficients of variation range up to 36%, and the proposed tolerances have not been varied to account for covermeter accuracy. That variability will in any case be inherent in cover surveys using electromagnetic covermeters.

6.4 COVER TOLERANCES

Figures A6.50 to A6.52 present the cover tolerances from Table A6.2 with least squares lines of best fit for a constant difference from specified cover. Results are summarised in Table A6.5.

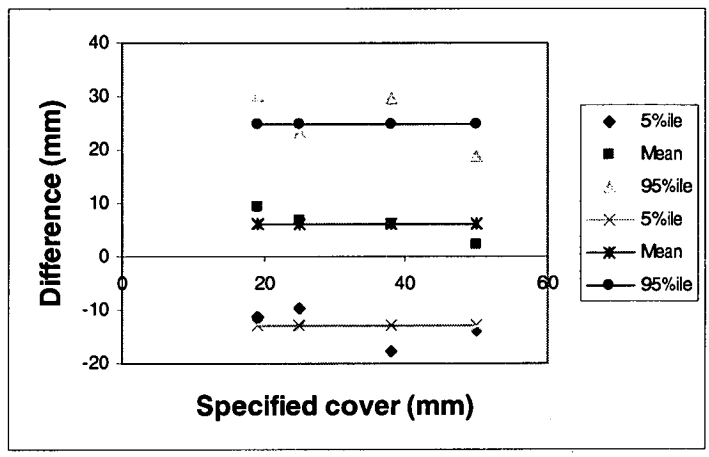

Figure A6.50 – Cover compliance for insitu elements

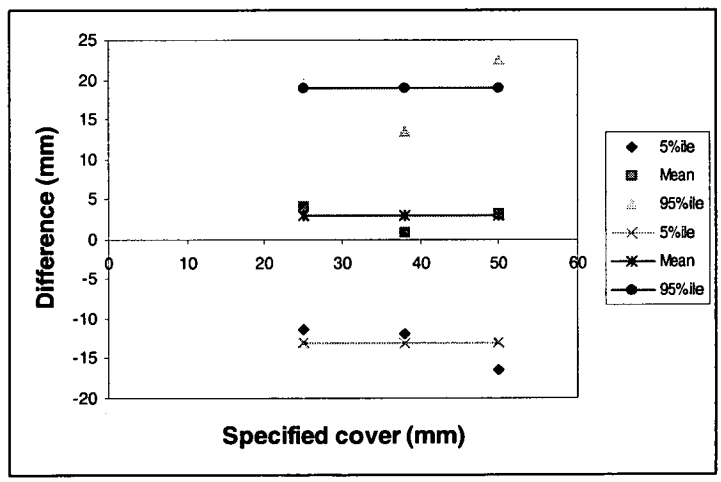

Figure A6.51 – Cover compliance for precast elements

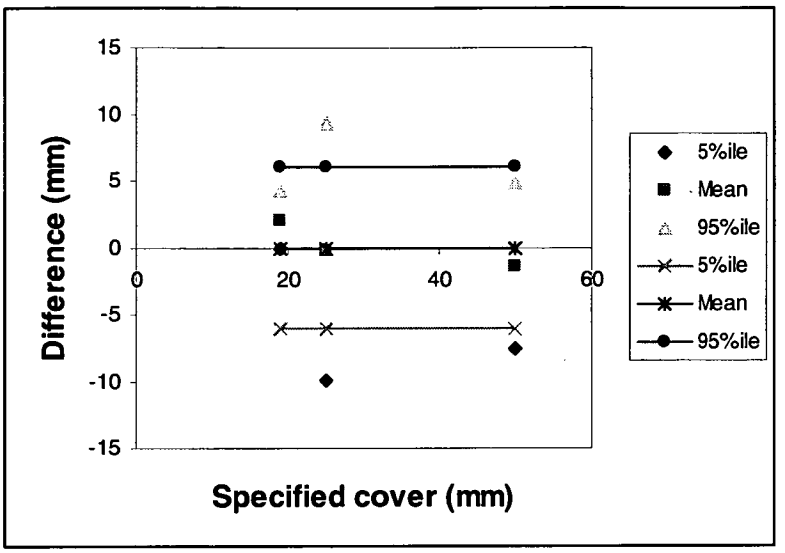

Figure A6.52 – Cover compliance for precast culverts

Element type	Constant difference	
	Negative	Positive
Insitu	-13	25
Precast	-13	19
Culverts	-6	6

Table A6.5 – Cover tolerances (90% compliance)

7 SERVICE LIFE MODELLING

7.1 INTRODUCTION

This section includes graphs of corrosion probabilities and reliability indices.

7.2 PROBABILISTIC MODELLING

7.2.1 CHLORIDE INGRESS

Figures A7.1 to A7.17 of show probabilities of corrosion initiation for a range of values of height above mean water level, distance from the coast, threshold chloride concentration for corrosion initiation, element type, truncation of cover negative tolerance, diffusion coefficient and reduced coefficients of variation. The mean value of the diffusion coefficient is 1 x 10^{-12} m/s^2 for all but figure 7.16.

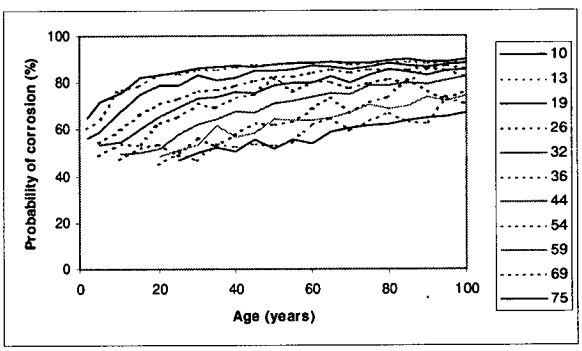

Figure A7.1 – Probability of corrosion for distance from coast 0 km, height ≤ 2m, insitu, threshold concentration 0.05 %

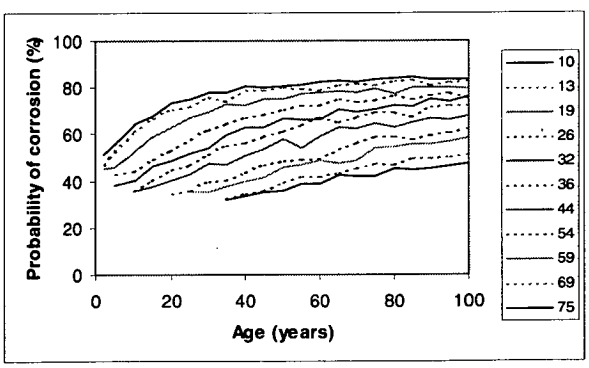

Figure A7.2 – Probability of corrosion for distance from coast 0 km, height ≤ 2m, insitu, threshold concentration 0.1 %

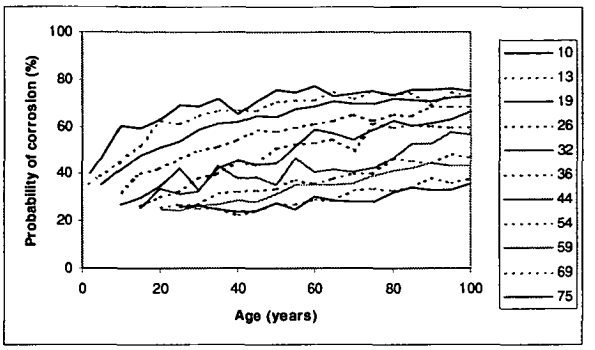

Figure A7.3 – Probability of corrosion for distance from coast 0 km, height ≤ 2m, insitu, threshold concentration 0.15 %

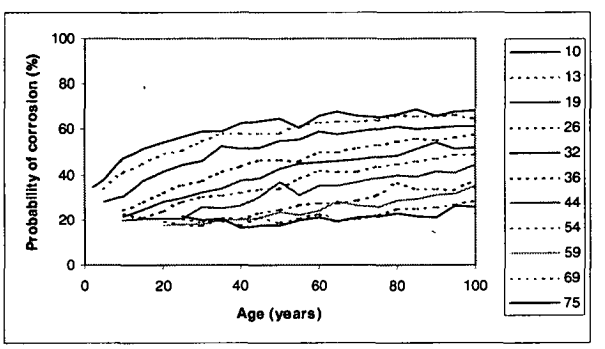

Figure A7.4 – Probability of corrosion for distance from coast 0 km, height ≤ 2m, insitu, threshold concentration 0.2 %

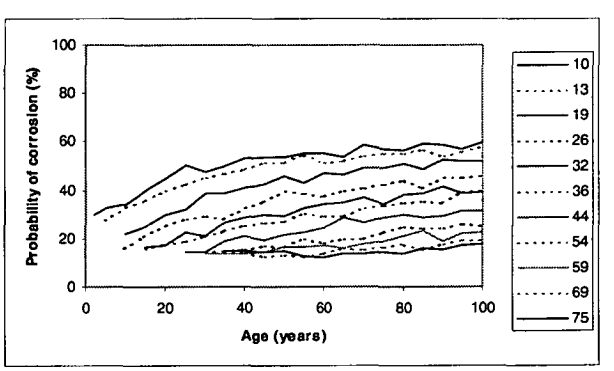

Figure A7.5 – Probability of corrosion for distance from coast 0 km, height ≤ 2m, insitu, threshold concentration 0.25 %

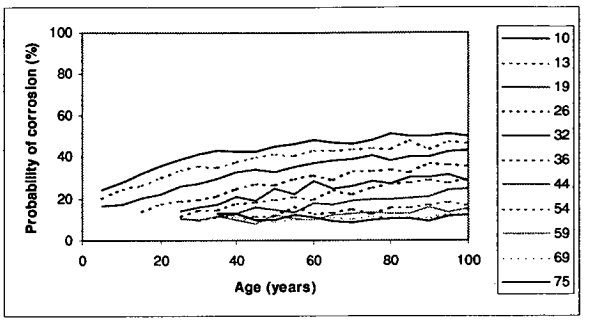

Figure A7.6 – Probability of corrosion for distance from coast 0 km, height ≤ 2m, insitu, threshold concentration 0.3 %

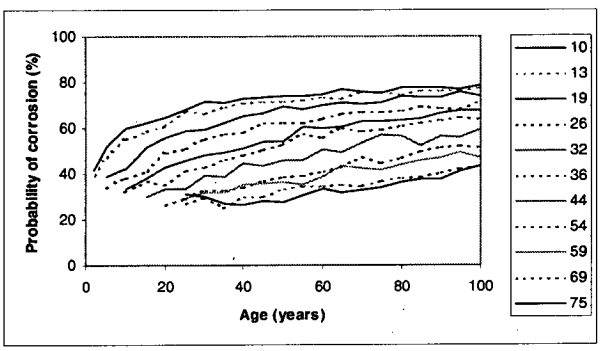

Figure A7.7 – Probability of corrosion for distance from coast 0 km, 2m<height ≤ 4m, insitu, threshold concentration 0.05 %

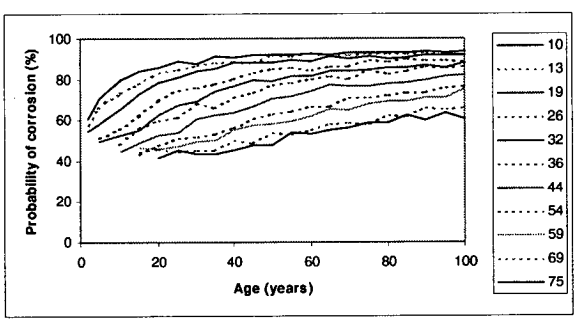

Figure A7.8 – Probability of corrosion for distance from coast 0.1 km, insitu, threshold concentration 0.05 %

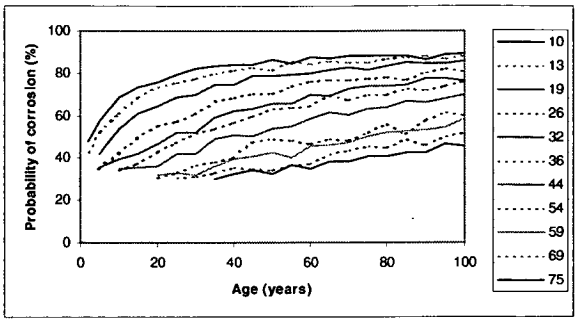

Figure A7.9 – Probability of corrosion for distance from coast 0.5 km, insitu, threshold concentration 0.05 %

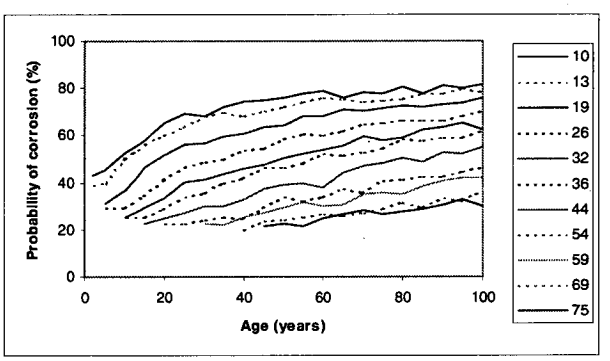

Figure A7.10 – Probability of corrosion for distance from coast 1.0 km, insitu, threshold concentration 0.05 %

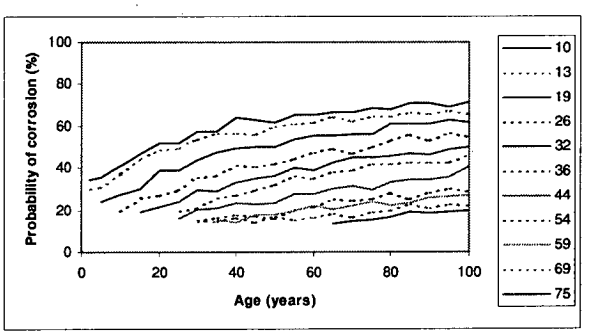

Figure A7.11 – Probability of corrosion for distance from coast 1.5 km, insitu, threshold concentration 0.05 %

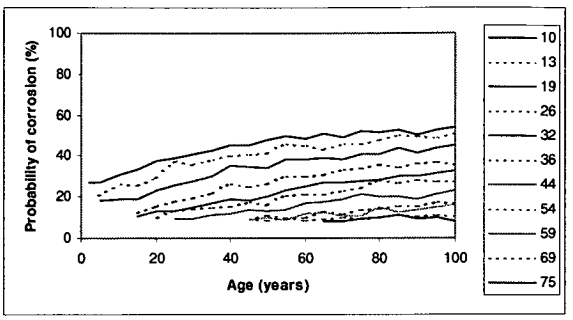

Figure A7.12 – Probability of corrosion for distance from coast 2.0 km, insitu, threshold concentration 0.05 %

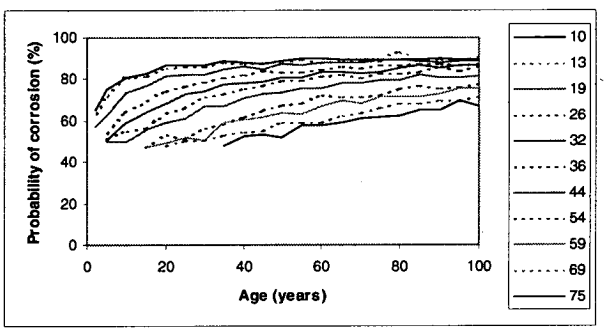

Figure A7.13 – Probability of corrosion for distance from coast 0 km, height ≤ 2m, precast, threshold concentration 0.05 %

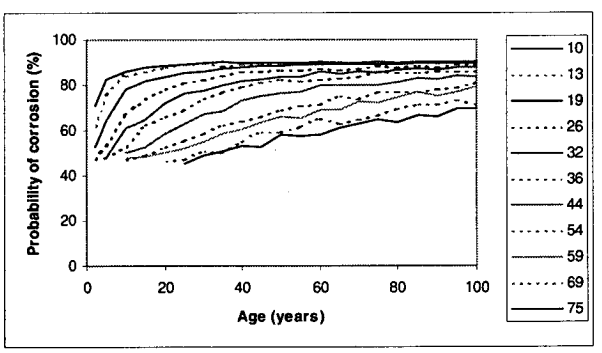

Figure A7.14 – Probability of corrosion for distance from coast 0 km, height ≤ 2m, precast culverts, threshold concentration 0.05 %

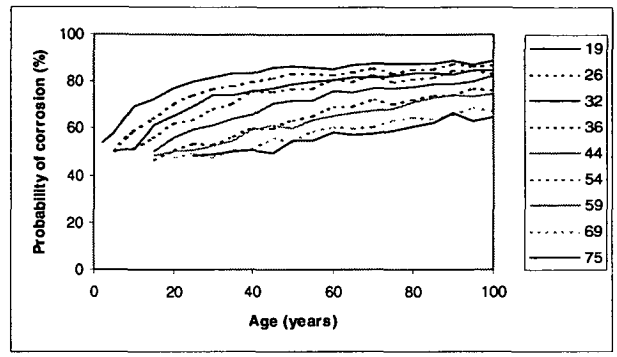

Figure A7.15 – Probability of corrosion for distance from coast 0 km, height ≤ 2m, threshold concentration 0.05 %, cover variability truncated at –15+30mm from specified

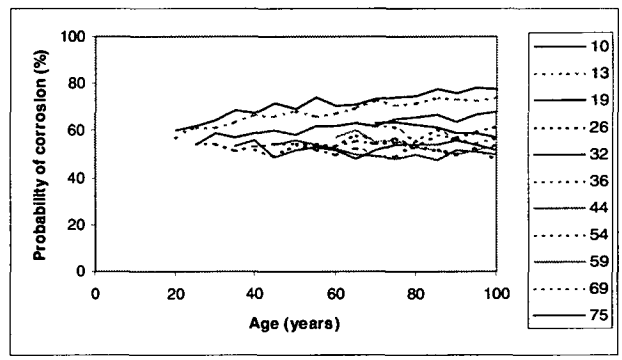

Figure A7.16 – Probability of corrosion for distance from coast 0 km, height ≤ 2m, threshold concentration 0.05 %, mean D_{eff} $1x10^{-13}$ m/s^2, standard deviation of transformed (log_{10}) distribution 0.48

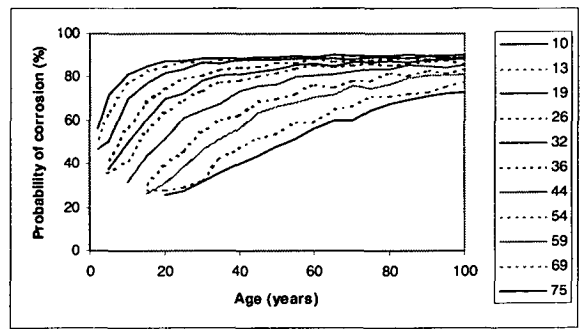

Figure A7.17 – Probability of corrosion for distance from coast 0 km, height ≤ 2m, threshold concentration 0.05 %, D_{eff} $1x10^{-12}$ m/s^2, standard deviation of transformed (log_{10}) distribution 0.25

Figures A7.18 to A7.34 show Figures A7.1 to A7.17 transformed to reliability indices.

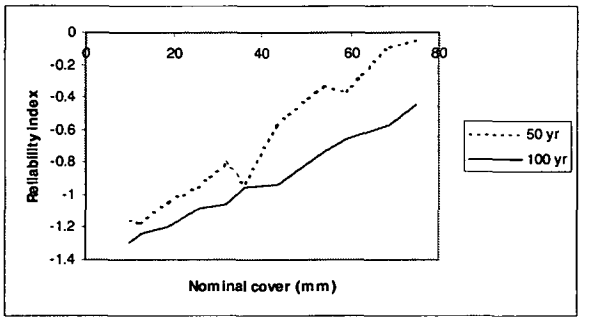

Figure A7.18 – Reliability indices for distance from coast 0 km, height ≤ 2m, insitu, threshold concentration 0.05 %

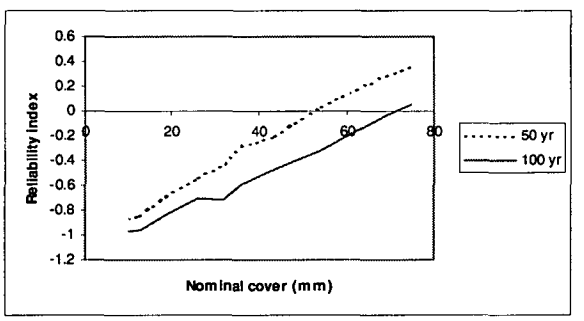

Figure A7.19 – Reliability indices for distance from coast 0 km, height ≤ 2m, insitu, threshold concentration 0.1 %

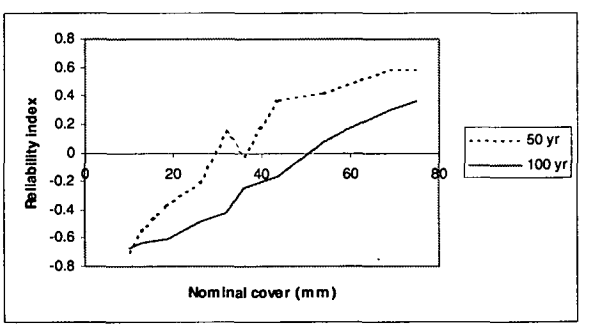

Figure A7.20 – Reliability indices for distance from coast 0 km, height ≤ 2m, insitu, threshold concentration 0.15 %

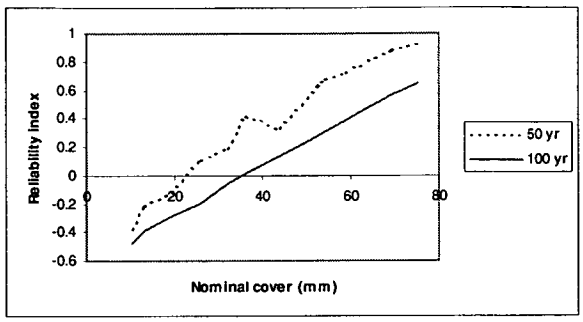

Figure A7.21 – Reliability indices for distance from coast 0 km, height ≤ 2m, insitu, threshold concentration 0.2 %

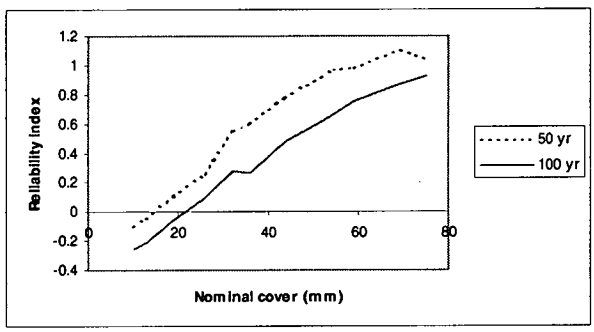

Figure A7.22 – Reliability indices for distance from coast 0 km, height ≤ 2m, insitu, threshold concentration 0.25 %

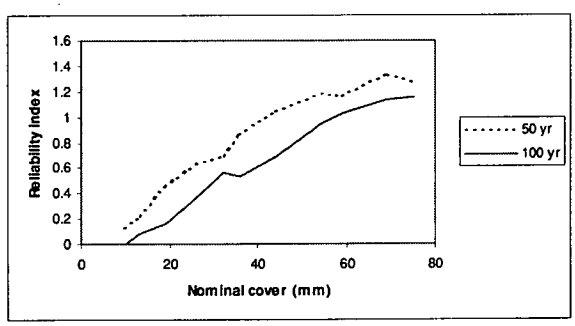

Figure A7.23 – Reliability indices for distance from coast 0 km, height ≤ 2m, insitu, threshold concentration 0.3 %

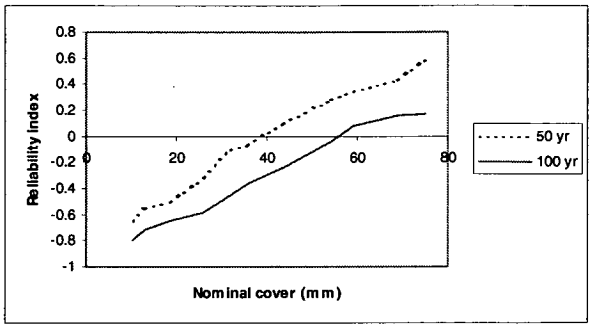

Figure A7.24 – Reliability indices for distance from coast 0 km, 2m<height ≤ 4m, insitu, threshold concentration 0.05 %

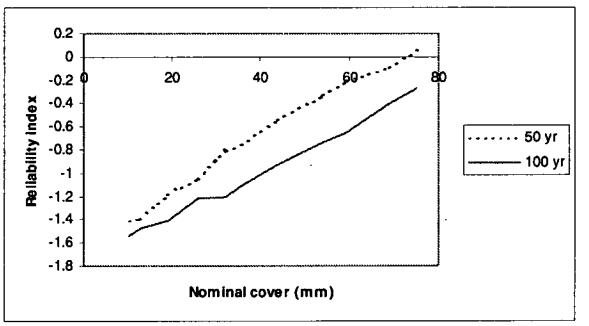

Figure A7.25 – Reliability indices for distance from coast 0.1 km, insitu, threshold concentration 0.05 %

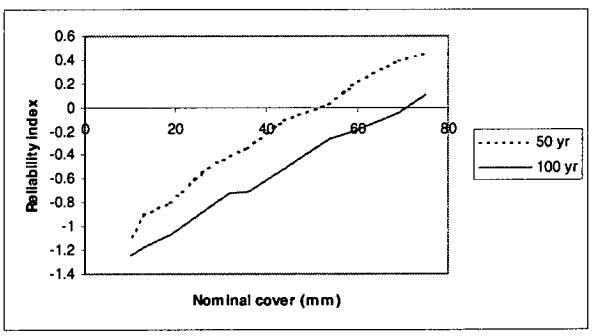

Figure A7.26 – Reliability indices for distance from coast 0.5 km, insitu, threshold concentration 0.05 %

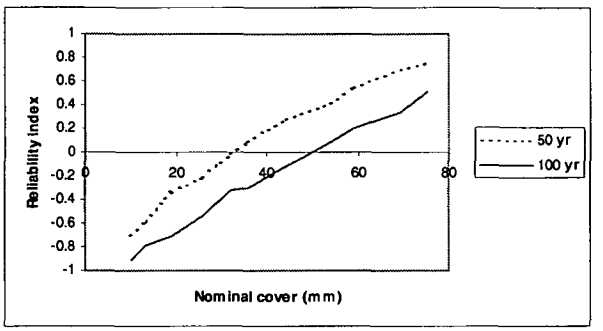

Figure A7.27 – Reliability indices for distance from coast 1.0 km, insitu, threshold concentration 0.05 %

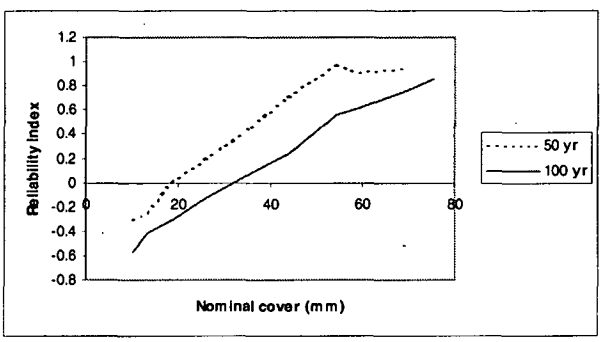

Figure A7.28 – Reliability indices for distance from coast 1.5 km, insitu, threshold concentration 0.05 %

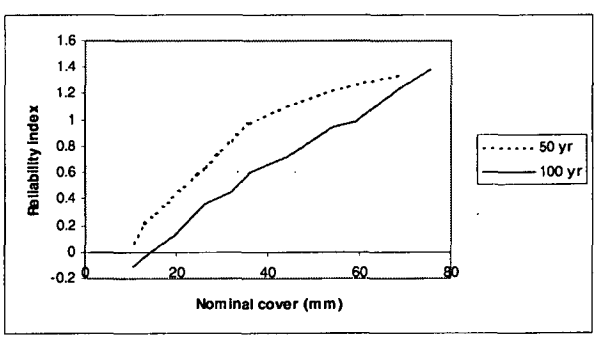

Figure A7.29 – Reliability indices for distance from coast 2.0 km, insitu, threshold concentration 0.05 %

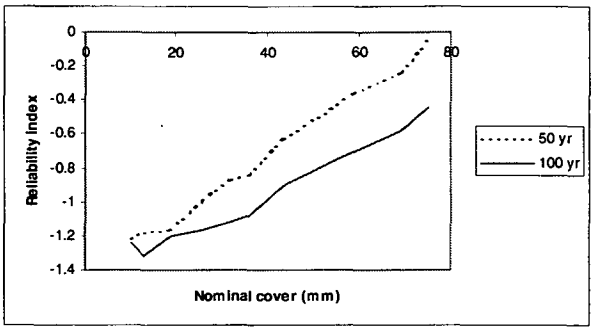

Figure A7.30 – Reliability indices for distance from coast 0 km, height ≤ 2m, precast, threshold concentration 0.05 %

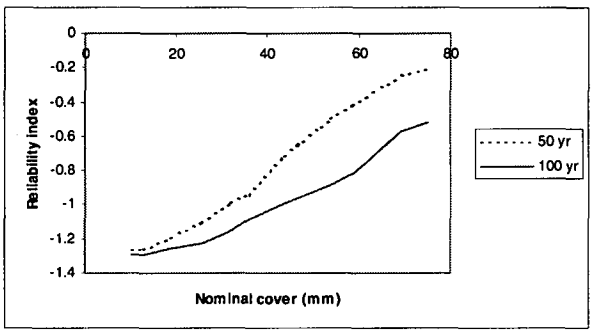

Figure A7.31 – Reliability indices for distance from coast 0 km, height ≤ 2m, precast culverts, threshold concentration 0.05 %

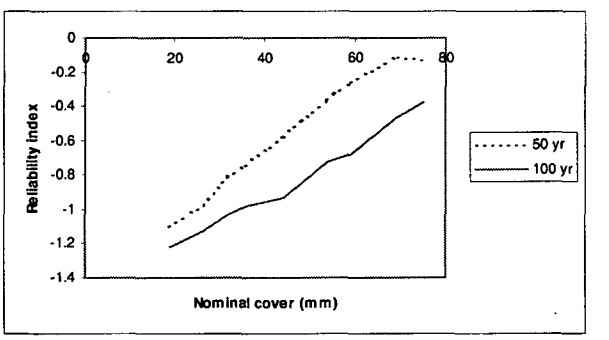

Figure A7.32 – Reliability indices for distance from coast 0 km, height ≤ 2m, threshold concentration 0.05 %, cover variability truncated at –15+30mm from specified

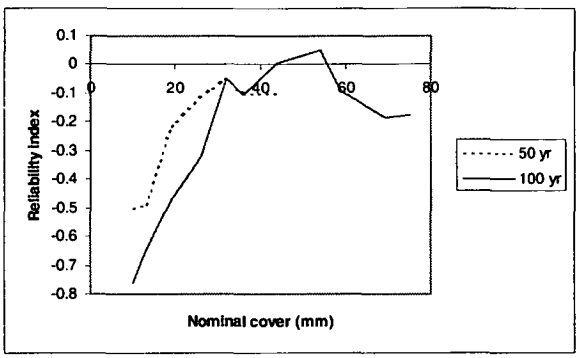

Figure A7.33 – Reliability indices for distance from coast 0 km, height ≤ 2m, threshold concentration 0.05 %, Deff $1x10^{-13}$ m/s^2, standard deviation of transformed (log_{10}) distribution 0.48

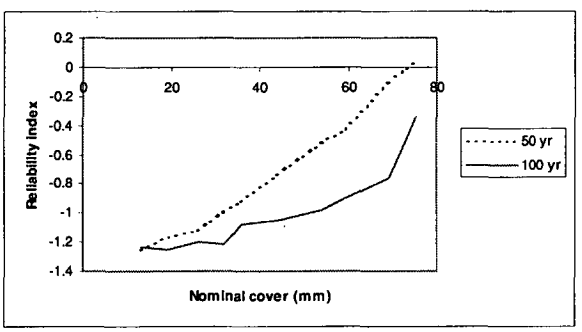

Figure A7.34 – Reliability indices for distance from coast 0 km, height ≤ 2m, threshold concentration 0.05 %, Deff $1x10^{-12}$ m/s^2, standard deviation of transformed (log_{10}) distribution 0.25

7.3 TASMANIAN BRIDGES

Table A7.1 details the bridges investigated in this study together with the times of first reports of visible distress and of remedial works, either in the form of repairs or replacement, as obtained from available records. Because of the reasons detailed above, times to visible distress provide an upper bound as, in most cases, cracking or staining will have appeared many years earlier.

Structure	YOC	Design cover	Visible distress		Remedial measures		Remarks
			Year	Age	Year	Age	
Faggs Gully Creek Culvert	1943	19	}		-	-	No distress in any
Faggs Gully Creek Culvert	1951	25	}		-	-	First extension
Faggs Gully Creek Culvert	1975	25	}		-	-	Second extension
Camp Creek Bridge	1934	19	1991	57	-	-	First inspection report

Structure	YOC	Design cover	Visible distress		Remedial measures		Remarks
			Year	Age	Year	Age	
Leven River Bridge	1934	51	1991	57	-	-	First inspection report
Porky Creek Bridge	1935	19	1991	56	-	-	Not identified 1980
Peggs Creek Bridge	1938	19	1982	44	-	-	First report – refers to
Orielton Rivulet Bridge	1938	-	-	-	-	-	Replaced – T-beam,
Saltwater Creek Bridge	1939	-	-	-	-	-	Replaced – T-beam,
Emu River Bridge	1939	30	-		1976	37	
Detention River Bridge	1940	19	1982	42	1983	43	First inspection report
Mountain Creek Bridge	1942/3	25	1987	45	1994	52	First inspection report
Surges Creek Bridge	1944	19	1990	46	-	-	First inspection report
Higgins Creek Bridge	1944	19	1990	46	-	-	First inspection report
Carlton River Culvert	1945	19	1992	47	-	-	First inspection report
Carlton River Bridge	1945	19	1991	47	-	-	First inspection report
Rileys Creek Bridge	1945	19	1990	45	-	-	First inspection report
Scopus Creek Bridge	1947	19	-	-	-	-	OK 1990; subsequent
Bridgewater Bridge	1947	19	1991	44	1998	51	First inspection report
Lilla Villa Bridge	1947	-	1965	18	-	-	First report of fence
Maclaines Creek Bridge	1948	19	1992	44	-	-	First inspection report
Stanley Dock	1950	32	1991	41	-	-	First inspection report
Stanley dock extension	1964	32	1991	41	-	-	First inspection report
Tasman Highway Culverts	1950	-	1990	40	-	-	First inspection report
Wardlaws Creek Bridge	1951	-	1991	40	1994	43	First inspection report
Flights Creek Bridge	1951	25	1990	39	-	-	First inspection report
King Island Main Road	1953	32	1996	43	-	-	First inspection report
East Arm Creek Culvert	1956	38			-	-	
Argent River Bridge	1957	35	1991	34	-	-	First inspection report
Ralphs Bay Canal Bridge	1956	30	1990	34	-	-	First inspection report
Egg Island Creek Bridge	1956	38			-	-	
Sorell Causeway Bridge	1957	-	1978	21	1982	25	First report, epoxy
Ringarooma River Bridge	1957	25	1990	33	1997	40	First inspection report
Pats River Bridge	1957	-	1988	31	1996	39	First report of damage
Cormiston Creek Bridge	1958	32			-	-	
Golden Fleece Bridge	1958	51	1996	38	1999	41	First reference; CP
Wrinklers Bridge	1959	38	1990	31	-	-	First inspection report
Reedy Creek Bridge	1959	38	1990	31	-	-	First inspection report
Princess River Bridge	1959	32	1991	32	-	-	Carbonation at testing
Symons Creek Bridge	1959	38	1990	31	-	-	First inspection report
Denison River Bridge	1960	38	1990	30	-	-	First inspection report
Boggy Creek Bridge	1960	40	1990	30	-	-	First inspection report
Tasman Bridge	1964	127	C1974	10	1976	12	Corrosion in Western
Cam River Bridge	1964	32	1990	26	1999	35	First report
Newmans Creek Bridge	1969	25	1991	22	1997	28	Pile cracking at first
Huon Highway Stock	1969	13	-	-	-	-	No file
Hunterston Culvert	1969	25	1993	24	-	-	First inspection report
Victoria Bridge	1970	28	1993	23	-	-	First inspection from
Grassy Wharf	1972	50	1980	8	1992	20	Extensive cracking
Freestone Point Road	1975	25	1991	16	-	-	First inspection report
Faulkners Rivulet Culvert	1976	25	1994	18	-	-	OK 1991
Cusicks Creek Culvert	1982	25	1994	12	-	-	OK 1991
Runnymede Culvert	1992	25	-	-	-	-	No corrosion distress
Burnie Port Access Bridge	1975	-	-	-	-	-	Cored with collision
Vale River Culvert	1986	25	1995	9	-	-	OK 1994
Deloraine Rail Underpass	1989	25	-	-	-	-	No distress 1995

Note: Design cover is minimum cover in most severe environment

Table 12.6 - Times to visible distress and remediation

8 TECHNICAL PAPERS

Modelling of Durability Performance of Tasmanian Bridges – International Conference on the Application of Statistics and Probability, Sydney, December 1999

Modelling of Chloride Ingress in Tasman Bridges – RILEM 2nd International Workshop on Testing and Modelling Chloride Ingress into Concrete, Paris, September 2000

Modelling of durability performance of Tasmanian bridges

R.W.M^{c}Gee
Asset Management Branch, Department of Infrastructure, Energy and Resources, Tasmania

ABSTRACT: The durability of concrete is a significant issue for asset owners throughout the world, particularly where structures are exposed directly to chlorides. This paper describes investigations of cover to reinforcement, chloride ingress and carbonation in bridges managed by the Tasmanian Department of Infrastructure, Energy and Resources and the application of the data to service life modelling of concrete structures. Enhancements in design and construction practices are proposed to increase the service lives of new structures.

1 INTRODUCTION

Tasmania is the southernmost State of Australia and is an island with an area of 68,332 square kilometres located around a latitude of 42^{0}S. The Tasmanian Department of Infrastructure, Energy and Resources (DIER) is the government agency responsible for the management of the State's classified road network and associated bridges, and previously had responsibility for a number of wharves and jetties. Concrete is the dominant material of construction for the structures, and a number of them have been affected by corrosion induced by chlorides from exposure to seawater, necessitating repairs or replacement. Data from the corrosion investigations used to determine appropriate management strategies for affected bridges and from sampling of other bridges have been analysed to assist with assessing the durability performance of and managing the overall bridge stock and to provide a basis for improving the durability of new structures.

2 TASMANIAN BRIDGE STOCK

At 1 July 1998, the bridge stock managed by DIER comprised 1158 bridges, major culverts and other civil engineering structures with an estimated replacement cost of A$1.1b. The distributions of bridge type by numbers and replacement cost are shown in Figures 1 and 2 which show that concrete, in the form of reinforced and prestressed concrete bridges and culverts, is the dominant material of construction. The average age of the bridge stock is 35 years.

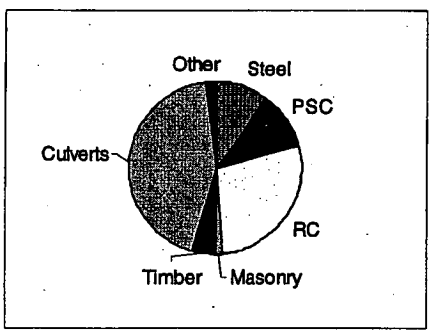

Figure 1 – Bridges by Number

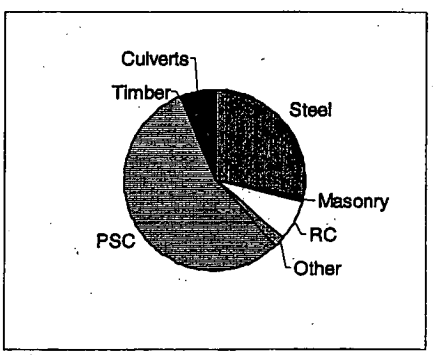

Figure 2 – Bridges by Replacement Cost

The Tasmanian climate is classed as temperate. Mean annual temperatures at bridge sites throughout the State range from 9^{0}C to 14^{0}C, with annual average rainfall between 760 and 2340 mm per annum.

3 CONCRETE DETERIORATION

Concrete is the most commonly used construction material throughout the world and generally performs well from both structural and durability perspectives. Reinforcing or prestressing is incorporated in most structures to address the low tensile capacity of concrete and is generally protected from corrosion by a thin layer of cover concrete, with the highly alkaline environment of the surrounding pore water creating a passive oxide layer. There is however a number of mechanisms by which concrete can degrade, either by corrosion of the steel or by deterioration of the concrete matrix. The primary distress mechanisms are summarised in Table 1.

Table 1 – Concrete Deterioration Mechanisms

Reinforcement corrosion	Chloride ingress Carbonation
Disintegration of matrix	Alkali aggregate reaction Sulphate attack Delayed ettringite formation Acid attack Freeze-thaw
Physical damage	Overloading Impact Abrasion

This paper discusses deterioration from reinforcement corrosion due to both chloride ingress and carbonation.

4 BRIDGE CONDITION

Figure 3 shows the distance of the bridge stock from the coastline in terms of both numbers and structures and their replacement cost (value), highlighting the high exposure to chlorides.

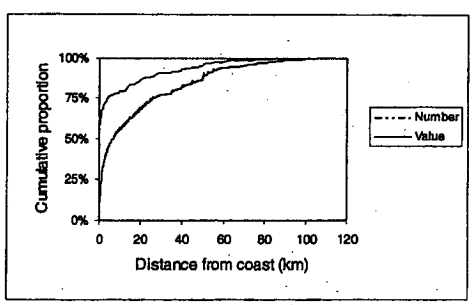

Figure 3 – Bridge Exposures

Because of the proximity to salt water and the age of the bridge stock, a number of the State's bridges are affected to some degree by one of more of the various deterioration mechanisms, particularly chloride ingress. Concrete durability is thus a significant issue for the Department with options for affected structures ranging from do nothing, through coatings, sealers and patch repair to cathodic protection and replacement.

Figure 4 – Chloride induced corrosion in a wharf structure

Corrosion investigations have been undertaken to determine appropriate management strategies for a number of structures, with those investigations including surveys of visual distress and concrete delamination, measurement of cover to reinforcement, concrete coring and analysis, half cell potential surveys and resistivity measurements. Data from the various studies and additional cover measurements have been collated and analysed, with the analysis providing the basis for this paper.

Locations of bridges for which corrosion investigations have been undertaken are shown in figure 5.

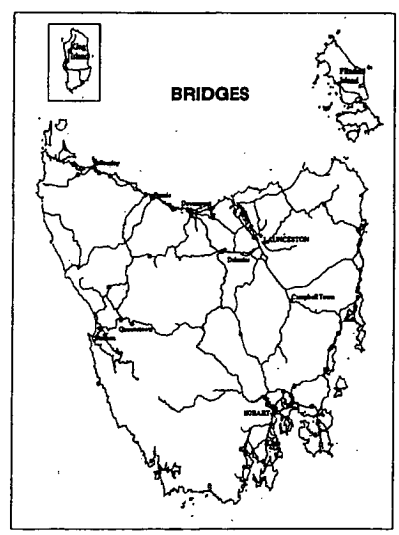

Figure 5 – Locations of surveyed bridges (corrosion investigations)

5 COVER TO REINFORCEMENT

5.1 *Background to research*

Durable concrete relies on the adequacy of both the quality and quantity of the cover concrete.

Tolerances on the placement of reinforcement from its specified position in structures in both specifications and codes have progressively increased from –0+5mm to –5+10mm over about the last 20 years. There is however strong evidence that even the increased tolerances are not generally achievable in practice (Kompen, 1997; Marrosszeky and Chew, 1990; Morgan et al, 1982; Ohta et al, 1992; Sirivivantnanon and Cao, 1991).

The published data and surveys of cover during and extensive program of testing on the Princess River Bridge on Tasmania's west coast during 1991 indicated that the reported variability in cover to reinforcement also occurred in the Tasmanian bridge stock. A program of collection and analysis of data on cover was thus initiated through cover surveys as part of the following processes:

- corrosion investigations
- acceptance audits at practical completion of bridge construction projects
- sampling of other bridges to provide statistically significant samples for longitudinal analysis.

5.2 *Surveyed structures*

Surveyed structures were built between 1931 and 1997 and represent the soope of the State's bridge stock, encompassing reinforced concrete T-beam bridges, steel girder bridges, concrete slabs, insitu and precast culverts, and prestressed concrete plank, I-beam and trough girder bridges. Figure 6 shows the distribution of sampled structures throughout Tasmania.

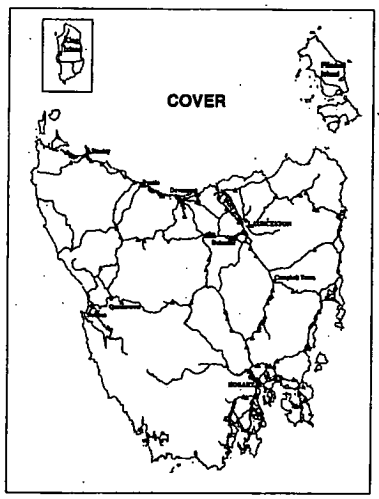

Figure 6 – Locations of surveyed bridges (cover surveys)

The number of cover measurements is summarised in Table 2.

Table 2 – Cover measurements

Description	No. structures	No. measurements
Insitu concrete	83	12,897
Precast elements	37	3,485
Precast box culverts	56	16,382
Total	143[1]	24,055

Note: 1. Some elements common to individual structures

5.3 *Analysis of data*

Preliminary analysis considered the accuracy of reinforcement placement, both in terms of the proportions of measurements complying with various tolerances and of the percentage exceeding various proportions of specified cover (N), given that the negative tolerances are relevant to the durability of structures. Results of the analysis are illustrated in figures 7 to 12.

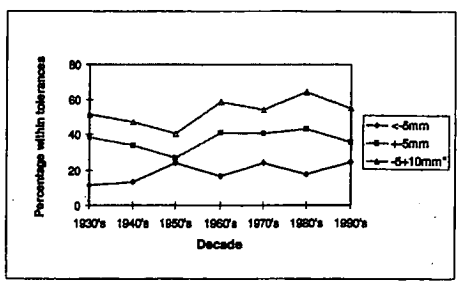

Figure 7 – Insitu Element Compliance

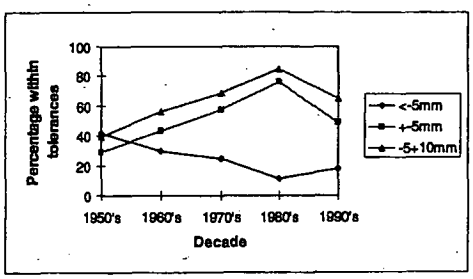

Figure 8 – Precast Element Compliance

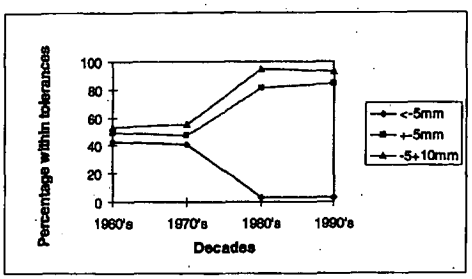

Figure 9 – Precast Culvert Compliance

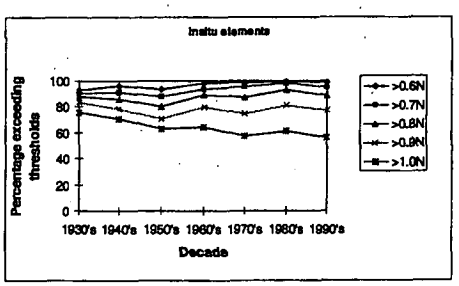

Figure 10 – Insitu Element Compliance

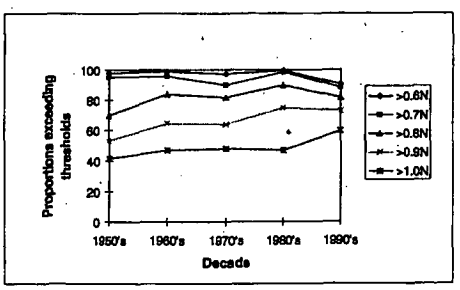

Figure 11 – Precast Element Compliance

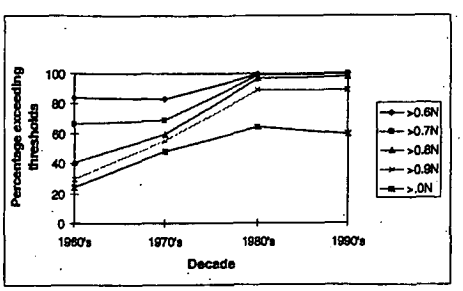

Figure 12 – Precast Culvert Compliance

Initial statistical analysis of data, normalised to a proportion of specified cover, was inconclusive and subsequent analysis disaggregated the data into insitu, precast and precast culvert element types and into nominal covers of 19, 25, 38 and 50mm. A sample frequency distribution for 50mm nominal cover for insitu elements, plotted with a normal distribution curve using the SPSS statistical software package, is shown in Figure 13. Tests for normality generally involved the use of normal quantile and probability plots. The analysis did not indicate a correlation between age and variability for the various subsets of the data.

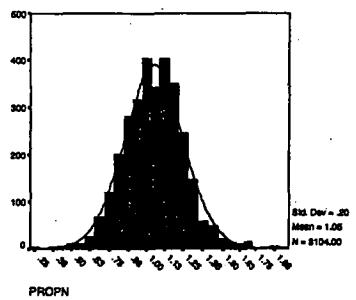

Figure 13 - Frequency distribution for 50mm nominal cover, insitu elements

Figures 14 to 16 show the mean and 5 and 95 percentile values of normal distributions fitted to the three structural categories and lines of best fit for a constant difference from the specified cover determined using least squares analysis.

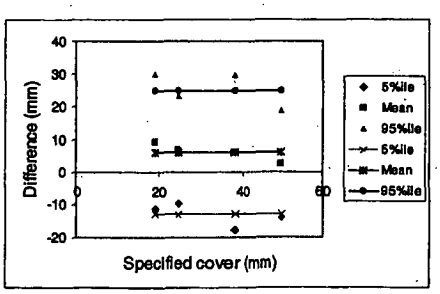

Figure 14 – Cover compliance, insitu elements

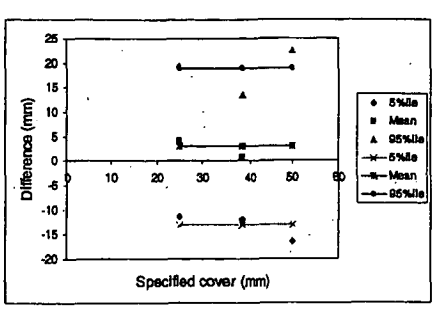

Figure 15 – Cover compliance, precast elements

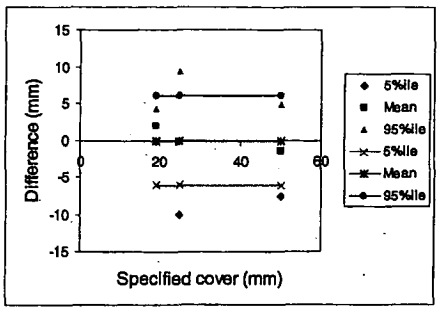

Figure 16 – Cover compliance, precast culverts

5.4 *Discussion and models for analysis*

The analysis showed that normal distributions could be used to describe the accuracy of placement of reinforcement, with the variability in cover being expressed in absolute values rather than being proportional to the quantum of specified cover. While it would be expected that specialisation in steel fixing and the introduction of quality assurance in the 1990's would lead to improved compliance with specifications and reduced variability, this was not found to be the case. Models used for subsequent analysis consequently consider only the form of construction and not the time at which it occurred.

The models are described in Table 3.

Table 3 – Cover models for analysis

Element type	Mean cover	Std deviation
Insitu	Specified + 6mm	11.5mm
Precast	Specified + 3mm	9.7mm
Precast culvert	Specified	3.6mm

6 CHLORIDES

6.1 *Chloride penetration models*

The penetration of chlorides into concrete is the result of a number of transport and binding processes, with concentrations at various depths being a time dependent function of environmental conditions, the design of a structure and its material properties. Chlorides which have penetrated and are in contact with the reinforcing or prestressing steel locally penetrate the passive oxide layer, triggering dissolution of the layer and thence the steel.

Below water level for structures located in salt water, environmental chloride concentrations are essentially uniform giving constant boundary conditions and thus the penetration of chlorides can be considered as a pure diffusion process. In tidal and splash zones however, where the most severe corrosion generally occurs, boundary conditions change as salt water splashes and is blown onto surfaces, rain water washes the surface free of chlorides and evaporation increases their concentration. Chlorides may also be present in the concrete mix from the aggregates, mixing water, admixtures and salt deposits on reinforcement.

While the penetration of chlorides into concrete is a complex process, it is commonly modelled using Fick's 2nd law of diffusion. For the purposes of this study, the apparent surface chloride concentration c_s and effective diffusion coefficient D are taken as constant and the chloride concentration c(x,t) at depth x and time t given by the common error function solution to Fick's law given in equation (1).

$$c(x, t) = c_s [1 - \mathrm{erf}(\frac{x}{2\sqrt{D.t}})] \quad (1)$$

6.1.1 *Chloride threshold concentration*

In laboratory tests, a chloride threshold for corrosion has been measured in terms of the chloride/hydroxyl ratio, with a ratio of 0.6 reported by Broomfield (1997). This approximates to a concentration of 0.4% of chloride by mass of cement if the chlorides are cast into the concrete, because of the effects of the cement hydration process, and 0.2% if they diffuse in. Studies by Clear (1974) suggest a threshold level of 0.2% by mass of cement. Other researchers have reported critical chloride concentrations between 0.06% and 2.02% by mass of cement (Petterson, 1992). Henriksen and Stoltzner (1993) found that 0.05% chloride by dry concrete weight was the minimum level for corrosion in reinforcement. On the basis of the published results and the cement contents of the mixes in the investigated bridges, service life modelling focussed on a threshold concentration of 0.05% by mass of concrete, with a sensitivity analysis up to 0.3%. Proportions by mass of concrete were used because of the correspondence with reporting from corrosion investigations.

6.2 *Analysis*

The corrosion investigations, which had been undertaken on 56 structures, had provided 241 chloride profiles for analysis. Chloride concentrations were determined as a proportion by mass of concrete using acid titration. Thicknesses were generally 20mm for the two slices closest to the surface, 30mm for the next two slices, and 40mm at greater depths, with chloride concentrations taken as being at the mid-point of the slice. Least squares analysis was used to determine c_s and D for each profile.

It was expected that, on the basis of published research, there would be a correlation between chloride penetration and other factors, particularly and cement content and water cement ratio. Correlations were not however found between c_s and D and any of the following factors: age, maturity, density, cement content, water cement ratio, compressive strength, Young's modulus, volume of permeable voids, annual rainfall, mean temperature, site humidity, chloride concentrations in the surrounding water, height above mean water level and the two parameters themselves. A relationship was identified between distance from the coast and the apparent surface chloride concentration. For structures directly in contact with salt water, the surface concentrations could be further subdivided into locations less than 2m above mean water level, and between 2m and 4m above mean water level. The number of samples from higher locations was insufficient to draw reliable conclusions. With tidal ranges in Tasmania ranging from 0.8m to 3.5m, the lower band is predominantly within the tidal range and the next in the splash zone. Figure 17 shows the relationship between the effective diffusion coefficient and cement content as an example of the lack of correlation.

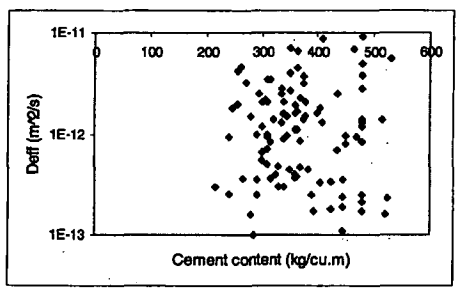

Figure 17 – Relationship between diffusion coefficient and cement content

Likely reasons for the lack of correlation include:

- variability in the concrete used for each structure, both within and between batches, with site batching likely to have been used for the majority of structures assessed
- variations in concrete properties within structural elements
- variations in cement compositions and grinding practices
- effects of placing and compacting concrete
- differences in finishing and curing
- environmental differences between structures
- effects of securing cores
- the use of different cores for the various tests
- accuracies of the various test methods
- effects of the curve fitting process.

Variability in concrete proportioning is illustrated in Figure 18, which shows the variation in measured cement contents for structures with a nominal cement content of 330 kg/m^3, being a 1:2:4 mix. The mean value is 341 kg/m^3 and the standard deviation 55 kg/m^3. Similar variabilities occurred with water cement ratio.

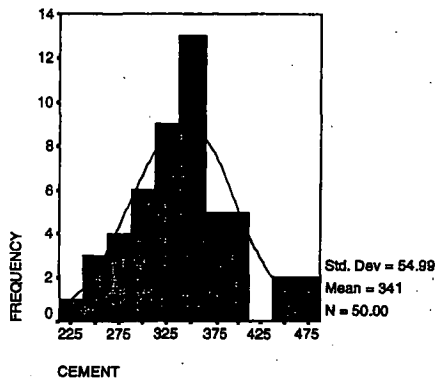

Figure 18 - Cement Contents

6.3 *Models for analysis*

In the absence of correlations with the various factors considered, the model adopted for the effective diffusion coefficient was a lognormal distribution, with a mean of –12.0 and standard deviation of 0.48 for the transformed values. The mean value equates to a diffusion coefficient of 1.0×10^{-12} m/s^2.

Parameters adopted for apparent surface concentrations are given in Table 4, with the concentrations being normally distributed.

Table 4 – Apparent chloride surface concentrations

Distance from coast ,d(km)	Height (m)	c_s (%m/m)	COV (%)	N
0	<=2	0.380	65.3	102
0	>2, <=4	0.148	71.5	62
0.1 to 2.84	All	-0.0729ln(d) +0.1161	48.7	16
>2.84	All	0.04	48.7	10

7 CARBONATION

Carbonation occurs when carbon dioxide from the atmosphere reacts with calcium hydroxide produced from the cement hydration reactions. As a result, the pH of the pore solution decreases with the potential to affect the passive oxide layer on the surface of the steel, leading to corrosion. In solution, the reaction between calcium hydroxide and carbon dioxide is rapid, and thus the carbon dioxide is unlikely to penetrate beyond pores in the cement paste which contain calcium hydroxide. A distinct boundary, known as the 'carbonation front', between reacted and unreacted calcium hydroxide thus forms

facilitating the accurate measurement of carbonation depth, typically with phenolpthalein solution. Measurements using the technique on freshly split cores were been used for the investigation.

Previous research has identified relationships between the depth of carbonation and age, water cement ratio, and concrete compressive strength. As with the analysis of chloride penetration, it was not however possible to identify a correlation between the depth of carbonation and the various factors considered. The analysis did show that a normal distribution could be used to describe kin equation (2).

$$X = k\sqrt{t} \qquad (2)$$

where X = carbonation depth
t = age
k = carbonation parameter

The mean value of k is 2.01 mm/yr$^{1/2}$ with a standard deviation of 1.24.

8 SERVICE LIFE MODELLING

8.1 *Definition*

The service life of a concrete structure can be defined by a number of criteria, which include:

- initiation of corrosion
- corrosion products becoming visible on the surface of the concrete
- cracking and spalling due to concrete corrosion
- compromising of public safety due to spalling concrete falling from a structure
- loss of structural capacity due to corrosion compromising public safety
- adverse aesthetic impacts of rust staining
- public perceptions of reduced safety arising from staining, cracking and spalling
- the minimum period for which the structure can be expected to perform its intended function, without significant loss of utility and not requiring too much maintenance (Somerville, 1986).

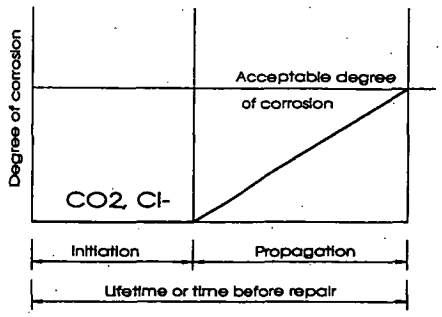

Figure 19 – Tuutti Corrosion Model

The Tuutti model in figure 19 is commonly used to describe corrosion processes in concrete. During the propagation phase, the corrosion rate is controlled by the rate of oxygen diffusion to the cathode, resistivity of the pore solution and temperature. Evaluations of corrosion rates and the effects of corrosion on structural capacity are beyond the scope of this paper. The time for initiation and propagation can be short, with extensive cracking and delamination having occurred in one structure within 8 years of completion.

Because of the aggressive nature of chloride induced corrosion, possible adverse effects on the mechanical properties of prestressing and reinforcing steel and the complexity of calculations and lack of data associated with the propagation phase, this paper defines service life as the time to initiation.

Deterministic modelling used the mean values of the relevant parameters (cover, apparent surface chloride concentration, effective diffusion coefficient, carbonation parameter).

Probabilistic modelling used the principles of limits states and structural reliability. In structural terms, the failure of an element occurs when the load effect (S) exceeds the resistance (R). Reliability can thus be expressed as a probability of failure (p_f) or 'reliability index' (β), defined as:

$$\begin{aligned} p_f &= \Phi(-\beta) \\ &= \Pr(R \le S) \\ &= \Pr(R-S \le 0) \\ &= \Pr(G(R,S) \le 0) \\ &= \int_0^\infty F_R(r) f_s(r) dr \end{aligned}$$

where Φ is the standard normal distribution function, G() is the 'limit state function' [which is equal to R-S in this case], $f_s(R)$ is the probability density function of the load and $F_R(R)$ is the cumulative probability density function of the resistance. For the purposes of the analysis, the load effects are those of chloride or carbon dioxide penetration and

the resistance is the cover to reinforcement so that the probability of failure is the proportion of reinforcement for which chloride concentrations exceed the threshold or where the carbonation front has reached the reinforcement. Both chloride ingress and carbonation are time dependent, while reinforcement location is fixed. Simulation software, using the Latin hypercube technique, was used for the probabilistic analysis.

8.2 *Chloride modelling*

8.2.1 *Deterministic modelling*

Figure 20 shows, for structures in direct contact with salt water, the expected time to initiation of corrosion for a range of specified covers and chloride threshold concentrations. It indicates that a 100 year service life with a threshold concentration of 0.05% requires a specified cover of the order of 126mm; alternatively a 100 year service life would be achieved with a specified cover of 88mm for a threshold concentration of 0.1% and a cover of 63mm for a concentration of 0.15%.

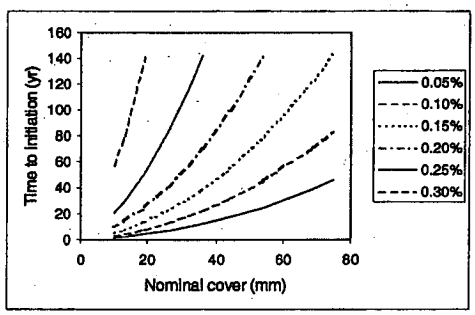

Figure 20 – Effect of Threshold Concentration on Time to Initiation for Corrosion due to Chlorides

Figure 21 shows the effect of distance from the coast to time to initiation for a threshold concentration of 0.05%. It indicates that, to achieve a 100 year service life, specified covers of 80mm, 58mm and 40mm would be required at distances from the coast of 0.5km, 1km and 1.5km respectively.

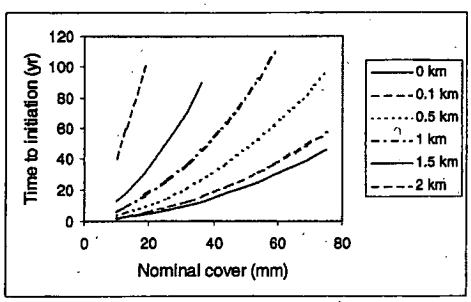

Figure 21 – Effect of Distance from Coast on Time to Initiation of Corrosion due to Chlorides

8.2.2 *Probabilistic modelling*

The probability of corrosion for insitu elements directly exposed to chlorides for a range of specified covers and ages is shown in figure 22. It highlights the high probability of corrosion (45% to 90%) in chloride rich environments arising from the variability in the concrete and cover parameters. Increasing the threshold concentration to 0.3% by mass of concrete reduces the probability of corrosion range to between 10% and 50%. The probability of corrosion similarly reduces as the distance from the coast and/or height above mean water level increase, but remains comparatively high. Probabilities of corrosion for precast elements and culverts are also high.

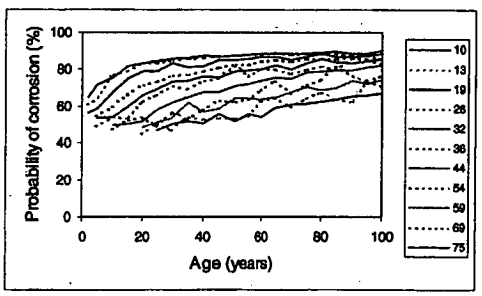

Figure 22 - Probability of Corrosion of Insitu Elements due to Chlorides, Distance from coast 0, Height ≤ 2m, Threshold Concentration 0.05%

8.3 *Carbonation*

8.3.1 *Deterministic modelling*

Figure 23 shows the expected time to initiation of corrosion due to carbonation of the cover concrete for insitu and precast elements and for precast culverts. It indicates that a service life of 100 years would be achieved using specified covers of 15mm, 17mm and 20mm for insitu and precast elements and precast culverts respectively.

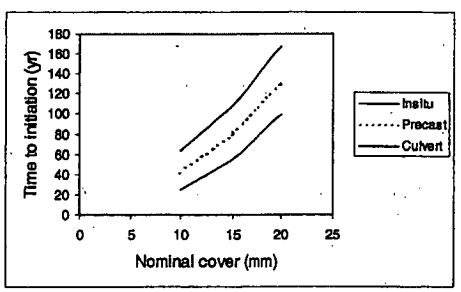

Figure 23 – Time to Initiation for Carbonation

8.3.2 *Probabilistic modelling*

As with probabilistic modelling of chloride induced corrosion, figure 24 shows comparatively high probabilities of corrosion due to carbonation, with a 62% probability of corrosion for 10mm speci-

fied cover at 100 years with insitu elements. Probabilities are slightly higher for precast elements and culverts because the mean value of cover is closer to the specified value than for insitu elements. By contrast with chloride induced corrosion however, probabilities of corrosion approach zero for specified covers of the order of 50mm or more.

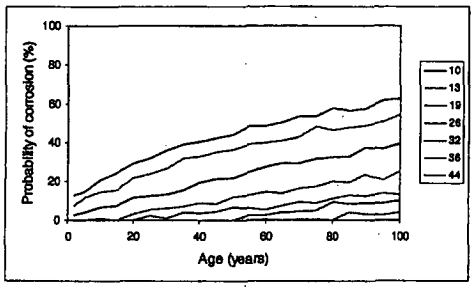

Figure 24 - Probability of Corrosion for Insitu Elements due to Carbonation

8.4 *Discussion*

Bridge structures in Australia have a nominal design life of 100 years, which is based on an acceptable probability of structural failure. Probabilities are generally expressed through the safety or reliability index, β, with the objective of code calibration being to achieve uniform failure probabilities for a range of load combinations and mechanisms. Eurocode 1 is based on a risk of failure of 7×10^{-5} for a life of 50 years, equating to a value of β of 3.8. This would imply that safety indices for materials aspects should be comparable with those for structural aspects, depending upon the consequences of failure.

By contrast, the investigation has found that probabilities of initiation of corrosion in bridges exposed to chlorides exceed 10%, meaning that values of β are less than 1.3 and are in many cases negative. The likelihood of corrosion due to carbonation is similarly high.

The acceptable probability of corrosion occurring is however likely to be higher than that for failure from structural effects as there will usually be visual signs of corrosion well before there are significant safety implications. Bamforth (1999) proposes a probability at the onset of corrosion of 10^{-2} ($\beta = 2.3$). A conservative approach is nevertheless required with prestressed structures because of the probability of chloride related embrittlement of the steel.

Implications of the high probabilities of initiation of corrosion are primarily economic because of the need to implement remedial measures, such as the installation of cathodic protection systems, before corrosion leads to significant reductions in structural capacity. The analysis also indicates that the economic lives of structures exposed to chlorides are likely to be determined by material, rather than structural, factors.

Analysis of concrete samples has generally involved structures more than 20 years old. In many cases, concrete would have been site batched leading to variability within and between batches. The influence of premixed concrete used in contemporary structures in reducing that variability was not assessed as part of the study. Other possible contributory factors in the variability include differences in properties within elements, effects of placing and compaction, differences in finishing and curing, environmental differences between structures, effects of securing cores and the use of different cores for the various tests.

While the general use of premixed concrete and increases in specified cement contents to enhance durability are expected to reduce the penetrability of the cover concrete, subject to adequate curing, the accuracy of reinforcement placement across decades is consistent and its high variability would be expected to lead to relatively high probabilities of initiation of corrosion in more recent structures because of the proportions of reinforcing bars with high negative tolerances. It is considered unlikely that enhancements in concrete properties to date would be sufficient to reduce probabilities of initiation of corrosion to a level consistent with those for structural failure or those proposed by Bamforth.

Achievement of an appropriate corrosion related reliability of structures, particularly those exposed to chlorides, is likely to require consideration of a number of strategies, including:

- the use of supplementary cementitious materials
- effective curing
- protection of concrete from initial contact with chlorides
- incorporation of corrosion inhibitors, such as calcium nitrite, in concrete mixes to increase the corrosion threshold concentration
- developments in reinforcing spacers to truncate the negative tolerances for cover
- recognition of variability in specifying cover to reinforcement for both insitu and precast elements
- use of stainless steel reinforcing
- the use of cathodic prevention
- enhancements in construction, supervision and quality assurance practices
- changes in design approaches from a menu type qualitative approach to one which more closely parallels a structural design approach.

This paper has only considered chloride and carbonation induced corrosion of reinforcing steel. Enhancements in design practices would also need to include the other concrete deterioration mechanisms.

9 SUMMARY AND CONCLUSIONS

The Tasmanian Department of Infrastructure, Energy and Resources is responsible for the management of a significant bridge stock, with much of it exposed directly to chlorides. Data from investigations into the durability performance of a number of structures have been analysed to assist with managing the existing bridge stock and as a basis for improvements in new structures.

The investigation showed high variability in materials properties related to chloride ingress and carbonation and in the placement of reinforcement leading to relatively high probabilities of initiation of corrosion.

Enhancements in design and construction practices so that materials related reliabilities are consistent with those for structural aspects are proposed.

10 ACKNOWLEDGMENTS

The permission of the Secretary of the Department of Infrastructure, Energy and Resources to publish this paper is gratefully acknowledged. The views expressed are however those of the author and do not necessarily reflect those of the Department.

REFERENCES

Bamforth P. 1999. Double standards in design. In *Concrete*. The Concrete Society. Slough. UK

Broomfield J P. *Corrosion of Steel in Concrete – Understanding, investigation and repair*. E & FN Spon. London. UK

Browne R D. 1988. Carbonation. *In Manual for Life Cycle Aspects of Concrete in Buildings and Structures*. Taywood Engineering. Perth. Western Australia

Bureau of Meteorology. 1993. *Climate of Tasmania*. Commonwealth of Australia. Canberra. Australia

Clear K C. 1974. *Evaluation of Portland Cement Concrete for Permanent Bridge Deck Repair*. Federal Highway Administration. USA

Henriksen C F and Stoltzner E. 1993. Chloride Corrosion in Danish Road Bridge Columns. In *Concrete International*. American Concrete Institute. USA

HETEK. 1996. *Chloride penetration into concrete - State of the art - Transport processes, corrosion initiation, test methods and prediction models*. The Road Directorate. Copenhagen. Denmark

Kompen R. 1997. *How to Achieve Proper Reinforcement Cover in Concrete Bridges – New Specifications*. Road Research Laboratory. Public Roads Administration, Norway

Marrosszeky M and Chew M. 1990. *Site Investigation of Reinforcement Placement on Buildings and Bridges*. Concrete International. American Concrete Institute. USA

Melchers R. 1987. *Structural Reliability – Analysis and Prediction*. Ellis Horwood Limited. Chichester. UK

Morgan P R, Ng T E, Smith H M N and Base G D. 1982. *How Accurately can Reinforcing Steel be Placed? Field Tolerance Measurement Compared to Codes*. Concrete International. American Concrete Institute. USA

Ohta T, Sakai K, Obi M and Ono S. 1992. *Deterioration in a Rehabilitated Prestressed Concrete Bridge*. ACI Materials Journal. American Concrete Institute. USA

Petterson K. 1992. *Corrosion Threshold Value and Corrosion Rates in Reinforced Concrete*. Swedish Cement and Concrete Research Institute. Stockholm. Sweden

Sirivivantnanon V and Cao H T. 1991. *Quality Assurance of Concrete Structures – Analysis of Insitu Concrete Cover*. Civil Engineering Transactions. The Institution of Engineers, Australia.. Canberra

Somerville G. 1986. The Design Life of Concrete Structures. In The Structural Engineer Vol 64A No.2. Institution of Structural Engineers. UK

MODELLING OF CHLORIDE INGRESS IN TASMANIAN BRIDGES

Rod M°Gee
University of Tasmania and Department of Infrastructure, Energy and Resources, Australia

Abstract
The durability of concrete structures is a significant issue for asset owners throughout the world. The Department of Infrastructure, Energy and Resources of Tasmania, Australia is responsible for the management of a large number of concrete bridges and major culverts with many located in close proximity to salt water. Corrosion is evident in many structures and the Department has an ongoing program of cathodic protection, replacement, repair and applying coatings and penetrating sealers to address corrosion related defects. Chloride induced corrosion is the dominant deterioration mechanism.

Data from corrosion investigations of affected structures and surveys of others have been used to develop models for the durability related performance of the bridge asset to assist with its management. Chloride ingress has been described in terms of Fick's 2nd law of diffusion. Comparable models have also been developed for cover to reinforcement and deterministic and probabilistic models for corrosion initiation developed. Variability in the parameters used for modelling leads to high probabilities of corrosion initiation for structures exposed to chlorides. Those probabilities are consistent with the observed performance of the bridge asset.

Fax: +(61)362336657
E-mail:rod.mcgee@dier.tas.gov.au

1. Introduction

Concrete durability is a significant issue for asset owners throughout the world. The Department of Infrastructure, Energy and Resources (DIER) of Tasmania, Australia is the State road authority responsible for the management of a large number of concrete bridges and box culverts. Many of those structures are affected by chloride induced corrosion of reinforcing and prestressing steel, with examples of other forms of concrete deterioration including carbonation damage, alkali aggregate reaction and freeze thaw damage also present. An ongoing program of replacement, cathodic protection, sealing, coating and repair has been established for existing structures. The durability of new structures is also being addressed.

Corrosion investigations have been undertaken for almost 60 structures to assist with the development of management strategies and, where cathodic protection systems are adopted for chloride induced corrosion, to assist with design. The investigations typically involve visual, crack, delamination, cover and half-cell potential surveys, resistivity measurements and concrete coring with subsequent analysis of strength, density, cement content, water cement ratio, carbonation depth and chloride ingress. The majority of investigations have been undertaken for chloride affected structures.

This paper describes the modelling of the ingress of chlorides in Tasmanian bridges using data from the corrosion investigations.

2. Background to research

The bridge asset managed by DIER comprises over 1100 bridges and major culverts with an estimated replacement cost of approximately US$700m. Concrete is the dominant material of construction. Reinforced and prestressed concrete bridges and reinforced concrete box culverts comprise over 80% by number and approximately 70% by value of the asset, which has an average age of 35 years. As an island state with much of its population located close to the coastline, there are many larger bridges crossing tidal estuaries and about 1/4 by number and 2/3 by value of the asset is located within 1km of direct contact with salt water. 4% by number and 26% by value of the bridge stock is affected by significant corrosion of concrete. Many more bridges have some evidence of concrete deterioration. A number of bridges have been replaced and 8 cathodic protection systems installed to date to address corrosion related defects. The ongoing program of addressing deterioration has significant financial and resource implications.

Corrosion investigations, measurements of new structures at the time of completion and surveys of other bridges have provided comprehensive data for analysis to better understand the likely performance of the asset, to help predict the future demand for remedial measures and improve the expected performance of new structures.

Fax: +(61)362336657
E-mail:rod.mcgee@dier.tas.gov.au

3. Samples for analysis

Corrosion investigations on 56 structures provided 241 chloride profiles for analysis. The structures were built between 1932 and 1976, with ages at coring ranging from 62 to 20 years. Samples for measurement of chloride concentrations were generally 75mm diameter cores, with the remainder being dust samples. Chloride concentrations were determined as a proportion by mass of concrete using acid titration. As the samples were taken for the purposes of developing management strategies for affected structures and possible design of cathodic protection systems rather than research, slices from cores for chloride analysis were typically 20mm for the first two slices, 30mm for the next two, and 40mm at greater depths, with chloride concentrations taken as being at the mid-point of the slice.

Figure 1 shows the state of Tasmania and locations of structures of bridges for which corrosion investigations have been undertaken and highlights the proximity to the coastline of the majority of affected structures.

Figure 1 – Locations of surveyed bridges

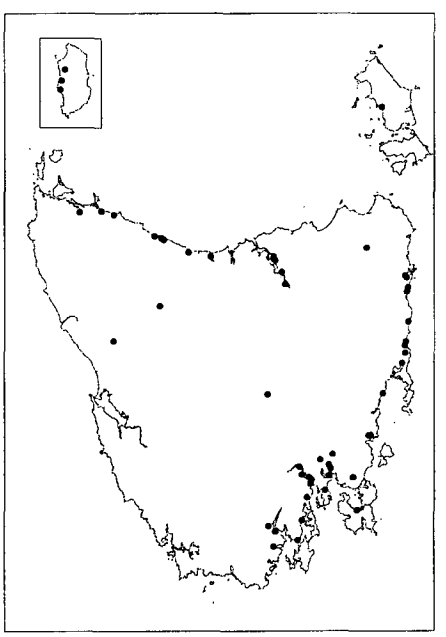

Fax: +(61)362336657
E-mail:rod.mcgee@dier.tas.gov.au

4. Chloride profiles

While the penetration of chlorides into concrete is a complex process, involving a number of transport and binding processes, it is commonly modelled using Fick's 2nd law of diffusion. For the purposes of the study, the apparent surface chloride concentration c_s and the effective diffusion coefficient D were assumed to be constant and the chloride concentration c(x,t) at depth x and time t given by the common error function solution to Fick's law given in equation (1).

$$c(x,t) = c_s\left[1 - erf\left(\frac{x}{2\sqrt{D.t}}\right)\right] \quad (1)$$

Least squares numerical curve fitting was used to determine c_s and D for each of the measured profiles. It is noted that the modelling of chloride ingress was an intermediate step, together with analysis of measurements of cover to reinforcement, in assessing expected times to and probabilities of corrosion initiation in accordance with Tuutti's model (Tuutti, 1982) and that any form of curve fitting could have been used. The use of Fick's law however provided values of surface chloride concentrations and diffusion coefficients that could be compared with other published results.

A skin effect (Andrade et al, 1997), in which a maximum chloride content is exhibited some millimetres inside the outer surface or an anomalously high concentration occurs at the surface, was observed in some cores. The effect can be modelled by using a two layer model. Anomalously high surface concentrations were not observed in any of the cores. Where a skin effect was observed, as shown in Figure 2, the surface layer was not included in the curve fitting to facilitate the subsequent modelling of chloride concentrations at the level of the reinforcement.

Figure 2 – Typical chloride profile

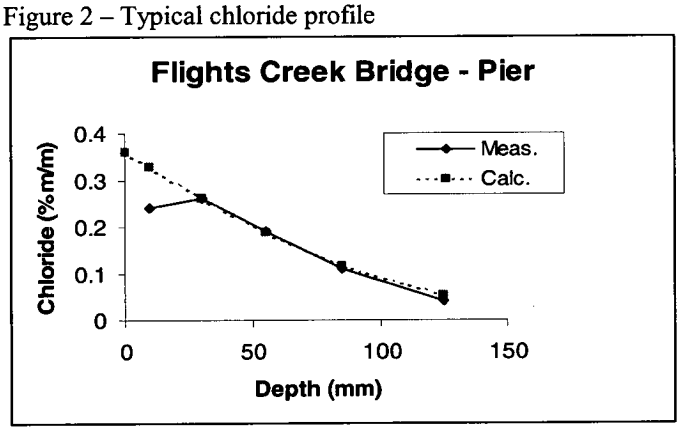

Fax: +(61)362336657
E-mail:rod.mcgee@dier.tas.gov.au

The two parameters, c_s and D, were examined for possible correlations with the following factors reflecting both concrete properties and environment:

- age
- concrete density
- cement content
- water cement ratio
- concrete strength
- concrete maturity
- Young's modulus
- permeable voids ratio
- height above mean water level
- distance from the coast
- chloride concentration in water at the bridge site
- annual rainfall at bridge site
- mean temperature at bridge site
- site humidity.

Estimates of 28 day compressive strength were made using data presented by Washa et al (1989), Wood (1991) and Taylor (1977) and comparisons of compressive strengths of cylinders cast at the time of construction of Tasmanian bridges built in 1938, 1942, 1944, 1946 and 1989 with cores taken at the time of investigation.

At the times of construction of the bridges involved in the study, Tasmania did not have ready access to supplementary cementitious materials (SCM's) and their use was limited to specific projects for other authorities where factors such as heat generation in massive concrete structures were an issue. The use of SCM's was also precluded in DIER specifications at the time of construction of the bridges, and the majority were built by direct labour. It is considered likely that all the structures in the study incorporated plain cement binders.

Tasmania is located around a latitude of 42^0S and has a cool temperate climate. Mean annual temperatures at sites of bridges for which corrosion investigations were undertaken range from 9^0C to 13^0C with mean humidities in the localities ranging from 63% to 76%. Days on which frost may occur range from nil to 120. Only limited parts of the network however are subject to snow. These are generally lowly trafficked roads and disruption is limited to a maximum of a few days. Deicing salts are consequently not used and chloride exposure arises from direct contact with seawater or associated airborne salts. Tidal ranges in Tasmania vary from 0.9m to 3.5m. There may be some isolated cases of calcium chloride being used as a set accelerator.

Fax: +(61)362336657
E-mail:rod.mcgee@dier.tas.gov.au

Figure 3 – Relationship between D and water cement ratio

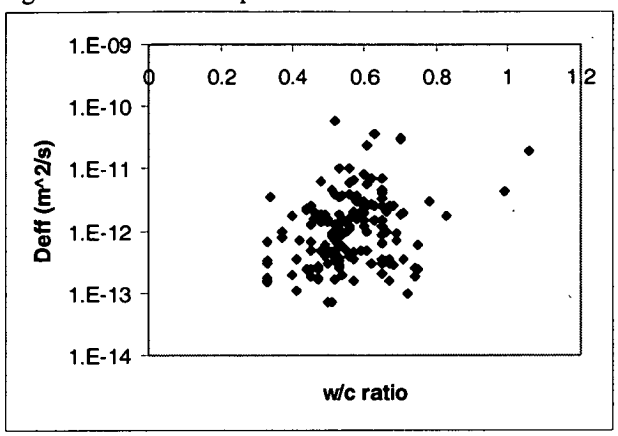

Analysis did not indicate any correlation between the surface chloride concentration and the diffusion coefficient and the factors age, density, cement content, water cement ratio, concrete strength, concrete maturity, Young's modulus, permeable voids ratio, rainfall, temperature, humidity and chloride concentration in the water at the bridge site. Figure 3 shows the relationship between the effective diffusion coefficient and water cement ratio; plots for the other factors examined were of similar form.

Figure 4 – Relationship between apparent surface chloride concentration and height above MWL (All cores)

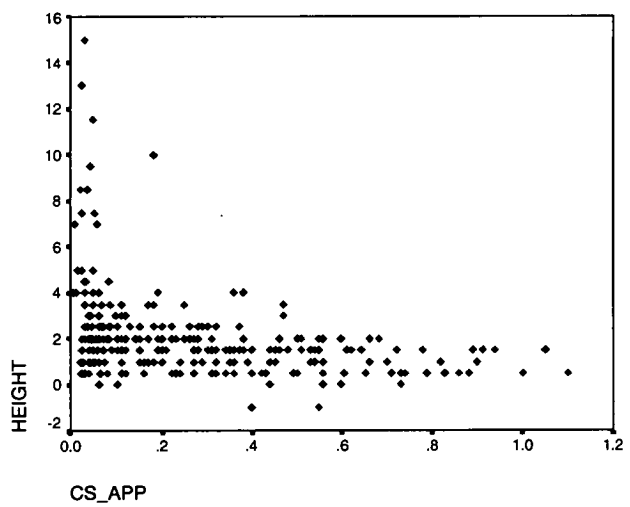

Fax: +(61)362336657
E-mail:rod.mcgee@dier.tas.gov.au

Figure 4 plots apparent surface chloride concentration against height above mean water level for all cores. Relationships were found between the surface chloride concentration, height of the core above mean water level and distance from coast using subsets of the full data set. Results of the analysis are shown in Table 1. Irregular profiles in the cores that were excluded from the subsets may have been attributable to factors such as cracking in the vicinity of the sample permitting other ingress paths for chlorides or the accuracy of measurement and curve fitting at relatively low chloride concentrations.

Table 2 shows the results of similar analysis for diffusion coefficients. For distances of at least 3km from the coast, apparent surface chloride concentrations were small and generally below a value of 0.05% by mass of concrete

Fax: +(61)362336657
E-mail:rod.mcgee@dier.tas.gov.au

Table 1 – Apparent surface chloride concentrations (%m/m)

Data set	Mean	SD	COV (%)	Range	N
All cores	0.273	0.251	91.9	0.01 – 1.10	264
Subsets of data					
• Irregular chloride profiles excluded	0.380	0.248	65.3	0.05-1.05	102
• Distance from coast 0km, height above MWL ≤ 2m	0.464	0.253	54.5	0.08-1.10	62
• Distance from coast 0km, 2m ≤ height above MWL ≤ 4m	0.207	0.148	71.5	0.05-0.42	16
• Distance from coast 0.1km	0.287	0.136	47.4	0.10-0.50	12
• Distance from coast > 0.5km (0.6-0.8km)	0.135	0.024	17.8	0.11-0.16	4

Table 2 – Chloride diffusion coefficients (m^2/s)

Data set	Mean[1]	SD[1]	Range[1]	N
All cores	-11.9	0.60	-13.2 to –10.0	241
Subsets of data				
• Irregular chloride profiles excluded	-12.0	0.48	-13.0 to –11.0	102
• Distance from coast 0km, height above MWL ≤ 2m	-11.9	0.46	-12.8 to –11.0	62
• Distance from coast 0km, 2m ≤ height above MWL ≤ 4m	-12.2	0.43	-12.7 to –11.3	16
• Distance from coast 0.1km	-12.2	0.47	-13.0 to –11.5	12
• Distance from coast > 0.5km	-12.2	0.41	-12.6 to –11.8	4

Note: 1. $\log_{10}$ transform

5. Models for analysis

As noted previously, chloride diffusion parameters were derived as an intermediate step in estimating the expected time to and probabilities of initiation of corrosion in accordance with Tuutti's model.

The subsets in Table 2 indicate a consistent value of diffusion coefficient. For the purposes of the subsequent modelling, D was taken to have a lognormal distribution, with a mean of –12.0 and standard deviation of 0.48 for the transformed values. The mean value equates to a diffusion coefficient of 1.00×10^{-12} m^2/s.

Fax: +(61)362336657
E-mail:rod.mcgee@dier.tas.gov.au

Parameters adopted for the apparent surface chloride concentration are detailed in Table 3. Note that there is a discontinuity between 0 and 0.1km. A logarithmic curve provides an estimate of surface chloride concentration for structures between 0.1km and 2.84km from the coast. Probability distributions are normal.

Table 3 – Apparent surface chloride concentrations (%m/m)

Distance from coast, d (km)	Height above MWL (m)	c_s (%m/m)	COV (%)
0	< 2	0.380	65.3
0	> 2, < 4	0.148	71.5
0	> 4	0.116	79.0
0.1 to 2.84	All	-0.0729ln(d) + 0.116	48.7
>2.84	All	0.04	48.7

6. Discussion

The values of surface chloride concentration and diffusion coefficient are consistent with published data reported by Bamforth (1996) from laboratory tests, natural exposure trials and structures up to 60 years old. Mean surface chloride concentrations ranged from 0.11 to 0.82% m/m. He suggested the use of effective diffusion coefficients in the range of $5x10^{-12}$ m^2/s to $1x10^{-13}$ m^2/s for design purposes.

The results are characterised by high variability, indicated by the coefficients of variation. Similar variability was found in the examination of other physical and compositional properties of the hardened concrete and is likely to be attributable to a number of factors, including:

- variability in the concrete manufactured for each structure, both within and between batches
- variations in cement compositions and grinding practices over the period of construction of the bridges; as discussed previously it is unlikely that supplementary cementitious materials were used in any of the structures
- effects of placing and compacting the concrete
- effects of differences in finishing and curing, including differences in weather
- differences in local environments between structures
- effects of securing cores
- cracking or other damage to cores
- the use of different cores for different tests, so that chloride profiles were not measured on the same cores as those used for determining cement content, water cement ratio, strength or permeable voids ratio
- accuracies of the various test methods

Fax: +(61)362336657
E-mail:rod.mcgee@dier.tas.gov.au

- the effects of the curve fitting process used to calculate the diffusion parameters.

In particular, it had been expected that there would be a degree of correlation between diffusion coefficient and cement content and/or water cement ratio.

A review of drawings and other documentation for the bridges involved in the study showed that most did not have job specific specifications. For those where concrete composition or strength were specified, a 3000 psi/20 MPa concrete mix using a 4:2:1 coarse aggregate:fine aggregate:cement ratio was commonly used, although specified strengths ranged from 10.4 MPa (1500 psi) to 44.9 MPa (6500 psi). Compressive strengths are for 150mm diameter by 300mm high cylinders. Virtually all of the structures were built by direct labour using site batched concrete and it is likely that similar mix designs were used for the various bridges. This is reflected in the analysis of measured cement contents which can reasonably be represented by normal distributions for all samples (mean 355 kg/m^3, standard deviation 70 kg/m^3, N=273) and or for those which were specified as a 4:2:1 mix (mean 341 kg/m^3, standard deviation 50 kg/m^3, N=70). Variations of up to 185 kg/m^3 were observed in measured cement contents for one structure. Water contents of 245 analysed cores could similarly be represented by a normal distribution with a mean of 195 l/m^3 and standard deviation of 26.2 l/m^3. The mean water cement ratio of 0.57 is high by contemporary standards and is likely to reflect the absence or limited availability of water reducers at the time of construction of and the need to use water to provide adequate workability, especially where the bridges predated the ready availability of powered compaction equipment.

The analysis indicated that similar mixes had been used for the structures involved in the study and it was considered that the variability in and between mixes and the use of different cores for different tests would outweigh the probable small differences in nominal cement contents and obviate the likelihood of identifying the expected correlation. Increases in specified cement contents for Departmental bridges did not occur until the 1980's as awareness of durability deficiencies in concrete structures increased.

It is nevertheless likely that the variability in the properties and performance of concrete in the structures is indicative of the inherent variability of concrete as a material.

Analysis of a large number of measurements of cover to reinforcement also showed high variability. For insitu bridge elements, approximately 50% of measurements complied with a tolerance of –5+10 mm on specified cover, with the compliance consistent for structures built from the 1930's through to the 1990's. The –5+10 mm tolerance is embodied in current Australian codes for concrete design and construction. For 90% compliance, a tolerance range of –15+25mm would be required. The variability was found to be independent of specified cover, which ranged from 13mm to 100mm. The 90% compliance range for precast bridge components was –15+20mm.

Fax: +(61)362336657
E-mail:rod.mcgee@dier.tas.gov.au

Figure 5 – Probabilities of initiation of corrosion for specified covers, distance from coast 0km, height ≤ 2m, threshold concentration 0.05%

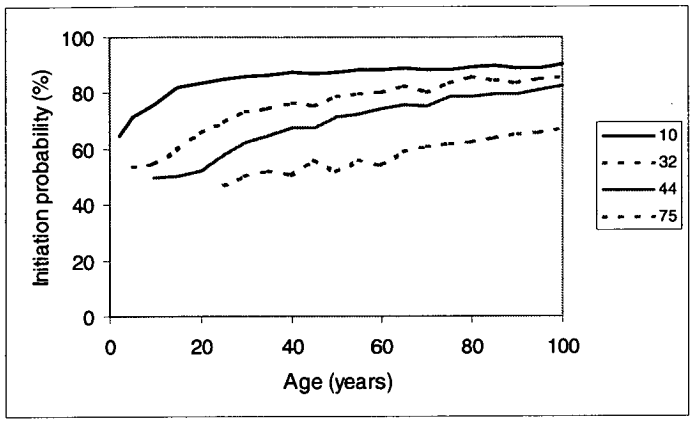

Probabilistic modelling showed high probabilities of corrosion initiation for structures exposed to chlorides, even with relatively large specified covers to reinforcement, because of the variabilities in the modelling parameters for chloride ingress and cover. Figure 5 shows probabilities of corrosion initiation for elements in the tidal zone with specified covers of 10, 32, 44 and 75mm. The results of the modelling were consistent with the observed frequency of corrosion related defects in the bridge stock. For concrete elements in contact with salt water less than 2m above mean water level, a specified cover of 50mm and a threshold concentration of 0.05% by mass of concrete, the expected time to initiation of corrosion was 22 years with a probability of corrosion initiation at 100 years of 78%.

7. Conclusions

Concrete durability is a major issue for asset owners throughout the world. Activities undertaken as part of the investigation of corrosion affected structures can provide a body of data for modelling to assist with the management of concrete assets.

Analysis of such data shows significant variability in the physical properties of concrete and the parameters used to model chloride ingress. That variability leads to high expected probabilities of corrosion initiation, which is consistent with the observed performance of the structures.

Fax: +(61)362336657
E-mail:rod.mcgee@dier.tas.gov.au

8. References

1. Andrade C, Diez J M and Alonso C, 'Mathematical Modelling of a Concrete Surface Skin Effect on Diffusion in Chloride Contaminated Media', Advanced Cement Based Materials, (Elsevier Science Ltd, USA, 1997;6)

2. Bamforth P B, 'Definition of Exposure Classes and Concrete Mix Requirements for Chloride Contaminated Environments', SCI 4th International Symposium on Corrosion of Reinforcement in Concrete Construction, (Cambridge, UK, 1996)

3. HETEK, 'Chloride penetration into concrete, State of the art, Transport processes, corrosion and initiation, test methods and prediction models', (The Road Directorate, Copenhagen, Denmark, 1996)

4. Taylor W H, 'Concrete Technology and Practice', (McGraw-Hill Book Company, Sydney, Australia, 1977)

5. Tuutti K, 'Corrosion of Steel in Concrete, Cement och Betong Institutet, Stockholm, (1982)

6. Washa G W, Saemann J C and Cramer S M, 'Fifty Year Properties of Concrete made in 1937', ACI Materials Journal, (American Concrete Institute, USA, 1989)

7. Wood S L, 'Evaluation of the Long-Term Properties of Concrete', ACI Materials Journal 88(6), (American Concrete Institute, USA, 1991)

Fax: +(61)362336657
E-mail:rod.mcgee@dier.tas.gov.au